(ISSN 0161-8202)

# Journal of ARACHNOLOGY

PUBLISHED BY THE AMERICAN ARACHNOLOGICAL SOCIETY

VOLUME 46 2018 NUMBER 2

The *Journal of Arachnology* (ISSN 0161-8202), a publication devoted to the study of Arachnida, is published three times each year by *The American Arachnological Society*. **Memberships (yearly):** Membership is open to all those interested in Arachnida. A subscription to the *Journal of Arachnology* and annual meeting notices are included with membership in the Society. Regular, $55; Students, $30; Institutional, $125. Inquiries should be directed to the Membership Secretary (see below). **Back Issues:** James Carrel, 209 Tucker Hall, Missouri University, Columbia, Missouri 65211-7400 USA. Telephone: (573) 882-3037. **Undelivered Issues:** Allen Press, Inc., 810 E. 10th Street, P.O. Box 368, Lawrence, Kansas 66044 USA.




---

*Cover photo: Araneus diadematus* (Araneidae) male and female hanging from the male's mating thread, which is attached to the periphery of the female's web. See *A review of the mechanisms and functional roles of male silk use in spider courtship and mating*, pp. 173-206; photo by Maria Hiles.

---


Publication date: 17 July 2018

♾ **This paper meets the requirements of ANSI/NISO Z39.48-1992 (Permanence of Paper).**

2018. Journal of Arachnology 46:173–206

## REVIEW

# A review of the mechanisms and functional roles of male silk use in spider courtship and mating

**Catherine E. Scott**[1], **Alissa G. Anderson**[2] and **Maydianne C.B. Andrade**[1]: [1]Department of Biological Sciences, University of Toronto Scarborough, 1265 Military Trail, Scarborough, Ontario Canada M1C 1A4; E-mail: catherine.elizabeth.scott@gmail.com; [2]School of Biological Sciences, Manter Hall, Rm 402, University of Nebraska, Lincoln, Nebraska 68588-0118

**Abstract.** Spiders are well known for using chemical, vibratory, tactile, and visual signals within mating contexts. All spiders produce silk, and even in non-web building spiders, silk is intimately tied to courtship and mating. Silk produced by females provides a transmission channel for male vibratory courtship signals, while webs and draglines provide a substrate for female sex pheromones. Observations of male spiders producing silk during sexual interactions are also common across phylogenetically widespread taxa. However, the function of male-produced silk in mating has received very little study. Exploring the function of male silk use during mating will provide a deeper understanding of the complex mating systems of spiders and allow tests of hypotheses about the evolution of male and female traits under sexual selection and/or conflict. In this review, we outline functional hypotheses that may explain each of the following three main categories of silk deposition males exhibit during courtship and mating: (1) silk deposition on females' webs or other silk structures, (2) silk deposition on females ('bridal veils') and (3) silk associated with nuptial gifts. We then summarize the current knowledge of silk use by male spiders within these three categories and the types of mechanisms that may lead to functional effects, and discuss areas where future work can be targeted.

**Keywords:** Nuptial gifts, web modification, bridal veils, mating behavior, sexual selection

TABLE OF CONTENTS

1. Introduction ..... 174
1.1 Overview ..... 174
1.2 Properties of spider silk ..... 174
1.3 Female silk and mating ..... 175
1.3.1 Substrate for pheromones ..... 175
1.3.2 Substrate for transmission of vibratory signals ..... 175
1.3.3 Structural effects on courtship & mating activity ..... 175
2. Male silk and Mating ..... 176
2.1 Overview ..... 176
2.2 Fitness effects of silk use ..... 176
2.2.1 Fitness effects—current mating ..... 176
2.2.2 Fitness effects—decreased polyandry ..... 176
2.3 Mechanisms of effect ..... 176
2.3.1 Indirect effects—chemical signals/cues ..... 176
2.3.2 Indirect effects—visual signals/cues ..... 178
2.3.3 Indirect effects—tactile cues ..... 179
2.3.4 Indirect effects—correlated effects of silk-laying behaviors ..... 179
2.3.5 Direct effects—structural modifications ..... 179
2.3.6 Direct effects—physical effects ..... 179
3. Silk deposition on females' webs or other silk structures ..... 179
3.1 Overview and descriptions of behaviors ..... 179
3.2 Proposed mechanisms and functions ..... 188
3.3 Current evidence and future directions ..... 188
4. Silk deposition on females ..... 190
4.1 Overview and descriptions of behaviors ..... 190
4.2 Proposed mechanisms and functions ..... 191
4.3 Current evidence and future directions ..... 192
5. Silk associated with nuptial gifts ..... 193
5.1 Overview and descriptions of behaviors ..... 193
5.2 Proposed mechanisms and functions ..... 195
5.3 Current evidence and future directions ..... 195

6. Other examples of male silk use during mating interactions ..... 197
7. Conclusions and future directions ..... 197
7.1 Summary ..... 197
7.2 Functions and mechanisms of effect ..... 197
7.3 Improving our understanding of male silk use ..... 198
7.4 Concluding remarks ..... 199

## 1. INTRODUCTION

**1.1 Overview.**—Mating in animals that are generally solitary, like spiders, necessarily involves a number of shifts in behavior to facilitate locating, approaching, and mating with the opposite sex (Elias et al. 2011; Schneider & Andrade 2011). These shifts provide interesting opportunities to test general aspects of theory related to communication (Hauser 1996; Bradbury & Vehrencamp 2011; Herberstein et al. 2014), mate choice (Bateson 1983), sexual conflict (Arnqvist & Rowe 2005), and sexual selection (Andersson 1994). In many species, males use a range of behavioral, morphological, sensory, and physiological traits when approaching females to seek matings (Andersson 1994). These traits may enhance the success of the male through their effects on the behavior of potential mates or rivals. For example, females' mating decisions may be based on the nature or intensity of male courtship displays or ornaments if these reflect desirable (female-fitness-enhancing) characteristics in a potential mate (Bateson 1983; Andersson 1994; Jennions & Petrie 1997; York & Baird, 2017). Moreover, in many taxa, courtship is a public event (Herberstein et al. 2002), vulnerable to interruption or interference by other males (e.g., Hibler & Houde 2006; Stoltz & Andrade 2009). Sexual selection on males to achieve matings is often intense and may lead to the evolution of remarkable adaptations to overcome competition or persuade females to mate (Andersson 1994). In addition, it is now clear that males may adjust investment in courtship as a function of the perceived fitness payoff (quality or risk) associated with approaching or mating with a given female (Johnson et al. 2011; Moskalik & Uetz 2011; Lane et al. 2015; McGhee et al. 2015; Rundus et al. 2015; Cross 2016; Rypstra et al. 2016). In cannibalistic spiders, there is an added dimension of risk to the male associated with approaching the wrong female (Herberstein et al. 2002; Johnson et al. 2011; Kralj-Fiser et al. 2016). The result is a rich interplay of male and female fitness interests that may be intertwined in different ways at different stages of courtship.

In general, spiders offer interesting opportunities for studying the 'mating dance' between the sexes in detail, since mating behavior varies considerably among taxa (Schneider & Andrade 2011), and courtship often includes multimodal communication (e.g., visual, vibratory, chemical, and tactile; Witt & Rovner 1982). Silk is a tangible, measurable, and manipulable medium that can convey information in all of these modalities and thus has been frequently studied in this context—but almost exclusively from the perspective of females. Thus, it is well known that female silk plays a central role in many aspects of communication and mating outcomes across spider taxa (Gaskett 2007; Elias & Mason 2010; Uhl & Elias 2011; Schulz 2013). In addition to its communicative role, for many spider species female silk is the substrate on which mating interactions occur (Foelix 2011) and this also has implications for its functional role.

What is less well known is the variety of ways in which male silk may mediate sexual interactions in spiders. In this review, we highlight accumulating evidence, from a variety of spider taxa, that male silk also has a significant role in mate attraction, courtship, and mating. We outline the ways in which male silk is used in these interactions and suggest tractable approaches to testing a range of hypotheses to explain the evolution of male silk use in terms of sexual selection and/or sexual conflict. Finally, we identify, where possible, taxa where additional study may be particularly illuminating, both in terms of our understanding of silk use in spiders, and in terms of a more general understanding of male and female mating tactics.

We start by briefly summarizing some salient features of spider silk, and the well-known uses of silk by females during mating interactions. We then provide an overview of the main functional hypotheses for male silk use in mating, and the mechanisms that may lead to functional outcomes. We follow this with a description of the ways males use silk in mating, split into three broad categories (silk deposition on the female's web or other silk structures, silk deposition on the female, and silk associated with nuptial gifts), with examples from a range of taxa. Each category ends with a qualitative evaluation of the hypotheses given the available data. Finally, we briefly discuss a few other ways males use silk in mating interactions (e.g., sperm webs).

**1.2 Properties of spider silk.**—Spider silk consists of protein-based fibers, is energetically costly to produce (Peakall & Witt 1976; Prestwich 1977), is unique in its combination of strength and elasticity, and is one of the toughest known biological substances (Gosline et al. 1999; Rising et al. 2011). The physical properties of spider silk vary among taxa and among contexts within taxa (Craig 2003). Years of research show the biophysical properties of silk are strongly dependent on links between ecological context, evolutionary history (e.g., Wolff et al. 2017), and the physiology of the spider at the time of silk production (Blamires et al. 2017). This may explain why, despite recent progress (Rising et al. 2011; Hsia et al. 2012), attempts to develop industrial production methods to synthesize spider silk have been challenging (Kluge et al. 2008; Koeppel & Holland 2017). Features such as the silk tensile strength and elasticity depend on which glands are used to produce the silk (e.g., aciniform, ampullate, flagelliform, tubuliform, or piriform) and how it is extruded, which varies with use (e.g., egg sacs, structural web silk, capture silk, or drag lines; Vollrath & Knight 2001; Foelix 2011).

Spiders produce silk at every life history phase, and in most cases, leave silk draglines behind them as they move through their habitat (Foelix 2011). Thus, most spider behaviors have the potential to create and leave behind information associated with silk in a variety of modalities. Variation in reflectance properties (Blackledge & Wenzel 2000; Barrantes

et al. 2013) and color (e.g., Craig et al. 1996) of silk can have implications for visibility or attractiveness to prey, predators and conspecifics under a variety of light conditions. However, functional effects have primarily been investigated with regard to predator/prey dynamics (e.g., Craig & Barnard 1990; Blackledge 1998; Persons & Rypstra 2001; Rypstra & Buddle 2013; Bucher et al. 2014; Lai et al. 2017). The structure of silk makes it well-suited as a delivery vehicle for contact or airborne semiochemicals (Gaskett 2007; Schulz 2013; Henneken et al. 2017a) with interesting implications for function arising from variation in how long pheromones remain active after deposition, and whether rain (i.e., a polar solvent) can wash them away (e.g., water soluble pheromones in some wolf spiders: Dondale & Hegdekar 1973; Tietjen 1977; Baruffaldi et al. 2010; water-resistant pheromones in fishing spiders and some wolf spiders: Roland & Rovner 1983; Lizotte & Rovner 1989). Finally, silk also serves as a medium for vibratory communication and detection of vibratory cues, particularly in web-building species (Uhl & Elias 2011).

**1.3 Female silk and mating.**—As a substrate for pheromones, transmission of vibratory signals, and the structure on which mating may take place, female silk is well known for its role within courtship and mating contexts in web-building spiders (Locket 1926; Foelix 2011). Webs or other silk structures (e.g., the silk associated with burrows) provide the stage for vibratory courtship displays by males in many spider taxa in which females are sedentary (Uhl & Elias 2011). Similarly, among cursorial spiders, female drag-line silk provides information to conspecific males (Bristowe & Locket 1926; Kaston 1936; Anderson & Morse 2001; Nelson et al. 2012; Rundus et al. 2015; Bell & Roberts 2017). Draglines can convey chemical (chemo-tactile; e.g., Nelson et al. 2012) or tactile (mechanical; e.g., Anderson & Morse 2001; Leonard & Morse 2006) information about the location and identity of the signaler.

*1.3.1 Substrate for pheromones:* Spiders are predatory and generally solitary, and thus face the challenge of attracting or finding mates. Behavioral evidence indicates that sex pheromones provide the solution to this problem in many spiders (Gaskett 2007; Uhl & Elias 2011; Trabalon 2013). Indeed, since chemical signaling is the most ancient form of communication (Wyatt 2014), sex pheromone production is likely ubiquitous in spiders. Pheromones associated with female silk include those that release volatile, airborne chemicals, and those that require contact by the receiver (Gaskett 2007; Schulz 2013).

Airborne sex pheromones typically attract mates at long range and may also reveal information about the identity and quality of the signaler (Gaskett 2007; Uhl & Elias 2011; Uhl 2013). Volatile, attractive sex pheromones have been identified from the bodies and/or silk of females in only three species: *Argiope bruennichi* (Scopoli, 1772) (Araneidae; Chinta et al. 2010), *Agelenopsis aperta* (Gertsch, 1934) (Agelenidae; Papke et al. 2001), and *Pholcus beijingensis* Zhu & Song, 1999 (Pholcidae; Xiao et al. 2009). Although these chemically identified pheromones come from web-builders, cursorial spiders including lycosids and salticids also produce volatile sex attractants associated with their bodies and/or silk (e.g., Searcy et al. 1999; Nelson et al. 2012). Behavioral studies with *Latrodectus* Walckenaer, 1805 spp. (Theridiidae) indicate that volatile, silk-borne female pheromones allow males to discriminate between females of different age, mating status, body condition, and population of origin (Kasumovic & Andrade 2004; Andrade & Kasumovic 2005; MacLeod & Andrade 2014).

Silk-borne contact pheromones elicit male searching and courtship behavior in both cursorial and web-building spiders (e.g., Tietjen 1978; Suter & Renkes 1982; Taylor 1998), and may provide information about female identity, mating status, receptivity, diet, gravidity, and reproductive potential (Riechert & Singer 1995; Roberts & Uetz 2005; Baruffaldi & Costa 2010; Trabalon 2013; Henneken et al. 2015, 2017b). Contact sex pheromones have been identified from the silk of female spiders in four families: *Linyphia triangularis* (Clerck, 1757) (Linyphiidae; Schulz & Toft 1993), *Latrodectus hasselti* Thorell, 1870 and *L. hesperus* Chamberlin & Ivie, 1935 (Theridiidae; Jerhot et al. 2010; Scott et al. 2015a), *Eratigena atrica* (C.L. Koch, 1843) (Agelenidae; Prouvost et al. 1999), and *Cupiennius salei* (Keyserling, 1877) (Ctenidae; Papke et al. 2000).

*1.3.2 Substrate for transmission of vibratory signals:* Substrate-borne vibrations are extremely important for spiders (Barth 2002; Elias & Mason 2010), which are highly sensitive to vibrations detected via receptors on their legs (Barth 1982; Foelix 2011). Spiders that build webs or snares or simply extend the silk lining of their burrow can essentially expand their field of sensory perception and create their own specialized signaling environments (Elias & Mason 2010; Krafft & Cookson 2012). The silk in these contexts transmits vibrations both from prey and courting males. The types of vibratory behaviors in spiders include percussion, stridulation, and tremulation, and these may transmit seismic and/or near-field airborne vibratory signals (reviewed in Uhl & Elias 2011). Vibratory courtship signals produced on webs have been recorded in only a small number of studies (Masters & Markl 1981; Masters 1984; Suter & Renkes 1984; Naftilan 1999; Wignall & Herberstein 2013a; Vibert et al. 2014). However, our understanding of the biomechanical properties of spider silk with respect to vibration transmission has expanded rapidly in recent years (primarily for orb-webs, e.g., Landolfa & Barth 1996; Watanabe 2000; Alam et al. 2007; Mortimer et al. 2014, 2015, 2016). For example, Mortimer and colleagues (2016) examined trade-offs between signal transmission and the structure of orb-webs; their work led them to conclude that silk tension and stiffness can affect vibration amplitude. This led them to the intriguing suggestion that females could construct webs to optimally balance multiple signal transmission functions (Mortimer et al. 2016).

*1.3.3 Structural effects on courtship & mating activity:* In web-building spiders, the female's web and/or retreat is often the location of courtship and mating. Thus, the structure of the web or retreat may constrain the type of courtship, approach vector, or mobility of males. For example, in some species females rest with their genital opening in close proximity to dense silk sheets such that mating requires a postural change (e.g., *Latrodectus*; Andrade & MacLeod 2015). Similarly, mating by non-web-building spiders may take place inside the female's burrow or silk retreat, where the movement of males and females is constrained (e.g., *Phidippus* C.L. Koch, 1846; Hoefler 2007). To our knowledge, there has

been no investigation of female web or retreat structure in relation to mobility during mating.

## 2. MALE SILK AND MATING

**2.1 Overview.**—Male spiders from diverse and distantly related families use silk during courtship and mating (Fig. 1). We review the main contexts in which males use silk in mating, with an emphasis on what is known about the effects of silk on males and/or females (Table 1). We start with a brief overview of the general types of effects that are recurrent themes, which suggest a number of (non-exclusive) hypotheses about male silk use in mating. We then arrange existing data on male silk use during mating into three main categories: (I) silk addition to females' webs (with or without web reduction; Table 2), (II) application of silk to female mating partners ('bridal veils'; Table 3), and (III) presentation of silk associated with nuptial gifts (or silk itself) to females (Table 4). For each type of silk use, we end by considering the specific types of effects predicted by each hypothesis and suggest where additional study would be fruitful. We then briefly discuss other ways silk is used by males during mating interactions that do not fall into these categories (Table 5). Finally, we provide general conclusions and suggestions for future directions.

**2.2 Fitness effects of silk use.**—There are a number of different hypotheses for the function of male silk use during mating interactions (Table 1). These are not mutually exclusive; as male silk use could have multiple functions in a given species. We consider these in terms of the way in which the behavior may increase the fitness of the silk-laying male, and the mechanism that leads to effects on fitness.

*2.2.1 Fitness effects—current mating:* Silk may increase a male's fitness if it increases his mating success with a given female (see columns 1–3 in Table 1). We consider three ways males might use silk to increase their fitness during interactions with a potential mate. (1) Silk may increase the likelihood of copulation by increasing or accelerating female receptivity to mating (i.e., affect female preference). More receptive females may also copulate more quickly. Rapid copulation may decrease the risk of interference by other males or by predators, and/or reduce the energetic investment in courtship. (2) Silk use may increase male fitness if it increases sperm transfer via longer or more frequent copulations (total copulation duration is linked to paternity or fertilization success in some species; Andrade 1996; Elgar et al. 2000; Anderson & Hebets 2017). We predict these functions would have the most significant effects on male fitness in species in which females are very choosy, courtship is costly and possibly prolonged, where rival males commonly approach females that are being courted by other males, and/or where copulation frequency or duration is related to paternity or fertilization success. (3) Silk use might increase male fitness by reducing the risk of male injury or death. These effects may arise through decreased risk of sexual cannibalism or attacks by rival males. Clearly, these effects would be most important in species where females frequently attack males during courtship or copulation, and/or where direct or escalated inter-male competition is coincident with courtship and mating attempts.

*2.2.2 Fitness effects—decreased polyandry:* Males may also benefit from silk use through a reduced risk of polyandry and thus a reduced risk of losing paternity to rival males (see columns 4–5 in Table 1). We divide this fitness benefit into two categories. (4) Silk use may decrease the risk of rival males courting or mating by interfering with the female's attractiveness to rivals, causing ineffective courtship by rivals, or decreasing physical access to females for rival males. (5) Alternatively, male silk use may decrease the likelihood of females remating by decreasing the receptivity of mated females. These effects would be most significant in species where females typically have the opportunity for polyandry, where sperm of rival males mix or last-male sperm precedence is relatively common (so males that mate after the first male will secure some paternity).

**2.3 Mechanisms of effect.**—In terms of mechanisms of effect (Table 1), fitness benefits of silk use can be derived indirectly through communication, where beneficial changes in the behavior of females or rival males arise from assessment of the information content of silk use. Information may be encoded in chemical, visual, tactile, or vibratory modalities. This may involve assessment of qualities of the male silk in itself (chemical, visual, and/or tactile modalities), or assessment of the performance of male behaviors involved in silk addition (vibratory and/or visual modalities). Finding evidence for fitness consequences of silk addition, or understanding the implications in terms of vibrations, may be less challenging than unravelling underlying mechanism(s) related to chemical or tactile signalling. Demonstrating the presence of pheromones on silk and differentiating between chemical and tactile cues requires carefully designed experiments (e.g., Anderson & Morse 2001). While identifying spider pheromones remains a challenge, other approaches include temporary or permanent ablation of the female's tactile or chemosensory receptors (Zhang et al. 2011; Aisenberg et al. 2015).

Fitness benefits may also derive directly through physical effects of male silk addition to the female, her web, or a nuptial gift. This may arise if structural changes to the web affect courtship and mating mobility, if silk acts as a physical constraint on movement, or if it functions to hide the contents of a nuptial gift (deception). In this category, we also include effects of silk addition on efficacy of communication that may arise through structural changes to the web.

*2.3.1 Indirect effects—chemical signals/cues:* Behavioral evidence suggests that, like female silk, silk produced by males can transmit chemical information as part of intersexual communication. Only one male spider pheromone has been chemically identified to date, an aphrodisiac isolated from whole-body extracts of *Pholcus beijingensis* (Pholcidae) males (Xiao et al. 2010). However, behavioral evidence demonstrates or supports the existence of silk-borne male sex pheromones in seven families (Fig. 1; Table 6). Like female pheromones, these putative male pheromones have diverse functions. Contact with male silk elicits courtship behavior in female *L. hesperus* (Theridiidae; Ross & Smith 1979). A pheromone from the male's body and/or silk induces quiescence in female *Agelenopsis aperta* (Agelenidae; Becker et al. 2005). Tactile and/or chemical information on male silk facilitates orientation in female *Tegenaria domestica* (Clerck, 1757) and *Coelotes terrestris* (Wider, 1834) (Agelenidae; Roland 1983). Similarly, in the lycosid spider *Pardosa milvina*

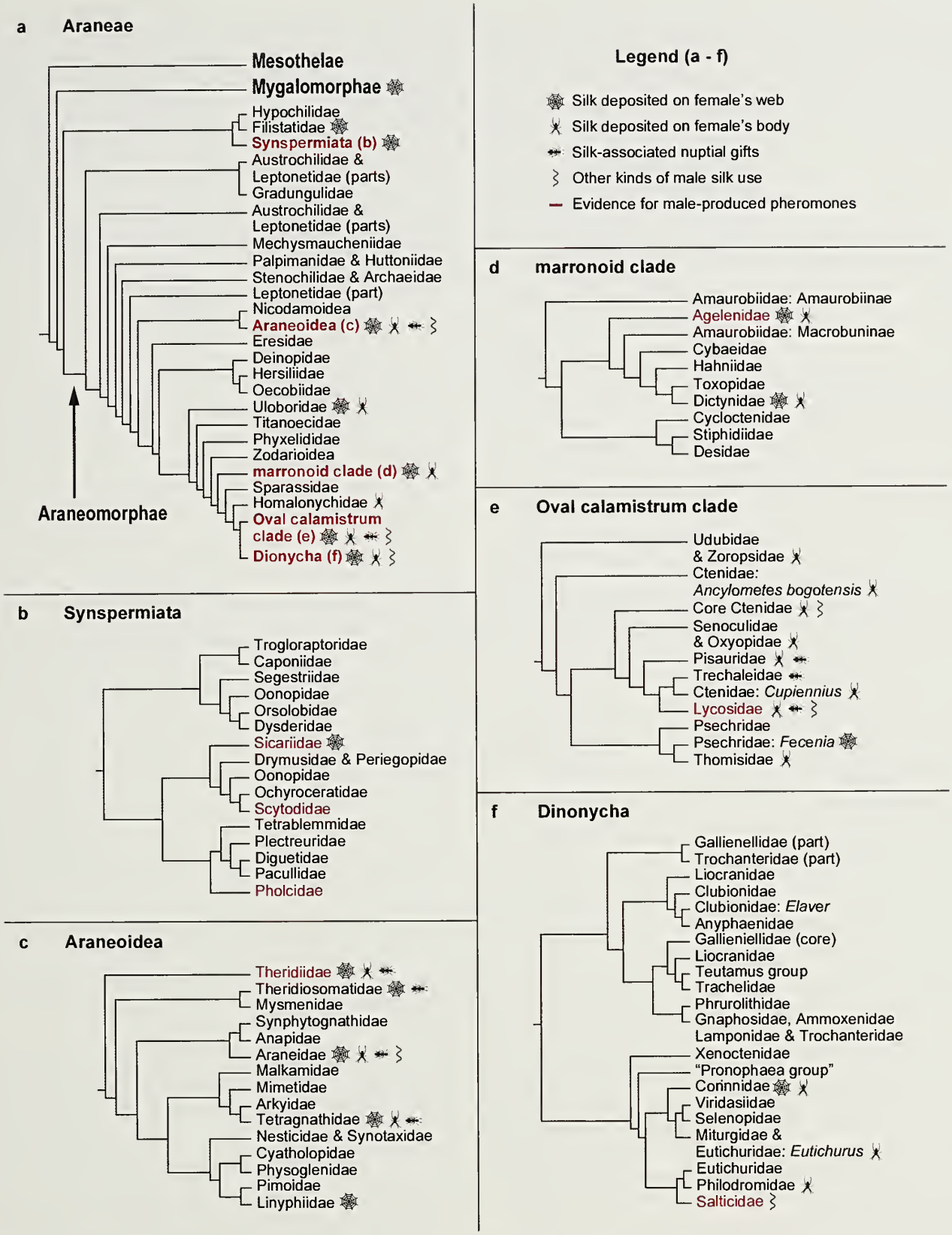


Figure 1.—Cladograms illustrating relationships between araneomorph spider families (based on Wheeler et al. 2016) and the occurrence of male silk and pheromone use. (a) Overview of the order Araneae. (b) Families in clade Synspermiata. (c) Families in clade Araneoidea. (d) Families in the marronoid clade. (e) Families in the Oval Calamistrum clade. (f) Families in clade Dionycha. Red type or symbols next to a clade (see legend) indicates that there is evidence for a given type of male silk use or the presence of male pheromones in at least one species in that clade (see Tables 2–5 for lists of species and references). Note that in the Mygalomorphae (families not shown on the figure) there are records of male silk deposition on the female's web or silk for species in the following three families: Dipluridae, Porrhothelidae, and Theraphosidae.

Table 1.—Cross tabulation of potential functions (columns) and mechanisms (rows) of silk use by male spiders in courtship and mating. Symbols in filled cells indicate functions and their mechanisms for which there is experimental evidence. Symbols are as in Fig. 1 (web indicates silk addition to or reduction of the female's web; spider indicates silk deposition on the female's body; insect indicates silk-associated nuptial gift). ✗ indicates experimental evidence against a specific function/mechanism and "nt" indicates that, to our knowledge, no test has been conducted.

| Function → | Increased success: current mating | | | Decreased polyandry | |
|---|---|---|---|---|---|
| Mechanisms | Increased female receptivity/ probability of mating | Increased sperm transfer (copulation # or duration) | Decreased risk of injury or death | Decreased risk of rival males courting/mating | Decreased female receptivity to remating |
| **INDIRECT: Communication** | | | | | |
| Chemical | (1) | (2) | (2) | (3,4) | nt |
| Visual | (5-7) | | | nt | nt |
| Tactile | nt | (2) | (2) | nt | nt |
| Vibratory (correlated effect) | nt | nt | nt | nt | nt |
| **DIRECT: Structural effects** | | | | | |
| Mobility | nt | nt | nt | nt | nt |
| Signal Transmission | nt | nt | nt | (3,4) | nt |
| **DIRECT: Physical effects** | | | | | |
| Physical constraints | ✗ (8) | (8) | (9) | nt | nt |
| Deceit | (10,11) | (10,11) | nt | nt | nt |

(1) *Paratrechalea ornata* (Trechaleidae); Brum et al. 2012 (silk extract alone is sufficient to elicit female gift acceptance)
(2) *Nephila pilipes* (Araneidae); Zhang et al. 2011 (chemical and tactile effects of veil on cannibalism and sperm transfer duration)
(3) *Neriene litigiosa* (Linyphiidae); Watson 1986 (female pheromone emission/attractiveness decreased by web reduction and females remain unattractive after mating)
(4) *Latrodectus hesperus* (Theridiidae); Scott et al. 2015b (female pheromone emission/attractiveness decreased by web reduction and females remain unattractive after mating)
(5) *Pisaura mirabilis* (Pisauridae); Stålhandske 2002 (females accept brighter gifts more quickly)
(6) *Paratrechalea ornata* (Trechaleidae); Trillo et al. 2014 (males with white painted chelicerae had higher mating success than those without, in absence of prey item)
(7) *Paratrechalea ornata* (Trechaleidae); Klein et al. 2014 (small bright gifts accepted more quickly than large dark ones, but does not exclude chemical/tactile cues)
(8) *Pisaurina mira* (Pisauridae); Anderson & Hebets 2017 (male silk does not affect copulation success but males that produce a bridal veil achieve increased sperm transfer and fertilization success)
(9) *Pisaurina mira* (Pisauridae); Anderson & Hebets 2016 (silk wrapping physically restrains females, reducing male's risk of cannibalism following/during sperm transfer and increasing the number of insertions achieved)
(10) *Pisaura mirabilis* (Pisauridae); Albo et al. 2011a (males presenting worthless gifts achieve similar copulation success to those with prey gifts, and significantly higher copulation success than males without gifts; males with worthless gifts achieve longer copulation duration than those without gifts, but shorter duration than those with prey gifts)
(11) *Paratrechalea ornata* (Trechaleidae); Albo et al. 2014 (males with worthless gifts achieve copulations while males without gifts do not; copulation duration—correlated with sperm transfer amount—is similar for males with worthless gifts and prey gifts)

(Hentz, 1844) females discriminate between silk of courting and non-courting males, increasing their own silk production in response to contact with the male's silk (Khan & Persons 2015). Airborne pheromones from the bodies and silk of *Scytodes* Latreille, 1804 sp. (Scytodidae) and *Evarcha culicivora* Wesolowska & Jackson, 2003 (Salticidae) males function in mate recognition and mate choice (Cross & Jackson 2009; Koh et al. 2009).

Pheromones on male silk may also be important for intrasexual communication (Table 7), including assessment of male-male competition. Airborne chemical cues from *Latrodectus hasselti* (Theridiidae) males and/or their silk provide information about the competitive environment and trigger shifts in development in other males (Kasumovic & Andrade 2006). Male *Nephila senegalensis* (Walckenaer, 1841) (Araneidae) use silk cues left behind by rival males to choose which females' webs to visit. They avoid webs previously visited by another male, irrespective of the female's quality (Schneider et al. 2011). Male courtship behavior is inhibited by a pheromone that can be extracted with methanol from the silk of *Schizocosa ocreata* (Hentz, 1844) (Lycosidae) males (Ayyagari & Tietjen 1987), and *Frontinella communis* (Hentz, 1850) (Linyphiidae) males respond to compounds on male cuticle with aggressive behavior (Suter et al. 1987).

*2.3.2 Indirect effects—visual signals/cues:* For spider species with well-developed vision, male silk could play a role in visual signaling, or provide cues about the state of the male that produced the silk, and thus affect female receptivity or choice.

For example, the density of silk male pisaurids and trechaleids use to wrap nuptial gifts (see section 4 below), affects the color of the gift (bright white to dark grey), and may provide information about the physiological state of the gift-giving male (Stålhandske 2002; Albo et al. 2011a; Trillo et al. 2014). White silk in itself may be highly visible, and so attract the attention of females, as has been shown in the crepuscular *Paratrechalea ornata* (Mello-Leitão, 1943) (Stålhandske 2002; Trillo et al. 2014).

*2.3.3 Indirect effects—tactile cues:* When silk comes in contact with females directly, or when females manipulate, touch, or move across silk laid down by males, that contact may provide information. For example, tactile cues on silk draglines allow male crab spiders to follow females, with recognition depending on mechanical characteristics of the silk (Anderson & Morse 2001).

*2.3.4 Indirect effects—correlated effects of silk-laying behaviors:* The behaviors associated with silk deposition may have functions independent of the silk itself. For many species, typical male abdominal movements have been described in association with silk application (see 'abdomen waggle' in Table 2), and these may produce vibrational or visual signals. In an analogous example, Vollrath (1979) showed that prey-wrapping by web-building spiders creates a characteristic pattern of vibrations that are exploited by the kleptoparasite *Argyrodes elevatus* Taczanowski, 1873. Here we focus primarily on the way in which male silk itself may affect mating outcomes, but also outline behaviors that are reliably associated with silk deposition where relevant.

*2.3.5 Direct effects—structural modifications:* Males of many species modify the webs or other silk structures of females, and this may involve the use of male silk in various ways, including covering or wrapping females' silk, or adding new silk lines to existing structures. Modifications to web structure are traditionally described in terms of how they affect the behavior or possible movement (mobility) of the female and/or rival males during a mating attempt. However, these structural changes may also affect the nature, directionality or efficacy of vibrational or chemical signals or cues. Thus, changes in signal transmission may be the primary mechanism by which silk use affects male fitness.

*2.3.6 Direct effects—physical effects:* Males produce a range of different types of silks, and comparable to the use of silk in prey-capture, male silk may be applied directly to the female in such a way that it restrains, impedes or slows the movement of females or even of rival males (physical constraints). Silken constructions may also support or adjust the posture of females in a way that facilitates genital coupling. Alternatively, silk wrapped around nuptial gifts may allow males to hide their contents when the gift is of low nutritional value (deceit).

## 3. SILK DEPOSITION ON FEMALES' WEBS OR OTHER SILK STRUCTURES

**3.1 Overview and descriptions of behaviors.**—In web-dwelling spiders, mating generally takes place on the female's web or in her retreat. During courtship, males in several families representing the full range of web architectures lay silk on the female's web, leading to modification of existing web structure (Figs. 1 & 2). Web modification with silk addition varies from the addition of a single line (a mating thread) to destruction of large areas of the female's web and replacement with male silk (web reduction). Similarly, in burrow-dwellers like some mygalomorph and lycosid spiders, silk lines the burrow and may extend from its entrance, providing the substrate on which courtship occurs. Males of these taxa may also deposit silk onto the female's silk during mating interactions, although modification of the overall architecture of the female's silk structures has not been reported. Descriptions of silk-spinning behavior of males when courting on webs or on other silk structures have many similarities, and thus we consider them together in this section.

Among the Mygalomorphae, silk deposition by males during courtship has been reported for the web-building Dipluridae and Porrhothelidae (formerly Hexathelidae) and the burrow-dwelling Theraphosidae. In the diplurid spiders *Thelechoris karschi* (Simon, 1889) and *Microhexura montigava* Crosby & Bishop, 1925, both males and females spin silk as they move about the web during courtship (Coyle 1985; Coyle & O'Shields 1990). *Porrhothele antipodiana* (Walckenaer, 1837) (Porrhothelidae) males spin silk during interactions with females on their webs (both before and after copulation), and also during interactions with other males. Silk spinning behavior in this species is accompanied by obvious lateral movements of the abdomen (Jackson & Pollard 1990). In the burrow-dwelling theraphosid spiders *Grammostola vachoni* Schiapelli & Gerschman, 1961 and *Brachypelma klaasi* (Schmidt & Krause, 1994), courting males lay down silk over the female's silk around the burrow entrance (Yáñez et al. 1999; Ferretti & Ferrero 2008).

Descriptions of silk deposition in some araneomorph spiders that build sheet webs are similar to those for the Mygalomorphae. Upon contact with the web of a virgin female, the crevice weaver *Kukulcania hibernalis* (Hentz, 1842) (Filistatidae) pulls swaths of silk threads from his spinnerets with his last pair of legs and deposits them on her web (Barrantes & Ramirez 2013). Less obvious silk deposition occurs during the courtship of the funnel weaver *Eratigena agrestis* (Walckenaer, 1802) (Agelenidae). Males deposit silk as they move around on the female's web, periodically anchoring it to the sheet (C.E. Scott, pers. obs.). Lateral 'abdomen wagging' behavior is associated with silk deposition in *E. agrestis*, and this behavior is common during the courtship of several other agelenids, most notably the genus *Agelenopsis* C.L. Koch, 1837 (Table 2; Galasso 2012). This 'wagging' that occurs as males move around the web is usually accompanied by silk emission in these agelenids (S. Riechert, pers. comm.).

In orb-weavers (family Araneidae, including subfamily Nephilinae, formerly Nephilidae), courtship is grouped into three types (A–C), two of which involve male alteration of web architecture (Robinson & Robinson 1980). Type A courtship occurs on the female's web and typically involves addition of silk near the hub. In type B courtship, the male cuts a hole in the web close to the hub and constructs a mating thread across it. Type C courtship does not involve any web cutting; the male constructs a mating thread that he attaches to the periphery of the web. In both type B and C courtship, the male engages in vibratory courtship on the mating thread (which may be multi-stranded; Table 2). Eventually the female joins the male on the mating thread, where copulation takes place. Typically, males of a given species use one type of courtship,

Table 2.—Spider taxa in which males modify the female's web or other silken structures by adding and/or removing silk (web reduction). Y = yes; N = no; P = probable; *n* = number of mating interactions observed. Where data are available, the specific behavior is described in brackets, as is the percentage of males that engage in that behavior, with a superscript indicating the reference specific to these data where necessary.

| Taxon | Addition of silk | Web reduction | Citations |
|---|---|---|---|
| **Agelenidae** | | | |
| *Agelenopsis actuosa* (Gertsch & Ivie, 1936) | P (abdomen waggle) | N | Galasso 2012 |
| *Agelenopsis aperta* (Gertsch, 1934) | Y (abdomen waggle) | N | Singer et al. 2000; Galasso 2012; S. Reichert pers. comm. |
| *Agelenopsis aleenae* Chamberlin & Ivie, 1935 | P (abdomen waggle) | N | Galasso 2012 |
| *Agelenopsis emertoni* Chamberlin & Ivie, 1935 | P (abdomen waggle) | N | Galasso 2012 |
| *Agelenopsis kastoni* Chamberlin & Ivie, 1941 | P (abdomen waggle) | N | Galasso 2012 |
| *Agelenopsis naevia* (Walckenaer, 1841) | P (abdomen waggle) | N | Galasso 2012 |
| *Agelenopsis oklahoma* (Gertsch, 1936) | P (abdomen waggle) | N | Galasso 2012 |
| *Agelenopsis pennsylvanica* (C. L. Koch, 1843) | P (abdomen waggle) | N | Galasso 2012 |
| *Agelenopsis potteri* (Blackwall, 1846) | P (abdomen waggle) | N | Galasso 2012 |
| *Agelenopsis spatula* Chamberlin & Ivie, 1935 | P (abdomen waggle) | N | Galasso 2012 |
| *Agelenopsis utahana* (Chamberlin & Ivie, 1933) | P (abdomen waggle) | N | Galasso 2012 |
| *Barronopsis texana* (Gertsch, 1934) | P (abdomen waggle) | N | Galasso 2012 |
| *Eratigena agrestis* (Walckenaer, 1802) | Y (depositing silk) | N | Vibert et al. 2014 |
| **Araneidae** | | | |
| *Aetrocantha falkensteini* Karsch, 1879 | Y (mating thread) | N | Robinson & Robinson 1980 |
| *Alpaida veniliae* (Keyserling, 1865) | Y (mating thread) | N | Benamú et al. 2012, 2015 |
| *Araneus diadematus* Clerck, 1757 | Y (mating thread) | N | Elgar & Nash 1988 |
| *Araneus quadratus* Clerck, 1757 | Y (mating thread) | N | Elgar 1991 |
| *Argiope aemula* (Walckenaer, 1841) | Y ('miniweb' within web & silk at hub) | N | Robinson & Robinson 1980 |
| *Argiope aetherea* (Walckenaer, 1841) | Y (mating thread) | Y (small hole) | Robinson & Robinson 1980 |
| *Argiope argentata* (Fabricius, 1775) | Y (dragline silk on web & female's dragline or multistranded mating thread inside or outside web) | Y (small hole) or N | Robinson & Robinson 1980 |
| *Argiope aurantia* Lucas, 1833 | Y (miniweb within web & silk on web) | Y (small hole) | Robinson & Robinson 1980 |
| *Argiope aurocincta* Pocock, 1898 | Y (mating thread & silk dep. during walkabouts) | Y (small hole) | Robinson & Robinson 1980 |
| *Argiope bruennichi* (Scopoli, 1772) | Y (mating thread) | Y (small hole) | Elgar 1991 |
| *Argiope cuspidata* Thorell, 1859 | Y (mating thread & silk dep. during walkabouts) | Y (small hole) | Robinson & Robinson 1980 |
| *Argiope flavipalpis* (Lucas, 1858) | Y (mating thread) | Y (small hole) | Robinson & Robinson 1980 |
| *Argiope florida* Chamberlin & Ivie, 1944 | Y (mating thread; silk dep. during walkabouts) | Y (small hole) | Robinson & Robinson 1980 |
| *Argiope keyserlingi* Karsch, 1878 | Y (mating thread) | Y (small hole) or N | Herberstein et al. 2002 |
| *Argiope ocyaloides* L. Koch, 1871 | Y (mating thread) | Y (small hole) | Robinson & Robinson 1980 |
| *Argiope picta* L. Koch, 1871 | Y (multistranded mating thread) | Y (large hole; male may increase size between courtship bouts) | Robinson & Robinson 1980; Elgar 1991 |
| *Argiope radon* Levi, 1983 | Y (mating thread) | Y (small hole) | Robinson & Robinson 1980; Wignall et al. 2014 |
| *Argiope reinwardti* (Doleschall, 1859) | Y (extensive silk dep. at hub) | N | Robinson & Robinson 1980 |
| *Argiope submaronica* Strand, 1916 | Y (mating thread & silk dep. on web) | Y (small hole) | Robinson & Robinson 1980 |
| *Argiope submaronica* Strand, 1916 | Y (mating thread) | Y (small hole) | Robinson & Robinson 1980 (as *Argiope savignyi*) |

Table 2.—Continued.

| Taxon | Addition of silk | Web reduction | Citations |
|---|---|---|---|
| *Cyclosa caroli* (Hentz, 1850) | Y (mating thread) | N | Robinson & Robinson 1980 |
| *Cyclosa insulana* (Costa, 1843) | Y (multistranded mating thread) | N | Robinson & Robinson 1980 |
| *Cyclosa insulana* (Costa, 1843) | Y (silk laid down onto guylines of web; $n = 4$) | Y (cuts threads of rival males, web size reduced by 40%; $n = 1$) | McClintock & Dodson 1999 |
| *Cyrtophora moluccensis* (Doleschall, 1857) | Y (mating thread) | N | Berry 1987 |
| *Eriophora fuliginea* (C. L. Koch, 1838) | Y (mating thread) | N | Robinson & Robinson 1980 |
| *Eriophora transmarina* (Keyserling, 1965) | Y (mating thread) | Y (small hole) | Elgar 1991 (as *Eriophora transmarinus*) |
| *Gasteracantha cancriformis* (Linnaeus, 1758) | Y (mating thread) | N | Robinson & Robinson 1980; Bukowski et al. 2001 |
| *Gasteracantha curvispina* (Guérin, 1837) | Y (mating thread) | N | Robinson & Robinson 1980 |
| *Gea* C. L. Koch, 1843 sp. | Y (mating thread) | N | Robinson & Robinson 1980 |
| *Herennia multipuncta* (Doleschall, 1859) | Y (dragline silk) | N | Robinson & Robinson 1980 (as *Herennia ornatissima*) |
| *Isoxya cicatricosa* (C. L. Koch, 1844) | Y (mating thread) | N | Robinson & Robinson 1980 (as *Isoxya cicatrosa*) |
| *Isoxya tabulata* (Thorell, 1859) | Y ('treadmill'-type mating thread) | Y (cuts some web elements) | Robinson & Robinson 1980 |
| *Kapogea sexnotata* (Simon, 1895) | Y (multistranded mating thread & silk dep. on web) | Y (cuts away extensive portion of lower snare) | Robinson & Robinson 1980 (as *Cyrtophora nympha*) |
| *Leviellus thorelli* (Ausserer, 1871) | Y (mating thread) | N | Kralj-Fišer et al. 2013 |
| *Mangora bimaculata* (O. Pickard-Cambridge, 1889) | Y (converts radius to mating thread; $n = 3$) | Y (removes viscid spiral elements on either side of mating thread; $n = 3$) | Robinson & Robinson 1980 |
| *Mecynogea lemniscata* (Walckenaer, 1841) | Y (mating thread & silk deposition on snare) | N | Robinson & Robinson 1980 |
| *Micrathena clypeata* (Walckenaer, 1805) | Y (mating thread) | N | Robinson & Robinson 1980 |
| *Micrathena duodecimspinosa* (O. Pickard-Cambridge, 1890) | Y (mating thread) | N | Robinson & Robinson 1980 |
| *Micrathena gracilis* (Walckenaer, 1805) | Y (mating thread) | N | Bukowski & Christenson 2000 |
| *Micrathena sagittata* (Walckenaer, 1841) | Y (mating thread) | N | Robinson & Robinson 1980 |
| *Micrathena schreibersi* (Perty, 1833) | Y (mating thread) | N | Robinson & Robinson 1980 |
| *Micrathena sexspinosa* (Hahn, 1822) | Y (converts one radius to thick, multistranded mating thread) | Y (removes viscid spiral elements on either side of mating thread radius) | Robinson & Robinson 1980 |
| *Nephila edulis* (Labillardière, 1799) | Y (dragline silk) | N | Robinson & Robinson 1980 |
| *Nephila pilipes* (Fabricius, 1793) | Y (dragline silk; extensive, incl. on females' dragline) | N | Robinson & Robinson 1980 |
| *Nephila pilipes* (Fabricius, 1793) | Y (dragline silk) | N | Robinson & Robinson 1980 (as *Nephila maculata*) |
| *Nephila clavipes* (Linnaeus, 1767) | Y (dragline silk) | N | Robinson & Robinson 1980 |
| *Nephilengys malabarensis* (Walckenaer, 1841) | Y (dragline silk) | N | Robinson & Robinson 1980 |

Table 2.—Continued.

| Taxon | Addition of silk | Web reduction | Citations |
|---|---|---|---|
| *Scoloderus cordatus* (Taczanowski, 1879) | Y ('treadmill'-type mating thread) | N | Stowe 1978 |
| *Thelacantha brevispina* (Dolesehall, 1857) | Y (mating thread) | N | Robinson & Robinson 1980 (as *Gasterocantha brevispina*) |
| *Zilla* spp. C. L. Koch, 1834 | Y (multistranded mating thread) | N | Robinson & Robinson 1980 |
| *Zygiella x-notata* (Clerek, 1757) | Y (mating thread) | N | Blanke 1986 as eited by Dondale et al. 2003 |
| **Corrinidae** | | | |
| *Nyssus coloripes* Walekenaer, 1805 | Y (zigzags of silk laid down onto female's web) | N | Jaekson & Poulsen 1990 (as *Snpuna picta*) |
| **Dictynidae** | | | |
| *Dictyna arundinacea* (Linnaeus, 1758) | Y (small 'eanopy') | Y (small hole) | Loeket 1926; Bristowe 1958 |
| *Dictyna tridentata* Bishop & Ruderman, 1946 | Y | N | Jaekson 1979 |
| *Dictyna volucripes* Keyserling, 1881 | Y | N | Starr 1988 |
| *Mallos gregalis* (Simon, 1909) | Y | N | Jaekson 1979 |
| *Mexitlia trivittata* (Banks, 1901) | Y | N | Jaekson 1979 (as *Mallos trivittatus*) |
| **Dipluridae** | | | |
| *Microhexura montivaga* Crosby & Bishop, 1925 | Y (sometimes apply silk to female's web) | N | Coyle 1985 |
| *Thelechoris striatipes* (Simon, 1889) | Y (spin silk while eourting; 4%; $n = 45$) | N | Coyle & O'Shields 1990 (as *Thelechoris karschi*) |
| **Filistatidae** | | | |
| *Kukulcania hibernalis* (Hentz, 1842) | Y (83%; $n = 6$) | N | Barrantes & Ramirez 2013 |
| **Linyphiidae** | | | |
| *Florinda coccinea* (Hentz, 1850) | Y | Y (part of web; 75%; $n = 20$) | Willey Robertson & Adler 1994 |
| *Lepthyphantes leprosus* (Ohlert, 1865) | Y | Y (90-100% of web; 45%; $n = 29$) | van Helsdingen 1965 |
| *Linyphia triangularis* (Clerek, 1757) | Y | Y (part or all of web[2]; 68%; $n = 60$[3]) | [2]Rovner 1968 [3]Weldingh et al. 2011 |
| *Neriene litigiosa* (Keyserling, 1886) | Y | Y (large portions of web; 28%; $n = 50$) | Watson 1986 (as *Linyphia litigiosa*) |
| *Pityohyphantes phrygianus* (C. L. Koch, 1836) | unknown | Y (web reduced to a small wad; $n = 18$)[4] | [4]Stålhandske & Gunnarsson 1996; Gunnarsson et al. 2004 |
| *Porrhomma egeria* Simon, 1884 | Y (adds threads to web) | N | Bourne 1978 |
| **Porrhothelidae** | | | |
| *Porrhothele antipodiana* (Walekenaer, 1837) | Y (spins silk on web before & after copulation; 47%; $n = 186$) | N | Jaekson & Pollard 1990 |
| **Psechridae** | | | |
| *Fecenia* Simon, 1887 sp. | N | Y (most of web, leaving single thread; $n = 1$) | Robinson & Lubin 1979 |
| **Sicariidae** | | | |
| *Loxosceles gaucho*, Gertseh, 1967 | N | Y (often eut some threads of web) | Rinaldi & Stropa 1998 |
| **Tetragnathidae** | | | |
| *Metellina segmentata* (Clerek, 1757) | Y (mating thread & wrapping silk around prey item) | Y (small section of web eut out) | Prenter et al 1994b; Bristowe 1929 |
| **Theraphosidae** | | | |
| *Brachypelma klaasi* (Schmidt & Krause, 1994) | Y (deposits silk around female's burrow & over her silk) | N | Yáñez et al. 1999 |

Table 2.—Continued.

| Taxon | Addition of silk | Web reduction | Citations |
|---|---|---|---|
| *Grammostola vachoni* Schiapelli & Gerschman, 1961 | Y (lays silk over female's silk) | N | Ferretti & Ferrero 2008 (as *Grammostola schulzei*) |
| **Theridiidae** | | | |
| *Argyrodes antipodianus* O. Pickard-Cambridge, 1880 | Y | Y | Whitehouse & Jackson 1994 (as *Argyrodes antipodiana*) |
| *Argyrodes argyrodes* (Walckenaer, 1841) | Y (web-spinning; 14%; $n = 7$) | Y | Knoflach 2004 |
| *Dipoena melanogaster* (C. L. Koch, 1837) | Y (mating web) | N | Knoflach 2004 |
| *Echinotheridion gibberosum* (Kulczyński, 1899) | Y (mating web) | N | Knoflach 2004 |
| *Enoplognatha afrodite* Hippa & Oksala, 1983 | Y (mating web; $n = 4$) | N | Knoflach 2004 |
| *Enoplognatha diversa* (Blackwall, 1859) | Y (mating web; $n = 3$) | N | Knoflach 2004 |
| *Enoplognatha latimana* Hippa & Oksala, 1982 | Y (mating web; $n = 1$) | N | Knoflach 2004 |
| *Enoplognatha macrochelis* Levy & Amitai, 1981 | Y (mating web; $n = 5$) | N | Knoflach 2004 |
| *Enoplognatha ovata* (Clerck, 1757) | Y (mating web; $n = 5$) | N | Knoflach 2004 |
| *Enoplognatha quadripunctata* Simon, 1884 | Y (mating web; $n = 2$) | N | Knoflach 2004 |
| *Enoplognatha thoracica* (Hahn, 1833) | Y (mating web; $n = 1$) | N | Knoflach 2004 |
| *Kochiura aulica* (C. L. Koch, 1838) | Y (mating thread; $n = 6$) | Y (hole cut for mating thread) | Knoflach 2004 (as *Anelosimus aulicus*) |
| *Latrodectus dahli* Levi, 1959 | Y (50%; $n = 2$) | N | Knoflach & van Harten 2002 |
| *Latrodectus geometricus* C. L. Koch, 1841 | Y | Y ('less commonly') | Segoli et al. 2008 |
| *Latrodectus hasselti* Thorell, 1870 | Y | Y | Forster 1992, 1995 |
| *Latrodectus hesperus* Chamberlin & Ivie, 1935 | Y | Y (up to 50% of web; 58%; $n = 12$[1]) | Ross & Smith 1979; [1]Scott et al. 2012 |
| *Latrodectus mactans* (Fabricius, 1775) | Y | Y | Breene & Sweet 1985 |
| *Latrodectus pallidus* O. Pickard-Cambridge, 1872 | Y | Y | Harari et al. 2009 |
| *Latrodectus reviveusis* Shulov, 1948 | Y (69% of males) | Y (up to 50% of barrier web) | Anava & Lubin 1993 |
| *Paidiscura* Archer, 1950 sp. | Y (mating web) | | Knoflach 2004 |
| *Paidiscura pallens* (Blackwell, 1834) | Y | Y | Locket 1927 (as *Theridion palleus*) |
| *Parasteatoda tepidariorum* (C. L. Koch, 1841) | Y (web-spinning; $n = 3$) | N | Knoflach 2004 (as *Achaearanea tepidariorum*) |
| *Parasteatoda wau* (Levi, Lubin & Robinson, 1982) | Y (small mating arena) | Y (small area reduced) | Lubin 1986 (as *Achaearanea wau*) |
| *Steatoda bipunctata* (Linnaeus, 1758) | Y (mating web; $n = 3$) | Y (removed threads) | Knoflach 2004 |
| *Steatoda castanea* (Clerck, 1757) | Y (mating web; $n = 1$) | | Knoflach 2004 |
| *Steatoda grossa* (C. L. Koch, 1838) | Y (all males added silk to female's web; $n = 23$) | Y (>50% of web; 74%; $n = 23$) | Scott et al. 2017 |
| | Y (mating web &/or web-spinning; $n = 4$[2]) | N | [2]Knoflach 2004; Gwinner-Hanke 1970 (as *Tentana grossa*) |
| *Steatoda paykulliana* (Walckenaer, 1806) | Y (silk-throwing; 66%; $n = 3$) | N | Knoflach 2004 |
| *Steatoda triangulosa* (Walckenaer, 1802) | Y (mating thread; $n = 4$) | Y (removed threads; 50%; $n = 4$) | Knoflach 2004 |
| *Sinitidion simile* (C. L. Koch, 1836) | Y | N | Locket 1927 (as *Theridion simile*) |
| *Theridion varians* Hahn, 1833 | Y | Y | Locket 1927 |
| *Tidarren argo* Knoflach & van Harten, 2001 | Y (mating web) | N | Knoflach 2004 |
| *Tidarren cuneolatum* (Tullgren, 1910) | Y (multistranded mating thread) | N | Knoflach & van Harten 2000 |
| **Uloboridae** | | | |
| *Octonoba sinensis* (Simon, 1880) | Y (mating thread) | N | Peaslee & Peck 1983 (as *Octonoba octonarius*) |
| *Uloborus* Latreille, 1806 sp. | Y (mating thread) | N | Bristowe 1958 |

Table 3.—Spider taxa in which males deposit silk 'bridal veils' onto the female during courtship.

| Taxon | Context | Type of 'veil' | Reference |
|---|---|---|---|
| **Agelenidae** | | | |
| *Eratigena agrestis* (Walckenaer, 1802) | female's web | some silk on legs & carapace | S. Vibert unpublished data |
| **Araneidae** | | | |
| *Argiope aemula* (Walckenaer, 1841) | female's web | silk on carapace, legs & abdomen (extensive) | Robinson & Robinson 1980 |
| *Argiope aurantia* Lucas, 1833 | female's web | draglines attached to abdomen | Robinson & Robinson 1980 |
| *Argiope picta* L. Koch, 1871 | female's web | some silk on legs | Robinson & Robinson 1980 |
| *Argiope* Audouin, 1826 spp. | female's web | silk on legs | Robinson & Robinson 1980 |
| *Caerostris darwini* Kuntner & Agnarsson, 2010 | female's web | silk on legs & body (extensive) | Gregorič et al. 2016 |
| *Hereniia multipuncta* (Doleschall, 1859) | female's web | silk on & around abdomen | Robinson & Robinson 1980 (as *Hereniia ornatissima*) |
| *Nephila pilipes* (Fabricius, 1793) | female's web | silk between legs, between base of abdomen & dorsal surface of cephalothorax (extensive) | Robinson & Robinson 1980 (as *Nephila maculata*) |
| *Nephila pilipes* (Fabricius, 1793) | female's web | silk on carapace, legs & abdomen; connected to web (extensive) | Robinson & Robinson 1980; Kuntner et al. 2009; Zhang et al. 2011 |
| **Corrinidae** | | | |
| *Nyssus coloripes* Walckenaer, 1805 | female's web | zigzags of silk placed on female's body as male walks over her | Jackson & Poulsen 1990 (as *Supunna picta*) |
| **Ctenidae** | | | |
| *Aucyloucetes bogotensis* (Keyserling, 1877) | substrate | silk rings around front tibiae & patellae (extensive) | Merrett 1988 |
| *Cteuus longipes* Keyserling, 1891 | substrate | silk on forelegs, pedipalps, chelicerae, & eyes (later consumed) | Trillo 2016 |
| *Cupiennius coccineus* F. O. Pickard-Cambridge, 1901 | substrate | some silk on legs | Schmitt 1992 |
| **Dictynidae** | | | |
| *Dictyna volucripes* Keyserling, 1881 | female's web | some silk on female | Starr 1988 |
| **Eutichuridae** | | | |
| *Eutichurus ibiuna* Bonaldo, 1994 | substrate | legs I, II & palps tied to substrate | Laborda & Simo 2015 |
| **Homalonychidae** | | | |
| *Homalonychus selenopoides* Marx, 1891 | substrate | silk ring around legs | Alvarado-Castro & Jiménez 2011 |
| *Homalonychus theologus* Chamberlin, 1924 | substrate | silk ring around legs | Domínguez & Jiménez 2005 |
| **Lycosidae** | | | |
| *Schizocosa malitiosa* (Tullgren, 1905) | substrate | legs I & II tied to substrate & silk near mouthparts | Aisenberg et al. 2008 |
| **Oxyopidae** | | | |
| *Oxyopes scheukeli* Lessert, 1927 | hanging on dragline | silk spun around legs I, II, & III | Preston-Mafham 1999 |
| **Philodromidae** | | | |
| *Tibellus oblongus* (Walckenaer, 1802) | substrate | some silk on female | Kaston 1936; Preston-Mafham 1999 |
| *Tibellus* Simon, 1875 sp. | substrate | some silk on female | Platnick 1971 |
| **Pisauridae** | | | |
| *Dolomedes triton* (Walckenaer, 1837) | substrate | legs I & II tied to substrate | Carico 1993 |
| *Pisaurina mira* (Walckenaer, 1837) | substrate or hanging on dragline | silk spun around legs I & II (extensive) | Bruce & Carico 1988; Anderson & Hebets 2016 |
| *Nilus curtus* (O. Pickard-Cambridge, 1876) | female's mating web | silk ring around patellae | Sierwald 1988 (as *Thalassius spinosissimus*) |
| **Tetragnathidae** | | | |
| *Metellina segmentata* (Clerck, 1757) | female's web | female wrapped with fine silk | Bristowe 1929; Lopez 1987 |
| **Theridiidae** | | | |
| *Euryopis episinoides* (Walckenaer, 1847) | female's web | some silk on female | Knoflach 2004 |

Table 3.—Continued.

| Taxon | Context | Type of 'veil' | Reference |
|---|---|---|---|
| *Latrodectus geometricus* C. L. Koch, 1841 | female's web | some silk on legs & body | Knoflach & van Harten 2002; Segoli et al. 2008 |
| *Latrodectus hasselti* Thorell, 1870 | female's web | some silk on legs & body | Forster 1992 |
| *Latrodectus hesperus* Chamberlin & Ivie, 1935 | female's web | some silk on legs & body | Ross & Smith 1979; Kaston 1970; Herms et al. 1935; Scott et al. 2012 |
| *Latrodectus indistinctus* O. Pickard-Cambridge, 1904 | female's web | some silk on legs & body | Smithers 1944 |
| *Latrodectus mactans* (Fabricius, 1775) | female's web | some silk on legs & body | Breene & Sweet 1985 |
| *Latrodectus pallidus* O. Pickard-Cambridge, 1872 | female's web | some silk on legs & body | Shulov 1940 |
| *Latrodectus revivensis* Shulov, 1948 | female's web | some silk on legs & body | Anava & Lubin 1993 |
| *Latrodectus tredecimguttatus* (Rossi, 1790) | female's web | some silk on legs & body | Shulov 1940 |
| *Steatoda bipunctata* (Linnaeus, 1758) | female's web | some silk on female | Knoflach 2004 |
| *Steatoda grossa* (C. L. Koch, 1838) | female's web | some silk on legs & body | Scott et al. 2017 |
| *Steatoda paykulliana* (Walckenaer, 1806) | female's web | some silk on legs & body | Knoflach 2004 |
| *Steatoda triangulosa* (Walckenaer, 1802) | female's web | some silk on female | Knoflach 2004 |
| **Thomisidae** | | | |
| *Bassaniana versicolor* (Keyserling, 1880) | substrate | female tied to substrate | Kaston 1936 (as *Coriarachne versicolor*) |
| *Xysticus cristatus* (Clerck, 1757) | substrate | legs I & II tied to substrate | Bristowe 1931; Bristowe 1958 |
| *Xysticus lanio* C. L. Koch 1835 | substrate | legs I & II tied to substrate | Gerhardt 1924 as cited by Bristowe 1926 |
| *Xysticus audax* (Schrank, 1803) | substrate | female tied to substrate | Thomas 1930 as cited by Kaston 1936 (as *Xysticus pini*) |
| *Xysticus striatipes* L. Koch, 1870 | substrate | female tied to substrate | Sytschewskaja 1935 as cited by Kaston 1936 |
| *Xysticus triguttatus* Keyserling, 1880 | substrate | female tied to substrate | Kaston 1936 |
| *Xysticus tristrani* (O. Pickard-Cambridge, 1872) | substrate | female tied to substrate | Gerhardt 1933 as cited by Kaston 1936 |
| *Pycnaxis krakatauensis* (Bristowe, 1931) | substrate | legs I & II tied to substrate | Bristowe 1931 (as *Xysticus krakatauensis*) |
| **Uloboridae** | | | |
| *Uloborus* Latreille, 1806 sp. | female's web | not described | Gerhardt 1933 (as cited by Berendonck 2003) |
| **Zoropsidae** | | | |
| *Tengella perfuga* Dahl, 1901 | female's web | some silk on legs & carapace | Mallis & Miller 2017 |

but in *Argiope argentata* (Fabricius, 1775), for instance, males switch types depending on context (Robinson & Robinson 1980). Some males do type A, and others type B, or the same male might do both types on different days. If another male is already courting on the web (type A or type B courtship), a second male will engage in type C courtship with a mating thread attached to the periphery of the web. Interestingly, when engaging in type B courtship, the male may add dragline silk to his mating thread after a courtship bout to which the female did not respond. Similarly, in *Argiope picta* L. Koch, 1871, males may enlarge the hole across which they spun their mating thread between bouts of unsuccessful courtship (Robinson & Robinson 1980).

In *Isoxya tabulata* (Thorell, 1859) and *Scoloderus cordatus* (Taczanowski, 1879) the mating thread is employed in a different way. The male situates himself such that the female walks onto a silk line still attached to his spinnerets, which he pays out as she tries to approach, resulting in a 'treadmill effect' (Robinson & Robinson 1980). The female attempts to walk along the line but makes no progress, rather she accumulates a bundle of the male's silk below her cephalothorax (this silk may constitute a nuptial gift; see section 5).

Male cobweb weavers (Theridiidae) also commonly construct mating threads during courtship on the female's web (Table 2). As in type C courtship of the orb-weavers, the male installs a silk line and then engages in vibratory courtship on it until the female eventually moves onto the thread, where copulation occurs (Knoflach 2004). In some species, the male reinforces the thread several times, or he constructs a larger area of threads referred to as a mating web, which is used similarly to mating threads (Knoflach 2004). In a few species, the male cuts some of the female's threads, but in general, theridiids modify the web by adding their own silk without excising sections of the female's web (Knoflach 2004). Exceptions include the widow and false widow spiders *Latrodectus* and *Steatoda* Sundevall, 1833, which engage in extensive web reduction behavior (discussed below) and males of the social theridiid spider *Parasteatoda wau* (Levi, Lubin & Robinson, 1982), which build courtship 'arenas' in their communal webs by cutting out small areas of the barrier web

Table 4.—Spider taxa in which males present females with silk-associated nuptial gifts, including silk-wrapped prey, silk alone, or silk-lined burrows.

| Taxon | Type of gift | Reference |
|---|---|---|
| **Araneidae** | | |
| *Isoxya tabulata* (Thorell, 1859) | mating thread silk (probably) | Robinson & Robinson 1980 |
| *Scoloderus cordatus* (Taczanowski, 1879) | mating thread silk (probably) | Stowe 1978 |
| **Ctenidae** | | |
| *Ctenus longipes* Keyserling, 1891 | bridal veil silk | Trillo 2016 |
| **Lycosidae** | | |
| *Allocosa alticeps* (Mello-Leitão, 1944) | silk-lined burrow | Aisenberg et al. 2010 |
| *Allocosa senex* (Mello-Leitão, 1945) | silk-lined burrow | Aisenberg et al. 2007 (as *Allocosa brasiliensis*); Carballo et al. 2017 |
| **Pisauridae** | | |
| *Pisaura lama* Bösenberg & Strand, 1906 | silk-wrapped prey | Itakura 1993 (as cited by Costa-Schmidt et al. 2008) |
| *Pisaura mirabilis* (Clerck, 1757) | silk-wrapped prey | Bristowe & Lockett 1926; Bristowe 1958 |
| *Perenethis fascigera* (Bösenberg & Strand, 1906) | silk-wrapped prey | Itakura 1998 |
| *Thaumasia argenteonotata* (Simon, 1898) | silk-wrapped prey | Nitzsche 1988 (as cited by Nitzsche 2011) |
| *Tinus peregrinus* (Bishop, 1924) | silk-wrapped prey | J. Carico pers. comm. in Nitzsche 2011 |
| **Tetragnathidae** | | |
| *Metellina segmentata* (Clerck, 1757) | silk-wrapped prey or rival male | Prenter et al. 1994a |
| **Theridiidae** | | |
| *Argyrodes elevatus* Taczanowski, 1873 | spider lightly wrapped in silk | Cobbold & Su 2010 |
| | stolen silk-wrapped prey | Uetz et al. 2010 |
| **Theridiosomatidae** | | |
| *Theridiosoma gemmosum* (L. Koch, 1877) | silk | Hajer & Řeháková 2011 |
| **Trechaleidae** | | |
| *Paratrechalea azul* Carico, 2005 | silk-wrapped prey | Costa-Schmidt et al. 2008 |
| *Paratrechalea galianoe* Carico, 2005 | silk-wrapped prey | Costa-Schmidt et al. 2008 |
| *Paratrechalea ornata* (Mello-Leitão, 1943) | silk-wrapped prey | Costa-Schmidt et al. 2008 |
| *Trechalea amazonica* F. O. Pickard-Cambridge, 1903 | silk-wrapped prey | Silva & Lise 2009 |
| *Trechalea bucculenta* (Simon, 1898) | silk-wrapped prey | Silva 2005 (as cited by Silva & Lise 2009) |
| *Trechalea* Thorell, 1869 sp. | silk-wrapped prey | Lapinski & Tschapka, 2009 (as cited by Nitzsche 2011) |

threads and laying down one or more of their own threads (Lubin 1986). Courtship occurs on these threads and they are considered functionally equivalent to the mating threads of araneid spiders (Lubin 1986).

Variations on the theme of mating threads and webs can also be found in cribellate web-dwellers (Table 2). In *Fecenia* Simon, 1887 sp. (Psechridae), which constructs an orb-web, the courting male cuts away most of the web, leaving only a single thread on which courtship and mating proceed (Robinson & Lubin 1979). Males of the meshweaver *Dictyna arundinacea* (Linnaeus, 1758) (Dictynidae) cut a hole in the web and construct a 'canopy' of their own threads on which they mate (Locket 1926). In other dictynid spiders in the genera *Dictyna* Sundevall, 1833, *Mallos* O. Pickard-Cambridge, 1902, and *Mexitlia* Lehtinen, 1967, however, there are records of silk addition to the female's web but no mention of males cutting the female's silk (Jackson 1979).

Web reduction is a behavior involving extreme web modification with silk addition that has been recorded for sheet weavers (Linyphiidae) and some cobweb weavers (Theridiidae; Table 2). During web reduction, the male moves around the web cutting threads with his chelicerae, then he bundles dismantled sections of the web into thick ropes or balls and, in some cases, wraps them extensively with his own

Table 5.—Other behaviors involving male silk deposition during courtship and mating. Note that silk deposition on the substrate is likely widespread in cursorial spiders but is rarely explicitly mentioned in descriptions of courtship behavior.

| Taxon | Behavior | Reference |
|---|---|---|
| **Araneidae** | | |
| *Manogea porracea* (C. L. Koch, 1838) | Male builds web above female's & protects egg sacs from predators | Moura et al. 2017 |
| **Ctenidae** | | |
| *Ctenus longipes* Keyserling, 1891 | Male deposits silk on the substrate prior to mounting the female (82% of males; $n = 11$ matings) | Trillo 2016 |
| **Lycosidae** | | |
| *Pardosa milvina* (Hentz, 1844) | Male deposits silk on substrate in response to female silk cues | Khan & Persons 2015 |
| **Salticidae** | | |
| *Plexippus paykulli* (Audouin, 1826) | Male spins silk as he walks around outside/near female's nest | Jackson & Macnab 1989 |

Table 6.—Spider taxa in which there is behavioral evidence for male-produced sex pheromones. These families are also indicated in red in Fig. 1

| Taxon | Source | Type | Female response | Reference |
|---|---|---|---|---|
| **Agelenidae** | | | | |
| *Agelenopsis aperta* (Gertsch, 1934) | body | airborne | quiescence/catalepsis | Becker et al. 2005 |
| *Coelotes terrestris* (Wider, 1834) | silk | contact | orientation | Roland 1983 |
| *Tegenaria domestica* (Clerck, 1757) | silk | contact | orientation | Roland 1983 |
| **Lycosidae** | | | | |
| *Allocosa alticeps* (Mello-Leitão, 1944) | body | airborne | courtship | Aisenberg et al. 2010 |
| *Allocosa brasiliensis* (Petrunkevitch, 1910) | body | airborne | courtship | Aisenberg et al. 2010 |
| *Pardosa milvina* (Hentz, 1844) | silk | contact | increased silk production | Khan & Persons 2015 |
| *Trochosa* C. L. Koch, 1847 sp. | silk | contact | mate recognition | Engelhardt 1964 (as cited by Uhl & Elias 2011) |
| **Pholcidae** | | | | |
| *Pholcus beijingensis* Zhu & Song, 1999 | body | airborne | stimulates mating behaviour | Xiao et al. 2010 |
| **Saltieidae** | | | | |
| *Evarcha culicivora* Wesolowska & Jackson, 2003 | body & silk | airborne + contact | courtship & attraction/ mate recognition | Cross & Jackson 2013 |
| **Scytodidae** | | | | |
| *Scytodes* Latreille, 1804 sp. | body & silk | airborne | mate choice | Koh et al. 2009 |
| **Theridiidae** | | | | |
| *Latrodectus hesperus* Chamberlin & Ivie, 1935 | silk | contact | courtship | Ross & Smith 1979 |
| **Sicariidae** | | | | |
| *Loxosceles intermedia* | body | unknown | mate recognition & avoiding cannibalism | Fischer et al. 2009 |

silk (first described by Van Helsdingen 1965 and later studied in detail by Watson 1986; Fig. 2b). The frequency at which this behavior occurs is variable within and among species, as is the extent to which the web is destroyed (Table 2). For instance, web reduction in *Lepthyphantes leprosus* (Ohlert, 1865) results in a web area decrease of 90% or more, but 55% of males do not engage in web reduction at all (Van Helsdingen 1965). In a field experiment, 69% of *Neriene litigiosa* (Keyserling, 1886) males reduced a large portion of the female's web, but web reduction only occurred in 28% of laboratory trials (Watson 1986). In *Latrodectus,* removal of 50% or less of the female's web is typical, with ~60–70% of males engaging in web reduction behavior (Anava & Lubin 1993; Scott et al. 2012). *Steatoda grossa* (C.L. Koch, 1838) males also engage in extensive web reduction, but unlike in *Latrodectus*, mating tends to take place on a rope or bridge-like section of the web that has been covered with male silk (Scott et al. 2017). Previous workers have described the construction of a mating web in *S. grossa* (Gwinner-Hanke 1970; Knoflach 2004), but not the removal of large sections of the female's capture web.

Behavior much like web reduction has also been reported for some araneids that build both typical and irregular orb webs. In the process of constructing their mating threads, males of *Micrathena sexspinosa* (Hahn, 1822) and *Mangora bimaculata* (O. Pickard-Cambridge, 1889) engage in extensive web modification (Robinson & Robinson 1980). They break the threads of the viscid spiral on both sides of one radius, such that the web ends up looking like the missing sector webs of *Zygiella* sp. The resulting analog to the missing sector web's signal thread is reinforced with up to 30 layers of the male's silk until it is conspicuously thickened and white in color before being used as a mating thread (Robinson & Robinson 1980). The installation of the mating thread in the irregular orb-webs of *Kapogea sexnotata* (Simon, 1895) also show

Table 7.—Spider taxa in which there is behavioral evidence for males responding to silk cues of conspecific males.

| Taxon | Source | Type | Male response | Citations |
|---|---|---|---|---|
| **Araneidae** | | | | |
| *Nephila senegalensis* (Walckenaer, 1841) | silk | contact | avoidance/mate choice | Schneider et al. 2011 |
| **Linyphiidae** | | | | |
| *Frontinella communis* (Hentz, 1850) | silk | contact | positive geotaxis | Suter & Hirscheimer 1986 (as *Frontinella pyramitela*) |
| | cuticle | contact | aggressive behavior | Suter et al. 1987 |
| **Lycosidae** | | | | |
| *Pardosa amentata* (Clerck, 1757) | silk | contact | increased silk production | Richter & Kraan 1970 |
| *Rabidosa rabida* (Walckenaer, 1837) | body | airborne | reduces exploratory behavior | Tietjen 1978 (as *Lycosa rabida*) |
| *Schizocosa ocreata* (Hentz, 1844) | silk | airborne & contact | inhibits courtship | Ayyagari & Tietjen 1987 |
| **Theridiidae** | | | | |
| *Latrodectus hasselti* (Thorell, 1870) | body &/or silk | airborne | shift in development | Kasumovic & Andrade 2006 |

parallels to web reduction in the Theridiidae and Linyphiidae. Males first cut away extensive portions of the lower snare of the female's web and attach silk to the surface of the web periodically during 'walkabouts.' The male continues to cut away sections of the female's web as he installs his mating thread, which he reinforces several times (Robinson & Robinson 1980).

**3.2 Proposed mechanisms and functions.**—A number of hypotheses that focus on effect of the male's silk on female receptivity or aggressive behavior have been proposed, mainly for species that engage in web reduction behavior (Table 2). However, these hypotheses may also apply to mating thread production or any behavior that may allow females to come in contact with male silk. Assuming that there are chemical signals or cues associated with the male silk produced during courtship, silk addition to the female's web, retreat, or burrow entrance may function in several non-mutually exclusive ways. First, pheromones on male silk might increase or accelerate female receptivity, either by stimulating the female to mate (e.g., initiate receptive postures or behaviors), or by inducing catalepsis (which always precedes successful mating in some species) (Gering 1953; Robinson & Robinson 1973; Ross & Smith 1979, Anava & Lubin 1993). Second, silk addition could also decrease female aggression and the risk of injury to males. For example, in both *Lepthyhphantes leprosus* and *Latrodectus hesperus*, web reduction (accompanied by extensive silk deposition) is associated with fewer instances of female aggression (Van Helsdingen 1965; Scott et al. 2012). However, it is not clear whether this is because 'shy' or more receptive females tolerate web reduction while aggressive or unreceptive females prevent it, or whether chemical signals associated with male silk decrease female aggression or induce receptivity. In addition, for each of these proposed functions, if females come in contact with the male's silk, it is also possible that behavioral changes are triggered by tactile (mechanical) cues on the silk rather than by chemical cues. Finally, chemicals (e.g., anti-aphrodisiacs) associated with the male's silk may deter rival males or render the female's silk unattractive (Yañez et al. 1999).

Clearly, silk addition to the web leads to structural alterations ranging from the addition of a single line (mating threads) to the major modification of web architecture that results from web reduction behavior (Table 2). Changing web architecture via web reduction and/or silk addition may generally function to improve the transmission of vibratory courtship signals (Robinson & Robinson 1980; Berendonck 2003). By plucking or moving on an isolated mating thread rather than engaging in vibratory courtship on the female's capture web, signal attenuation and degradation may be reduced. Similarly, constructing a mating web may allow a male to produce a transmission medium with properties that minimize courtship signal attenuation or degradation; these properties may differ from those that maximize capture efficiency for a hunting female. Isolating the female from extraneous vibrations, such as those produced by prey or other males arriving at the web, is a function proposed for web reduction behavior (Rovner 1968; Lubin 1986), but it could also apply to mating threads and webs. For instance, males in several orb-weaver species cut the mating threads of simultaneously courting rivals (Robinson & Robinson 1980).

Rather than improving transmission properties of the web, vibrations associated with cutting silk lines or adding silk could themselves transmit information to the female or attract her attention; that is, silk modification activities may in themselves be courtship signals (Forster 1995; Berendonck 2003). The materials and behaviors involved in silk addition may be energetically costly and provide the female with information about male quality (Anava & Lubin 1993; Harari et al. 2009). Silk is metabolically expensive to produce (Craig 2003), and adult males of web-building spiders apparently reduce or stop foraging after maturity (Foelix 2011), so they have limited energetic resources. When males invest considerable time and large amounts of silk during courtship, this could provide honest information about male nutritional status or vigor.

Fitness benefits of structural changes to the web may be less related to communication, and more related to restricting the mobility of a potentially dangerous female (Van Helsdingen 1965; Ross & Smith 1979; Breene & Sweet 1985). For example, the male may reduce the risk of cannibalism by altering the web in a way that restricts the female's movements prior to or just after mating. For species that construct a mating thread (Table 2; Fig. 2a), a male may cut the silk line between himself and an aggressive female to remove the immediate risk of attack (Robinson & Lubin 1979; Robinson & Robinson 1980). Alternatively, the "treadmill"-type mating threads of some araneids may provide the male with some control over the female's predatory response and thus decrease the likelihood of cannibalism (Robinson & Robinson 1980).

Similarly, structural modifications may reduce the likelihood of females mating with rivals and thus reduce the risk of losing paternity due to polyandry. This effect may also arise through effects on mobility, as altering the web may allow males to control the avenue of approach for a rival male attempting to court the female. If the female is on a mating thread or if web reduction has reduced the web's surface area, then altering web structure reduces the area that must be defended from competitors (Van Helsdingen 1965; Ross & Smith 1979; Breene & Sweet 1985). Rather than affecting mobility, a similar benefit would arise if web reduction decreases the attraction of rivals in the first place by interfering with the release of the female's airborne pheromones. Cutting out portions of the female's web could reduce the surface area of pheromone-laden silk (Watson 1986), and wrapping bundles of the female's silk with a layer of the male's own silk may also block the release of pheromones (Scott et al. 2015b).

*3.3 Current evidence and future directions.*—Male silk deposition onto webs or other silk structures has been hypothesized to increase female receptivity and the probability of mating, decrease the likelihood of polyandry, and/or decrease the risk of cannibalism by the female. These effects may arise via indirect means (communication, in a number of modalities) or directly through the structural changes to the web, but there is scant experimental evidence supporting these ideas to date (see Table 1).

Of the numerous examples of silk deposition and web modification described above, the only experimental work to

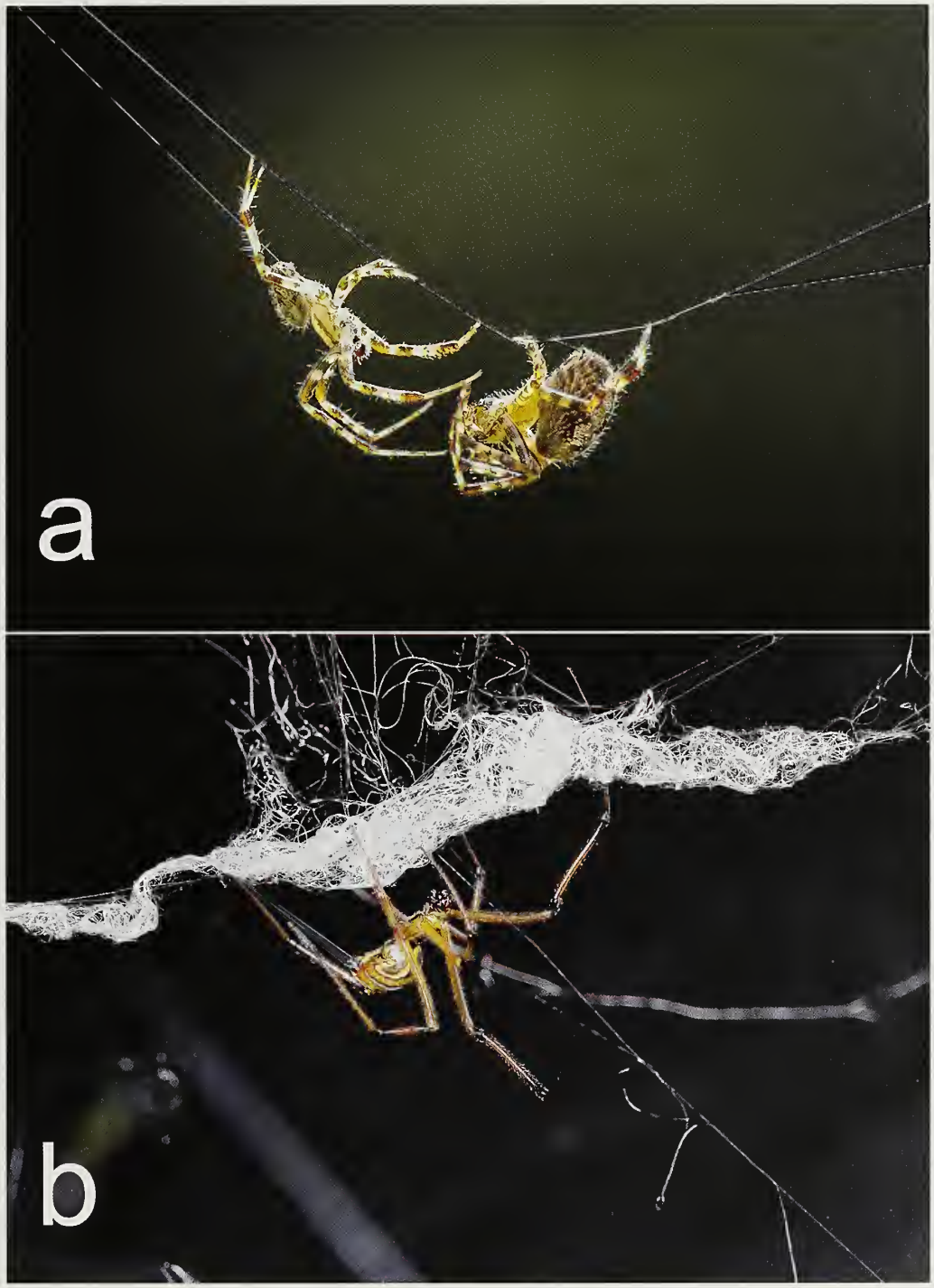


Figure 2.—Examples of silk deposition onto females' webs during courtship. (a) *Araneus diadematus* (Araneidae) male and female hanging from the male's mating thread, attached to the periphery of the female's web (photo: Maria Hiles). (b) Web reduction with silk addition by a *Latrodectus hesperus* (Theridiidae) male. The male has dismantled part of the capture web (which would have filled the lower half of the photograph before he began web reduction behavior) and is wrapping it with his own silk (photo: Sean McCann).

determine functions and mechanisms has focused on web reduction in *Neriene litigiosa* (Watson 1986) and *Latrodectus hesperus* (Scott et al. 2015b). In both species, reduced webs are less attractive to males than intact webs, indicating that males that engage in web reduction decrease the probability of their long (often several hours) courtship displays being interrupted by rival males. The effect of web reduction is presumably long lasting because mated females rebuild their webs without pheromones, so web-reducing males also benefit by decreasing the probability of sperm competition (Watson 1986). For *N. litigiosa*, Watson (1986) argued that web reduction limits female silk pheromone emission by decreasing the exposed surface area of the female's silk. Conversely, the results of a series of field experiments by Scott et al. (2015b) suggest that

physical alteration of the web and male silk addition both play roles in the function of web reduction as a mate monopolization tactic. Further work is required to determine the mechanism(s) by which web reduction decreases female attractiveness, and to what extent chemical cues affecting conspecifics (females or males) are involved.

The fitness benefits of web reduction for males are clear; decreasing female attractiveness limits sperm competition in two ways. First, it acts to quickly reduce the arrival rate of rival males, decreasing direct competition for access to females and increasing the likelihood of being first to copulate, which is important in spiders with long pre-copulatory courtship and first-male sperm precedence like *Latrodectus* and *Neriene litigiosa* (Watson 1991; Watson & Lighton 1994; Snow & Andrade 2005; MacLeod 2013). Second, mated females rebuild their webs without attractive pheromones (Watson 1986; MacLeod & Andrade 2014), decreasing the likelihood that males will face sperm competition from subsequently mating males. The fitness consequences for females, however, may be positive or negative. Females may benefit from the ability to quickly become unattractive after mating if they suffer costly harassment from subsequent males arriving at their webs. However, if females benefit from polyandry, web reduction may be costly; it may be a form of manipulation. Experimental studies are needed to explicitly test the fitness consequences to females to determine whether this is an example of cooperation or conflict between the sexes.

Other potential functions of silk addition with and without web modification remain to be experimentally investigated. A number of approaches would be valuable in future studies. First, tests of hypotheses related to vibrational signalling or signal transmission could harness Laser Doppler Vibrometry, which allows precise measurement of silk-borne vibrations with minimal loading of the web, unlike earlier methods based on accelerometers (Masters & Markl 1981; also see alternative methods in Vollrath 1979). Assessment of transmission properties of webs (e.g., Vibert et al. 2016) with and without male silk addition and the attendant web modifications (reduction and mating threads/webs) would be valuable for explicit tests of hypotheses associated with vibration transmission. For example, in recent work, Mortimer et al. (2015) combined laser vibrometry, electron microscopy, tensile testing, and behavioral assays to understand the function and biomechanical properties of the (predation-related) signal thread of *Zygiella x-notata* (Clerck, 1757). This study could be used as a model for exploring the characteristics of mating threads, and comparisons of signal threads used for predation and those used in mating may produce valuable insights. Second, once vibrations created during silk addition are characterized, synthesized vibrations can then be used in playback experiments to gauge male and female responses (e.g., see Uhl & Elias 2011; Wignall & Herberstein 2013b; Vibert et al. 2014) and how male fitness is affected. Third, behavioral experiments in the laboratory or field that focus on whether the silk itself affects female attractiveness or male mating success could utilize the experimental addition of male silk (e.g., Scott et al. 2015b), or experimental blocking of male silk production by covering the spinnerets of courting males with wax or glue (e.g., Zhang et al. 2011).

## 4. SILK DEPOSITION ON FEMALES

**4.1 Overview and description of behaviors.**—Males may deposit silk directly on the female's body during courtship or copulation—a widespread behavior reported in 16 families, including web-building and cursorial spiders (Figs. 1 & 2; Table 3). The term 'bridal veil' was coined by Bristowe (1931) as a descriptor for male silk-laying on females during mating in *Xysticus cristatus* (Clerck, 1757) and *Pycnaxis krakatauensis* (Bristowe, 1931) (Thomisidae). Other descriptions for bridal veil spinning behavior include 'tying', 'mate-binding', 'silk-binding', 'copulatory silk-wrapping', and 'trussing' (Table 3). We use 'bridal veil' and 'veil' to refer to this behavior because this is the original term and to avoid using terms that imply particular functions. There are several types of bridal veils, and species in which they have been reported vary in the context in which they are used, the part of the body on which the silk is applied, the predictability of silk-laying patterns, and the volume of silk used in the behavior (Table 3).

Extensive silk-wrapping behavior, often focused on the female's legs, is seen across a number of families of cursorial spiders and some web-builders (Table 3; Fig. 3). Males deposit silk over the female's first two pairs of legs and anchor the silk to the substrate in several crab spiders, including *Xysticus* C.L. Koch, 1835 spp., *Pycnaxis krakatauensis*, and *Bassaniana versicolor* (Keyserling, 1880) (Thomisidae; Bristowe 1931, 1958; Kaston 1936). Comparable veiling behavior has been described for the wolf spider *Schizocosa malitiosa* (Tullgren, 1905) (Lycosidae; Aisenberg et al. 2008) and the fishing spider *Dolomedes triton* (Walckenaer, 1837) (Pisauridae; Carico 1993). Similarly, males of *Ctenus longipes* Keyserling, 1891 (Ctenidae) concentrate silk deposition on the female's forelegs and also spin silk over the palps, chelicerae, and eyes (Trillo 2016). Intriguingly, the female apparently eats the veil silk after copulation in this species (discussed below in section 5). In *Oxyopes schenkeli* Lessert, 1927 (Oxyopidae; Preston-Mafham 1999) and in some cases, *Pisaurina mira* (Walckenaer, 1837) (Pisauridae; Bruce & Carico 1988; A.G. Anderson pers. obs.), both mates will hang from a dragline below a plant as the male deposits silk on the first two or three pairs of the female's legs. Males systematically deposit a ring-like veil around the female's legs as she stands on the ground in *Homalonychus selenopoides* Marx, 1891 and *H. theologus* Chamberlin, 1924 (Homalonychidae; Domínguez & Jiménez 2005; Alvarado-Castro & Jiménez 2011), or as the female hangs from her mating web in *Nilus curtus* (O. Pickard-Cambridge, 1876) (Pisauridae; Sierwald 1988). Males of *Ancylometes bogotensis* (Keyserling, 1877) (Ctenidae) wrap the distal segments of the female's legs first with an outer ring of silk, and then add a second inner ring around the patellae (Merrett 1988). Complex, extensive veiling behavior has also been described for several orb-weaver genera (Araneidae; Table 3; Fig. 3a). The diminutive males move around on the dorsum of the female, spinning silk between the bases of her legs, over her cephalothorax, and between her cephalothorax and abdomen (e.g., Robinson & Robinson 1980; Gregorič et al. 2016).

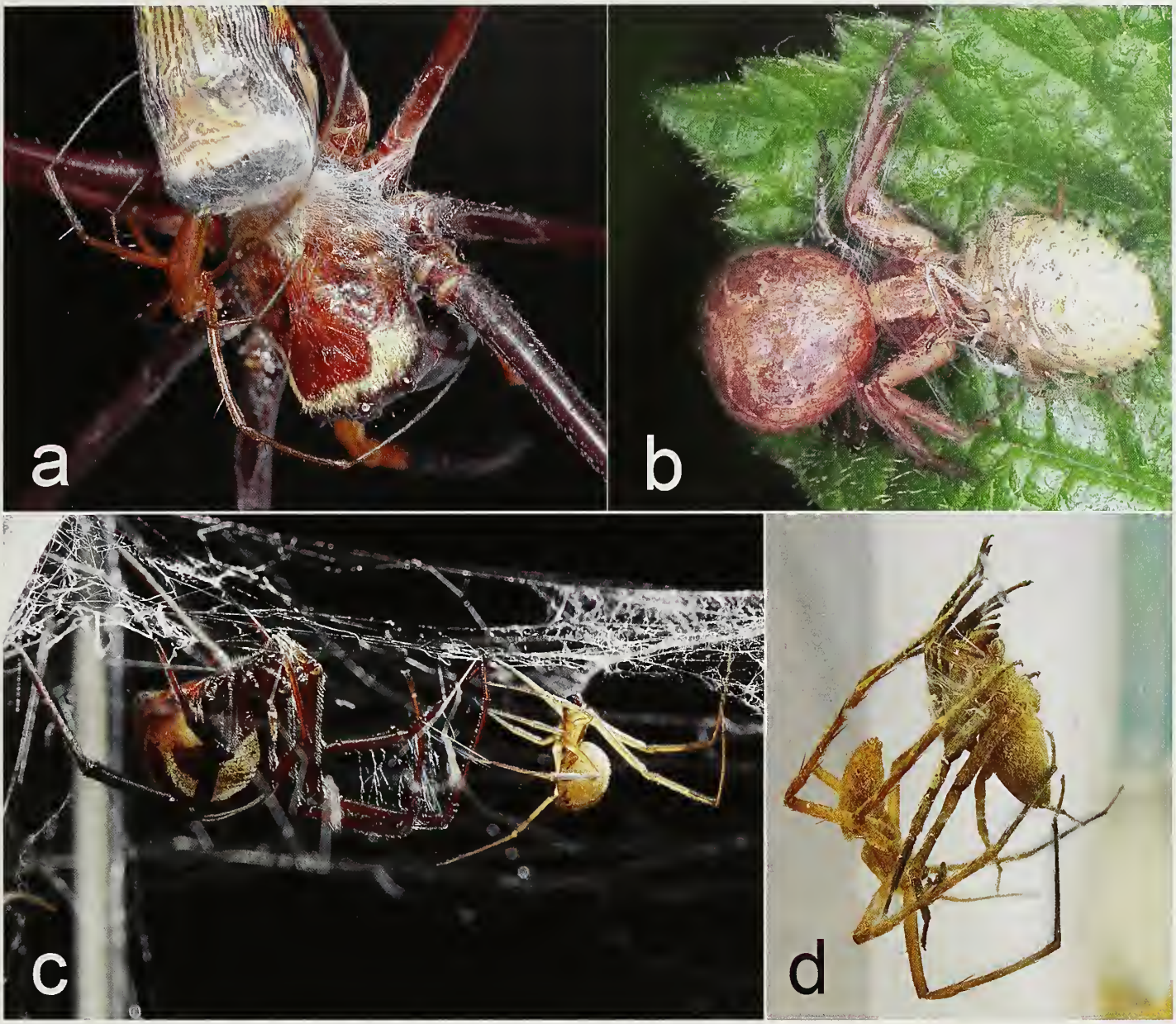


Figure 3.—Examples of silk 'bridal veils' applied to females' legs and bodies during courtship. (a) *Nephila pilipes* (Araneidae) male depositing silk onto the female's carapace, legs, and abdomen (photo: Shichang Zhang). (b) *Xysticus cristatus* (Thomisidae) female with silk on her forelegs and abdomen as she feeds on a prey item—note that the male is underneath her abdomen (photo: Ed Niewenhuys). (c) *Latrodectus hesperus* ("texanus" morph, formerly *Latrodectus mactans texanus*; Theridiidae) male depositing silk onto the female's legs (photo: Sean McCann). (d) *Pisaurina mira* (Pisauridae) male wrapping a female's legs with silk prior to sperm transfer (Photo: Alissa Anderson).

Less extensive silk deposition on females has been described for species in the Agelenidae, Corrinidae, Dictynidae, Philodromidae, Tetragnathidae, Theridiidae and Zoropsidae (see Table 3 for details and references). In these taxa veiling behavior occurs on the female's web and seems to be less ritualized or more variable than the types described above. In the Theridiidae, for example, there is variation in the occurrence of silk deposition behavior within and across species. Veiling took place in about 33% of courtship observations in *Latrodectus revivensis* Shulov, 1948 (Anava & Lubin 1993), in 50% of *Steatoda bipunctata* (Linnaeus, 1758) pairings (Knoflach 2004), and only occasionally in *Steatoda grossa* (Scott et al. 2017). Intriguingly, application of a bridal veil appears to be an obligate behavior in *Nephila pilipes* (Fabricius, 1793), as well as in *Pisaurina mira* (Bruce & Carico 1988; Kuntner et al. 2009; Anderson & Hebets 2016). Conversely, *Cupiennius coccineus* F.O. Pickard-Cambridge, 1901 (Ctenidae) males normally do not use veils in laboratory trials, but in an inter-species mating experiment, some male *C. coccineus* deposited silk on *C. salei* females, which are larger than conspecific females (Schmitt 1992).

**4.2 Proposed mechanisms and functions.**—Bridal veils may increase female receptivity and the probability of mating. The veil may also act as a physical restraint that increases mating success or decreases the risk of sexual cannibalism. Finally, it is also possible that application of a veil decreases the

likelihood of polyandry. Typically, silk used in veils is not placed within the female's field of view and is removed shortly after copulation, so visual cues are unlikely to play a functional role, but chemical or tactile information may be important to either the female or rival males. Below, although we focus on hypotheses that suggest mechanisms involving chemical cues, we note that all the proposed effects could also arise from female detection of tactile cues or signals, or perhaps even improved seismic signal transmission via direct contact with male silk.

Females may be more likely to mate with males that produce veils due to information in the silk itself (chemical or tactile modalities), due to mechanical stimulation of structures in the location of the veil (e.g., if silk is laid across particular sensory regions on the female's body), or due to information in the activity associated with laying silk (tactile cues/signals). Silk-laying may increase female receptivity if the veil allows females to identify males as potential mates (e.g., rather than prey), or if the veil is instrumental in female choice among conspecifics. In terms of mating with rather than attacking the male, it has been proposed that pheromones on the male's silk may lead to a general reduction in the female's predatory or aggressive behaviors (e.g., Schmitt 1992; Dominguez & Jiminez 2005). In a more extreme proposal, chemicals in the veil could inhibit movements of the female so that she remains in a cataleptic state during copulation (Ross & Smith 1979; Aisenberg et al. 2008; Preston-Mafham 1999). Silk-borne pheromones could also provide the female with information about the male's quality (Ross & Smith 1979; Anava & Lubin 1993) and thus increase her receptivity to mating with particular males. Both of these types of functional hypotheses are consistent with previous mechanistic arguments that bridal veils 'stimulate' the female or trigger physiological changes that prepare the female for mating (Robinson & Robinson 1973; Preston-Mafham 1999).

As has been proposed for web reduction (Scott et al. 2015b), the male's silk could also function to deter rival males, possibly via pheromones (Aisenberg et al. 2008) that remain on the female's body. 'Antiaphrodisiacs' (e.g., in butterflies; Estrada et al. 2011) may be particularly effective in species with first-male sperm precedence (such as many spiders), since this predicts the evolution of tactics that allow males to avoid previously-mated females (Parker 1970).

In many species, silk deposition by males seems to target the distal segments of the female's legs (usually the first two or three pairs) and sometimes the pedipalps (see Table 3) (Aisenberg et al. 2008). Spider chemoreceptors are concentrated on the distal segments of the legs and pedipalps (Trabalon 2013), thus the pattern of silk deposition supports the hypothesis of chemical information delivery to females. In a twist on this idea, Lopez (1987) argued that the female's sensory hairs might be incapacitated by direct contact with the silk. This argument suggests that reduced predatory responses could be the result of silk-mediated impairment of the female's sensory system (but see Zhang et al. 2011).

Independent of any signal function of veils, the application of silk to the female's body could directly affect female positioning or mobility during mating interactions in ways that are beneficial for the male. Silken restraints may facilitate copulation by ensuring the female's abdomen is supported in a posture that simplifies intromission. However, silk may also reduce female mobility, which could increase copulation duration and thus fertilization success (Anderson & Hebets 2017) or reduce the risk of injury or sexual cannibalism (Anderson & Hebets 2016). There has been some debate as to whether the veil is able to physically restrain the female. Most descriptions indicate that females are quickly and easily able to break free of their silken bonds (e.g., Ross & Smith 1979; Preston-Mafham 1999), making this interpretation seem unlikely for many species, but other authors argue that the brief moments of struggling free from the veil may provide the male with just enough time to escape from a potentially cannibalistic female (Breene & Sweet 1985; Bruce & Carico 1988; Anderson & Hebets 2016; Gregorič et al. 2016). The efficacy of the veil in interfering with female movement may depend on how this tactic is employed and to which body parts the veil is applied. It is worth noting that extensive binding of the female's legs, common in some species (see Table 3), is also consistent with the idea of an effective restraint.

**4.3 Current evidence and future directions.**—The function of the silk bridal veil has been investigated experimentally in only two studies, one with *Nephila pilipes* (Zhang et al. 2011) and another with *Pisaurina mira* (Anderson & Hebets 2016). Both studies found that the veil reduced the risk of sexual cannibalism and allowed males to obtain a second sperm transfer opportunity, and in *P. mira*, this led to higher fertilization success (Anderson & Hebets 2017). Zhang et al. (2011) ablated or occluded the female's tactile and chemical receptors, revealing that tactile cues associated with tying behavior may be critical for this effect, with chemical cues playing a secondary role. Zhang et al. (2011) conclude that the veil in *N. pilipes* reduces the risk of sexual cannibalism and allows males to overcome resistance of females to repeated copulations. While Anderson & Hebets (2016) did not directly test for chemical cues, their observations are consistent with the silk wrapping acting as a physical restraint, rather than effects mediated by chemical signals. Female *P. mira* attempt to free themselves from the silk wrapping (rather than showing reduced activity), and sexual cannibalism attempts occur whether or not the silk wrapping is present (Anderson & Hebets 2016).

For most species in which males apply silk to the female's body during mating, the fitness consequences are unclear. The varied terms used to describe this behavior in the literature suggests that authors have inferred a range of possible functions from their observations. This is a fascinating phenomenon, and we suggest a number of different approaches could be fruitful for future study.

First, the phylogenetic distribution of the behavior is broad (Fig. 1; Table 3) and may suggest more than one evolutionary origin, so comparative analysis of the behavior and underlying physiology among taxa may be informative. For example, there are many species where extensive leg wrapping is typical, and physical restraint functions should be more likely in these species than in those where wrapping concentrates on the abdomen. We predict that leg-wrapping, but not abdomen-wrapping, will be more likely in taxa with a higher occurrence of sexual cannibalism.

Second, silk wrapping in the context of mating has been proposed to have its evolutionary origin in silk wrapping of prey (Lopez 1987; Schmitt 1992). Prey-wrapping has a similar underlying function, that is, reduced risk of injury from dangerous prey (Foelix 2011). This gives rise to a mechanistic prediction that bridal veils that function as physical restraints should be constructed from aciniform silk (the toughest type of silk, also used in prey capture; Craig 2003). Testing this supporting prediction may involve comparative analysis of silk structure (e.g., Parkhe et al. 1997; Hayashi et al. 2004), or analysis of the glandular origin of bridal veil silks.

Third, careful experimental designs that manipulate the male's ability to produce the veil, or the female's ability to detect it (e.g., Zhang et al. 2011; Anderson & Hebets 2016, 2017; and see Aisenberg et al. 2015) can be combined with assessments of female aggression, mating outcomes (e.g., proxies for female choice), or the opportunity for polyandry (e.g., assessments of anti-aphrodisiac effects) to estimate effects on male fitness. Comparative approaches may be valuable here as well. If bridal veils are primarily related to female choice, then they should be more common in taxa with higher levels of inter-male competition over mates, or low overall mating rates.

Fourth, similar types of manipulations can be employed to assess which functions of the bridal veils are related to communication (rather than restraint), and which modalities are most important. Disentangling possible effects of tactile and chemical cues will be particularly interesting. For this work, examination of behavioral effects of extracts of bridal veil silk may also be informative. Moreover, given recent improvement of techniques for nerve recordings from spiders, there is the exciting potential to measure female responses to chemicals vs. tactile cues directly (Menda et al. 2014).

## 5. SILK ASSOCIATED WITH NUPTIAL GIFTS

**5.1 Overview and descriptions of behaviors.**—Nuptial gifts are material items transferred during mating that function as paternal effort (increasing male offspring number or success) or mating effort (increasing the likelihood of mating; reviewed in Vahed 1998, 2007; Gwynne 2008). Although rare in spiders, the types of gifts reported include the male's body, glandular secretions from the male's cephalothorax, and silk-wrapped prey (reviewed in Albo et al. 2013b). Here we will focus on silken nuptial gifts, in particular the wrapped-prey gifts reported in one theridiid, one tetragnathid and in several species in the closely related families Trechaleidae and Pisauridae. We also include silk produced by males and consumed by females (Theridiosomatidae, Lycosidae, and probably Araneidae provide examples of this phenomenon) and silk-lined burrows (provided by males in a sex-role reversed wolf spider) as examples of nuptial gifts. Our focus will be on the function of the silk associated with these nuptial gifts rather than the gifts themselves.

Silk-wrapped nuptial gifts have been well studied in both *Pisaura mirabilis* (Clerck, 1757) (Pisauridae; Fig. 4a) and *Paratrechalea ornata* (Mello-Leitão, 1943) (Trechaleidae). Female silk cues (probably sex pheromones) elicit courtship and gift construction in males of both *P. ornata* (Albo et al. 2009) and *P. mirabilis* (Albo et al. 2011a). However, female silk is not required to elicit gift-wrapping by *P. mirabilis* males, who sometimes prepare nuptial gifts before they encounter a female or her draglines (Lang, 1996; Albo et al. 2011a). When a *P. mirabilis* or *P. ornata* male finds a female, he presents his gift by holding it in his chelicerae and raising his front legs in a characteristic display. If the female accepts his gift, she grasps it with her chelicerae and copulation ensues while she is feeding on the gift.

Whereas nuptial gifts are the norm for *Pisaura mirabilis* and *Paratrechalea ornata,* in *Metellina segmentata* (Clerck, 1757) (Tetragnathidae) silk-wrapped prey items are used as an alternative mating tactic (Prenter et al. 1994b; reviewed in Neff & Svensson 2013; Fig. 4b). In this species, males guard females and normally wait until she has captured a prey item before initiating courtship. Once the female has captured and wrapped a prey item in silk, the male takes it from her, adds his own silk, and then incorporates the silk-wrapped prey item into his mating thread (Prenter et al. 1994a); he may also wrap the female in a light bridal veil as he does this (Bristowe 1929; Lopez 1987). Clearly, the prey in this situation is not a nuptial gift since the female captures it herself, although once the male steals it from her, he can prevent her from eating it if she does not mate with him (Schneider & Lubin 1998). In rare cases, however, when two males are present on a female's web (in the field, 7% of females are guarded by two males simultaneously) the male captures the prey item himself and waits for the female to approach it before beginning courtship (Prenter et al. 1994b). In some cases, one male kills and wraps his rival male into a package with another prey item, using this silk-wrapped package to initiate courtship with the female (Prenter et al. 1994b; Fig. 4b).

In the kleptoparasitic and araneophagic spider *Argyrodes elevatus* (Theridiidae), two anecdotal reports of nuptial gifts are available. One *A. elevatus* male used a stolen prey item as a gift, and the other used the silk-wrapped carcass of a host spider (Cobbold & Su 2010; Uetz et al. 2010). In the case of the stolen prey item, the male was observed to present the gift to a female, wait until she began feeding on it, and then copulate with her (Uetz et al. 2010). Whether this functions as an alternative mating tactic or simply represents an occasional occurrence in this species remains to be seen.

Silk-wrapped prey gifts have most commonly been reported for pisaurids in the genera *Pisaura* Simon, 1886 (*P. lama* in addition to *P. mirabilis*), *Perenethis* L. Koch, 1878, *Thaumasia* Perty, 1833, and *Tinus* F.O. Pickard-Cambridge, 1901 (Table 4). In addition to *Paratrechalea ornata,* two congeners and members of the genus *Trechalea* Thorell, 1869 also use silk-wrapped nuptial gifts (Table 4). The families Pisauridae and Trechaleidae are closely related members of the Lycosoidea (Wheeler et al. 2016; see Fig. 1) hinting at silk-wrapped nuptial gift-giving as a synapomorphy, however, spotty reports of silk-wrapped nuptial gifts in other species suggest that silk-wrapped nuptial gifts may have evolved more than once in spiders.

There a few examples of apparent nuptial gifts in which the male's silk itself, rather than a prey item, constitutes the gift. In the ray spider *Theridiosoma gemmosum* (L. Koch, 1877) (Theridiosomatidae), males feed silk directly to the female between repeated copulations (Hajer & Řeháková 2011). This silk is considered a nutrient gift, because araneoids can recycle silk proteins by consuming silk (Craig 2003). Intriguingly, in one ctenid spider species where males deposit a bridal veil, the

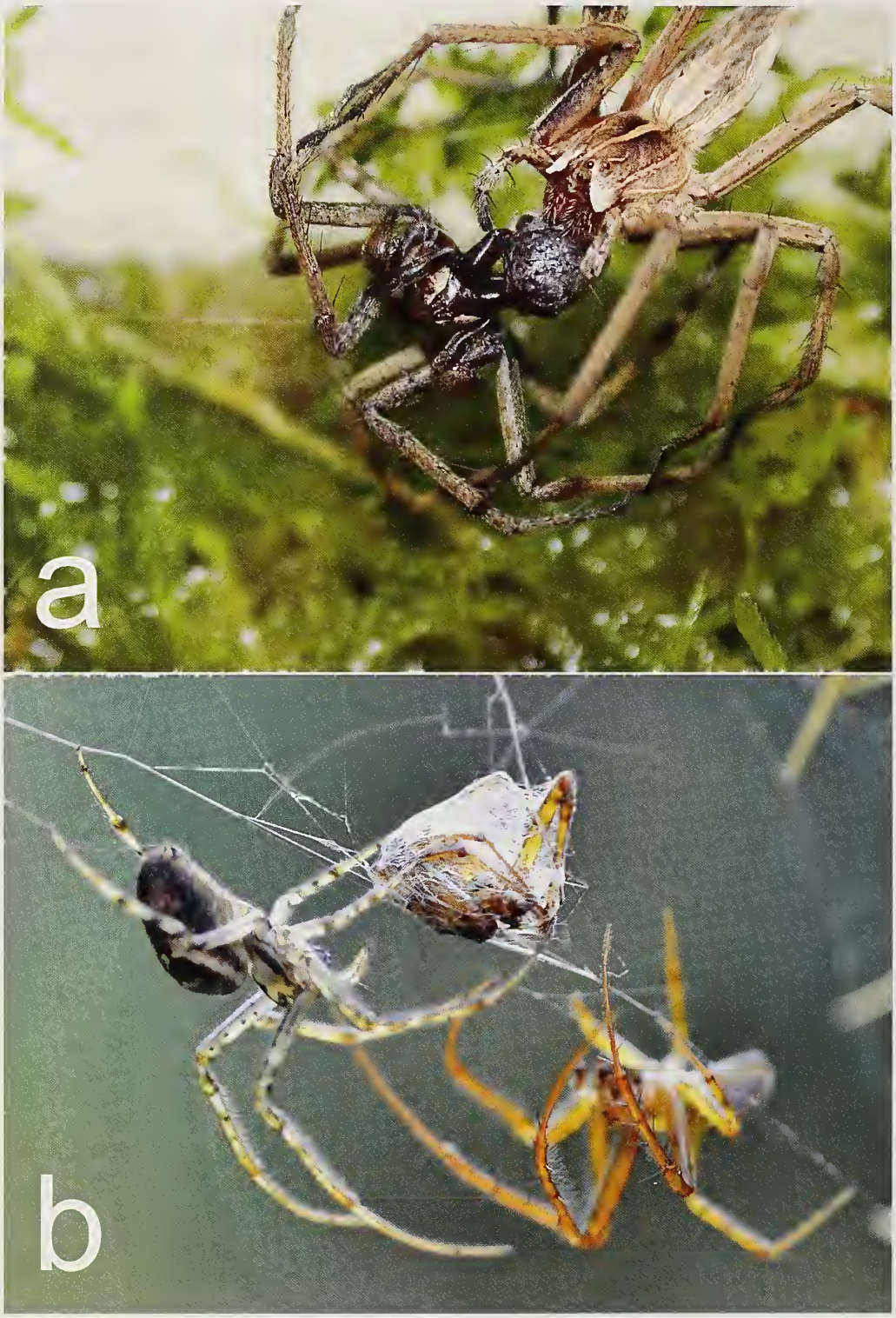


Figure 4.—Examples of silk-wrapped nuptial gifts. (a) Female (right) *Pisaura mirabilis* (Pisauridae) accepts a silk-wrapped gift from a male (photo: Alan Lau). (b) A male (right) *Metellina segmentata* (Tetragnathidae) has wrapped a rival male in silk as a nuptial gift for the female (photo: Conall McCaughey).

silk is apparently consumed after copulation. Trillo (2016) describes females of *Ctenus longipes* grooming the silk veil off of their legs and palps after mating and then bringing the silk to their mouthparts until it disappears. In the araneid spiders *Scoloderus cordatus* (Stowe 1978) and *Isoxya tabulata* (Robinson & Robinson 1980) males employ "treadmill"-type mating threads that they pay out as the female attempts to walk toward them on the thread. Robinson & Robinson (1980) note that during this process the female accumulates a conspicuous ball of silk under her cephalothorax, and though

they do not mention it being consumed, it seems probable that females eat the silk as in the examples above.

Finally, the silk-lined burrows provided by males of the sex role reversed wolf spiders in the genus *Allocosa* Sundevall, 1833 are nuptial gifts (reviewed in Aisenberg 2014). In *Allocosa senex* (Mello-Leitão, 1945) and *A. alticeps* (Mello-Leitão, 1944), males construct silk-lined burrows in which females oviposit and brood their egg sacs, providing both female and offspring with protection from predators (Aisenberg 2014). Females prefer males that provide longer burrows (Aisenberg et al. 2007) and males lengthen their burrows after experiencing rejection by a female (Carballo et al. 2017).

**5.2 Proposed mechanisms and functions.**—The most likely function for silk-wrapped nuptial gifts is to increase female receptivity and thus male mating success. Related to this may be a decreased risk of sexual cannibalism, which is a demonstrated function of gifts in *Pisaura mirabilis* (Toft & Albo 2016). Both of these are forms of mating effort. The silk wrapping of nuptial gifts may in general provide females with information about males via visual, tactile, or chemical cues. Proposed mechanisms for such effects in pisaurids and trechaleids generally fall into two categories. In both cases, silk wrapping may function in several non-mutually exclusive ways that either conflict or align with the female's interests. First, silk may have direct physical effects if it disguises gift contents and thus increases mating success even if prey items are insufficient (or missing). When silk is wrapped around a non-prey item, it may serve to hide the contents of a 'worthless package' (e.g., Ghislandi et al. 2017; Prokov & Semelbauer 2017), through visual obstruction and/or creating a barrier (physical or chemical) between the female and the contents. Males may thus deceive females into mating in the absence of a nutritious gift. However, recent work argues that such 'worthless' gifts may be most common in species where the nuptial gift has evolved to serve a signal function rather than a direct benefit (e.g., Albo et al. 2017; Pandulli-Alonso et al. 2017). Another possible physical effect of the silk wrapping is to allow males to maintain a firm grip on the gift to avoid it being stolen by the female (Andersen et al. 2008) or rival males (Nitzsche 2011).

Second, silk may have indirect effects through communication, whereby visual, tactile or chemical cues increase the likelihood of gift acceptance and mating by females. For example, the brightness of the silk wrapping around the gift or its chemo-tactile qualities may provide the female with information about the male's quality, since silk and/or associated pheromones may provide an honest signal of male body condition (Stålhandske 2002; Albo et al. 2011a; Trillo et al. 2014). Moreover, the amount of silk a male can spin before or during mating may also provide information about body condition (Albo et al. 2011a; Klein et al. 2014). In this context, silk wrapping around prey may also provide a method for delivery of chemicals to female chemosensory organs.

Third, rather than providing information about the male, the silk wrapping may include cues that exploit female sensory biases by mimicking egg sacs (Stålhandske 2002), which females carry in their chelicerae in pisaurids and attached to the spinnerets in trechaleids (Carico 1993).

Fourth, when silk itself is a nuptial gift, it may also function as paternal effort. When the female consumes the silk as in ray spiders (Hajer & Řeháková 2011), at least one ctenid (Trillo 2016) and possibly some araneids that use 'treadmill'-type mating threads (Stowe 1978; Robinson & Robinson 1980), it may provide additional nutrients to females that are incorporated into the male's offspring. However, the thick silk wrapping of the nuptial gift apparently does not itself provide a significant source of protein to the female in pisaurids (Nitzsche 1988 as cited by Nitzsche 2011). The silk burrows provided by *Allocosa* males clearly provide material benefits to females (safe places to oviposit and brood egg sacs) but may also represent mating effort, with males lengthening their burrows (requiring addition of costly silk) in response to rejection by females (Carballo et al. 2017).

In *Argyrodes elevatus*, silk-wrapped nuptial gifts may be an alternative mating tactic as in *Metellina segmentata*. Males of some spider species mate opportunistically with females engaged in feeding as a way to avoid sexual cannibalism (e.g., Austin & Anderson 1978; Fromhage & Schneider 2004), and the presentation of nuptial gifts may be a refinement of this mating strategy.

**5.3 Current evidence and future directions.**—Experimental studies of the function of nuptial gifts in spiders are restricted to a few species. There is experimental evidence for several functions of nuptial gifts in both *Paratrechalea ornata* and *Pisaura mirabilis*. Nuptial gifts in *P. mirabilis* and *P. ornata* may have evolved by sexual selection through cryptic female choice for sperm storage (Albo & Costa 2010; Albo et al. 2013a). In both species, males that provide nuptial gifts to mates have longer copulations and transfer more sperm than males who do not provide gifts (Albo & Costa 2010; Albo et al. 2013a), and nuptial gifts are also correlated with accelerated oviposition in *P. ornata* (Albo & Costa 2010). We note here the interesting functional parallel with the bridal veil in *Pisaurina mira* (Anderson & Hebets 2016, 2017).

Nuptial gift silk may provide information via visual signals or cues. *Paratrechalea ornata* females accept smaller, brighter gifts more quickly than larger gifts that are darker in color—but the mechanism is not clear (Klein et al. 2014). Brighter gifts (painted white to match egg sacs) are more quickly accepted than unmanipulated silk-wrapped gifts, which in turn are more readily accepted than gifts painted brown (*P. mirabilis*, Stålhandske 2002). In some species, visual signals alone may be insufficient to elicit gift acceptance, but ether-extractable chemical compounds specific to nuptial gift silk elicit female acceptance of filter paper 'gifts' (*Paratrechalea ornata*; Brum et al. 2012). Moreover, females more often accepted gifts wrapped by males than gifts wrapped with silk experimentally reeled from males' spinnerets, suggesting that males control the type of silk they use or the compounds they add to the silk during gift construction (Brum et al. 2012). This suggests that pheromones on male silk stimulate females to accept gifts, thereby increasing mating success of males. In no-choice tests, females responded similarly to silk extracts and prey extracts, implying that the pheromone either has chemical similarities to prey cues and exploits the female's foraging response, or comprises unrelated compounds that elicit the same response—the acceptance of and feeding on the gift (Brum et al. 2012).

The pheromone on silk-wrapped nuptial gifts may provide information about a male's quality even if the gift itself does

not necessarily honestly indicate prey capture ability (males can steal gifts from rivals or from the female herself; Prenter et al. 1994b; Nitzsche 2011). The extent of silk-wrapping during gift construction depends on male condition in *P. mirabilis*, with males in better condition adding more silk, and thus this may be an honest signal of male quality (Albo et al. 2011a). As expected if this is the case, *P. mirabilis* feed longer on gifts wrapped with more silk, and most males already carrying wrapped prey wrap it again after encountering a female (Lang 1996; Albo & Costa 2010), as do males that were previously rejected (Bilde et al. 2007), which appears to increase the attractiveness of the gift (Bilde et al. 2007; Brum et al. 2012). This suggests that visual, tactile and/or chemical cues associated with the male's silk affect female acceptance of the gift (Bilde et al. 2007).

Similarly, wrapping low-quality gifts in pheromone-laden silk may be a strategy of males that minimizes the costs of providing a gift while maintaining its attractiveness. In some species females will not copulate unless males provide a gift (*P. mirabilis*, Prokop & Maxwell 2009; Albo et al. 2011b). Such effects may be limited however, as males that present a silk-wrapped gift containing a prey carcass or plant material instead of prey may obtain a short copulation, but, in *P. mirabilis*, it ends as soon as the female detects that there is no prey inside the silk (Albo et al. 2011b; Brum et al. 2012). Consistent with this, field studies of *P. mirabilis* found no evidence for 'sham' gifts concealed in silk, instead, 40% of males carried gifts, all of these were freshly killed arthropods (Prokop & Maxwell 2009), and gift size was correlated with male body size (Prokop & Semelbauer 2017). The idea that the gift is a sensory trap exploiting female maternal care behavior (Stålhandske 2002) was not supported in this species; experimental evidence suggests that the gift exploits female foraging motivation instead (Bilde et al. 2007; Toft & Albo 2015).

In strong contrast to *P. mirabilis*, 70% of gifts carried by *Paratrechalea ornata* males are nutritionally worthless in nature. However, in *P. ornata*, female receptivity does not depend on hunger, as might be expected if females are permitting copulations with gift-bearing males because they are seeking food (Pandulli-Alonso et al. 2017). Albo et al. (2017) suggest that nuptial gifts may evolve initially due to direct benefits to females, but in some species, gifts may evolve a signal function (Bradbury & Vehrenkamp 2011). Thus *P. mirabilis* and *P. ornata* represent different points in the evolutionary ritualization of a direct benefit into a signal (Albo et al. 2017). Alternatively, the provision of worthless gifts may be maintained in a basically honest, direct-benefits system as long as the frequency of these deceptions remains sufficiently low (negative frequency dependence; Dawkins & Guilford 1991; Neff & Svensson 2013). If this is the case, then receiving deceitful gifts will be costly for females, but elevated discrimination would be even more costly than accepting worthless gifts at low frequency. Moreover, at equilibrium, the fitness of males using deceitful or honest tactics should be equal, as part of a mixed ESS (Evolutionarily Stable Strategy; Neff & Svensson 2013). Finally, a high frequency of worthless gifts may occur as a transient outcome of sexually-antagonistic coevolution (Ghislandi et al. 2014). In this case, receiving worthless gifts is costly for females, and the high frequency of male deceit would eventually lead to the evolution of increased female discrimination (Lindstedt & Mokkonen 2014).

In addition to other functions, silk-wrapping apparently affords *P. mirabilis* males greater control over their gifts by improving their grip, thus decreasing the risk of the female stealing the gift without mating. Moreover, the rounded shape of the wrapped gift facilitates access to the female's genitalia for copulation, thus increasing their mating success (Andersen et al. 2008). The gift itself may also function as a "shield" preventing cannibalism; cannibalism is six times more likely to occur when males do not provide the female with a gift (Toft & Albo 2016), although it is unclear whether silk wrapping is required for this effect.

Visual cues, chemical cues, and physical properties of the silk have all been implicated in the gift-giving systems of *P. ornata* and *P. mirabilis*. Given that the type of silk appears to be important (Brum et al. 2012), future studies could compare the chemical and biophysical properties of silk used to wrap nuptial gifts to those of other silk types. This will facilitate consideration of the origin of gifts, and the identification of putative pheromones on the silk and study of their specific function(s). Whether chemical cues are important in other species that produce silk-wrapped nuptial gifts (or when silk alone acts as a gift) remains to be investigated. In the *Allocosa* species providing burrows as nuptial gifts, the silk lining alone (i.e., in the absence of the male's body, which emits a volatile pheromone) is not sufficient to elicit female courtship behavior, but the potential role of the silk in female assessment of males has not been further tested (Aisenberg et al. 2010). Studies of the mechanisms by which nuptial gift silk influences female responses would benefit from experiments that systematically manipulate the possible cues presented in gift silk, and/or ablate the female's sensory receptors and examine the effect on mating success, cannibalism risk, and female reproductive output (e.g., in the case of species where females consume the male's silk).

Understanding the evolutionary trajectory of nuptial gift evolution in spiders will require a more explicitly comparative approach, with the addition of studies of more taxa that vary in the type of gift involved in mating. In the broadest sense, this may include males that wait until females are feeding before attempting to mate, those that steal prey from females and then present those same prey at mating, those that wrap nutritive prey to present to females, and those that frequently present non-nutritive, silk-wrapped items to females. A theoretical evolutionary sequence would predict co-occurrence of a number of features in species at different stages (e.g., Albo et al. 2017). In this case, silk wrapping may originally function to subdue prey or for easy manipulation of prey to facilitate gift giving as a direct benefit to females. Hungry females may be more likely to mate and accept these prey items, and most gifts carried by males should be nutritive. In such species, male honesty may be further augmented by the risk of cannibalism from hungry females who do not receive a gift. Later in the evolutionary sequence, silk wrapped packages may provide information to females (via visual, chemical or tactile cues), thus triggering receptive behavior regardless of female's hunger, and in the absence of a risk of cannibalism. Under this scenario, these species should show a relatively high frequency of 'worthless' gifts, but features of the silk package

itself would be correlated with male quality (e.g., Pandulli-Alonso et al. 2017). In contrast, species with a relatively high frequency of 'worthless' gifts may not be those in which the gift has evolved a signal function; rather this may be an exploitative behavior of males maintained through negative frequency dependence. If silk wrapping serves a deceptive function, it is expected that receptivity of females will be linked to hunger, and gifts should deter sexual cannibalism. This can be tested in experiments that measure the fitness payoff to males bearing worthless gifts as a function of natural or manipulated variation in the relative frequency of the tactic.

## 6. OTHER EXAMPLES OF MALE SILK USE DURING MATING INTERACTIONS

The three types of silk use discussed above do not include all of the ways that male spiders can use silk during courtship and mating interactions. Below we briefly discuss some other kinds of silk use related to spider mating (see Table 5).

We have not considered sperm webs in this review because their production is rarely observed and described, and, to our knowledge, there have been no suggestions or investigations of functions other than the required one of charging the palps in preparation for sperm transfer (Foelix 2011). Indeed, in many spider taxa males charge their palps with sperm before they set off in search of mates, and thus the silk involved clearly has no effect on females during courtship (Foelix 2011). However, in those species where males build sperm webs on the female's web and/or charge the palps in between mating bouts (e.g., in the Linyphiidae; Van Helsingden 1965; Watson & Lighton 1994), we cannot exclude the possibility that this silk plays some additional role.

Cursorial spiders trail dragline silk as they move around, periodically anchoring it to the substrate (Richman & Jackson 1992; Foelix 2011), and undoubtedly do so in close proximity to one another during mating interactions. In these taxa, where courtship occurs on substrates other than the female's silk, male silk function could overlap substantially with those where males deposit silk on the female's web or body. Explicit studies of male silk use in such contexts are rare, but the following example is illustrative. In the wolf spider *Pardosa milvina* (Lycosidae), the structure of male silk produced during courtship differs from typical dragline silk (e.g., in the number of attachment disks), and females respond to contact with courtship silk by spinning more of their own pheromone-laden silk (Khan & Persons 2015). Females increase their own silk production in response to males who court less intensively (i.e., males depositing less silk), suggesting that silk-bound pheromones and/or contact cues may mediate a two-way "conversation" between the sexes (Havrilak et al. 2015). Additional studies analyzing the structural and/or chemical differences between silk deposited by males during courtship and other contexts, as well as the behavioral responses of females to these different silk types (as in Khan & Persons 2015) would be very useful. Such studies may reveal that bi-directional communication mediated by silk is common across spider taxa

The orb-weaver *Manogea porracea* (Araneidae) provides a unique example of male silk use that facilitates paternal care (Moura et al. 2017). After mating, the male builds his own capture web above that of the female and remains there until the end of the reproductive season. The female then hangs her egg sacs between the two webs and the male provides parental care by protecting the egg sacs from predators. Both parents provide protection, but females frequently die before spiderlings emerge, such that egg sacs attended by males are most common at the end of the season (Moura et al. 2017). This example has clear overlap with nuptial gifts that constitute paternal effort.

## 7. CONCLUSIONS AND FUTURE DIRECTIONS

**7.1 Summary.**—Here we reviewed evidence that male silk use during courtship and mating is taxonomically widespread, diverse in possible function and mechanism (Fig. 1; Table 1), and may play an important part in the mating dynamics in many spider species (Tables 2–7). The widespread occurrence of silk deposition by male spiders during courtship and mating (Fig. 1) suggests an important, but often neglected, function of male silk in behavioral interactions between males and females, and among competing males. Moreover, the evidence for ritualized silk use in both the Mygalomorphae and Araneomorphae and its prevalence across the phylogeny (Fig. 1) presents the intriguing possibility that functional roles for male silk use are plesiomorphic among spiders. Systematic use of silk in mating by males includes the addition of silk to females' webs or other silk structures, silk deposition on females' bodies, and the use of silk associated with nuptial gifts. In the former two types of silk use, the silk is invariably deposited in close proximity to the female, often in direct contact with her chemoreceptors or proprioreceptors, and in the latter case, female manipulation and/or consumption of gifts places male silk against the sensory receptors on her palps. Thus, simply considering these patterns of silk use suggests hypotheses regarding the role of silk in intersexual communication during mating. Perhaps not surprisingly, thus far, the bulk of experimental studies have focused on the potential importance of male-produced sex pheromones in such communication (Table 1). These studies suggest that silk produced by males can play an important role in inter-sexual communication (see Gaskett 2007). However, chemical communication is just one possible mechanism by which silk use can affect the fitness of mating males (Table 1). Unfortunately, as is common in reviews of spider biology and behavior, our ability to make general inferences is limited because of the relatively narrow taxonomic range of the species that have been well-studied (Huber 2005; Schneider & Andrade 2011). Moreover, while in many spiders the role of the female's silk is clear and relatively easy to measure, the role of male silk may be more challenging to untangle from correlated activities, even in those species that are relatively well-studied. For example, since silk deposition co-occurs with courtship or nuptial gift presentation, elegant experimentation is required to make clear inferences about the independent effects of the silk itself. Nonetheless, based on the available evidence, we conclude that male silk serves a number of important functions during courtship and mating, and these may be mediated through direct or indirect mechanisms (Table 1).

**7.2 Functions and mechanisms of effect.**—Male silk use during mating may evolve or be maintained because it increases male success in the current mating or reduces the

risk of losing paternity through polyandry (Table 1). The (scant) current evidence suggests an interesting pattern of segregation of benefits from different types of silk use. The data show that silk addition to the female's web affects the likelihood of polyandry (and risk of paternity losses to sperm competition) but not the outcome of the mating attempt of the silk-laying male. In contrast, the data suggest that silk addition to the female's body (bridal veils) and silk associated with nuptial gifts function exclusively to increase the likelihood of favorable outcomes in the current mating, but do not affect polyandry. It seems unlikely that this is a real division, however, given the small number of experimental studies. We consider two examples in which additional work might quickly remove this pattern. First, one of the two mechanisms for which there is currently no experimental support is the hypothesis that silk use could affect female mobility. However, the creation of mating threads in orb-weaving spiders has often been described anecdotally in terms of constraints on the movement of potentially cannibalistic mates, and this makes intuitive sense. Nevertheless, this does not appear in Table 1 because, to our knowledge, there are no experimental tests of this hypothesis, nor of any other way in which male silk use might reduce female mobility (e.g., web modifications that reduce the area of the web). Second, very few studies have examined long-term effects of exposure to male silk on females. So, although in the short term, mate attraction or female receptivity to polyandry may not change, there could be longer-term effects that do confer benefits on silk-spinning males through decreased polyandry. This may be particularly likely if tactile or chemical cues trigger physiological (e.g., hormonal) changes in females that, over time, lead to changes in receptivity (e.g., in *Drosophila*; Wolfner 2002).

While it is possible that functional effects may arise through indirect effects (communication) or direct effects (physical or structural), the majority of studies to date have focused on indirect effects mediated by chemical communication (Tables 1, 5). There is experimental evidence that chemical communication is involved in all three types of silk use (web modification, veils, gifts). However, in most cases, these studies showed that chemicals are sufficient to elicit an effect but did not exclude other possible mechanisms that might also be operating simultaneously in nature. This is problematic since the hypotheses and mechanisms we suggest for male silk use may overlap, as males may acquire benefits in more than one way, context may determine which function has the strongest effect on male fitness, and more than one mechanism may operate simultaneously. Thus, it is unclear whether these results suggest the critical importance of indirect chemical information relative to other possible mechanisms of effect. Another possibility is that, since male silk is apparently pheromone-laden (Table 6), chemical communication effects may overlay other effects that also affect male fitness.

**7.3 Improving our understanding of male silk use.**—To better understand male silk use in courtship and communication, the functional roles of both the silk itself and the behaviors associated with its deposition must be investigated. Preventing males from depositing silk during courtship by occluding their spinnerets with wax or glue is a good technique for investigating the function of male silk (e.g., Anderson & Hebets, 2016). Ablating female chemoreceptors may also be useful in determining the function and importance of chemical signals (e.g., Zhang et al. 2011; Aisenberg et al 2015). Testing the responses of males to the silk of rival males in the context of mate-searching and mate choice (e.g., Schneider et al. 2011) will allow us to determine the function of silk in intra-sexual communication. In species where behavioral evidence indicates the presence of a male silk-borne pheromone, pheromone identification should be pursued. Comparative pheromone analyses of male and female silk may be especially fruitful in those species in which the female pheromone is already known. Recent evidence that silk gene expression and morphology of the spinning apparatus differ between males and females in *Steatoda* and *Latrodectus* (Correa-Garwhal et al. 2017) provide the opportunity to link silk structure with function in taxa for which sexual behavior and chemical communication is already well studied. Tichy et al. (2001) have obtained electrophysiological responses to volatile components from tarsal chemoreceptors in *Cupiennius salei*, and 'electrolegograms' have already been developed for whip spiders (Amblypygi; Hebets & Chapman 2000). As our knowledge of spider chemoreception improves, we should strive to develop an analog of the gas chromatographic-electroantennographic detection (GC-EAD) system previously invented for analyses of insect pheromone (Struble & Arn 1984; see Hebets & Chapman 2000). This technique would entail using a spider's chemoreceptive appendage in place of an insect antenna as a sensor to determine the volatiles that elicit sensory responses. Such a technique would allow rapid screening for potential pheromones in extracts from spider silk or cuticle. Future studies should also attempt to determine the glandular origins of silks and associated pheromones that males produce during courtship and mating behavior. We still do not know where and how spiders synthesize pheromones, but comparative morphology and careful experimentation (e.g., assaying extracts of individual silk glands or body parts) should help us begin to address this major gap in our knowledge.

An intriguing suggestion that appears frequently in the literature is that males may use silk to manipulate females; that is, to partially or completely control female behavior (*sensu* Dawkins 1978) and thus mating outcomes. Here, 'manipulation' is a useful functional concept if the induced female behaviors are beneficial to males but decrease female fitness. In the context of mating, such an outcome may arise through an evolutionary history of sexual conflict (Arnqvist & Rowe 2005). This may be contrasted with communication, which increases the likelihood of a particular female behavior because the behavior is, on average, beneficial for the female as well as the male (Bradbury & Vehrencamp 2011). Manipulation is discussed frequently for the silk-wrapping around nuptial gifts, which can, and often does, conceal 'worthless' (nutritionless) items (Ghislandi et al 2017; Pandulli-Alonso et al. 2017). In some species such 'worthless' gifts are common and they may nonetheless increase mating success (Albo et al 2017; Pandulli-Alonso et al 2017). However, these deceptive gifts should be considered manipulative only if females mating with males carrying 'worthless' gifts have reduced reproductive fitness, and this has not been examined experimentally. Particularly if 'worthless' gifts are common, it

may be that the gift itself is a ritualized representation of male quality (e.g., Albo et al. 2011a; Pandulli-Alonso et al. 2017). Studies of this aspect of male silk use may be particularly valuable, given that ritualization is thought to be the widespread basis of a wide range of signals (Bradbury & Vehrenkamp 2011), but there is very little empirical evidence for this phenomenon (e.g., Scott et al. 2010).

Another common discussion of manipulation arises in the context of silk-borne pheromones that may 'induce receptivity' in females, or otherwise change the outcome of the current mating (e.g., Becker et al. 2005). However, when chemical cues induce a behavioral change in females that increases mating success of the silk-laying male, this may also represent a normal, or necessary coordination of male and female behavior that is not maladaptive for females (e.g., Bradbury & Vehrencamp 2011). For example, a small proportion of female agelenids fail to recover from the state of catalepsis following mating (S. Riechert pers. comm.), an observation consistent with manipulation. However, Gehring (1953) suggests the complexity of the agelenid genitalia makes female immobility a necessity for copulation success. Showing a mechanism by which silk leads to negative effects on females does not necessarily demonstrate manipulation. Nevertheless, in general, the phenomena associated with male silk use during mating suggests intriguing questions regarding the role that sexual conflict plays in the evolution of male silk use during mating. Studies of fitness effects on males and females may advance our understanding of this interplay.

Unfortunately, we have insufficient data to analyze comparative patterns regarding male silk use, nor to test hypotheses about evolutionary sequences for current modes of silk use (e.g., nuptial gifts; Albo et al. 2017). We are limited because the bulk of our knowledge of spider mating behavior comes from extensive study of a small number of families including the Araneidae, Ctenidae, Linyphiidae, Lycosidae, Pholcidae, Pisauridae, Salticidae, and Theridiidae (Schneider & Andrade 2011; and see references in this review). Taxa for which we do not report male silk use are as likely to represent the absence of study as the absence of male silk use. Arguably, since males leave behind draglines when they move, and courtship and mate searching often involves extensive movement (Foelix 2011), male silk use during mating may be the rule rather than the exception, despite the limited literature now available. The more ritualized forms of silk use described here (silk deposition, bridal veils, nuptial gifts) may have arisen when more common uses that are found across spiders were coopted for mating. What is clear is that we critically need more phylogenetic coverage in studies of mating, to test these and other hypotheses (Huber 2005; Schneider & Andrade 2011).

Although there are challenges with initiating studies with new species, there may be ways to offset the risk, while maximizing the likely payoff in terms of comparative analyses that increase our understanding. Studies of new species that document the prevalence of male silk use and conduct at least preliminary examinations of the functional importance would be valuable (e.g., by comparing behaviors and mating outcomes for males with and without occluded spinnerets; Zhang et al. 2011; or females with or without ablated sensory structures; Aisenberg et al. 2015). One approach that may be particularly useful would be to focus new efforts on representative species in little-known families within taxa that already have relatively extensive records of a variety of types of male silk use. Two examples are the superfamily Araneoidea, and the Oval Calamistrum clade (Fig. 1), each of which includes records of all three categories of male silk use. Choosing new species to study within these groups would benefit from strategic thinking. Among the web-building Araneoidea, it may be more feasible to stage laboratory matings of spiders that weave irregular webs rather than orb webs since the structural requirements for appropriate web frames may be less stringent (e.g., Nesticidae: scaffold-web weavers; Cyatholipilidae: sheet-web weavers), or, among the less well-known orb-weavers, those that build small webs may be more tractable for laboratory study (e.g., Mysmenidae and Anapidae). Another approach would be to focus on studying multiple species within families in which there are already records of all categories of male silk use (e.g., Theridiidae and Tetragnathidae). Either of these approaches would move us closer to valid comparative tests for understanding the evolution of silk use.

**7.4 Concluding remarks.**—Overall, this review provides a functional and mechanistic framework for understanding the diversity of male silk use behaviors, and suggests fruitful approaches and taxa for study. Spiders are models for studies of sexual selection, and how choice, competition, and communication are affected by ecology, cannibalism, and sexual conflict more broadly (Herberstein et al. 2002; Schneider & Andrade 2011; Uhl & Elias, 2011; Kralj-Fiser et al. 2016). As in other fields, insight is limited by what we choose to study (Huber 2005). While technological limitations created challenges in the past, particularly to the study of silk, vibrations, or pheromones, a number of novel approaches now make these studies more feasible (e.g., Hebets & Chapman 2000; Menda et al. 2014; Mortimer et al. 2015). Harnessing these techniques and expanding the range of taxa studied may lead to big advances in understanding. The strong evidence presented here for various effects of male silk in mating suggests that we currently have only part of the picture with respect to spider mating behavior in most taxa. Understanding how male-produced silk may influence, constrain, or manipulate interactions with females and with rival males could provide significant new insights into mating behavior, the evolution of traits related to mating, and fuel new tests of a wide range of theory in sexual selection and sexual conflict.

## ACKNOWLEDGMENTS

We thank Samantha Vibert for conversations inspiring the topic of the review and Rick Vetter for inviting us to write it. Anita Aisenberg, Gerhard Gries, and two anonymous reviewers provided helpful comments on earlier versions of the manuscript. We also thank Maria Hiles, Alan Lau, Sean McCann, Conall McCaughey, Ed Niewenhuys, and Shichang Zhang for the photographs. Funding was provided by a Natural Sciences and Engineering Research Council of Canada (NSERC) Alexander Graham Bell Canada Graduate Scholarship (to CES), and the Canada Research Chairs Program (to MCBA).

## LITERATURE CITED


Aisenberg, A. 2014. Adventurous females and demanding males: sex role reversal in a Neotropical spider. Pp. 163–182. *In* Sexual Selection: Perspectives and Models from the Neotropics. (R. Macedo & G. Machado, eds.). Academic Press, London, UK.

Aisenberg, A., G. Barrantes & W.G. Eberhard. 2015. Hairy kisses: tactile cheliceral courtship affects female mating decisions in *Lencauge mariana* (Araneae, Tetragnathidae). Behavioral Ecology and Sociobiology 69:313–323.

Aisenberg, A., L. Baruffaldi & M. González. 2010. Behavioural evidence of male volatile pheromones in the sex-role reversed wolf spiders *Allocosa brasiliensis* and *Allocosa alticeps*. Naturwissenschaften 97:63–70.

Aisenberg, A., N. Estramil, M. González, C.A. Toscano-Gadea & F.G. Costa. 2008. Silk release by copulating *Schizocosa malitiosa* males (Araneae, Lycosidae): a bridal veil. Journal of Arachnology 36:204–206.

Aisenberg, A., C. Viera & F.G. Costa. 2007. Daring females, devoted males, and reversed sexual size dimorphism in the sand-dwelling spider *Allocosa brasiliensis* (Araneae, Lycosidae). Behavioral Ecology and Sociobiology 62:29–35.

Alam, M.S., M.A. Wahab, & C.H. Jenkins. 2007. Mechanics in naturally compliant structures. Mechanics of Materials 39:145–160.

Albo, M.J & F.G. Costa. 2010. Nuptial gift-giving behaviour and male mating effort in the Neotropical spider *Paratrechalea ornata* (Trechaleidae). Animal Behaviour 79:1031–1036.

Albo, M.J., T. Bilde & G. Uhl. 2013a. Sperm storage mediated by cryptic female choice for nuptial gifts. Proceedings of the Royal Society B 280:20131735.

Albo, M.J., L.E. Costa-Schmidt & F.G. Costa. 2009. To feed or to wrap? Female silk cues elicit male nuptial gift construction in a semiaquatic trechaleid spider. Journal of Zoology 277:284–290.

Albo, M.J., N. Macías-Hernández, T. Bilde & S. Toft. 2017. Mutual benefit from exploitation of female foraging motivation may account for the early evolution of gifts in spiders. Animal Behaviour 129:9–14.

Albo, M.J., V. Melo-González, M. Carballo, F. Baldenegro, M.C. Trillo & F.G. Costa. 2014. Evolution of worthless gifts is favoured by male condition and prey access in spiders. Animal Behaviour 92:25–31.

Albo, M.J., S. Toft & T. Bilde. 2011a. Condition dependence of male nuptial gift construction in the spider *Pisaura mirabilis* (Pisauridae). Journal of Ethology 29:473–479.

Albo, M.J., S. Toft & T. Bilde. 2013b. Sexual selection, ecology, and evolution of nuptial gifts in spiders. Pp. 183–200. *In* Sexual Selection: Perspectives and Models from the Neotropics. (R. Macedo & G. Machado, eds). Academic Press, London, UK.

Albo, M.J., G. Winther, C. Tuni, S. Toft & T. Bilde. 2011b. Worthless donations: male deception and female counter play in a nuptial gift-giving spider. BMC Evolutionary Biology 11:329.

Alvarado-Castro, J.A. & M.L. Jiménez. 2011. Reproductive behavior of *Homalonychus selenopoides* (Araneae: Homalonychidae). Journal of Arachnology 39:118–127.

Anava, A. & Y. Lubin. 1993. Presence of gender cues in the web of a widow spider *Latrodectus revivensis*, and a description of courtship behaviour. Bulletin of the British Arachnological Society 9:119–122.

Andersen, T., K. Bollerup, S. Toft & T. Bilde. 2008. Why do males of the spider *Pisaura mirabilis* wrap their nuptial gifts in silk: Female preference or male control? Ethology 114:775–781.

Anderson, A.G. & E.A. Hebets. 2016. Benefits of size dimorphism and copulatory silk wrapping in the sexually cannibalistic nursery web spider, *Pisaurina mira*. Biology Letters 12:20150957.

Anderson, A.G. & E.A. Hebets. 2017. Increased insertion number leads to increased sperm transfer and fertilization success in a nursery web spider. Animal Behaviour 132:121–127.

Anderson, J.T. & D.H. Morse. 2001. Pick-up lines: cues used by male crab spiders to find reproductive females. Behavioral Ecology 12:360–366.

Andersson, M.B. 1994. Sexual Selection. Princeton University Press, Princeton, NJ.

Andrade, M.C.B. 1996. Sexual selection for male sacrifice in the Australian redback spider. Science 271:70–71.

Andrade, M.C.B. & M.M. Kasumovic. 2005. Terminal investment strategies and male mate choice: extreme tests of Bateman. Integrative and Comparative Biology 45:838–847.

Andrade, M.C.B. & E.C. MacLeod. 2015. Potential for CFC in black widows (genus *Latrodectus*): mechanisms and social context. Pp. 27–53. *In* Cryptic Female Choice in Arthropods (A.V. Peretti & A. Aisenberg, eds.). Springer International Publishing, Switzerland.

Arnqvist, G. & L. Rowe. 2013. Sexual Conflict. Princeton University Press, Princeton, NJ.

Austin, A.D., & D.T. Anderson. 1978. Reproduction and development of the spider *Nephila edulis* (Koch)(Arancidae: Araneae). Australian Journal of Zoology 26:501–518.

Ayyagari, L.R. & W.J. Tietjen. 1987. Preliminary isolation of male-inhibitory pheromone of the spider *Schizocosa ocreata* (Araneae, Lycosidae). Journal of Chemical Ecology 13:237–244.

Barrantes, G. & M.J. Ramírez. 2013. Courtship, egg sac construction, and maternal care in *Kukulcania hibernalis*, with information on the courtship of *Misionella mendensis* (Araneae, Filistatidae). Arachnology 16:72–80.

Barrantes, G., L. Sandoval, C. Sánchez-Quirós, P.P. Bitton & S.M. Doucet. 2013. Variation and possible function of egg sac coloration in spiders. Journal of Arachnology 41:342–348.

Barth, F.G. 1982. Spiders and vibratory signals: sensory reception and behavioral significance, Pp. 67–120. *In* Spider Communication: Mechanisms and Ecological Significance. (P. Witt & J. Rovner, eds.). Princeton University Press, Princeton, NJ.

Barth, F.G. 2002. A Spider's World: Senses and Behavior. Springer, Heidelberg, Germany.

Baruffaldi, L. & F.G. Costa. 2010. Changes in male sexual responses from silk cues of females at different reproductive states in the wolf spider *Schizocosa malitiosa*. Journal of Ethology 28:75–85.

Baruffaldi, L., F.G. Costa, A. Rodríguez & A. González. 2010. Chemical communication in *Schizocosa malitiosa*: evidence of a female contact sex pheromone and persistence in the field. Journal of Chemical Ecology 36:759–767.

Bateson, P.P.G. 1983. Mate Choice. Cambridge University Press, Cambridge, UK.

Becker, E., S. Riechert & F. Singer. 2005. Male induction of female quiescence/catalepsis during courtship in the spider, *Agelenopsis aperta*. Behaviour 142:57–70.

Bell, R.D. & J.A. Roberts. 2017. Trail-following behavior by males of the wolf spider, *Schizocosa ocreata* (Hentz). Journal of Ethology 35:29–36.

Benamú, M.A., N.E. Sánchez, C. Viera & A. González. 2012. Sexual behavior of *Alpaida veniliae* (Araneae: Arancidae). Revista de Biología Tropical 60:1259–1270.

Benamú, M.A., N.E. Sánchez, C. Viera & A. González. 2015. Sexual cannibalism in the spider *Alpaida veniliae* (Keyserling 1865)(Araneae: Araneidae). Journal of Arachnology 43:72–76.

Berendonck, B. 2003. Reproductive strategies in *Latrodectus revivensis* (Araneae; Theridiidae): functional morphology and sexual cannibalism. PhD Thesis. Heinrich-Heine-Universität Düsseldorf.

Berry, J.W. 1987. Notes on the life history and behavior of the communal spider *Cyrtophora moluccensis* (Doleschall)(Araneae, Arancidae) in Yap, Caroline Islands. Journal of Arachnology, 15:309–319.

Bilde, T., C. Tuni, R. Elsayed, S. Pekar & S. Toft. 2007. Nuptial gifts

of male spiders: sensory exploitation of the female's maternal care instinct or foraging motivation? Animal Behaviour 73:267–273.

Blackledge, T.A. 1998. Signal conflict in spider webs driven by predators and prey. Proceedings of the Royal Society B 265:1991–1996.

Blackledge, T.A. & J.W. Wenzel. 2000. The evolution of cryptic spider silk: a behavioral test. Behavioral Ecology 11:142–145.

Blamires, S.J., T.A. Blackledge & I.M. Tso. 2017. Physicochemical property variation in spider silk: Ecology, evolution, and synthetic production. Annual Review of Entomology 62:443–460.

Blanke, R. 1986. Homologien im fortpflanzungsverhalten von kreuzspinnen (Araneae, Araneidae) und deren interpretation im kontext von systematic und der existenz von artbarrieren. Pp. 69–94. *In* Proceedings of the 10th International Arachnological Congress. (J.A. Barrientos, ed.). Instituto Pirenaico de Ecología and Grupo de Araenología, Barcelona.

Bourne, J.D. 1978. Observations on the sexual behaviour of *Porrhomma egeria* Simon (Araneae: Linyphiidae). Bulletin of the British Arachnological Society 4:221–225.

Bradbury, J.W. & S.L. Vehrencamp. 2011. Principles of Animal Communication. Sinauer Associates, Sunderland, MA.

Breene, R. & M. Sweet. 1985. Evidence of insemination of multiple females by the male black widow spider, *Latrodectus mactans* (Araneae, Theridiidae). Journal of Arachnology 13:331–335.

Bristowe, W.S. 1926. XIII.—The mating habits of British thomisid and sparassid spiders. Journal of Natural History 18:114–131.

Bristowe, W.S. 1929. The mating habits of spiders, with special reference the problems surrounding sex dimorphism. Proceedings of the Zoological Society of London 1929:309–358.

Bristowe, W.S. 1931. The mating habits of spiders: a second supplement, with the description of a new thomisid from Krakatau. Proceedings of the Zoological Society of London 1931:1401–1412.

Bristowe, W.S. 1958. The World of Spiders. Collins, London, UK.

Bristowe, W.S. & G.H. Locket. 1926. The courtship of British lycosid spiders, and its probable significance. Proceedings of the Zoological Society of London 22:317–347.

Bruce, J. & J. Carico. 1988. Silk use during mating in *Pisaurina mira* (Walckenaer) (Araneae, Pisauridae). Journal of Arachnology 16:1–4.

Brum, P.E.D., L.E. Costa-Schmidt & A.M. de Araújo. 2012. It is a matter of taste: chemical signals mediate nuptial gift acceptance in a neotropical spider. Behavioral Ecology 23:442–447.

Bucher, R., H. Binz, F. Menzel, & M.H. Entling. 2014. Effects of spider chemotactile cues on arthropod behavior. Journal of Insect Behavior 27:567–580.

Bukowski, T.C., & T.E. Christenson. 2000. Determinants of mating frequency in the spiny orbweaving spider, *Micrathena gracilis* (Araneae: Araneidae). Journal of Insect Behavior 13:331–352.

Bukowski, T.C., C.D. Linn, & T.E. Christenson. 2001. Copulation and sperm release in *Gasteracantha cancriformis* (Araneae: Araneidae): differential male behaviour based on female mating history. Animal Behaviour 62:887–895.

Carballo, M., F. Baldenegro, F. Bollatti, A.V. Peretti & A. Aisenberg. 2017. No pain, no gain: male plasticity in burrow digging according to female rejection in a sand-dwelling wolf spider. Behavioural Processes 140:174–180.

Carico, J.E. 1993. Revision of the genus *Trechalea* Thorell (Araneae, Trechaleidae) with a review of the taxonomy of the Trechaleidae and Pisauridae of the western hemisphere. Journal of Arachnology 21:226–257.

Chinta, S.P., S. Goller, J. Lux, S. Funke, G. Uhl & S. Schulz. 2010. The sex pheromone of the wasp spider *Argiope bruennichi*. Angewandte Chemie International Edition 49:2033–2036.

Cobbold, S.M. & Y.C. Su. 2010. The host becomes dinner: possible use of *Cyclosa* as a nuptial gift by *Argyrodes* in a colonial web. Journal of Arachnology 38:132–134.

Correa-Garhwal, S.M., R.C. Shaw, T.H. Clarke III, N.A. Ayoub & C.Y. Hayashi. 2017. Silk gene expression of theridiid spiders: implications for male-specific silk use. Zoology 122:107–114.

Costa-Schmidt, L.E., J.E. Carico & A.M. de Araújo. 2008. Nuptial gifts and sexual behavior in two species of spider (Araneae, Trechaleidae, *Paratrechalea*). Naturwissenschaften 95:731–739.

Coyle, F.A. 1985. Observations on the mating behaviour of the tiny mygalomorph spider, *Microhexura montivaga* Crosby & Bishop (Araneae, Dipluridae). Bulletin of the British Arachnological Society 6:328–330.

Coyle, F.A. & T.C. O'Shields. 1990. Courtship and mating behavior of *Thelechoris karschi* (Araneae, Dipluridae), an African funnelweb spider. Journal of Arachnology 18:281–296.

Craig, C.L. 2003. Spiderwebs and Silk: Tracing Evolution from Molecules to Genes to Phenotypes. Oxford University Press, Oxford, UK.

Craig, C.L. & G.D. Bernard. 1990. Insect attraction to ultraviolet-reflecting spider webs and web decorations. Ecology 71:616–623.

Craig, C.L., R.S. Weber & G.D. Bernard. 1996. Evolution of predator-prey systems: spider foraging plasticity in response to the visual ecology of prey. American Naturalist 147:205–229.

Cross, F.R. 2016. Discrimination of draglines from potential mates by *Evarcha culicivora*, an East African jumping spider. New Zealand Journal of Zoology 43:84–95.

Cross, F.R. & R.R. Jackson. 2009. Mate-odour identification by both sexes of *Evarcha culicivora*, an East African jumping spider. Behavioural Processes 81:74–79.

Cross, F.R. & R.R. Jackson. 2013. The functioning of species-specific olfactory pheromones in the biology of a mosquito-eating jumping spider from East Africa. Journal of Insect Behavior. 26:131–148.

Dawkins, R. 1978. Replicator selection and the extended phenotype. Zeitschrift für Tierpsychologie 47:61–76.

Dawkins, M.S. & T. Guilford. 1991. The corruption of honest signalling. Animal Behaviour 41:865–873.

Domínguez, K. & M.L. Jiménez. 2005. Mating and self-burying behavior of *Homalonychus theologus* Chamberlin (Araneae, Homalonychidae) in Baja California sur. Journal of Arachnology 33:167–174.

Dondale, C.D. & B.M. Hegdekar. 1973. The contact sex pheromone of *Pardosa lapidicina* Emerton (Araneida: Lycosidae). Canadian Journal of Zoology 51:400–401.

Dondale, C.D., J.H. Redner, P. Paquin & H.W. Levi. 2003. Orb-Weaving Spiders of Canada and Alaska The Insects and Arachnids of Canada Series, Part 23: Araneae: Uloboridae, Tetragnathidae, Araneidae, Theridiosomatidae. NRC Research Press, Ottawa, ON, Canada.

Elgar, M.A. 1991. Sexual cannibalism, size dimorphism, and courtship behavior in orb-weaving spiders (Araneidae). Evolution 45:444–448.

Elgar, M.A. & D.R. Nash. 1988. Sexual cannibalism in the garden spider *Araneus diadematus*. Animal Behaviour 36:1511–1517.

Elgar, M.A., J.M. Schneider & M.E. Herberstein. 2000. Female control of paternity in the sexually cannibalistic spider *Argiope keyserlingi*. Proceedings of the Royal Society B 267:2439–2443.

Elias, D.O. & A.C. Mason. 2010. Signaling in variable environments: substrate-borne signaling mechanisms and communication behavior in spiders. Pp. 25–46. *In* The Use of Vibrations in Communication: Properties, Mechanisms and Function Across Taxa. (C.E. O'Connell-Rodwell, ed.). Research Signpost, Kerala, India.

Elias D.O., M.C.B. Andrade & M.M. Kasumovic. 2011. Dynamic population structure and the evolution of spider mating systems. Advances in Insect Physiology. 41:65–114.

Engelhardt, W. 1964. Die mitteleuropäischen arten der gattung

*Trochosa* CL Koch, 1848 (Araneae, Lycosidae). Morphologie, chemotaxonomie, biologie, autökologie. Zoomorphology 54:219–392.

Estrada, C., S. Schulz, S. Yildizhan & L.E. Gilbert. 2011. Sexual selection drives the evolution of antiaphrodisiac pheromones in butterflies. Evolution 65:2843–2854.

Ferretti, N.E. & A.A. Ferrero. 2008. Courtship and mating behavior of *Grammostola schulzei* (Schmidt 1994) (Araneae, Theraphosidae), a burrowing tarantula from Argentina. Journal of Arachnology 36:480–483.

Fischer, M.L., A. Čokl, E.N. Ramires, E. Marques-da-Silva, C. Delay, J.D. Fontana et al. 2009. Sound is involved in multimodal communication of *Loxosceles intermedia* Mello-Leitão, 1934 (Araneae; Sicariidae). Behavioural Processes 82:236–243.

Foelix, R.F. 2011. Biology of Spiders. Oxford University Press, Oxford, UK.

Forster, L. 1992. The stereotyped behavior of sexual cannibalism in *Latrodectus hasselti* Thorell (Araneae, Theridiidae), the Australian redback spider. Australian Journal of Zoololgy 40:1–11.

Forster, L. 1995. The behavioral ecology of *Latrodectus hasselti* (Thorell), the Australian redback spider (Araneae: Theridiidae): A review. Records of the Western Australia Museum Supplement 52:13–24.

Fromhage, L. & J.M. Schneider. 2004. Safer sex with feeding females: sexual conflict in a cannibalistic spider. Behavioral Ecology 16:377–382.

Galasso, A.B. 2012. Comparative analysis of courtship in *Agelenopsis* funnel-web spiders (Araneae, Agelenidae) with an emphasis on potential isolating mechanisms. PhD thesis. University of Tennessee, Knoxville.

Gaskett, A.C. 2007. Spider sex pheromones: emission, reception, structures, and functions. Biological Reviews 82:27–48.

Gerhardt, U. 1924. Weitere Studien über die Biologie der Spinnen. Archiv für Naturgeschichte 90:85–192.

Gerhardt, U. 1933. Neue untersuchungen zur sexualbiologie der spinnen, insbesondere an arten der mittelmeerländer und der tropen. Zeitschrift für Morphologie und Ökologie der Tiere 27:1–75.

Gering, R. 1953. Structure and function of the genitalia in some American agelenid spiders. Smithsonian Miscellaneous Collections 121:1–84.

Ghislandi, P.G., M.J. Albo, C. Tuni & T. Bilde. 2014. Evolution of deceit by worthless donations in a nuptial gift-giving spider. Current Zoology 60:43–51.

Ghislandi, P.G., M. Beyer, P. Velado & C. Tuni. 2017. Silk wrapping of nuptial gifts aids cheating behaviour in male spiders. Behavioral Ecology 28:744–749.

Gosline, J.M., P.A. Guerette, C.S. Ortlepp & K.N. Savage. 1999. The mechanical design of spider silks: from fibroin sequence to mechanical function. Journal of Experimental Biology 202:3295–3303.

Gregorič, M., K. Šuen, R.C. Cheng, S. Kralj-Fišer & M. Kuntner. 2016. Spider behaviors include oral sexual encounters. Scientific Reports 6:25128.

Gunnarsson, B., G. Uhl & K. Wallin. 2004. Variable female mating positions and offspring sex ratio in the spider *Pityohyphantes phrygianus* (Araneae: Linyphiidae). Journal of Insect Behavior 17:129–144.

Gwinner-Hanke, H. 1970. Zum Verhalten zweier stridulierender Spinnen *Steatoda bipunctata* Linné und *Teutana grossa* Koch (Theridiidae, Araneae), unter besonderer Berücksichtigung des Fortpflanzungsverhaltens. Ethology 27:649–678.

Gwynne, D.T. 2008. Sexual conflict over nuptial gifts in insects. Annual Review of Entomology 53:83–101.

Hajer, J. & D. Řeháková. 2011. Mating behavior of *Theridiosoma gemmosum* (Araneae: Theridiosomatidae): The unusual role of the male dragline silk. Archives of Biological Sciences 63:199–208.

Harari, A.R., M. Ziv & Y. Lubin. 2009. Conflict or cooperation in the courtship display of the white widow spider, *Latrodectus pallidus*. Journal of Arachnology 37:254–260.

Hauser, M.D. 1996. The Evolution of Communication. MIT Press, Cambridge, MA.

Havrilak, J.A., K.M. Shimmel, A.L. Rypstra & M.H. Persons. 2015. Are you paying attention? Female wolf spiders increase dragline silk advertisements when males do not court. Ethology 121:345–352.

Hayashi, C.Y., T.A. Blackledge & R.V. Lewis. 2004. Molecular and mechanical characterization of aciniform silk: uniformity of iterated sequence modules in a novel member of the spider silk fibroin gene family. Molecular Biology and Evolution 21:1950–1959.

Hebets, E.A. & R.F. Chapman. 2000. Electrophysiological studies of olfaction in the whip spider *Phrynus parvulus* (Arachnida, Amblypygi). Journal of Insect Physiology 46:1441–1448.

Henneken, J., J.Q. Goodger, T.M. Jones & M.A. Elgar. 2017a. The potential role of web-based putrescine as a prey-attracting allomone. Animal Behaviour 129:205–210.

Henneken, J., J.Q. Goodger, T.M. Jones & M.A. Elgar. 2017b. Variation in the web-based chemical cues of *Argiope keyserlingi*. Journal of Insect Physiology 101:15–21.

Henneken, J., T.M. Jones, J.Q. Goodger, D.A. Dias, A. Walter & M.A. Elgar. 2015. Diet influences female signal reliability for male mate choice. Animal Behaviour 108:215–221.

Herberstein, M.E., J.M. Schneider & M.A. Elgar. 2002. Costs of courtship and mating in a sexually cannibalistic orb-web spider: female mating strategies and their consequences for males. Behavioral Ecology and Sociobiology 51:440–446.

Herberstein, M.E., A.E. Wignall, E.A. Hebets & J.M. Schneider. 2014. Dangerous mating systems: signal complexity, signal content and neural capacity in spiders. Neuroscience & Biobehavioral Reviews 46:509–518.

Herms, W., S. Bailey & B. McIvor. 1935. The black widow spider. University of California Agricultural Experiment Station Bulletin 591:1:30.

Hibler, T.L. & A.E. Houde. 2006. The effect of visual obstructions on the sexual behaviour of guppies: the importance of privacy. Animal Behaviour 72:959–964.

Hsia, Y., E. Gnesa, R. Pacheco, K. Kohler, F. Jeffery & C. Vierra. 2012. Synthetic spider silk production on a laboratory scale. Journal of Visualized Experiments: JoVE 65:4191.

Hoefler, C.D. 2007. Male mate choice and size-assortative pairing in a jumping spider, *Phidippus clarus*. Animal Behaviour 73:943–954.

Huber, B.A. 2005. Sexual selection research on spiders: progress and biases. Biological Reviews 80:363–385.

Itakura, Y. 1993. The life history and nuptial feeding of a nursery web spider, *Pisaura lama*. Insectarium 30:88–93.

Itakura, Y. 1998. Discovery of nuptial feeding in the spider, *Perenethis fascigera* (Araneae: Pisauridae). Acta Arachnologica 47:173–175.

Jackson, R.R. 1979. Comparative studies of *Dictyna* and *Mallos* (Araneae, Dictynidae) II. The relationship between courtship, mating, aggression and cannibalism in species with differing types of social organization. Revue Arachnologique 2:103–132.

Jackson, R.R. & A.M. Macnab. 1989. Display, mating, and predatory behaviour of the jumping spider *Plexippus paykulli* (Araneae: Salticidae). New Zealand Journal of Zoology 16:151–168.

Jackson, R.R. & S.D. Pollard. 1990. Intraspecific interactions and the function of courtship in mygalomorph spiders: a study of *Porrhothele antipodiana* (Araneae: Hexathelidae) and a literature review. New Zealand Journal of Zoology 17:499–526.

Jackson, R.R. & B.A. Poulsen. 1990. Predatory versatility and

intraspecific interactions of *Supunna picta* (Araneae: Clubionidae). New Zealand Journal of Zoology 17:169–184.

Jennions, M.D. & M. Petrie. 1997. Variation in mate choice and mating preferences: a review of causes and consequences. Biological Reviews 72:283–327.

Jerhot, E., J.A. Stoltz, M.C.B. Andrade & S. Schulz. 2010. Acylated serine derivatives: a unique class of arthropod pheromones of the Australian redback spider, *Latrodectus hasselti*. Angewandte Chemie International Edition 49:2037–2040.

Johnson, J.C., P. Trubl, V. Blackmore & L. Miles. 2011. Male black widows court well-fed females more than starved females: silken cues indicate sexual cannibalism risk. Animal Behaviour 82:383–390.

Kaston, B.J. 1936. The senses involved in the courtship of some vagabond spiders. Entomologica Americana 16:97–159.

Kaston, B. 1970. Comparative biology of American black widow spiders. Transactions of the San Diego Society of Natural History 16:33–82.

Kasumovic, M.M. & M.C.B. Andrade. 2004. Discrimination of airborne pheromones by mate-searching male western black widow spiders (*Latrodectus hesperus*): species- and population-specific responses. Canadian Journal of Zoology 82:1027–1034.

Kasumovic, M.M. & M.C.B. Andrade. 2006. Male development tracks rapidly shifting sexual versus natural selection pressures. Current Biology 16:R242–R243

Khan, R. & M.H. Persons. 2015. Female *Pardosa milvina* wolf spiders increase silk advertisements when in the presence of silk from courting males. Journal of Arachnology 43:168–173.

Klein, A.L., M.C. Trillo, F.G. Costa & M.J. Albo. 2014. Nuptial gift size, mating duration and remating success in a Neotropical spider. Ethology Ecology & Evolution 26:29–39.

Kluge, J.A., O. Rabotyagova, G.G. Leisk & D.L. Kaplan. 2008. Spider silks and their applications. Trends in Biotechnology 26:244–251.

Knoflach, B. 2004. Diversity in the copulatory behaviour of comb-footed spiders (Araneae, Theridiidae). Denisia 12:161–256.

Knoflach, B., & A. van Harten. 2000. Palpal loss, single palp copulation and obligatory mate consumption in *Tidarren cuneolatum* (Tullgren, 1910)(Araneae, Theridiidae). Journal of Natural History 34:1639–1659.

Knoflach, B. & A. van Harten. 2002. The genus *Latrodectus* (Araneae: Theridiidae) from mainland Yemen, the Socotra Archipelago and adjacent countries. Fauna of Arabia 19:321–362.

Koeppel, A. & C. Holland. 2017. Progress and trends in artificial silk spinning: a systematic review. ACS Biomaterials Science and Engineering 3:226–237.

Koh, T.H., W.K. Seah, L.M.Y. Yap & D. Li. 2009. Pheromone-based female mate choice and its effect on reproductive investment in a spitting spider. Behavioral Ecology and Sociobiology 63:923–930.

Krafft, B. & L.J. Cookson. 2012. The role of silk in the behaviour and sociality of spiders. Psyche 2012:529564. Online at http://dx.doi.org/10.1155/2012/529564

Kralj-Fišer, S., K. Čandek, T. Lokovšek, T. Čelik, R.C. Cheng, M.A. Elgar et al. 2016. Mate choice and sexual size dimorphism, not personality, explain female aggression and sexual cannibalism in raft spiders. Animal Behaviour 111:49–55.

Kralj-Fišer, S., M. Gregorič, T. Lokovšek, T. Čelik & M. Kuntner. 2013. A glimpse into the sexual biology of the "zygiellid" spider genus *Leviellus*. Journal of Arachnology 41:387–391.

Kuntner, M., S. Kralj-Fišer, J.M. Schneider & D. Li. 2009. Mate plugging via genital mutilation in nephilid spiders: an evolutionary hypothesis. Journal of Zoology 277:257–266.

Laborda, A. & M. Simo. 2015. Description of the female of *Eutichurus ibiuna* Bonaldo, 1994 (Araneae: Eutichuridae) with notes on natural history and sexual behavior. Zootaxa 4021:591–596.

Lai, C.W., S. Zhang, D. Piorkowski, C.P. Liao & I.M. Tso. 2017. A trap and a lure: dual function of a nocturnal animal construction. Animal Behaviour 130:159–164.

Landolfa, M.A. & F.G. Barth. 1996. Vibrations in the orb web of the spider *Nephila clavipes*: cues for discrimination and orientation. Journal of Comparative Physiology A 179:493–508.

Lane, S.M., J.H. Solino, C. Mitchell, J.D. Blount, K. Okada, J. Hunt et al. 2015. Rival male chemical cues evoke changes in male pre- and post-copulatory investment in a flour beetle. Behavioral Ecology 26:1021–1029.

Lang, A. 1996. Silk investment in gifts by males of the nuptial feeding spider *Pisaura mirabilis* (Araneae: Pisauridae). Behaviour 133:697–716.

Lapinski, W. & M. Tschapka. 2009: Erstnachweis von Brautgeschenken bei *Trechalea* sp. (Trechaleidae, Araneae) in Costa Rica. Arachne 14:4–13.

Leonard, A.S. & D.H. Morse. 2006. Line-following preferences of male crab spiders, *Misumena vatia*. Animal Behaviour 71:717–724.

Lindstedt, C. & M. Mokkonen. 2014. The evolutionary strategy of deception. Current Zoology 60:1–5.

Lizotte, R. & J.S. Rovner. 1989. Water-resistant sex pheromones in lycosid spiders from a tropical wet forest. Journal of Arachnology 17:122–125.

Locket, G.H. 1926. Observations on the mating habits of some web-spinning spiders, with some corroborative notes by W.S. Bristowe. Proceedings of the Zoological Society of London 1926:1125–1146.

Locket, G.H. 1927. XII.—On the mating habits of some spiders in the family Theridiidae. Annals and Magazine of Natural History 20:91–99.

Lopez, A. 1987. Glandular aspects of sexual biology, Pp. 121–132. *In* Ecophysiology of Spiders. (W. Nentwig, ed.). Springer, Heidelberg, Germany.

Lubin, Y. D. 1986. Courtship and alternative mating tactics in a social spider. Journal of Arachnology 14:239–257.

MacLeod, E.C. 2013. New insights in the evolutionary maintenance of male mate choice behaviour using the western black widow, *Latrodectus hesperus*. PhD thesis, University of Toronto, Canada.

MacLeod, E.C. & M.C.B. Andrade. 2014. Strong, convergent male mate choice along two preference axes in field populations of black widow spiders. Animal Behaviour 89:163–169.

Mallis, R.E. & K.B. Miller. 2017. Natural history and courtship behavior in *Tengella perfuga* Dahl, 1901 (Araneae: Zoropsidae). Journal of Arachnology 45:166–176.

Masters, W.M. 1984. Vibrations in the orbwebs of *Nuctenea sclopetaria* (Araneidae). Behavioral Ecology and Sociobiology 15:207–215.

Masters, W.M. & H. Markl. 1981. Vibration signal transmission in spider orb webs. Science 213:363–365.

McClintock, W.J. & G.N. Dodson. 1999. Notes on *Cyclosa insulana* (Araneae, Araneidae) of Papua New Guinea. Journal of Arachnology 27:685–688.

McGhee, K.E., S. Feng, S. Leasure & A.M. Bell. 2015. A female's past experience with predators affects male courtship and the care her offspring will receive from their father. Proceedings of the Royal Society B 282:20151840.

Menda, G., P.S. Shamble, E.I. Nitzany, J.R. Golden & R.R. Hoy. 2014. Visual perception in the brain of a jumping spider. Current Biology 24:2580–2585.

Merrett, P. 1988. Notes on the biology of the neotropical pisaurid, *Ancylometes bogotensis* (Keyserling) (Araneae: Pisauridae). Bulletin of the British Arachnological Society 7:197–201.

Mortimer, B., S.D. Gordon, C. Holland, C.R. Siviour, F. Vollrath & J.F. Windmill. 2014. The speed of sound in silk: linking material performance to biological function. Advanced Materials 26:5179–5183.

Mortimer, B., C. Holland, J.F. Windmill & F. Vollrath. 2015.

Unpicking the signal thread of the sector web spider *Zygiella x-notata*. Journal of The Royal Society Interface 12:20150633.

Mortimer, B., A. Soler, C.R. Siviour, R. Zaera & F. Vollrath. 2016. Tuning the instrument: sonic properties in the spider's web. Journal of The Royal Society Interface 13:20160341.

Moskalik, B. & G.W. Uetz. 2011. Experience with chemotactile cues indicating female feeding history impacts male courtship investment in the wolf spider *Schizocosa ocreata*. Behavioral Ecology and Sociobiology 65:2175–2181.

Moura, R.R., J. Vasconcellos-Neto & M. de Oliveira Gonzaga. 2017. Extended male care in *Manogea porracea* (Araneae: Araneidae): the exceptional case of a spider with amphisexual care. Animal Behaviour 123:1–9.

Naftilan, S.A. 1999. Transmission of vibrations in funnel and sheet spider webs. International Journal of Biological Macromolecules 24:289–293.

Neff, B.D. & E.I. Svensson. 2013. Polyandry and alternative mating tactics. Philosophical Transactions of the Royal Society B 368:20120045.

Nelson, X.J., C.M. Warui & R.R. Jackson. 2012. Widespread reliance on olfactory sex and species identification by lyssomanine and spartaeine jumping spiders. Biological Journal of the Linnean Society 107:664–677.

Nitzsche, R.O.M. 1988. "Brautgeschenk" und umspinnen der beute bei *Pisaura mirabilis*, *Dolomedes fimbriatus* und *Thaumasia uncata* (Arachnida, Araneida, Pisauridae). Verhandlungen des Naturwissenschaftlichen Vereins Hamburg 20:353–393.

Nitzsche, R.O.M. 2011. Courtship, mating and agonistic behaviour in *Pisaura mirabilis* (Clerck, 1757). Arachnology 15:93–120.

Pandulli-Alonso, I., A. Quaglia & M.J. Albo. 2017. Females of a gift-giving spider do not trade sex for food gifts: a consequence of male deception? BMC Evolutionary Biology 17:112.

Papke, M.D., S.E. Riechert & S. Schulz. 2001. An airborne female pheromone associated with male attraction and courtship in a desert spider. Animal Behaviour 61:877–886.

Papke, M., S. Schulz, H. Tichy, E. Gingl & R. Ehn. 2000. Identification of a new sex pheromone from the silk dragline of the tropical wandering spider *Cupiennius salei*. Angewandte Chemie International Edition 39:4339–4341.

Parker, G.A. 1970. Sperm competition and its evolutionary consequences in the insects. Biological Reviews 45:525–567.

Parkhe, A.D., S.K. Seeley, K. Gardner, L. Thompson & R.V. Lewis. 1997. Structural studies of spider silk proteins in the fiber. Journal of Molecular Recognition 10:1–6.

Peakall, D.B. & P.N. Witt. 1976. The energy budget of an orb web-building spider. Comparative Biochemistry and Physiology Part A: Physiology 54:187–190.

Peaslee, J.E. & W.B. Peck. 1983. The biology of *Octonoba octonarius* (Muma) (Araneae: Uloboridae). Journal of Arachnology 11:51–67.

Persons, M.H. & A.L. Rypstra. 2001. Wolf spiders show graded antipredator behavior in the presence of chemical cues from different sized predators. Journal of Chemical Ecology 27:2493–2504.

Platnick, N. 1971. The evolution of courtship behaviour in spiders. Bulletin of the British Arachnological Society 2:40–47.

Prenter, J., R. Elwood & S. Colgan. 1994a. The influence of prey size and female reproductive state on the courtship of the autumn spider, *Metellina segmentata*: a field experiment. Animal Behaviour 47:449–456.

Prenter, J., R.W. Elwood & W.I. Montgomery. 1994b. Alternative mating behaviour in *Metellina segmentata* (Clerck). Newsletter of the British Arachnological Society 70:10–11.

Preston-Mafham, K.G. 1999. Notes on bridal veil construction in *Oxyopes schenkeli* Lessert, 1927 (Araneae: Oxyopidae) in Uganda. Bulletin of the British Arachnological Society 11:150–152.

Prestwich, K.N. 1977. The energetics of web-building in spiders. Comparative Biochemistry and Physiology Part A: Physiology 57:321–326.

Prokop, P. & M.R. Maxwell. 2009. Female feeding regime and polyandry in the nuptially feeding nursery web spider, *Pisaura mirabilis*. Naturwissenschaften 96:259–265.

Prokop, P. & M. Semelbauer. 2017. Biometrical and behavioural associations with offering nuptial gifts by males in the spider *Pisaura mirabilis*. Animal Behaviour 129:189–196.

Prouvost, O., M. Trabalon, M. Papke & S. Schulz. 1999. Contact sex signals on web and cuticle of *Tegenaria atrica* (Araneae, Agelenidae). Archives of Insect Biochemistry and Physiology 40:194–202.

Richman, D.B. & R.R Jackson. 1992. A review of the ethology of jumping spiders (Araneae, Salticidae). Bulletin of the British Arachnological Society 9:33–37.

Richter, C.J. & C. Van Der Kraan. 1970. Silk production in adult males of the wolf spider *Pardosa amentata* (CL.) (Araneae, Lycosidae). Netherlands Journal of Zoology 20:392–400.

Riechert, S.E. & F.D. Singer. 1995. Investigation of potential male mate choice in a monogamous spider. Animal Behaviour 49:715–723.

Rinaldi, I.M., & A.A. Stropa. 1998. Sexual behaviour in *Loxosceles gaucho* Gertsch (Araneae, Sicariidae). Bulletin of the British Arachnological Society 11:57–61.

Rising, A., M. Widhe & J. Johansson. 2011. Spider silk proteins: recent advances in recombinant production, structure–function relationships and biomedical applications. Cellular and Molecular Life Sciences 68:169–184.

Roberts, J.A. & G.W. Uetz. 2005. Information content of female chemical signals in the wolf spider, *Schizocosa ocreata*: male discrimination of reproductive state and receptivity. Animal Behaviour 70:217–223.

Robinson M.H. & Y.D. Lubin. 1979. Specialists and generalists: the ecology and behavior of some web-building spiders from Papua New Guinea. Pacific Insects 21:133–164.

Robinson, M.H. & B. Robinson. 1973: Ecology and behavior of the giant wood spider *Nephila maculata* (Fabricius) in New Guinea. Smithsonian Contributions to Zoology 149:1–176.

Robinson, M.H. & B. Robinson. 1980. Comparative studies of the courtship and mating behavior of tropical araneid spiders. Pacific Insects Monograph 36:1–218.

Roland, C. 1983. Chemical signals bound to the silk in spider communication (Arachnida, Araneae). Journal of Arachnology 11:309–314.

Roland, C. & J.S. Rovner. 1983. Chemical and vibratory communication in the aquatic pisaurid spider *Dolomedes triton*. Journal of Arachnology 11:77–85.

Ross, K. & R.L. Smith. 1979. Aspects of the courtship behavior of the black widow spider, *Latrodectus hesperus* (Araneae: Theridiidae), with evidence for the existence of a contact sex pheromone. Journal of Arachnology 7:69–77.

Rovner, J. 1968. Territoriality in the sheet-web spider *Linyphia triangularis* (Clerck) (Araneae, Linyphiidae). Zeitschrift für Tierpsychologie 25:232–242.

Rundus, A.S., R. Biemuller, K. DeLong, T. Fitzgerald & S. Nyandwi. 2015. Age-related plasticity in male mate choice decisions by *Schizocosa retrorsa* wolf spiders. Animal Behaviour 107:233–238.

Rypstra, A.L. & C.M. Buddle. 2013. Spider silk reduces insect herbivory. Biology Letters 9:20120948.

Rypstra, A.L., S.E. Walker & M.H. Persons. 2016. Cautious versus desperado males: predation risk affects courtship intensity but not female choice in a wolf spider. Behavioral Ecology 27:876–885.

Schmitt, A. 1992. Conjectures on the origins and functions of a bridal veil spun by the males of *Cupiennius coccineus* (Araneae, Ctenidae). Journal of Arachnology 20:67–68.

Schneider, J.M. & M.C.B. Andrade. 2011. Mating behaviour and

sexual selection. Pp. 215–274. *In* Spider Behaviour: Flexibility and Versatility. (M.E. Herberstein, ed.). Cambridge University Press, Cambridge, UK.

Schneider, J.M. & Y. Lubin. 1998. Intersexual conflict in spiders. Oikos 83:496–506.

Schneider, J.M., C. Lucass, W. Brandler & L. Fromhage. 2011. Spider males adjust mate choice but not sperm allocation to cues of a rival. Ethology 117:970–978.

Schulz, S. 2013. Spider pheromones—a structural perspective. Journal of Chemical Ecology 39:1–14.

Schulz, S. & S. Toft. 1993. Identification of a sex pheromone from a spider. Science 260:1635–1637.

Scott, C., C. Gerak, S. McCann & G. Gries. 2017. The role of silk in courtship and chemical communication of the false widow spider, *Steatoda grossa* (Araneae: Theridiidae). Journal of Ethology, available online at https://link.springer.com/article/10.1007/s10164-017-0539-3

Scott, C., D. Kirk, S. McCann & G. Gries. 2015b. Web reduction by courting male black widows renders pheromone-emitting females' webs less attractive to rival males. Animal Behaviour 107:71–78.

Scott, C., S., McCann, R., Gries, G., Khaskin & G. Gries, 2015a. *N*-3-Methylbutanoyl-*O*-methylpropanoyl-*L*-serine methyl ester pheromone component of western black widow females. Journal of Chemical Ecology 41:465–472.

Scott, C., S. Vibert & G. Gries. 2012. Evidence that web reduction by western black widow males functions in sexual communication. Canadian Entomologist 144:672–678.

Scott, J.L., A.Y. Kawahara, J.H. Skevington, S.H. Yen, A. Sami, M.L. Smith & J.E. Yack. 2010. The evolutionary origins of ritualized acoustic signals in caterpillars. Nature Communications 1:1–9.

Searcy, L.E., A.L. Rypstra & M.H. Persons. 1999. Airborne chemical communication in the wolf spider *Pardosa milvina*. Journal of Chemical Ecology 25:2527–2533.

Segoli, M., R. Arieli, P. Sierwald, A.R. Harari & Y. Lubin. 2008. Sexual cannibalism in the brown widow spider (*Latrodectus geometricus*). Ethology 114:279–286.

Shulov, A. 1940. On the biology of two *Latrodectus* species in Palestine. Proceedings of the Linnean Society of London 152:309–328.

Sierwald, P. 1988. Notes on the behavior of *Thalassius spinosissimus* (Arachnida: Araneae: Pisauridae). Psyche 95:243–252.

Silva, E.L.C. 2005. New data on the distribution of *Trechalea cezariana* Mello-Leitão, 1931 in Southern Brazil. Acta Biologica Leopoldensia 27:127–128.

Silva, E.L.C. & A.A. Lise. 2009. New record of nuptial gift observed in *Trechalea amazonica* (Araneae, Lycosoidea, Trechaleidae). Revista Peruana de Biología 16:119–120.

Singer, F., S.E. Riechert, H. Xu, A.W. Morris, E. Becker, J.A. Hale et al. 2000. Analysis of courtship success in the funnel-web spider *Agelenopsis aperta*. Behaviour 137:93–117.

Smithers, R.H.N. 1944. Contribution to our knowledge of the genus *Latrodectus* (Araneae) in South Africa. Annals of the South African Museum 36:263–312.

Snow, L.S. & M.C.B. Andrade. 2004. Pattern of sperm transfer in redback spiders: implications for sperm competition and male sacrifice. Behavioral Ecology 15:785–792.

Stålhandske, S. 2002. Nuptial gifts of male spiders function as sensory traps. Proceedings of the Royal Society of London B 269:905–908.

Stålhandske, P. & B. Gunnarsson. 1996. Courtship behaviour in the spider *Pityohyphantes phrygianus* (Linyphiidae Araneae): do females discriminate injured males? Pp. 617–625. *In* Revue Suisse de Zoologie Proceedings of the XIIIth Congress of Arachnology.

Starr, C.K. 1988. Sexual behaviour in *Dictyna volucripes* (Araneae, Dictynidae). Journal of Arachnology 16:321–330.

Stoltz, J.A. & M.C.B. Andrade. 2009. Female's courtship threshold allows intruding males to mate with reduced effort. Proceedings of the Royal Society B 277:585–592.

Stowe, M. K. 1978. Observations of two nocturnal orbweavers that build specialized webs: *Scoloderus cordatus* and *Wixia ectypa* (Araneae: Araneidae). Journal of Arachnology 6:141–146.

Struble, D.L. & H. Arn. 1984. Combined gas chromatography and electroantennogram recording of insect olfactory responses. Pp. 161–178. *In* Techniques in Pheromone Research. (H.E. Hummel & T.A. Miller, eds.). Springer, New York, NY.

Suter, R.B. & A.J. Hirscheimer. 1986. Multiple web-borne pheromones in a spider *Frontinella pyramitela* (Araneae: Linyphiidae). Animal Behaviour 34:748–753.

Suter, R.B. & G. Renkes. 1982. Linyphid spider courtship: releaser and attractant functions of a contact sex pheromone. Animal Behaviour 30:714–718.

Suter, R.B. & G. Renkes. 1984. The courtship of *Frontinella pyramitela* (Araneae, Linyphiidae): patterns, vibrations and functions. Journal of Arachnology 12:37–54.

Suter, R.B., C.M. Shane & A.J. Hirscheimer. 1987. Communication by cuticular pheromones in a linyphiid spider. Journal of Arachnology 15:157–162.

Sytshevskaja, V.J. 1928. Fauna of spiders in the environs of the biological station at Bolshevo. Bulletin of the Bolshevo Biological Station 2:57–58.

Taylor, P.W. 1998. Dragline-mediated mate-searching in *Trite planiceps* (Araneae, Salticidae). Journal of Arachnology 26:330–334.

Thomas, M. 1930. L'instinct chez les araignées: L'accouplement de *Xysticus pini* Hahn. Bulletin & Annales de la Société Entomologique de Belgique 70:183–187.

Tichy, H., E. Gingl, R. Ehn, M. Papke & S. Schulz. 2001. Female sex pheromone of a wandering spider (*Cupiennius salei*): identification and sensory reception. Journal of Comparative Physiology A 187:75–78.

Tietjen, W.J. 1977. Dragline-following by male lycosid spiders. Psyche 84:165–178.

Tietjen, W.J. 1978. Tests for olfactory communication in four species of wolf spiders (Araneae, Lycosidae). Journal of Arachnology 6:197–206.

Trabalon, M. 2013. Chemical communication and contact cuticular compounds in spiders. Pp. 125–140. *In* Spider Ecophysiology. (W. Nentwig, ed.) Springer, Heidelberg.

Toft, S. & M.J. Albo 2015. Optimal numbers of matings: the conditional balance between benefits and costs of mating for females of a nuptial gift-giving spider. Journal of Evolutionary Biology 28:457–467.

Toft, S. & M.J. Albo 2016. The shield effect: nuptial gifts protect males against pre-copulatory sexual cannibalism. Biology Letters 12:20151082.

Trillo, M.C. 2016. Comportamiento sexual y deposición de velo nupcial en la araña errante *Ctenus longipes* (Ctenidae). Unpublished thesis. Universidad de la República Uruguay.

Trillo, M.C., V. Melo-González & M.J. Albo 2014. Silk wrapping of nuptial gifts as visual signal for female attraction in a crepuscular spider. Naturwissenschaften 101:123–130.

Uetz, G.W., A. McCrate & C.S. Hieber. 2010. Stealing for love? Apparent nuptial gift behavior in a kleptoparasitic spider. Journal of Arachnology 38:128–131.

Uhl, G. 2013. Spider olfaction: attracting, detecting, luring and avoiding. Pp. 141–157. *In* Spider Ecophysiology (W. Nentwig, ed.) Springer, Heidelberg.

Uhl, G. & D.O. Elias. 2011. Communication. Pp. 127–189. *In* Spider Behaviour: Flexibility and Versatility. (M.E. Herberstein, ed.). Cambridge University Press, Cambridge, UK.

Vahed, K. 1998. The function of nuptial feeding in insects: a review of empirical studies. Biological Reviews 73:44–78.

Vahed, K. 2007. All that glisters is not gold: Sensory bias, sexual conflict and nuptial feeding in insects and spiders. Ethology 113:105–127.

Van Helsdingen, P.J. 1965. Sexual behaviour of *Lepthyphantes leprosus* (Ohlert) (Araneida, Linyphiidae) with notes on the function of the genital organs. Zoologische Mededelingen 41:15–44.

Vibert, S., C. Scott & G. Gries. 2014. A meal or a male: the 'whispers' of black widow males do not trigger a predatory response in females. Frontiers in Zoology 11:4.

Vibert, S., C. Scott & G. Gries. 2016. Vibration transmission through sheet webs of hobo spiders (*Eratigena agrestis*) and tangle webs of western black widow spiders (*Latrodectus hesperus*). Journal of Comparative Physiology A 202:749–758.

Vollrath, F. 1979. Vibrations: their signal function for a spider kleptoparasite. Science 205:1149–1151.

Vollrath, F. & D.P. Knight. 2001. Liquid crystalline spinning of spider silk. Nature 410:541–548.

Watanabe, T. 2000. Web tuning of an orb-web spider, *Octonoba sybotides*, regulates prey-catching behaviour. Proceedings of the Royal Society B 267:565–569.

Watson, P.J. 1986. Transmission of a female sex pheromone thwarted by males in the spider *Linyphia litigiosa* (Linyphiidae). Science 233:219–221.

Watson, P.J. 1991. Multiple paternity and first mate sperm precedence in the sierra dome spider, *Linyphia litigiosa* Keyserling (Linyphiidae). Animal Behaviour 41:135–148.

Watson, P.J. & J.R. Lighton. 1994. Sexual selection and the energetics of copulatory courtship in the Sierra dome spider, *Linyphia litigiosa*. Animal Behaviour 48:615–626.

Weldingh, D.L., S. Toft & O.N. Larsen. 2011. Mating duration and sperm precedence in the spider *Linyphia triangularis*. Journal of Ethology 29:143–152.

Wheeler, W.C., J.A. Coddington, L.M. Crowley, D. Dimitrov, P.A. Goloboff, C.E. Griswold et al. 2016. The spider tree of life: phylogeny of Araneae based on target-gene analyses from an extensive taxon sampling. Cladistics 2016:1–43.

Whitehouse, M. & R.R. Jackson. 1994. Intraspecific interactions of *Argyrodes antipodiana*, a kleptoparasitic spider from New Zealand. New Zealand Journal of Zoology 21:243–168.

Wignall, A.E. & M.E. Herberstein. 2013a. The influence of vibratory courtship on female mating behaviour in orb-web spiders (*Argiope keyserlingi*, Karsch 1878). PLoS ONE 8:e53057.

Wignall, A.E. & M.E. Herberstein. 2013b. Male courtship vibrations delay predatory behaviour in female spiders. Scientific Reports 3:3557.

Wignall, A.E., D.J. Kemp & M.E. Herberstein. 2014. Extreme short-term repeatability of male courtship performance in a tropical orb-web spider. Behavioral Ecology 25:1083–1088.

Willey Robertson, M. & P.H. Adler. 1994. Mating behavior of *Florinda coccinea* (Hentz) (Araneae: Linyphiidae). Journal of Insect Behavior 7:313–326.

Witt, P.N. & J.S. Rovner. 1982. Spider Communication: Mechanisms and Ecological Significance. Princeton University Press, Princeton, NJ.

Wolff, J.O., M. Řczáč, T. Krejčí & S.N. Gorb. 2017. Hunting with sticky tape: functional shift in silk glands of araneophagous ground spiders (Gnaphosidae). Journal of Experimental Biology 220:2250–2259.

Wolfner, M.F. 2002. The gifts that keep on giving: physiological functions and evolutionary dynamics of male seminal proteins in *Drosophila*. Heredity 88:85–93.

Wyatt, T. 2014. Pheromones and Animal Behavior, 2nd ed. Cambridge University Press, Cambridge, UK.

Xiao, Y., J. Zhang & S. Li. 2009. A two-component female-produced pheromone of the spider *Pholcus beijingensis*. Journal of Chemical Ecology 35:769–778.

Xiao, Y.H., J.X. Zhang & S.Q. Li. 2010. Male-specific (*Z*)-9-tricosene stimulates female mating behaviour in the spider *Pholcus beijingensis*. Proceedings of the Royal Society B 277:3009–3018.

Yáñez, M., A. Locht & R. Macías-Ordóñez. 1999. Courtship and mating behavior of *Brachypelma klaasi* (Araneae, Theraphosidae). Journal of Arachnology 27:165–170.

York, J.R. & T.A. Baird. 2017. Sexual selection on male collared lizard (*Crotaphytus collaris*) display behaviour enhances offspring survivorship. Biological Journal of the Linnean Society 122:176–183.

Zhang, S., M. Kuntner & D. Li. 2011. Mate binding: male adaptation to sexual conflict in the golden orb-web spider (Nephilidae: *Nephila pilipes*). Animal Behaviour 82:1299–1304.

*Manuscript received 31 October 2017, revised 23 March 2018.*

2018. Journal of Arachnology 46:207 213

# Sexual dimorphism in the spinning apparatus of *Allocosa senex* (Araneae: Lycosidae), a wolf spider with a reversal in typical sex roles

**Andrea Albín**[1,2], **Anita Aisenberg**[1], **Miguel Simó**[2] and **Petr Dolejš**[3]: [1]Laboratorio de Etología, Ecología y Evolución, Instituto de Investigaciones Biológicas Clemente Estable, Avenida Italia 3318, PC 11600, Montevideo, Uruguay. E-mail: andrea.r.albin@gmail.com; [2]Sección Entomología, Facultad de Ciencias, Universidad de la República, Iguá 4225 PC 11400, Montevideo, Uruguay; [3]Department of Zoology, National Museum-Natural History Museum, Praha 9-Horní Počernice CZ-19300, Czech Republic

**Abstract.** *Allocosa senex* (Mello-Leitão, 1945) is a sex role-reversed wolf spider that inhabits sandy water-margin environments of southern South America. Males are larger than females and dig deeper burrows. Females are the courting sex and they prefer to mate with males that build deep burrows, suggesting high selective pressures on male digging behavior. Our aim was to investigate the external morphology and histological constitution of the spinning apparatus of males, females and juveniles of *A. senex*. Our results showed that *A. senex* adult males possess more piriform glands and spigots than adult females and juveniles. These glands produce silk for attachment discs that are crucial for the stability of the burrows. The differences according to the sex could be related to females' and males' digging strategies and strong selection on male burrow length in this species.

**Keywords:** spinnerets, spigots, spinning glands, digging behavior

One of the synapomorphies of spiders is the presence of silk glands situated in the ventral part of opisthosoma (Marples 1967). The glands are connected to the outside through thin tubes called the spigots, which are located on the spinnerets (Foelix 2011). The spider spinnerets are thought to arise evolutionarily from biramous opisthosomal appendages, similar to those reported for other arthropods (Shultz 1987). The order Araneae is represented by three clades, Mesothelae, Mygalomorphae, and Araneomorphae (Wheeler et al. 2017). These groups present structural differences in the spinning apparatus (e.g., Glatz 1972, 1973; Haupt & Kovoor 1993; Hajer et al. 2017). The spinnerets in the mesothelids are located at the middle of the opisthosoma, whereas in most mygalomorphs and araneomorphs they are located at the posterior end of the opisthosoma (Marples 1967). The number of spinnerets varies in different groups. The mesothelids present four pairs of spinnerets: anterior median (AMS), anterior lateral (ALS), posterior median (PMS), and posterior lateral (PLS), representing the ancestral state in spiders (Haupt & Kovoor 1993). The araneomorphs, however, possess only three pairs of spinnerets: ALS, PMS and PLS (e.g., Foelix 2011).

In spite of the ecological and evolutionary importance of silk production in spiders, the spinning apparatus has been well studied only in a few taxa, such as orb web spiders and their relatives (Araneoidea) (Kovoor 1977). There are only few studies regarding the spinning apparatus in wolf spiders (Richter 1970; Townley & Tillinghast 2003; Dolejš et al. 2014), which belong to the araneomorph family Lycosidae. Wolf spiders have four types of silk glands: piriform, ampullate, aciniform and tubuliform (Richter 1970). The piriform glands are connected to the ALS and produce attachment discs. Based on histochemical differences, the ampullate glands can be divided into the major ampullate glands (MA) and minor ampullate glands (mA) (Kovoor 1987; Kovoor & Peters 1988). The ducts of the MA glands are connected to spigots located on the ALS, while the ducts of the mA glands are connected to spigots on the PMS. The function of both types of ampullate glands is to produce draglines (silk threads that some spiders release while walking) and attach the egg sac to the spinnerets, as is typical in wolf spiders (Townley & Tillinghast 2003). On the other hand, the aciniform glands are connected to the PMS and PLS (Richter 1970), and one of their possible functions is to produce a scaffold that secures the spider when molting (Dolejš et al. 2014). The tubuliform glands are connected to the PMS and PLS and occur only in adult females; their function is to produce the fibers that constitute egg sacs (Richter 1970; Foelix 2011).

Both types of ampullate glands (MA and mA) can be divided into the primary (1°A) and secondary (2°A) glands (Townley et al. 1993). During the inter-ecdysial period, the ampullate glands that produce the draglines are the primary ampullate glands (1°MA and 1°mA). The primary spigots are not functional during ecdysis and molt *in situ*. The ampullate glands that produce draglines during proecdysis (beginning of molting), are the secondary ampullate glands (2°MA and 2°mA) (Townley et al. 1993). There are two secondary ampullate glands associated with each ALS (two 2°MA) and PMS (two 2°mA), but only one of each pair is functional at a given instar. The other pair of ampullate secondary glands (both 2°MA and 2°mA) is not functional at a given instar, but was functional during the preceding proecdysis. When nonfunctional, these glands are not represented externally by spigots, but only by post-functional tartipores: cuticle openings that allow the glands' ducts to remain connected to spigots on the old exoskeleton during the preceding proecdysis. As a consequence, the two secondary ampullate glands associated with one spinneret take turns functioning from instar to instar (Townley et al. 1993). After the final molt of lycosid males, one of the 2°A spigots turns into a nonfunctional structure called the nubbin (Townley & Tillinghast 2003). Tartipores are associated not only with the secondary ampullate glands but also with piriform and aciniform glands. Tubuliform glands are found only in adult

females, therefore are never tartipore-accommodated (e.g., Dolejš et al. 2014).

*Allocosa senex* (Mello-Leitão, 1945) is a wolf spider that inhabits the sandy coastal areas of northeastern Argentina, southern Brazil and Uruguay (Simó et al. 2017). This species was originally described as *Glieschiella senex* Mello-Leitão, 1945, later it was considered a junior synonym of *Allocosa brasiliensis* (Petrunkevitch, 1910) (Capocasale 2001), and has been recently revalidated (Simó et al. 2017). Individuals construct burrows where they stay during the day, becoming active during the summer nights (Aisenberg 2014). This species is characterized by a reversal in typical sex roles and expected sexual size dimorphism in spiders (Aisenberg et al. 2007, 2011; Aisenberg 2014). Males are larger than females and dig deep tubular burrows, while females construct superficial silk capsules (Aisenberg et al. 2007). Females of *A. senex* prefer to mate with males that present longer burrows (Aisenberg et al. 2007). Copulation occurs within the male burrow; after mating, the males exit and the females remain inside. The male burrows are mating refuges but also breeding nests because the females will lay their egg sac there and will not leave before spiderling dispersal (Aisenberg 2014).

According to previous observations on this species, individuals show longer ALS (anterior lateral spinnerets) compared to other burrowing wolf spider species (Simó et al. 2017). This could be an adaptation for digging in the sand and releasing large quantities of silk. The construction of male burrows in this species begins with the extraction of the sand using chelicerae, pedipalps and occasionally tibiae, metatarsi and tarsi of the first pair of legs (Aisenberg & Peretti 2011). Males combine the extraction of sand with the deposition of multiple layers of silk on the walls and around the entrance of the burrow (Aisenberg & Peretti 2011). The deposition of multiple layers of silk during burrow construction has been described also for other wolf spiders (Gwynne & Watkiss 1975; Henschel 1990) and is probably necessary to maintain a stable burrow in the sandy habitat where *A. senex* is found. Taking into account that males of *A. senex* need to construct long burrows and that this trait is selected under female choice, we could expect differences in spigot morphology according to the sex in this species. Thus, our aim was to investigate the external morphology and histological constitution of the spinning apparatus of males, females and juveniles of *A. senex*, with focus on the sexual strategies in this species.

## METHODS

We collected 22 individuals of *Allocosa senex* (7 adult males, 8 adult females, 2 subadult males, 2 subadult females and 3 juveniles) in November 2016 at the coastal area of San José de Carrasco, Canelones, Uruguay (34°51′06.06" S, 55°58′46.71" W). Spiders were captured by hand during the night using headlamps. We housed each individual in Petri dishes 9.5 cm in diameter and 1.5 cm tall, with sand as substrate and cotton soaked in water, under controlled conditions of temperature and humidity. We fed the spiders three times a week with *Tenebrio molitor* larvae (Coleoptera; Tenebrionidae). When individuals molted, we preserved the shed exuviae dry in an Eppendorf tube with their corresponding identification. We deposited voucher specimens in the National Museum, Prague (Czech Republic) under the inventory number P6d-2/2017.

The methodology follows Dolejš et al. (2014). We examined the spinning glands of males, females, and juveniles histologically (light microscopy), and the exterior of their spinnerets through scanning electron microscopy (SEM). For both types of microscopy spiders were fixed in modified Bouin-Dubosque-Brasil fluid (Smrž 1989) for 5 days, rinsed in 80% ethanol that was changed every 12 hours for 5 days, and stored in propanol until further processing. For histological evaluation, the specimens were embedded in Paraplast Plus (Fluka) and sectioned by sledge microtome (Reichert-Jung 407) at 7 µm. We stained sections in two triple-stains: Masson-Goldner's (Masson 1929; Foot 1933; Goldner 1938) and Gomori's (Gomori 1950) trichrome to discriminate between the gland types based on their color, to observe their position in the spider's opisthosoma and to detect carboxyl groups by hematoxylin present in both triple-stains. We also applied the ferric ferricyanide reaction – FFR (Adams 1956) to test for reducing groups of secreted proteins. We inspected the preparations under a light microscope (Olympus BX50) and photographed selected sections using a 3CCD color video camera (Olympus DP70).

For SEM examination, we transferred fixed specimens into acetone, air-dried, and inspected them using a scanning electron microscope (HITACHI S-3700N). Terminology of silk glands, spigots, tartipores, and nubbins follows Townley & Tillinghast (2003). We obtained additional images of juvenile spinning apparatus from exuviae. The exuviae were treated in a glycine SDS buffer (Novex, Invitrogen) for two weeks. Subsequently, we detached distal parts of the opisthosomal exuviae containing spinneret cuticle. Each spinneret was re-expanded by using watchmaker pincers to pull the spinneret down onto the pointed end of an appropriately sized pin embedded in and protruding from dark wax in a Petri dish (Townley & Tillinghast 2009). The cuticles of re-expanded spinnerets were rinsed in distilled water, dehydrated through an ascending ethanol series to propanol, and prepared for SEM examination as described above. We identified the spigots generally according to the spinnerets on which they appeared, and based on their shape, size and number. To distinguish between the aciniform and tubuliform spigots that are similar and present on the same spinnerets of adult females, we compared the spinning fields of adult females, subadult females and adult males.

## RESULTS

The silk glands in *Allocosa senex* opened in three pairs of spinnerets (Fig. 1A) through four types of spigots. Anterior lateral spinnerets (ALS) were the largest, notably prolonged spinnerets (Fig. 1A). We observed the spigots corresponding to the major ampullate glands, 1°MA and 2°MA in juveniles, females and subadult males. The bases of both types of MA spigots were relatively small (Fig. 1B) and difficult to locate at the spinning field. However, the base of the 2°MA spigot is larger than that of the 1°MA spigot. Beside the spigots, the spinning field was densely covered by setae. The presence of the 2°MA tartipore was recorded. The 2°MA glands and tartipores persisted in adult females. In adult males, however, only 1°MA spigot was present and the nubbin appeared

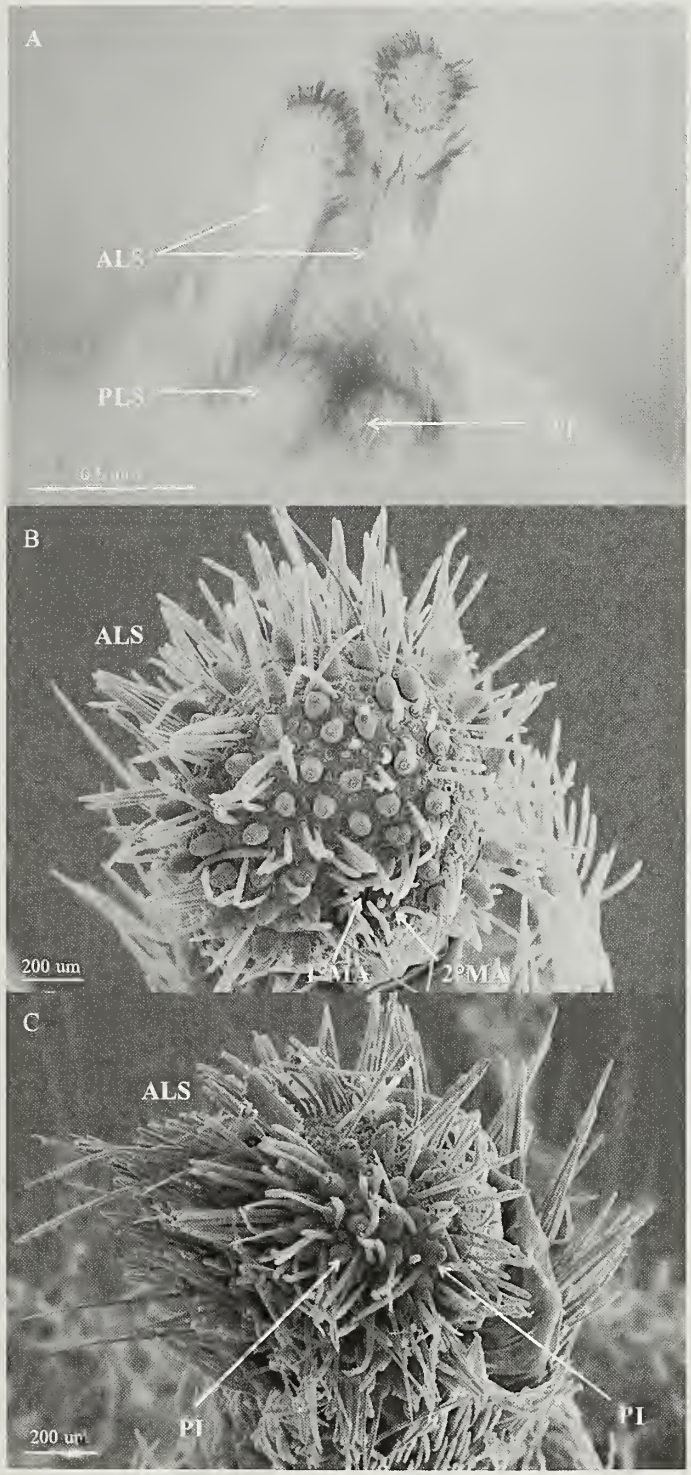


Figure 1.—*Allocosa senex*: A. Spinnerets, note extremely prolonged anterior lateral spinnerets. B. Anterior lateral spinneret of a female, with relatively small major ampullate spigots. C. Anterior lateral spinneret of a male, with higher number of piriform spigots; 1°MA = primary major ampullate spigot, 2°MA = secondary major ampullate spigot, ALS = anterior lateral spinnerets, AT = anal tubercle, PI = piriform spigots, PLS = posterior lateral spinnerets.

instead of the 2°MA spigot. We counted the spigots belonging to the piriform glands (Table 1). Adult males possessed a greater number of piriform glands (Fig. 1C), compared to juveniles and adult females (Table 1). Histologically, the piriform glands appeared as oval or bean-shape structures with a clearly bipartite epithelium (Fig. 2A, B). The proximal part stained dark purple via hematoxylin, revealing carboxyl groups present in the secretory cells. The basophilic distal part of the gland stained grey or greenish. The FFR revealed reducing groups of medium intensity present in the proximal part, as well as in the lumen of the gland. The piriform glands were located not only at the ventral area of the spinning apparatus, but also on the dorsal area, together with the aciniform glands (Fig. 2A). Relative diameter of piriform glands was larger than that of aciniform glands, being apparent already in subadult males (Fig. 2B).

Posterior middle spinnerets (PMS) were short and extremely reduced. In juveniles, females and subadult males of *A. senex*, we observed the spigots corresponding to the minor ampullate glands: 1°mA and 2°mA, and the 2°mA tartipore. The bases of both types of mA spigots were relatively large; the base of the 2°mA spigot was larger than that of the 1°mA (Fig. 3A). Intensive dark blue color of the FFR revealed that silk present in the ampullate glands (both MA and mA) consisted of proteins containing strong reducing groups (Fig. 2C) enabling clear identification of the ampullate glands in the histological slides (cf. Fig. 2D). In adult males, the 2°mA glands were reduced, and the nubbin could also be observed (Fig. 3B). The number of spigots corresponding to the aciniform and tubuliform (the latter only in adult females) glands was relatively low compared to other wolf spider species (Table 1; Dolejš et al. 2014). The aciniform glands appeared histologically as small roundish structures with a bipartite epithelium situated at the dorsal area of the spinning apparatus, close to the PMS, PLS and the anal tubercle. The proximal area stained darker red than the distal area, differing in a degree of acidity. The lumen stained pinkish orange (Fig. 2A, B) and the result of the FFR was negative. The tubuliform spigots appeared at the periphery of the spinning field and their shafts were thicker than those of the aciniform spigots (Fig. 3A).

At the posterior lateral spinnerets (PLS), we observed the spigots corresponding to aciniform and tubuliform glands (the latter in adult females only). In adult females, aciniform and tubuliform spigots could not be accurately discriminated due to its poor visualization and/or breakage of the shafts (Table 1). Beside the spigots, the spinning field was covered densely by setae (Fig. 3C). Histologically, however, the tubuliform glands were easily distinguishable as a cluster of glands with a thin epithelium, filled with a green substance. These glands were situated ventral to the ovaries.

## DISCUSSION

We found differences in the spinning apparatus, namely in number of piriform glands, between males and females of *A. senex*. The spinning apparatus of *A. senex* differs in comparison to other wolf spider species regarding the size of ALS, PMS and number of spigots occurring on those spinnerets (Dolejš et al. 2014). Based on our results, *A. senex* adult males possess more piriform glands and spigots than

Table 1.—Number of spigots per each spinneret of *Allocosa senex*; ac, aciniform spigot; pi, piriform spigot; tu, tubuliform spigot. The juveniles examined were on their 5th to 9th instar.

| Spinnerets | Juvenile (n = 8) | Sub-adult ♂ (n = 4) | Adult ♂ (n = 8) | Sub-adult ♀ (n = 4) | Adult ♀ (n = 4) |
|---|---|---|---|---|---|
| ALS | 21–45 pi | 36–38 pi | 64–86 pi | 43–50 pi | 49–52 pi |
| PMS | 5–9 ac | 7–9 ac | 5–9 ac | 13–14 ac | 7–9 ac, 11–12 tu |
| PLS | 20–27 ac | 22–27 ac | 23–28 ac | 31–46 ac | 33–47 ac+tu |

adult females. Probably the higher quantity of piriform glands in males compared to females of *A. senex* is closely related to the construction of the burrow, i.e., the need for deposition of several silk layers and the function of these glands (producing attachment discs). This result is contrary to that reported by Dolejš et al. (2014) for four species of lycosids from Europe with traditional sex roles, in which adult females had a greater number of piriform glands. In their study, one of the species, *Tricca lutetiana* (Simon, 1876), is a burrowing wolf spider also possessing large piriform glands (Dolejš et al. 2014), which, however, present a smaller number of piriform, aciniform and tubuliform glands compared to *A. senex*. One of the probable reasons why *T. lutetiana* has a smaller number of piriform glands could be that its burrow is not covered with silk (Dolejš et al. 2008, 2014). Likewise, possibly the increase in the number of piriform glands in the adult males of *A. senex* could be determined by its habitat: sandy substrate instead of soil as it occurs in *T. lutetiana* typical habitat (Dolejš et al. 2008). Also, the spider's life history can increase the number of piriform glands as it was observed in gnaphosids that use piriform silk for prey capture (Wolff et al. 2017). In general, the number of glands increases from sub-adult to adult wolf spider stages (Dolejš et al. 2014), but in *A. senex*, we did not find differences in the number of spigots between subadult and adult spiders (with the exception of newly formed tubuliform glands in adult females and increased number of piriform glands in adult males).

Standard histochemical characteristics (e.g., Kovoor & Peters 1988; Haupt & Kovoor 1993) of all four types of silk glands observed in *A. senex* resemble those of other wolf spiders (Richter 1970; Dolejš et al. 2014 and references therein). A region containing carboxyl groups seems to be

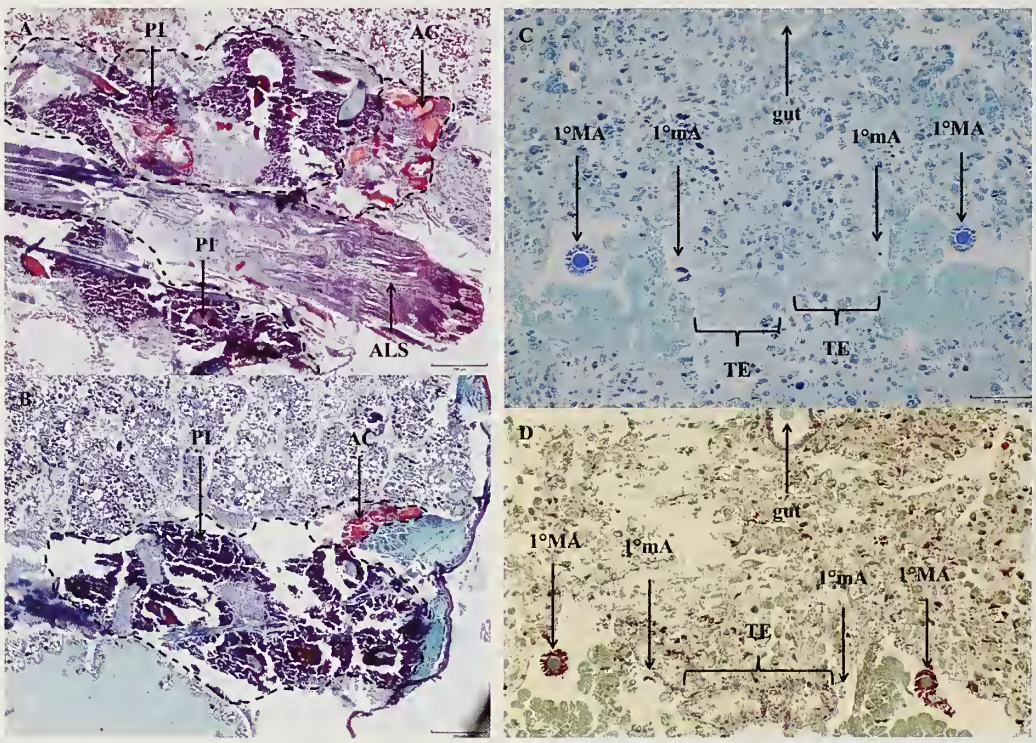


Figure 2.—Spinning glands of *Allocosa senex*: A. Adult male (sagittal section, Gomori trichrome), note large piriform glands (PI) located also very close to the aciniform glands (AC); dashed line = approximate borders of piriform and aciniform glands; ALS = retracted anterior lateral spinneret. B. Subadult male (sagittal section, Gomori trichrome), note the difference in size between piriform (PI) and aciniform (AC) glands; dashed line = approximate borders of piriform and aciniform glands. C. Transversal section of an adult male (Ferric-ferricyanide reaction) showing reducing content in dark blue, of primary ampullate glands. D. Corresponding (more anterior) image as in C providing general histological overview (Masson-Goldner trichrome). Despite comprehensible depiction, the minor ampullate glands are hardly visible: 1°MA = primary major ampullate gland, 1°mA = primary minor ampullate gland, TE = testis.

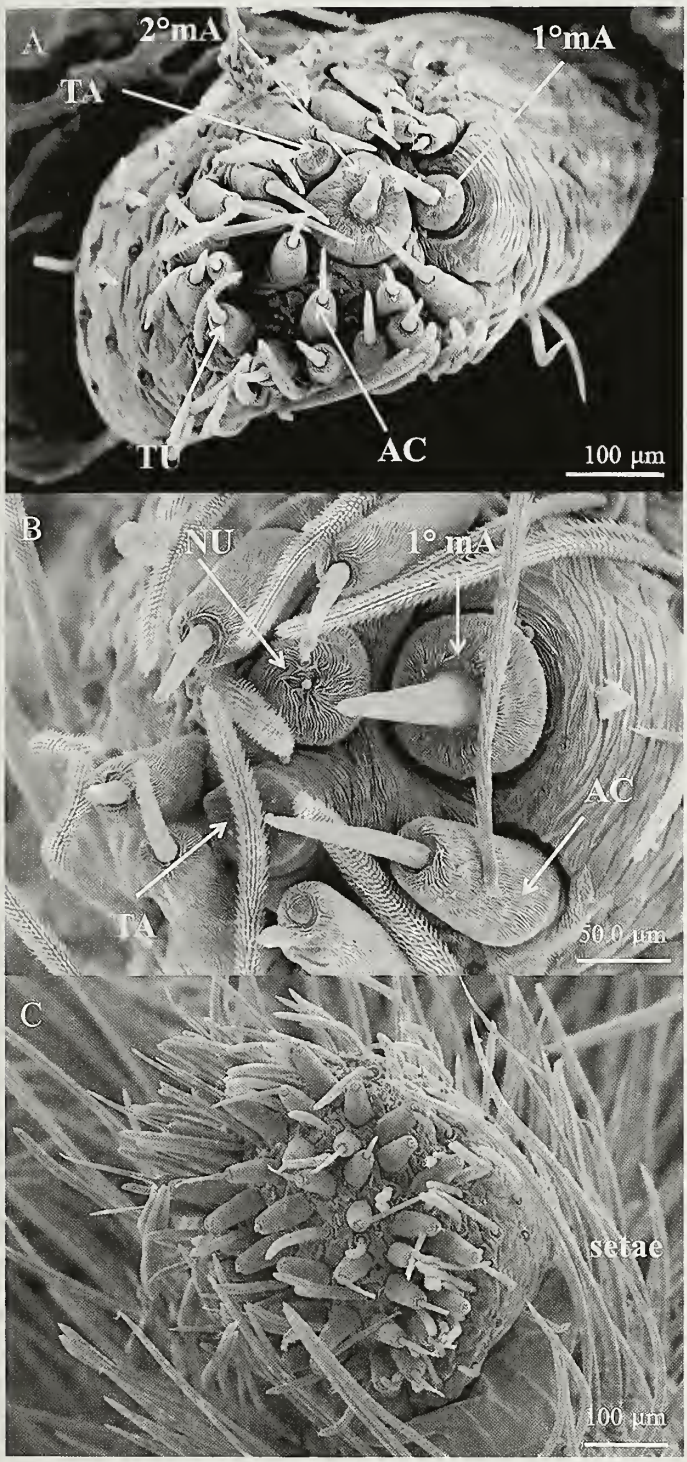


Figure 3.—*Allocosa senex*: A. Posterior median spinneret of a female, note large base of secondary minor ampullate spigot and position of tubuliform spigots. B. Posterior median spinneret of a male, with secondary minor ampullate nubbin. C. Posterior lateral spinneret of a female, see the spinning field densely covered by setae. 1°mA = primary minor ampullate spigot, 2°mA = secondary minor ampullate spigot, AC = aciniform spigot, NU = nubbin, TA = tartipore, TU = tubuliform spigot.

typical for piriform glands, as well as acidophilic reaction of aciniform glands (Kovoor 1987). Content of proteins rich on reducing groups increase from proximal to distal of any prolonged (e.g., ampullate) glands (e.g., Kovoor 1990; Haupt & Kovoor 1993). Thus, the FFR can be used for visualization of ampullate glands (not only) on transversal sections.

Simó et al. (2017) reported that *A. senex* possesses anterior lateral spinnerets twice as long as the rest. Studies under the electron microscope revealed that burrow silk in this species is composed by hundreds of thin silk lines that cover each sand grain (Foelix et al. 2017). The enlarged ALS and reduced PMS seem to be a common feature among sand-dwelling spiders across families as described by Peters (1992) for an eresid of the genus *Seothyra* (Purcell, 1903) and the sparassid *Leucorchestris arenicola* (Lawrence, 1962).

In araneoids, contrary to the lycosids, the 2° ampullate glands produce silk only during proecdysis (Townley et al. 1993) and, therefore, these glands are not necessary and nonfunctional in adults of both sexes. In lycosids (and also in pisaurids, agelenids, amaurobiids, thomisids and some dionychans), the 2°MA and 2°mA are transformed into nonfunctional nubbins in males only, whereas females' glands and spigots are maintained as they produce silk to attach the eggsacs to the spinnerets (Townley & Tillinghast 2003). Our results indicate that the bases of the MA spigots in males, females and juveniles of *A. senex* are relatively small and difficult to locate in the spinning field even with SEM, due the high density of hairs. It could be expected that their size is limited by spatial constrictions and as a way to generate more space for the piriform spigots. However, the MA spigots, while relatively small, differ in size with the 2°MA spigot base which is clearly wider than the 1°MA spigot base. Next to the spigots, the spinning field was densely covered by setae, and it can be inferred that the large number of setae would have the function of protecting the spigots. Small MA spigots as well as ALS densely covered with setae were also recorded in other sand-dwelling spiders (Peters 1992).

Simó et al. (2017) reported the presence of the 2°mA spigots at the PMS of *A. senex* (therein see 'MAP' in Figure 7E). The bases of both types of mA spigots are relatively large and the base of the 2°mA spigot is greater than that of the 1°mA. Generally, 2°A (both 2°MA and 2°mA) spigots with wider bases have been observed to coincide with larger diameter silk fibers produced by these 2°A as compared with fibers from the 1°A (Townley & Tillinghast 2003). Thus, as in some other lycosids, the 2°A likely play an important role compared to the 1°A in attaching the egg sac to the spinnerets in *A. senex*. However, the 2°A spigot bases can be notably larger (genus *Pardosa* C.L. Koch, 1847) or only slightly larger (or even of similar size) compared to 1°A spigots (other genera) (Townley & Tillinghast 2003; Dolejš et al. 2014).

The small size of the PMS and a small number of aciniform glands on them were observed. The function of the small PMS in *A. senex* is probably limited to carrying the egg sac due to enlarged bases of mA spigots, whereas the anchor threads that support the body of the spider during the molting process, as was suggested by Dolejš et al. (2014) for other wolf spider species, could be supplied mostly by aciniform glands on the PLS.

Finally, Alfaro et al. (2018) reported that the number of piriform gland spigots of females in several spider families increased with adulthood. Also these authors observed sexual dimorphism in this type of spigots in *Dolonnedes tenebrosus* Hentz, 1884 (Pisauridae), in which males have lower number of spigots than females. In our study, we observed the opposite: males with larger number of spigots compared to females. We could infer that the large number of piriform glands in males of this species is responsible for producing and depositing silk to keep the burrow stable in fine sand, the typical substrate of *A. senex* (Aisenberg & Peretti 2011). It can be assumed that digging activity would bear an important associated cost in the production of large amounts of protein, similarly to what has been reported for other burrowing spider species (Prestwich 1977; Henschel & Lubin 1992; Peters 1992). For example, it has been reported that the burrow of *C. rechenbergi* lasts approximately one month before being replaced, and if it is damaged the spider repairs it instead of constructing a new one (Foelix et al. 2017). The burrowing spider *Geolycosa missouriensis* (Banks, 1895) stays practically all its life in the same burrow and only maintains and enlarges the tube (Wallace 1942). Unfortunately, the total excavation time-period and the associated costs of burrow construction in *A. senex* are still unknown and remain to be determined. Future studies will focus on determining whether there are differences in spinneret size and the number of spigots in *A. senex* spiders that live on sandy substrates with different grain size or in Allocosinae species inhabiting different substrates.

## ACKNOWLEDGMENTS

We thank M. González, R. Postiglioni and C. Toscano for their help during field-work. L. Váchová helped us with the scanning electron microscopy. We are grateful to both reviewers and the Editor Peter Michalik for their suggestions that improved the final version of the manuscript. A. Albín was financially supported by the ANII (Agencia Nacional de Investigación e Innovación) under the code POS_NAC_2013_1_555. This scholarship was financially supported by PEDECIBA, Facultad de Ciencias, Universidad de la República and Department of Zoology, National Museum-Natural History Museum. A. Aisenberg and M. Simó acknowledge financial support by PEDECIBA (Programa de Desarrollo de Ciencias Básicas), and SNI (Sistema Nacional de Investigadores, ANII). P. Dolejš was financially supported by Ministry of Culture of the Czech Republic (DKRVO 2017/15, National Museum, 00023272).

## LITERATURE CITED

Adams, C.W.M. 1956. A strieter interpretation of the ferrie ferrieyanide reaction with particular referenee to the demonstration of protein-bound sulphydryl and di-sulphide groups. Journal of Histoehemistry and Cytoehemistry 4:23–35.

Aisenberg, A. 2014. Adventurous females and demanding males: sex role reversal in a Neotropical spider. Pp. 163–182. *In* Sexual Seleetion, Perspeetives and Models from the Neotropies. (R. Maeedo, G. Maehado (eds.)) Waltham (MA). Elsevier.

Aisenberg, A. & A.V Peretti. 2011. Male burrow digging in a sex role reversed spider inhabiting water-margin environments. Bulletin of the British Arachnological Society 15:201–204.

Aisenberg, A., M. González, Á. Laborda, R. Postiglioni & M. Simó. 2011. Spatial distribution, burrow depth and temperature: implications for the sexual strategies in two *Allocosa* wolf spiders. Studies on Neotropical Fauna and Environment 46:147–152.

Aisenberg, A., C. Viera & F.G. Costa. 2007. Daring females, devoted males, and reversed sexual size dimorphism in the sand dwelling spider *Allocosa brasiliensis* (Araneae, Lycosidae). Behavioral Ecology and Sociobiology 62:29–35.

Alfaro, R.E., C.E. Griswold & K.B. Miller. 2018. Comparative spigot ontogeny across the spider tree of life. PeerJ 6:e4233, online at https://doi.org/10.7717/peerj.4233

Capocasale, R.M. 2001. Review of the South American species of the genera *Aulonia* and *Allocosa* (Araneae, Lycosidae). Journal of Arachnology 29:270–272.

Dolejš, P., J. Buehar, L. Kubcová & J. Smrž. 2014. Developmental changes in the spinning apparatus over the life eyele of wolf spiders (Araneae: Lycosidae). Invertebrate Biology 133:281–297.

Dolejš, P., L. Kubcová & J. Buehar. 2008. Subterrestrial life of *Arctosa lutetiana* (Araneae, Lycosidae). Journal of Arachnology 36:202–203.

Foelix, R.F. 2011. Biology of Spiders. 3rd Edition. Oxford University Press, New York.

Foelix, R., I. Reehenberg, B. Erb, A. Albín & A. Aisenberg. 2017. Sand transport and burrow construction in sparassid and lycosid spiders. Journal of Arachnology 45:255–264.

Foot, N.C. 1933. The Masson trichrome staining methods in routine laboratory use. Stain Technology 8:101–110.

Glatz, L. 1972. Der Spinnapparat haplogyner Spinnen (Arachnida, Araneae). Zeitschrift für Morphologie der Tiere 72:1–25.

Glatz, L. 1973. Der Spinnapparat der Orthognatha (Arachnida, Araneae). Zeitschrift für Morphologie der Tiere 75:1–50.

Goldner, J. 1938. A modifieation of the Masson trichrome teehnique for routine laboratory purposes. American Journal of Pathology 14:237–243.

Gomori, G. 1950. A rapid one-step trichrome stain. American Journal of Clinieal Pathology 20:661–664.

Gwynne, D.T. & J. Watkiss. 1975. Burrow-blocking behaviour in *Geolycosa wrightii* (Araneae: Lycosidae). Animal Behaviour 23:953–956.

Hajer J., L. Foberová & D. Řeháková. 2017. Silk-producing organs of cribellate and cribellate nymphal stages in *Austrochilus* sp. (Araneae: Austrochilidae): Notes on the transformation of the anterior median spinnerets into the cribellum. Israel Journal of Entomology 47:21–33.

Haupt, J. & J. Kovoor. 1993. Silk-gland system and silk production in Mesothelae (Araneae). Annales des Sciences Naturelles, Zoologie, Paris, 13th série, 14:35–48.

Henschel, J.R. 1990. The biology of *Leucorchestris arenicola* (Araneae: Heteropodidae), a burrowing spider of the Namib dunes. Pp. 115–127. *In* Namib Ecology 25 Years of Namib Research. (M.K. Seely (ed.)). Transvaal Museum Monograph No. 7 Transvaal Museum Pretoria.

Henschel, J.R. & Y.D. Lubin. 1992. Environmental factors affecting the web and activity of a psammophilous spider in the Namib Desert. Journal of Arid Environments 22:173–189.

Kovoor, J. 1977. La soie et les glandes sérieigènes des Arachnides. Annee Biologique, 16:97–171.

Kovoor, J. 1987. Comparative structure and histochemistry of silk-producing organs in arachnids. Pp. 160–186. *In* Ecophysiology of Spiders. (W. Nentwig (ed.)). Springer, Berlin.

Kovoor, J. 1990. The silk-gland system in some Tetragnathinae (Araneae: Araneidae): Comparative anatomy and histochemistry. Acta Zoologica Fennica 190:215–221.

Kovoor, J. & H.M. Peters.1988. The spinning apparatus of *Polenecia producta* (Araneae-Uloboridae): Structure and histochemistry. Zoolomorphology 108:47–59.

Marples, B.J. 1967. The spinnerets and epiandrous glands of spiders. Journal of the Linnean Society of London (Zoology) 46:209–222.

Masson, P. 1929. Some histological methods, trichrome staining and their preliminary technique. Journal of Technical Methods and Bulletin of the International Association of Medical Museums 12:75–90.

Peters, H.M. 1992. On the burrowing behaviour and the production and use of silk in *Scotlyra*, a sand-inhabiting spider from the Namib Desert (Arachnida, Araneae, Eresidae). Verhandlungen naturwissenschaften Vereins Hamburg (NF) 33:191–211.

Prestwich, K.N. 1977. The energetics of web-building in spiders. Comparative Biochemistry and Physiology 57:321–326.

Richter, C.J.J. 1970. Morphology and function of the spinning apparatus of the wolf spider *Pardosa amentata* (Cl.) (Araneae, Lycosidae). Zeitschrift für Morphologie der Tiere 68:37–68.

Shultz, J.W. 1987. The origin of the spinning apparatus in spiders. Biological Reviews 62:89–113.

Simó, M., A.A. Lise, G. Pompozzi & Á. Laborda. 2017. On the taxonomy of southern South American species of the wolf spider genus *Allocosa* (Araneae: Lycosidae: Allocosinae). Zootaxa 4216:261–278.

Smrž, J. 1989. Internal anatomy of *Hypochthonius rufulus* (Acari: Oribatida). Journal of Morphology 200:215–230.

Townley, M.A. & E.K. Tillinghast. 2003. On the use of ampullate gland silks by wolf spiders (Araneae, Lycosidae) for attaching the egg sac to the spinnerets and a proposal for defining nubbins and tartipores. Journal of Arachnology 31:209–245.

Townley, M.A. & E.K. Tillinghast. 2009. Developmental changes in spider spinning fields: a comparison between *Mimetus* and *Araneus* (Araneae: Mimetidae, Araneidae). Biological Journal of the Linnean Society 98:343–383.

Townley, M.A., E.K. Tillinghast & N.A. Cherim. 1993. Moult-related changes in ampullate silk gland morphology and usage in the araneid spider *Araneus cavaticus*. Philosophical Transactions of the Royal Society, London, Series B 340:25–38.

Wallace, H.K. 1942. A revision of the burrowing spiders of the genus *Geolycosa* (Araneae, Lycosidae). American Midland Naturalist 27:1–62.

Wheeler, W.C., J.A. Coddington, L.M. Crowley, D. Dimitrov, P.A. Goloboff, C.E. Griswold, H. Hormiga, L. Prendini, M.J. Ramírez, P. Sierwald, L. Almeida-Silva, F. Alvarez-Padilla, M.A. Arnedo, L.R. Benavides Silva, S.P. Benjamin, J.E. Bond, C.J. Grismado, E. Hasan, M. Hedin, M.A. Izquierdo, F.M. Labarque, J. Ledford, J. Lopardo, W.P. Maddison, J.A. Miller, L.N. Piacentini, N.I. Platnick, D. Polotow, D. Silva-Dávila, N. Scharff, T. Szuts, D. Ubick, C.J. Vink, H.M. Wood & J. Zhang. 2017. The spider tree of life: phylogeny of Araneae based on target-gene analyses from an extensive taxon sampling. Cladistics 33:574–616.

Wolff, J.O., M. Řezáč, T. Krejčí & S.N. Gorb. 2017. Hunting with sticky tape: functional shift in silk glands of araneophagous ground spiders (Gnaphosidae). Journal of Experimental Biology 220:2250–2259.

*Manuscript received 3 November 2017, revised 27 February 2018.*

2018. Journal of Arachnology 46:214 225

# Morphology of setae on the coxae and trochanters of theraphosine spiders (Mygalomorphae: Theraphosidae)

**Arthur Galleti Lima** and **José Paulo Leite Guadanucci**: Department of Zoology, Institute of Biosciences, São Paulo State University (UNESP – Rio Claro), Rio Claro, São Paulo, Brazil. E-mail: arthurgalletilima6@hotmail.com

**Abstract.** Mygalomorphae spiders have several cuticular structures, such as stridulating, sensory and urticating setae, which offer great potential for phylogenetic studies. Spiders of the subfamily Theraphosinae have stridulating setae that aid in group taxonomy, having been found in numerous genera including: *Acanthoscurria* Ausserer, 1871, *Aguapanela* Perafán, Cifuentes & Estrada-Gomez, 2015, *Citharacanthus* Pocock, 1901, *Cyrtopholis* Simon, 1892, *Grammostola* Simon, 1892, *Hemirrhagus* Simon, 1903, *Lasiodora* C. L. Koch, 1850, *Longilyra* Gabriel, 2014, *Pamphobeteus* Pocock, 1901, *Phormictopus* Pocock, 1901 and *Theraphosa* Thorell, 1870. Some distinct bristle-like setae were examined using scanning electron microscopy with the following objectives: (1) to sample and describe the diversity of setae on the coxae and trochanters of representatives of the subfamily Theraphosinae; and (2) to code morphological characters useful for phylogenetics. We used a previously published phylogenetic matrix, with modifications to those characters that scored stridulatory setae, and analyzed these data using parsimony with implied weighting. Setae of the same type were found in *Acanthoscurria*, *Brachypelma* Simon, 1891, *Cyrtopholis*, *Phormictopus* and *Theraphosa* (claviform stridulating setae). A second type, which we name velvet stridulating setae, emerged as an autapomorphy of the genus *Lasiodora*, and spiniform stridulating setae were recovered as an autapomorphy of the genus *Pamphobeteus*. Some other setae similar to those of *Lasiodora*, named plumose stridulating setae, were found in *Nhandu* Lucas, 1983, *Proshapalopus* Mello-Leitão, 1923, *Pterinopelma* Pocock, 1901 and *Vitalius* Lucas, Silva & Bertani, 1993.

**Keywords:** Theraphosinae, stridulating setae, phylogeny, cladistics

Mygalomorph spiders, as well as other arthropods, present cuticular structures with great morphological variation and phylogenetic information (Raven 1994; Ferretti et al. 2011; Guadanucci 2014; Bertani & Guadanucci 2013). Among these structures, we find different types of setae with different functions, such as chemosensory, mechanosensory and adhesive (Seyfarth 1985; Barth 2002). Many species of Mygalomorphae use sound production, presumably for sexual behavior or for protection against possible predators (Legendre 1963; Uetz & Stratton 1982; Marshall et al. 1995). Sounds are produced as a result of a phenomenon known as stridulation, and made by stridulatory organs that consist of specialized setae and antagonistic structures on the integument (Jocqué 2005). Other varieties of setae may also act in the stridulating process, such as the long spiniform setae of spiders of the genus *Grammostola* Simon, 1892 (Ferretti et al. 2011) and the spiniform setae found in *Acanthoscurria suina* Pocock, 1903 (Pérez-Miles et al. 2005). These organs are arranged on opposing surfaces and rub against each other, causing vibrations that are captured by trichobothria (Uetz & Stratton 1982).

The systematics and taxonomy of the family Theraphosidae have been heavily influenced by the presence and variations of stridulatory setae (Pocock 1895, 1897, 1899; Simon 1903; Pérez-Miles et al. 1996; Schmidt 1999). One of the earliest records of stridulatory setae in a theraphosid spider can be found in the work of Simon (1892), who cites a description made by Wood-Mason (1876) for some 'Avicularíides' spiders. Among representatives of the subfamily Selenocosmiinae, Raven (1985) recorded different stridulatory setae in the form of a lyra, on the retrolateral face of the chelicerae and the prolateral face of the maxillae.

Stridulatory organs are found in at least 22 families of spiders (Uetz & Stratton 1982). The taxonomy of spiders of the subfamily Theraphosinae (family Theraphosidae) is largely based on the presence and distribution of stridulating organs (Pocock 1895, 1897, 1899; Simon 1903; Bücherl 1957; Pérez-Miles et al. 1996, Schmidt 1999, 2000), along with differences in the leg and body measurements, the disposition of eyes and scopulae, coloration (Simon 1892; Pocock 1903; Mello-Leitão 1923; Schiapelli & Gerschman de Pikelin 1979; Raven 1985; Smith 1995; Prentice 1997), the type of urticating setae (Cooke et al. 1972; Pérez- Miles et al. 1996), the morphology of the spermathecae (Schiapelli & Gerschman de Pikelin 1962), and the shape of the tibial apophysis and male palpal bulb (Raven 1985; Perez-Miles et al. 1996; Guadanucci 2014). With respect to stridulating setae, the presence of such structures has hitherto been reported for 11 theraphosinae genera: *Acanthoscurria* Ausserer, 1871; *Aguapanela* Perafán, Cifuentes & Estrada-Gomez, 2015; *Citharacanthus* Pocock, 1901; *Cyrtopholis* Simon, 1892; *Grammostola*; *Hemirrhagus* Simon, 1903; *Lasiodora* C. L. Koch, 1850; *Longilyra* Gabriel, 2014; *Pamphobeteus* Pocock, 1901; *Phormictopus* Pocock, 1901; and *Theraphosa* Thorell, 1870.

Pocock (1901) noticed the presence of plumose setae, which he did not name or recognize as stridulatory, on the retrolateral face of the palpal trochanter and on the prolateral coxa I of spiders of the genus *Pterinopelma* Pocock, 1901 (similar to those of *Brachypelma* Simon, 1891). Bücherl (1957) also noticed varieties of these setae on some Theraphosinae. In *Acanthoscurria*, the setae were drawn by Bücherl (1957) as spear-shaped, with a smooth proximal portion and barbs covering the apical half, these barbs becoming denser at the apex. These stridulating setae are currently called claviform (Pérez-Miles et al. 2005). In the genus *Lasiodora*, Bücherl (1957) described the setae as having a velvet surface, and provided with many short barbs. Bertani (2001) also reported

the presence of distinct setae in *Lasiodora* on the upper prolateral faces of coxae I and II.

After examining specimens of the genera *Nhandu* Lucas, 1983, *Proshapalopus* Mello-Leitão, 1923, *Pterinopelma* and *Vitalius* Lucas, Silva & Bertani, 1993, a conspicuous tuft of setae on the trochanters and coxae drew our attention. Thereafter, our objective was to examine the variations of stridulating setae of the coxae and trochanters of Theraphosinae using scanning electron microscopy. In this study, we present these data, and analyze and interpret our results in a phylogenetic context.

## METHODS

Material was examined from the following scientific collections: IBSP, Instituto Butantan, São Paulo, Brazil (A. Brescovit); MCN, Museu de Ciências Naturais, Fundação Zoobotânica do Rio Grande do Sul, Porto Alegre, Brazil (R. Ott); CNAN, Colección Nacional de Arácnidos UNAM, México DF, México (O. F. Ballvé); CCEN, Centro de Ciências Exatas e da Natureza, Universidade Federal da Paraíba, João Pessoa, Paraíba, Brazil (M. B. da Silva); CAD, Coleção Aracnológica Diamantina, Diamantina, Minas Gerais, Brazil (J. P. L Guadanucci).

**Material examined.**—*Acanthoscurria gomesiana* Mello-Leitão, 1923. BRAZIL: *Minas Gerais*: 1 ♂, Diamantina, November 2008 (CAD 021); 1 ♀, São Gonçalo do Rio Preto, 11 November 2009 (CAD 472).

*Acanthoscurria juruenicola* Mello-Leitão, 1923. BRAZIL: *Mato Grosso*: 1 ♂, Alta Floesta, 4 December 1979 (IBSP 4474).

*Acanthoscurria natalensis* Chamberlin, 1917. BRAZIL: *Mato Bahia*: 1 ♂, Riachão das Neves, 18 February 1974, A. Pereira Filho (IBSP 4234); 1 ♀, Irerê, September 1980, M. Guimarães (IBSP 4558).

*Acanthoscurria paulensis* Mello-Leitão, 1923. BRAZIL: *Minas Gerais*: 1 ♂, Alpinópolis, February 1983, J. Oliveira (IBSP 4759); 1 ♀, Campo Grande, 13 March 1972 (IBSP 2117).

*Brachypelma smithi* (F. O. Pickard-Cambridge, 1897). MEXICO: *Guerrero*: 2 ♂, Zihuatanejo, June 2015 (CNAN).

*Cyrtopholis* species. DOMINICAN REPUBLIC: *La Veja Contanza*: 1 ♂, La Piramide Paque Nacional Valle Nuevo, 18°42′27.7″N, 70°36′01.6″W, 19 October 2011, G. Santos (IBSP). *San Juan*: 1 ♀, Parque Nacional José del Carmen Pramiras, 14 November 2009 (IBSP).

*Eupalaestrus* species. BRAZIL: *São Paulo*: 1 ♂, Serra do Mar, 12 May 1976 (IBSP 4200).

*Lasiodora parahybana* Mello-Leitão, 1917. BRAZIL: *Paraíba*: 1 ♂, João Pessoa, 22 April 2015 (CCEN 854). *Piauí*: 1 ♀, Oeiras, July 2008, T. Porto, H. Yamaguti & M. B. da Silva (CCEN 180).

*Nhandu cerradensis* Bertani, 2001. BRAZIL: *Piauí*: 1 ♂, Parque Nacional da Serra das Confusões, January 2002 (IBSP 11847); 1 ♀, 'Brazil', January 1994, A. P. da Silva (IBSP 13971).

*Proshapalopus multicuspidatus* Mello-Leitão, 1929. BRAZIL: *Minas Gerais*: 1 ♂, Mendanha, P. S. Moreira (CAD 094).

*Pterinopelma felipeleitei* Bertani & Leal, 2016. BRAZIL: *Minas Gerais*: 1 ♂, Diamantina, 5 June 2011 (CAD 441); 1 ♀, Diamantina (CAD 584).

*Pterinopelma sazimai* Bertani, Nagahama & Fukushima, 2011. BRAZIL: *Minas Gerais*: 1 ♂, Diamantina, C. A. Bispo (CAD); 1 ♀, Diamantina (CAD).

*Pterinopelma vitiosum* Keyserling, 1891. BRAZIL: *Rio Grande do Sul*: 1 ♂, Encantado, 17 April 1992, L. Dacroce (MCN 22145); 1 ♀, Caxias do Sul, 18 December 1991, F. Becker (MCN 22102).

*Theraphosa blondi* Latreille, 1804. BRAZIL: *Pará*: 1 ♂, Caxiuanã-Melgaço, 17–30 March 2002 (MPEG 000176); 1 ♀, Almerim, 01°1′33.1″S, 52°34′2.8″W, 22 June 2005, T. Gardner & M. A. R. Junior (MPEG 007558).

*Vitalius* species. BRAZIL: *São Paulo*: 1 ♂, Jaú, R. Benetti (CAD).

**Morphological methods.**—The pro- and retrolateral faces of coxae and trochanters were surveyed in search of distinct types of setae. The articles were dissected and manually cleaned with thin brushes (synthetic fibers) towards the same direction of setal alignment to remove visible particles and debris. The articles were then cleaned in an ultrasonic vibrator after soaking for 12 hours in a water/detergent solution. Dehydration in ethanol series was done before critical-point drying. Each article was mounted on a separate aluminum stub with copper double-sided tape and finally sputter coated with gold. The preparations were examined under a Hitachi TM-1000 scanning electron microscope (SEM) at the Electronic Microscopy Laboratory of the Institute of Biosciences of Sao Paulo State University, campus Rio Claro, São Paulo, Brazil.

**Cladistics.**—To study the evolution of stridulating setae, we used the matrix assembled by Bertani et al. (2011) with the following changes regarding the terminal taxa: *Acanthoscurria geniculata* C. L. Koch, 1841 and *Acanthoscurria sternalis* Pocock, 1903 were replaced by *Acanthoscurria gomesiana*, *A. juruenicola*, *A. natalensis* and *A. paulensis*; and the terminal taxon *Pterinopelma felipeleitei* was added. The presence/absence of setae for species not examined under the SEM was checked under the stereomicroscope, with comparisons to the micrographs obtained. We treated the presence/absence of setae on the legs (coxae and trochanters) as a whole, without distinction between the legs or palps and the surfaces (prolateral and retrolateral), considering that the repetition of the structures (cuticular setae) is a case of serial homology, and that scoring the presence of such setae on different legs as distinct characters would be misleading.

Regarding the characters, the following changes were applied to the original matrix of Bertani et al. (2011): characters 21 (presence of stridulating setae on the trochanters) and 22 (presence of stridulating setae on the coxae) were inactivated as they didn't distinguish different types of setae (see Results, below). Seven new characters referring to observed stridulating setae were added to the original matrix and numbered from the last character, as follows (all '0' absent and '1' present): (36) stridulating plumose setae on the coxae; (37) stridulating plumose setae on the trochanters; (38) stridulating claviform setae on the coxae; (39) stridulating claviform setae on the trochanters; (40) stridulating velvet setae on the coxae; (41) stridulating spiniform setae on the coxae; and (42) stridulating spiniform setae on the trochanters. The matrix for this revised and expanded dataset is shown in Table 1.

Table 1.—Character matrix edited from Bertani et al. (2011), composed of 35 terminals and 42 characters. See Bertani et al. (2011) for description of characters 1-35; see text for description of characters 36-42.

| | Characters > | | | | | | | | | | | | | | | | | | | | | | | | | | | | | | | | | | | | | | | |
|---|---|---|---|---|---|---|---|---|---|---|---|---|---|---|---|---|---|---|---|---|---|---|---|---|---|---|---|---|---|---|---|---|---|---|---|---|---|---|---|---|
| Taxa | 1 | 2 | 3 | 4 | 5 | 6 | 7 | 8 | 9 | 10 | 11 | 12 | 13 | 14 | 15 | 16 | 17 | 18 | 19 | 20 | 21 | 22 | 23 | 24 | 25 | 26 | 27 | 28 | 29 | 30 | 31 | 32 | 33 | 34 | 35 | 36 | 37 | 38 | 39 | 40 | 41 | 42 |
| *A. seemanni* | 0 | 0 | 0 | 0 | 0 | 0 | 1 | 0 | 0 | 0 | 0 | 0 | 0 | 0 | 0 | 0 | 0 | 0 | 0 | 0 | 0 | 0 | 0 | 0 | 0 | 0 | 0 | 0 | 0 | 0 | 0 | 0 | 0 | 0 | 0 | 0 | 0 | 0 | 0 | 0 | 0 | 0 |
| *S. hoffmanni* | 0 | 0 | 0 | 0 | 0 | 0 | 1 | 0 | 0 | 0 | 0 | 0 | - | 0 | 1 | 0 | 0 | 0 | 0 | 0 | 0 | 0 | 0 | 0 | 0 | 0 | 0 | 0 | 0 | 0 | 0 | 0 | - | - | 0 | 0 | 0 | 0 | 0 | 0 | 0 | 0 |
| *P. cancerides* | 0 | 0 | 0 | 0 | 0 | 0 | 0 | 0 | 0 | 0 | 1 | 0 | 0 | 0 | 0 | 0 | 0 | 0 | 0 | 0 | 1 | 1 | 1 | 0 | 0 | 0 | 0 | 0 | 0 | 0 | 1 | 0 | 0 | 1 | 1 | 0 | 0 | 1 | 1 | 0 | 0 | 0 |
| *C. portoricae* | 0 | - | 0 | 0 | 0 | 0 | 0 | 0 | 0 | 0 | 0 | 0 | 3 | 0 | 0 | 0 | 0 | 0 | 0 | 0 | 1 | 0 | 1 | 0 | 0 | 0 | 0 | 1 | 0 | 0 | 0 | 0 | 0 | 0 | 0 | 0 | 0 | 0 | 1 | 0 | 0 | 0 |
| *A. gomesiana* | 0 | 0 | 0 | 0 | 0 | 0 | 0 | 0 | 0 | 0 | - | 0 | - | 0 | - | 1 | 0 | 1 | 0 | 0 | 1 | 0 | 1 | 0 | 0 | 0 | 0 | 0 | 0 | 0 | 1 | 0 | 0 | 0 | 1 | 0 | 0 | 1 | 1 | 0 | 0 | 0 |
| *A. paulensis* | 0 | 0 | 0 | 0 | 0 | 0 | 0 | 0 | 0 | 0 | - | 0 | - | 0 | - | 1 | 0 | 1 | 0 | 0 | 1 | 0 | 1 | 0 | 0 | 0 | 0 | 0 | 0 | 0 | 1 | 0 | 1 | 0 | 1 | 1 | 1 | 1 | 1 | 0 | 0 | 0 |
| *A. juruenicola* | 0 | 0 | 0 | 0 | 0 | 0 | 0 | 0 | 0 | 0 | - | 0 | - | 0 | - | 1 | 0 | 1 | 0 | 0 | 1 | 0 | 1 | 0 | 0 | 0 | 0 | 0 | 0 | 0 | 1 | 0 | 0 | 0 | 1 | 1 | 1 | 1 | 1 | 0 | 0 | 0 |
| *A. natalensis* | 0 | 0 | 0 | 0 | 0 | 0 | 0 | 0 | 0 | 0 | - | 0 | - | 0 | - | 1 | 0 | 1 | 0 | 0 | 1 | 0 | 1 | 0 | 0 | 0 | 0 | 0 | 0 | 0 | 1 | 0 | 1 | 0 | 1 | 1 | 1 | 1 | 1 | 0 | 0 | 0 |
| *Pauphobeteus* spp. | 0 | 2 | 0 | 2 | 0 | 0 | 0 | 2 | 0 | 0 | 0 | 0 | 2 | 0 | 2 | 0 | 2 | 0 | 0 | 0 | 0 | 0 | 1 | 0 | 0 | 0 | 0 | 0 | 0 | 0 | 0 | 0 | 0 | 0 | 1 | 0 | 0 | 0 | 0 | 0 | 1 | 1 |
| *B. emilia* | 0 | 2 | 0 | 0 | 0 | 0 | 0 | 2 | 0 | 0 | 0 | 0 | 2 | 0 | 1 | 0 | 3 | - | - | - | 0 | 0 | 1 | 0 | 0 | 0 | 0 | 0 | 0 | 0 | 0 | 0 | 0 | 1 | 0 | 0 | 0 | 1 | 1 | 0 | 0 | 0 |
| *X. immanis* | 0 | 2 | 0 | 2 | 0 | 0 | 0 | 2 | 0 | 0 | 0 | 0 | 2 | 0 | 2 | 0 | 2 | 0 | 0 | 0 | 0 | 0 | 1 | 0 | 0 | 0 | 0 | 0 | 0 | 0 | 0 | 0 | 0 | 1 | 1 | 0 | 0 | 0 | 0 | 0 | 0 | 0 |
| *T. bloudi* | - | 2 | 0 | 0 | 0 | 0 | 0 | 2 | 1 | 0 | 0 | 1 | - | 2 | - | - | 3 | - | - | - | 0 | 1 | 1 | - | 1 | 0 | 0 | 0 | 0 | 0 | 0 | 0 | 0 | 1 | 0 | 0 | 1 | 1 | 0 | 1 | 0 |
| *T. apophysis* | - | 2 | 0 | 0 | 0 | 0 | 0 | 2 | 1 | 0 | 0 | 1 | 2 | 0 | 0 | 0 | 3 | - | - | - | 0 | 1 | 1 | - | 1 | 0 | 0 | 0 | 0 | 0 | 0 | 0 | 0 | 1 | 0 | 0 | 1 | 1 | 0 | 1 | 0 |
| *E. caupestratus* | 0 | 0 | 0 | 1 | 0 | 0 | 0 | 1 | 0 | 0 | 1 | 0 | 0 | 0 | 0 | 0 | 0 | 0 | 0 | 0 | 0 | 0 | 1 | 0 | 0 | 1 | 0 | 0 | 0 | 0 | 0 | 0 | 1 | 0 | 1 | 0 | 0 | 0 | 0 | 0 | 0 | 0 |
| *E. weijenberghi* | 0 | 0 | 0 | 1 | 0 | 0 | 0 | 1 | 0 | 0 | 1 | 0 | - | 0 | 0 | 0 | 0 | 0 | 0 | 0 | 0 | 0 | 1 | 0 | 0 | 1 | 0 | 0 | 0 | 0 | 0 | 0 | 1 | 0 | 1 | 0 | 0 | 0 | 0 | 0 | 0 | 0 |
| *P. amazonicus* | 0 | 0 | 0 | 1 | 1 | 1 | 0 | 1 | 0 | 1 | 0 | 0 | 0 | 0 | 1 | 0 | 0 | 0 | 0 | 0 | 0 | 0 | 0 | 0 | 0 | 1 | 0 | 0 | 0 | 1 | 0 | 0 | 1 | 0 | 1 | 1 | 1 | 0 | 0 | 0 | 0 | 0 |
| *P. anomalus* | 1 | 0 | 0 | 1 | 1 | 1 | 0 | 1 | 0 | 0 | 0 | 0 | 0 | 0 | 1 | 0 | 0 | 0 | 0 | 0 | 0 | 0 | 1 | 1 | 0 | 0 | 0 | 1 | 0 | 0 | 0 | 1 | 0 | 0 | 1 | 1 | 1 | 0 | 0 | 0 | 0 | 0 |
| *P. multicuspidatus* | 1 | 0 | 0 | 1 | 1 | 1 | 0 | 1 | 0 | 1 | 0 | 0 | 1 | 0 | 0 | 0 | 0 | 0 | 0 | 0 | 0 | 0 | 1 | 1 | 0 | 0 | 1 | 1 | 0 | 0 | 0 | 1 | 0 | 0 | 1 | 1 | 1 | 0 | 0 | 0 | 0 | 0 |
| *Lasiodora* spp. | 0 | 0 | 0 | 2 | 1 | 0 | 0 | 1 | 0 | 0 | 0 | 0 | 0 | 0 | 1 | 0 | 1 | 0 | 0 | 0 | 0 | 1 | 1 | 0 | 0 | 0 | 0 | 0 | 0 | 0 | 0 | 0 | 0 | 1 | 1 | 1 | 1 | 0 | 0 | 1 | 0 | 0 |
| *N. carapoensis* | 1 | 1 | 1 | 2 | 1 | 0 | 0 | 1 | 0 | 0 | 0 | 0 | - | 2 | - | - | 1 | 0 | 0 | 1 | 0 | 0 | 0 | 0 | 0 | 0 | 0 | 0 | 1 | 1 | 0 | 0 | 0 | 0 | 1 | 1 | 1 | 0 | 0 | 0 | 0 | 0 |
| *N. tripepii* | 1 | 1 | 1 | 2 | 1 | 0 | 0 | 1 | 0 | 0 | 0 | 0 | 0 | 0 | 0 | 0 | 1 | 0 | 1 | 1 | 0 | 0 | 1 | 0 | 0 | 0 | 0 | 0 | 1 | 1 | 0 | 0 | 1 | 1 | 1 | 1 | 1 | 0 | 0 | 0 | 0 | 0 |
| *N. coloratovillosus* | 1 | 1 | 1 | 2 | 1 | 0 | 0 | 1 | 0 | 0 | 0 | 0 | 0 | 0 | 1 | 0 | 1 | 0 | 1 | 1 | 0 | 0 | 1 | 0 | 0 | 0 | 0 | 0 | 1 | 1 | 0 | 0 | 1 | 1 | 1 | 1 | 1 | 0 | 0 | 0 | 0 | 0 |
| *N. cerradensis* | 1 | 1 | 1 | 2 | 1 | 0 | 0 | 1 | 0 | 0 | 0 | 0 | 0 | 0 | 1 | 0 | 1 | 0 | 0 | 0 | 0 | 0 | 1 | 0 | 0 | 0 | 0 | 0 | 1 | 1 | 0 | 0 | 0 | 1 | 1 | 1 | 1 | 0 | 0 | 0 | 0 | 0 |
| *V. sorocabae* | 1 | 1 | 0 | 2 | 1 | 0 | 0 | 1 | 0 | 0 | 0 | 0 | 1 | 0 | 0 | 0 | 1 | 0 | 0 | 0 | 0 | 0 | 0 | 0 | 0 | 0 | 0 | 0 | 1 | 0 | 0 | 0 | 0 | 0 | 1 | 1 | 1 | 0 | 0 | 0 | 0 | 0 |
| *V. wacketi* | 0 | 1 | 0 | 2 | 1 | 0 | 0 | 1 | 0 | 0 | 0 | 0 | 1 | 0 | 0 | 0 | 1 | 0 | 0 | 0 | 0 | 0 | 0 | 0 | 0 | 0 | 0 | 0 | 0 | 0 | 0 | 0 | 0 | 0 | 1 | 1 | 1 | 0 | 0 | 0 | 0 | 0 |
| *V. dubius* | 1 | 1 | 1 | 2 | 1 | 0 | 0 | 1 | 0 | 0 | 0 | 0 | 1 | 0 | 0 | 0 | 1 | 0 | 0 | 0 | 0 | 0 | 0 | 0 | 0 | 0 | 0 | 0 | 0 | 0 | 0 | 0 | 0 | 0 | 1 | 1 | 1 | 0 | 0 | 0 | 0 | 0 |
| *V. roseus* | 1 | 1 | 0 | 2 | 1 | 0 | 0 | 1 | 0 | 0 | 0 | 0 | - | 1 | - | 0 | 1 | 0 | 0 | 0 | 0 | 0 | 0 | 0 | 0 | 0 | 1 | 0 | 0 | 0 | 0 | 0 | 1 | 0 | 1 | 1 | 1 | 0 | 0 | 0 | 0 | 0 |
| *V. vellutinus* | 1 | 1 | 0 | 2 | 1 | 0 | 0 | 1 | 0 | 0 | 0 | 0 | - | 1 | - | 0 | 1 | 0 | 0 | 0 | 0 | 0 | 0 | 0 | 0 | 0 | 1 | 0 | 0 | 0 | 0 | 0 | 0 | 0 | 1 | 1 | 1 | 0 | 0 | 0 | 0 | 0 |
| *V. longisternalis* | 0 | 1 | 0 | 2 | 1 | 0 | 0 | 1 | 0 | 0 | 0 | 0 | 1 | 0 | 0 | 0 | 1 | 0 | 0 | 0 | 0 | 0 | 0 | 0 | 0 | 0 | 0 | 0 | 0 | 0 | 0 | 0 | 1 | 0 | 1 | 1 | 1 | 0 | 0 | 0 | 0 | 0 |
| *V. lucasae* | 1 | 1 | 0 | 2 | 1 | 0 | 0 | 1 | 0 | 1 | 0 | 0 | 0 | 0 | 0 | 1 | 1 | 0 | 0 | 0 | 0 | 0 | 0 | 0 | 0 | 1 | 0 | 0 | 0 | 0 | 0 | 0 | 0 | 1 | 1 | 1 | 1 | 0 | 0 | 0 | 0 | 0 |
| *V. buecherli* | 1 | 1 | 1 | 2 | 1 | 0 | 0 | 1 | 0 | 0 | 0 | 0 | 1 | 0 | 0 | 0 | 1 | 0 | 0 | 0 | 0 | 0 | 0 | 0 | 0 | 0 | 0 | 1 | 0 | 0 | 0 | 0 | 0 | 0 | 1 | 1 | 1 | 0 | 0 | 0 | 0 | 0 |
| *V. paranaensis* | 1 | 1 | 0 | 2 | 1 | 0 | 0 | 1 | 0 | 0 | 0 | 0 | 1 | 0 | 0 | 0 | 1 | 0 | 0 | 0 | 0 | 0 | 0 | 0 | 0 | 0 | 1 | 0 | 0 | 0 | 0 | 0 | 0 | 0 | 1 | 1 | 1 | 0 | 0 | 0 | 0 | 0 |
| *P. felipeleitei* | 0 | 0 | 0 | 1 | 0 | 0 | 1 | 1 | 0 | 0 | 0 | 0 | 0 | 0 | 1 | 0 | 1 | 0 | 0 | 0 | 0 | 0 | 1 | 0 | 0 | 0 | 0 | 0 | 0 | 0 | 0 | 0 | 0 | 1 | 1 | 1 | 1 | 0 | 0 | 0 | 0 | 0 |
| *P. vitiosum* | 0 | 0 | 0 | 1 | 1 | 0 | 1 | 1 | 0 | 0 | 0 | 0 | 0 | 0 | 0 | 0 | 1 | 0 | 0 | 0 | 0 | 0 | 1 | 0 | 0 | 0 | 0 | 0 | 0 | 0 | 0 | 0 | 1 | 0 | 1 | 1 | 1 | 0 | 0 | 0 | 0 | 0 |
| *P. sazimai* | 1 | 1 | 1 | 1 | 1 | 0 | 1 | 1 | 0 | 0 | 0 | 0 | 0 | 0 | 1 | 0 | 1 | 0 | 0 | 0 | 0 | 0 | 0 | 0 | 0 | 0 | 0 | 0 | 0 | 0 | 0 | 0 | 0 | 1 | 1 | 1 | 1 | 0 | 0 | 0 | 0 | 0 |

Table 2.—Results obtained from the trees found in the analyses.

| K-Values | % of character weights | N° of trees | Total fit |
|---|---|---|---|
| 3.061 | 75 | 1 | 8.687 |
| 3.459 | 77.222 | 1 | 8.087 |
| 3.944 | 79.444 | 1 | 7.467 |
| 4.545 | 81.667 | 1 | 6.825 |
| 5.313 | 83.889 | 1 | 6.153 |
| 6.327 | 86.111 | 1 | 5.440 |
| 7.726 | 88.333 | 1 | 4.696 |
| 9.784 | 90.556 | 1 | 3.917 |
| 13.108 | 92.778 | 1 | 3.095 |
| 19.388 | 95 | 1 | 2.221 |

The most parsimonious trees were searched with heuristic methods and with implied weighting under different parameters (K-values), in order to perform a sensitivity analysis of the dataset. To decide upon which K-values to apply, we used TNT software 1.1 (Goloboff et al. 2008), with the script designed by Mirande (2009), which finds the K-values that divide the values of fit/distortion at regular intervals (script command line aaa 3 10 70 95 7). In order to avoid zero length branches (Coddington & Scharff 1995), nodes without support were collapsed (collapsing rule 1) and suboptimal trees were discarded. The K-values, percentages of the weights of the characters, number of trees and fit values are shown in Table 2. Character optimization and tree editing were done using Winclada 1.00.08 (Nixon 2002).

## RESULTS

According to Pérez-Miles et al. (2005), a stridulatory seta needs to have a strong and rigid appearance, so that it can withstand the intense friction of stridulation. Studies such as those by Bücherl (1957), Pérez-Miles et al. (2005) and Bertani et al. (2008) show that stridulatory setae are always present on the coxae and trochanters. Genera examined and the types of stridulating setae they possess are shown in Table 3.

**Setal morphology.**—The types of stridulating setae found in our study are named and described below.

*Claviform stridulating setae (Figs. 1–4, 15–18):* The claviform stridulating setae have the appearance of a club, with the apical third slightly wider than the basal portion. The basal half is bare and the apical half is covered with coarse barbs, which are directed towards the apical end, where there is a short area without barbs and with marked grooves. The claviform stridulating setae were first named by Pérez-Miles et al. (2005) for *Acanthoscurria suina*. The occurrence of these setae did not show any phylogenetic pattern in our study, however in all species analyzed they were found on the pro- and retrolateral faces of the trochanters of the palp and leg I in *Acanthoscurria*, *Cyrtopholis*, *Brachypelma*, *Theraphosa* and *Phormictopus*.

*Plumose stridulating setae (Figs. 6–13, 19–22):* The plumose stridulating setae were named by Perafán et al. (2015) for the genus *Aguapanela*. They are very slender, with the same width along their whole length, and the apical half is covered with many fine and long barbs, giving the appearance of a plume. Similar to the claviform setae, they have the apical end bare. In our dataset, the occurrence of this character did not show any phylogenetic pattern, however in all species analyzed they were found on the pro-and retrolateral faces of the frontal coxae and trochanters in *Lasiodora*, *Nhandu*, *Proshapalopus*, *Pterinopelma*, *Vitalius*, *Acanthoscurria juruenicola*, *A. natalensis* and *A. paulensis*.

*Velvet stridulating setae (Figs. 5, 23–26):* The velvet stridulating setae are characterized by having a robust appearance, being thick and densely covered with fine and short barbs, giving them a velvety appearance. The apex is bare or partially covered by these fine barbs. These setae, named here as velvet stridulating setae (Figs. 23–26) in accordance with Bücherl (1957) (who also drew attention to their velvety morphology), are reported on the prolateral surfaces of coxae I and II in *Lasiodora*.

*Spiniform stridulating setae (Figs. 14, 27–30):* Similar in shape to a leg spine, the spiniform stridulating setae are thick, with a typical surface marked with longitudinal striae. Spines are conspicuously present on theraphosid spider legs, mainly on the tibiae and metatarsi. The spiniform stridulating setae are short, present on the coxae and trocanthers (which is unusual), and interspersed with many fine barbs. We found the spiniform setae on the coxae of *Theraphosa*, and this character was also previously reported by Bertani et al. (2008), who reported their presence in *Pamphobeteus crassifemur* Bertani, Fukushima & Silva, 2008.

**Cladistics.**—The parsimony analyses resulted in a single tree of 103 steps (Fig. 31) with the same topology for all K-values (Table 2), and a consistency index of 0.49 and a retention index of 0.78. For the new characters added to the original

Table 3.—Genera examined and their types of stridulating setae.

| Genera | Claviform | Plumose | Velvet | Spiniform | Figures |
|---|---|---|---|---|---|
| *Acanthoscurria* | X | X | - | - | Figs. 1, 11–13 |
| *Cyrtopholis* | X | - | - | - | Fig. 2 |
| *Theraphosa* | X | - | - | X | Figs. 3, 14 |
| *Brachypelma* | X | - | - | - | Fig. 4 |
| *Phormictopus* | X | - | - | - | Ortiz & Bertani (2005) |
| *Pamphobeteus* | - | - | - | X | Bertani et al. (2008); Figs. 9–12 |
| *Proshapalopus* | - | X | - | - | Fig. 6 |
| *Pterinopelma* | - | X | - | - | Fig. 7 |
| *Lasiodora* | - | X | X | - | Figs. 5, 8 |
| *Nhandu* | - | X | - | - | Fig. 9 |
| *Vitalius* | - | X | - | - | Fig. 10 |

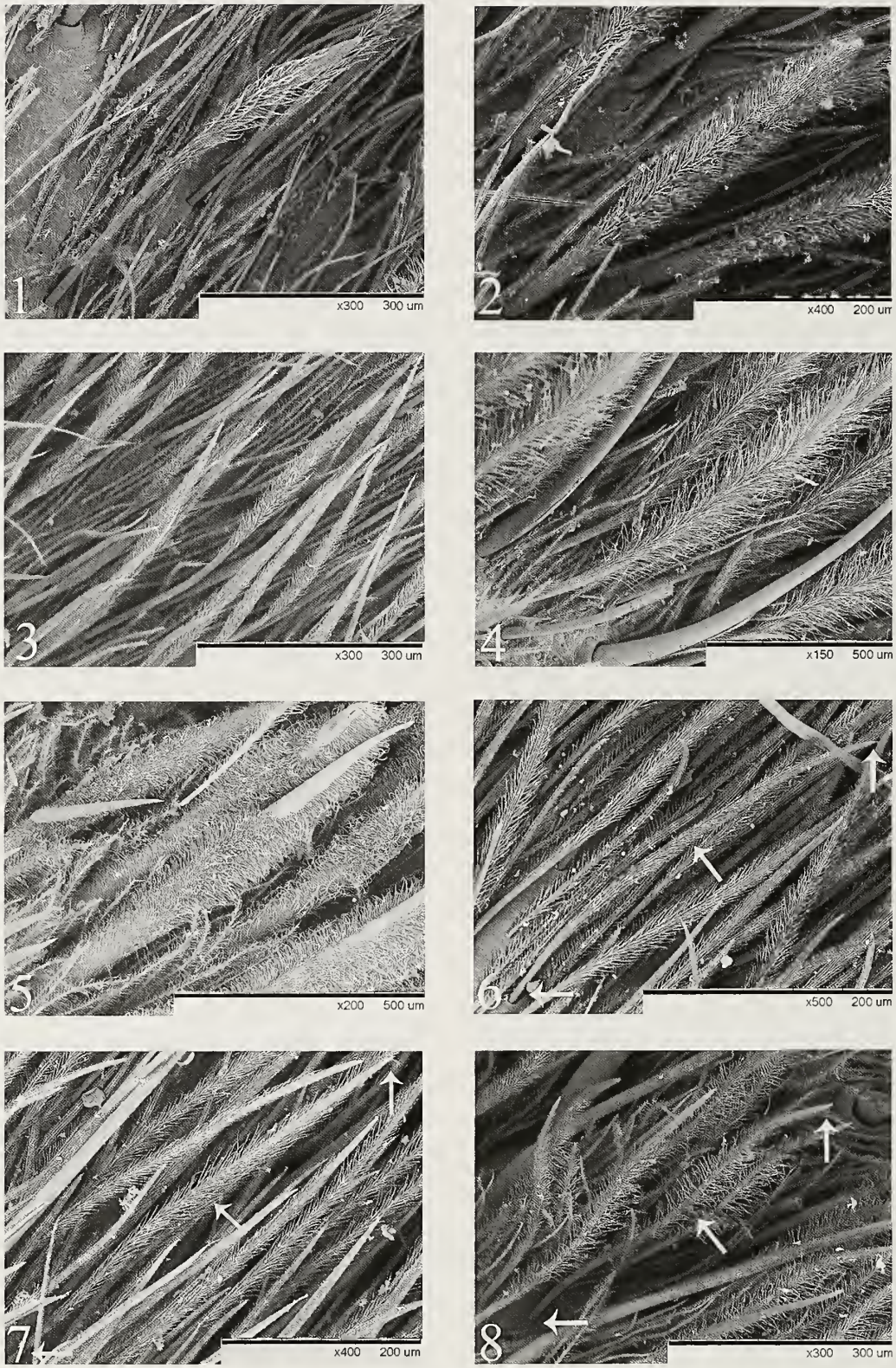


Figures 1–8.—Variations of stridulating setae: (1) claviform stridulating setae of *Acanthoscurria*; (2) claviform stridulating setae of *Cyrtopholis*; (3) claviform stridulating setae of *Brachypelma*; (4) claviform stridulating setae of *Theraphosa*; (5) velvet stridulating setae of *Lasiodora*; (6) plumose stridulating setae of *Proshapalopus*; (7) plumose stridulating setae of *Pterinopelma*; (8) plumose stridulating setae of *Lasiodora*. Arrows show the stridulating setae. Images: A. Galleti-Lima.

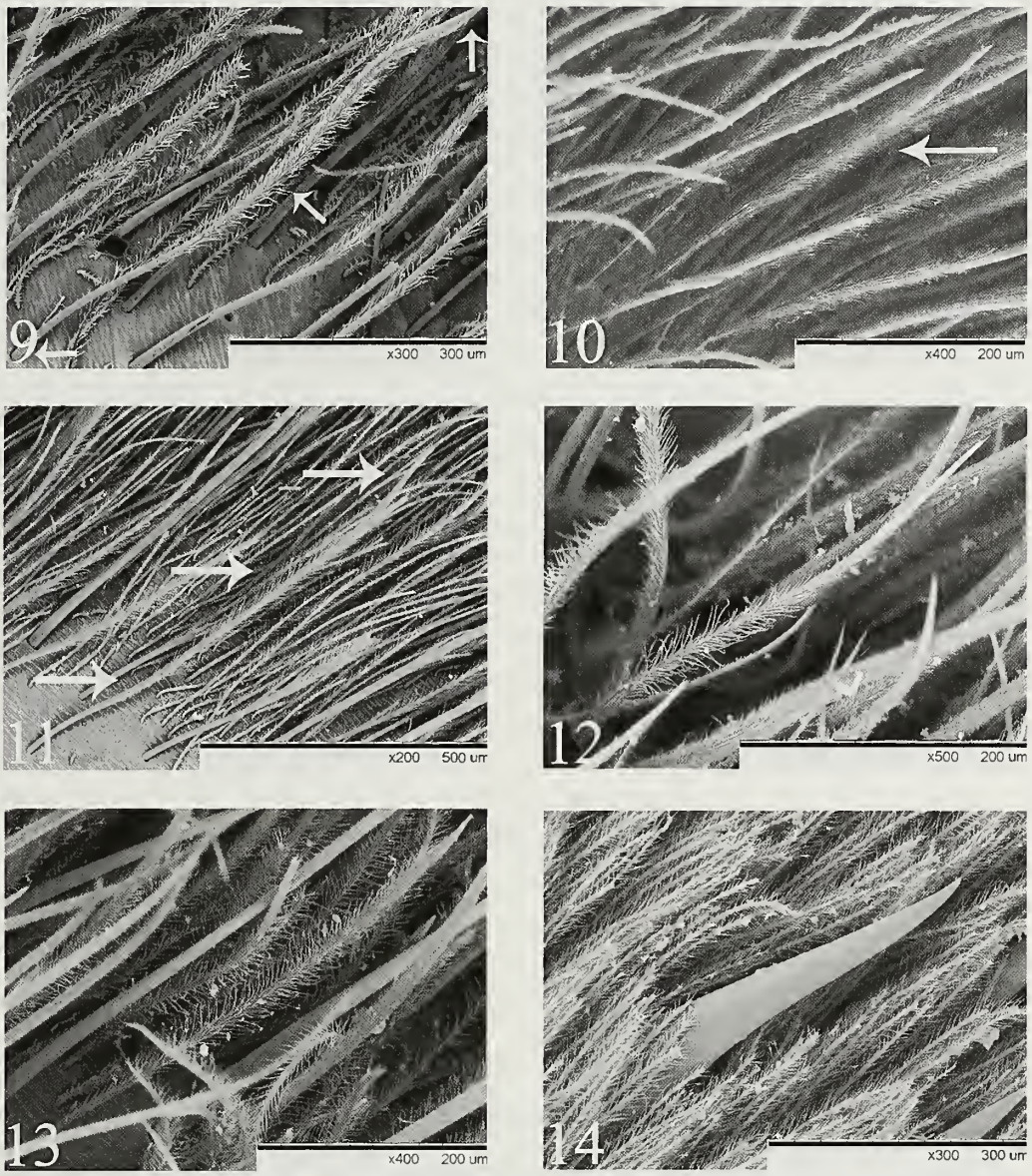


Figures 9–14.—Variations of stridulating setae: (9) plumose stridulating setae of *Nhandu*; (10) plumose stridulating setae of *Vitalius*; (11) plumose stridulating setae of *Acanthoscurria paulensis*; (12) plumose stridulating setae of *Acanthoscurria natalensis*; (13) plumose stridulating setae of *Acanthoscurria juruenicola*; (14) spiniform stridulating setae of *Theraphosa*. Arrows show the stridulating setae. Images: A. Galleti-Lima.

matrix of Bertani et al. (2011), optimizations are as follows: characters 36 (plumose setae on coxae) and 37 (plumose setae on trochanters) emerged as homoplastic synapomorphies that support the clades (*Lasiodora* + *Nhandu* + *Proshapalopus* + *Pterinopelma* + *Vitalius*) and (*Acanthoscurria juruenicola* + *A. natalensis* + *A. paulensis*). Character 38 (claviform setae on coxae) emerged as a homoplastic synapomorphy supporting the clades (*Acanthoscurria* + *Phormictopus cancerides* (Latreille, 1806)) and (*Brachypelma emilia* (White, 1856) + *Theraphosa*). Character 39 (claviform setae on trochanters) emerged as a homoplastic synapomorphy of the clades (*Acanthoscurria* + *Cyrtopholis portoricae* Chamberlin, 1917 + *Phormictopus cancerides*) and (*Brachypelma* + *Theraphosa*). Character 40 (velvet setae on coxae) emerged as an autapomorphy of the genus *Lasiodora*. Character 41 (spiniform setae on coxae) emerged as a homoplastic character, shared by the genera *Pamphobeteus* and *Theraphosa*, whereas character 42 (spiniform setae on trochanters) emerged as an autapomorphy of the genus *Pamphobeteus*.

## DISCUSSION

According to Pérez-Miles et al. (2005), a stridulating seta needs to be strong enough to withstand the intense friction of stridulation. Despite their barbed morphology, these setae can be difficult to recognize under the stereomicroscope. We observed that all setae described here as stridulating present a rigid structure that is most noticeable when one attempts to bend them with fine forceps. Moreover, all stridulating setae documented in this study show a bare basal portion, a distal portion covered with numerous barbs, differing mainly in density among the distinct types, and an apex with a rough surface. However, distinguishing among the setal types is only possible when their ultrastructure has been previously well

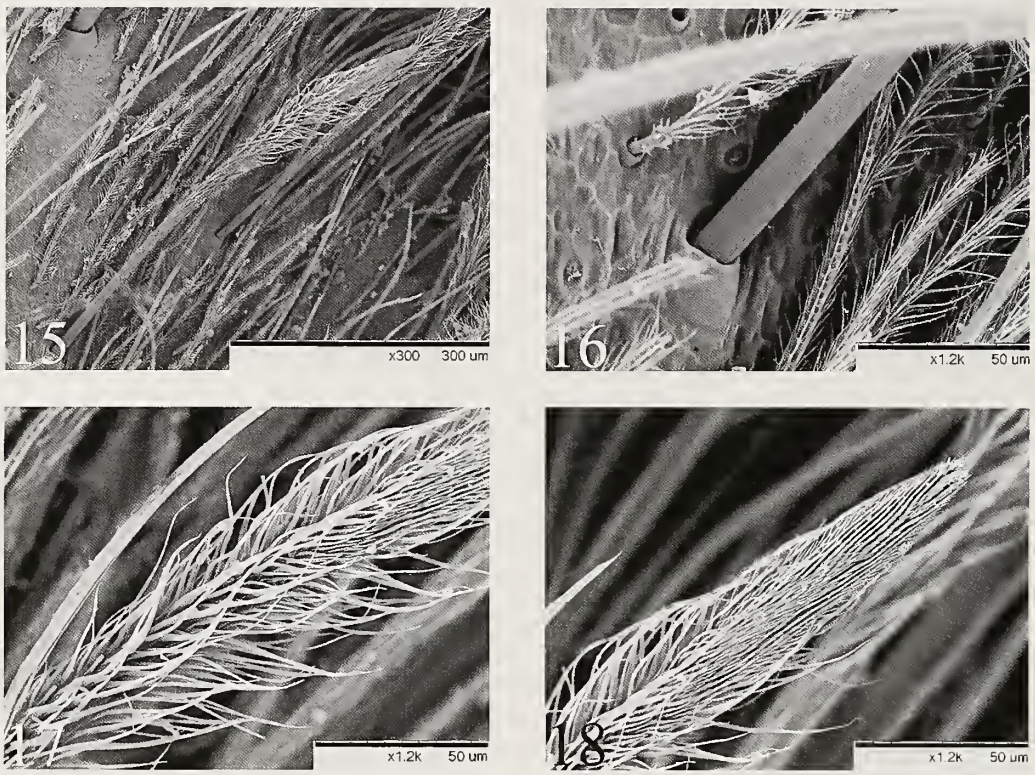


Figures 15–18.—Morphology of claviform stridulating setae; *Acanthoscurria* shown as an example. (15) Overview (arrows indicate a stridulating seta); (16) Base; (17) Middle region; (18) Apex. Photos: A. Galleti-Lima.

examined under the SEM for later comparison under the stereomicroscope. Since the first arachnologists started to notice the presence of distinct setae on the basal leg articles of Theraphosidae (Pocock 1901), there have been numerous proposals for naming these structures. Our study is the first descriptive account that includes examinations under SEM. Therefore, the setal types described above are an attempt to formalize the classification of the distinct variations of these setae.

Table 4.—Changes in terminology of stridulating setae of some Theraphosinae.

| Genera | Name of stridulating setae (literature) | Name of stridulating setae (named in this work) |
|---|---|---|
| ***Lasiodora*** C. L. Koch, 1850 | Plumose<br>Mello-Leitão 1921, Bertani 2001,<br>Perez-Miles et al. 1996 | Velvet |
| ***Acanthoscurria*** Ausserer, 1871 | Clavate<br>Pocock 1903;<br>Claviform<br>Pérez-Miles et al. 2005 | Claviform |
| ***Theraphosa*** Thorell, 1870 | Black spine and plumose setae Gersehman & Schiapelli 1966,<br>Marshall et al. 1995,<br>Tinter 1991,<br>Perez-Miles et al. 1996, Rudloff & Weinmann 2010 | Spiniform and Claviform |
| ***Pamphobeteus*** Pocock, 1901 | Spiniform<br>Bertani et al. 2008 | Spiniform |
| ***Phoruictopus*** Pocock, 1901 | Plumose<br>Perez-Miles et al. 1996, Ortiz & Bertani 2005 | Claviform |
| ***Cyrtopholis*** Simon, 1892 | Clavate<br>Pocock 1903;<br>Plumose<br>Rudloff 1994,<br>Perez-Miles et al. 1996 | Claviform |
| *Aguapauela* Perafán, Cifuentes & Estrada-Gomez 2015 | Plumose<br>Perafán et al. 2015 | Plumose |


Figures 19–22.—Morphology of plumose stridulating setae; *Lasiodora* shown as an example. (19) Overview (arrows indicate a stridulating seta); (20) Base; (21) Middle region; (22) Apex. Photos: A. Galleti-Lima.

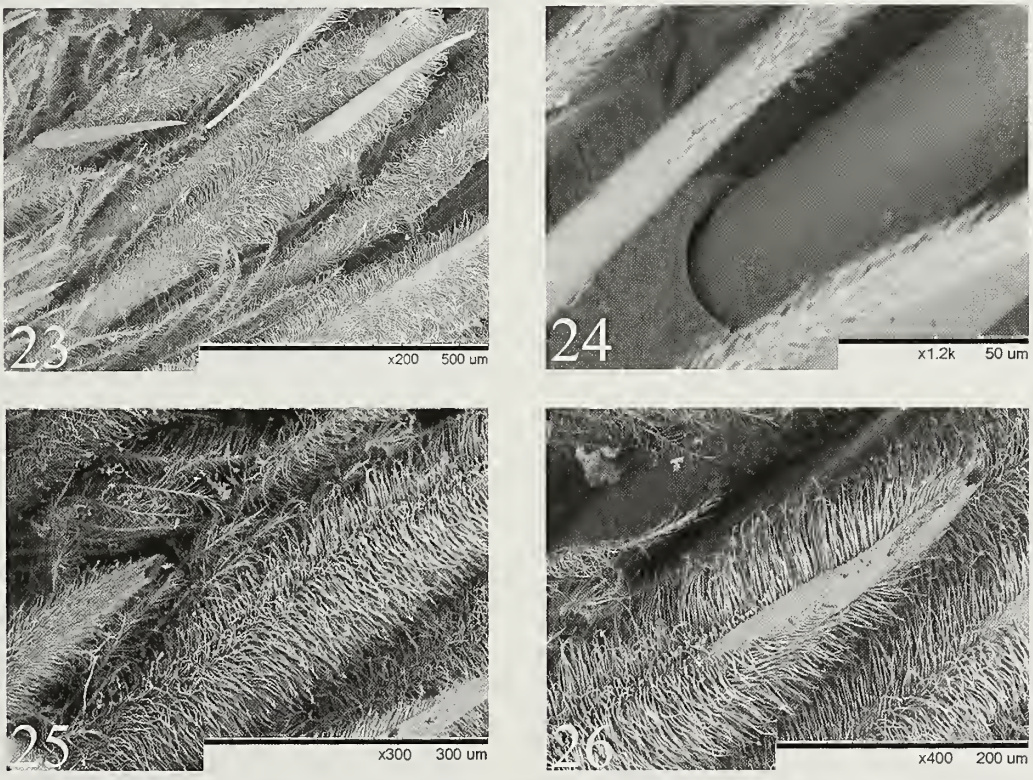


Figures 23–26.—Morphology of velvet stridulating setae; *Lasiodora* shown as an example. (23) Overview (arrows indicate stridulating setae); (24) Base; (25) Middle region; (26) Apex. Photos: A. Galleti-Lima.


Figures 27–30.—Morphology of spiniform stridulating seta: *Theraphosa* shown as an example. (27) Overview; (28) Base; (29) Middle region; (30) Apex. Photos: A. Galleti-Lima.

The variation known as claviform stridulating setae (Figures 15–18) was described by Pérez-Miles et al. (2005) for *Acanthoscurria suina*, on the retrolateral palpal trochanter and on the prolateral trochanter 1, and they were also found on other species of *Acanthoscurria*, *Cyrtopholis* and *Phormictopus*, corroborating their close relationships (Pérez-Miles et al. 1996; Bertani 2000; Perafán et al. 2015). The homoplastic presence of claviform setae in *Brachypelma* and *Theraphosa* was unexpected, as representatives of these two genera have already been reported as possessing a stridulatory apparatus (Pocock 1901; Gerschman & Schiapelli 1966), but were never previously examined under SEM. Ortiz & Bertani (2005) and Rudloff (1994), when describing new species of *Cyrtopholis* and *Phormictopus*, respectively, used the term plumose to refer to the claviform setae, which according to our characterization should be referred to with the latter name.

The plumose setae, considered here, are hardly noticeable in some spiders as they are very thin and may be interspersed with other body and stridulating setae. First reported in the genus *Aguapanela* (Perafán et al. 2015), we also found these setae in *A. jurutenicola*, *A. natalensis*, *Acanthoscurria paulensis*, *Lasiodora*, *Nhandu*, *Proshapalpus*, *Pterinopelma* and *Vitalius*. Other types of setae, such as the velvet setae of *Lasiodora*, were also previously called plumose by Bertani (2001).

The velvet setae are clearly visible on all representatives of the genus *Lasiodora*, being restricted to the upper portion of the prolateral coxae I and II, and characterized mainly by their thick morphology. The velvet setae were resolved as autapomorphic for *Lasiodora*, which are known to produce an audible sound (pers. obs.). Interestingly, velvet setae, along with plumose setae, had not been noticed before in Theraphosinae, and spiders of the genera *Nhandu*, *Proshapalopus*, *Pterinopelma* and *Vitalius* bear only the plumose type, which are rather delicate compared to the velvet type; these genera are not yet known to produce an audible stridulating sound. According to Bücherl et al. (1971) and Bertani et al. (2008), there are other cases of theraphosine spiders producing audible stridulating sounds, and they all bear two distinct types of stridulating setae: *Theraphosa blondi*, which has claviform and spiniform types; some species of *Acanthoscurria*, with plumose and claviform types; and *Pamphobeteus* species, with the spiniform type and possibly also the plumose type. Although we did not have any specimens of *Pamphobeteus* available to scan, the illustrations in Bertani et al. (2008) show some setae very similar to the spiniform type that we describe herein. It is important to note that different stridulating setae may be present on the same individual, as in representatives of *Acanthoscurria jurutenicola*, *A. natalensis* and *A. paulensis* (claviform setae and plumose setae), *Theraphosa blondi* (claviform setae and spiniform setae), and *Lasiodora* species (velvet setae and plumose setae).

The lack of a comparative study including both distinct types of stridulating setae and descriptions of their ultrastructure, and the recognition of these setae by many authors, has resulted in a confusing terminology. As discussed above, the terminology we use for each seta is a proposal to formalize the terminology for similar structures. Table 4 shows the changes in the nomenclature of stridulating setae and the genera in which they occur, according to the literature.

The character coding that we adopt for stridulating setae (i.e., without appendage and surface discrimination) is justified

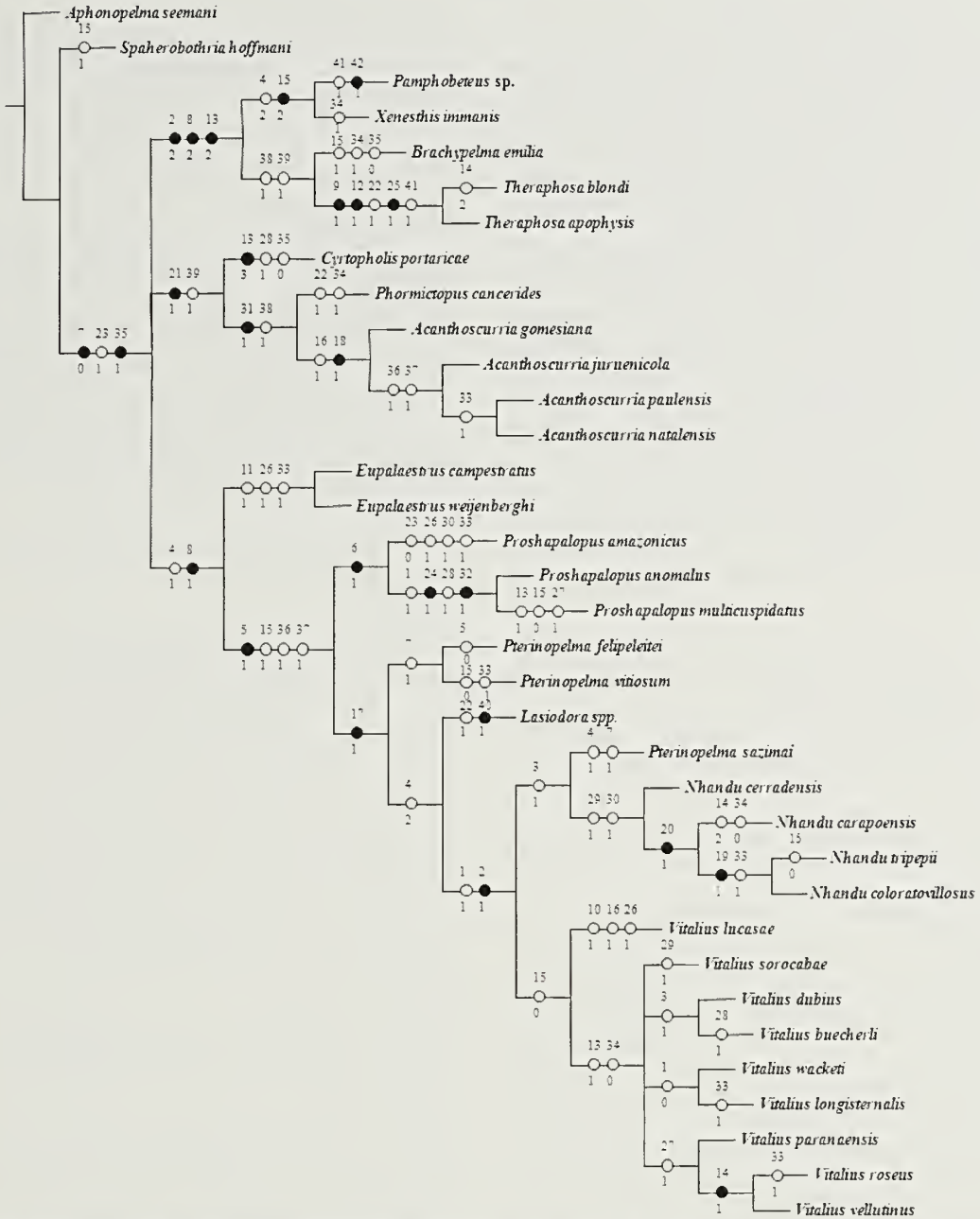


Figure 31.—Cladogram for some species of Theraphosinae, following re-analysis of Bertani et al. (2011). White circles indicate homoplastic character states, and black circles indicate synapomorphies.

by the likely evolution of these structures under serial or iterative homology (Wagner 1989). According to Van Valen (1993), the repetition of homologous structures is, in many cases, guided by copies of the structure on which they originate. Starck (1985) observed that stridulating setae are morphologically different and found in distinct positions, and suggested that these organs aren't homologous, having developed independently within Theraphosinae. However, Haszprunar (1992) explains that during evolution, localized copies of these setae may undergo changes into more specialized structures, as also suggested by Van Valen (1994) based on studies by de Beer (1971) and Roth (1988). Wagner (1989) recognized two types of homology: (1) serial homology, whereby shared similar structures are present on the same organism; and (2) evolutionary homology, whereby shared similar structures are present on different taxa. In the case of evolutionary homology, we should consider the possibility that stridulating setae are modifications of the covering setae, as proposed for the origin and evolution of urticating setae in Theraphosinae (Bertani & Guadanucci 2013).

A more extensive survey with a comparative approach including other representatives of Theraphosinae and Theraphosidae may reveal additional variation among these setae. Moreover, behavioral and functional morphology studies would clarify whether theses setae are in fact stridulating and whether distinct setae produce different vibrating sound wave frequencies. Such a study would require specific and precise equipment for soundwave recording.

## ACKNOWLEDGMENTS

Thanks to Coordenação de Aperfeiçoamento de Pessoa de Nível Superior (CAPES), for financing AGL's Masters degree course, and Conselho Nacional de Desenvolvimento Científico e Tecnológico (CNPq) for funding the project "Atlas morfológico de estruturas cuticulares em aranhas Mygalomorphae (process 479377/2012-0)". Thanks also the Department of Zoology and the Laboratory of Electronic Microscopy (Mônika Iamonte, Antônio Yabuki and Professor Odair Correa Bueno) from the Institute of Biosciences of São Paulo State University (UNESP-Rio Claro); the British Tarantula Society; and the curators of all scientific collections that have helped with this work. Thanks to Dr. Oscar Francke Ballvé, Jorge Mendonza and David Ortiz for their help with the materials of the Colección Nacional de Arácnidos. In particular, we thank Rick West for his help in revising the manuscript; Stuart Longhorn, Rafael Indicatti, Sylvia Lucas, Facundo Labarque, Alexasandro Santana Vieira and Marcio Bolfarine for suggestions for improvements to the manuscript; and Robert Raven for his insightful review of the manuscript.

## LITERATURE CITED

Barth, F.G. 2002. A Spider's World: Senses and Behavior. Springer-Verlag, Berlin, Heidelberg, New York.

Bertani, R. 2000. Male palpal bulbs and homologous features in Theraphosinae (Araneae, Theraphosidae). Journal of Araehnology 28:29–42.

Bertani, R. 2001. Revision, eladistie analysis, and zoogeography of *Vitalius*, *Nhandu*, and *Proshapalopus*; with notes on other Theraphosinae genera (Aranae, Theraphosidae). Arquivos de Zoologia 36:265–356.

Bertani, R. & J.P.L. Guadanueei. 2013. Morphology, evolution and usage of urticating setae by tarantulas (Araneae: Theraphosidae). Zoologia 30:403–418.

Bertani, R., C.S. Fukushima & P.I. Silva-Júnior. 2008. Two new speeies of *Pauphobeteus* Poeoek1901 (Araneae: Mygalomorphae: Theraphosidae) from Brazil, with a new type of stridulatory organ. Zootaxa 1826:45–58.

Bertani, R., R.H. Nagahama & C.S. Fukushima. 2011. Revalidation of *Pterinopelma* Poeoek 1901 with description of a new speeies and the female of *Pterinopelma vitiosum* (Keyserling 1891) (Araneae: Theraphosidae: Theraphosinae). Zootaxa 2814:1–18.

Bücherl, W. 1957. Sobre a importância dos bulbos eopuladores e das apófises tibiais dos maehos na sistemátiea das aranhas earanguejeiras (Orthognatha). Anais da Academia Brasileira de Ciêneias 29:377–416.

Bücherl, W., A. Timotheo Da Costa & S. Lucas. 1971. Revisão de alguns tipos de aranhas earanguejeiras (Orthognatha) estabeleeidos por Cândido de Mello-Leitão e depositados no Museu Naeional do Rio. Memórias do Instituto Butantan 35:117–138.

Coddington, J.A. & N. Seharff. 1995. Problems with zero-length branehes. Cladisties 10:415–423.

Cooke, J.A.L., V.D. Roth & F.H. Miller. 1972. The urticating hairs of theraphosid spiders. Ameriean Museum Novitates 2498:1–43.de Beer, G.R. 1971. Homology, An Unsolved Problem. Oxford Biology Readers 11. London: Oxford University Press.

Ferretti, N., G. Pompozzi & F. Pérez-Miles. 2011. The speeies of *Grammostola* (Araneae: Theraphosidae) from eentral Argentina: taxonomy, distribution, and surfaee ultrastrueture of eoxal setae. Zootaxa 2828:1–18.

Gersehman de Pikelin. B.S. & R.D. Sehiapelli. 1966. Contribueión al eonoeimiento de *Theraphosa lebloudi* (Latreille), 1804 (Aranea: Theraphosidae). Memórias do Instituto Butantan 33:667–674.

Goloboff, P.A., J.S. Farris & J.S. Nixon. 2008. TNT, a free program for phylogenetie analysis. Cladisties 24:774–786.

Guadanueei, J.P.L. 2014. Theraphosidae phylogeny: relationships of "Isehnoeolinae" genera (Mygalomorphae). Zoologiea Scripta 43:508–518.

Haszprunar, G. 1992. The types of homology and their signifieanee for evolutionary biology and phylogeneties. Journal of Evolutionary Biology 5:13–24.

Joequé, R. 2005. Six stridulating organs on one spider (Araneae, Zodariidae): is this the limit? Journal of Araehnology 33:597–603.

Legendre, R. 1963. L'audition et l'émission de sons ehez les Aranéides. L'Année Biologique 2:371–390.

Marshall, S.D., E.M. Thoms & G.W. Uetz. 1995. Setal entanglement: an undeseribed method of stridulation by a neotropieal tarantula (Araneae: Theraphosidae). Journal of Zoology 235:587–595.

Mello-Leitão, C.F. 1921. On the genus *Lasiodora*, C. Koch. Annals and Magazine of Natural History (9)8:337–350.

Mello-Leitão, C.F. 1923. Theraphosoideas do Brasil. Revista do Museo Paulista 13:1–438.

Mirande, J.M. 2009. Weighted parsimony phylogeny of the family Characidae (Teleostei: Characiformes). Cladisties 25:574–613.

Nixon, K.C. 2002. WinClada ver. 1.00.08. Ithaea, NY: Published by the authors.

Ortiz, D. & R. Bertani. 2005. A new speeies in the spider genus *Phormictopus* (Theraphosidae: Theraphosinae) from Cuba. Revista Ibérica de Araenología 11:29–36.

Perafán, C., Y. Cifuentes & S. Estrada-Gomez. 2015. *Aguapanela*, a new tarantula genus from the Colombian Andes (Araneae, Theraphosidae). Zootaxa 4033:529–542.

Pérez-Miles, F., F.G. Costa, C. Toseano-Gadea & A. Mignone. 2005. Eeology and behavior of the "road tarantulas" *Eupalaestrus weijenberghi* and *Acanthoscurria suina* (Aranea, Theraphosidae) from Uruguay. Journal of Natural History 39:483–498.

Pérez-Miles, F., S.M. Lucas, P.I. Silva & R. Bertani. 1996. Systematie revision and eladistie analysis of Theraphosinae (Araneae: Theraphosidae). Mygalomorph 1:33–68.

Poeock, R.I. 1895. Musieal boxes in spiders. Natural Science, London, 6:44–50.

Poeock, R.I. 1897. On the spiders of the suborder Mygalomorphae from the Ethiopian Region, eontained in the eolleetion of the British Museum. Proeeedings of the Zoologieal Soeiety of London 65:724–774.

Poeock, R.I. 1899. A new stridulating theraphosid spider from South Ameriea. Annals and Magazine of Natural History 3:347–349.

Poeock, R.I. 1901. Some new and old genera of South Ameriean Avicularidae. Annals and Magazine of Natural History 7:540–555.

Poeock, R.I. 1903. On some genera and speeies of South Ameriean Aviculariidae. Annals and Magazine of Natural History 7:81–115.

Prentiee, T.R. 1997. Theraphosidae of the Mojave Desert west and north of the Colorado River (Araneae, Mygalomorphae, Theraphosidae). Journal of Araehnology 25:137–176.

Raven, R.J. 1985. The spider infraorder Mygalomorphae (Araneae): eladisties and systematies. Bulletin of the Ameriean Museum of Natural History 182:1–180.

Raven, R.J. 1994. Mygalomorph spiders of the Baryehelidae in Australia and the western Paeifie. Memoirs of the Queensland Museum 35:291–706.

Roth, V.L. 1988. The biologieal basis of homology. Pp. 1–26. *In* Ontogeny and Systematies. (C.J. Humphries (ed.)). Columbia University Press, New York.

Rudloff, J.P. 1994. Two new speeies of *Cyrtopholis* from Cuba (Araneida: Theraphosidae: Theraphosinae). Gareiana 22:7–16.

Rudloff, J.P. & D. Weinmann. 2010. A new giant tarantula from Guyana. Arthropoda Scientia 1:21–40.

Sehiapelli, R.D. & B.S. Gersehman de Pikelin. 1962. Importaneia de

las espermatecas en la sistematica de las arañas del suborden Mygalomorphae (Araneae). Physis 23:69–75.
Schiapelli, R.D. & B.S. Gerschman de Pikelin. 1979. Las arañas de la subfamília Theraphosinae (Araneae, Theraphosidae). Revista del Museo Argentino de Cieneias Naturales 'Bernardino Rivadavia' 5:287–300.
Schmidt, G. 1999. Eine Klassifizierung der Stridulationsorgane. Mitteilungen bei der Deutschen Arachnologischen Gesellschaft 4:3–5.
Schmidt, G. 2000. Zur Klassifizierung der Stridulationsorgane bei Vogelspinnen (Araneae: Theraphosidae). Entomologische Zeitschrift 110:58–61.
Seyfarth, E.A. 1985. Spider proprioception: receptors, reflexes, and control of locomotion. Pp. 230–248. *In* Neurobiology of Arachnids: Springer-Verlag.
Simon, E. 1892. Histoire Naturelle des Araignés. Paris 1:256.
Simon, E. 1903. Histoire Naturelle des Araignées. Paris 2:669–1080.
Smith, A.M. 1995. Tarantula Spiders: Tarantulas of the U.S.A. and Mexico. Fitzgerald Publishing, London.
Starek, J.M. 1985. Stridulationsapparate einiger Spinnen–Morphologie und evolutionsbiologische Aspekte. Zeitschrift für zoolische Systematik und Evolutionsforschung 23:115–135.
Tinter, A. 1991. Eine neue Vogelspinne aus Venezuela *Pseudotheraphosa apophysis* n. gen. n. sp. (Araneae: Theraphosidae: Theraphosinae). Arachnologischer Anzeiger 16:6–10.
Uetz, G.W. & G.E. Stratton. 1982. Acoustic communication and reproductive isolation in spiders. Pp. 123–159. *In* Spider Communication: Mechanisms and Ecological Significance. (P.N. Witt, J.S. Rovner, eds.), Princeton University Press, Princeton, New Jersey.
Van Valen, L.M. 1993. Serial homology: the crests and cusps of mammalian teeth. Acta Palaeontologica Polonica 38:145–158.
Wagner, G.P. 1989. The origin of morphological characters and the biological meaning of homology. Evolution 43:1157–1171.
Wood-Mason, J. 1876. On the gigantic stridulating spider. Annals and Magazine of Natural History 16:96.

*Manuscript received 14 March 2017, revised 23 June 2017.*

2018. Journal of Arachnology 46:226 230

# Response of the eastern sand scorpion, *Paruroctonus utahensis*, to air movement from a moth analog

**Kathryn Ashford, Raven Blankenship, Wyatt Carpenter, Isaac Wheeler** and **Douglas Gaffin**: Department of Biology, University of Oklahoma, Norman, Oklahoma 73019 USA; E-mail: ddgaffin@ou.edu

**Abstract.** Arachnids have many setae that are used as sensory organs. Spiders have been shown to use trichobothria to sense air movements. Scorpions also have trichobothria, located solely on their pedipalps. In scorpions, these trichobothria have been used for taxonomic purposes, due to their systematic variations across taxa. In the lab, buthid scorpions respond to moth-like air vibrations by "hunting" a dummy prey, but scorpionids retreat. The eastern sand scorpion, *Paruroctonus utahensis* (Williams, 1968) is a member of the family Vaejovidae; by measuring its responses to air movements, we can begin to compare behavior of scorpion families. To determine the responses of *P. utahensis* to air stimulus, we created a piston-driven moth analog. To assess the trichobothria as candidate detectors of our air stimulus, we also monitored trichobothrial deflection in response to the moth analog. In behavioral trials, we ran this device for 10 seconds and recorded each scorpion's immediate responses as negative, neutral, or positive. For a control, we ran the device without its piston. Scorpions experienced both conditions. We found a significant difference between scorpions' responses under experimental and control conditions. On average, scorpions responded more negatively to experimental conditions as compared to control conditions. These data suggest that vaejovids, like scorpionids, retreat when they encounter a moth. We also found that our device was effective in stimulating appropriate trichobothrial deflection. Our moth analog could therefore be useful in further studies investigating the physiological mechanisms of prey detection.

**Keywords:** Trichobothria, sensory, orientation, Scorpiones, Vaejovidae

Scorpions hunt primarily by detecting ground vibrations (Brownell 1977). However, scorpions also catch prey such as moths and butterflies when they are in flight (Polis 1979). When the only stimulus is air movement, buthid scorpions exhibit prey-catching behaviors, whereas scorpionids react defensively (Krapf 1988). Other studies show that scorpions also orient themselves with a constant angle to a wind current (Linsenmair 1972).

To sense these air movements, scorpions appear to use thin, hair-like structures called trichobothria that are located on the pedipalps (Hoffman 1967). When researchers removed all the trichobothria from one side of a scorpion's body and presented a stimulus, the scorpion responded by moving toward its intact side (Krapf 1988). The arrangement and number of these trichobothria vary greatly from species to species, making trichobothria useful in systematics (Fet et al. 2005). However, this array certainly has more importance than just as a way to determine relatedness. Scant information exists on the physiological relevance of the trichobothria or how their arrangement and patterns of deflections translate to a behavioral response. As a start, we have produced a simple mechanical device that simulates moth wing flapping movements to generate a relevant air stimulus. We used this moth analog to test the behavioral response of a vaejovid scorpion.

An ecological analysis of a scorpion species of the family Vaejovidae, *Smeringurus mesaensis* (Stahnke, 1957), shows that moths and butterflies make up around 3% of these animals' diet (Polis 1979). Anecdotal field evidence suggests that *Paruroctonus utahensis* (Williams, 1968), another vaejovid, orients toward moths flying overhead. In light of this, we hypothesized that vaejovids would, like buthids, react to our moth analog with prey-catching behaviors. However, our experiment showed that the scorpions exhibited defensive behavior in response to the moth analog.

## METHODS

**Animals.**—We used 20 female *P. utahensis*. Each scorpion was kept in a 3.8 L (14.0 cm diameter, 25.5 cm tall) glass jar containing sand to a depth of about 2.5–5.0 cm and a piece of clay pot. We moistened the sand with 5 mL of water three times weekly. We exposed the animals to a 14:10 hour light:dark cycle and shifted the cycle back one hour a day until the dark part of the cycle began at 1300. We began our trials between 1400 and 1500 and finished them no later than 1600 to take advantage of the time when the animals were most active (Polis 1980). We grouped our animals so half experienced the control condition a day before experiencing the experimental condition, and half vice versa. To control for scorpion hunger level affecting expression of hunting behavior, we deprived the animals of food for 5–7 days prior to testing.

**Apparatus.**—We ran our trials in a 20 cm x 20 cm x 20 cm wooden box, made of ¾ inch (1.9 cm) plywood (Fig. 1A). The wooden box had a large hole in the center of the top for an infrared camera (Nest Cam Indoor, Nest Labs) and a smaller hole for the piston holding the simulated moth. On two opposite sides of the box, a hole 14 cm above the bottom of the box and 8 cm from one side allowed for the crankshaft of the moth analog to go through the box. The interior of the box was dark. The box was set on top of "memory foam" (low-resilience polyurethane foam) to minimize any vibrations.

During the trial, the scorpion being tested was contained within a circular glass bowl (11.3 cm diameter at widest point, 4.50 cm tall) containing sand to a depth of about 5 mm. The sides of the bowl curved out from the bottom and back in at the top. The bowl sat near one corner of the box, with the bowl's outer edge 4 cm from either wall of the box. The bowl sat on top of a small Lazy Susan, for a combined height of 6.3 cm. The piston with the moth analog was centered over the bowl, with the piston's tip 2 cm below the lip of the bowl.

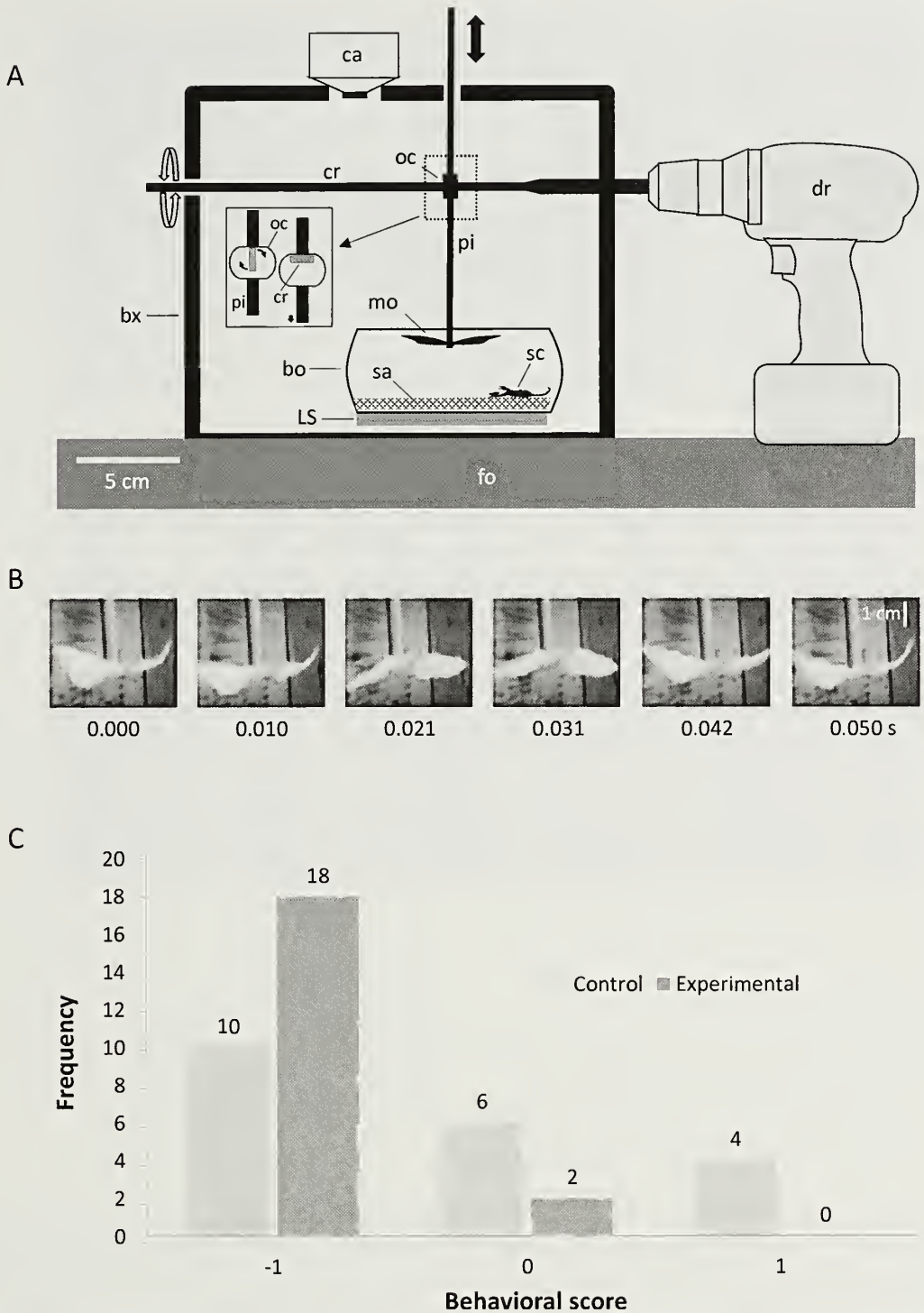


Figure 1.—Experimental apparatus and behavioral results. A: Diagram of the experimental apparatus. The wooden box (bx) covers the experiment and sits atop a 5-em thick layer of memory foam (fo). An infrared camera (ca) is installed at the top of box for monitoring the trials. A drill (dr) powers the crankshaft (cr) that enters the box horizontally. The oblong cuff (oc) surrounds the crankshaft and is attached to the vertical piston (pi) which has the paper towel moth (mo) secured to its lower end. Under the moth is the bowl (bo) that sits on a Lazy Susan (LS) and contains sand (sa) and a test scorpion (sc). The inset shows an expanded, end-on view of the oblong cuff and the resulting vertical displacement of the piston during a quarter turn of the crankshaft. B: Moth wing movement. One flap of the paper towel moth's wings as the piston moves up and down. The wings flapped at a speed of about 20 times per second, and the range of the moth's vertical movement was about 2 cm. C: Frequency of behavioral scores in control and experimental trials. An experimental trial denotes the use of the moth analog, while a control trial denotes the use of the crankshaft without the piston and moth analog. A score of -1 represents movement away from the center of the bowl; 1 denotes movement toward the center of the bowl; 0 means no movement occurred. The mean behavioral scores were significantly different ($P = 0.0039$).

To create the air stimulus, we used a piston-driven moth analog (the "Blankenship device"; Fig. 1A). The piston was connected to the crankshaft by an oblong cuff, which allowed for rotation of the shaft while allowing for only vertical motion of the piston. To further decrease any horizontal movement, the piston came out of a small hole in the top of the box. A drill rotated the crankshaft, driving the piston at 1200 rpm or 1200 "flaps" of the moth's wings each minute (Fig. 1B); this is roughly the same speed at which the geometer moth flaps its wings (Mountcastle & Daniel 2009). Attached to the piston were the two paper towel "wings;" paper towels have a density similar to a moth's wings (Henningson & Bomphrey 2013). The wings, about 2 cm in length, were approximately the same dimensions as the wings of geometer moths, which are known to be eaten by *S. mesaensis* (Polis 1979). To simulate the wing angle of a real moth, the wings were affixed by Scotch Tape (3M Co., Maplewood, MN, USA) to one end of an unfolded paper clip at a 15-degree angle from horizontal. The other end of the paper clip was fastened to the piston by hot glue.

**Trials.**—For each trial, we placed the scorpion in the bowl under an empty film canister and gave it one minute to acclimate. After the acclimation time, we removed the canister, placed the box over the bowl, and allowed for 30 more seconds of acclimation. During this time, the scorpions usually moved from their original position to the edge of the bowl. After the second acclimation period, we began the trial by turning on the Blankenship device for 10 seconds. Our experimental and control trials were the same, except the piston and attached moth were removed in control trials. Between trials, we changed out the sand to eliminate the possibility of influence by the chemicals or footstep patterns left by the previous animal. Each animal underwent both control and experimental conditions; we randomly selected half to experience control conditions first, and the other half experienced experimental conditions first.

**Scoring.**—The infrared camera recorded each trial. After all trials were complete, we analyzed the recordings of the scorpions, assigning them a -1, 0, or 1 based on their behavior. The trial was given a score of -1 if the scorpion moved away from the stimulus in the first 2 seconds of the trial or if the scorpion had an immediate motion around the edge of the bowl. The trial was given a score of 1 if the scorpion moved towards the stimulus in the first 2 seconds of the trial or if the scorpion was located under the stimulus and rotated or moved its claws without moving away from the stimulus. If a scorpion exhibited no response to the stimulus, the trial was given a neutral score of 0. All movement directions were determined by measuring whether movement was toward or away from the center of the bowl, where the moth was centered. Animals that continued moving along the edge of the bowl were scored -1; the only way that an animal starting at the edge of the bowl could be scored a 1 is if it moved toward the center of the bowl. At first, four researchers scored each trial, but after determining that there was high inter-scorer reliability, two researchers (WC, IW) scored the remaining trials in near-real time. In the event of a scoring discrepancy, all four researchers reviewed the footage and resolved the score through a unanimous decision. A two-tailed, Wilcoxon matched pairs test was used to determine whether treatment differences were statistically significant ($P < 0.05$).

**Trichobothrial response.**—To determine if the moth analog produced an effective air stimulus for deflecting the trichobothria, we used foam rubber to restrain a live scorpion and position its right pedipalp about 1 cm from one of the moth's wings (Fig. 2A). Since the microscope precluded use of the wooden box support, we assembled ring stands and various clamps and sleeves to hold the shafts of the crankshaft and piston. We used a 40x dissecting microscope and an adaptor to mount a cell phone to view and video trichobothrial deflection both with and without the drill activated.

## RESULTS

Before the drill was activated at the start of every experimental and control trial, the scorpions tended to move away from their original position in the middle of the bowl. They would often spend a lot of time around the rim of the bowl, trying to climb out. In the experimental trials, the scorpions would often start moving more quickly when the stimulus began, whereas in control conditions they typically continued moving in the same way as they had been moving before. Only one scorpion remained motionless for both its experimental and control trial.

The mean behavioral score was significantly different for the experimental trials as compared to the control trials (experimental: -0.9 ± 0.18 SE, control: -0.3 ± 0.07 SE; $P = 0.0039$, paired two-tailed Wilcoxon test, $n = 20$). The frequency of behavioral scores in control and experimental trials is shown in Fig. 1C. While many scorpions in both trials responded negatively, there were many more positive responses in the control trials than in the experimental trials.

The trichobothrial response to movement of the moth analog is shown in Fig. 2. We monitored the movement of individual trichobothria while the moth analog was on (drill activated) and during the intervening no-stimulus periods (Fig. 2B). A plot of the hair deflections shows slow wafting movements during no-stimulus periods and quick side-to-side deflections consistent with the 1200 wing flaps per minute while the stimulus was on (Fig. 2C).

## DISCUSSION

Other species in the vaejovid family, such as *S. mesaensis*, are known to eat moths occasionally (Polis 1979) and individuals of *P. utahensis* have been seen orienting toward moths in the field (B. Brayfield, pers. comm.). The animals in this study, however, consistently retreated under experimental conditions. Our result was surprising, as it suggests that when exposed to a moth in the field, *P. utahensis* may initially retreat.

There were some limitations to our experiment. Due to their availability, we tested only females' responses. Additionally, since we don't have specific information on the typical diet of *P. utahensis*, our moth analog may not be similar to the kinds of moths these scorpions may encounter and eat in the field. Ideally, we would have exposed the scorpions to air movements from the wings of an actual moth, but it was not feasible to control for potential olfactory or auditory sensory influences when using a real moth.

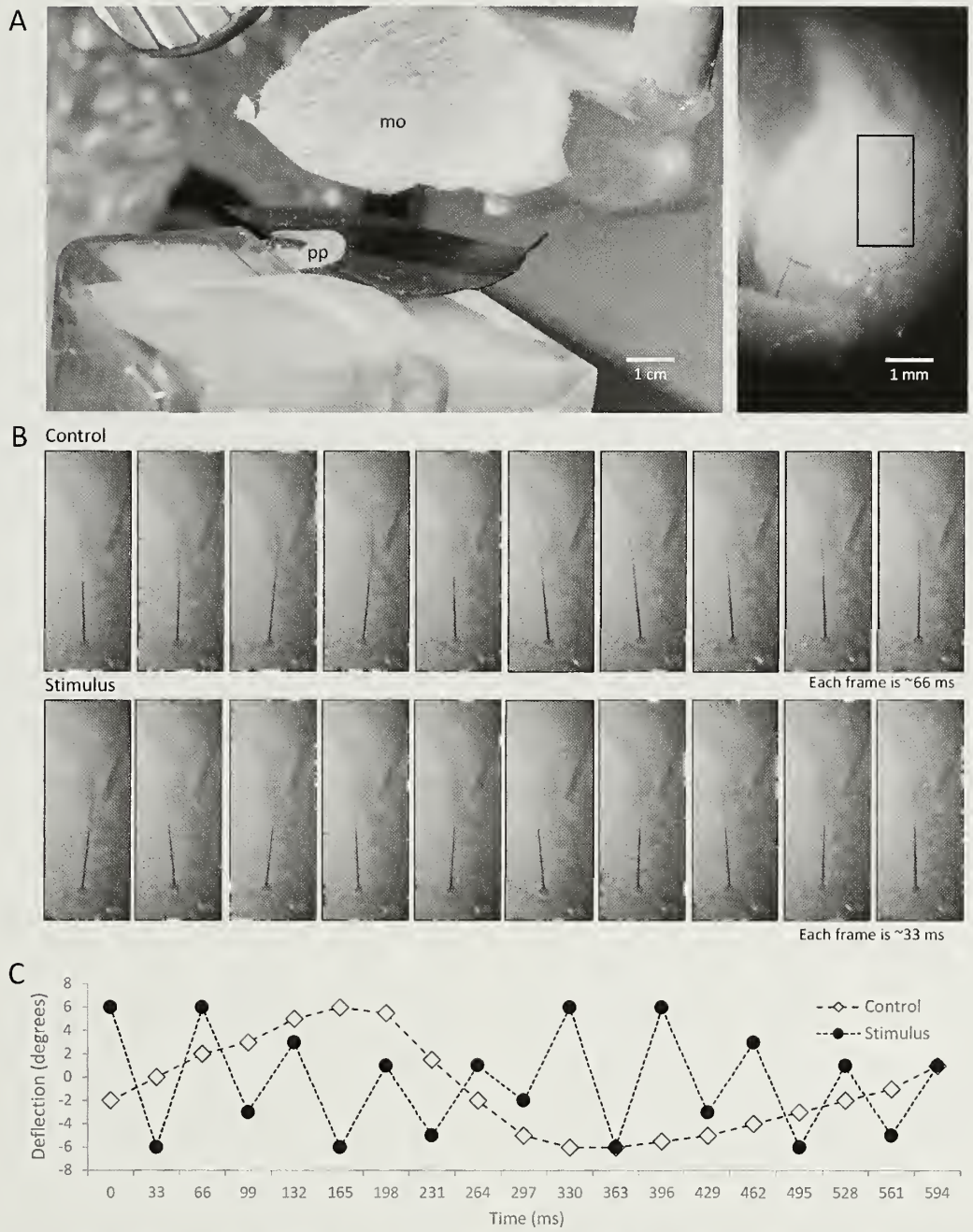


Figure 2.—Trichobothrium response to moth analog. A: A live female *P. utahensis* is restrained within foam inside of a plastic chamber with its right pedipalp (pp) exposed. A set of ring stands and supports allowed operation of the moth analog (mo) within a few cm of the pedipalp. Right: expanded view of pedipalp with the focal trichobothrium highlighted in box. B: Movements of trichobothrium before and during moth stimulation. The upper set of images show normal, baseline swaying of trichobothrium while the moth was stationary (66 ms between each frame). The lower set of images shows a segment of activity while the moth was activated (33 ms between each frame). Highlighting has been added to the lower portion of the trichobothrium shaft to help visualize deflection. C: Comparison of trichobothrial deflection change during stimulus and control situations. The deflection in degrees of a trichobothrium is plotted for both a non-stimulated control section of record across its full breadth of angular movement and for a section of movement during stimulation by the moth analog.

This research could take many future paths. For example, studying the responses of scorpion families other than buthids or vaejovids could uncover a pattern in, or an explanation of, behavioral differences between species. Other studies could focus on perfecting the moth analog; by conducting ecological analyses on different species of scorpions, we could match the analog's size and speed to that of a moth that a scorpion species is known to eat in the field. Additionally, varying the size, wing speed, duration of wing movement, or distance of the moth stimulus to the scorpion would contribute to a better understanding of the kinetics of the scorpions' behavioral responses. A longer

stimulus exposure could allow scorpions to show a changing response, such as an initial retreat followed by a return to the area of stimulus.

The mocked-up test we used to visualize trichobothrial deflection showed that the moth analog did in fact cause commensurate deflections of trichobothria. Here we report the deflection of a single trichobothrium; however, when panned out we saw that several trichobothria reacted to the stimulus. Each trichobothrium has its own plane of oscillation, which means that it takes two or more trichobothria working in concert to provide the scorpion with directional information about the source of a movement (Hoffmann 1967). While the trichobothria remain candidate receptors, additional behavioral tests involving animals with their trichobothria removed or covered are necessary to determine if these sensilla are responsible for sensing the air movements of the moth analog or if another sensory organ may be involved, such as the constellation array on the fixed finger of the scorpion (Fet et al. 2006).

## ACKNOWLEDGMENTS

We thank Brad Brayfield for his guidance and encouragement through every step of this process and Mariëlle Hoefnagels for her critical review of the manuscript. We also thank the University of Oklahoma Department of Biology and the University of Oklahoma Honors College for making this project—and the class in which it was conceived and executed—possible. Finally, we thank Julie Chen and the University of Oklahoma Innovation Hub for their instrumental part in designing and producing the Blankenship Device.

## LITERATURE CITED

Brownell, P.H. 1977. Compressional and surface waves in sand: Used by desert scorpions to locate prey. Science 197:479–482.

Fet, V., M.S. Brewer, M.E. Soleglad & D.P.A. Neff. 2006. Constellation array: a new sensory structure in scorpions (Arachnida: Scorpiones). Boletín Sociedad Entomológica Aragonesa 38:269–278.

Fet, V., M.E. Soleglad & G. Lowe. 2005. A new trichobothrial character for the high-level systematics of Buthoidea (Scorpiones: Buthida). Euscorpius 23:1–40.

Henningson, P. & R.J. Bomphrey. 2013. Span efficiency in hawkmoths. Journal of the Royal Society Interface 10:1–9.

Hoffmann, C. 1967. Bau und function der trichobothrien von *Euscorpius carpathicus* L. Zeitschrift für Vergleichende Physiologie 54:290–352.

Krapf, D. 1988. Prey localization by trichobothria of scorpions. Proceedings of the European Society of Arachnology 11:29–34.

Linsenmair, K.E. 1972. Anemomenotactic orientation in beetles and scorpions. Pp. 501–510. *In* Animal Orientation and Navigation. (S. Galler, K. Schmidt-Koenig, G. Jacobs & R. Belleville, eds.) NASA, Washington, D.C.

Mounteastle, A.M. & T.L. Daniel. 2009. Aerodynamic and functional consequences of wing compliance. Experiments in Fluids 46:873–882.

Polis, G.A. 1979. Prey and feeding phenology of the desert sand scorpion *Paruroctonus mesaensis*. Journal of Zoology 118:333–346.

Polis, G.A. 1980. Seasonal patterns and age-specific variation in the surface activity of a population of desert scorpions in relation to environmental factors. Journal of Animal Ecology 49:1–18.

Stahnke, H.L. 1957. A new species of scorpion of the Vejovidae: *Paruroctonus mesaensis*. Entomology News 68:253–259.

Williams, S.C. 1968. Scorpion preservation for taxonomic and morphological studies. Wasmann Journal of Biology 26:133–36.

*Manuscript received 8 July 2017, revised 15 December 2017.*

2018. Journal of Arachnology 46:231–239

# From storage to delivery: sperm volume and number of spermatozoa inside storage organs and ejaculates in males of *Timogenes elegans* (Scorpiones: Bothriuridae)

**David Eduardo Vrech**[1,2,3], **Paola Andrea Olivero**[1,2], **Camilo Iván Mattoni**[1,2] and **Alfredo Vicente Peretti**[1,2,3]: [1]Universidad Nacional de Córdoba, Facultad de Ciencias Exactas, Físicas y Naturales, Departamento de Diversidad Biológica y Ecología, Córdoba, Argentina; E-mail: dvrech@gmail.com; [2]Consejo Nacional de Investigaciones Científicas y Técnicas (CONICET), Instituto de Diversidad y Ecología Animal (IDEA), Laboratorio de Biología Reproductiva y Evolución, Córdoba, Argentina; [3]Catedra de Diversidad Biológica II.

**Abstract.** Sperm competition influences the evolution of many reproductive traits such as gonads, sperm or genitalia. Many sperm competition analyses concentrate in testes and ejaculates. Among arachnids, scorpions constitute an intriguing taxon for examining sperm production and usage. For example, in the family Bothriuridae the females of *Timogenes elegans* Mello-Leitão, 1931 accept more than one male per reproductive season and males produce spermatozoa continuously, storing them inside two elastic storage organs (i.e., two seminal vesicles plus two deferent ducts) before inseminating females, using a sclerotized spermatophore. In this study, we analyzed the sperm storage organs and the ejaculate volume transferred by *T. elegans*. We described the volume and number of spermatozoa at storage sites and in ejaculates, and investigated ejaculate volume and concentration in remating experiences. Storage organs varied in total size. Inside the spermatophore, the volume of the sperm drop represented 38% of the volume of both sperm storage sites. The remaining space around the sperm drop is filled with a gel-like substance. The ejaculate volume and spermatozoa number did not vary significantly between consecutive matings. *Timogenes elegans* stored abundant sperm inside the seminal vesicles. Available sperm was divided equally between both storage organs, and ejaculates were diluted in the spermatophore, presumably, with the gel stored in the trunk. There was no effect of body condition over any of the variables analyzed. Male sperm storage and ejaculate production are discussed considering the sperm depletion hypothesis and the sperm competition theory.

**Keywords:** Scorpion, storage organs, ejaculates, sperm transfer, sperm numbers.

Sperm competition is an important evolutionary driver in postcopulatory sexual selection, which occurs in polyandrous species when the sperm of different males compete for the access to the ova (Parker 1970; Birkhead & Moller 1998; Parker & Pizzari 2010). Sperm competition influences the evolution of many morphological, physiological, and behavioral traits that are directly related to reproduction (Andersson 1994; Birkhead & Moller 1998; Wigby & Chapman 2004; Simmons 2014). Most studies have focused on the effect of sperm competition on testes mass, followed by the analysis of ejaculate production (Parker & Ball 2005; Simmons 2014). Testes mass is accepted as a good proxy for sperm competition risk (Parker et al. 1997; Parker & Ball 2005). However, the dynamics of sperm production can vary (Moller 1991; Schärer & Vizoso 2007; Vahed & Parker 2012) and thus sperm production is challenging to assess, mainly because the production rate of sperm is often hard to quantify (Schärer et al. 2004).

Seminal vesicles are storage organs usually found in males of many arthropods (Wedell et al. 2002). Seminal vesicles are thought to influence the outcome of sperm competition in many taxa, mainly through seminal secretions that may help, for example, sperm maintenance and viability (Ramm et al. 2005). Besides, and linked to sperm competition, it has been shown that males of species that store sperm seem to produce more sperm than species that do not store it (Orr & Zuk 2013). The seminal secretions may be generated in an accessory gland or be a product of secretory cells in the primary reproductive system (Leopold 1976). In spiders, the seminal fluid is comprised of spermatozoa and secretions, which are produced by the somatic cells of the testis (e.g., Michalik & Huber 2006; Michalik & Ramirez 2014). In solpugids, the genital chamber seems to produce a secretion that is thought to be essential for sperm transfer. The deferent ducts and the glandular part of testes contribute to the secretion that helps to form the sperm droplet, similar to what happens in actinotrichid mites (Alberti & Coons 1999; Klann 2009).

Although males can produce, maintain, and store sperm, they may become depleted of sperm at some point during the reproductive season. For example, sperm depletion may arise as a consequence of the energetic demand of generating an ejaculate (Dewsbury 1982; Rubolini et al. 2007; Parker & Pizarri 2010). This cost is a result of spermatozoa being delivered together with accessory fluids (Dewsbury 1982). These fluids may be involved in many tasks, like maintaining spermatozoa, generating reluctance to mate with a subsequent male, (Chapman 2001; Arnqvist & Andrés 2006), or contributing to the formation of a genital plug (Kaufman et al. 2008; Dennenmoser & Thiel 2015).

Males may also become sperm depleted because of their inability to produce sperm continuously during adulthood (Barr 1974; Chapman 1998; Manogem 2002; Boomsma et al. 2005; Bressac et al. 2008). For example, spiders produce sperm during adulthood (Michalik & Uhl 2005), but there are some unusual cases in which spermatogenesis ends before the final molt (Michalik et al. 2010; Michalik & Rittschof 2011). The testes decrease in size and degenerate towards the end of adulthood. As a result, the amount of sperm available for mating is limited to the sperm inside the pedipalps, and adults lose their ability to fertilize eggs once it is used. For example,

Schneider & Michalik (2011) discussed the evolution of mating tactics in three species of *Nephila* Leach, 1815. They suggested that males that can reverse to polygamy developed the potential to economize their limited sperm supply, but they failed to produce sperm as adults. In other arachnids, such as solpugids, it has been suggested that spermatogenesis is completed after reaching adulthood (Klann et al. 2005). In this scenario, males should allocate sperm strategically over successive matings because it is a limited resource (Simmons 2014).

Among arachnids, scorpions constitute an intriguing taxon for analyzing sperm production. Males produce sperm continuously in paired testes (Jespersen & Hartwick 1973; Alberti 1983; Michalik & Mercati 2010; Vrech et al. 2014) and store it in two seminal vesicles (Polis & Sissom 1990; Peretti & Battán-Horenstein 2003; Vrech 2013). Males of some species may produce seminal secretions that are transferred to the female during mating (Peretti & Battán-Horenstein 2003). In some species, the cylindrical gland may secrete substances that can contribute to the formation of a genital plug inside the genital atrium of inseminated females (Vachon 1953; Hjelle 1990; Peretti 2010). Sperm is transferred indirectly inside a sclerotized spermatophore deposited on the ground (Francke 1979; Hjelle 1990; Peretti 2010).

In the family Bothriuridae, *Timogenes elegans* Mello-Leitão, 1931 is in many aspects an exciting species for analyzing sperm production. Firstly, each female copulates with more than one male per reproductive season (Peretti 1993; Vrech et al. 2011). At the same time, males can accept more than one female during the entire reproductive season (Peretti 2003). Secondly, males produce sperm continuously in their paired testes and store them in two elastic storage organs (i.e., two seminal vesicles plus two deferent ducts) (Peretti & Battán-Horenstein 2003). However, contrary to the situation in other bothriurid species, *T. elegans* males lack accessory glands inside their genital system, and there is no production of a visible genital plug (Peretti & Battán-Horenstein 2003). Finally, *T. elegans* is a suitable model species, as individuals show a considerable body size, respond adequately to laboratory conditions, perform complete mating sequences, and are abundant in the Chaco region of Argentina (Acosta 1995; Ojanguren-Affilastro 2005).

Data on *T. elegans* suggest that males show relatively small testes mass compared to other closely related species (Vrech et al. 2014). So far, studies on *T. elegans* have only focused on the description of the reproductive system (Peretti & Battán-Horenstein 2003), sperm conjugation and its morphology (Vrech et al. 2011), as well as on the effects of polyandry on testes mass (Vrech et al. 2014). However, the volume of the storage organs and ejaculates, their concentration, and the dynamics of sperm production in light of consecutive mating events have never been evaluated.

In this study we (1) analyze the volume of the seminal vesicles and calculated the number of spermatozoa inside them; (2) measure the volume and number of spermatozoa of the male's ejaculate and (3) present data on ejaculate volume and sperm numbers in subsequent multiple matings. We hypothesize that (1) sperm production will be abundant since males of *T. elegans* may be under sperm competition and will produce and store a high amount of sperm; (2) Sperm number will not vary from storage organs to ejaculates, as this species lacks accessory glands that may produce diluents; (3) Sperm volume will not decrease in successive multiple matings due to continuous sperm production, and may in fact increase due to sperm competition (Parker & Pizzari 2010).


Figure 1a.—Adult male of *Timogenes elegans*.

## METHODS

**Specimen sampling and rearing.**—Adult males ($n = 20$) and females ($n = 10$) of *T. elegans* (Fig. 1a) were collected during the night using ultraviolet lamps in the Parque Provincial and Reserva Forestal Chancaní (31°22′13.21″ S, 65°27′13.75″ W, Córdoba, Argentina) in January 2011. Captured individuals were kept in cylindrical plastic vials (8 cm height x 10 cm diameter) with sand as the substrate and moistened cotton as a water supply. Specimen were fed on a 15-day basis with larvae of *Tenebrio* sp. (Insecta, Coleoptera). Voucher specimens are deposited in the scorpion collection of the Laboratorio de Biología Reproductiva y Evolución of the Universidad Nacional de Córdoba (IDEA, UNC-CONICET; curated by C. I. Mattoni).

**Sperm storage organs and ejaculates.**—Adult males were dissected dorsally, and the paraxial organs were removed ($n = 20$). Then, both testes were cut at the base of the deferent duct (Fig. 2a). The dissection at this level avoided massive sperm loss (Vrech, pers. obs.). The volumes of the deferent ducts were negligible, mainly due to their small magnitude. Therefore, we focused only on seminal vesicles (Fig. 2a). Finally, right and left storage organs were isolated from their respective paraxial organ.

For the volume of sperm inside the storage organ, we took pictures of the seminal vesicles contained in the paraxial organs (Fig. 2a). The length and width of these vesicles were measured, and we used the volume of a cylinder as a proxy to the total volume of the seminal vesicle. The formula used was $V = \pi\ r^2\ h$. The radius (r) was an average obtained by measuring the diameter of the seminal vesicle at three places along the entire seminal vesicle length (h). We then divided the mean diameter by two to get the average radius of the structure. All measurements were taken three times by the same person for consistency. After calculating the volume of each vesicle, we evaluated the difference in volume between them with a Wilcoxon signed-rank test. We used the

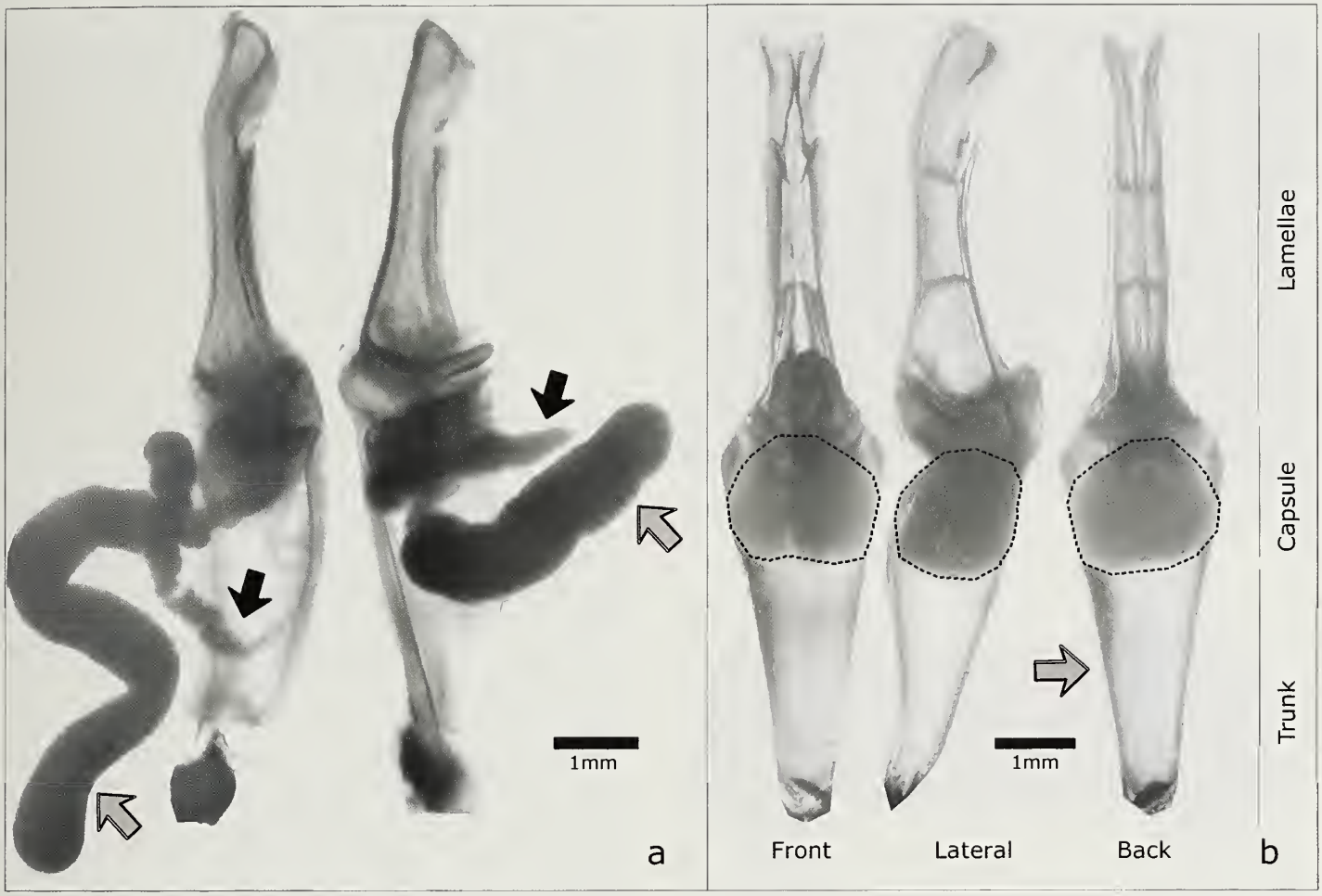


Figure 2.—Seminal vesicles and ejaculates in males from *T. elegans*. (a) Two left paraxial organs from two different males of *T. elegans*. Seminal vesicles (gray arrows). Notice that both vesicles are full of sperm. The small pouches (black arrows) are the vas deferens and correspond to the connections between seminal vesicles and testes. (b) Pre-insemination spermatophore of *T. elegans* in three different views. Three zones can be observed: the lamella, the capsule, containing the ejaculate (dotted polygon), and the trunk, filled with a transparent gel-like substance (gray arrow).

*wilcox.test* function of the package stats in R (R Core Team 2016).

For measuring ejaculates, spermatophores were obtained in laboratory matings ($n = 16$) performed in a mating arena (18 cm x 30 cm with 30 cm height) with sand as the substrate with bark and stones to resemble the natural habitat (Maury 1982). For acclimation, the female was placed in the arena one hour before starting the trial. The mating trial started when we placed the male in the test arena and was stopped after spermatophore deposition on the substrate, but right before sperm transfer. After each mating trial, the arena was washed with ethanol 70%, and the substrate was changed. Each spermatophore was removed from the soil, photographed, and manually deployed over a slide, obtaining the entire ejaculate content. We measured the volume of the sperm drop inside the spermatophore (Fig. 2b) and after extraction (ejaculate) (Fig. 3a) to see if the volume is modified with spermatophore deployment. To estimate the volume of the sperm drop inside the spermatophore, we used the volume of a sphere ($V = 4/3\ \pi\ r^3$). The radius (r) was obtained dividing the diameter of the sperm drop by two in a picture of the frontal view of the spermatophore. All measurements were taken three times by the same person for consistency.

To estimate the volume of the ejaculate, we adapted a technique based on Gage (1994). We used two microscope slides separated by the height of a single coverslip (Fig. 3b). Coverslips were put on each side of the sperm storage organs or the ejaculate to avoid collapsing. After deposition, a second slide was placed over the coverslips resulting in a controlled crush of the sample. The pressure on the slides was uniform due to the use of four binder clips, each placed in a corner. The space between the coverslips was controlled on each analysis by measuring three sites along the length of the slide. The space remained uniform in all measurements ($0.1729 \pm 0.0054$, $n = 48$; i.e., 16 spermatophores, three measurements each). The pressure of crushing scattered sperm homogeneously within an area ($mm^2$). We measured this area with the Image J 64 bits image-processing software (Schindelin et al. 2015). The volume ($mm^3$) was obtained by multiplying the measured area by the height left between the coverslips. All volumes obtained in $mm^3$ were converted to ml ($1\ mm^3 = 0.001$ ml).

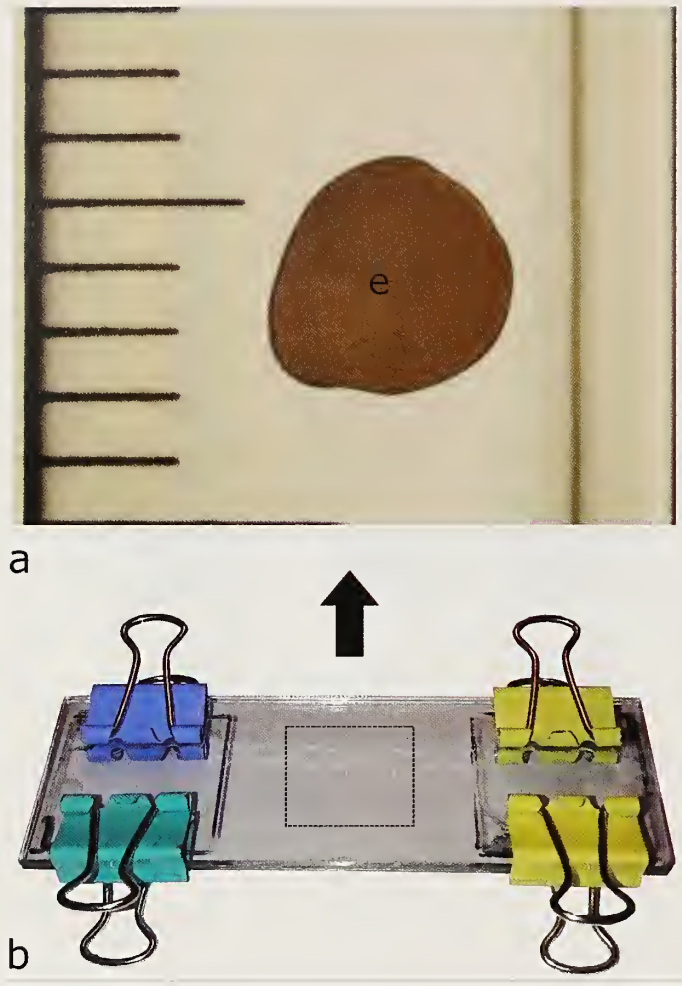


Figure 3.— Ejaculate and device used for measuring its volume. (a) Sperm drop from a manually deployed spermatophore (ejaculate). This ejaculate lays between two microscope slides. (b) Device used to measure the volume of the sperm drop. The zone occupied by the coverslips is delineated with a black marker and is pressed with binder clips. The dotted square represents the area shown in Figure 3a. Abbreviation: e: ejaculate.

*Spermatozoa number:* Fresh storage organs were immersed in saline solution ($NaCl_2$ 0.9 gm/ 100 ml distilled water) and cut to liberate sperm packages. Sperm packages were collected using a 10 µl micropipette with 1 µl gradations (Finnpipette, Thermo Scientific) and mixed with 100 µl of saline solution. Spermatozoa were released from sperm packages after 5 minutes of vortexing. Spermatozoa were counted using a Neubauer counting chamber, following the basic protocol for counting cells (Bukowski & Christenson 1997; Bastidas 2014). Spermatozoa were counted in the four big squares at the corners of the chamber's grid. Additionally, the variation coefficient was used to evaluate the changeability in sperm supply in the storage organs as well as in the ejaculate. To compare the spermatozoa numbers of storage sites and the ejaculate, a Negative Binomial Generalized Linear Model test was performed using the *MASS* package (Venables & Ripley 2002) in R (R Core Team 2016).

*Male body weight:* Variables of storage organs, ejaculate volume, and sperm counts were regressed against body weight to analyze the possible influence of an energy trade-off in sperm production ($n = 13$). Data were modeled using GLM function from the *stats* package in R. For each variable, the distribution was assessed graphically with a Cullen and Frey graph in R using the *descdist* function from the *fitdistrplus* package (skewness-kurtosis plot) (Delignette-Muller & Dutang 2015), and statistically with a chi-square test. We used a gamma distribution for vesicle volume, gaussian for ejaculate volume, and negative binomial for counts of spermatozoa in the seminal vesicles and ejaculates. We used the package *glmmADMB* for R (Bolker et al. 2012).

*Sperm volume and number over two consecutive matings:* Adult males were captured in January 2011 and 2012 ($n = 10$). Mating trials were scheduled weekly during the mating season (January-February) to obtain more than one spermatophore per male. The volume of the sperm drop inside the spermatophore and number of spermatozoa were measured on each of the spermatophores produced by the males following the techniques described in the previous section. A generalized linear mixed model approach with the packages *lme4* (Bates et al. 2014) and *glmmADMB* was used to evaluate differences between successive matings. The volume and number of sperm were the response variables, and mating (first or second) was the fixed factor. We used the identity of the male as a random factor, and in both models the variance of the random effect was negligible.

Table 1.—Absolute values of the volume of seminal vesicles, sperm drop (drop contained inside the spermatophore), ejaculate (sperm drop that came out of the spermatophore) and full spermatophore volume expressed in ml. Here, values are shown as the sum of both seminal vesicles. Spermatophore relates to the total volume that a spermatophore can contain. Values are given as mean± SD. cv: coefficient of variation

| | Vesicles ($x10^3$ ml) | Sperm drop ($x10^3$ ml) | Ejaculate ($x10^3$ ml) | Spermatophore ($x10^3$ ml) |
|---|---|---|---|---|
| *Mean* | 9.54 ± 3.35 | 2.35 ± 0.99 | 2.04 ± 0.74 | 6.23 ± 1.03 |
| *cv* | 35% | 42% | 36% | 17% |

## RESULTS

**Sperm volume in storage organs and spermatophore.**—In the storage organs, the seminal vesicle was always filled with sperm (Fig. 2a). The deferent ducts were usually less fully filled (black arrows in Fig. 2a). The volumes of the seminal vesicles showed a coefficient of variation of 35% among males (Table 1). Both seminal vesicles (right and left) had similar volumes (Wilcoxon rank paired test; $V = 76$, $P = 0.38$). Seminal vesicles stored 4.67 times the volume of the ejaculate delivered inside the spermatophore (see Table 1).

Sperm inside the spermatophore (sperm drop) did not differ with the ejaculate that was extruded from the spermatophore (Wilcoxon rank paired test; $V = 71$, $P = 0.90$) (Table 1). The sperm drop inside the spermatophore represented a part (38%) of the total volume of the spermatophore (Fig. 2b). The total volume of the available storage place within the spermatophore was larger than the volume of the sperm drop and the ejaculate (Table 1). This remaining space inside the spermatophore was filled with a gel-like substance, mainly located at the

Table 2.—Volume and numbers of spermatozoa inside spermatophores deposited in two consecutive mating events.

| Matings | Ejaculate volume ($x10^3$ ml) | Spermatozoa number ($x10^{10}$) |
|---|---|---|
| *Male 01* | | |
| 1 | 2.58 | 0.56 |
| 2 | 2.44 | 0.23 |
| *Male 05* | | |
| 1 | 2.41 | 1.84 |
| 2 | 3.56 | 3.25 |
| *Male 06* | | |
| 1 | 2.29 | 1.03 |
| 2 | 2.40 | 2.89 |
| *Male 09* | | |
| 1 | 3.13 | 0.17 |
| 2 | 3.14 | 0.05 |

bottom of the capsule, filling the trunk, around the sperm drop (Fig. 2b, grey arrow). The ejaculate consisted of the sperm drop inside the spermatophore and part of the gel-like substance, which comes out with sperm after spermatophore activation.

Male body weight did not correlate with the volume of the storage organs (GLM $z = 1.35$; $P = 0.18$). There was a positive influence of male body weight on the ejaculate volume (GLM $z = 2.89$; $P = 0.0039$).

**Sperm counts inside storage organs and spermatophores.**—Inside the seminal vesicle, sperm number was $1.32 \pm 9.41 \times 10^{11}$, and inside the spermatophore $1.67 \pm 1.13 \times 10^{10}$ spermatozoa. The coefficient of variation of spermatozoa numbers was 0.71 and 0.67 respectively, and there was a difference between both counts (Negative Binomial GLM, $z = 7.151$, $P = 8.59 \times 10^{-13}$). The number of spermatozoa contained inside the spermatophore represented 13% of the spermatozoa stored inside both storage organs.

Male body weight did not influence sperm number within the storage organs or ejaculates (GLM sperm count in storage organs, $z = -0.05$, $P = 0.96$; GLM sperm count in ejaculates, $z = 0.57$, $P = 0.57$).

**Volume and sperm number of successive matings.**—Four males mated a second time (Table 2). The rest of the males did not remate ($n = 6$). Ejaculate volume, and spermatozoa numbers did not vary significantly between successive matings (GLMM (ejaculate volume) $z = 1.15$, $P = 0.25$; (spermatozoa numbers) $z = 0.76$, $P = 0.44$).

## DISCUSSION

The present study focused on sperm storage and ejaculate production in the male of the neotropical scorpion *T. elegans*. By measuring the total volume and number of spermatozoa, we could gather information about the pattern of sperm production in this species. The sperm volume inside the seminal vesicles (storage organs) was higher than inside the spermatophore. The ejaculate showed a decrease in the number of spermatozoa inside the spermatophore compared to the seminal vesicles. In contrast, the analysis of successive matings revealed that ejaculate size was maintained and did not change substantially in volume and sperm number, at least in two spermatophore depositions. Additionally, we found that the body weight influenced the ejaculate volume positively but did not affect the other variables analyzed.

**Sperm storage organs and ejaculates.**—The size of the storage organs limits the amount of sperm available for each spermatophore production. In *T. elegans*, storage organs are full and vary in size between males (this was also seen when analyzing the coefficient of variation). At first glance, in *T. elegans*, each storage organ could store the equivalent volume of at least four ejaculates. However, since spermatozoa were more diluted in the ejaculate, storage organs may store more, and the total potential ejaculates that storage organs can produce might be higher.

As expected, sperm drop volumes inside the spermatophore and ejaculate volume are equivalent. Inside the spermatophore, sperm seems to be already mixed with the gel-like substance before coming out. This fact could explain the similarity in the volume of the sperm drop inside the spermatophore and the ejaculate. The rest of the gel-like substance that remains might help to extrude the ejaculate (Francke 1979). Besides, this gel-like substance may have other functions, similar to those of seminal fluids in other arthropods (Svärd & Wiklund 1989). Sperm numbers decreased inside the ejaculates in one order of magnitude. We did not expect a dilution inside the ejaculate, regarding the further addition of secretory products, as males of *T. elegans* lack accessory glands connected with the capsular region of the hemispermatophores inside the paraxial organs (Peretti & Battán-Horenstein 2003). Nevertheless, in many taxa, seminal secretions can be generated in other parts of male's reproductive tract like testes or ejaculatory ducts (Chapman & Davies 2004; den Boer et al. 2008; Avila et al. 2011). In fact, in spiders, seminal secretions are added to the sperm in testes and deferent ducts (Herberstein et al. 2011; Michalik & Lipke 2013; Michalik & Ramirez 2014). As we previously stated, the gel-like substance that fills the trunk comes out mixed with the sperm drop. Thus, the gel-like substance inside the spermatophore may serve as the diluent of the spermatozoa of the ejaculate. Still, further analysis of the secretory tissues along the distal part of the storage organs, and the detailed examination of the gel-like substance are needed. These analyses may help to reveal the formation process of the seminal fluid as well as the origin of the gel-like substance.

In our study, the male's body weight influenced the volume of the ejaculate positively, suggesting that heavier males produce ejaculates with higher volume. Using similar approaches, most studies in arthropods found that the ejaculate or spermatophore size may covary positively with body size or weight of the male (e.g., Wedell 1993; Bissoondath & Wiklund 1996; MacDiarmid & Butler 1999; Gosselin et al. 2003; Jivoff 2003; Rubolini et al. 2006). Our results suggest that males with higher reserves can allocate more resources to sperm production. Ejaculates are costly to produce and force the organism to be in an optimal condition having energetic reserves to compensate for the production of ejaculates (Jiménez-Pérez & Wang 2004; Gress & Pitnick 2017).

**Sperm counts.**—Here, we reported a sperm count on the order of $1 \times 10^{11}$ inside the storage organs and $1 \times 10^{10}$ in an ejaculate. Among arachnids, we did not find data on sperm counts inside the male's storage organs. However, there are many excellent works analyzing spermatozoa numbers of

ejaculates. For example, in spiders, spermatozoa count from ejaculates inside the male's palps are lower than we found in the present study, ranging from $1 \times 10^3$ to $1 \times 10^5$ (Arnaud et al. 2001; Bukowski et al. 2001; Snow & Andrade 2004; Ceballos et al. 2015). Bukowski & Christenson (1997) also showed that sperm stored inside the female's spermatheca were on the order of $1 \times 10^4$. However, sperm counts in scorpions more closely resembled ejaculates of other arthropods (e.g., Brown & Knouse 1973; Swallow & Wilkinson 2002; Sato et al. 2006; Vahed 2006; Dallai et al. 2009; Aron et al. 2016). Similar to what happened with scorpions' seminal vesicles, Snow & Andrade (2004) also reported a correlation between the number of spermatozoa in the right and left pedipalps. They show that both charged an equivalent number of spermatozoa, but with a few orders of magnitude lower than what we reported here for the volume of right and left storage organs.

**Successive matings.**—Regarding our analysis of successive matings in *T. elegans*, sperm depletion is not evident in the two observed consecutive matings. This result may be expected in a species that has continuous sperm production, like *T. elegans*. Similarly, in a study that involved a tephritid dipteran, sperm reserves did not drop over successive matings (Pérez-Staples & Aluja 2006). In fact, sperm reserves did not become depleted even after three matings in a single day. Males partitioned their sperm production avoiding sperm depletion and maintaining sperm reserves.

Besides sperm depletion, males can allocate sperm strategically in response to sperm competition (Parker & Pizzari 2010; Simmons 2014). Again, males from *T. elegans* seem not to respond to sperm competition, as ejaculate volume and sperm numbers remain unaltered in successive matings. If this is the case, we would have found different strategies and patterns of sperm allocation (Abe & Kamimura 2015). For example, in lepidopterans, sperm number could decline over successive matings (Cook & Gage 1995) or could increase in the second mating and finally decrease in the third (Watanabe et al. 1998).

Preliminary analyses in other Bothriuridae suggests that sperm depletion may be present in scorpions (D. Vrech et al., unpublished). Scorpions show a refractory period that lasts until both paraxial organs have regenerated their contents. Data in *Bothriurus bonariensis* (C.L. Koch, 1842) suggests that males need approximately five days for the regeneration plus two more days to regain receptiveness to mate (Peretti & Acosta 1998). Males from *T. elegans* in the present study remated within this same period. In *B. bonariensis*, ejaculate depletion was observed in the course of three spermatophore depositions. However, the pattern of sperm depletion in *T. elegans* may not be equally evident after only two successive matings. Thus, in the present study, the number of achieved matings may have been insufficient to allow a conclusion about sperm depletion in this scorpion species. More data on successive spermatophore depositions, as well as precise data on the actual mating systems in the field, are subjects that should be strictly assessed in future works of scorpions.

**Ejaculate dynamics.**—The question that arises in *T. elegans* is: why do males produce such large number of spermatozoa? Indeed, the number of produced spermatozoa in animals is much higher compared to the number needed to fertilize the female's entire set of ova (Brown & Knouse 1973; Parker 1982; Thornhill & Alcock 1983; Pizzari & Parker 2009; Xu & Wang 2010). *Timogenes elegans* has a male-biased sex ratio (Nime et al. 2014). Besides, females may mate with multiple males (Polis & Sissom 1990; Peretti 2010), can store sperm inside paired spermathecae (Volschenk et al. 2008), and receive a relatively ineffective genital plug (Peretti & Battán-Horenstein 2003; Mattoni & Peretti 2004). These characteristics show a system with a potentially high risk of sperm competition (Parker 2000). As many other scorpions, males of *T. elegans* live as adults for only one mating season (Maury 1982; Peretti 1996; Polis & Sissom 1990). Thus, the need to produce a significant number of spermatozoa would be linked to the possibility of filling many spermatophores and thus being able to inseminate many different females (Parker & Pizzari 2010; Vahed & Parker 2012). A high successive ejaculate investment often reduces the number of females that a male can inseminate and may reduce the male's longevity (Scharf et al. 2013). Although the spermatophore is a sclerotized structure, the volume of ejaculate may change as the variation coefficient of the ejaculate in our analysis suggests.

The dilution of sperm observed in the ejaculate of *T. elegans* may help to fill more spermatophores with a fixed number of spermatozoa. Following Acosta & Maury (1990), we calculated an average of 110 days as the total effective reproductive period in *T. elegans* (i.e., end of November to the beginning of March). Males of this species need five days to regenerate the hemispermatophores (Peretti & Acosta 1998), and approximately two more days to regain willingness to mate (Peretti 1993). In a maximum scenario, spermatophore production would result in approximately 16 spermatophores for the entire reproductive season (110 divided by 7). Our data suggest that both storage organs may store a volume close to that of five spermatophores. Sperm is continuously produced, and seminal vesicles will never be empty. Unfortunately, we do not have precise data on sperm dynamics inside the storage organs to know how many spermatophores males can produce in the entire season. Sperm measured in one sample of the two seminal vesicles was nearly 33% of the quantity found in the spermatophore contents calculated for the entire season (16 spermatophores). So, with only filling both seminal vesicles once, the males assure a third (i.e., the volume of 4.67 spermatophores) of the whole sperm production for the entire reproductive season. We should bear in mind that five spermatophores represent a great production for males, and, that this theoretical number of spermatophores may be difficult to reach in nature, as other variables may be affecting this capacity. For example, the rate of predation may vary daily (Nime et al. 2013). Besides, the operational sex ratio is thought to be biased towards males, and female availability for mating can be reduced.

There is another hypothesis that states that a male can have an increased sperm production to counter the effect of interspecific sperm competition, between two closely related species that are living in sympatry. For example, Carretero et al. (2006) and Kaliontzopoulou et al. (2007) found that sympatric males of two reptile species of *Podarcis* produced relatively more sperm, suggesting there may be a sexual interaction between them. Naretto et al. (2016) found something similar in male *Salvator* lizards, but this time testes mass was affected but sperm number was not. Although there

are studies in arthropods about reproductive interference (e.g., Costa-Schmidt & Machado 2012, Shuker et al. 2015), to our knowledge, there are no studies that evaluate sperm production between similar species. *Timogenes elegans* may live in sympatry with one sister species, *T. dorbignyi* (Guérin-Méneville, 1843). In this scenario, both species could incur in interspecific sperm competition. However, this may rarely be the case. *Timogenes dorbignyi* is substantially smaller than *T. elegans* (Ojanguren-Affilastro 2005) and heterospecific mating trials rarely result in courtship (Peretti 2003; Vrech pers. obs.). Besides, the level of mating synchrony is apparently low (C. Mattoni, A. Peretti pers. obs.). Finally, courtship displays are different between them (Peretti 2003).

We could confirm some of our hypotheses. Males from *T. elegans* show a high and continuous sperm production. Sperm is divided equally between both storage organs. Contrary to our presumptions, the data showed that the ejaculates became diluted when passing to the spermatophore. Secretory tissue throughout the reproductive system, as well as the gel-like substance, may be candidates for aiding to dilute sperm. We should not discard the presence of secretory tissues in some other part of the reproductive system. We do not know the location and mechanism as accessory glands are not present. Future studies may answer if the gel-like substance inside the trunk acts as the diluent. Successive matings did not suggest sperm depletion. However, investigations of ejaculate dynamics in more scorpions and other arachnids are still lacking. For this reason, further studies in other species of Bothriuridae and other families would be beneficial to offer a comparative survey of sperm production across the entire order.

## ACKNOWLEDGMENTS

We thank Matias Izquierdo, Lucia Calbacho-Rosa, Fedra Bollatti, Silvana Burela and Monica Nime for their help during field samplings. We also thank Martín Ramírez, Margarita Chiaraviglio, Alejandro Guidobaldi, Peter Michalik and two anonymous reviewers for critics and suggestions that contributed to improve previous versions of the manuscript. We are also very thankful with Germán Gonzalez with his help on statistical modeling, and with David Lee who helped improve the language. Finally, we acknowledge funding by CONICET, Foncyt, and Secyt-UNC.

## LITERATURE CITED

Abe, J. & Y. Kamimura. 2015. Sperm economy between female mating frequency and male ejaculate allocation. American Naturalist 185:406–416.

Acosta, L.E. 1995. The scorpions of the Argentinian western Chaco. I. Diversity and distributional patterns. Biogeographica 71:49–59.

Acosta, L.E. & E.A. Maury. 1990. Estridulación en *Timogenes elegans*. Boletín de La Sociedad Biológica de Concepción, Chile 61:29–37.

Alberti, G. 1983. Fine structure of scorpion spermatozoa. Journal of Morphology 212:205–212.

Alberti, G. & L.B. Coons. 1999. Acari: mites. Microscopic anatomy of invertebrates 8:515–1265.

Andersson, M.B. 1994. Sexual Selection. Princeton University Press.

Arnaud, L., E. Haubruge & M.J.G. Gage. 2001. Sperm size and number variation in the red flour beetle. Zoological Journal of the Linnean Society 133:369–375.

Arnqvist G. & J.A. Andrés. 2006. The effects of experimentally induced polyandry on female reproduction in a monandrous mating system. Ethology 112:748–756.

Aron, S., P. Lybaert, C. Baudoux, M. Vandervelden & D. Fournier. 2016. Sperm production characteristics vary with level of sperm competition in *Cataglyphis* desert ants. Functional Ecology 30:614–624.

Avila, F.W., L.K. Sirot, B.A. Laflamme, C.D. Rubinstein & M.F. Wolfner. 2011. Insect seminal fluid proteins: identification and function. Annual Review of Entomology 56:21–40.

Barr, A.R. 1974. Symposium on reproduction of arthropods of medical and veterinary importance: V. Reproduction in Diptera of medical importance with special reference to mosquitoes. Journal of Medical Entomology 11:35–40.

Bastidas, O. 2014. Cell counting with Neubauer Chamber. Technical note. Online at http://www.celeromics.com/en/resources/docs/Articles/Cell-counting-Neubauer-chamber.pdf

Bates, D., M. Maechler, B. Bolker & S. Walker. 2014. lme4: Linear mixed-effects models using Eigen and S4. R package version 1(7):1–23.

Birkhead, T.R. & A.P. Moller. 1998. Sperm Competition and Sexual Selection. Academic Press, Massachusetts.

Bissoondath, C.J. & C. Wiklund. 1996. Effect of male mating history and body size on ejaculate size and quality in two polyandrous butterflies, *Pieris napi* and *Pieris rapae* (Lepidoptera: Pieridae). Functional Ecology 10:457–464.

Bolker, B., H. Skaug, A. Magnusson & A. Nielsen. 2012. Getting started with the glmmADMB package. Available at glmmadmb.r-forge.r-project.org/glmmADMB.pdf.

Boomsma, J.J., B. Baer & J. Heinze. 2005. The evolution of male traits in social insects. Annual Review of Entomology 50:395–420.

Bressac C., D. Damiens & C. Chevrier. 2008. Sperm stock and mating of males in a parasitoid wasp. Journal of Experimental Zoology part B-Molecular and Developmental Evolution 310b:160–166.

Brown, G.G. & J.R. Knouse. 1973. Effects of sperm concentration, sperm aging, and other variables on fertilization in the horse-shoe crab, *Limulus polyphemus* L. Biological Bulletin 144:462–470.

Bukowski, T.C. & T.E. Christenson. 1997. Determinants of sperm release and storage in a spiny orbweaving spider. Animal Behaviour 53:381–395.

Bukowski, T.C., C.D. Linn & T.E. Christenson. 2001. Copulation and sperm release in *Gasteracantha cancriformis* (Araneae: Araneidae): differential male behaviour based on female mating history. Animal Behaviour 62:887–895.

Carretero, M.A., R. Ribeiro, D. Barbosa, P. Sá-Sousa & D.J. Harris. 2006. Spermatogenesis in two iberian *Podarcis* lizards: relationships with male traits. Animal Biology 56:1–12.

Ceballos, L., T.M. Jones & M.A. Elgar. 2015. Patterns of sperm transfer in the golden orb-weaver *Nephila edulis*. Ethology 121:617–624.

Chapman, R.F. 1998. The Insects: Structure and Function. Cambridge University Press.

Chapman, T. 2001. Seminal fluid-mediated fitness traits in *Drosophila*. Heredity 87:511–521.

Chapman, T. & S.J. Davies. 2004. Functions and analysis of the seminal fluid proteins of male *Drosophila melanogaster* fruit flies. Peptides 25:1477–1490.

Cook, P.A. & M.J.G. Gage. 1995. Effects of risks of sperm competition on the numbers of eupyrene and apyrene sperm ejaculated by the moth *Plodia interpunctella* (Lepidoptera: Pyralidae). Behavioral Ecology and Sociobiology 36:261–268.

Costa-Schmidt, L.E. & G. Machado. 2012. Reproductive interference between two sibling species of gift-giving spiders. Animal Behaviour 84:1201–1211.

Dallai, R., Z.V. Zizzari & P.P. Fanciulli. 2009. Different sperm number in the spermatophores of *Orchesella villosa* (Geoffroy)

(Entomobryidae) and *Allacma fusca* (L.) (Sminthuridae). Arthropod Structure and Development 38:227–234.

Delignette-Muller, M.L. & C. Dutang. 2015. fitdistrplus: An R package for fitting distributions. Journal of Statistical Software 64(4):1–34.

den Boer, S.P.A., J.J. Boomsma & B. Baer. 2008. Seminal fluid enhances sperm viability in the leafcutter ant *Atta colombica*. Behavioral Ecology and Sociobiology 62:1843–1849.

Dennenmoser, S. & M. Thiel. 2015. Cryptic female choice in crustaceans. Pp. 203–237. *In* Cryptic Female Choice in Arthropods (A.V. Peretti & A Aisenberg, eds.). Springer International Publishing, Switzerland.

Dewsbury, D.A. 1982. Ejaculate cost and male choice. American Naturalist 119:601–610.

Franeke, O.F. 1979. Spermatophores of some north American scorpions (Arachnida, Scorpiones). Journal of Arachnology 7:19–32.

Gage, M.J.G. 1994. Associations between body size, mating pattern, testis size and sperm lengths across butterflies. Proceedings of the Royal Society of London. Series B: Biological Sciences 258:247–254.

Gosselin, T., B. Sainte-Marie & L. Bernatchez. 2003. Patterns of sexual cohabitation and female ejaculate storage in the American lobster (*Homarus americanus*). Behavioral Ecology and Sociobiology 55:151–160.

Gress, B.E. & S. Pitnick. 2017. Size-dependent ejaculation strategies and reproductive success in the yellow dung fly, *Scathophaga stercoraria*. Animal Behaviour 127:281–287.

Herberstein, M.E., J.M. Schneider, G. Uhl & P. Michalik. 2011. Sperm dynamics in spiders. Behavioral Ecology 22:692–695.

Hjelle, J.T. 1990. Anatomy and morphology. Pp. 9–63. *In* The Biology of Scorpions (G.A. Polis, ed.). Stanford University Press, Stanford.

Jespersen, Å. & R. Hartwick. 1973. Fine structure of spermiogenesis in scorpions from the family Vejovidae. Journal of Ultrastructure Research 45:366–383.

Jiménez-Pérez, A. & Q. Wang. 2004. Effect of body weight on reproductive performance in *Cnephasia jactatana* (Lepidoptera: Tortricidae). Journal of Insect Behavior 17:511–522.

Jivoff, P. 2003. A review of male mating success in the blue crab, *Callinectes sapidus*, in reference to the potential for fisheries-induced sperm limitation. Bulletin of Marine Science 72:273–286.

Kaliontzopoulou, A., M.A. Carretero & G.A. Llorente. 2007. Multivariate and geometric morphometries in the analysis of sexual dimorphism variation in *Podarcis* lizards. Journal of Morphology 268:152–165.

Kaufman, W.R., A.S. Bowman & P.A. Nuttall. 2008. Factors that determine sperm precedence in ticks, spiders and insects: a comparative study. Pp. 164–185. *In* Ticks: Biology, Disease and Control. (A.S. Bowman & P.A. Nuttall, eds.). Cambridge University Press, Cambridge.

Klann, A.E. 2009. Histology and ultrastructure of solifuges: Comparative studies of organ systems of solifuges (Arachnida, Solifugae) with special focus on functional analyses and phylogenetic interpretations. PhD thesis, University of Greifswald.

Klann, A.E., A.V. Peretti & G. Alberti. 2005. Ultrastructure of male genital system and spermatozoa of a Mexican camel-spider of the *Ereniobates pallipes* species group (Arachnida, Solifugae). Journal of Arachnology 33:613–621.

Leopold, R.A. 1976. Role of male accessory glands in insect reproduction. Annual Review of Entomology 21:199–221.

MacDiarmid, A.B. & M.J. Butler. 1999. Sperm economy and limitation in spiny lobsters. Behavioral Ecology and Sociobiology 46:14–24.

Manogem, E.M. 2002. Dynamics of spermiogenesis in *Spodoptera mauritia* Boisd. (Lepidoptera: Noctuidae) Thesis. Department of Zoology, University of Calicut.

Mattoni, C.I. & A.V. Peretti. 2004. The giant and complex genital plug of the *asper* group of *Bothriurus* (Scorpiones, Bothriuridae): morphology and comparison with other genital plugs in scorpions. Zoologischer Anzeiger 243:75–84.

Maury, E.A. 1982. El género *Timogenes* Simon 1880 (Scorpiones, Bothriuridae). Revista de la Sociedad Entomológica Argentina 41:23–48.

Michalik, P. & B.A. Huber. 2006. Spermiogenesis in *Psilochorus simoni* (Berland, 1911) (Pholcidae, Araneae): evidence for considerable within-family variation in sperm structure and development. Zoology 109:14–25.

Michalik, P. & D. Mercati. 2010. First investigation of the spermatozoa of a species of the superfamily Scorpionoidea (*Opistophthalmus penrithorum*, Scorpionidae) with a revision of the evolutionary and phylogenetic implications of sperm structures in scorpions (Chelicerata, Scorpiones). Journal of Zoological Systematics and Evolutionary Research 48:89–101.

Michalik, P. & E. Lipke. 2013. Male reproductive system of spiders. Pp. 173–187. *In* Spider Ecophysiology (W. Nentwig, ed.). Springer Berlin Heidelberg.

Michalik, P. & M.J. Ramírez. 2014. Evolutionary morphology of the male reproductive system, spermatozoa and seminal fluid of spiders (Araneae, Arachnida) - Current knowledge and future directions. Arthropod Structure & Development 43:291–e322.

Michalik, P. & C.C. Rittschof. 2011. A comparative analysis of the morphology and evolution of permanent sperm depletion in spiders. PLoS ONE 6(1) e16014

Michalik, P. & G. Uhl. 2005. The male genital system of the cellar spider *Pholcus phalangioides* (Fuesslin, 1775) (Pholcidae, Araneae): development of spermatozoa and seminal secretion. Frontiers in Zoology 2:1–12.

Michalik, P., B. Knoflach, K. Thaler & G. Alberti. 2010. Live for the moment adaptations in the male genital system of a sexually cannibalistic spider (Theridiidae, Araneae). Tissue and Cell 42:32–36.

Moller, A.P. 1991. Sperm competition, sperm depletion, paternal care, and relative testis size in birds. American Naturalist 137:882–906.

Naretto, S., C.S. Blengini, G. Cardozo & M. Chiaraviglio. 2016. Pre and postcopulatory traits of *Salvator* male lizards in allopatry and sympatry. Scientifica 2016:1–9.

Nime, M.F., F. Casanoves, D.E. Vrech & C.I. Mattoni. 2013. Relationship between environmental variables and surface activity of scorpions in the Arid Chaco ecoregion of Argentina. Invertebrate Biology 132:145–155.

Nime, M.F., F. Casanoves & C.I. Mattoni. 2014. Scorpion diversity in two different habitats in the Arid Chaco, Argentina. Journal of Insect Conservation 18:373–384.

Ojanguren-Affilastro, A.A. 2005. Estudio monográfico de los escorpiones de la República Argentina. Revista Ibérica de Aracnología 11:75–241.

Orr, T.J. & M. Zuk. 2013. Does delayed fertilization facilitate sperm competition in bats? Behavioral Ecology and Sociobiology 67:1903–1913.

Parker, G.A. 1970. Sperm competition and its evolutionary consequences in the insects. Biological Reviews 45:525–567.

Parker, G.A. 1982. Why are there so many tiny sperm - sperm competition and the maintenance of 2 sexes. Journal of Theoretical Biology 96:281–294.

Parker, G.A. 2000. Sperm competition games between related males. Proceedings of The Royal Society B: Biological Sciences 267:1027–1032.

Parker, G.A. & M.A. Ball. 2005. Sperm competition, mating rate and

the evolution of testis and ejaculate sizes: a population model. Biological Letters 1:235–238.

Parker, G.A. & T. Pizzari. 2010. Sperm competition and ejaculate economics. Biological Reviews 85:897–934.

Parker, G.A., M.A. Ball, P. Stockley & M.J.G. Gage. 1997. Sperm competition games: a prospective analysis of risk assessment. Proceedings of the Royal Society B: Biological Sciences 264:1793–1802.

Peretti A.V. 1993. Estudio de la biología en escorpiones argentinos (Arachnida, Scorpiones): un enfoque etológico. PhD Thesis. UNC FCEFyN CDAI.

Peretti, A.V.1996. Una probable estrategia para inseminar más hembras en machos de *Bothriurus bonariensis* (Scorpiones, Bothriuridae). Journal of Arachnology 24:167–169.

Peretti, A.V. 2003. Functional morphology of spermatophores and female genitalia in bothriurid scorpions: genital courtship, coercion and other possible mechanisms. Journal of Zoology 261:135–153.

Peretti, A.V. 2010. An ancient indirect sex model: single and mixed patterns in the evolution of scorpion genitalia. Pp. 218–248. *In* The Evolution of Primary Sexual Characters in Animals (J. Leonard, A. Córdoba-Aguilar, eds.). Oxford University Press, New York.

Peretti, A.V. & L.E. Acosta. 1998. Comparative analysis of mating in scorpions the post transfer stage. Zoologischer Anzeiger 237:259–265.

Peretti, A.V. & M. Battán-Horenstein. 2003. Comparative analysis of the male reproductive system in Bothriuridae scorpions: structures associated with the paraxial organs and the presence of sperm packages (Chelicerata, Scorpiones). Zoologischer Anzeiger 242:21–31.

Pérez-Staples, D. & M. Aluja. 2006. Sperm allocation and cost of mating in a tropical tephritid fruit fly. Journal of Insect Physiology 52:839–845.

Pizzari, T. & G.A. Parker. 2009. Sperm competition and sperm phenotype. Pp. 207–245. *In* Sperm Biology: an Evolutionary Perspective (T.R. Birkhead, D.J. Hosken & S.S. Pitnick, eds.). Academic Press, Oxford.

Polis, G.A. & W.D. Sissom. 1990. Life history. Pp. 161–223. *In* The Biology of Scorpions (G.A. Polis, ed.). Stanford University Press.

R Core Team. 2016. R: A language and environment for statistical computing. R Foundation for Statistical Computing, Vienna, Austria. Online at https://www.R-project.org/

Ramm, S.A., G.A. Parker & P. Stockley. 2005. Sperm competition and the evolution of male reproductive anatomy in rodents. Proceedings of the Royal Society of London B: Biological Sciences 272:949–955.

Rubolini, D., P. Galeotti, G. Ferrari, M. Spairani, F. Bernini & M. Fasola. 2006. Sperm allocation in relation to male traits, female size, and copulation behaviour in freshwater crayfish species. Behavioral Ecology and Sociobiology 60:212–219.

Rubolini, D., P. Galeotti, F. Pupin, R. Sacchi, P.A. Nardi & M. Fasola. 2007. Repeated matings and sperm depletion in the freshwater crayfish *Austropotamobius italicus*. Freshwater Biology 52:1898–1906.

Sato, T., M. Shidate, T. Jinbo & S. Goshima. 2006. Variation of sperm allocation with male size and recovery rate of sperm numbers in spiny king crab *Paralithodes brevipes*. Marine Ecology Progress Series 312:189–199.

Schärer, L. & D.B. Vizoso. 2007. Phenotypic plasticity in sperm production rate: there's more to it than testis size. Evolutionary Ecology 21:295–306.

Schärer, L., P. Ladurner & R.M. Rieger. 2004. Bigger testes do work more: experimental evidence that testis size reflects testicular cell proliferation activity in the marine invertebrate, the free-living flatworm *Macrostomum* sp. Behavioral Ecology and Sociobiology 56:420–425.

Scharf, I., F. Peter & O.Y. Martin. 2013. Reproductive trade-offs and direct costs for males in arthropods. Evolutionary Biology 40:169–184.

Schindelin, J., C.T. Rueden, M.C. Hiner & K.W. Eliceiri. 2015. The ImageJ ecosystem: An open platform for biomedical image analysis. Molecular reproduction and development 82 (7–8):518–529.

Schneider, J.M. & P. Michalik. 2011. One-shot genitalia are not an evolutionary dead end — Regained male polygamy in a sperm limited spider species. BMC Evolutionary Biology 11(197):1–8.

Shuker, D.M., N. Currie, T. Hoole & E.R. Burdfield-Steel. 2015. The extent and costs of reproductive interference among four species of true bug. Population Ecology 57:321–331.

Simmons, L.W. 2014. Sperm competition. Pp. 193–218. *In* The Evolution of Insect Mating Systems. (D.M. Shuker & L.W. Simmons, eds.). Oxford University Press, USA.

Snow, L.S.E. & M.C.B. Andrade. 2004. Pattern of sperm transfer in redback spiders: Implications for sperm competition and male sacrifice. Behavioral Ecology 15:785–792.

Svärd, L. & C. Wiklund. 1989. Mass and production rate of ejaculates in relation to monandry/polyandry in butterflies. Behavioral Ecology and Sociobiology 24:395–402.

Swallow, J.G. & G.S. Wilkinson. 2002. The long and short of sperm polymorphisms in insects. Biological Reviews 77:153–182.

Thornhill, R. & J. Alcock. 1983. The Evolution of Insect Mating Systems. Harvard University Press.

Vachon, M. 1953. The biology of scorpions. Endeavour 12(46):80–89.

Vahed, K. 2006. Larger ejaculate volumes are associated with a lower degree of polyandry across bushcricket taxa. Proceedings of the Royal Society B: Biological Sciences 273:2387–2394.

Vahed, K. & D.J. Parker. 2012. The evolution of large testes: sperm competition or male mating rate? Ethology 118:107–117.

Venables, W.N. & B.D. Ripley. 2002. Modern Applied Statistics with S. Fourth Edition. Springer, New York.

Volschenk, E.S., C.I. Mattoni & L. Prendini. 2008. Comparative anatomy of the mesosomal organs of scorpions (Chelicerata, Scorpiones), with implications for the phylogeny of the order. Zoological Journal of the Linnean Society 154:651–675.

Vrech, D.E. 2013. Patrones de producción espermática en escorpiones (Arachnida, Scorpiones): una aproximación comparada y experimental. PhD Dissertation, Facultad Ciencias Exactas, Físicas y Naturales. Universidad Nacional de Córdoba.

Vrech, D.E., A.V. Peretti & C.I. Mattoni. 2011. Sperm package morphology in scorpions and its relation to phylogeny. Zoological Journal of the Linnean Society 161:463–483.

Vrech, D.E., P.A. Olivero, C.I. Mattoni & A.V. Peretti. 2014. Testes mass, but not sperm length, increases with higher levels of polyandry in an ancient sex model. PLoS ONE 9(4).

Watanabe, M., C. Wiklund & M. Bon'no. 1998. The effect of repeated matings on sperm numbers in successive ejaculates of the cabbage white butterfly *Pieris rapae* (Lepidoptera: Pieridae). Journal of Insect Behavior 11:559–570.

Wedell, N. 1993. Spermatophore size in bushcrickets: comparative evidence for nuptial gifts as a sperm protection device. Evolution 47:1203–1212.

Wedell, N., M.J.G. Gage & G.A. Parker. 2002. Sperm competition, male prudence and sperm limited females. Trends in Ecology and Evolution 17:313–320.

Wigby, S. & T. Chapman. 2004. Sperm competition. Current Biology 14(3):R100–R103.

Xu, J. & Q. Wang. 2010. Thiotepa, a reliable marker for sperm precedence measurement in a polyandrous moth. Journal of Insect Physiology *56*:102–106.

*Manuscript received 30 December 2016, revised 17 November 2017.*

2018. Journal of Arachnology 46:240 248

# A new, relictual *Antilloides* from Mexican caves: first mainland record of the genus and revised placement of the fossil *Misionella didicostae* (Araneae: Filistatidae)

**Ivan L. F. Magalhaes**: División Aracnología, Museo Argentino de Ciencias Naturales "Bernardino Rivadavia"–CONICET, Av. Ángel Gallardo 470, C1405DJR, Buenos Aires, Argentina. E-mail: magalhaes@macn.gov.ar

**Abstract.** Cave organisms are often relictual, ancient lineages that conserve characters no longer represented in their closest relatives. I here present a new species of Filistatidae from Mexican caves with a notable suite of characters that preclude its placement in any of the filistatid genera currently recorded from North America. A detailed study of its morphology using light and scanning electron microscopy indicates that this is the first mainland species of *Antilloides* Brescovit, Sánchez-Ruiz & Alayón, 2016 and I describe it as *Antilloides chupacabras* sp. nov. The genus was previously known only from the Antilles, and its presence in Mexico is evidence of a wider distribution. I here identify some characters which are novel putative synapomorphies of *Antilloides*, and the phylogenetic affinities of the genus are discussed. Finally, the presence of a modified metatarsus II in males of the new species, among other characters, suggests that the only known fossil filistatid, *Misionella didicostae* Penney, 2005 from Dominican amber, is misplaced in this genus and the new combination *Antilloides didicostae* comb. nov. is proposed.

**Keywords:** Araneomorphae, Caribbean, Prithinae, taxonomy

http://zoobank.org/?lsid=urn:lsid:zoobank.org:pub:308D8616-BC63-4621-884E-9BCF0A0BC956

The fauna associated with caves is often relictual, containing species representing old lineages that have been evolving separately from their closest relatives for long periods of time. Two recent examples from the North American fauna include the first New World harvestman of the family Pyramidopidae, a lineage previously known only from Africa, identified in caves in Belize (Cruz-López et al. 2016), and the new spider family Trogloraptoridae described from caves in Oregon and California (Griswold et al. 2012). These relictual organisms offer valuable insights into the evolution and biogeography of the clades to which they belong, especially as troglobitic species can retain characters that have been lost in their more widespread relatives.

The Mexican fauna associated with caves is a rich one, and includes several species of Filistatidae (Reddell 1981). This medium-sized spider family includes around 150 species in 19 genera (World Spider Catalog 2017), most of which inhabit arid and semi-arid regions of the subtropics; some species are known to be associated to caves (Brescovit et al. 2016a; Magalhaes 2016). The North American fauna includes three genera but is still poorly known, as extensive taxonomic revisions are lacking and only *Filistatinella* Gertsch & Ivie, 1936 has been recently revised (Magalhaes & Ramírez 2017).

Among filistatid material collected from limestone caves in south-western Coahuila State (Fig. 1), I found some particularly interesting specimens. At first glance, they seemed to belong to yet another undescribed species of *Filistatoides* F. O. Pickard-Cambridge, 1899. However, a closer look at their fine morphology suggested that they belonged to the recently described genus *Antilloides* Brescovit, Sánchez-Ruiz & Alayón, 2016, which was previously recorded only from the Antilles. The aims of this paper are thus to describe this new species, to discuss its generic placement, and to document its unique suite of characters and their implications for the taxonomy of New World Filistatidae.

## METHODS

Specimens of the new species and comparative material of *Antilloides* and *Filistatoides* (Appendix 1) were borrowed from the collections of the American Museum of Natural History, New York, USA (AMNH; curator L. Prendini), the Field Museum of Natural History, Chicago, USA (FMNH; P.


Figure 1.—Distribution of *Antilloides chupacabras* sp. nov. (stars; detailed in lower panel), other *Antilloides* species (white circles) and the fossil species *Misionella didicostae* Penney, 2005 (cross).

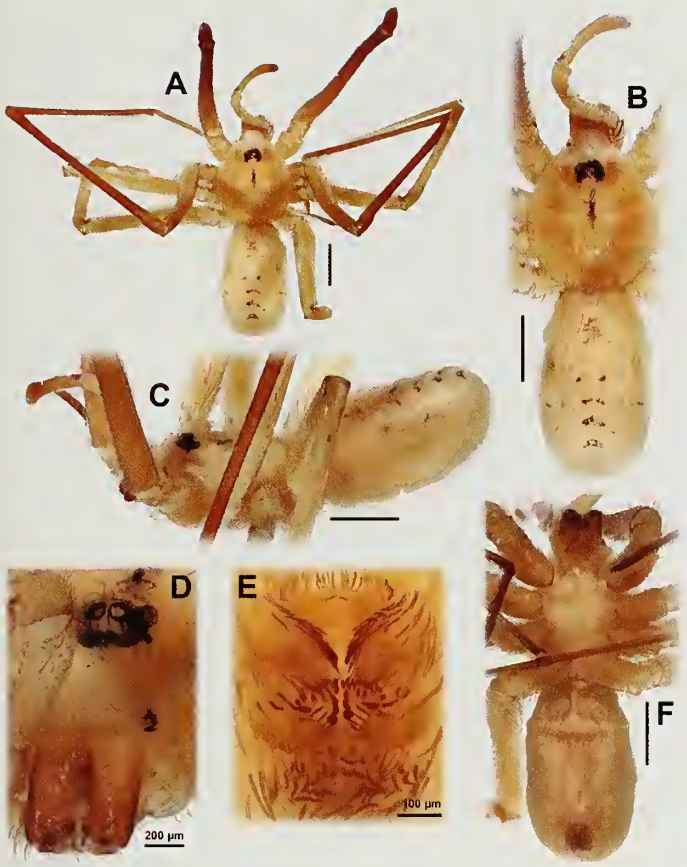


Figure 2.—*Antilloides chupacabras* sp. nov., male holotype from Cueva de Yeso, Coahuila (AMNH, IFM-1302). A–C, F, habitus: A, B, dorsal view; C, lateral view; F, ventral view. D, clypeus and eye region, sub-anterior view. E, spinnerets, ventral view. Scale bars = 1.0 mm except where noted.

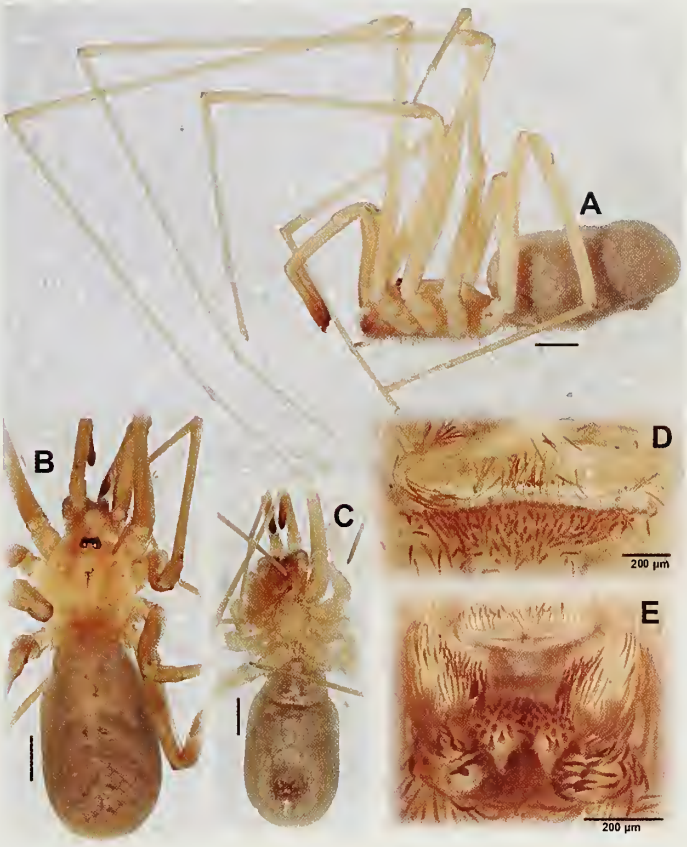


Figure 3.—*Antilloides chupacabras* sp. nov., female paratype from Cueva de Empalme, Coahuila (AMNH, IFM-1303). A–C, habitus: A, lateral view; B, dorsal view; C, ventral view. D, genital area, ventral view. E, spinnerets, ventral view. Scale bars = 1.0 mm except where noted.

Sierwald), the Instituto Nacional de Biodiversidad, San José, Costa Rica (INBIO; C. Víquez) and the Museum of Comparative Zoology, Cambridge, USA (MCZ: G. Giribet).

Measurements and habitus photos were taken using a Leica M165C stereoscopic microscope and Leica Application Suite 3.6. Female genitalia were digested in a pancreatin solution and examined in lactic acid, and the male palp was cleared in clove oil. Genitalia were photographed using an Olympus BH–2 compound microscope and drawn with the aid of a *camera lucida*. Multi-focus photo stacks were constructed in Helicon Focus 6. The format of descriptions follows Magalhaes & Ramírez (2017). Exact locations for some Mexican caves were taken from Reddell (1981). For scanning electronic microscopy images, specimens were dehydrated in solutions of increasing concentration of ethanol, critical point-dried, mounted on aluminium stubs using copper adhesive tape, gold-paladium sputter-coated, and examined using a Philips FEI XL 30 TMP scanning electron microscope.

## RESULTS AND DISCUSSION

The reduced cymbium, feathery setae, lack of tarsal macrosetae and wide cribellum, among other characters, suggest that the specimens from Coahuila belong to Prithinae, one of the two subfamilies of Filistatidae (see Gray 1995;

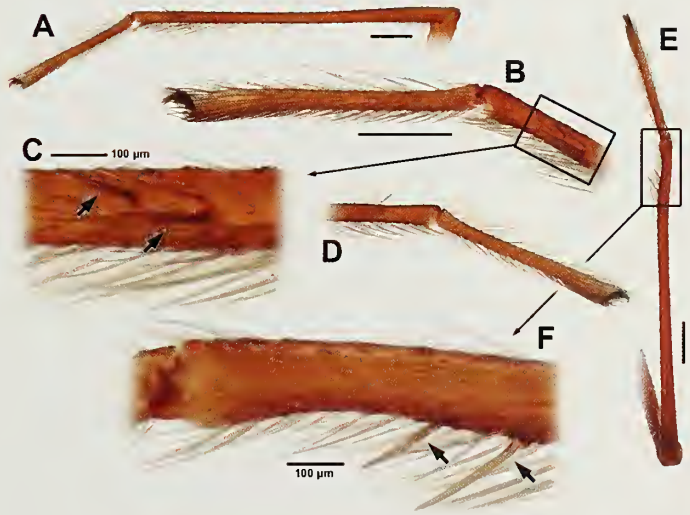


Figure 4.—*Antilloides chupacabras* sp. nov., male holotype from Cueva de Yeso, Coahuila (AMNH, IFM-1302), leg II, metatarsus and tarsus: A–C, retrolateral view; D, prolateral view; E–F, dorsal view. Arrows to macrosetae. Scale bars = 0.5 mm except where noted.

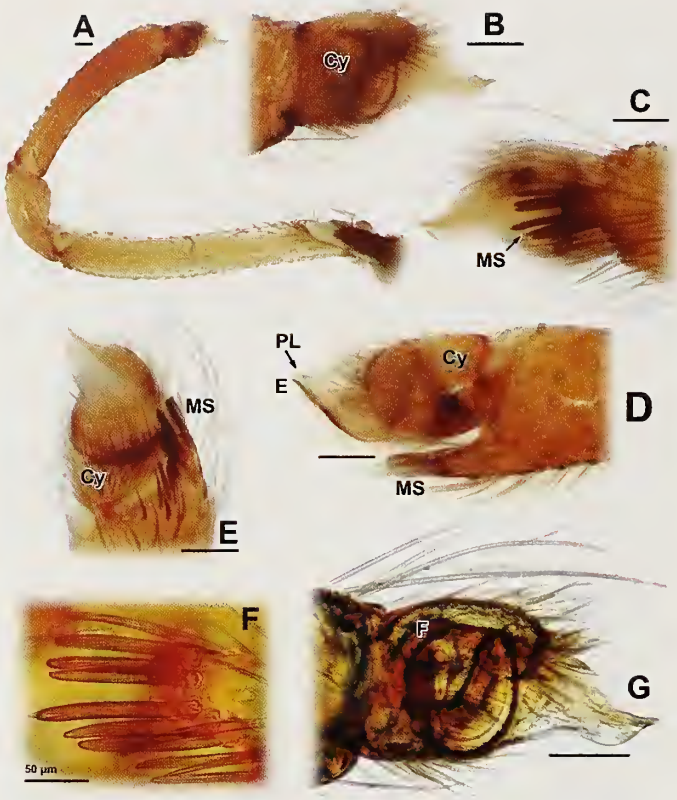


Figure 5.—*Antilloides chupacabras* sp. nov., male holotype from Cueva de Yeso, Coahuila (AMNH, IFM-1302), pedipalp: A, entire palp, prolateral view; B, bulb, prolateral view; C, same, retrolateral view; D, same, dorsal view; E, same, ventral view; F, detail of retrolateral modified setae, clove oil cleared; G, bulb, prolateral view, clove oil cleared. Abbreviations: Cy = cymbium, E = embolus, F = fundus, MS = modified setae, PL = paraembolic lamina. Scale bars = 0.1 mm except where noted.

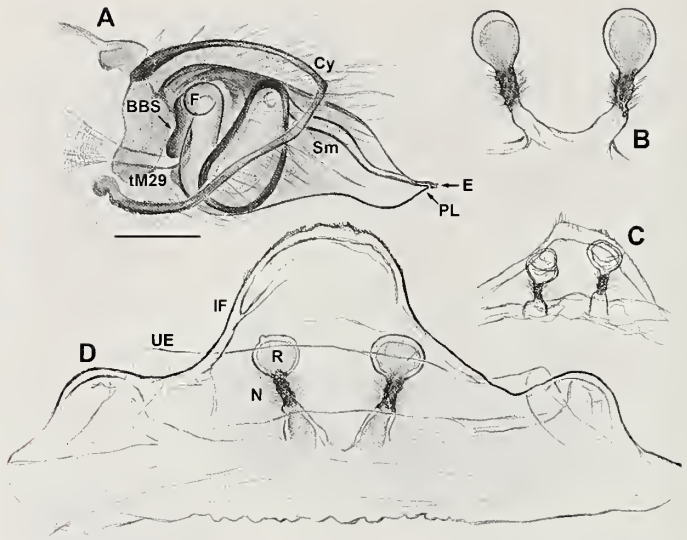


Figure 6.—*Antilloides chupacabras* sp. nov., genitalia. A, Male holotype from Cueva de Yeso, Coahuila (AMNH, IFM-1302), palpal bulb, prolateral view, clove oil cleared. B–D, paratypes, spermathecae, dorsal view, digested and lactic acid cleared: B, female from Cueva del Guano, Coahuila (AMNH, IFM-1286); C, subadult female from Cueva de los Grillos, Coahuila (AMNH, IFM-1283). D, female from Cueva de Empalme, Coahuila (AMNH, IFM-1304). Abbreviations: BBS = basal bulb sclerite, Cy = cymbium, E = embolus, F = fundus, IF = interpulmonary fold, N = spermathecal 'neck', PL = paraembolic lamina, R = receptacle, Sm = spermophore, tM29 = tendon of the claw flexor muscle, UE= uterus externus. Scale bar = 1.0 mm, and all figures to scale.

Magalhaes & Ramírez 2017). The spiders are pale in color and have elongate palps and legs (Figs. 2, 3), characters observed in some *Filistatoides* but also frequently associated with cave-dwelling species. However, a closer inspection of the male revealed it had modifications to metatarsus II, with a retrolateral excavation and a pair of macrosetae (Fig. 4). In Filistatidae, these modifications are so far unknown outside of the South American genera *Pikelinia* Mello-Leitão, 1946 and *Misionella* Ramírez & Grismado, 1997 (see Ramírez & Grismado 1997). The male palpal morphology is also modified and quite unlike most known Filistatidae species (Figs. 5, 6). The tibia bears a small projection with strong setae (Figs. 5C–E: MS), as in *Pikelinia* (see Ramírez & Grismado 1997, figs. 25, 27, 33) and *Antilloides* (see Brescovit et al. 2016b, figs. 11A, 16G). The bulb is small and globose and covered dorsally by an extension of the cymbium (Figs. 5B, D, 6A: Cy); the latter has a dorsal area devoid of setae and is not fused to the bulb. A small unsclerotized outgrowth near the apex of the embolus is probably a reduced paraembolic lamina (Figs. 5A, 6A: PL). The sperm duct has a single coil and the fundus points ventrally and attaches to a very reduced basal bulb sclerite (Figs. 5G, 6A: F, BBS), as in many prithines. The female has a pair of simple receptacles each with a narrowed 'neck', as in *Filistatoides* and *Antilloides* (see Brescovit et al. 2016b, figs. 1B, 9F), but also an enlarged interpulmonary fold, a diagnostic character of the latter genus (Figs. 6–8: IF). Interestingly, the receptacles lack glandular pores, which are restricted to the 'neck' region (Figs. 7–8: N). The body is further covered in feathery setae (Fig. 9A), as in *Filistatoides, Antilloides, Pikelinia* and relatives (see Ramírez & Grismado, 1997, fig. 80; Brescovit et al. 2016a, fig. 10G).

The phylogenetic relationships among New World filistatid genera, and the limits of some of the genera themselves, are still largely untested or unknown. Existing studies have a limited sampling of taxa and/or characters (Gray 1995; Ramírez & Grismado 1997; Magalhaes & Ramírez 2017) and do not include some of the characteristics mentioned in the previous paragraph. However, the polarity of some of these characters can be inferred by comparison with other filistatid genera, some of which are becoming better-known due to recent redescriptions and revisions of several taxa worldwide (e.g., Zonstein & Marusik 2015, 2016; Brescovit et al. 2016a, b; Magalhaes 2016; Legittimo et al. 2017; Magalhaes & Ramírez 2017). From these revisions, it can be inferred that some characters are of particular interest for placing the new species. For example, the presence of modified setae on a small projection of the male palpal tibia combined with a modified metatarsus II in the male have hitherto been observed only in *Pikelinia* (Ramírez & Grismado 1997) – a genus that belongs to a clade (along with *Misionella* and *Lihuelistata* Ramírez & Grismado, 1997) where the cymbium is fused to the bulb (Ramírez & Grismado 1997). Thus, if the new species belongs to *Pikelinia*, the presence of an unfused

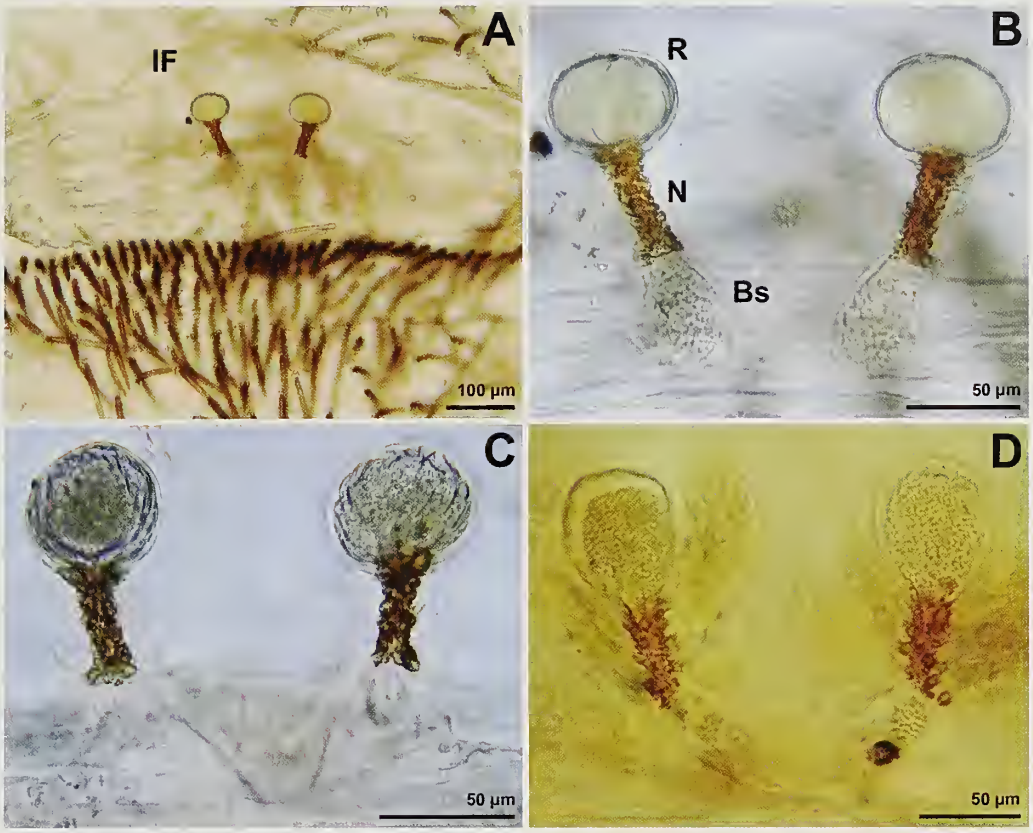


Figure 7.—*Antilloides chupacabras* sp. nov., paratypes, spermatheeae, dorsal view, digested and lactic acid cleared. A B, female from Cueva de Empalme, Coahuila (AMNH, IFM-1304; this is the same genitalia prepared for SEM, see Fig. 8); C, female from Cueva del Guano, Coahuila (AMNH, IFM-1286); D, female from Cueva de Empalme, Coahuila (AMNH, IFM-1287). Abbreviations: Bs = spermatheeae base, IF = interpulmonary fold, N = spermatheeal 'neek', R = receptacle.

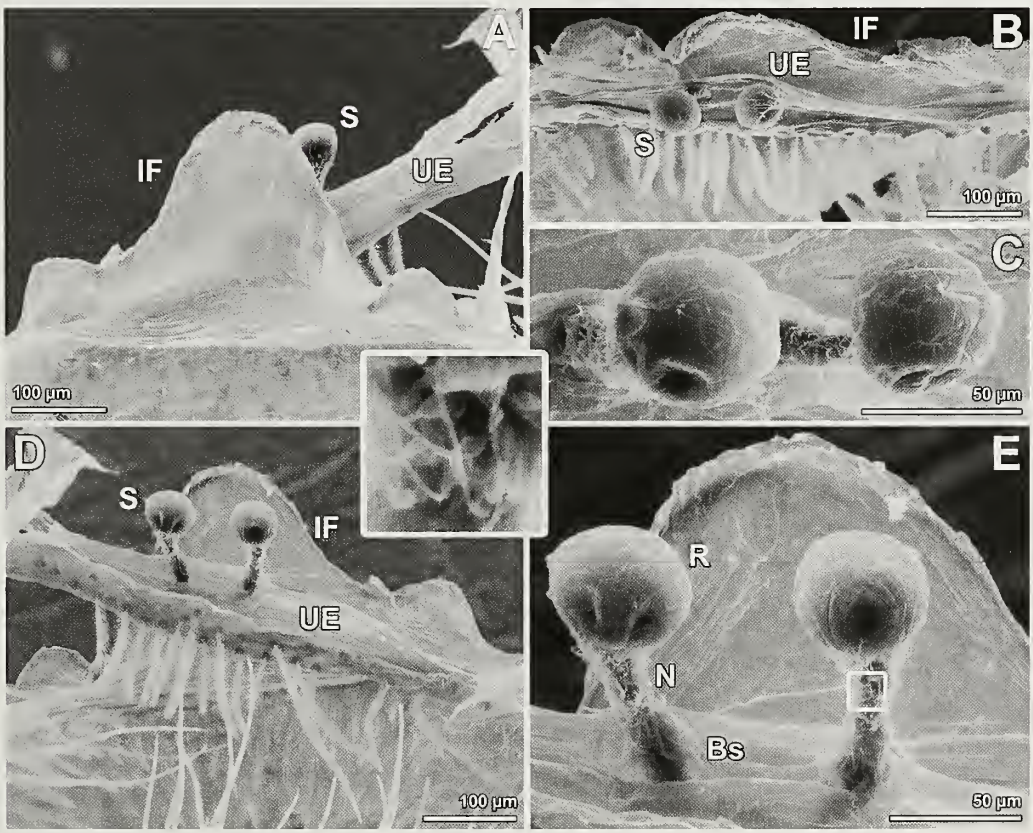

cymbium would represent at least one instance of homoplasy. On the other hand, the new species shows a particular shape of the cymbium: large, anteriorly convex, covering the bulb dorsally, and with an area devoid of setae. We have recently argued (Magalhaes & Ramírez 2017) that an anteriorly concave cymbium (the "horseshoe-shaped cymbium" that Lehtinen (1967) suggested to be diagnostic of *Pritha* Lehtinen, 1967) is widespread among prithine genera, including *Pikeliuia* and *Filistatiuella*, and is probably a synapomorphy of the subfamily. Thus, an anteriorly projected, convex cymbium covering the bulb is a rare character among the Prithinae, to my knowledge present only in *Antilloides* (see Brescovit et al. 2016b, figs. 11A–C). The anteriorly elongate interpulmonary fold (termed "uterus externus" by Brescovit et al. 2016b) is also a diagnostic feature of some (though not all) *Antilloides* species. Finally, the new species lacks pores in the receptacles of the spermathecae; these are restricted to the 'necks'. My own observations of *Antilloides* females (including *A. abeli* Brescovit, Sánchez-Ruiz & Alayón, 2016, *A. mesoliticus* Brescovit, Sánchez-Ruiz & Alayón, 2016, and a morphospecies similar to *A. cubitas* Brescovit, Sánchez-Ruiz & Alayón, 2016) show that at least these species have the glandular pores restricted to the 'necks' of the spermathecae; this character is unknown to me in other filistatid genera.

Taken together, these observations suggest that this species belongs to *Antilloides*, the first to be described from mainland North America, as all previously known species are restricted to the Antilles. It is likely that the genus had a wider distribution in the past, and now survives on the Caribbean islands and as a relict in Mexican caves in dry areas. In addition, I report a novel putative synapomorphy for *Antilloides* (or at least a group of species within the genus): the glandular pores restricted to the 'neck' of the spermathecae. The presence of a modified metatarsus II in the new species – the first to be described outside of *Pikeliuia* and *Misionella* – suggests that *Antilloides* is closely related to these genera, or that metatarsal modifications evolved independently several times within Prithinae. Both hypotheses should be tested within a phylogenetic framework that includes a wide sample of taxa and characters.

Finally, the finding of this new *Antilloides* species with a modified metatarsus II in males calls for a reappraisal of the only fossil Filistatidae known to date, *Misionella didicostae* Penney, 2005. This fossil comes from amber deposits from the Dominican Republic (where at least two extant species of *Antilloides* can still be found) and date from the Miocene. Penney (2005a) placed the fossil species in *Misionella* based on the modified metatarsus II combined with the absence of a tibial apophysis. However, the new extant species here described also combines these characters. Furthermore, in the specimen PRC A-10-255 of *M. didicostae*, the cymbium is convex and covers almost half of the bulb; setae can be observed along its margin (Fig. 12D, arrow). This indicates *M. didicostae* also belongs in *Antilloides*, and a new combination is here proposed.

## TAXONOMY

**Family Filistatidae** Ausserer, 1867
**Genus *Antilloides*** Brescovit, Sánchez-Ruiz & Alayón, 2016
*Antilloides* Brescovit, Sánchez-Ruiz & Alayón, 2016: 413.

**Type species.**—*Antilloides abeli* Brescovit, Sánchez-Ruiz & Alayón, 2016, by original designation.

**Diagnosis.**—*Antilloides* males can be recognized by the combination of a retrolateral projection bearing thick setae on the palpal tibia (Figs. 5C, D, F) and a convex, anteriorly drawn cymbium partly covering the bulb dorsally and bearing a glabrous dorsal area (Fig. 5B, D); the metatarsus II may or may not present modifications such as a retrolateral excavation and macrosetae (Fig. 4). *Antilloides* females are similar to *Filistatoides* in having a single pair of spermathecae, usually with a narrow 'neck' between the base and the receptacle (Fig. 7); they differ from *Filistatoides* by having at least one of the two following characters: a large, anteriorly drawn interpulmonary fold covering the spermathecae (Figs. 6D, 8A) (short, not covering the spermathecae in *A. cubitas, A. zozo* Brescovit, Sánchez-Ruiz & Alayón, 2016 and *A. mesoliticus*) or glandular pores restricted to the 'neck' and absent from the receptacles (Figs. 7, 8E) (pores present on the receptacles of *A. haitises* Brescovit, Sánchez-Ruiz & Alayón, 2016).

***Antilloides chupacabras*** sp. nov.
http://zoobank.org/?lsid=urn:lsid:zoobank.org:act:22339F8C-FDB5-4922-9D50-A78D178CE200
(Figs. 2–11)
*Filistatoides* sp. Reddell, 1981: 25.

**Type material.**—*Holotype male*. MEXICO: *Coahuila:* Sierra de Mayrán, Cueva de Yeso, [102.8°W, 25.5°N], 24 July 1965, J. Fish & J. Reddell (AMNH, IFM-1302).

*Paratypes*. MEXICO: *Coahuila:* 6 ♀, 1 juvenile, La Cuchilla, Sierra de Mayrán, Cueva de Empalme, 24 February 1966, W. Bell & J. Reddell (AMNH IFM-1303, 1304); subadult ♀, 50 km E. of Torreon, September 1964, B. Russell (AMNH); 2 ♀, Sierra de Mayrán, 0.25 miles W. of Cueva de Yeso, Cueva de Los Grillos, 24 July 1965, J. Reddell & J. Fish (AMNH); subadult ♂, Sierra San Lorenzo, 4 km E. of Coyote, Cueva del Vapor, [103.15°W, 25.65°N], 9 June 1980, J. Reddell (AMNH); 1 ♀, Cueva del Guano (AMNH); 1 ♀, 4.5 km E. of Coyote, Cueva Granjero (AMNH).

**Note.**—The labels associated with the specimens have no geographical coordinates, or exact locations other than the cave names. For instance, the label of the holotype reads only "Cueva de Yeso, Coah., MEX. / 7-24-65. J Fish, J. Reddell". I have traced their approximate placement using the list of Mexican caves provided by Reddell (1981; see caves listed under Sierra de Mayrán Region, p. 294; see also map on page 18, pinpointing the location of Sierra de Mayrán). Reddel collected most of the specimens himself, and was the first to

Figure 8.—*Antilloides chupacabras* sp. nov., female paratype from Cueva de Empalme, Coahuila (AMNH, IFM-1304), spermathecae, digested: A, dorsal view; B, anterior view; C, antero-lateral view; D–E, ventral view. Inset shows detail of glandular pores. Abbreviations: Bs = spermathecae base, IF = interpulmonary fold, N = spermathecal 'neck', R = receptacle, UE = uterus externus.

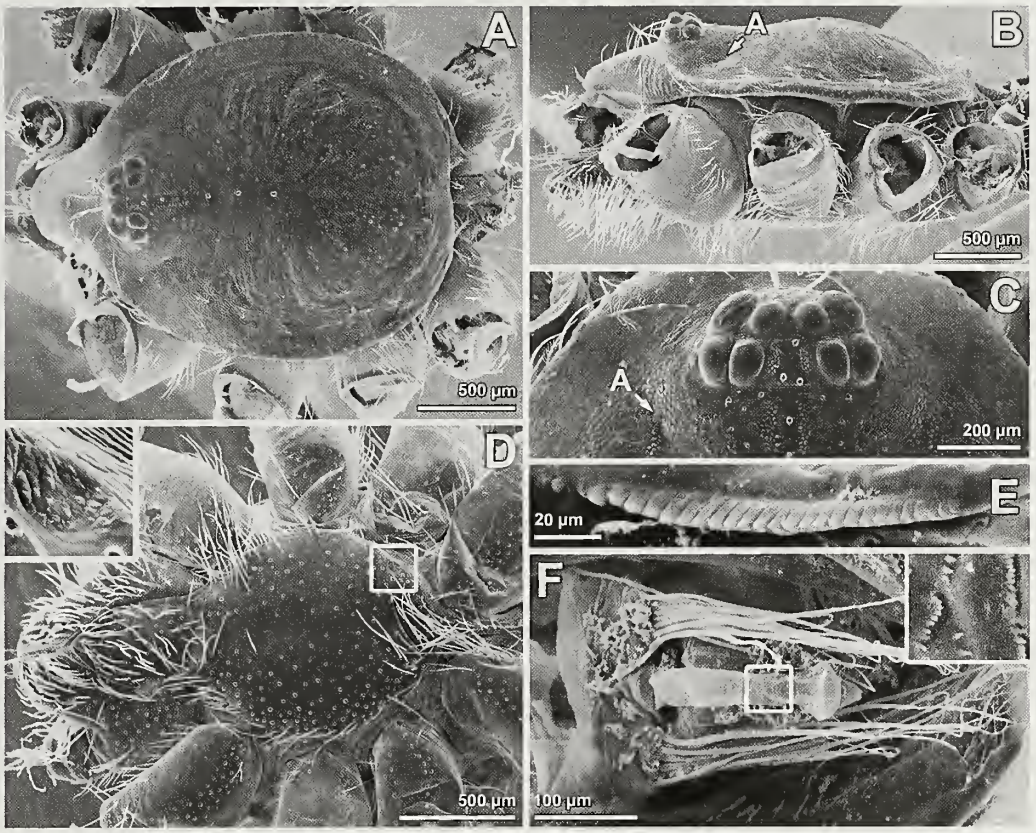


Figure 9.—*Antilloides chupacabras* sp. nov., female paratype from Cueva de Empalme, Coahuila (AMNH, IFM-1304): A, cephalothorax, dorsal view; B, same, lateral view; C, eye region, dorsal view; D, cephalothorax, ventral view (inset shows sternal sigillum); E, serrula, anterior view; F, labrum, subdorsal view (inset shows texture of labral tongue). Abbreviation: A = eye apodeme.

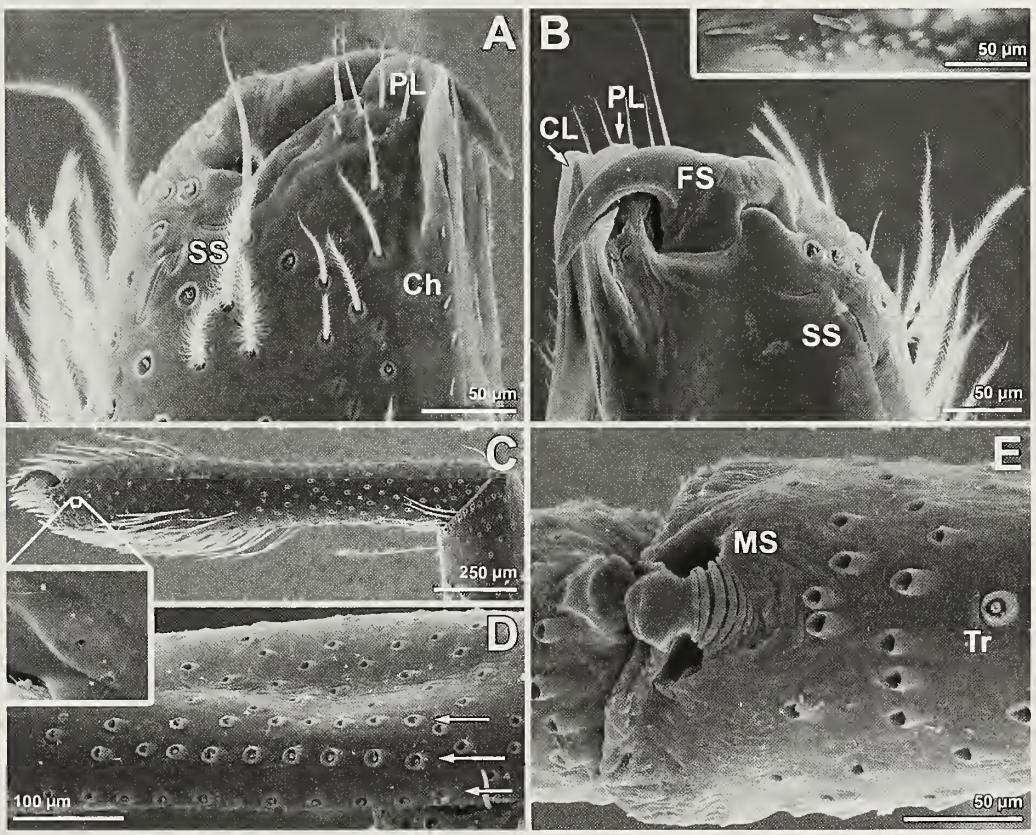

notice that this was an undescribed species, although he listed it under *Filistatoides* (Reddell 1981).

**Etymology.**—The 'chupacabras' is the name of a mythological creature from an urban legend that is widespread in Latin America; it holds that this strange, reptilian creature roams around rural areas and feeds by sucking the blood of livestock. The new species is given this name because it has a strange morphological appearance, feeds by sucking the fluids of its prey, and is the only known species to have been separated from its closest relatives in the Antilles. The specific epithet is to be treated as a noun in apposition.

**Diagnosis.**—Individuals of this species are pale-colored, with reduced pigmentation, and both sexes have more elongate legs than any other *Antilloides* (femur-carapace length ratios of 3.02 and 2.24 in *A. chupacabras* sp. nov. males and females, respectively; at most 2.3 and 1.4 in other *Antilloides* males and females, respectively; Figs. 2–3). Males are easily distinguished from other extant species of *Antilloides* by the metatarsus II bearing two macrosetae on the retrolateral face (Fig. 4) and by the long palp with a short bulb (Fig. 5). Females can be distinguished by the deep furrow bearing setae in the genital region (Fig. 3D), and by the internal genitalia, which have slender, straight 'necks' leading to globose receptacles (Figs. 6B–D, 7, 8) .

**Description.**—*Male holotype* (Figs. 2–4, 6A). Coloration pale yellowish cream except where noted (Fig. 2). Carapace with dark coloration around eyes and a median elongate spot dorsally. Chelicerae orange. Legs pale yellowish cream, except for light orange legs I and II. Abdomen dorsum light cream, with faint brown chevron markings posteriorly. Anterior margin of the carapace unmodified (Fig. 2D). Sternum oval, narrowest posteriorly, sigilla not visible. Total length 5.03. Carapace length 2.30; width 1.85. Clypeus length 0.57. Eye diameters and interdistances: anterior median eye (AME) 0.11; posterior median eye (PME) 0.12; anterior lateral eye (ALE) 0.15; posterior lateral eye (PLE) 0.13; AME–AME 0.03; PME–PME 0.15. Sternum length 1.26; width 1.00. Palp: femur (fe) length 1.67, height 0.25; tibia (ti) length 1.15, height 0.20. Leg I: fe 6.95; patella (pa) 0.85; missing from tibia–tarsus. II: fe 4.50; pa 0.83; ti 5.48; metatarsus (mt) 3.94; tarsus (ta) 1.48. III: fe 3.51, pa 0.81, ti 3.58, mt 3.85, ta 1.49. IV: fe 4.19, pa 0.85, ti 4.03, mt 4.85, ta 2.57. Abdomen: length 2.88; width 1.65. Leg II modified: metatarsus II with a shallow retrolateral apical excavation, a strong retrolateral condyle, and two macrosetae, one more proximal, ventral and parallel to the metatarsus, and the other more distal, dorsal, and pointing dorso-apically (Fig. 4). Leg macrosetae otherwise absent. Palp (Figs. 5, 6A): femur and tibia unusually slender; cymbium convex, covering at least half of the bulb, unfused to bulb (Figs. 5C, D); bulb short and globose, bent slightly upwards distally (Figs. 5G, 6A); sperm duct N-shaped, proximally with a ventral bend (Fig. 6A); paraembolic lamina a small triangular projection situated prolateral to the embolus (Fig. 6A); embolus short. The specimen is in relatively poor condition, with most setae lost, both legs I missing from the tibiae, femora I broken in the midline, left leg III and right leg IV disarticulated from the tibiae, and the left palp dissected.

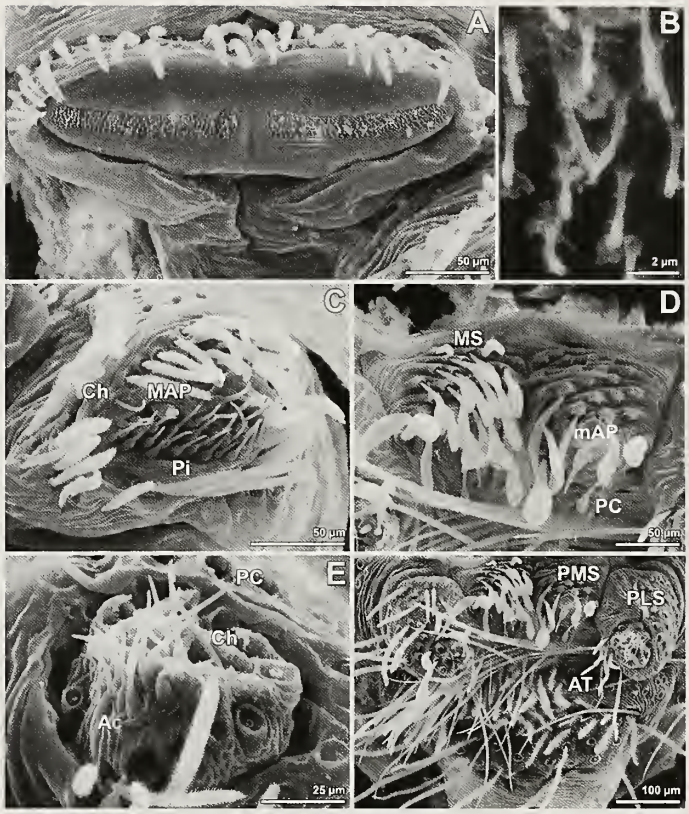


Figure 11.—*Antilloides chupacabras* new species, female paratype from Cueva de Empalme, Coahuila (AMNH, IFM-1304), spinnerets: A, cribellum, ventral view; B, cribellum spigots, ventral view; C, left anterior lateral spinneret, ventral view; D, posterior median spinnerets, ventral view; E, left posterior lateral spinnerets, subventral view; F, anal tubercle and posterior spinnerets. Abbreviations: AT = anal tubercle, Ch = chemosensory seta, MAP = major ampullate gland spigot, mAP = minor ampullate gland spigot, MS = modified setae, PC = paracribellar gland spigot, Pi = piriform gland spigot, PLS = posterior lateral spinnerets, PMS = posterior median spinnerets.

*Female paratype* (AMNH, IFM-1303). Coloration as in male except for more yellowish legs and chelicerae (Fig. 3). Anterior margin of the carapace unmodified, eye apodemes present (Fig. 9A). Sternum oval, narrowest posteriorly, sigilla not visible, but detected in another specimen examined under SEM (Fig. 9D). Total length 7.16. Carapace length 2.83; width 2.03. Clypeus length 0.72. Eye diameters and interdistances: AME 0.06; PME 0.10; ALE 0.13; PLE 0.13; AME–AME 0.06; PME–PME 0.17. Sternum length 1.40; width 1.09. Palp: fe length 2.31, height 0.47; ti length 1.65, height 0.34. Leg I: fe 6.35; pa 0.95; ti 8.88; mt 8.07; ta 2.93. II: fe 4.19; pa 0.83; ti 4.83; mt 4.09; ta 1.54. III: fe 3.33, pa 0.91, ti 3.20, mt 3.48, ta 1.49. IV: fe 3.91, pa 0.93, ti 3.70, mt 4.07, ta 1.76. Abdomen: length 4.47; width 2.65.

Figure 10.—*Antilloides chupacabras* sp. nov., female paratype from Cueva de Empalme, Coahuila (AMNH, IFM-1304), appendages: A, left chelicera, anterior view; B, same, posterior view (inset shows chelicera gland); C, left palp, retrolateral view (inset shows tarsal organ); D, left calamistrum, setae have fallen off (arrows to setal rows); E, metatarsus IV apex, dorsal view. Abbreviations: CL = apex of chelicera lamina, Ch = chemosensory seta, MS = metatarsus stopper, PL = promarginal lobe, SS = slit sensila, Tr = trichobothria socket.

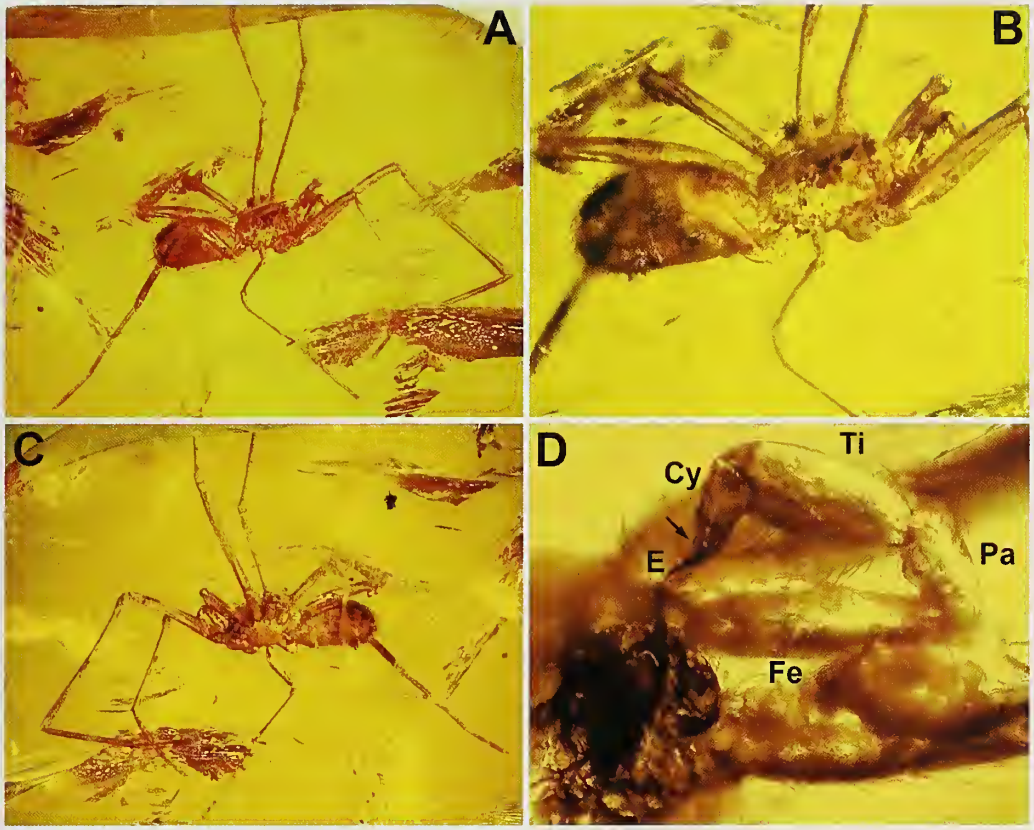


Figure 12.—*Antilloides didicostae* (Penney, 2005), male from Dominican Amber (Oregon State University, PRC A-10-255). Photos courtesy of George Poinar. A B, habitus, dorso-lateral view; C, habitus, sub-ventral view; D, right palp, sub-prolateral view (arrow indicates setae at the apex of cymbium). Abbreviations: Cy = cymbium, E = embolus, Fe = palpal femur, Pa = palpal patella, Ti = palpal tibia.

Chelicerae with a posterior row of chemosensory setae, and gland with projected openings (Fig. 10B). Palp and leg macrosetae absent. Tarsal organ capsulate (Fig. 10C), metatarsus stopper narrowed (Fig. 10E). Calamistrum three-rowed (Fig. 10D), missing most setae. Cribellum very wide, with narrow spinning fields (Fig. 11 A), posterior median spinnerets with spatulate setae (Fig. 11D), posterior lateral spinnerets with several aciniform gland spigots (Fig. 11E). Epigastric furrow unsclerotized, with a fold delimiting a depression bearing many setae (Fig. 3D). The specimen is in relatively good condition, but most setae are missing.

*Female paratype* (AMNH, IFM-1304). Interpulmonary fold enlarged anteriorly, covering the spermathecae, with ragged anterior margin, and laterally subsquarish (Figs. 6D, 7A, 8); with a single pair of receptacles, each connected to the uterus externus through a long and thin spermathecal 'neck' covered by glandular pores; receptacles globose, without glandular pores, set close to each other (Figs. 7B, 8E).

**Variation.**—Females ($n = 5$): total length 6.55–7.16 (mean 6.84), carapace length 2.43–3.01 (2.72), femur 1 length 5.54–6.70 (6.14), tibia 1 length 7.62–9.22 (8.62), femur/carapace length ratio 2.15–2.41 (2.26). The receptacles in the female genitalia can be rounded (Fig. 7B) to oval (Fig. 7D); subadult females have simpler, smaller genitalia (Fig. 6C).

**Natural history.**—All of the specimens of *A. clupacabras* I examined come from caves. They are much more lightly coloured than other species of *Antilloides*, and also have much longer legs (see Diagnosis). It is tempting to suspect that these aspects represent troglomorphisms, but the lack of epigean records might be a consequence of undercollecting outside the caves. More studies on the region should reveal whether this species also occurs outside caves or is a cave obligate, but for now this species should be considered a potential troglophile.

Reddell (1981: 25) stated that the caves in the Sierra de Mayrán are formed by a solution of gypsum beds in Cretaceous limestone, stand at an elevation of ca. 1150 m above sea level, and are very dry, with a fauna typical of Mexican arid areas.

***Antilloides didicostae*** (Penney, 2005), comb. nov.
(Fig. 12)

*Misionella didicostae* Penney, 2005a: 95, figs. 1–5. Male holotype deposited in the Museo del Ámbar Dominicano, not examined; Penney 2005b, fig. 1.

**Note.**—I could not examine the holotype of this species directly, but have examined photos by G. Poinar of a second specimen (Oregon State University, PRC A-10-255), examined and identified by Penney (2005b) shortly after his original description. The palpal morphology (Fig. 12D) fits with the original description. The new combination is here proposed because the examined specimen has a convex cymbium covering the bulb, as do other *Antilloides*. The two characters originally used for placing the species in *Misionella* (the modified second metatarsus and lack of tibial apophysis) are also shared with *Antilloides clupacabras* sp. nov.

## ACKNOWLEDGMENTS

I am indebted to L. Prendini, N. Platnick and L. Sorkin (AMNH), P. Sierwald and J. Boone (FMNH), C. Víquez (INBIO) and G. Giribet and L. Leibensperger (MCZ) for making specimens available for this study. Peter Sprouse helped with finding the exact location of some Mexican caves. George Poinar kindly photographed the *Misionella didicostae* specimen and authorized use of his pictures. I thank D. Penney for suggesting some references and pointing out the existence of the second specimen of *M. didicostae*. Fabián Tricárico helped with the acquisition of SEM images. Earlier versions of the manuscript have been improved by commentaries from M.J. Ramírez and A. Pérez-González, and by a careful revision by A. Sánchez-Ruiz, an anonymous reviewer and the editor, M. Rix. I have been supported by a CONICET doctoral fellowship and by grants from CONICET (2012–0943) and FONCyT (2011–1007) to Martín J. Ramírez.

## LITERATURE CITED

Brescovit, A.D., I.L.F. Magalhaes & I. Cizauskas. 2016a. Three new species of *Misionella* from northern Brazil (Araneae, Haplogynae, Filistatidae). ZooKeys 589:71–96.

Brescovit, A.D., A. Sánchez-Ruiz & G. Alayón. 2016b. The Filistatidae in the Caribbean region, with a description of the new genus *Antilloides*, revision of the genus *Filistatoides* F. O. P.-Cambridge and notes on *Kukulcania* Lehtinen (Arachnida, Araneae). Zootaxa 4136:401–432.

Cruz-López, J.A., D.N. Proud & A. Pérez-González. 2016. When troglomorphism dupes taxonomists: morphology and molecules reveal the first pyramidopid harvestman (Arachnida, Opiliones, Pyramidopidae) from the New World. Zoological Journal of the Linnean Society 177:602–620.

Gray, M.R. 1995. Morphology and relationships within the spider family Filistatidae (Araneae: Araneomorphae). Records of the Western Australian Museum 52:79–89.

Griswold, C.E., T. Audisio & J.M Ledford. 2012. An extraordinary new family of spiders from caves in the Pacific Northwest (Araneae, Trogloraptoridae, new family). ZooKeys 215:77–102.

Legittimo, C.M., E. Simeon, P.D.I. Pompeo & A. Kulczycki. 2017. The Italian species of *Pritha* (Araneae, Filistatidae): a critical revision and description of two new species. Zootaxa 4243:201–248.

Lehtinen, P.T. 1967. Classification of the cribellate spiders and some allied families, with notes on the evolution of the suborder Araneomorpha. Annales Zoologici Fennici 4:199–468.

Magalhaes, I.L.F. 2016. On new or poorly known Australian Filistatidae spiders (Araneae: Araneomorphae), including a study on the fine morphology of *Waudella*. Journal of Natural History 50:1815–1858.

Magalhaes, I.L.F. & M.J. Ramírez. 2017. Relationships and phylogenetic revision of *Filistatinella* spiders (Araneae: Filistatidae). Invertebrate Systematics 31:665–712. doi/full/10.1071/IS16083

Penney, D. 2005a. First fossil Filistatidae: a new species of *Misionella* in Miocene Amber from the Dominican Republic. Journal of Arachnology 33:93–100.

Penney, D. 2005b. Fossil blood droplets in Miocene Dominican amber yield clues to speed and direction of resin secretion. Palaeontology 48:925–927.

Ramírez, M.J. & C.J. Grismado. 1997. A review of spider family Filistatidae in Argentina (Arachnida, Araneae), with a cladistic reanalysis of filistatid genera. Entomologica Scandinavica 28:319–349.

Reddell, J.R. 1981. A review of the cavernicole fauna of Mexico, Guatemala, and Belize. Bulletin of the Texas Memorial Museum, the University of Texas at Austin 27:1–327.

World Spider Catalog. 2017. World Spider Catalog. Version 18. Natural History Museum, Bern. Online at http://wsc.nmbe.ch.

Zonstein, S. & Y.M. Marusik. 2015. The first record of *Audoharano* Lehtinen, 1967 (Araneae: Filistatidae) from mainland Africa. African Invertebrates 56:483–489.

Zonstein, S. & Y.M. Marusik. 2016. A revision of the spider genus *Zaituna* (Araneae, Filistatidae). European Journal of Taxonomy 214:1–97.

*Manuscript received 29 May 2017, revised 18 August 2017.*

## APPENDIX 1

**Material examined.**—The following comparative material of *Antilloides* and *Filistatoides* was examined for this study:

*Antilloides abeli* Brescovit, Sánchez-Ruiz & Alayón, 2016. CUBA: *Piñar del Río*: 5 ♀, Viñales, San Vincente, cave entrance, [83.7166°W, 22.6166°N], 9 January 1954, L. Ross (FMNH 2857656).

*Antilloides mesoliticus* Brescovit, Sánchez-Ruiz & Alayón, 2016. CUBA: *Piñar del Río*: 5 ♀, San Diego de Los Baños, Cueva de los Indios, [83.36558°W, 22.64661°N] (AMNH IFM-1310).

*Antilloides* morphotype 'IFMsp114' (cf. *A. cubitas* Brescovit, Sánchez-Ruiz & Alayón, 2016). BRITISH VIRGIN ISLANDS: *Virgin Gorda*: 3 ♀, Baths & Devil's Bay, [64.44336°W, 18.42663°N], 25 June 1966, Island Project Staff (AMNH IFM-1285).

*Antilloides* morphotype 'IFMsp151'. FRENCH WEST INDIES: *Saint Barthéleuy*: 3 ♀, [62.83333°W, 17.9°N], 2008, K. Questel (MCZ 79820).

*Antilloides* morphotype 'IFMsp153'. BRITISH VIRGIN ISLANDS: *West Dog Seal*. 1 ♀, [64.43467°W, 18.50665°N], Island Project Staff (AMNH IFM-1309).

*Filistatoides insignis* (O. Pickard-Cambridge, 1896). GUATEMALA: *Tijax*: 3 ♀, [89.26903°W, 15.37521°N], C. Víquez (INBIO IFM-1189).

*Filistatoides* morphotype 'IFMsp23'. MEXICO: *Nuevo León*: 1 ♂, 9 ♀, 5 juveniles, near Mt. El Candela, Gruta del Carrizal, in darkness, [100.57037°W, 26.77644°N], B. Russell (AMNH IFM-1282).

2018. Journal of Arachnology 46:249–344

# Systematics of the spiny trapdoor spider genus *Bungulla* (Mygalomorphae: Idiopidae): revealing a remarkable radiation of mygalomorph spiders from the Western Australian arid zone

**Michael G. Rix**[1,2,3], **Robert J. Raven**[1], **Andrew D. Austin**[2], **Steven J. B. Cooper**[2,4] and **Mark S. Harvey**[3,5,6]: [1]Biodiversity and Geosciences Program, Queensland Museum, South Brisbane, Queensland 4101, Australia. E-mail: michael.rix@qm.qld.gov.au; [2]Australian Centre for Evolutionary Biology and Biodiversity, and Department of Ecology and Evolutionary Biology, School of Biological Sciences, The University of Adelaide, Adelaide, South Australia 5005, Australia; [3]Department of Terrestrial Zoology, Western Australian Museum, Welshpool, Western Australia 6106, Australia; [4]Evolutionary Biology Unit, South Australian Museum, Adelaide, South Australia 5005, Australia; [5]School of Biological Sciences, The University of Western Australia, Crawley, Western Australia 6009, Australia; [6]School of Natural Sciences, Edith Cowan University, Joondalup, Western Australia 6027, Australia

**Abstract.** The aganippine spiny trapdoor spiders of the genus *Bungulla* Rix, Main, Raven & Harvey are revised, and 30 new species are described from Western Australia: *B. ajana* sp. nov., *B. aplini* sp. nov., *B. banksia* sp. nov., *B. bella* sp. nov., *B. bidgemia* sp. nov., *B. biota* sp. nov., *B. bringo* sp. nov., *B. burbidgei* sp. nov., *B. dipsodes* sp. nov., *B. disrupta* sp. nov., *B. ferraria* sp. nov., *B. fusca* sp. nov., *B. gibba* sp. nov., *B. hameliaeusis* sp. nov., *B. harrisonae* sp. nov., *B. hillyerae* sp. nov., *B. inermis* sp. nov., *B. iota* sp. nov., *B. keigheryi* sp. nov., *B. keirani* sp. nov., *B. kendricki* sp. nov., *B. laevigata* sp. nov., *B. mckenziei* sp. nov., *B. oraria* sp. nov., *B. parva* sp. nov., *B. quobba* sp. nov., *B. sampeyae* sp. nov., *B. weld* sp. nov., *B. westi* sp. nov. and *B. yeni* sp. nov. The type species, *B. bertmaini* Rix, Main, Raven & Harvey, 2017, is re-illustrated and re-diagnosed, and *B. riparia* (Main, 1957) is re-described. Molecular data from seven genes for a subset of taxa are analyzed with Bayesian methods, to complement the morphological descriptions, to help delimit three species known only from female specimens, and to generate a provisional phylogeny of the genus. Species of *Bungulla* exhibit a remarkable range of genitalic and somatic morphologies, and we here document this diversity, demonstrating that the characteristic loss of the retrolateral tibial apophysis has not been associated with a concomitant loss of genitalic complexity. We further provide a key to all known species and highlight the southern Carnarvon Basin (including the western Yalgoo and northern Geraldton Sandplains) as a hotspot of diversity.

**Keywords:** Taxonomy, tribe Aganippini, subfamily Arbanitinae, biogeography, Shark Bay

http://zoobank.org/?lsid=urn:lsid:zoobank.org:pub:8544DABD-1B89-47C9-A4DC-09E552329F5D

The spiny trapdoor spiders of the Western Australian endemic genus *Bungulla* Rix, Main, Raven & Harvey, 2017 (Figs. 1–10) are a major component of the idiopid fauna of western continental Australia (Fig. 11), and among the genera of Aganippini, second only to *Idiosoma* Ausserer, 1871 in known diversity (Rix et al. 2017d; M. Rix unpubl. data). Prior to 2017, the only described species in the genus, *B. riparia* (Main, 1957), was placed in the genus *Eucyrtops* Pocock, 1897, along with numerous recognized but undescribed species present in Australian collections. The molecular phylogenetic study of Rix et al. (2017b) was the first to highlight the presence of two main clades of *Eucyrtops* (Fig. 10), and subsequent morphological analysis clarified the identity of the *Bungulla*-clade relative to *E. latior* (O. P.-Cambridge, 1877) and its closest relatives (i.e., *Eucyrtops* s. s.). As a result, Rix et al. (2017d) formally described *Bungulla* (for which a genus-group name was not previously available), and removed the closely related genus *Gaius* Rainbow, 1914 from synonymy with *Auidiops* Pocock, 1897.

As the only lineage of Arbanitinae without a retrolateral tibial apophysis (RTA) on the male pedipalp, species of *Bungulla* are among the most recognizable of Australasian Idiopidae. Thanks to collections made for environmental impact assessments since 2000, and to major biotic surveys throughout Western Australia since the 1990s (Burbidge et al. 2000; Keighery 2004; McKenzie et al. 2009), all of which utilized wet pitfall trapping methods and long-term sampling, we now know that the genus has a widespread distribution throughout much of western, central and south-western Western Australia (Fig. 11). Relatively few specimens were known prior to the 1990s, due in part to the rarity and low diversity of species from temperate regions, and a dearth of collections from more remote areas. However, during the then CALM (Department of Conservation and Land Management) 'Biodiversity Survey of the Southern Carnarvon Basin', run from 1994–1995 (Burbidge et al. 2000; Main et al. 2000), the remarkable diversity of arid zone *Bungulla* was revealed for the first time. This comprehensive biological survey resulted in the collection of over one third (i.e., 13) of all new species of *Bungulla* described in the current study, over 90% of which appear to be endemic to the region. At a number of sites (e.g., Zuytdorp and Nanga Station), unprecedented levels of sympatry or parapatry were documented (as '*Eucyrtops*'; Main et al. 2000). Additional survey work in subsequent years has resulted in the discovery of other new species, especially in the Murchison bioregion, however nowhere else exhibits the same level of species diversity as the southern Carnarvon Basin (including the adjacent western Yalgoo and northern Geraldton Sandplains). Documenting this remarkable diversity is therefore the aim of our study, not least because the conservation of Australian trapdoor spiders is dependent on a robust taxonomy (Rix et al. 2017c).


Figures 1–9.—Live habitus images and burrows of *Bungulla*: 1–3, holotype male (WAM T126205) and burrow of *B. biota* sp. nov. from Mount Richardson (Western Australia); 4, holotype male *B. lillyerae* sp. nov. (WAM T144352) from Madura Caravan Park (Western Australia); 5–6, burrow of holotype female *B. harrisonae* sp. nov. (WAM T129257) from John Forrest National Park (Western Australia), with Australian two dollar coin of diameter 20 mm for scale; 7–9, paratype female (WAM T143010) and burrow of *B. gibba* sp. nov. from Two Peoples Bay Nature Reserve (Western Australia). Images 1–3 by R. Teale; 4, 7 by M. Harvey; 5–6, 8–9 by M. Rix.

This paper is the fourth in a series of revisionary works to describe Western Australia's known species of *Bungulla*, *Cataxia* Rainbow, 1914 (see Rix et al. 2017a), *Eucanippe* Rix, Main, Raven & Harvey, 2017 (see Rix et al. 2018), *Eucyrtops*, *Euoplos* Rainbow, 1914, *Gaius* Rainbow, 1914 and *Idiosoma* (see Rix et al. 2017d). Thirty new species of *Bungulla* are here described, taking the total number of species in the genus to 32.

## METHODS

**Morphological methods.**—Morphological methods, including the format of species descriptions, follow Rix et al. (2017d). All species are distinguished and diagnosed according to a generalized species concept, whereby morphological and (where available) molecular data are combined to provide the operational criteria for distinguishing "separately evolving metapopulation lineages" (de Queiroz 2007: 880). Most species are described from only one sex, due largely to male collection biases in pitfall trap surveys, and to the requirement of molecular data for adequately distinguishing *Bungulla* females from similar females of *Eucyrtops*. Specimens were examined using a Zeiss Stemi SV11 stereomicroscope, and female genitalia were cleared in 100% lactic acid at room temperature. Measurements (in millimeters, to one decimal place) and digital automontage images were taken using a Leica M165C stereomicroscope with mounted DFC425 digital camera and processed using Leica Application Suite Version 3.7 software; one specimen (WAM T3961) was imaged using a Leica MZ16A stereomicroscope with mounted DFC500 digital camera and processed using Leica Application Suite Version 4.6.1 software. Species are presented in this paper in alphabetical order (following the generic type species), and leg segments were measured along the dorsal prolateral edge, in lateral view. Total body length measurements include the chelicerae, in dorsal view. Most available male specimens of

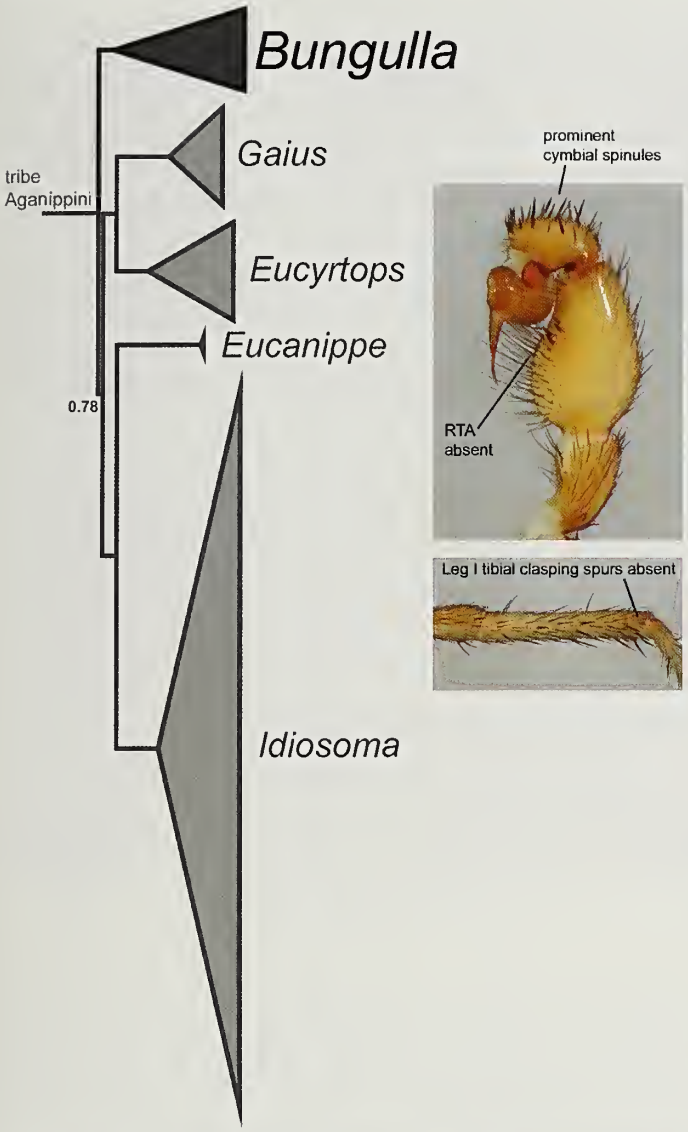


Figure 10.—Summary phylogeny of the tribe Aganippini, from the 'FULL' 12-gene Bayesian analysis of Rix et al. (2017b), showing the phylogenetic position of *Bungulla*. Inset images show the retrolateral pedipalp and prolateral leg I tibia of *B. bringo* sp. nov., and the three male apomorphies characteristic of all *Bungulla*. Unlabelled nodes have a posterior probability of 1.0.

*Bungulla* were illustrated for this study, either within the primary numbered plates or, for additional (non-holotype) specimens, as an 'Atlas' series of more rapidly assembled single-shot images in four standard views (see Supplementary File 1, Online at http://dx.doi.org/10.1636/JoA-S-17-057.s1). The latter are included for ease of comparison to the type specimens, to directly illustrate the subtle morphological variation in key characters typical of Mygalomorphae, and to provide a comprehensive digital compendium of the material available in collections. For records with multiple specimens per vial, in most cases only a single exemplar specimen was imaged. For the species *B. bertmaini* Rix, Main, Raven & Harvey, 2017 and *B. yeni* sp. nov., for which > 20 records were available, a geographically and morphologically representative selection of 22 (*B. bertmaini*) and 12 (*B. yeni* sp. nov.) specimens was imaged for each. Maps were generated using the online Atlas of Living Australia (online at http://www.ala.org.au/) and are reproduced under a Creative Commons Attribution 3.0 Australia license.

Specimens are lodged at the Western Australian Museum, Perth (WAM), the Queensland Museum, Brisbane (QMB) and the South Australian Museum, Adelaide (SAM), and the following abbreviations are used throughout the text: ALE, anterior lateral eye/s; AME, anterior median eye/s; *COI*, cytochrome *c* oxidase subunit I; *CYB*, cytochrome b; IBRA, Interim Biogeographic Regionalisation of Australia Version 7 (available online at https://www.environment.gov.au/land/nrs/science/ibra); ITS1–2, internal transcribed spacer 1–2; *MRPL45*, 39S ribosomal protein L45 mitochondrial; PLE, posterior lateral eye/s; PME, posterior median eye/s; *RPF2*, ribosome production factor 2 homolog; RTA, retrolateral tibial apophysis (of male pedipalp); *XPNPEP3*, probable Xaa-Pro aminopeptidase 3. For readability and ease of diagnosis, 'sp. nov.' epithets are removed from the body text after the key to species.

**Molecular methods.**—Nucleotide sequences for seven genes (*COI*, *CYB*, ITS1–2, *MRPL45*, *RPF2*, *XPNPEP3*) were generated for 19 specimens of *Bungulla* for which tissue was available (older pitfall trap material was not sequenced for this study), using a next-generation parallel tagged amplicon sequencing (TAS) approach, described in detail by Rix et al. (2017b). For each specimen sequenced, DNA voucher codes and GenBank accession numbers are provided next to repository registration numbers in the material examined section for each species (below), in the form: [Registration$^{DNA_Voucher_Code}$; GenB_COI_No., GenB_CYB_No., GenB_MRPL45_No., GenB_RPF2_No., GenB_XPNPEP3_No., GenB_ITS_No.]. Outgroup sequences were obtained from data previously published by Rix et al. (2017b). The ultimate outgroup for the molecular analyses was the diplurid spider *Cethegus fugax* (Simon, 1908), and other outgroups included an undescribed species of *Prothemenops* Schwendinger, 1991 and *Euoplos spinnipes* Rainbow, 1914. In total, sequences were analyzed for 22 specimens (see Supplementary File 2, online at http://dx.doi.org/10.1636/JoA-S-17-057.s2).

Individual gene alignments were conducted in Geneious R6 (Biomatters Ltd.; online at http://www.geneious.com/) using the MAFFT v7.017 plugin with default parameters, and these alignments were concatenated to generate a 'FULL' dataset (Supplementary File 2) which included all available data for all taxa, and a 'NUCLEAR' dataset (Supplementary File 3, online at http://dx.doi.org/10.1636/JoA-S-17-057.s3) which included only the nuclear sequences for 21 specimens (nuclear sequences were not available for '274_T131634_F_BU_~disrupta'). PartitionFinder Version 1.1.1 (Lanfear et al. 2012) was used to choose an optimal partitioning scheme, favoring a 10 partition model for the 'FULL' dataset; for the 'NUCLEAR' dataset, four mitochondrial partitions were excluded (see Supplementary Files 2, 3 for a detailed summary of the models used in each analysis). Both datasets (Supplementary Files 2, 3) were analyzed in MrBayes Version 3.2.6 (Huelsenbeck & Ronquist 2001; Ronquist & Huelsenbeck 2003) via the CIPRES Science Gateway (Miller et al. 2010), with substitution model parameters estimated independently for each partition

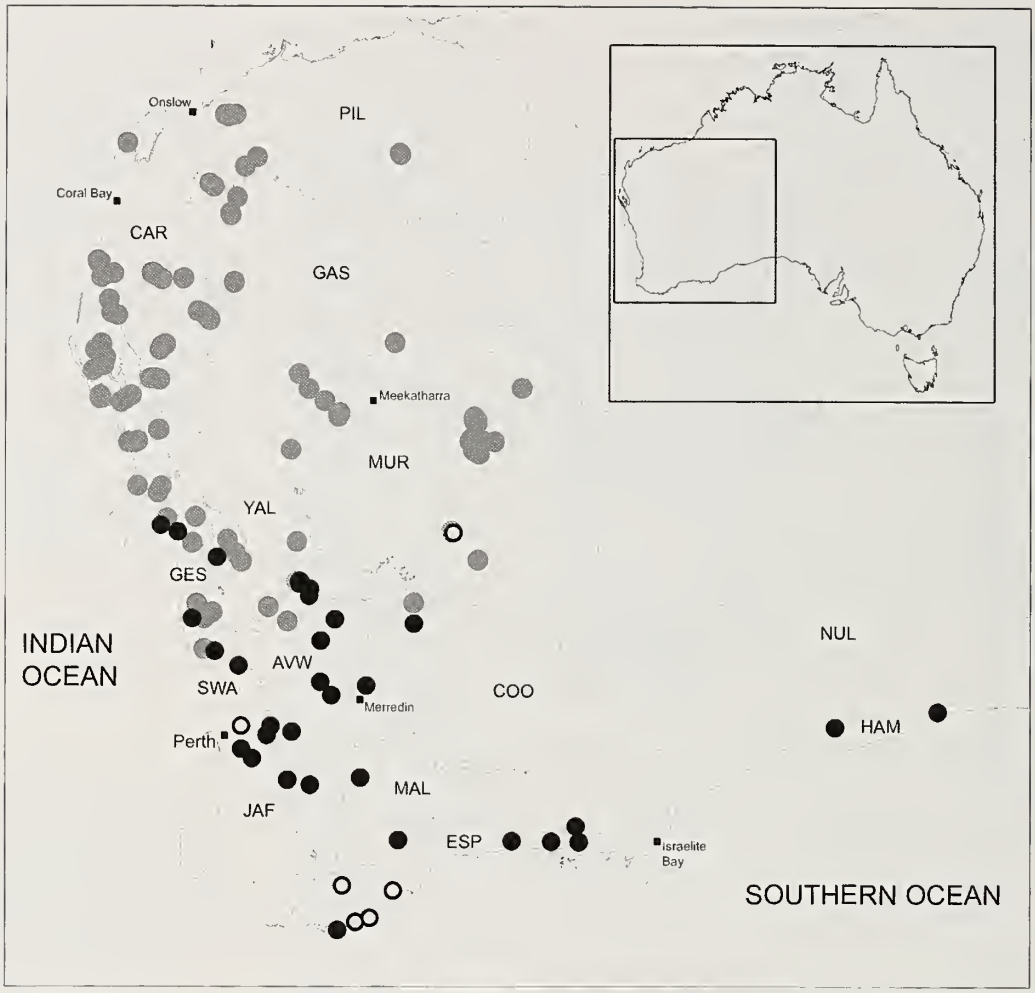


Figure 11.—Map showing collection records of *Bungulla* from Australia. Black circles denote temperate species with < 5 retrolateral spinules on the male palpal tibia (see Fig. 12); grey circles denote species with > 10 retrolateral spinules on the male palpal tibia (see Fig. 13); open circles denote species/sites represented only by female specimens (all of which are likely to have males with < 5 spinules; see Fig. 14). Relevant IBRA 7.0 bioregional acronyms are as follows: AVW, Avon Wheatbelt; CAR, Carnarvon; COO, Coolgardie; ESP, Esperance Plains; GAS, Gascoyne; GES, Geraldton Sandplains; HAM, Hampton; JAF, Jarrah Forest; MAL, Mallee; MUR, Murchison; NUL, Nullarbor; PIL, Pilbara; SWA, Swan Coastal Plain; YAL, Yalgoo.

([Unlink tratio = (all) pinvar=(all) shape=(all) statefreq=(all) revmat=(all)]) and rates allowed to vary across partitions ([Prset applyto=(all) ratepr=variable]). Four Markov Chain Monte Carlo (MCMC) chains were run for 10 million generations for each analysis, sampling every 1000 generations, with the first 10% of sampled trees discarded as 'burnin' ([burnin = 1000]). Two additional 40 million generation analyses were also run for each dataset, to ensure adequate sampling and topological congruence. Summary statistics of estimated parameters, including ESS values, were assessed using Tracer Version 1.6 (Rambaut et al. 2014), and FigTree Version 1.4.2 (online at http://tree.bio.ed.ac.uk/software/figtree/) was used to visualize 50% majority-rule consensus trees (Fig. 14).

## RESULTS AND DISCUSSION

Bayesian analyses of both the 'FULL' dataset (2 mitochondrial genes, 5 nuclear genes; 22 specimens for 4,265 bp) and the 'NUCLEAR' dataset (5 nuclear genes; 21 specimens for 2,912 bp) recovered a similar topology (Fig. 14) consistent with that inferred by Rix et al. (2017b) for a subset of the same taxa. Male specimens identified as conspecific according to morphological criteria were also inferred as monophyletic lineages, although overall coverage of the genus at the species level was low (22%). Early-branching lineages were temperate in distribution and, although no males of these lineages were directly sequenced for the molecular analyses, an absence of spinules on the male palpal tibia (Fig. 12) is inferred as symplesiomorphic for *Bungulla* given the distributions of sequenced females (relative to Fig. 14) and the phylogenetic position of *B. disrupta* sp. nov. (WAM T131634), the latter of which is tentatively linked to male conspecifics. Sequenced species with > 10 retrolateral spinules on the male palpal tibia (i.e., *B. bertmaini*, *B. biota* sp. nov. and *B. yeni* sp. nov.; Fig. 13) were derived relative to other taxa – a result consistent with a hypothesis of 'derived xeric adaptation' out of temperate south-western Australia (Rix et al. 2015, 2017b) in


Figure 12.—Montage of pedipalps of species of *Bungulla* with < 5 retrolateral spinules on the male palpal tibia. Note the two main types of cymbial spinules.

at least one clade of taxa with numerous spinules on the palpal tibia. Pronounced mitochondrial and to a lesser extent nuclear genetic structure was also evident among disparate populations of some arid species – namely *B. bertmaini* and *B. biota* sp. nov. (Fig. 14) – however, determining whether such uncorrected pairwise divergences for *COI* (up to 15.4% for *B. biota* sp. nov., and 15.6% for *B. bertmaini*) are the result of inadequate sampling, incipient or cryptic speciation and/or distance effects requires a much larger taxon sample. Future molecular sampling in this genus should therefore focus on genetically diverse (Fig. 14) and geographically widespread (Fig. 36) taxa like *B. bertmaini*, for which cryptic speciation cannot be ruled out, and on the highly diverse fauna of the southern Carnarvon Basin, for which molecular and phylogenetic data are currently lacking. Similarly, given the diversity and apparent levels of sympatry in the southern Carnarvon Basin (as revealed by pitfall trap data), future research exploring actual levels of syntopy, patterns of spatial segregation, micro-habitat preferences, size class distributions and burrow morphologies among different species would also be useful to understand how so many congeners can potentially occur in such close proximity.

## SYSTEMATICS

**Family Idiopidae** Simon, 1889
**Subfamily Arbanitinae** Simon, 1903

**Tribe Aganippini** Simon, 1903
**Genus *Bungulla*** Rix, Main, Raven & Harvey, 2017

*Bungulla* Rix, Main, Raven & Harvey, 2017 in Rix et al., 2017d: 602.

**Type species.**—*Bungulla bertmaini* Rix, Main, Raven & Harvey, 2017, by original designation.

**Diagnosis.**—Males of *Bungulla* can be distinguished from all other Arbanitinae by the absence of a retrolateral tibial apophysis (RTA) on the male pedipalp (Rix et al. 2017d) (Fig. 10). They can be further characterized by the absence of prolateral clasping spurs on the leg I tibia (Fig. 10; cf. Rix et al. 2017d, figs. 10, 139, 213), by the presence of a field of strong spinules on the dorsal cymbium (Fig. 10; cf. Rix et al. 2017d, figs. 48, 142, 218), and by the absence of a complete fringe of porrect setae around the lateral margins of the male carapace (Figs. 15, 99; cf. Rix et al. 2017d, figs. 35, 132, 178). Seven species have re-evolved a rudimentary RTA-like bulge on the male palpal tibia (Figs. 108, 134, 147, 280, 306, 406, 432), but can be easily placed in *Bungulla* by those features otherwise characteristic of the genus.

Females of *Bungulla* are very similar to females of *Eucyrtops* but can be distinguished from most species of *Idiosoma* and *Eucanippe* by the absence of sclerotized abdominal sigilla (Figs. 77, 200), and from species of *Gaius* by their smaller body size and relatively less setose somatic morphology. Seven autapomorphic nucleotide substitutions can also be used to


Figure 13.—Montage of pedipalps of species of *Bungulla* with > 10 retrolateral spinules on the male palpal tibia. Note the enormous variation in the shape of the tibia, the length and shape of the embolus, the distribution of tibial spinules, and the morphology of the cymbial spinules.

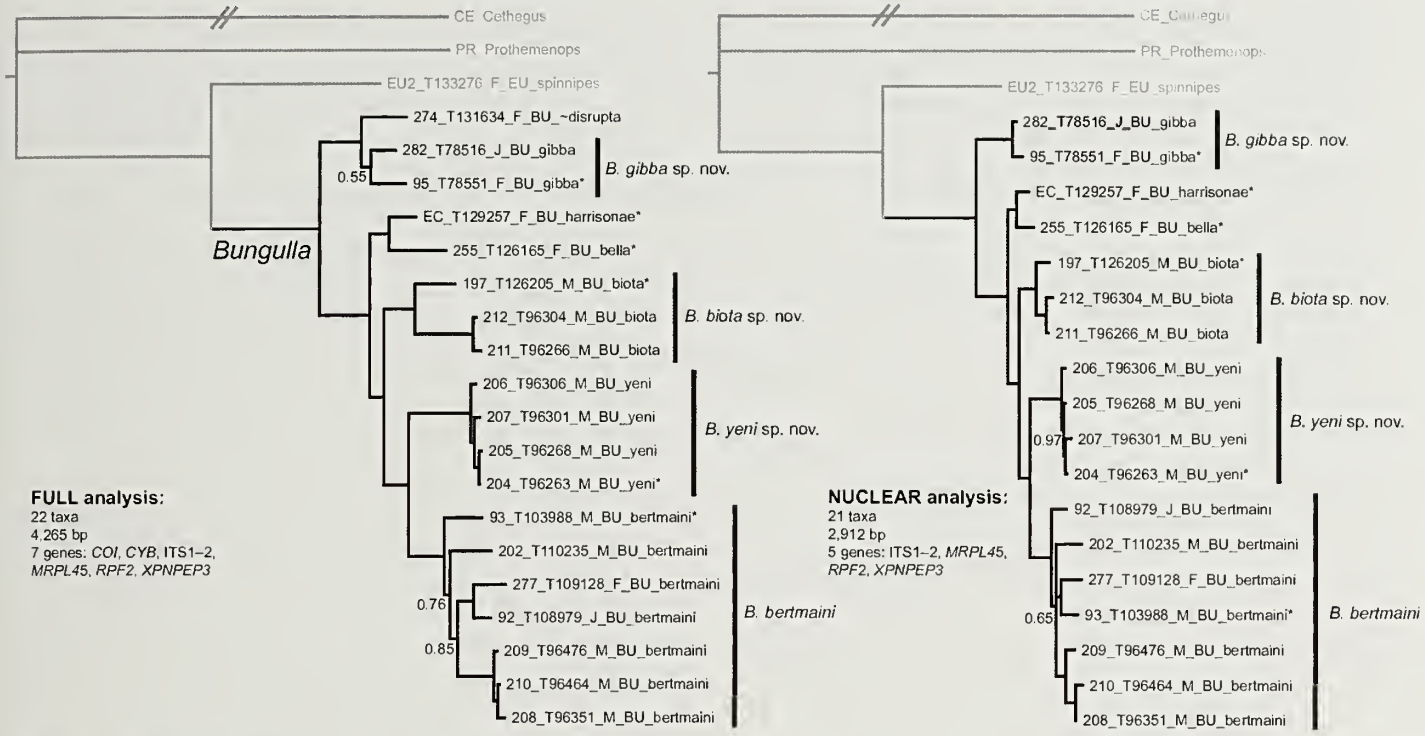


Figure 14.—Bayesian 50% majority-rule consensus trees resulting from partitioned phylogenetic analyses of the 7 gene 'FULL' dataset (at left) and the 5 gene 'NUCLEAR' dataset (at right). Posterior probabilities < 0.99 are shown adjacent to nodes (all other nodes have a posterior probability of 1.0), and holotype specimens are highlighted (*).

distinguish females, males and juveniles of *Bungulla* from species of *Eucyrtops* and all other Aganippini (see Rix et al. 2017d: 602).

**Description.**—See Rix et al. (2017d).

**Distribution.**—The genus *Bungulla* is endemic to Western Australia, with a broad distribution that extends from the temperate southern forests and south-eastern coastal heathlands, north to the Pilbara and east to the Murchison and Gascoyne bioregions (Fig. 11). Species of *Bungulla* are a major component of the idiopid fauna of central-western Western Australia, with the highest diversity of species found in the northern Geraldton Sandplains, western Yalgoo and southern Carnarvon Basin.

**Composition and remarks.**—*Bungulla* was found to be the sister-genus to all other Aganippini by Rix et al. (2017b; Fig. 10), and includes 32 known species, 30 of which are newly described in this study. The monophyly of the genus is strongly supported by both molecular and morphological characters, although females remain difficult to distinguish from *Eucyrtops* in the absence of molecular data. Most species are relatively small, pale trapdoor spiders (e.g., Figs. 1, 86, 87, 138, 139), although larger and darker taxa are known from some areas (e.g., Figs. 186, 187, 222, 223, 336, 337). The characteristic loss of the RTA has not been associated with a concomitant loss of genitalic complexity, and indeed species of *Bungulla* exhibit a remarkable range of genitalic and somatic morphologies, including male pedipalps which are often unusually autapomorphic and species-specific (Figs. 12, 13). While diverse throughout much of arid and semi-arid Western Australia, little is known of their biology or burrow-building behavior, due largely to the requirement of males for morphological identification (most of which have been collected in pitfall traps) and the remote distributions of most species.

## KEY TO THE AUSTRALIAN SPECIES OF *BUNGULLA* (MALES ONLY)

NB. Males of *Bungulla bella* sp. nov., *B. gibba* sp. nov. and *B. harrisonae* sp. nov. are unknown. See also Supplementary File 1 (online at http://dx.doi.org/10.1636/JoA-S-17-057.s1) for additional images of relevant character states.

1. Palpal tibia with < 5 (and usually without) retrolateral spinules (Fig. 12) ..... 2
– Palpal tibia with > 10 retrolateral spinules (Fig. 13) ..... 10
2. Spinules on cymbium porrect, thorn-like, covering most of dorsal surface of cymbium (Figs. 12, 121, 182, 393) ..... 3
– Spinules on cymbium curved, anteriorly-directed and restricted to distal half of segment (Figs. 12, 160, 195, 241, 254, 345, 358) ..... 5
3. Palpal tibia with very small field of < 5 retrolateral spinules (Figs. 121, 122) ..... ***B. bringo*** sp. nov.
– Palpal tibia without retrolateral spinules (Figs. 182, 393) ..... 4

4. Prolateral tibia I with staggered row of ≥ 4 medial spine-like setae (Fig. 392); palpal tibia relatively stout, without strongly concave disto-ventral margin in retrolateral view (Fig. 393)..... ***B. riparia*** (Main, 1957)
– Prolateral tibia I with 1–3 medial spine-like setae (Fig. 181); palpal tibia more tapered distally, with strongly concave disto-ventral margin in retrolateral view (Fig. 182)..... ***B. ferraria*** sp. nov.
5. Body size very small (carapace width < 2.5) (Fig. 349)..... ***B. parva*** sp. nov.
– Body size larger (carapace width ≥ 3.0) (Figs. 151, 186, 232, 245, 336)..... 6
6. Body coloration dark, carapace usually dark brown (depending on state of preservation) (Figs. 151, 186, 336; see also Supplementary File 1)..... 7
– Body coloration lighter, carapace usually shades of tan brown with darker caput (depending on state of preservation) (Figs. 232, 245; see also Supplementary File 1)..... 9
7. Legs bi-colored, leg I with dark femur and distinctly lighter patella, tibia, metatarsus and tarsus (Fig. 158); abdomen with ornate dorsal pattern of broad pale chevrons (Fig. 152; see also Supplementary File 1)..... ***B. disrupta*** sp. nov.
– Legs more uniformly-colored, without distinctly lighter patellae, tibiae, metatarsi and tarsi (Figs. 193, 343); abdomen with smaller, thinner dorsal chevrons (Figs. 187, 337; see also Supplementary File 1)..... 8
8. Palpal tibia sub-rectangular in retrolateral view, with strongly concave disto-ventral margin (Fig. 345); pro-ventral metatarsus I with 2 or more medial spine-like setae (Fig. 343)..... ***B. oraria*** sp. nov.
– Palpal tibia more bulbous in retrolateral view, with less strongly concave disto-ventral margin (Fig. 195); pro-ventral metatarsus I with at most 1 medial spine-like seta (Fig. 193)..... ***B. fusca*** sp. nov.
9. Tarsus I with row of small prolateral macrosetae (Fig. 239); ALE almost contiguous (Fig. 235)..... ***B. lillyerae*** sp. nov.
– Tarsus I without row of small prolateral macrosetae (Fig. 252); ALE more widely spaced (Fig. 248).. ***B. inermis*** sp. nov.
10. Palpal tibia with field of thorn-like spinules on disto-dorsal margin (Figs. 432–434)..... ***B. westi*** sp. nov.
– Palpal tibia without spinules on disto-dorsal margin (Figs. 24, 59, 108, 134, 445)..... 11
11. Embolus with broad, distally-flattened, truncate tip (Figs. 108, 109)..... ***B. biota*** sp. nov.
– Embolus otherwise, usually tapered, with or without distal modifications (Figs. 24, 95, 147, 280, 319)..... 12
12. Proximal half of palpal tibia with RTA-like ventral bulge in retrolateral view (Figs. 134, 147, 280, 306, 406)..... 13
– Palpal tibia piriform or sub-cylindrical, unmodified, without pronounced ventral bulge (Figs. 24, 46, 59, 95, 267, 393, 445)..... 17
13. RTA-like bulge of palpal tibia with field of porrect dagger-like spinules at apex (Figs. 134, 135).... ***B. burbidgei*** sp. nov.
– Spinules on RTA-like bulge of palpal tibia smaller, cuspule-like or thorn-like (Figs. 147, 280, 306, 406)..... 14
14. RTA-like bulge of palpal tibia developed into relatively acute, attenuate process (Figs. 280, 281) ... ***B. keigheryi*** sp. nov.
– RTA-like bulge of palpal tibia broadly rounded (Figs. 147, 306, 406)..... 15
15. Dorsal abdomen with mottled 'sandy' coloration and thin chevrons (Fig. 398; see also Supplementary File 1) ..... ***B. sampeyae*** sp. nov.
– Dorsal abdomen bi-colored, pale tan in color with dark anterior markings and dark posterior chevrons (Figs. 139, 298; see also Supplementary File 1)..... 16
16. Palpal tibia strongly arched dorsally, with 'pistol-like' profile in retrolateral view (Fig. 306)..... ***B. kendricki*** sp. nov.
– Palpal tibia less strongly arched dorsally, with relatively symmetrical, bulbous profile in retrolateral view (Fig. 147) ..... ***B. dipsodes*** sp. nov.
17. Palpal tibia with medial 'ledge' situated closely proximal to field of spinules, bearing brush of filiform setae (Figs. 46, 47, 59, 60, 293, 294, 332, 333)..... 18
– Palpal tibia without ledge (Figs. 24, 72, 95, 218, 267, 319, 371, 419, 445)..... 21
18. Palpal tibia stout, bulbous and strongly arched dorsally (Fig. 46); medial ledge broad, with relatively large brush of filiform setae (Figs. 46, 47)..... ***B. ajana*** sp. nov.
Palpal tibia longer (Figs. 59, 293, 332); medial ledge shorter with smaller brush of filiform setae (Figs. 59, 60, 293, 294, 332, 333)..... 19
19. Spinules on cymbium short, thorn-like (Fig. 293)..... ***B. keirani*** sp. nov.
– Spinules on cymbium poorly developed, with thinner, almost filiform morphology (Figs. 59, 332)..... 20
20. Palpal tibia long, with sub-cylindrical profile in retrolateral view (Fig. 59)..... ***B. aplini*** sp. nov.
– Palpal tibia broader proximally, with crescent-shaped field of spinules distally (Fig. 332)..... ***B. mckenziei*** sp. nov.
21. Palpal tibia with small field of spinules restricted to disto-ventral margin, situated closely proximal to small retro-distal bulge (Figs. 72, 73)..... ***B. banksia*** sp. nov.
– Palpal tibia with larger field of retrolateral spinules and retro-distal bulge absent (Figs. 24, 95, 218, 267, 319, 371, 419, 445) 22
22. Embolus relatively long (longer than bulb) (Figs. 24, 319, 371)..... 23
– Embolus relatively short (~length of bulb) (Figs. 95, 218, 267, 419, 445)..... 25
23. Embolus relatively straight in standard retrolateral view (Fig. 371); palpal tibia extended distally (distal to spinules), with strongly concave disto-ventral margin in retrolateral view (Fig. 371)..... ***B. quobba*** sp. nov.
– Embolus slightly longer and more strongly curved in standard retrolateral view (Figs. 24, 319); palpal tibia not as extended distally (Figs. 24, 319)..... 24
24. Abdomen usually relatively heavily pigmented (Fig. 16; see also Supplementary File 1); pars cephalica covered with short setae (Fig. 15)..... ***B. bertmaini*** Rix, Main, Raven & Harvey, 2017

– Abdomen lighter, with pale 'sandy' coloration and thin chevrons (Fig. 311; see also Supplementary File 1); pars cephalica glabrous, with relatively few setae (Fig. 310) ..... ***B. laevigata*** sp. nov.
25. Spinules on cymbium poorly developed, with thinner filiform morphology (Figs. 218–220)..... ***B. hamelinensis*** sp. nov.
– Spinules on cymbium relatively thick, spine-like (Figs. 95, 267, 419, 445) ..... 26
26. Palpal tibia with relatively small, rectangular field of retrolateral spinules on distal half of segment (Fig. 445) ..... ***B. yeni*** sp. nov.
– Palpal tibia with larger, crescent-shaped field of retrolateral spinules covering most of retro-ventral surface (Figs. 95, 267, 419)..... 27
27. Palpal tibia with uniformly crescent-shaped field of spinules in retrolateral view (Figs. 95, 267) ..... 28
– Palpal tibia with asymmetric 'wave-shaped' field of spinules in retrolateral view (Fig. 419)..... ***B. weld*** sp. nov.
28. Carapace with marginal lateral indentations between coxae II–III (Fig. 86); carapace width ≥ 2.0 (Fig. 86) ..... ***B. bidgemia*** sp. nov.
– Carapace without lateral indentations between coxae II–III (Fig. 258); carapace width < 2.0 (Fig. 258)... ***B. iota*** sp. nov.

***Bungulla bertmaini*** Rix, Main, Raven & Harvey, 2017
(Figs. 13–36)

*Bungulla bertmaini* Rix, Main, Raven & Harvey, 2017 in Rix et al., 2017d: 602, figs. 152, 159, 163–175.

**Type material.**—*Holotype male*. AUSTRALIA: *Western Australia*: Deception [Hill], 102.5 km N. of Koolyanobbing (IBRA_COO), 29°55′10″S, 119°15′26″E, leaf litter, 1 July 2010, Z. Hamilton, J. Cairnes (WAM T103988$^{DNA_Voucher_93}$; GenB–COI–KY295289, GenB–CYB–KY295410, GenB–MRPL45–KY295533, GenB–RPF2–KY295654, GenB–XPNPEP3- KY295782, GenB–ITS–KY295035).

**Other material examined.**—AUSTRALIA: *Western Australia*: 1 ♂, Ajana Back Road, site NO 7 (IBRA_GES), 27°59′57″S, 114°37′55″E, wet pitfall trap, 30 March–18 October 1999, N. Guthrie, CALM Survey (WAM T142987); 1 ♂, Albion Downs, 78.3 km NNW. of Leinster (IBRA_MUR), 27°12′25″S, 120°23′52″E, dry pitfall trap, 28 August–3 September 2008, Z. Hamilton & R. Teale (WAM T96351$^{DNA_Voucher_208}$; GenB–COI–MG516834, GenB–CYB–MG516845, GenB–MRPL45–MG516873, GenB–RPF2–MG516878, GenB–XPNPEP3–MG516894, GenB–ITS–MG516859); 1 ♂, same data (WAM T96477); 1 ♂, same data except 62.6 km NNW. of Leinster, 27°25′03″S, 120°23′45″E (WAM T96464$^{DNA_Voucher_210}$; GenB–COI–MG516832, GenB–CYB–MG516843, GenB–MRPL45–MG516872, GenB–RPF2–MG516877, GenB–XPNPEP3–MG516893, GenB–ITS–MG516857); 1 ♂, same data (WAM T96478); 1 ♂, same data (WAM T96481); 1 ♂, same data except 62.7 km NNW. of Leinster, 27°25′02″S, 120°23′41″E (WAM T96484); 1 ♂, same data except 66.3 km NNW. of Leinster, 27°24′06″S, 120°21′08″E (WAM T96474); 1 ♂, same data except 76.1 km NNW. of Leinster, 27°17′37″S, 120°22′09″E (WAM T96473); 1 ♂, same data (WAM T96471); 1 ♂, same data except 76.6 km NNW. of Leinster, 27°17′28″S, 120°21′51″E (WAM T96444); 1 ♂, same data except 78.8 km NNW. of Leinster, 27°14′45″S, 120°25′41″E (WAM T96476$^{DNA_Voucher_209}$; GenB–COI–MG516833, GenB–CYB–MG516844, GenB–MRPL45–MG516875, GenB–RPF2–MG516879, GenB–XPNPEP3–MG516896, GenB–ITS–MG516858); 1 ♂, same data except 79.0 km NNW. of Leinster, 27°14′42″S, 120°29′11″E (WAM T96482); 1 ♂, same data (WAM T96349); I ♂, same data except 81.3 km NNW. of Leinster, 27°15′33″S, 120°19′46″E (WAM T96480); 1 ♂, same data except 84.0 km NNW. of Leinster, 27°12′03″S, 120°18′48″E (WAM T96472); 1 ♂, same data except 84.9 km NNW. of Leinster, 27°14′38″S, 120°16′57″E (WAM T96511); 1 ♂, same data (WAM T96496); 1 ♂, same data except 27°14′40″S, 120°16′54″E (WAM T96479); 1 ♂, Barlee Range Nature Reserve, quadrat 9 (IBRA_GAS), 23°06′06″S, 116°00′28″E, wet pitfall trap, August 1993, S. van Leeuwen, B. Bromilow (WAM T57654); 2 ♂, Bidgemia Station, site GJ1 (IBRA_CAR), 25°12′34.5″S, 115°30′50.5″E, wet pitfall trap, 5 June–20 August 1995, N Hall, WAM/CALM Carnarvon Survey (WAM T98663); 3 ♂, same data except 3–8 June 1995 (WAM T98664); 2 ♂, same data (QMB); 2 ♂, same data except site GJ2, 25°10′30.9″S, 115°29′16.7″E, 4 June–20 August 1995 (WAM T98665); 1 ♂, same data except site GJ3, 25°07′08.1″S, 115°25′33.1″E, 6 June–20 August 1995 (WAM T98666); 2 ♂, same data (WAM T98667); 3 ♂, same data except 3–8 June 1995 (WAM T98668); 2 ♂, same data except site GJ5, 25°03′17.2″S, 115°17′37.5″E (WAM T98669); 1 ♂, same data except 6 June–20 August 1995 (WAM T98670); 3 ♂, Boolathana Station, site BO1 (IBRA_CAR), 24°24′48.4″S, 113°39′47.2″E, wet pitfall trap, 29 May–25 August 1995, N Hall, WAM/CALM Carnarvon Survey (WAM T98659); 5 ♂, same data (WAM T98660); 11 ♂, same data except site BO3, 24°24′48.5″S, 113°42′23.5″E (WAM T98661); 7 ♂, same data except site BO4, 24°24′48.7″S, 113°44′40.6″E, 31 May–25 August 1995 (WAM T98657); 1 ♂, same data except 15 January–31 May 1995 (WAM T98658); 1 ♂, Buntine Rocks Nature Reserve (IBRA_AVW), 29°59′06″S, 116°35′35″E, wet pitfall trap, 22 May–17 September 1996, M.S. Harvey & J.M. Waldock (WAM T38552); 1 ♂, same data (WAM T38553); 6 ♂, Bush Bay, site BB1 (IBRA_CAR), 25°07′30.8″S, 113°49′21.6″E, wet pitfall trap, 23 May–23 August 1995, N Hall, WAM/CALM Carnarvon Survey (WAM T98692); 1 ♂, same data except site BB3, 25°04′39.8″S, 113°42′36.9″E (WAM T98693); 1 ♂, Canna Nature Reserve, site MO 6 (IBRA_AVW), 28°52′45″S, 115°50′33″E, wet pitfall traps, 15 September 1998–18 October 1999, P. Van Heurck, CALM Survey (WAM T142962); 6 ♂, Cape Cuvier, Quobba Station, site CU2 (IBRA_CAR), 24°13′24.0″S, 113°30′13.1″E, wet pitfall trap, 30 May–24 August 1995, N. Hall, WAM/CALM Carnarvon Survey (WAM T142999); 1 ♂, same data (WAM T143000); 1 ♂, Cape Range, 8 m outside Cave C-118 (IBRA_CAR), 22°09′41″S, 113°59′41″E, pitfall trap, 27 July 1989, E.C. Pryor (WAM T28514); 1 ♂, same data except 3 August 1989 (WAM T28515); 1 ♂, 1 km SSE. of Cowra Line Camp, site RHNW13 (IBRA_PIL), 22°21′41.2″S, 119°00′24.5″E, wet pitfall trap, 28 August 2003–20 October 2004, CALM Pilbara Survey (WAM

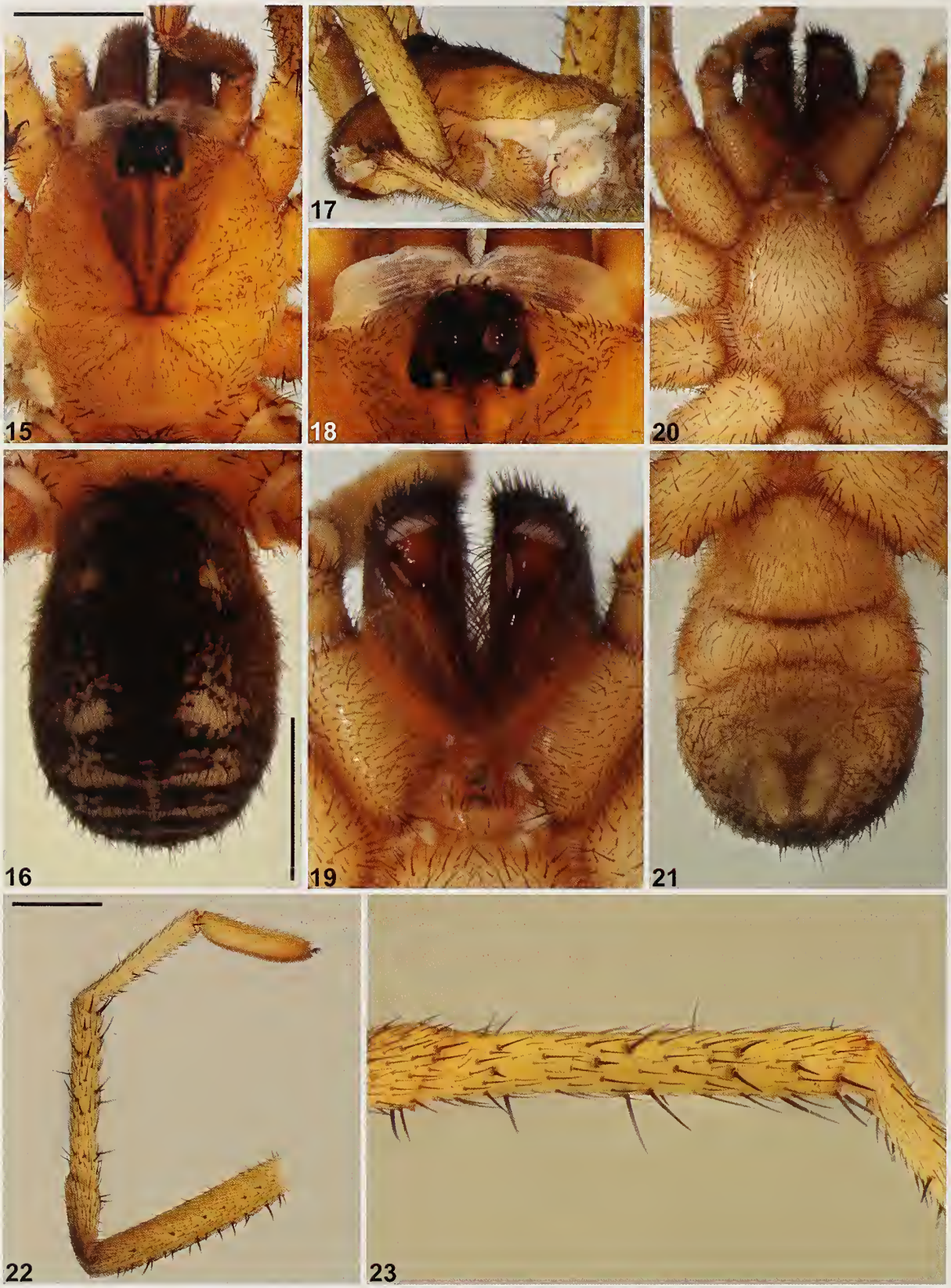


Figures 15–23.—*Bungulla bertmaini* Rix, Main, Raven & Harvey, 2017, male holotype (WAM T103988) from Deception Hill, 102.5 km N. of Koolyanobbing (Western Australia: COO), somatic morphology: 15–16, carapace and abdomen, dorsal view; 17, cephalothorax, lateral view; 18, eyes, dorsal view; 19, mouthparts, ventral view; 20–21, cephalothorax and abdomen, ventral view; 22, leg 1, prolateral view; 23, leg I tibia, prolateral view. Scale bars = 2.0 mm.

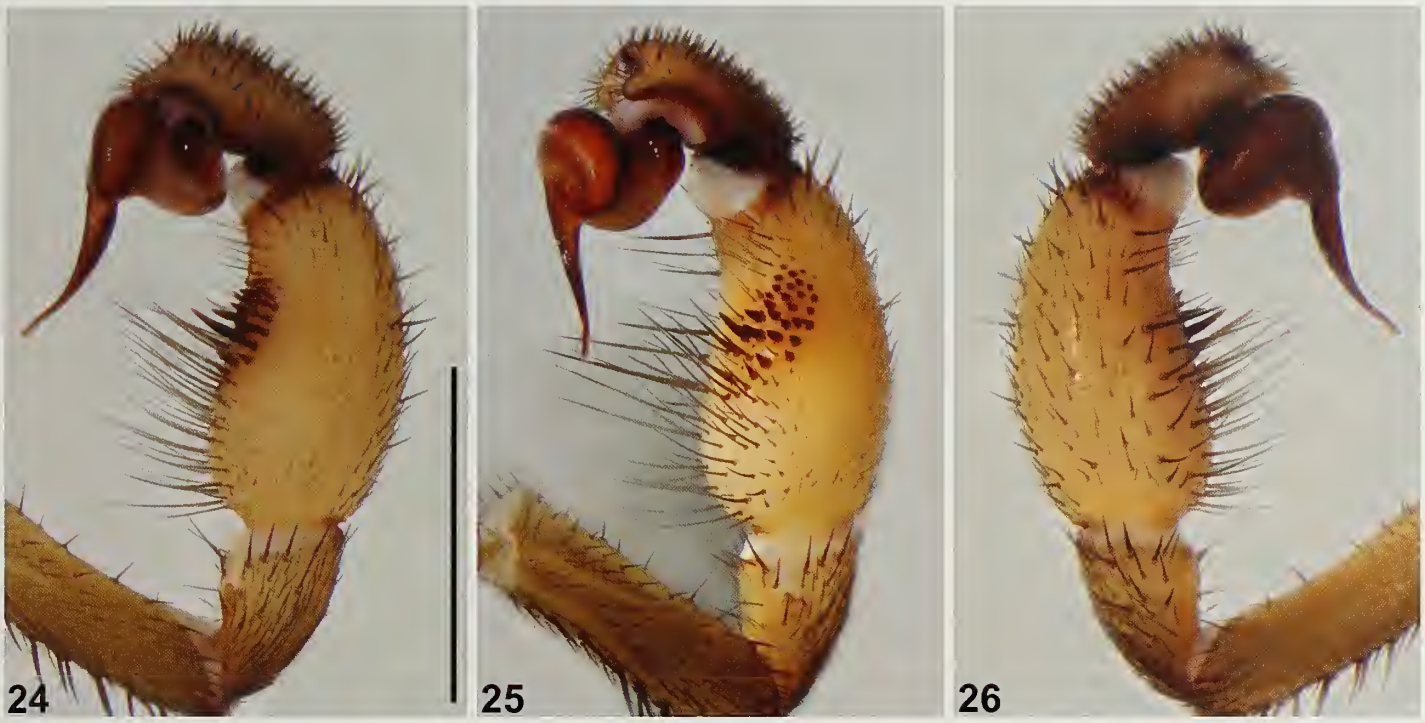


Figures 24–26.—*Bungulla bertmaini* Rix, Main, Raven & Harvey, 2017, male holotype (WAM T103988) from Deception Hill, 102.5 km N. of Koolyanobbing (Western Australia; COO), pedipalp: 24, retrolateral view; 25, retro-ventral view; 26, prolateral view. Scale bar = 2.0 mm.

T134982); 3 ♂, Francois Peron National Park, site PE2 (IBRA_CAR), 25°52′30.9″S, 113°32′59.0″E, wet pitfall trap, 25 May–30 August 1995, N Hall, WAM/CALM Carnarvon Survey (WAM T98683); 2 ♂, same data except site PE3, 25°49′14.1″S, 113°32′24.3″E, 24 May–30 August 1995 (WAM T98684); 1 ♂, same data except site PE4, 25°50′20.0″S, 113°36′23.1″E, 23 May–30 August 1995 (WAM T98685); 1 ♂, same data except site PE5, 25°58′33.6″S, 113°34′14.7″E, 26 May–30 August 1995 (WAM T98686); 1 ♂, Glen Florrie, 48 km WNW. of homestead, site WYW11 (IBRA_PIL), 22°51′48.6″S, 115°30′11.1″E, wet pitfall trap, 1 October 2003–30 September 2004, CALM Pilbara Survey (WAM T134978); 1 ♂, Glen Florrie Station, W. of homestead, Pilbara survey site WYW12 (IBRA_PIL), 22°55′05″S, 115°34′39″E, wet pitfall trap, 1 October 2003–October 2004, CALM Pilbara Survey (WAM T96996); 1 ♂, 53 km N. of Glen Station Homestead (1084) (IBRA_MUR), 26°34′22.51″S, 117°37′30.04″E, wet pitfall trap, 5 May–28 June 2009, N. Dight & L. Quinn (WAM T115190); 1 ♂, Highway Tod Bore (West Robe), ca. 50 km W. of Pannawonica (IBRA_PIL), site TOD01, 21°41′37.0″S, 115°49′55.7″E, 18–31 May 2015, M. Quinn (WAM T137423); 1 ♂, same data except site TOD03, 21°39′55.9″S, 115°50′56.9″E (WAM T137428); 1 ♂, Jack Hills, site 17 (IBRA_MUR), 26°07′S, 117°09′E, 24 August–24 November 2006, Ecologia staff (WAM T142973); 1 ♂, Kennedy Range National Park, site KE1 (IBRA_CAR), 24°29′33.7″S, 115°01′50.1″E, wet pitfall trap, 29 May–28 August 1995, N Hall, WAM/CALM Carnarvon Survey (WAM T98688); 4 ♂, same data except site KE2, 24°30′01.5″S, 115°01′07.1″E (WAM T98689); 1 ♂, same data (WAM T98690); 1 ♂, same data except site KE4, 24°33′03.5″S, 115°57′31.7″E (WAM T98691); 3 ♂, same data except site KE5, 24°34′14.3″S, 115°57′11.9″E (WAM T98687); 1 ♂, Lake Way Station, Honeymoon Well lease (IBRA_MUR), 26°53′49″S, 120°25′07″E, glycol pitfall trap, mulga-spinifex, 20 October 2006, S. Thompson (WAM T80619); 1 ♂, same data except 26°56′22″S, 120°24′35″E, spinifex (WAM T80612); 1 ♂, same data except 26°56′05″S, 120°24′11″E (WAM T80613); 12 ♂, same data except 26°55′41″S, 120°23′59″E (WAM T80620); 1 ♂, same data except 26°54′40″S, 120°23′14″E, open mulga (WAM T80617); 2 ♂, same data except 26°57′04″S, 120°24′45″E (WAM T80615); 1 ♂, same data except 26°54′50″S, 120°22′15″E (WAM T80614); 1 ♂, same data except 26°52′07″S, 120°21′49″E, chenopod vegetation (WAM T80611); 2 ♂, same data except 26°52′01″S, 120°21′16″E (WAM T80616); 3 ♂, same data except 26°51′01″S, 120°22′11″E (WAM T80618); 1 ♂, same data except 26°50′08″S, 120°21′59″E, sand dune (WAM T80610); 1 ♂, same data except 26°50′52″S, 120°22′53″E (WAM T80609); 1 ♂, Koolanooka Dam Road, SE. of Morawa, site MO 3 (IBRA_AVW), 29°14′40″S, 116°06′06″E, wet pitfall traps, 15 September 1998–18 October 1999, P. Van Heurck, CALM Survey (WAM T142961); 1 juvenile, Lake MacLeod (IBRA_CAR), 24°28′33.9″S, 113°31′32.7″E, dry pitfall trap, samphire flats, edge of salt lake, 5 November 2010, P.R. Langlands (WAM T108979$^{DNA_Voucher_92}$; GenB–COI–KY295290, GenB–MRPL45–KY295534, GenB–RPF2–KY295655, GenB–XPNPEP3–KY295783, GenB–ITS–KY295036); 1 ♂, Lorna Glen Station, site Sherwood 3 (IBRA_MUR), 26°21′17″S, 121°14′40″E, pitfall trap, 19 March 2004, G. Owen (WAM T60786); 1 ♂, Mardathuna Station, site MR1 (IBRA_CAR), 24°30′41.0″S, 114°38′13.8″E, wet pitfall trap, 26 May–26 August 1995, N Hall, WAM/CALM Carnarvon Survey (WAM T98671); 13 ♂, same data except site MR2, 24°26′35.7″S, 114°30′41.5″E, 25 May–26

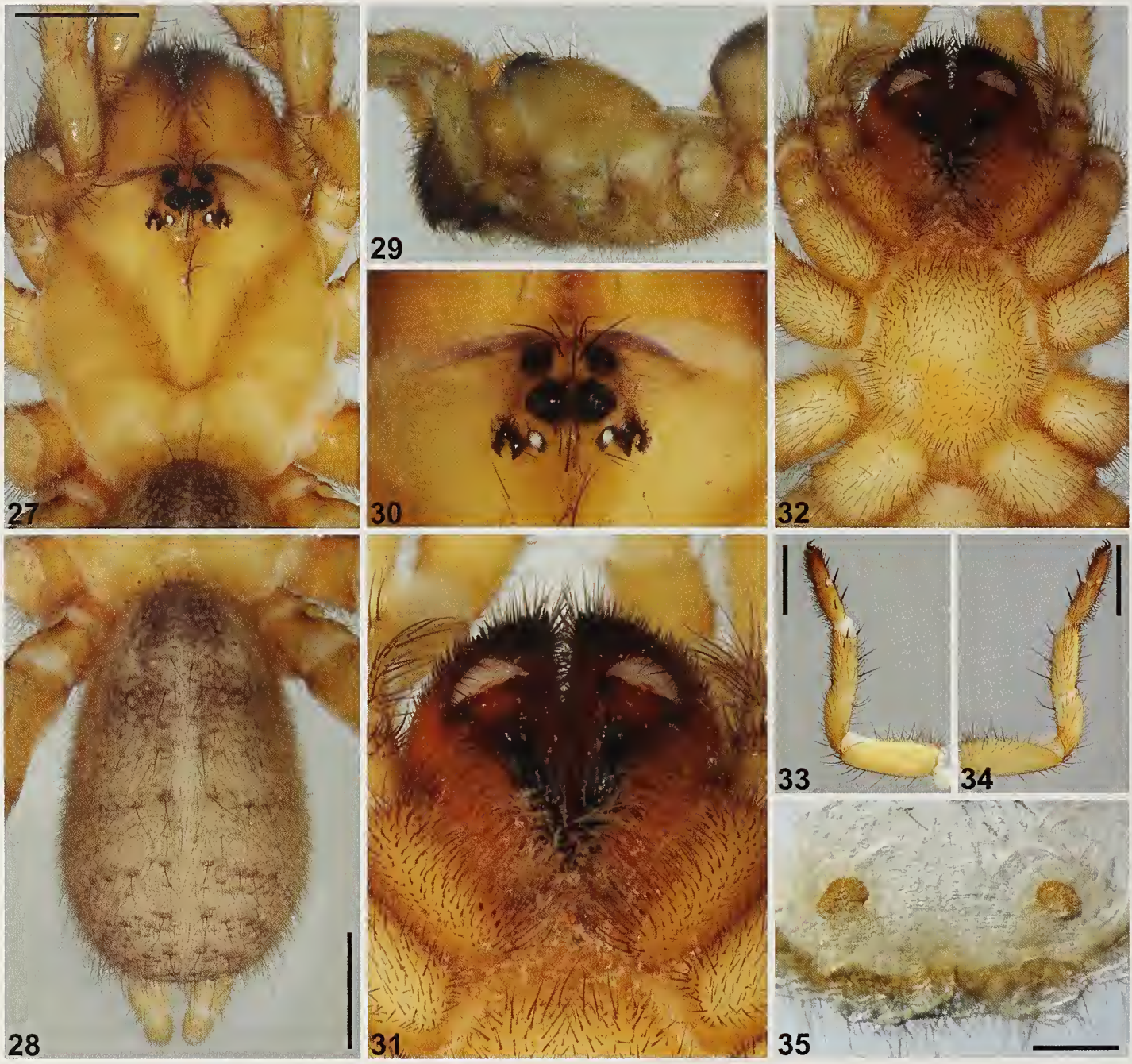


Figures 27–35.—*Bungulla bertmaini* Rix, Main, Raven & Harvey, 2017, female (WAM T109128) from Robe Valley, WSW. of Pannawonica (Western Australia; PIL): 27–28, carapace and abdomen, dorsal view; 29, cephalothorax, lateral view; 30, eyes, dorsal view; 31, mouthparts, ventral view; 32, cephalothorax, ventral view; 33, leg I, prolateral view; 34, leg I, retrolateral view; 35, spermathecae, dorsal view. Scale bars = 2.0 mm (27–28, 33–34), 0.5 mm (35).

August 1995 (WAM T98672); 2 ♂, same data except site MR3, 24°25′42.7″S, 114°30′00.5″E, 24 May–26 August 1995 (WAM T98673); 1 ♂, same data except site MR4, 24°24′42.7″S, 114°28′24.4″E (WAM T98674); 3 ♂, same data except site MR5, 24°24′23.3″S, 114°26′42.1″E (WAM T98675); 2 ♂, Meedo Station, site MD1 (IBRA_CAR), 25°37′31.3″S, 114°42′18.8″E, wet pitfall trap, 17 May–21 August 1995, N. Hall, WAM/CALM Carnarvon Survey (WAM T98695); 1 ♂, same data except site MD2, 25°37′23.4″S, 114°41′39.8″E, 18 May–21 August 1995 (WAM T98697); 2 ♂, same data except site MD3, 25°39′13.5″S, 114°37′37.5″E, 19 May–22 August 1995 (WAM T98696); 4 ♂, same data except site MD5, 25°42′41.6″S, 114°35′58.5″E (WAM T98694); 1 ♂, Meka Station, Shire of Murchison (IBRA_MUR), 27°23′09.92″S, 117°00′14.00″E, wet pitfall trap, 5 May–28 June 2009, N. Dight & L. Quinn (WAM T98145); 1 ♂, Mesa B C (West Robe), ca. 50 km W. of Pannawonica, site RVM05 (IBRA_PIL), 21°40′36.9″S, 115°55′23.3″E, 18–31 May 2015, M. Quinn (WAM T137417); 1 ♂, Mileura Station, Ejah

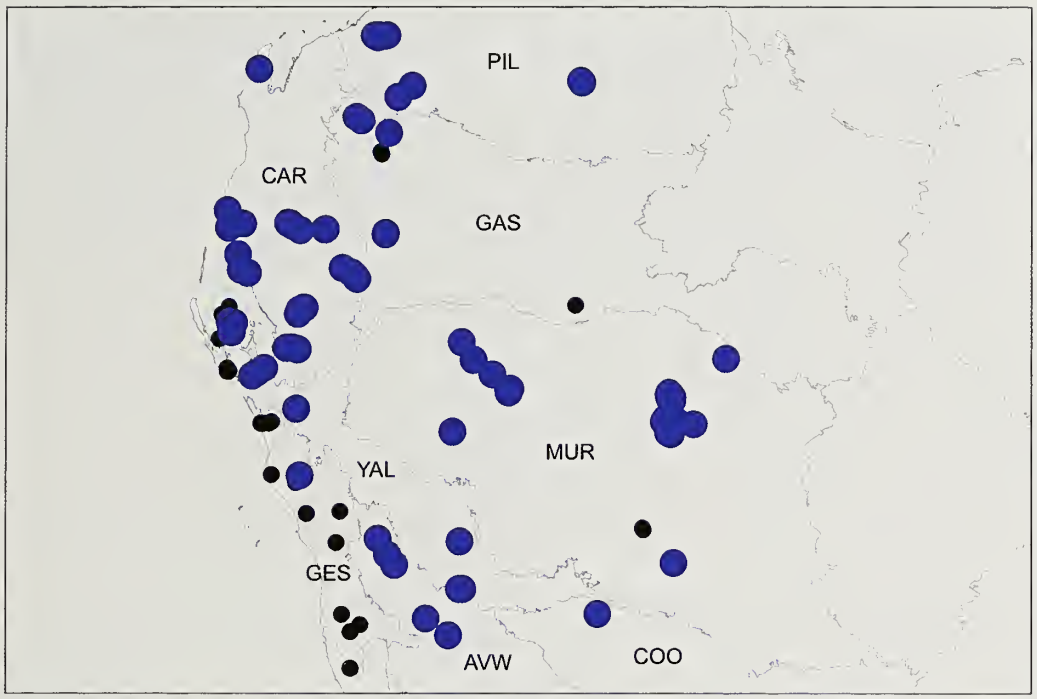


Figure 36.—Map showing collection records of *Bungulla bertmaini* Rix, Main, Raven & Harvey, 2017 (large blue circles), relative to other taxa with > 10 retrolateral spinules on the male palpal tibia (see Fig. 13). Relevant IBRA 7.0 bioregional acronyms are as follows: AVW, Avon Wheatbelt; CAR, Carnarvon; COO, Coolgardie; GAS, Gascoyne; GES, Geraldton Sandplains; MUR, Murchison; PIL, Pilbara; YAL, Yalgoo.

Paddock (IBRA_MUR), 26°22′S, 117°20′E, 1 June 1980, P.A. Woolley & T. Valente (WAM T28387); 1 ♂, same data (WAM T28388); 1 ♂, same data (WAM T28389); 1 ♂, same data (WAM T28390); 1 ♂, 8 km NNE. of Mount Edith, Mount Stuart Station, site WYE05 (IBRA_PIL), 22°34′16.9″S, 116°08′53.8″E, wet pitfall trap, 11 September 2003–7 October 2004, CALM Pilbara Survey (WAM T135152); 1 ♂, Mount Ida, 100 km WSW. of Leonora, site MI–08–8C (IBRA_MUR), 29°12′59″S, 120°26′10″E, active search, 29 July 2008, M. Quinn & G. Murray (WAM T110235[DNA_Voucher_202]; GenB–COI–MG516831, GenB–MRPL45–MG516874, GenB–RPF2–MG516883, GenB–XPNPEP3–MG516895, GenB–ITS–MG516860); 1 ♂, Mount Gibson iron-ore mine, Banded Ironstone Range, Extension Hill, east facing (IBRA_AVW), 29°34′27″S, 117°09′39″E, wet pitfall traps, 31 May–11 June 2005, S. Thompson (WAM T72327); 1 ♂, same data (WAM T71715); 1 ♂, same data (WAM T72317); 1 ♂, same data except Ironstone Slope, Extension Hill, west facing, 29°34′38″S, 117°09′35″E (WAM T72326); 1 ♂, same data except sandplains 4 (D), control site (N. of road), 29°34′34″S, 117°07′34″E, 30 May–11 June 2005 (WAM T71637); 1 ♂, same data except sandplains 1 (A), impact site (S. of road), 29°34′33″S, 117°06′35″E (WAM T71636); 1 ♂, 19.9 km E. of Mount Keith (IBRA_MUR), 27°16′56″S, 120°45′24″E, October 2003, R. Teale (WAM T88605); 1 ♂, NW. of Mount Wilkie, site DRW02, Crown Land Reserve (IBRA_PIL), 20°50′41.0″S, 116°22′03.0″E, wet pitfall trap, 23 September 2003–2 October 2004, CALM Pilbara Survey (WAM T135055); 1 ♂, 1.8 km SSE. of Mulga Downs Outcamp, site RHNW04 (IBRA_PIL), 22°20′04.7″S, 118°59′19.5″E, wet pitfall trap, 13 August 2003–18 October 2004, CALM Pilbara Survey (WAM T135003); 1 ♂, Nanga Station, site NA1 (IBRA_CAR), 26°28′40.1″S, 114°04′33.6″E, wet pitfall trap, 11 May–30 August 1995, N Hall, WAM/CALM Carnarvon Survey (WAM T98677); 3 ♂, same data except site NA4 (IBRA_YAL), 26°32′47.3″S, 113°57′47.0″E (WAM T98676); 2 ♂, same data except site NA5, 26°35′31.8″S, 113°53′22.3″E (WAM T98678); 2 ♂, Nerren Nerren Station, site NE2 (IBRA_YAL), 27°03′24.1″S, 114°34′22.6″E, wet pitfall trap, 11 May–18 August 1995, N Hall, WAM/CALM Carnarvon Survey (WAM T98662); 3 ♂, Paynes Find Rock [ca. 8 miles from junction of Yalgoo/Paynes Find Roads] (IBRA_YAL), 28°55′S, 117°07′E, pitfall trap, 4–5 July 1970, R. Jones (WAM T142975); 1 ♂, same data except 12 July 1969 (WAM T142976); 1 ♂, Paynes Find Rock on Yalgoo Road (site no. 6) (IBRA_YAL), 28°55′S, 117°07′E, pitfall trap, 24 July–27 August 1985, B.Y. & A.R. Main (WAM T 142974); 1 ♂, Pintharuka (IBRA_AVW), 29°06′03″S, 115°59′14″E, wet pitfall trap, 23 May 1996–17 September 1996, M.S. Harvey & J.M. Waldock (WAM T38502); 1 ♂, same data (WAM T44214); 1 ♀, Robe Valley, 36 km WSW. of Pannawonica (IBRA_PIL), 21°40′00″S, 115°58′37″E, dug from burrow, 26 October 2010, Z. Hamilton (WAM T109128[DNA_Voucher_277]; GenB–COI–KY295241, GenB–CYB–KY295366, GenB–MRPL45–KY295489, GenB–RPF2–KY295608, GenB–XPNPEP3–KY295735, GenB–ITS–KY304512); 1 ♂, Snake Gully Nature Reserve, site WU 11 (IBRA_AVW), 30°13′05″S, 116°56′36″E, wet pitfall traps, 15 September 1997–7 April 1998, N. Guthrie, CALM Survey (WAM T142963); 1 ♂, same data (WAM T142964); 1 ♂, ca. 5 km SW. of Warramboo, Alinta Dampier to Bunbury Natural Gas Pipeline (IBRA_PIL), 21°40′11.9″S, 115°46′50.3″E, in trench, 16 July 2007, P. Hinchy, C. Day (WAM T95784); 1 ♂, Water Supply Island (WSI), Gascoyne River, ca. 4 km NNE. of Carnarvon (IBRA_CAR), 24°51′36″S, 113°40′08″E, wet pitfall trap, 23–30 September 2002, I. Stemp (WAM T57304);

1 ♂, Weld Range North mine lease, site WN 12, 67 km SW. of Meekatharra (IBRA_MUR), 26°49′55.69″S, 117°52′30.47″E, wet pitfall trap, 30 August 2007, Ecologia staff (WAM T130912); 2 ♂, same data except site WN 15, 66 km SW. of Meekatharra, 26°48′34.52″S, 117°52′20.05″E, 29 August 2007 (WAM T130916); 1 ♂, same data except site WN 6, 63 km SW. of Meekatharra, 26°46′48.64″S, 117°53′54.99″E, 3 September 2007 (WAM T130896); 1 ♂, Weld Range (no specific locality) (IBRA_MUR), Ecologia staff (WAM T142966); 1 ♂, same data (WAM T142967); 1 ♂, same data (WAM T142968); 1 ♂, same data (WAM T142969); 2 ♂, same data (WAM T142970); 1 ♂, same data (WAM T142971); 1 ♂, same data (WAM T142972); 1 ♂, Woodleigh Station, site WO1 (IBRA_CAR), 26°13′01.2″S, 114°35′59.4″E, wet pitfall trap, 17 May–21 August 1995, N Hall, WAM/CALM Carnarvon Survey (WAM T98679); 2 ♂, same data except site WO2, 26°12′30.0″S, 114°34′35.0″E (WAM T98680); 2 ♂, same data except site WO4, 26°11′31.1″S, 114°30′33.0″E (WAM T98681); 2 ♂, same data except site WO5, 26°11′45.3″S, 114°25′23.6″E (WAM T98682); 1 ♂, 26.5 km SW. of Woodleigh Homestead (IBRA_CAR), 26°12′S, 114°32′E, 5 July 1997, M. Peterson (WAM T44353).

**Diagnosis.**—Males of *Bungulla bertmaini* can be distinguished from all other known congeners with > 10 retrolateral spinules on the palpal tibia (Fig. 13) – except *B. banksia*, *B. bidgemia*, *B. hamelinensis*, *B. iota*, *B. laevigata*, *B. quobba*, *B. weld* and *B. yeni* – by the shape of the proximal half of the palpal tibia, which is without a pronounced ventral bulge (Fig. 24), combined with the absence of a medial 'ledge' on the palpal tibia (Figs. 24, 25) (palpal tibia is with a ledge or bulges ventrally in other species). *Bungulla bertmaini* can be further distinguished from *B. banksia*, *B. bidgemia*, *B. hamelinensis*, *B. iota*, *B. weld* and *B. yeni* by the shape of the embolus, which is relatively long (i.e., longer than the bulb) (Fig. 24; cf. Figs. 72, 95, 218, 267, 419, 445); from *B. quobba* by the shape of the embolus, which is slightly longer and more strongly curved in standard retrolateral view (Fig. 24; cf. Fig. 371); and from *B. laevigata* by the morphology of the pars cephalica, which is covered in short setae (Fig. 15; cf. Fig. 310), combined with the (usually) darker coloration of the dorsal abdomen (Fig. 16; cf. Fig. 311 and Supplementary File 1).

**Description (male holotype).**—See Rix et al. (2017d).

**Description (female WAM T109128).**—Total length 14.3. Carapace 5.5 long, 4.7 wide. Abdomen 6.9 long, 4.3 wide. Carapace (Fig. 27) pale tan, with slightly darker ocular region; fovea strongly procurved. Eye group (Fig. 30) trapezoidal (anterior eye row strongly procurved), 0.8 x as long as wide, PLE PLE/ALE–ALE ratio 1.6; ALE separated by their own diameter; AME separated by their own diameter; PME separated by 4.5 x their own diameter; PME and PLE separated by diameter of PME, PME positioned slightly anterior to level of PLE. Maxillae with field of cuspules confined to inner corner (Fig. 31); labium without cuspules. Abdomen (Fig. 28) oval, sandy-beige in dorsal view with three darker olive-brown markings anteriorly and five pairs of thin, spotted, dark olive-brown chevrons posteriorly, each divided along midline; sclerotized sigilla absent. Legs (Figs. 33, 34) variable shades of tan; thick scopulae present on tarsus I (metatarsus II missing); tibia I with 2 stout prolateral macrosetae and 4 retro-ventral spine-like macrosetae; metatarsus I with 2 stout pro-ventral macrosetae and 2 longer retro-ventral macrosetae; tarsus I with distal cluster of 5 stout ventral macrosetae. Leg I: femur 2.9; patella 2.0; tibia 1.6; metatarsus 1.3; tarsus 1.1; total 8.8. Leg I femur–tarsus/carapace length ratio 1.6. Pedipalp pale tan, spinose on tibia and tarsus, with thick tarsal scopula. Genitalia (Fig. 35) with pair of short, widely spaced, mushroom-shaped spermathecae.

**Distribution and remarks.**—*Bungulla bertmaini* (formerly known by WAM identification codes 'MYG150' and 'MYG131') is a medium to large species with an extremely widespread distribution in arid Western Australia, in the northern Avon Wheatbelt, Coolgardie, Yalgoo, Murchison, Carnarvon, Gascoyne and Pilbara bioregions (Fig. 36; see also Rix et al. 2017d, fig. 175, for which fewer specimens were examined). Molecular data are consistent with morphology, and convincingly unite populations from the northern Coolgardie, central and southern Murchison, western Carnarvon and western Pilbara bioregions (Fig. 14). Specimens from subcoastal locations and lower latitudes are generally smaller than those from the arid inland, and there is some variation in the length of the cymbial spinules (see Supplementary File 1), but in the absence of consistent genitalic or somatic variation, this entire clade is regarded as representing a single species. No other congener has such an enormous distributional range, and *B. bertmaini* remains the only known species of *Bungulla* in the Pilbara (Fig. 36). However, despite this broad distribution, the vast majority of specimens have been collected from pitfall traps, and thus little is known of the biology of the species, other than that it is largely restricted to habitats that receive less than 300 mm of annual rainfall, and that males have been collected wandering in search of females in autumn, winter and spring, with a peak in winter.

***Bungulla ajana*** Rix, Raven & Harvey, sp. nov.
http://zoobank.org/?lsid=urn:lsid:zoobank.org:act:47244D2D-680A-4978-8246-CEE3103782C0
(Figs. 13, 37–49)

**Type material.**—*Holotype male*. AUSTRALIA: *Western Australia*: Ogilvie Road, west, c. 40 km SW. of Ajana, site NO 11 (IBRA_GES), 27°59′29″S, 114°11′40″E, wet pitfall trap, 16 September 1998–18 October 1999, P. Van Heurck et al., CALM Survey (WAM T143033).

*Paratypes.* AUSTRALIA: *Western Australia*: 5 ♂, same data as holotype (WAM T142977).

**Etymology.**—The specific epithet is a noun in apposition, in reference to the type locality of this species.

**Diagnosis.**—Males of *Bungulla ajana* can be distinguished from all other known congeners with > 10 retrolateral spinules on the palpal tibia (Fig. 13) – except *B. aplini*, *B. keirani* and *B. mckenziei* – by the shape of the proximal half of the palpal tibia, which is without a pronounced ventral bulge (Fig. 46), combined with the presence of a medial 'ledge' on the palpal tibia, this ledge situated closely proximal to the field of retrolateral spinules and bearing a brush of filiform setae (Figs. 46, 47) (palpal tibia is without a ledge or bulges ventrally in other species). *Bungulla ajana* can be further distinguished from *B. aplini*, *B. keirani* and *B. mckenziei* by the shape of the palpal tibia, which is stout, bulbous and strongly arched dorsally (Fig. 46; cf. Figs. 59, 293, 332), combined with the presence of a broad medial ledge bearing a relatively large

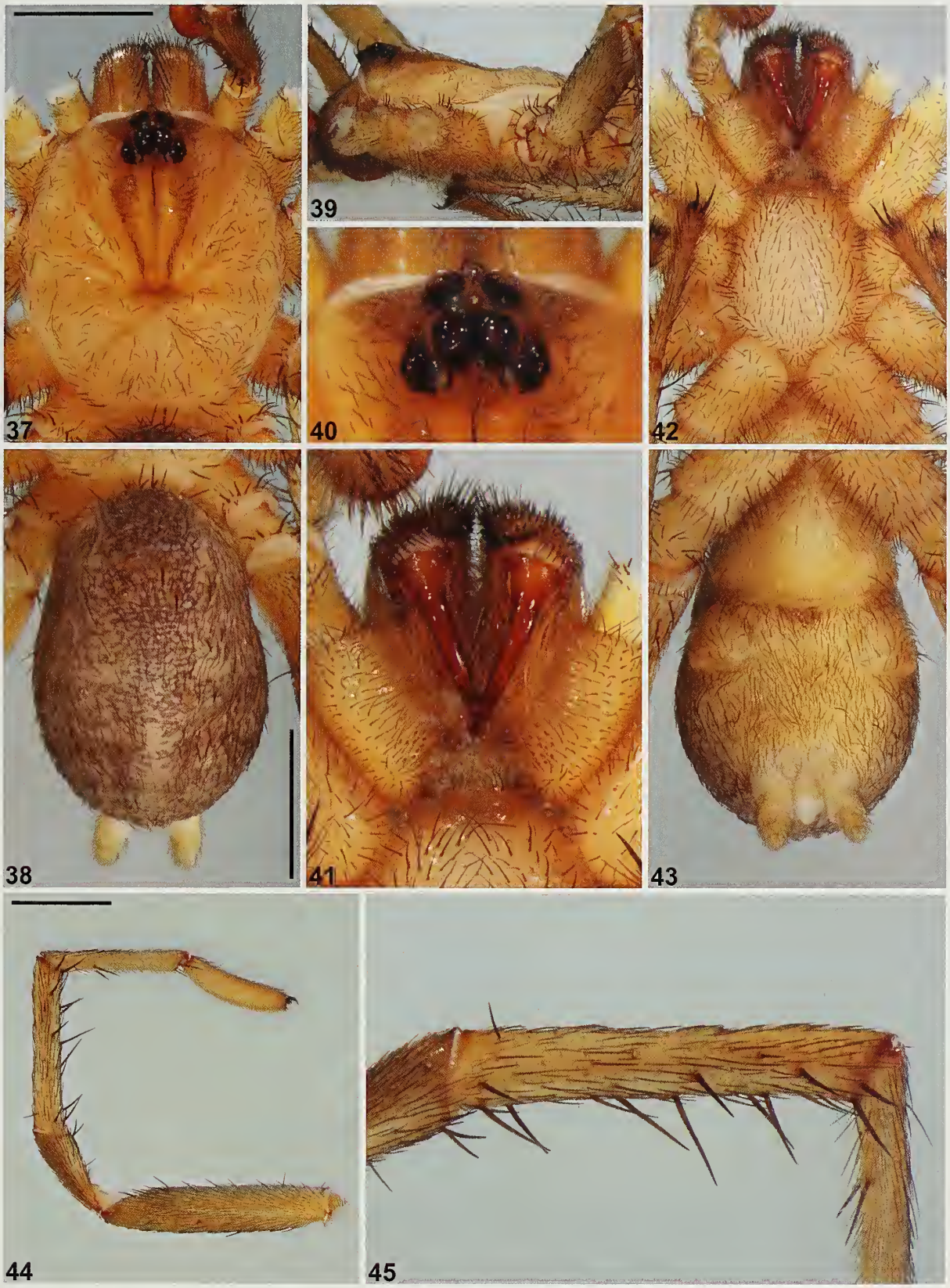


Figures 37–45.—*Bungulla ajana* sp. nov., male holotype (WAM T143033) from Ogilvie Road, SW. of Ajana (Western Australia, GES), somatic morphology: 37–38, carapace and abdomen, dorsal view; 39, cephalothorax, lateral view; 40, eyes, dorsal view; 41, mouthparts, ventral view; 42–43, cephalothorax and abdomen, ventral view; 44, leg I, prolateral view; 45, leg I tibia, prolateral view. Scale bars = 2.0 mm.


Figures 46–48.—*Bungulla ajana* sp. nov., male holotype (WAM T143033) from Ogilvie Road, SW. of Ajana (Western Australia; GES), pedipalp: 46, retrolateral view; 47, retro-ventral view; 48, prolateral view. Scale bar = 2.0 mm.

brush of filiform setae (Figs. 46, 47; cf. Figs. 59, 60, 293, 294, 332, 333). Females are unknown.

**Description (male holotype).**—Total length 9.8. Carapace 4.3 long, 3.8 wide. Abdomen 4.6 long, 3.1 wide. Carapace (Fig. 37) tan, with slightly darker pars cephalica, darker brown lyre-like pattern on pars cephalica and mostly black ocular region; postero-lateral corners near abdomen each with pair of porrect black setae; fovea straight. Eye group (Fig. 40) trapezoidal (anterior eye row strongly procurved), 0.9 x as long as wide, PLE–PLE/ALE–ALE ratio 1.5; ALE separated

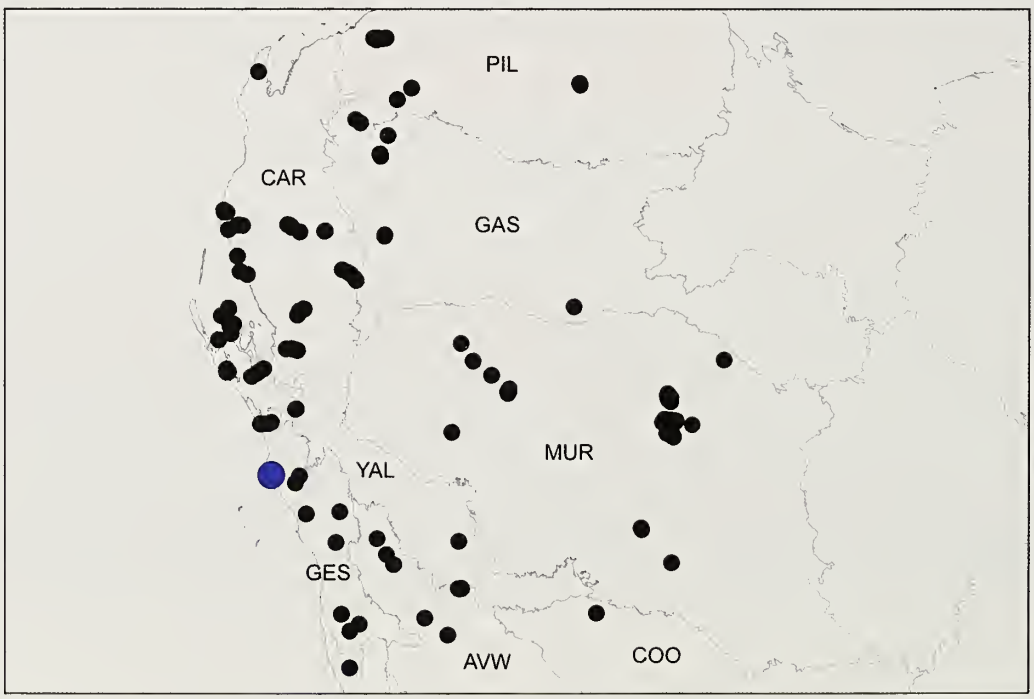


Figure 49.—Map showing collection records of *Bungulla ajana* sp. nov. (large blue circles), relative to other taxa with > 10 retrolateral spinules on the male palpal tibia (see Fig. 13). Relevant IBRA 7.0 bioregional acronyms are as follows: AVW, Avon Wheatbelt; CAR, Carnarvon; COO, Coolgardie; GAS, Gascoyne; GES, Geraldton Sandplains; MUR, Murchison; PIL, Pilbara; YAL, Yalgoo.

by ca. half their own diameter; AME separated by ca. half their own diameter; PME separated by 3.0 x their own diameter; PME and PLE separated by slightly less than diameter of PME, PME positioned in line with level of PLE. Maxillae with field of cuspules confined to inner corner (Fig. 41); labium without cuspules. Abdomen (Fig. 38) oval, dark olive-brown in dorsal view with beige-tan mottling, two pairs of beige-tan sigilla spots, and three indistinct pairs of beige-tan chevrons posteriorly, each divided along midline. Dorsal surface of abdomen (Fig. 38) with sparse arrangement of stiff, porrect black setae, each with slightly raised, dark brown sclerotic base; sclerotized sigilla absent. Legs (Figs. 44, 45) variable shades of tan, with light scopulae on tarsi I–II; tibia 1 spinose, without prolateral clasping spurs. Leg I: femur 4.6; patella 2.1; tibia 3.5; metatarsus 3.0; tarsus 2.2; total 15.2. Leg 1 femur–tarsus/carapace length ratio 3.5. Pedipalpal tibia (Figs. 46–48) stout, bulbous and strongly arched dorsally, nearly 2.0 x longer than wide, with broad medial 'ledge' bearing a relatively large brush of filiform setae; field of retrolateral spinules oval–subtriangular in shape, positioned medially (distal to medial ledge), consisting of > 50 spinules of varying length, the latter longest proximally; RTA absent. Cymbium (Figs. 46–48) setose, with dense field of long, slightly curved spine-like spinules covering most of dorsal surface. Embolus (Figs. 46–48) slightly longer than bulb, strongly curved, with slightly expanded tip; embolic apophysis absent.

**Distribution and remarks.**—*Bungulla ajana* is a rare and highly restricted species known only from south-west of Ajana, near Kalbarri National Park in the northern Geraldton Sandplains bioregion of south-western Australia (Fig. 49). Nothing is known of the biology of this species, other than that the known male specimens were collected wandering in search of females in spring.

***Bungulla aplini*** Rix, Raven & Harvey, sp. nov.
http://zoobank.org/?lsid=urn:lsid:zoobank.org:act:953F008F-4F27-4389-9513-F59D231CE404
(Figs. 13, 50–62)

**Type material.**—*Holotype male*. AUSTRALIA: *Western Australia*: Nerren Nerren Station, site NE2 (IBRA_YAL), 27°03′24.1″S, 114°34′22.6″E, wet pitfall trap, 11 May–18 August 1995, N. Hall, WAM/CALM Carnarvon Survey (WAM T142981).

*Paratypes*. AUSTRALIA: *Western Australia*: 2 ♂, same data as holotype (WAM T98653).

**Etymology.**—This species is named in honor of Ken Aplin, in recognition of his contributions to the Southern Carnarvon Basin Survey (Burbidge et al. 2000) and to the study of Australasian biodiversity.

**Diagnosis.**—Males of *Bungulla aplini* can be distinguished from all other known congeners with > 10 retrolateral spinules on the palpal tibia (Fig. 13) – except *B. ajana*, *B. keirani* and *B. mckenziei* – by the shape of the proximal half of the palpal tibia, which is without a pronounced ventral bulge (Fig. 59), combined with the presence of a medial 'ledge' on the palpal tibia, this ledge situated closely proximal to the field of retrolateral spinules and bearing a brush of filiform setae (Figs. 59, 60) (palpal tibia is without a ledge or bulges ventrally in other species). *Bungulla aplini* can be further distinguished from *B. ajana*, *B. keirani* and *B. mckenziei* by the shape of the palpal tibia, which is long with a sub-cylindrical profile in retrolateral view (Fig. 59; cf. Figs. 46, 293, 332). Females are unknown.

**Description (male holotype).**—Total length 10.8. Carapace 4.6 long, 3.8 wide. Abdomen 4.6 long, 3.0 wide. Carapace (Fig. 50) tan, with slightly darker pars cephalica, darker brown lyre-like pattern on pars cephalica, black lateral rims and mostly black ocular region; postero-lateral corners near abdomen each with pair of porrect black setae; fovea straight. Eye group (Fig. 53) trapezoidal (anterior eye row strongly procurved), as long as wide, PLE–PLE/ALE–ALE ratio 1.7; ALE almost contiguous; AME separated by less than their own diameter; PME separated by 2.4 x their own diameter; PME and PLE separated by diameter of PME, PME positioned slightly posterior to level of PLE. Maxillae with field of cuspules confined to inner corner (Fig. 54); labium without cuspules. Abdomen (Fig. 51) oval, sandy-beige-tan in dorsal view with darker brown-black markings anteriorly and five pairs of thin, spotted, brown-black chevrons posteriorly, each divided along midline. Dorsal surface of abdomen (Fig. 51) with sparse arrangement of stiff, porrect black setae, each with slightly raised, dark brown sclerotic base; sclerotized sigilla absent. Legs (Figs. 57, 58) variable shades of tan, with light scopulae on tarsi I–II; metatarsus 1 and tarsus I lighter in color; tibia I heavily spinose, without prolateral clasping spurs. Leg 1: femur 5.1; patella 2.1; tibia 4.0; metatarsus 3.7; tarsus 2.7; total 17.6. Leg I femur–tarsus/carapace length ratio 3.8. Pedipalpal tibia (Figs. 59–61) long and sub-cylindrical, 3.0 x longer than wide, with very small medial 'ledge' bearing a relatively small brush of filiform setae; field of retrolateral spinules rectangular in shape, positioned distally (distal to medial ledge), consisting of 18 spinules of varying length, the latter longest proximally; RTA absent. Cymbium (Figs. 59–61) setose, with field of slightly curved and relatively poorly developed (almost filiform) spinules covering most of dorsal surface. Embolus (Figs. 59–61) as long as bulb, relatively straight, with unmodified tip; embolic apophysis absent.

**Distribution and remarks.**—*Bungulla aplini* (formerly confused with WAM identification code 'MYG155') is a rare and highly restricted species known only from Nerren Nerren Station, in the north-western Yalgoo (Edel) bioregion of south-western Australia (Fig. 62). Nothing is known of the biology of this species, other than that the known male specimens were collected wandering in search of females in winter or possibly late autumn.

***Bungulla banksia*** Rix, Raven & Harvey, sp. nov.
http://zoobank.org/?lsid=urn:lsid:zoobank.org:act:B082E5B0-3F54-47E3-AA94-EECCAF2E4525
(Figs. 13, 63–75)

**Type material.**—*Holotype male*. AUSTRALIA: *Western Australia*: Cooljarloo Mining Lease, between Brand Highway, Cooljarloo Road and Wongonderrah Road (IBRA_GES), 30°40′S, 115°25′E, *Banksia* low woodland on sand, 17–21 August 2007, M. Bamford (WAM T67132).

*Paratype*. AUSTRALIA: *Western Australia*: 1 ♂, near Coomallo Hill, Cooljarloo lease (Tiwest Joint Venture) (IBRA_GES), 30°10′S, 115°25′E, dry pitfall trap, 16–21 August 2006, M. Bamford (WAM T77024).

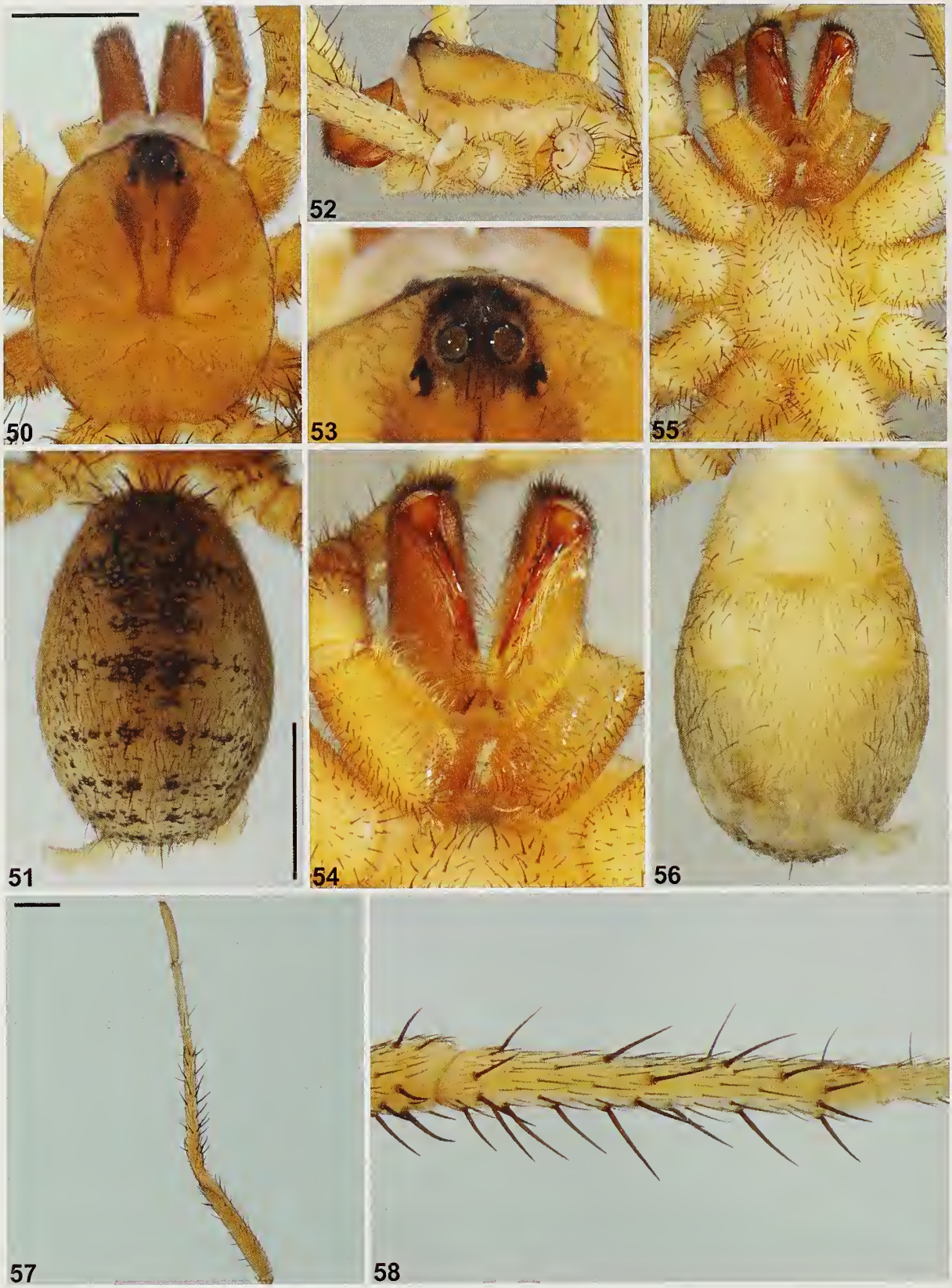


Figures 50–58.—*Bungulla aplini* sp. nov., male holotype (WAM T142981) from Nerren Nerren Station (Western Australia; YAL), somatic morphology: 50–51, carapace and abdomen, dorsal view; 52, cephalothorax, lateral view; 53, eyes, dorsal view; 54, mouthparts, ventral view; 55–56, cephalothorax and abdomen, ventral view; 57, leg 1, prolateral view; 58, leg 1 tibia, prolateral view. Scale bars = 2.0 mm.


Figures 59–61.—*Bungulla aplini* sp. nov., male holotype (WAM T142981) from Nerren Nerren Station (Western Australia; YAL), pedipalp: 59, retrolateral view; 60, retro-ventral view; 61, prolateral view. Scale bar = 2.0 mm.

**Other material examined.**—AUSTRALIA: *Western Australia*: 1 ♂, Bindoo Hill Nature Reserve, south boundary, site ML 11 (IBRA_GES), 28°30′12″S, 115°15′17″E, wet pitfall traps, 15 September 1998–15 January 1999, N. Guthrie, CALM Survey (WAM T142943); 1 ♂, Burma Road Reserve, 30 km E. of Walkaway (IBRA_GES), 28°56′S, 115°12′E, 15 September 1986, R.P. McMillan (WAM T27094); 1 ♂, S. of Coorow-Green Head Road, site DN 10 (IBRA_GES), 30°04′15″S, 115°34′07″E, wet pitfall traps, 15 October 1999–1 November 2000, P. Van Heurck, CALM Survey (WAM

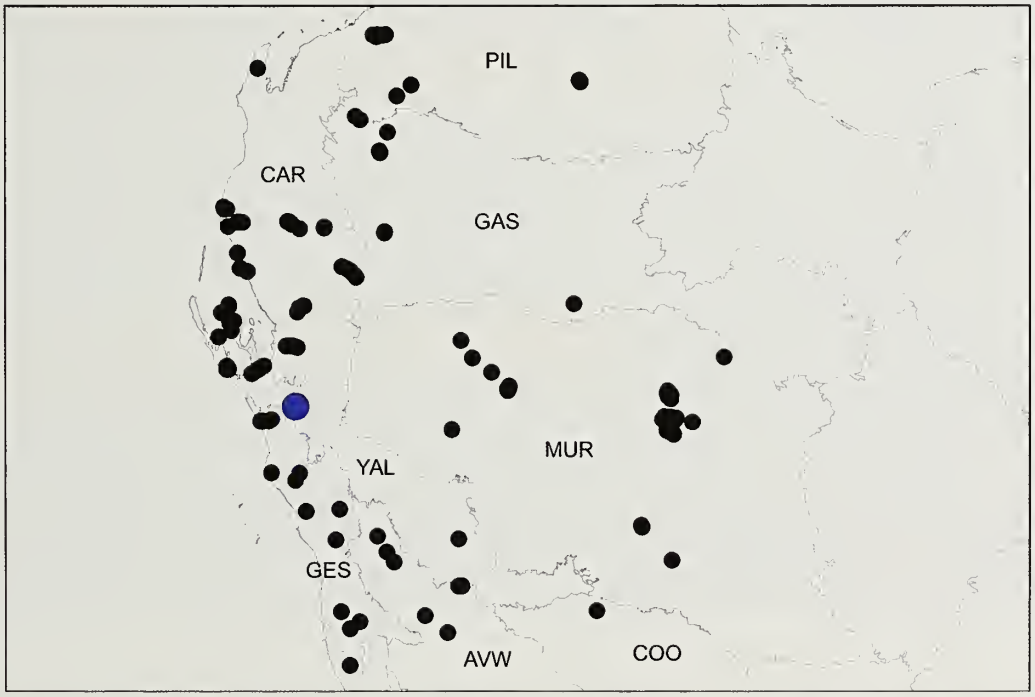


Figure 62.—Map showing collection records of *Bungulla aplini* sp. nov. (large blue circles), relative to other taxa with > 10 retrolateral spinules on the male palpal tibia (see Fig. 13). Relevant IBRA 7.0 bioregional acronyms are as follows: AVW, Avon Wheatbelt; CAR, Carnarvon; COO, Coolgardie; GAS, Gascoyne; GES, Geraldton Sandplains; MUR, Murchison; PIL, Pilbara; YAL, Yalgoo.

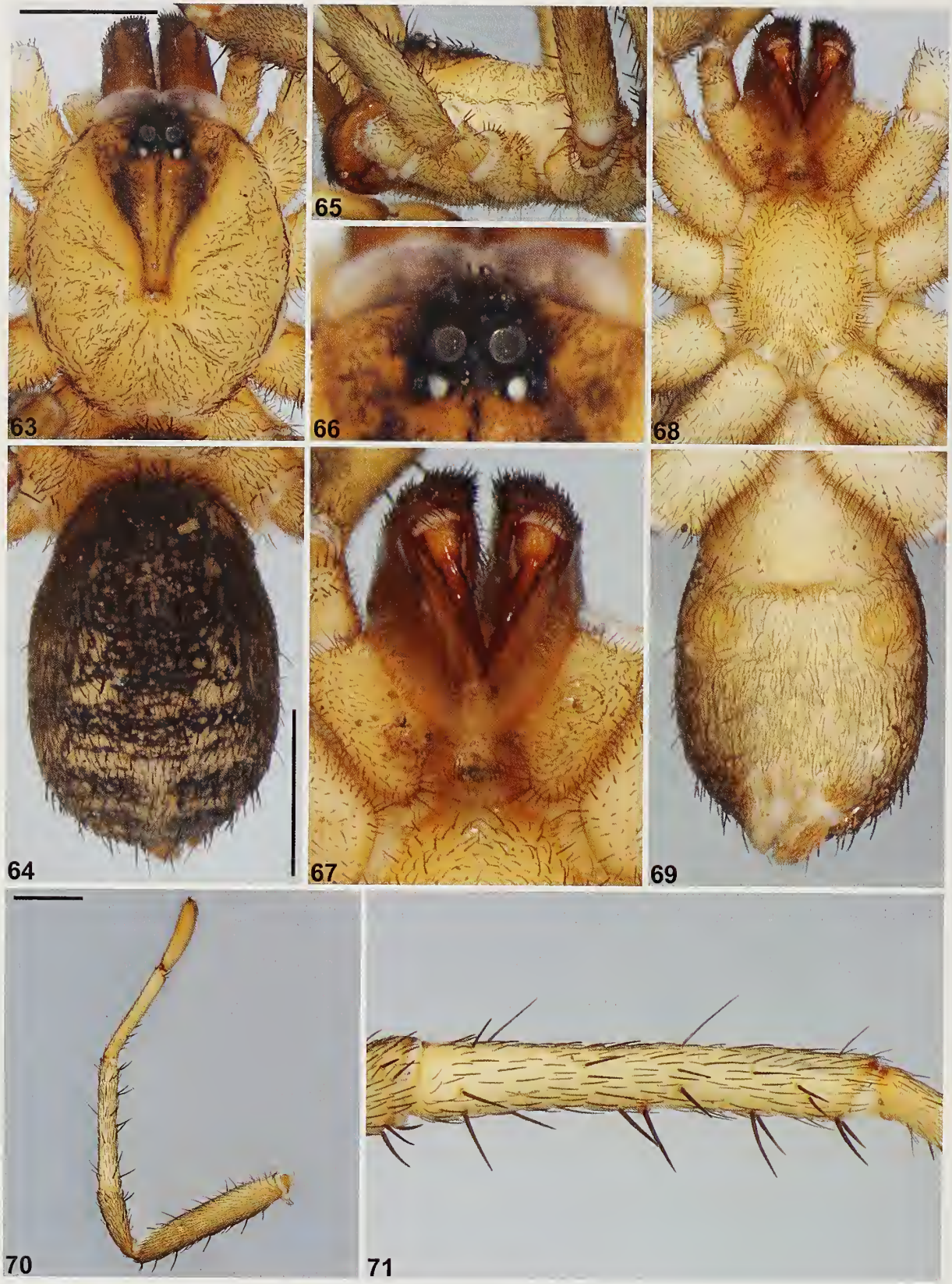


Figures 63–71.—*Bungulla banksia* sp. nov., male holotype (WAM T67132) from Cooljarloo Mining Lease (Western Australia; GES), somatic morphology: 63–64, carapace and abdomen, dorsal view; 65, cephalothorax, lateral view; 66, eyes, dorsal view; 67, mouthparts, ventral view; 68–69, cephalothorax and abdomen, ventral view; 70, leg I, prolateral view; 71, leg I tibia, prolateral view. Scale bars = 2.0 mm.


Figures 72–74.—*Bungulla banksia* sp. nov., male holotype (WAM T67132) from Cooljarloo Mining Lease (Western Australia; GES), pedipalp: 72, retrolateral view; 73, retro-ventral view; 74, prolateral view. Scale bar = 2.0 mm.

T142940); 1 ♂, same data (WAM T142941); 1 ♂, same data (WAM T142942); 2 ♂, Eneabba, R.G.C. Mineral Sands, site 8 (IBRA_GES), 29°56′S, 115°17′E, pitfall trap, 8 August 1998, P.L.J. West et al. (WAM T40636); 1 ♂, 10 km S. of Eneabba, R.G.C. Mineral Sands, site 6 (IBRA_GES), 29°56′S, 115°17′E, 9 August 1998, P.L.J. West et al. (WAM T44185); 2 ♂, Tip Road, SW. of Nabawa, site NO 6 (IBRA_GES), 28°31′57″S, 114°44′18″E, wet pitfall traps, 15 September 1998–18 October 1999, N. Guthrie, CALM Survey (WAM T142944).

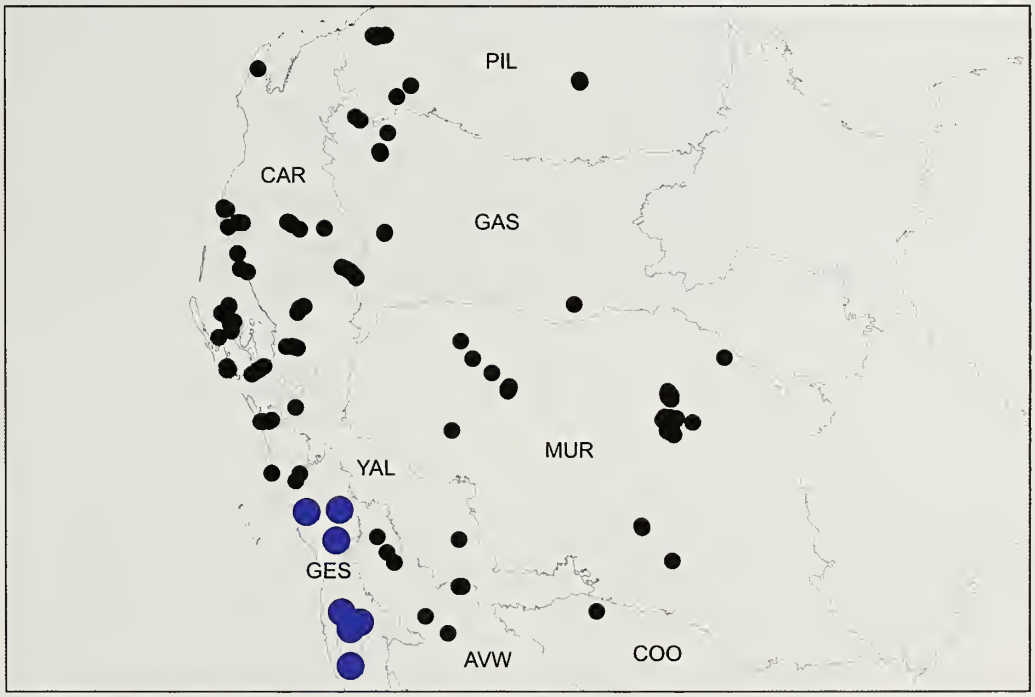


Figure 75.—Map showing collection records of *Bungulla banksia* sp. nov. (large blue circles), relative to other taxa with > 10 retrolateral spinules on the male palpal tibia (see Fig. 13). Relevant IBRA 7.0 bioregional acronyms are as follows: AVW, Avon Wheatbelt; CAR, Carnarvon; COO, Coolgardie; GAS, Gascoyne; GES, Geraldton Sandplains; MUR, Murchison; PIL, Pilbara; YAL, Yalgoo.

**Etymology.**—The specific epithet is a noun in apposition, in reference to the distribution of this species in the 'kwongan' *Banksia* heathlands of south-western Australia's northern sandplains.

**Diagnosis.**—Males of *Bungulla banksia* can be distinguished from all other known congeners with > 10 retrolateral spinules on the palpal tibia (Fig. 13) – except *B. bertmaini*, *B. bidgemia*, *B. hamelinensis*, *B. iota*, *B. laevigata*, *B. quobba*, *B. weld* and *B. yeni* – by the shape of the proximal half of the palpal tibia, which is without a pronounced ventral bulge (Fig. 72), combined with the absence of a medial 'ledge' on the palpal tibia (Figs. 72, 73) (palpal tibia is with a ledge or bulges ventrally in other species). *Bungulla banksia* can be further distinguished from *B. bertmaini*, *B. bidgemia*, *B. iota*, *B. hamelinensis*, *B. laevigata*, *B. quobba*, *B. weld* and *B. yeni* by the presence of a small field of spinules restricted to the disto-ventral margin of the palpal tibia, and situated closely proximal to a small retro-distal bulge (Figs. 72, 73; cf. Figs. 24, 95, 218, 267, 319, 371, 419, 445). Females are unknown.

**Description (male holotype).**—Total length 10.3. Carapace 4.6 long, 3.8 wide. Abdomen 4.5 long, 3.0 wide. Carapace (Fig. 63) tan, with darker pars cephalica, darker brown lyre-like pattern on pars cephalica, black lateral rims and black ocular region; fovea straight. Eye group (Fig. 66) trapezoidal (anterior eye row strongly procurved), 0.8 x as long as wide, PLE–PLE/ALE–ALE ratio 1.5; ALE separated by ca. half their own diameter; AME separated by less than their own diameter; PME separated by 3.0 x their own diameter; PME and PLE separated by slightly less than diameter of PME, PME positioned in line with level of PLE. Maxillae with field of cuspules confined to inner corner (Fig. 67); labium without cuspules. Abdomen (Fig. 64) oval, dark brown-black in dorsal view with beige-tan mottling, two pairs of beige-tan sigilla spots, and three pairs of beige-tan chevrons posteriorly. Dorsal surface of abdomen (Fig. 38) with sparse arrangement of stiff, porrect black setae, each with slightly raised, dark brown sclerotic base; sclerotized sigilla absent. Legs (Figs. 70, 71) variable shades of tan, with light scopulae on tarsi I–II; tibia I spinose, without prolateral clasping spurs. Leg I: femur 4.7; patella 2.3; tibia 3.8; metatarsus 3.1; tarsus 2.2; total 16.0. Leg I femur–tarsus/carapace length ratio 3.5. Pedipalpal tibia (Figs. 72–74) nearly 2.0 x longer than wide; field of retrolateral spinules rectangular in shape, positioned distally (along disto-ventral margin, closely proximal to a small retro-distal bulge), consisting of 18 spinules of largely similar length; RTA absent. Cymbium (Figs. 72–74) setose, with field of spine-like spinules covering most of dorsal surface. Embolus (Figs. 72–74) as long as bulb, curved, with unmodified tip; embolic apophysis absent.

**Distribution and remarks.**—*Bungulla banksia* has a relatively restricted distribution in the 'kwongan' heathlands of the Geraldton Sandplains bioregion of south-western Australia, from near Kalbarri in the north, south to Cooljarloo (Fig. 75). Nothing is known of the biology of this species, other than that the known male specimens were collected wandering in search of females in late winter and possibly early spring.

***Bungulla bella*** Rix, Raven & Harvey, sp. nov.
http://zoobank.org/?lsid=urn:lsid:zoobank.org:act:FC39EBF1-8FCD-4E5A-B8DF-3ABFEAB4F1CC
(Figs. 14, 76–85)

**Type material.**—*Holotype female*. AUSTRALIA: *Western Australia*: Mount Richardson, 225.8 km SE. of Mount Magnet (IBRA_MUR), 28°46′13″S, 119°59′09″E, dug from burrow, 24 June 2012, N. Watson & R. Teale (WAM T126165[DNA_Voucher_255]; GenB–COI–MG516838, GenB–CYB–MG516849, GenB–MRPL45–MG516865, GenB–RPF2–MG516876, GenB–XPNPEP3–MG516888, GenB–ITS–MG516853).

**Etymology.**—The specific epithet is derived from the Latin 'bellus' (adjective: 'pretty', 'lovely' or 'fine'; see Brown 1956), in reference to the attractive abdominal coloration of this species.

**Diagnosis.**—*Bungulla bella* is known from only a single female specimen, for which sequence data are available (Fig. 14). It can be distinguished from the other two species known only from females – *B. gibba* and *B. harrisonae* – by the ornate coloration of the dorsal abdomen (Fig. 77; cf. Figs. 200, 236). While it is possible that *B. bella* may be conspecific with a species here described separately from male specimens, we consider this highly unlikely given the size, coloration and morphology of those congeners known from the vicinity of the type locality.

**Description (female holotype).**—Total length 19.1. Carapace 6.7 long, 5.6 wide. Abdomen 9.9 long, 6.8 wide. Carapace (Fig. 76) light chocolate-brown with mostly black ocular region; fovea strongly procurved. Eye group (Fig. 79) trapezoidal (anterior eye row strongly procurved), 0.8 x as long as wide, PLE–PLE/ALE–ALE ratio 1.6; ALE separated by ca. half their own diameter; AME separated by their own diameter; PME separated by 3.2 x their own diameter; PME and PLE separated by diameter of PME, PME positioned in line with level of PLE. Maxillae with field of cuspules confined to inner corner (Fig. 80); labium without cuspules. Abdomen (Fig. 77) oval, beige in dorsal view with contrasting pattern of three darker purple-brown markings anteriorly and five pairs of thin, spotted, dark purple-brown chevrons posteriorly, each divided along midline; sclerotized sigilla absent. Legs (Figs. 82, 83) variable shades of tan; thick scopulae present on tarsi and metatarsi I–II; tibia I with 4 stout prolateral macrosetae and 4 retro-ventral spine-like macrosetae; metatarsus I with 3 stout pro-ventral macrosetae and 3 longer retro-ventral macrosetae; tarsus I with distal cluster of 2 stout ventral macrosetae. Leg I: femur 4.1; patella 2.7; tibia 2.4; metatarsus 1.8; tarsus 1.4; total 12.5. Leg I femur–tarsus/carapace length ratio 1.9. Pedipalp tan, spinose on tibia and tarsus, with thick tarsal scopula. Genitalia (Fig. 84) with pair of short, widely spaced, bud-shaped spermathecae.

**Distribution and remarks.**—*Bungulla bella* is an enigmatic species known only from Mount Richardson, in the southern-central Murchison bioregion of Western Australia (Fig. 85). Genetic data reveal that *B. bella* is closely related to *B. harrisonae* (Fig. 14), the latter found in the mesic jarrah forest east of Perth (Fig. 231). Nothing is known of the biology of this species.

***Bungulla bidgemia*** Rix, Raven & Harvey, sp. nov.
http://zoobank.org/?lsid=urn:lsid:zoobank.

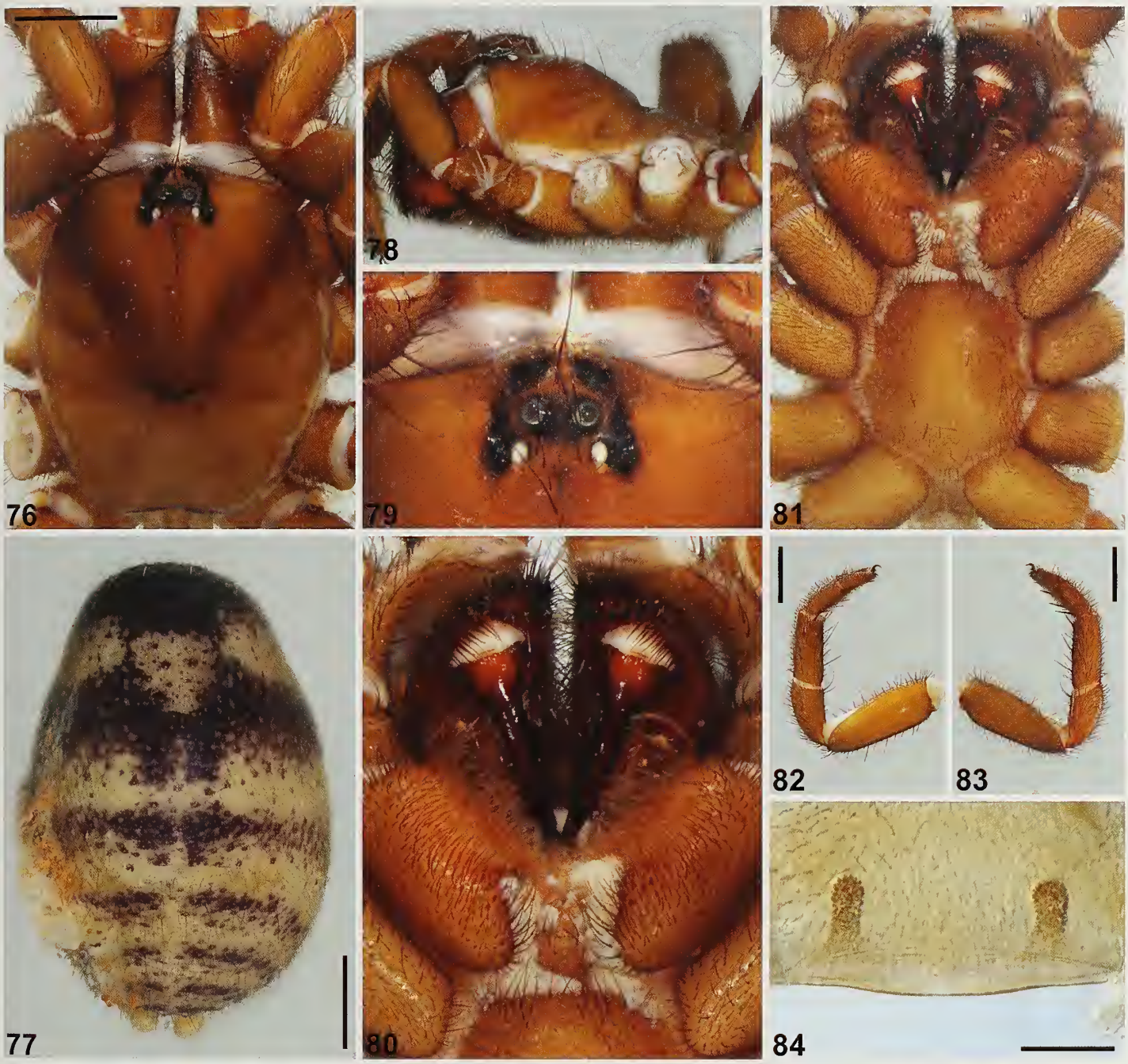


Figures 76–84.—*Bungulla bella* sp. nov., female holotype (WAM T126165) from Mount Richardson, SE. of Mount Magnet (Western Australia; MUR): 76–77, carapace and abdomen, dorsal view; 78, cephalothorax, lateral view; 79, eyes, dorsal view; 80, mouthparts, ventral view; 81, cephalothorax, ventral view; 82, leg I, prolateral view; 83, leg I, retrolateral view; 84, spermathecae, dorsal view. Scale bars = 2.0 mm (76–77, 82–83), 0.5 mm (84).

org:act:CB2AC8D2-4BB4-4339-8130-35E93E261155

(Figs. 13, 86–98)

**Type material.**—*Holotype male*. AUSTRALIA: *Western Australia*: Bidgemia Station, Gascoyne Junction, site GJ1 (IBRA_CAR), 25°12′34.5″S, 115°30′50.5″E, wet pitfall trap, 5 June–20 August 1995, N. Hall, WAM/CALM Carnarvon Survey (WAM T98533).

*Paratype*. AUSTRALIA: *Western Australia*: 1 ♂, same data as holotype (WAM T142979).

**Etymology.**—The specific epithet is a noun in apposition, in reference to the type locality of this species.

**Diagnosis.**—Males of *Bungulla bidgemia* can be distinguished from all other known congeners with > 10 retrolateral spinules on the palpal tibia (Fig. 13) – except *B. banksia*, *B. bertmaini*, *B. hamelinensis*, *B. iota*, *B. laevigata*, *B. quobba*, *B. weld* and *B. yeni* – by the shape of the proximal half of the palpal tibia, which is without a pronounced ventral bulge (Fig. 95), combined with the absence of a medial 'ledge' on the palpal tibia (Figs. 95, 96) (palpal tibia is with a ledge or bulges ventrally in other species). *Bungulla bidgemia* can be further

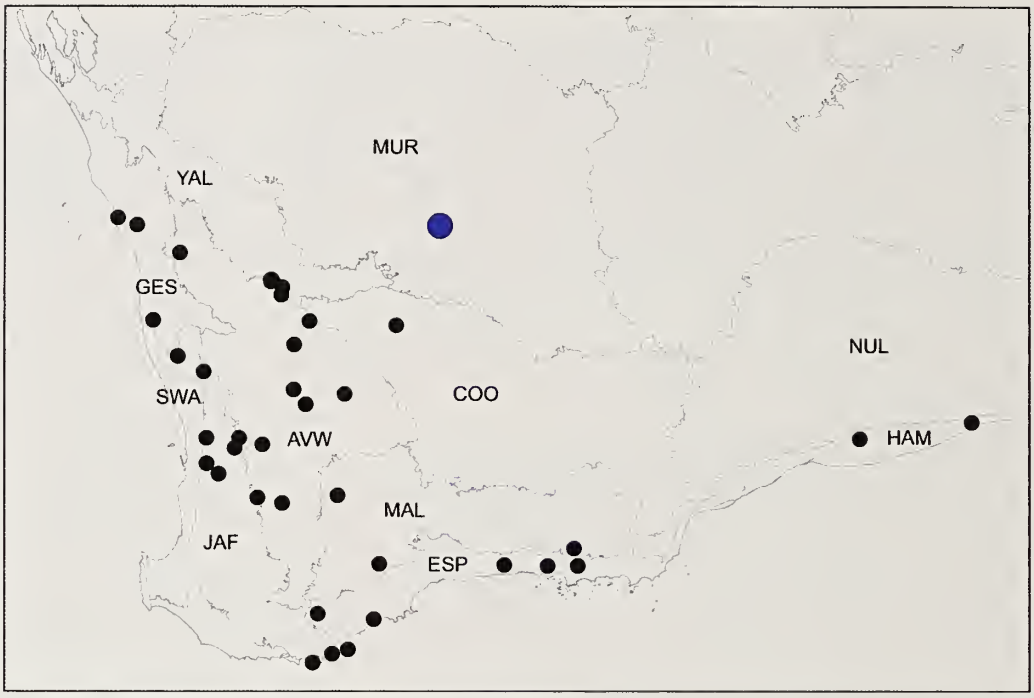


Figure 85.—Map showing collection records of *Bungulla bella* sp. nov. (large blue circle), relative to other taxa with < 5 retrolateral spinules on the male palpal tibia (see Fig. 12). Relevant IBRA 7.0 bioregional acronyms are as follows: AVW, Avon Wheatbelt; COO, Coolgardie; ESP, Esperance Plains; GES, Geraldton Sandplains; HAM, Hampton; JAF, Jarrah Forest; MAL, Mallee; MUR, Murchison; NUL, Nullarbor; SWA, Swan Coastal Plain; YAL, Yalgoo.

distinguished from *B. banksia* by the larger field of retrolateral spinules on the palpal tibia (Fig. 95; cf. Fig. 72); from *B. bertmaini*, *B. laevigata* and *B. quobba* by the shape of the embolus, which is relatively short (i.e., ~as long as bulb) (Fig. 95; cf. Figs. 24, 319, 371); from *B. hamelinensis* by the morphology of the cymbial spinules, which are thicker and more spine-like (Figs. 95–97; cf. Figs. 218–220); from *B. yeni* and by the presence of a larger, crescent-shaped field of retrolateral spinules on the palpal tibia (Fig. 95; cf. Fig. 445); from *B. weld* by the presence of relatively symmetric field of retrolateral spinules on the palpal tibia (Fig. 95; cf. Fig. 419); and from *B. iota* by its larger body size (carapace width ≥ 2.0) (Fig. 86; cf. Fig. 258), combined with the presence of marginal lateral indentations on the carapace between coxae II–III (Fig. 86; cf. Fig. 258). Females are unknown.

**Description (male holotype).**—Total length 7.1. Carapace 2.9 long, 2.2 wide. Abdomen 3.4 long, 2.0 wide. Carapace (Fig. 86) pale tan, with darker pars cephalica and mostly black ocular region; fovea straight; marginal lateral indentations present between coxae II–III. Eye group (Fig. 89) trapezoidal (anterior eye row strongly procurved), 0.8 x as long as wide, PLE–PLE/ALE–ALE ratio 1.5; ALE separated by nearly their own diameter; AME separated by less than their own diameter; PME separated by 2.9 x their own diameter; PME and PLE separated by diameter of PME, PME positioned in line with level of PLE. Maxillae with field of cuspules confined to inner corner (Fig. 90); labium without cuspules. Abdomen (Fig. 87) elongate-oval, beige-tan in dorsal view with five faded pairs of thin, spotted brown chevrons posteriorly, each divided along midline. Dorsal surface of abdomen (Fig. 87) with sparse arrangement of stiff, porrect black setae, each with slightly raised, dark brown sclerotic base; sclerotized sigilla absent. Legs (Figs. 93, 94) variable shades of pale tan, with light scopulae on incrassate tarsi I–II; tibia I spinose, without prolateral clasping spurs. Leg I: femur 2.7; patella 1.3; tibia 2.0; metatarsus 1.7; tarsus 1.5; total 9.3. Leg I femur–tarsus/carapace length ratio 3.2. Pedipalpal tibia (Figs. 95–97) 2.0 x longer than wide; field of retrolateral spinules large and symmetrically crescent-shaped in retrolateral view, positioned medially–distally (along most of retro-ventral margin), consisting of ca. 50 spinules of largely similar length; RTA absent. Cymbium (Figs. 95–97) setose, with sparse field of spine-like spinules covering most of dorsal surface. Embolus (Figs. 95–97) as long as bulb, slightly curved, with unmodified tip; embolic apophysis absent.

**Distribution and remarks.**—*Bungulla bidgemia* (formerly known by WAM identification code 'MYG138') is known only from Bidgemia Station in the far eastern Carnarvon bioregion (Western Australia), just west of the Gascoyne River near the junction of Pell Creek and Daurie Creek (Fig. 98). Nothing is known of the biology of this species, other than that the known male specimens were collected wandering in search of females in winter.

***Bungulla biota*** Rix, Raven & Harvey, sp. nov.
http://zoobank.org/?lsid=urn:lsid:zoobank.org:act:5138917E-CF75-46C7-8D54-D53CECF594AA
(Figs. 1–3, 13, 14, 99–111)

**Type material.**—*Holotype male.* AUSTRALIA: *Western Australia*: Mount Richardson, 222 km SE. of Mount Magnet (IBRA_MUR), 28°45′13″S, 119°57′55″E, dug from burrow, 28 June 2012, N. Watson & R. Teale (WAM T126205[DNA_Voucher_197]; GenB–CO1–MG516830, GenB–CYB–MG516852, GenB–MRPL45–MG516868, GenB–

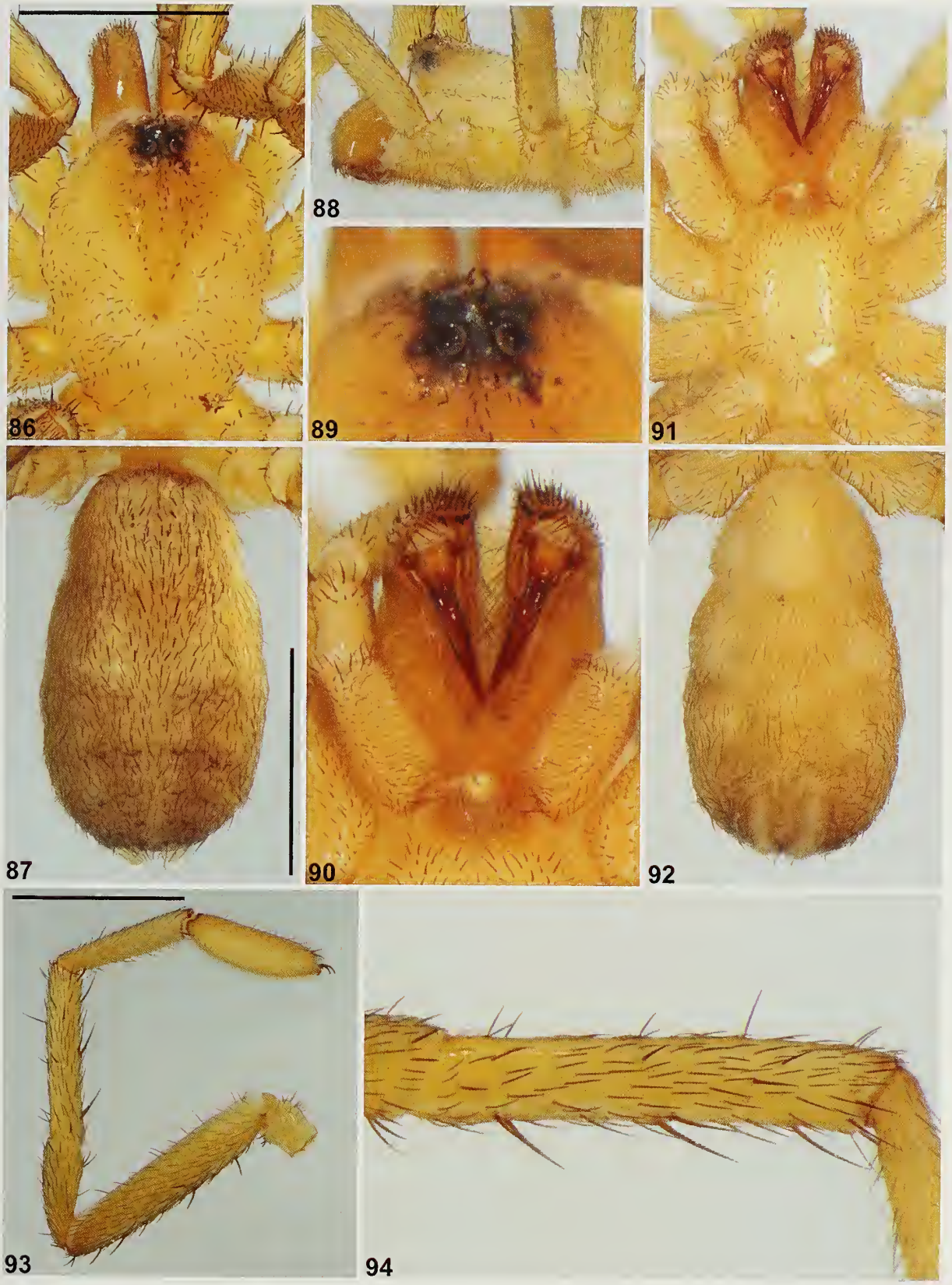


Figures 86–94.—*Bungulla bidgemia* sp. nov., male holotype (WAM T98533) from Bidgemia Station, Gascoyne Junction (Western Australia; CAR), somatic morphology: 86–87, carapace and abdomen, dorsal view; 88, cephalothorax, lateral view; 89, eyes, dorsal view; 90, mouthparts, ventral view; 91–92, cephalothorax and abdomen, ventral view; 93, leg 1, prolateral view; 94, leg 1 tibia, prolateral view. Scale bars = 2.0 mm.


Figures 95–97.—*Bungulla bidgemia* sp. nov., male holotype (WAM T98533) from Bidgemia Station, Gascoyne Junction (Western Australia; CAR), pedipalp: 95, retrolateral view; 96, retro-ventral view; 97, prolateral view. Scale bar = 2.0 mm.

RPF2–MG516886, GenB–XPNPEP3–MG516891, GenB–ITS–MG516856).

*Paratypes*. AUSTRALIA: *Western Australia*: 1 ♂, Albion Downs, 84.9 km NNW. of Leinster (IBRA_MUR), 27°14′40″S, 120°16′54″E, dry pitfall trap, 29 August 2008, Z Hamilton & R. Teale (WAM T96266[DNA_Voucher_211]; GenB–COI–MG516829, GenB–CYB–MG516851, GenB–MRPL45–MG516867, GenB–RPF2–MG516885, GenB–XPNPEP3–MG516890, GenB–ITS–MG516855); 1 ♂, same data except 28 August–3 September 2008 (WAM T96303); 1 ♂, same data except 62.6 km NNW. of

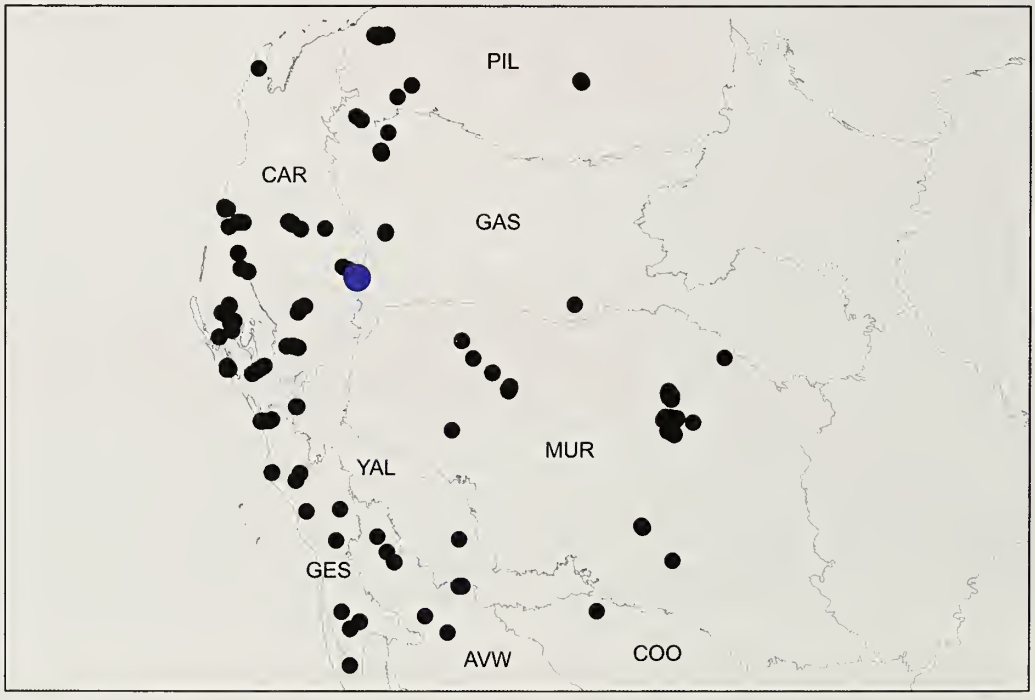


Figure 98.—Map showing collection records of *Bungulla bidgemia* sp. nov. (large blue circles), relative to other taxa with > 10 retrolateral spinules on the male palpal tibia (see Fig. 13). Relevant IBRA 7.0 bioregional acronyms are as follows: AVW, Avon Wheatbelt; CAR, Carnarvon; COO, Coolgardie; GAS, Gascoyne; GES, Geraldton Sandplains; MUR, Murchison; PIL, Pilbara; YAL, Yalgoo.

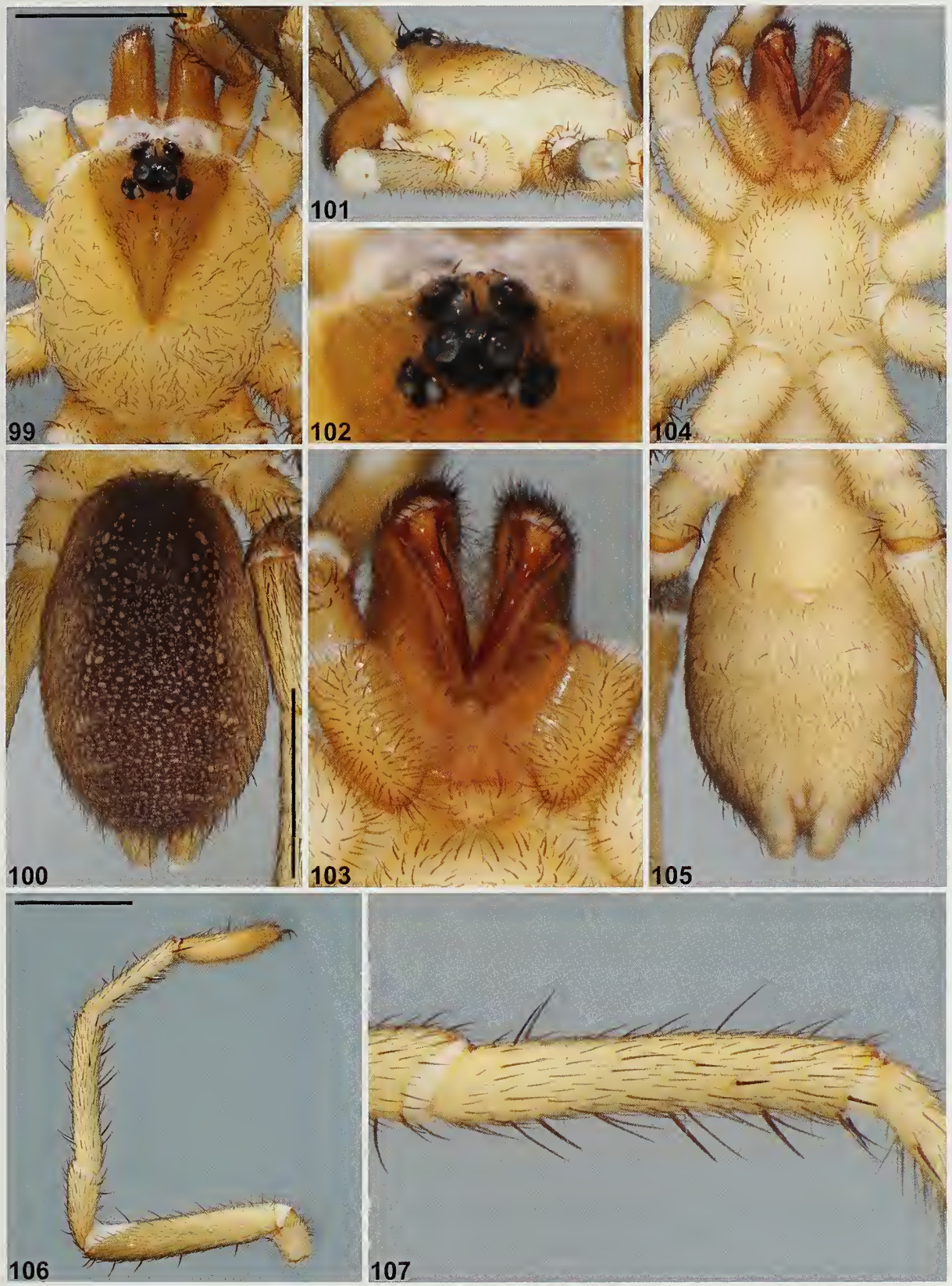


Figures 99–107.—*Bungulla biota* sp. nov., male holotype (WAM T126205) from Mount Richardson (Western Australia; MUR), somatic morphology: 99–100, carapace and abdomen, dorsal view; 101, cephalothorax, lateral view; 102, eyes, dorsal view; 103, mouthparts, ventral view; 104–105, cephalothorax and abdomen, ventral view; 106, leg 1, prolateral view; 107, leg 1 tibia, prolateral view. Scale bars = 2.0 mm.

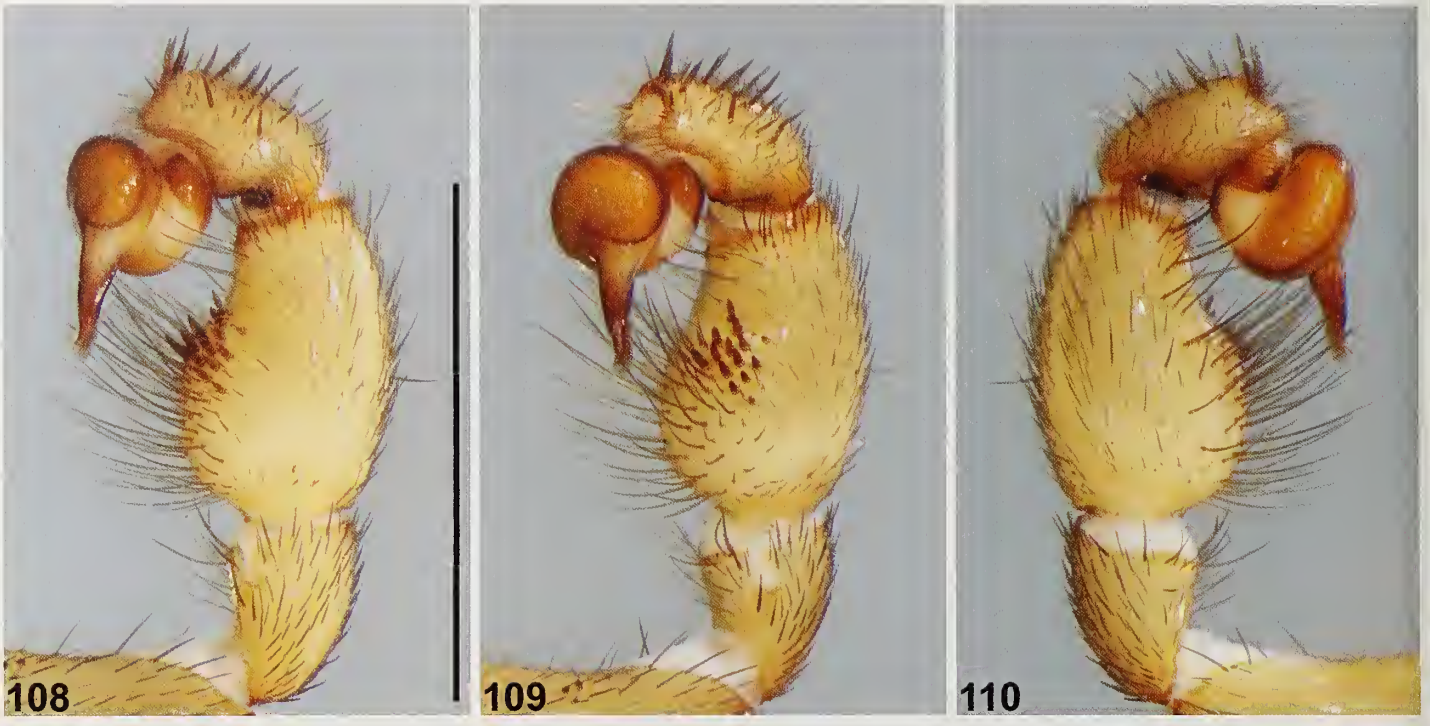


Figures 108–110.—*Bungulla biota* sp. nov., male holotype (WAM T126205) from Mount Richardson (Western Australia; MUR), pedipalp: 108, retrolateral view; 109, retro-ventral view; 110, prolateral view. Scale bar = 2.0 mm.

Leinster, 27°25′03″S, 120°23′45″E (WAM T96297); 1 ♂, same data (WAM T96304[DNA_Voucher_212]; GenB–COI–MG516828, GenB–CYB–MG516850, GenB–MRPL45–MG516866, GenB–RPF2–MG516884, GenB–XPNPEP3–MG516889, GenB–ITS–MG516854).

**Other material examined.**—AUSTRALIA: *Western Australia*: 1 ♂, Albion Downs, 62.7 km NNW. of Leinster (IBRA_MUR), 27°25′02″S, 120°23′41″E, dry pitfall trap, 28 August–3 September 2008, Z Hamilton & R. Teale (WAM T96307); 1 ♂, same data (WAM T96302); 1 ♂, same data

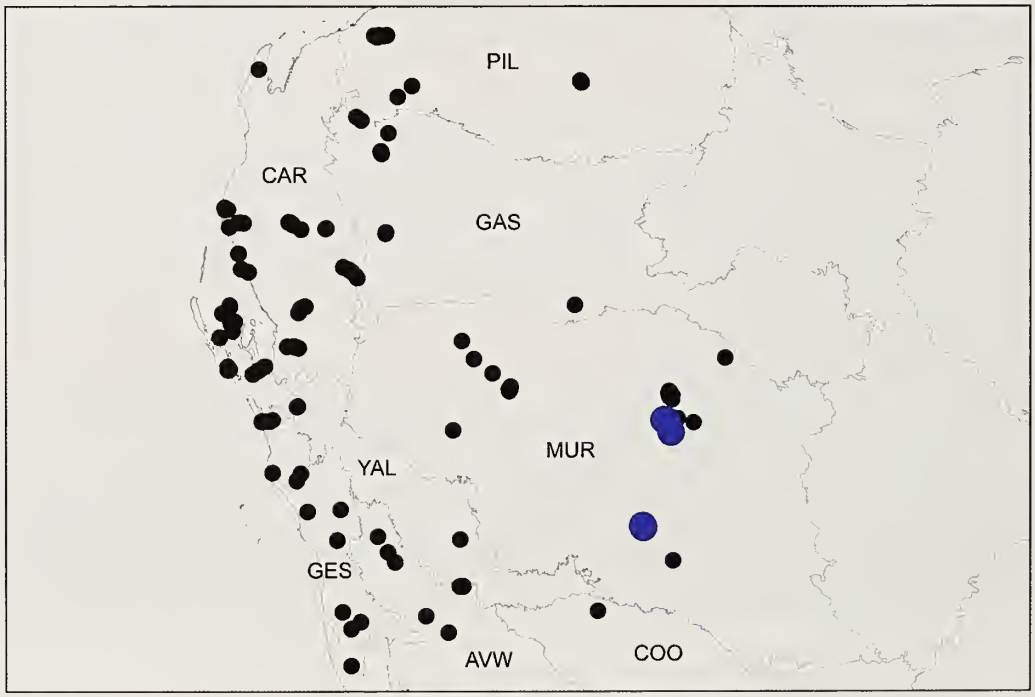


Figure 111.—Map showing collection records of *Bungulla biota* sp. nov. (large blue circles), relative to other taxa with > 10 retrolateral spinules on the male palpal tibia (see Fig. 13). Relevant IBRA 7.0 bioregional acronyms are as follows: AVW, Avon Wheatbelt; CAR, Carnarvon; COO, Coolgardie; GAS, Gascoyne; GES, Geraldton Sandplains; MUR, Murchison; PIL, Pilbara; YAL, Yalgoo.

except 81.2 km NNW. of Leinster, 27°15′32″S, 120°19′50″E (WAM T96293); 1 ♂, same data (WAM T96292); 1 ♂, same data (WAM T96296); 1 ♂, same data (WAM T96294); 1 ♂, Dingo North, ca. 63 km WNW. Mount Ida (IBRA_MUR), 28°43′47.88″S, 119°57′5.360″E, hand foraging, 14 September 2013, M.K. Curran & S.R. Bennett (WAM T135207).

**Etymology.**—The specific epithet is a noun in apposition, in reference to 'Biota Environmental Sciences', for their wonderful support of the Australian Research Council (ARC) idiopid project since its commencement in 2012, and whose staff first discovered and provided sequenceable specimens of this rare species in 2008.

**Diagnosis.**—Males of *Bungulla biota* can be distinguished from all other known congeners by the shape of the distal embolus, which is broad and distally-flattened with a truncate tip (Figs. 108, 109) (embolus is usually tapered, with or without distal modifications in other species). Females are unknown.

**Description (male holotype).**—Total length 8.4. Carapace 3.3 long, 2.7 wide. Abdomen 3.8 long, 2.4 wide. Carapace (Fig. 99) pale tan, with much darker olive-tan pars cephalica and mostly black ocular region (carapace tan with brown-black pars cephalica in life; Figs. 1, 2); postero-lateral corners near abdomen each with marginal cluster of longer black setae; fovea straight. Eye group (Fig. 102) trapezoidal (anterior eye row strongly procurved), 0.8 x as long as wide, PLE–PLE/ALE–ALE ratio 1.4; ALE separated by nearly their own diameter; AME separated by less than their own diameter; PME separated by 4.3 x their own diameter; PME and PLE separated by diameter of PME, PME positioned in line with level of PLE. Maxillae with field of cuspules confined to inner corner (Fig. 103); labium without cuspules. Abdomen (Fig. 100) oval, mostly dark purple-brown in dorsal view, lighter dorso-laterally (as in life; Figs. 1, 2), with beige-tan mottling, two pairs of small beige-tan sigilla spots, and four indistinct pairs of beige-tan chevrons posteriorly, each divided along midline. Dorsal surface of abdomen (Fig. 100) with sparse arrangement of stiff, porrect black setae, each with slightly raised, dark brown sclerotic base; sclerotized sigilla absent. Legs (Figs. 106, 107) variable shades of pale tan, with light scopulae on tarsi I–II; tibia I spinose, without prolateral clasping spurs. Leg I: femur 3.3; patella 1.6; tibia 2.5; metatarsus 2.0; tarsus 1.7; total 11.1. Leg I femur–tarsus/carapace length ratio 3.4. Pedipalpal tibia (Figs. 108–110) stout, 1.5 x longer than wide, with RTA-like ventral bulge proximally; field of retrolateral spinules sub-triangular in shape, positioned medially (at apex of RTA-like bulge), consisting of 14 spinules of largely similar length; RTA absent. Cymbium (Figs. 108–110) setose, with field of porrect, thorn-like spinules covering most of dorsal surface. Embolus (Figs. 108–110) as long as bulb, relatively straight, with broad, distally-flattened, truncate tip; embolic apophysis absent.

**Distribution and remarks.**—*Bungulla biota* (formerly known by WAM identification codes 'MYG270' and 'MYG032') has a relatively restricted distribution in the central Murchison bioregion of Western Australia, at Albion Downs (near Leinster) and in the vicinity of Mount Richardson (Fig. 111). Little is known of the biology of this unusual species, other than that the known male specimens were collected wandering in search of females in late winter and early spring, with a single male (Figs. 1–2) collected in its burrow (pre-emergence) in mid-winter.

***Bungulla bringo*** Rix, Raven & Harvey, sp. nov.
http://zoobank.org/?lsid=urn:lsid:zoobank.org:act:333DE2CC-8CF5-4A7A-B830-4ED18E505D88
(Figs. 10, 12, 112–124)

**Type material.**—*Holotype male*. AUSTRALIA: *Western Australia*: 1 km SE. of Bringo railway cutting (IBRA_GES), 28°45′S, 114°56′E, gully with York Gum, 13 May 2000, S. Slack-Smith (WAM T41571).

**Other material examined.**—AUSTRALIA: *Western Australia*: 1 ♂, Ebano Creek, ca. 22 miles SW. of Morawa on Morawa-Mingenew Road (IBRA_AVW), 29°10′S, 115°39′E, 5 August 1953, B.Y. Main (WAM T142938).

**Etymology.**—The specific epithet is a noun in apposition, in reference to the distribution of this species near Bringo, Western Australia.

**Diagnosis.**—Males of *Bungulla bringo* can be distinguished from all other known congeners by the presence of a very small field of < 5 retrolateral spinules on the palpal tibia (Figs. 121, 122) (> 10 spinules or spinules absent in other species). Females are unknown.

**Description (male holotype).**—Total length 13.5. Carapace 4.9 long, 4.3 wide. Abdomen 6.4 long, 4.3 wide. Carapace (Fig. 112) tan, with darker pars cephalica and slightly darker ocular region; postero-lateral corners near abdomen each with marginal cluster of longer black setae; fovea slightly recurved. Eye group (Fig. 115) trapezoidal (anterior eye row strongly procurved), 0.8 x as long as wide, PLE–PLE/ALE–ALE ratio 1.5; ALE separated by nearly their own diameter; AME separated by less than their own diameter; PME separated by 3.2 x their own diameter; PME and PLE separated by diameter of PME, PME positioned in line with level of PLE. Maxillae with field of cuspules confined to inner corner (Fig. 116); labium without cuspules. Abdomen (Fig. 113) oval, mostly dark grey in dorsal view, with beige mottling and large beige patch posteriorly (the latter a preservation artefact). Dorsal surface of abdomen (Fig. 103) with sparse arrangement of stiff, porrect black setae, each with slightly raised, dark brown sclerotic base; sclerotized sigilla absent. Legs (Figs. 119, 120) variable shades of tan, with light scopulae on tarsi I–II; tibia I spinose, without prolateral clasping spurs. Leg I: femur 5.3; patella 2.6; tibia 4.1; metatarsus 2.8; tarsus 2.8; total 18.7. Leg I femur–tarsus/carapace length ratio 3.8. Pedipalpal tibia (Figs. 121–123) stout, 1.6 x longer than wide, with very small field of 4 retrolateral spinules positioned medially; RTA absent. Cymbium (Figs. 121–123) setose, with field of porrect, thorn-like spinules covering most of dorsal surface. Embolus (Figs. 121–123) slightly longer than bulb, slightly curved, with unmodified tip; embolic apophysis absent.

**Distribution and remarks.**—*Bungulla bringo* (formerly known by WAM identification code 'MYG152') is a rare species known only from near Bringo railway cutting and Ebano Creek, east and south-east of Geraldton (Western Australia) (Fig. 124). Nothing is known of the biology of this species, other than that the known male specimens were collected wandering in search of females in late autumn and winter.

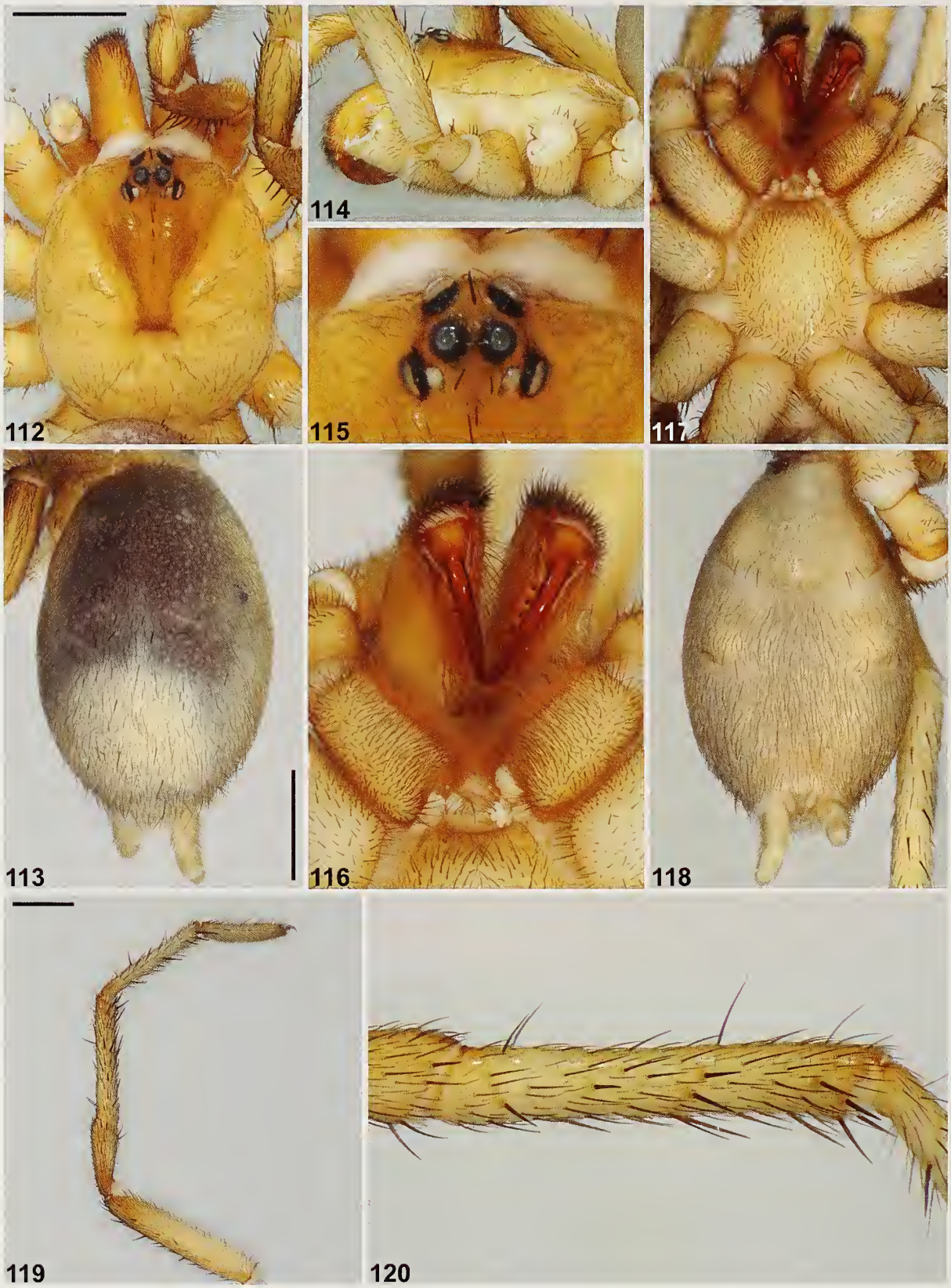


Figures 112–120.—*Bungulla bringo* sp. nov., male holotype (WAM T41571) from SE. of Bringo railway cutting (Western Australia; GES), somatic morphology: 112–113, carapace and abdomen, dorsal view; 114, cephalothorax, lateral view; 115, eyes, dorsal view; 116, mouthparts, ventral view; 117–118, cephalothorax and abdomen, ventral view; 119, leg I, prolateral view; 120, leg I tibia, prolateral view. Scale bars = 2.0 mm.


Figures 121–123.—*Bungulla bringo* sp. nov., male holotype (WAM T41571) from SE. of Bringo railway cutting (Western Australia; GES), pedipalp: 121, retrolateral view; 122, retro-ventral view; 123, prolateral view. Scale bar = 2.0 mm.

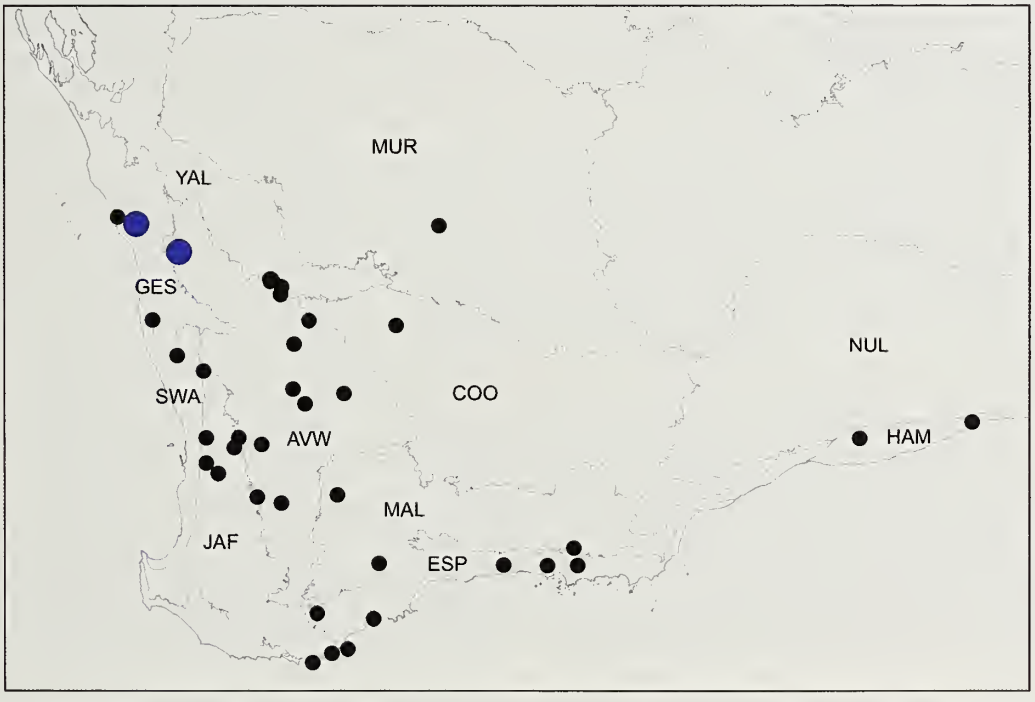


Figure 124.—Map showing collection records of *Bungulla bringo* sp. nov. (large blue circles), relative to other taxa with < 5 retrolateral spinules on the male palpal tibia (see Fig. 12). Relevant IBRA 7.0 bioregional acronyms are as follows: AVW, Avon Wheatbelt; COO, Coolgardie; ESP, Esperance Plains; GES, Geraldton Sandplains; HAM, Hampton; JAF, Jarrah Forest; MAL, Mallee; MUR, Murchison; NUL, Nullarbor; SWA, Swan Coastal Plain; YAL, Yalgoo.

***Bungulla burbidgei*** Rix, Raven & Harvey, sp. nov.
http://zoobank.org/?lsid=urn:lsid:zoobank.org:act:64FAAD08-2D57-46CF-848F-7B2D47EF1229
(Figs. 13, 125–137)

**Type material.**—*Holotype male*. AUSTRALIA: *Western Australia*: Zuytdorp, site ZU1 (IBRA_GES), 27°15′42″S, 114°01′09″E, dry pitfall trap, 14 October 1994, A. Sampey (WAM T142988).

*Paratype*. AUSTRALIA: *Western Australia*: 1 ♂, same data as holotype (142989).

**Other material examined.**—AUSTRALIA: *Western Australia*: 1 ♂, Zuytdorp, site ZU2 (IBRA_GES), 27°15′59.7″S, 114°01′82.2″E, wet pitfall trap, 26 August–15 October 1994, A. Sampey et al., WAM/CALM Carnarvon Survey (WAM T142990); 2 ♂, same data except dry pitfall trap, 14–19 October 1994 (WAM T142991); 2 ♂, same data except site ZU3, 27°15′49.9″S, 114°04′13.7″E, wet pitfall trap, 18 May–16 August 1995, N. Hall, WAM/CALM Carnarvon Survey (WAM T142992); 1 ♂, same data except 26 August–17 October 1994, A. Sampey et al., WAM/CALM Carnarvon Survey (WAM T142993).

**Etymology.**—This species is named in honor of Allan Burbidge, in recognition of his contributions to the Southern Carnarvon Basin Survey (Burbidge et al. 2000) and to the study of Australian biodiversity.

**Diagnosis.**—Males of *Bungulla burbidgei* can be distinguished from all other known congeners with > 10 retrolateral spinules on the palpal tibia (Fig. 13) – except *B. biota*, *B. dipsodes*, *B. keigheryi*, *B. kendricki*, *B. sampeyae* and *B. westi* – by the shape of the proximal half of the palpal tibia, which has a pronounced RTA-like ventral bulge in retrolateral view (Fig. 134) (palpal tibia is piriform and unmodified in other species). *Bungulla burbidgei* can be further distinguished from *B. biota*, *B. dipsodes*, *B. keigheryi*, *B. kendricki*, *B. sampeyae* and *B. westi* by the presence of a field of porrect, dagger-like spinules at the apex of the RTA-like bulge (Figs. 134, 135; cf. Figs. 108, 147, 280, 306, 406, 432). Females are unknown.

**Description (male holotype).**—Total length 12.1. Carapace 4.8 long, 4.1 wide. Abdomen 5.4 long, 3.4 wide. Carapace (Fig. 125) tan, with slightly darker pars cephalica, darker brown lyre-like pattern on pars cephalica and mostly black ocular region; fovea slightly procurved. Eye group (Fig. 128) trapezoidal (anterior eye row strongly procurved), 0.8 x as long as wide, PLE–PLE/ALE–ALE ratio 1.3; ALE separated by their own diameter; AME separated by less than their own diameter; PME separated by 4.4 x their own diameter; PME and PLE separated by diameter of PME, PME positioned in line with level of PLE. Maxillae with field of cuspules confined to inner corner (Fig. 129); labium without cuspules. Abdomen (Fig. 126) oval, dark charcoal-brown in dorsal view, with beige-tan mottling, two large pairs of beige-tan sigilla spots, and three pairs of large, beige-tan chevron-like bands posteriorly. Dorsal surface of abdomen (Fig. 126) with sparse arrangement of stiff, porrect black setae, each with slightly raised, dark brown sclerotic base; sclerotized sigilla absent. Legs (Figs. 132, 133) variable shades of tan, with light scopulae on tarsi I–II; tibia I largely aspinose, without prolateral clasping spurs. Leg I: femur 4.4; patella 2.3; tibia 3.3; metatarsus 2.8; tarsus 2.1; total 14.9. Leg 1 femur–tarsus/carapace length ratio 3.1. Pedipalpal tibia (Figs. 134–136) 2.0 x longer than wide, with RTA-like ventral bulge proximally; field of retrolateral spinules crescent-shaped, positioned medially (on and adjacent to RTA-like bulge), consisting of ca. 30 spinules, the latter longest and with dagger-like morphology at apex of RTA-like bulge; RTA absent. Cymbium (Figs. 134–136) setose, with field of spine-like spinules covering most of dorsal surface. Embolus (Figs. 134–136) slightly longer than bulb, strongly curved, with slightly expanded tip; embolic apophysis absent.

**Distribution and remarks.**—*Bungulla burbidgei* is a rare and highly restricted species known only from Zuytdorp, in the northern Geraldton Sandplains bioregion of south-western Australia (Fig. 137). Nothing is known of the biology of this species, other than that the known male specimens were collected wandering in search of females in winter, spring and possibly late autumn.

***Bungulla dipsodes*** Rix, Raven & Harvey, sp. nov.
http://zoobank.org/?lsid=urn:lsid:zoobank.org:act:A829DD35-85CF-4A23-A7A5-112DAF3413DD
(Figs. 13, 138–150)

**Type material.**—*Holotype male*. AUSTRALIA: *Western Australia*: Meekatharra, ca. 130 km N., site 3 (IBRA_GAS), 25°35′29.83″S, 118°54′36.64″E, forage, bulk sample, 6–16 November 2009, M. Peterson (WAM T100061).

**Etymology.**—The specific epithet is derived from the Greek 'dipsodes' ('thirsty' or 'the thirsty ones'; see Brown 1956), in reference to the arid landscape in which this species lives.

**Diagnosis.**—Males of *Bungulla dipsodes* can be distinguished from all other known congeners with > 10 retrolateral spinules on the palpal tibia (Fig. 13) – except *B. biota*, *B. burbidgei*, *B. keigheryi*, *B. kendricki*, *B. sampeyae* and *B. westi* – by the shape of the proximal half of the palpal tibia, which has a pronounced RTA-like ventral bulge in retrolateral view (Fig. 147) (palpal tibia is piriform and unmodified in other species). *Bungulla dipsodes* can be further distinguished from *B. biota* by the shape of the embolus, which is without a truncate tip (Figs. 147, 148; cf. Fig. 108); from *B. burbidgei* by the absence of dagger-like spinules at the apex of the RTA-like bulge (Fig. 147; cf. Fig. 134); from *B. keigheryi* by the broadly-rounded shape of the RTA-like bulge (Fig. 147; cf. Fig. 280); from *B. sampeyae* by the coloration of the dorsal abdomen, which is bi-colored (i.e., pale tan in color with dark anterior markings and dark posterior chevrons) (Fig. 139; cf. Fig. 398 and Supplementary File 1); from *B. kendricki* by the shape of the palpal tibia, which is less strongly arched dorsally, with a relatively symmetrical, bulbous profile in retrolateral view (Fig. 147; cf. Fig. 306); and from *B. westi* by the absence of spinules on the disto-dorsal margin of the palpal tibia (Figs. 147–149; cf. Fig. 432). Females are unknown.

**Description (male holotype).**—Total length 9.5. Carapace 3.2 long, 2.4 wide. Abdomen 5.1 long, 2.7 wide. Carapace (Fig. 138) tan, with slightly darker pars cephalica, darker olive lyre-like pattern on pars cephalica and mostly black ocular region; fovea straight. Eye group (Fig. 141) trapezoidal (anterior eye row strongly procurved), 0.8 x as long as wide, PLE–PLE/ALE–ALE ratio 1.3; ALE separated by nearly their own diameter; AME separated by less than their own diameter; PME separated by 2.3 x their own diameter; PME and PLE separated by diameter of PME, PME positioned in line with

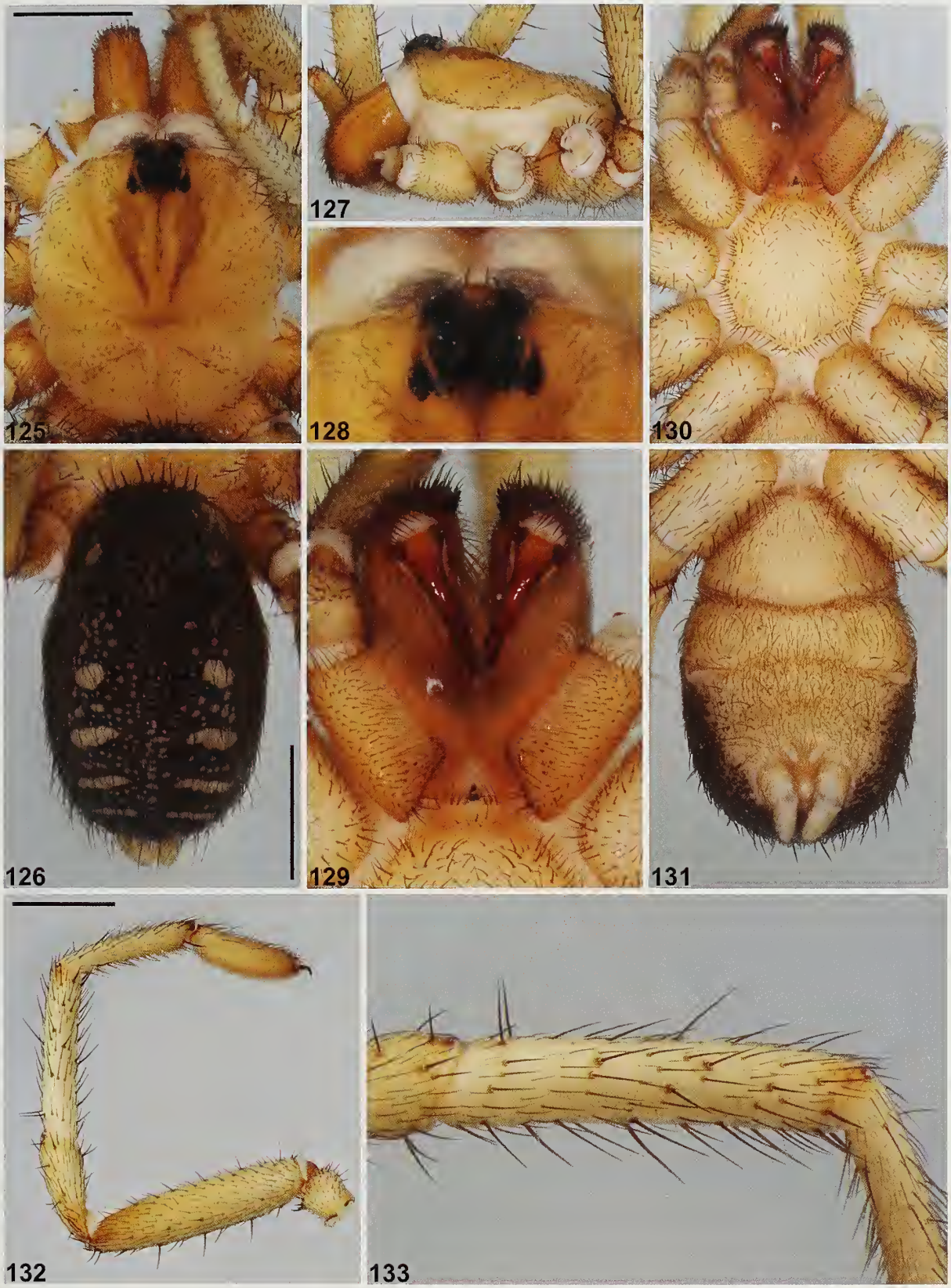


Figures 125–133.—*Bungulla burbidgei* sp. nov., male holotype (WAM T142988) from Zuytdorp (Western Australia; GES), somatic morphology: 125–126, carapace and abdomen, dorsal view; 127, cephalothorax, lateral view; 128, eyes, dorsal view; 129, mouthparts, ventral view; 130–131, cephalothorax and abdomen, ventral view; 132, leg I, prolateral view; 133, leg I tibia, prolateral view. Scale bars = 2.0 mm.


Figures 134–136.—*Bungulla burbidgei* sp. nov., male holotype (WAM T142988) from Zuytdorp (Western Australia; GES), pedipalp: 134, retrolateral view; 135, retro-ventral view; 136, prolateral view. Scale bar = 2.0 mm.

level of PLE. Maxillae with field of cuspules confined to inner corner (Fig. 142); labium without cuspules. Abdomen (Fig. 139) elongate-oval, pale beige-tan in dorsal view with contrasting pattern of four darker charcoal-grey markings anteriorly and five pairs of thin, spotted, dark charcoal-grey chevrons posteriorly, each divided along midline. Dorsal surface of abdomen (Fig. 139) with sparse arrangement of stiff, porrect black setae, each with slightly raised, dark brown sclerotic base; sclerotized sigilla absent. Legs (Figs. 145, 146) variable shades of pale tan, with light scopulae on incrassate

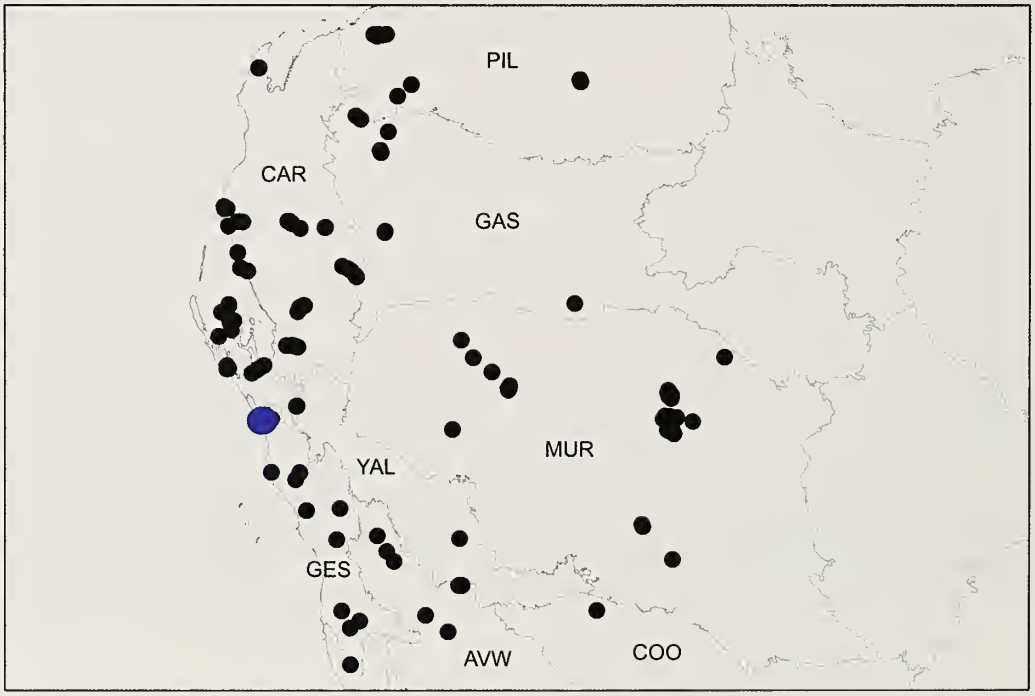


Figure 137.—Map showing collection records of *Bungulla burbidgei* sp. nov. (large blue circles), relative to other taxa with > 10 retrolateral spinules on the male palpal tibia (see Fig. 13). Relevant IBRA 7.0 bioregional acronyms are as follows: AVW, Avon Wheatbelt; CAR, Carnarvon; COO, Coolgardie; GAS, Gaseoyne; GES, Geraldton Sandplains; MUR, Murchison; PIL, Pilbara; YAL, Yalgoo.

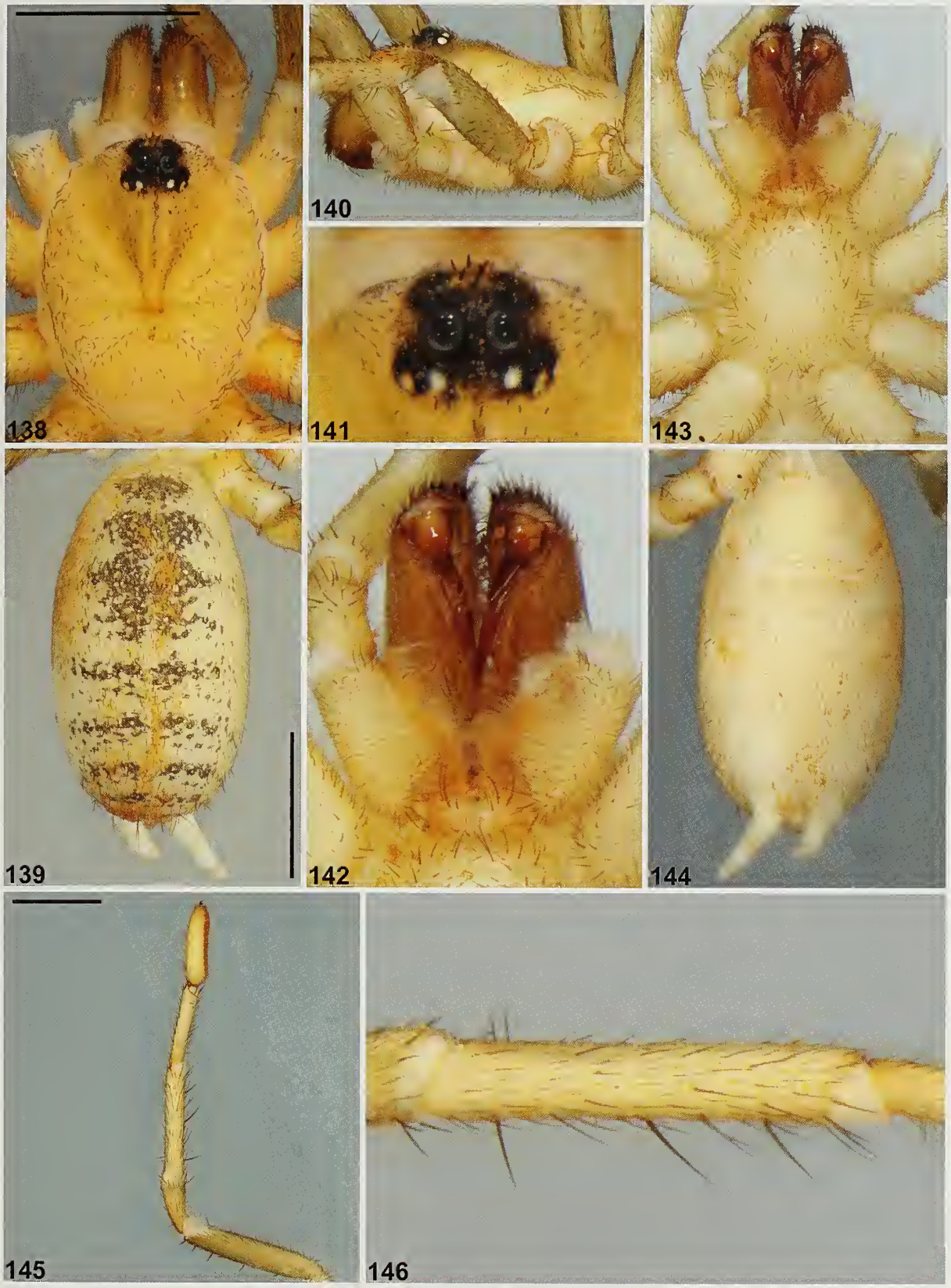


Figures 138–146.—*Bungulla dipsodes* sp. nov., male holotype (WAM T100061) from ca. 130 km N. of Meekatharra (Western Australia; GAS), somatic morphology: 138–139, carapace and abdomen, dorsal view; 140, cephalothorax, lateral view; 141, eyes, dorsal view; 142, mouthparts, ventral view; 143–144, cephalothorax and abdomen, ventral view; 145, leg I, prolateral view; 146, leg I tibia, prolateral view. Scale bars = 2.0 mm.


Figures 147–149.—*Bungulla dipsodes* sp. nov., male holotype (WAM T100061) from ca. 130 km N. of Meekatharra (Western Australia; GAS), pedipalp: 147, retrolateral view; 148, retro-ventral view; 149, prolateral view. Scale bar = 2.0 mm.

tarsi I–II; tibia I largely aspinose, without prolateral clasping spurs. Leg I: femur 3.0; patella 1.5; tibia 2.3; metatarsus 1.9; tarsus 1.8; total 10.5. Leg I femur–tarsus/carapace length ratio 3.2. Pedipalpal tibia (Figs. 147–149) stout, bulbous, 1.6 x longer than wide, with rounded RTA-like ventral bulge proximally; field of retrolateral spinules oval in shape, positioned medially (on and adjacent to RTA-like bulge), consisting of ca. 40 spinules, the latter longest at apex of RTA-like bulge; RTA absent. Cymbium (Figs. 147–149) setose, with field of porrect, thorn-like spinules covering most of dorsal

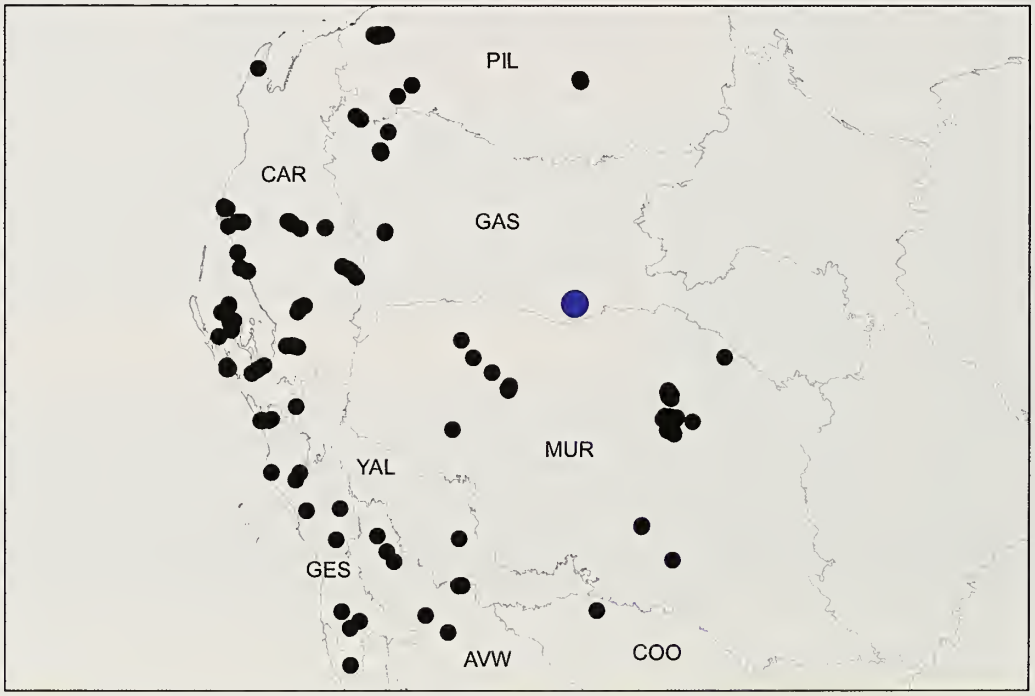


Figure 150.—Map showing collection records of *Bungulla dipsodes* sp. nov. (large blue circle), relative to other taxa with > 10 retrolateral spinules on the male palpal tibia (see Fig. 13). Relevant IBRA 7.0 bioregional acronyms are as follows: AVW, Avon Wheatbelt; CAR, Carnarvon; COO, Coolgardie; GAS, Gascoyne; GES, Geraldton Sandplains; MUR, Murchison; PIL, Pilbara; YAL, Yalgoo.

surface. Embolus (Figs. 147–149) slightly longer than bulb, strongly curved, with slightly expanded tip; embolic apophysis absent.

**Distribution and remarks.**—*Bungulla dipsodes* is known only from north of the Robinson Ranges, in the southern Gascoyne (Augustus) bioregion of Western Australia (Fig. 150). Nothing is known of the biology of this species, other than that the single known male specimen was collected wandering in search of females in late spring.

***Bungulla disrupta*** Rix, Raven & Harvey, sp. nov.
http://zoobank.org/?lsid=urn:lsid:zoobank.org:act:8DC29324-76A7-4E3C-8228-C63962534FED
(Figs. 12, 14, 151–172)

**Type material.**—*Holotype male*. AUSTRALIA: *Western Australia*: Lake Magenta Nature Reserve (S. Central), south, site PI 13 (IBRA_MAL), 33°42′11″S, 118°58′59″E, wet pitfall traps, 15 October 1999–1 November 2000, P. Van Heurck, CALM Survey (WAM T142954).

**Other material examined.**—AUSTRALIA: *Western Australia*: 1 ♂, Durokoppin Nature Reserve, Bencubbin-Kellerberrin Road, site KL 9 (IBRA_AVW), 31°24′37″S, 117°45′06″E, wet pitfall traps, 22 May–22 September 1998, N. Guthrie, CALM Survey (WAM T139539); 1 ♂, same data (WAM T139540); 1 ♂, Gillingarra (IBRA_JAF), 30°56′S, 116°03′E, 5 April 1956, B.Y. Main (WAM T142937); 1 ♂, Gura Road, north-east, NW. of Narrogin, site NR 10 (IBRA_JAF), 32°45′12″S, 116°56′43″E, wet pitfall traps, 30 October 1997–12 May 1998, E. Ladhams, CALM Survey (WAM T142959); 1 ♂, Hopkins Road, west, SE. of Kulin, site KN 2 (IBRA_MAL), 32°43′15″S, 118°16′59″E, wet pitfall traps, 15 May–22 September 1998, N. Guthrie, CALM Survey (WAM T 142955); 1 ♂, Mackie Creek Reserve, west, site YO 2 (IBRA_AVW), 31°59′33″S, 117°01′28″E, wet pitfall traps, 30 October 1997–26 May 1998, P. Van Heurck, N. Guthrie, CALM Survey (WAM T142958); 1 ♂, 3 km W. of Nembudding (IBRA_AVW), 31°11′49″S, 117°32′51″E, wet pitfall traps, 30 March–29 June 1999, M.S. Harvey et al. (WAM T40108); 1 ♂, Wambyn Nature Reserve, site YO 10 (IBRA_JAF), 31°54′02″S, 116°38′22″E, wet pitfall traps, 15 October 1997–25 May 1998, N. Guthrie, CALM Survey (WAM T142956); 1 ♂, Wardering Spring Nature Reserve, site WK 12 (IBRA_AVW), 32°50′17″S, 117°21′31″E, wet pitfall traps, 30 October 1997–14 May 1998, N. Guthrie, CALM Survey (WAM T142960); 1 ♂, Warrigal Road, SW. of Beverley, site YO 8 (IBRA_JAF), 32°02′40″S, 116°33′56″E, wet pitfall traps, 30 October 1997–20 May 1998, P. Van Heurck, N. Guthrie, CALM Survey (WAM T142957); 1 ♀, Stirling Range National Park, Talyuberlup Picnic Area (IBRA_ESP), 34°24′49″S, 117°57′22″E, dug from burrow in bank of gully, 24 October 2012, M.S. Harvey, A. Beavis, M. Castalanelli, D. Harms (WAM T131634[DNA_Voucher_274]; GenB–COI–MG516840, GenB–CYB–MG516842).

**Etymology.**—The specific epithet is derived from the Latin 'disruptus' (adjective: 'broken up' or 'separated'; see Brown 1956), in reference to the now highly fragmented distribution of this species in the heavily cleared Avon Wheatbelt and western Mallee bioregions.

**Diagnosis.**—Males of *Bungulla disrupta* can be distinguished from all other known congeners with < 5 retrolateral spinules on the palpal tibia (Fig. 12) – except *B. fusca*, *B. hillyerae*, *B. inermis*, *B. oraria* and *B. parva* – by the shape of the cymbial spinules, which are curved, anteriorly-directed and restricted to the distal half of the cymbium (Figs. 160–162) (spinules are porrect, thorn-like, and cover most of the dorsal surface of the cymbium in other species). *Bungulla disrupta* can be further distinguished from *B. parva* by its larger body size (carapace width ≥ 3.0) (Fig. 151; cf. Fig. 349); from *B. hillyerae* and *B. inermis* by the darker carapace coloration (depending on the state of preservation; see Supplementary File 1) (Fig. 151; cf. Figs. 232, 245); and from *B. fusca* and *B. oraria* by the color of the legs, which are bi-colored with pale patellae, tibiae, metatarsi and tarsi (Fig. 158; cf. Figs. 193, 343), combined with the color of the dorsal abdomen, which has an ornate pattern of broad pale chevrons (Fig. 152; cf. Figs. 187, 337 and Supplementary File 1).

**Description (male holotype).**—Total length 8.0. Carapace 4.2 long, 3.5 wide. Abdomen 3.2 long, 2.4 wide. Carapace (Fig. 151) chocolate-brown, with darker pars cephalica and black ocular region; fovea straight. Eye group (Fig. 154) trapezoidal (anterior eye row strongly procurved), 0.8 x as long as wide, PLE–PLE/ALE–ALE ratio 1.5; ALE separated by nearly their own diameter; AME separated by less than their own diameter; PME separated by 3.4 x their own diameter; PME and PLE separated by slightly less than diameter of PME, PME positioned in line with level of PLE. Maxillae with field of cuspules confined to inner corner (Fig. 155); labium without cuspules. Abdomen (Fig. 152) oval, dark brown in dorsal view with tan mottling, two pairs of tan sigilla spots and three pairs of tan chevrons posteriorly, each divided along midline. Dorsal surface of abdomen (Fig. 152) with sparse arrangement of stiff, porrect black setae, each with slightly raised, dark brown sclerotic base; sclerotized sigilla absent. Legs (Figs. 158, 159) variable shades of tan on patellae–tarsi, with darker brown femora and light scopulae on tarsi I–II; tibia 1 largely aspinose, without prolateral clasping spurs. Leg I: femur 4.1; patella 2.1; tibia 3.5; metatarsus 3.1; tarsus 2.1; total 14.9. Leg I femur–tarsus/carapace length ratio 3.5. Pedipalpal tibia (Figs. 160–162) sub-rectangular, 2.2 x longer than wide, without retrolateral spinules; RTA absent. Cymbium (Figs. 160–162) setose, with field of curved, anteriorly-directed spine-like spinules restricted to distal half of segment. Embolus (Figs. 160–162) nearly twice length of bulb, slightly curved, with unmodified tip; embolic apophysis absent.

**Description (female WAM T131634).**—Total length 17.3. Carapace 6.1 long, 5.6 wide. Abdomen 8.7 long, 6.7 wide. Carapace (Fig. 163) slightly damaged, light chocolate-brown with slightly darker ocular region; fovea strongly procurved. Eye group (Fig. 166) trapezoidal (anterior eye row strongly procurved), 0.7 x as long as wide, PLE–PLE/ALE–ALE ratio 1.7; ALE separated by their own diameter; AME separated by their own diameter; PME separated by 3.3 x their own diameter; PME and PLE separated by diameter of PME, PME positioned in line with level of PLE. Maxillae with field of cuspules confined to inner corner (Fig. 167); labium without cuspules. Abdomen (Fig. 164) oval, dark grey-brown in dorsal view with beige mottling, darker cardiac marking, two pairs of beige sigilla spots, and four pairs of beige chevrons posteriorly, each divided along midline; sclerotized sigilla absent. Legs (Figs. 169, 170) variable shades of tan; thick

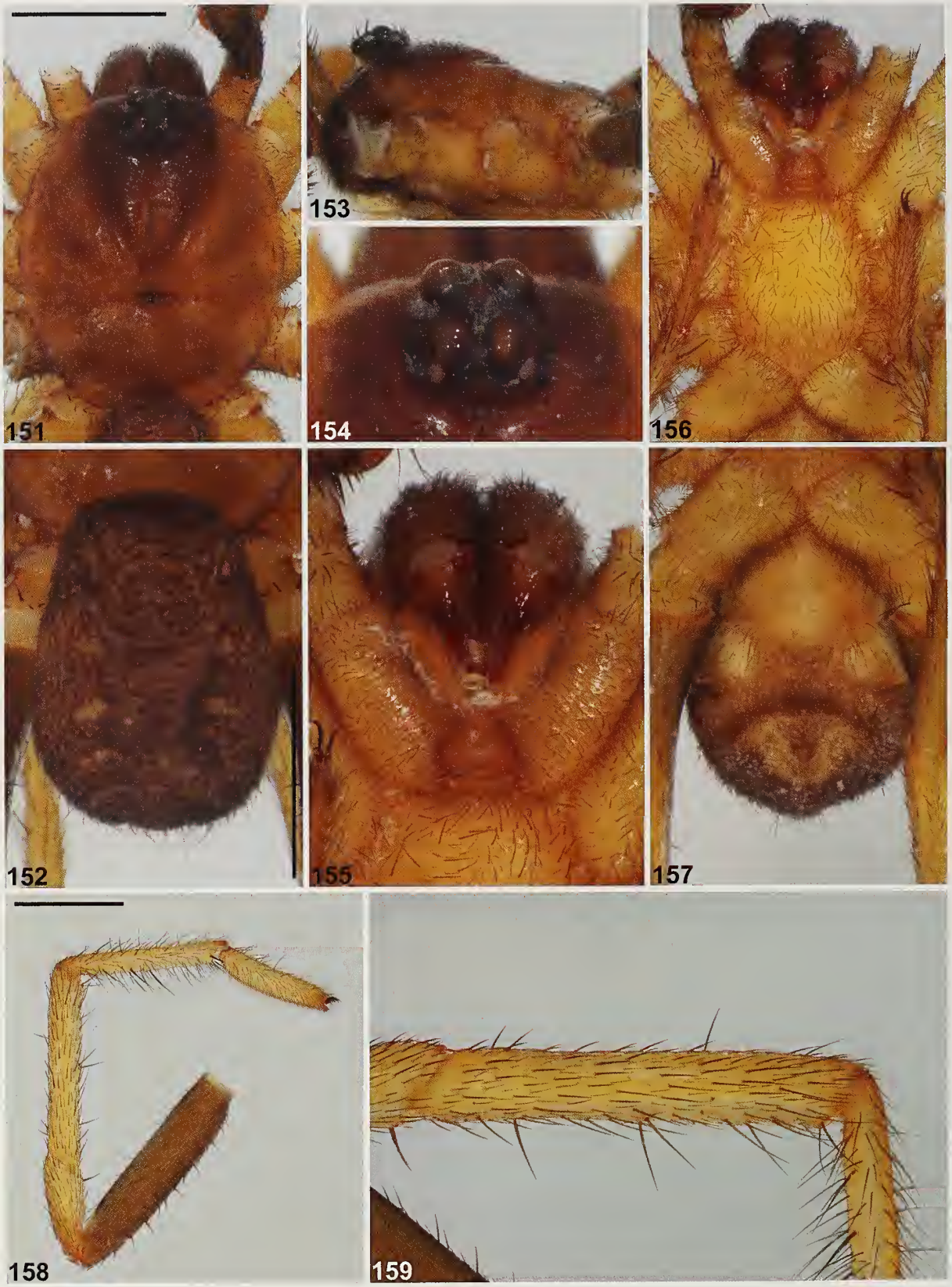


Figures 151–159.—*Bungulla disrupta* sp. nov., male holotype (WAM T142954) from Lake Magenta Nature Reserve (Western Australia: MAL), somatic morphology: 151–152, carapace and abdomen, dorsal view; 153, cephalothorax, lateral view; 154, eyes, dorsal view; 155, mouthparts, ventral view; 156–157, cephalothorax and abdomen, ventral view; 158, leg I, prolateral view; 159, leg I tibia, prolateral view. Scale bars = 2.0 mm.


Figures 160–162.—*Bungulla disrupta* sp. nov., male holotype (WAM T142954) from Lake Magenta Nature Reserve (Western Australia; MAL), pedipalp: 160, retrolateral view; 161, retro-ventral view; 162, prolateral view. Scale bar = 2.0 mm.

scopulae present on tarsi and metatarsi I–II; tibia I with distal cluster of 4 stout prolateral macrosetae and 2 retro-ventral spine-like macrosetae; metatarsus I with 2 stout pro-ventral macrosetae and 4 longer retro-ventral macrosetae; tarsus I with distal cluster of 4 stout ventral macrosetae. Leg 1: femur 3.6; patella 2.4; tibia 2.1; metatarsus 1.7; tarsus 1.4; total 11.3. Leg I femur–tarsus/carapace length ratio 1.8. Pedipalp tan, spinose on tibia and tarsus, with thick tarsal scopula. Genitalia (Fig. 171) with pair of obliquely-angled, handle-shaped spermathecae.

**Distribution and remarks.**—*Bungulla disrupta* has a moderately widespread but now highly fragmented distribution in the Avon Wheatbelt, western Mallee and eastern Jarrah Forest bioregions of south-western Australia, from Gillingarra and near Nembudding in the north, south to at least Lake Magenta (Fig. 172). A single female specimen from the Stirling Range National Park (Figs. 163–171), described above, is also tentatively assigned to this species, based on its abdominal coloration and distribution. Genetic data reveal that *B. disrupta* is likely closely related to *B. gibba*, together forming a deeply-divergent clade sister to all other *Bungulla* (Fig. 14). This relationship is further evidenced by the unusual morphology of the spermathecae (Fig. 171; cf. Fig. 207). Little is known of the biology of this species, other than that the known male specimens were collected wandering in search of females in autumn, winter and possibly early spring. The single, tentatively-assigned female specimen was unwittingly collected from the clay bank of a deep gully, while excavating a burrow of another mygalomorph.

***Bungulla ferraria*** Rix, Raven & Harvey, sp. nov.
http://zoobank.org/?lsid=urn:lsid:zoobank.org:act:7E7F242B-EF64-4967-92F2-A84D7CEB2DAC
(Figs. 12, 173–185)

**Type material.**—*Holotype male.* AUSTRALIA: *Western Australia*: Mount Gibson iron-ore mine, woodlands 1 (A), impact site (IBRA_AVW), 29°34′09″S, 117°10′36″E, wet pitfall trap, 30 April–11 May 2005, S. Thompson (WAM T72319).

*Paratype.* AUSTRALIA: *Western Australia*: 1 ♂, same data as holotype except Ironstone Slope, Mount Gibson, west facing, 29°35′36″S, 117°10′55″E, 31 May–11 June 2005 (WAM T72325).

**Other material examined.**—AUSTRALIA: *Western Australia*: 1 ♂, Mount Gibson Station, site 9 (IBRA_YAL), 29°41′13″S, 117°21′37″E, dry pitfall trap, 20–31 August 2001 (WAM T46011); 1 ♂, Mount Gibson Station, 93 km NE. of Wubin (IBRA_AVW), 29°48′02″S, 117°20′34″E, pitfall trap, 21–29 August 2001, K. Ottewell & R. Leys (SAM NN19643); 1 ♂, Regional Geraldton and Buller River, Ecologia Project 1102 (IBRA_GES), 28°38′36.61″S, 114°37′15.70″E, litter/soil sift, 10–14 July 2009, L. Roque-Albelo & S. White (WAM T97847); 1 ♂, Mount Jackson, site MJR5 (IBRA_COO), 30°15′S, 119°16′E, hand collected, 1 September 1979, R.A. How (WAM T16219).

**Etymology.**—The specific epithet is derived from the Latin 'ferrarius' (adjective: 'pertaining to iron'; see Brown 1956), in reference to the type locality of this species at the Mount Gibson iron-ore mine.

**Diagnosis.**—Males of *Bungulla ferraria* can be distinguished from all other known congeners with < 5 retrolateral spinules on the palpal tibia (Fig. 12) – except *B. bringo* and *B. riparia* – by the shape of the cymbial spinules, which are porrect, thorn-


Figures 163–171.—*Bungulla disrupta* sp. nov., tentatively assigned female (WAM T131634) from Stirling Range National Park, Talyuberlup Picnic Area (Western Australia: ESP): 163–164, carapace and abdomen, dorsal view; 165, cephalothorax, lateral view; 166, eyes, dorsal view; 167, mouthparts, ventral view; 168, cephalothorax, ventral view; 169, leg I, prolateral view; 170, leg I, retrolateral view; 171, spermatheeae, dorsal view. Scale bars = 2.0 mm (163–164, 169–170), 0.5 mm (171).

like, and cover most of the dorsal surface of the cymbium (Figs. 182–184) (spinules more curved, anteriorly-directed and restricted to distal half of cymbium in other species). *Bungulla ferraria* can be further distinguished from *B. bringo* by the absence of retrolateral spinules on the palpal tibia (Fig. 182; cf. Figs. 121, 122); and from *B. riparia* by the presence of only 1–3 prolateral (medial) spine-like setae on tibia I (Fig. 181; cf. Fig. 392), combined with the shape of the palpal tibia, which is relatively tapered distally, with a strongly concave disto-ventral margin in retrolateral view (Fig. 182; cf. Fig. 393). Females are unknown.

**Description (male holotype).**—Total length 10.6. Carapace 4.3 long, 3.3 wide. Abdomen 4.7 long, 2.9 wide. Carapace (Fig. 173) tan, with slightly darker pars cephalica and slightly darker ocular region; postero-lateral corners near abdomen each with marginal cluster of longer black setae; fovea straight. Eye group (Fig. 176) trapezoidal (anterior eye row strongly procurved), 0.8 x as long as wide, PLE–PLE/ALE–ALE ratio 1.6; ALE separated by their own diameter; AME

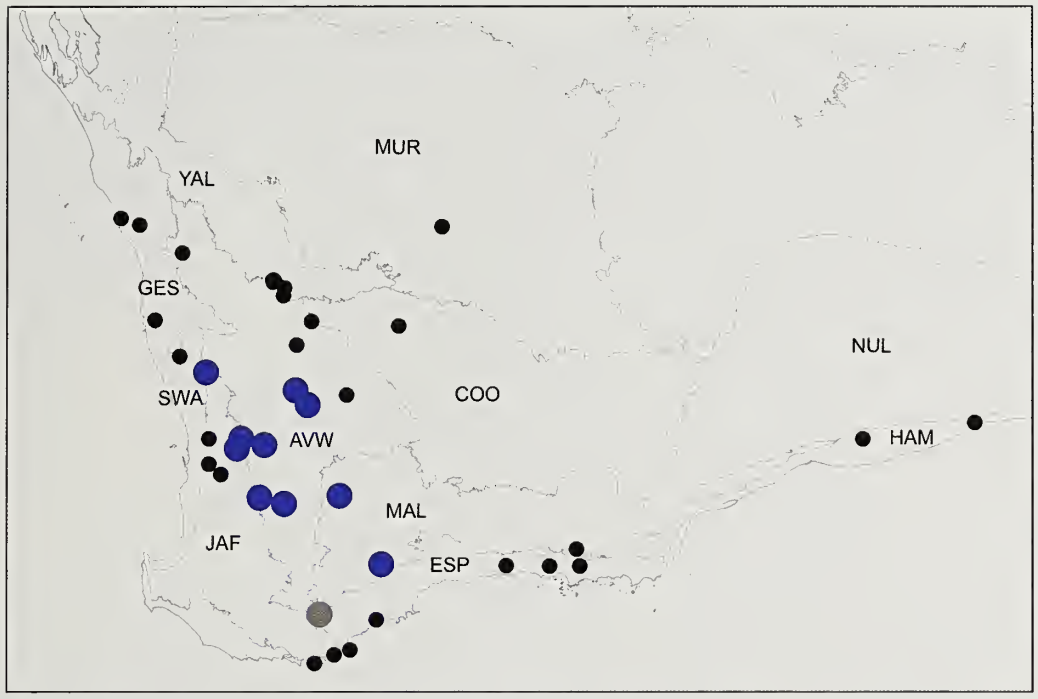


Figure 172.—Map showing collection records of *Bungulla disrupta* sp. nov. (large blue circles), relative to other taxa with < 5 retrolateral spinules on the male palpal tibia (see Fig. 12). The grey circle represents a tentatively assigned female specimen. Relevant IBRA 7.0 bioregional acronyms are as follows: AVW, Avon Wheatbelt; COO, Coolgardie; ESP, Esperance Plains; GES, Geraldton Sandplains; HAM, Hampton; JAF, Jarrah Forest; MAL, Mallee; MUR, Murchison; NUL, Nullarbor; SWA, Swan Coastal Plain; YAL, Yalgoo.

separated by less than their own diameter; PME separated by 3.1 x their own diameter; PME and PLE separated by diameter of PME, PME positioned in line with level of PLE. Maxillae with field of cuspules confined to inner corner (Fig. 177); labium without cuspules. Abdomen (Fig. 174) oval, dark grey in dorsal view with faint beige-tan mottling. Dorsal surface of abdomen (Fig. 174) with sparse arrangement of stiff, porrect black setae, each with slightly raised, dark brown sclerotic base; sclerotized sigilla absent. Legs (Figs. 180, 181) variable shades of tan, with light scopulae on tarsi I–II; tibia I spinose, without prolateral clasping spurs. Leg I: femur 4.7; patella 2.3; tibia 3.7; metatarsus 3.2; tarsus 2.4; total 16.3. Leg 1 femur–tarsus/carapace length ratio 3.8. Pedipalpal tibia (Figs. 182–184) 2.0 x longer than wide, without retrolateral spinules; RTA absent. Cymbium (Figs. 182–184) setose, with field of porrect, thorn-like spinules covering most of dorsal surface. Embolus (Figs. 182–184) as long as bulb, slightly curved, with unmodified tip; embolic apophysis absent.

**Distribution and remarks.**—*Bungulla ferraria* (formerly known by WAM identification code 'MYG149') has a disjunct distribution in the Avon Wheatbelt and Geraldton Sandplains bioregions of Western Australia, at Mount Gibson (near Lake Moore) and in the vicinity of Geraldton (Fig. 185). A single male specimen from Mount Jackson, in the northern Coolgardie bioregion, is also tentatively assigned to this species on the basis of its pedipalp and leg I morphology, however it is somewhat smaller than other specimens of *B. ferraria*, and the specimen is severely faded (see Supplementary File 1). Nothing is known of the biology of this species, other than that the known male specimens were collected wandering in search of females in late autumn and winter.

***Bungulla fusca*** Rix, Raven & Harvey, sp. nov.
http://zoobank.org/?lsid=urn:lsid:zoobank.org:act:27AA3A3D-0D19-4B7A-891A-5C6AA90EF13E
(Figs. 12, 186–198)

**Type material.**—*Holotype male*. AUSTRALIA: *Western Australia*: Junction of Neds Corner & Yerritup Roads, site GP 13 (IBRA_ESP), 33°43′21″S, 121°03′56″E, wet pitfall traps, 15 October 1999–26 November 2000, B. Durrant, CALM Survey (WAM T142947).

*Paratype*: 1 ♂, same data as holotype (WAM T142948).

**Other material examined.**—AUSTRALIA: *Western Australia*: 1 ♂, Backmans Road, nr Burdett Road junction, SE. of Mount Burdett, site ES 9 (IBRA_MAL), 33°29′05″S, 122°14′27″E, wet pitfall traps, 15 October 1999–1 November 2000, P. Van Heurck, CALM Survey (WAM T142946); 1 ♂, Brockway Road, Helms Arboretum Reserve, site ES 2 (IBRA_ESP), 33°43′42″S, 121°47′50″E, wet pitfall traps, 15 October 1999–1 November 2000, P. Van Heurck, CALM Survey (WAM T142949); 1 ♂, Coolinup Nature Reserve, east, site ES 11 (IBRA_ESP), 33°43′53″S, 122°17′50″E, wet pitfall traps, 15 October 1999–29 November 2000, P. Van Heurck, CALM Survey (WAM T142950).

**Etymology.**—The specific epithet is derived from the Latin 'fuscus' (adjective: 'dark', 'swarthy' or 'dusky'; see Brown 1956), in reference to the dark brown body coloration of this species.

**Diagnosis.**—Males of *Bungulla fusca* can be distinguished from all other known congeners with < 5 retrolateral spinules on the palpal tibia (Fig. 12) – except B. *disrupta*, *B. hillyerae*, *B. inermis*, *B. oraria* and *B. parva* – by the shape of the cymbial

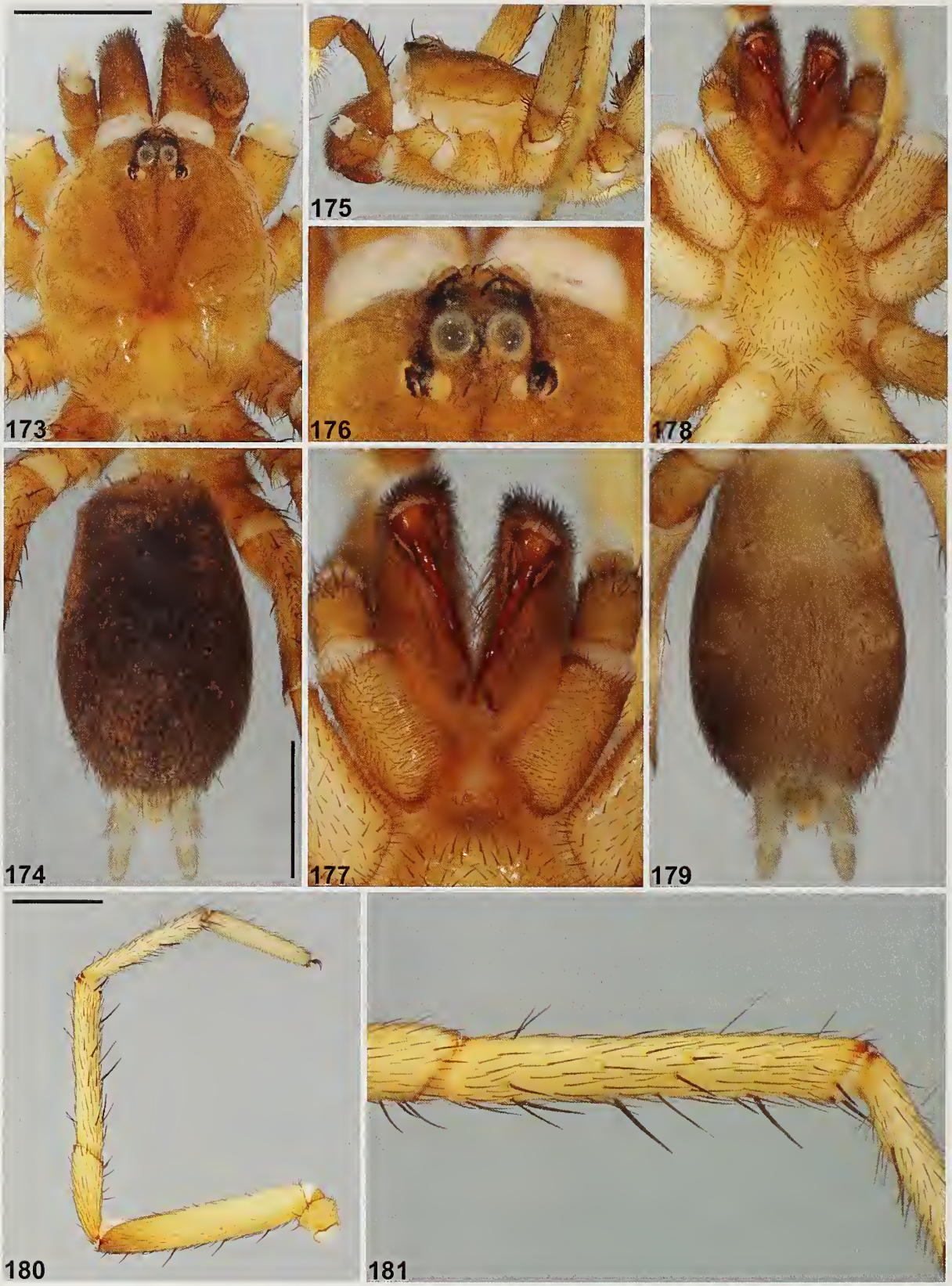


Figures 173–181.—*Bungulla ferraria* sp. nov., male holotype (WAM T72319) from Mount Gibson iron-ore mine (Western Australia; AVW), somatic morphology: 173–174, carapace and abdomen, dorsal view; 175, cephalothorax, lateral view; 176, eyes, dorsal view; 177, mouthparts, ventral view; 178–179, cephalothorax and abdomen, ventral view; 180, leg 1, prolateral view; 181, leg 1 tibia, prolateral view. Scale bars = 2.0 mm.


Figures 182–184.—*Bungulla ferraria* sp. nov., male holotype (WAM T72319) from Mount Gibson iron-ore mine (Western Australia; AVW), pedipalp: 182, retrolateral view; 183, retro-ventral view; 184, prolateral view. Scale bar = 2.0 mm.

spinules, which are curved, anteriorly-directed and restricted to the distal half of the cymbium (Figs. 195–197) (spinules are porrect, thorn-like, and cover most of the dorsal surface of the cymbium in other species). *Bungulla fusca* can be further distinguished from *B. parva* by its larger body size (carapace width $\geq$ 4.5) (Fig. 186; cf. Fig. 349); from *B. hillyerae* and *B. inermis* by the darker carapace coloration (depending on the state of preservation; see Supplementary File 1) (Fig. 186; cf.

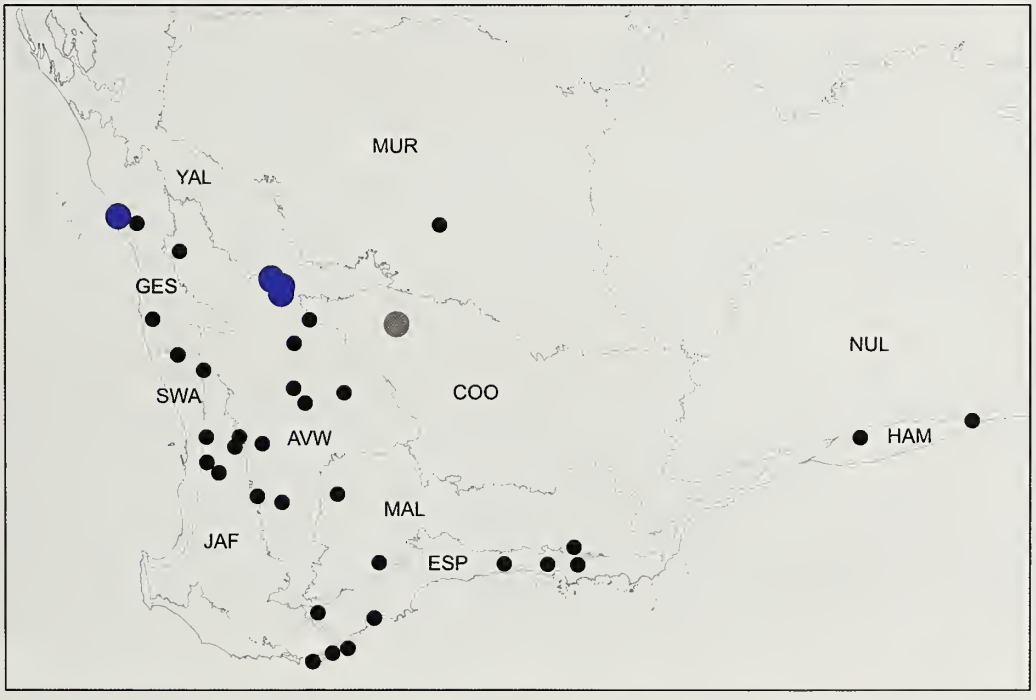


Figure 185.—Map showing collection records of *Bungulla ferraria* sp. nov. (large blue circles), relative to other taxa with < 5 retrolateral spinules on the male palpal tibia (see Fig. 12). The grey circle represents a tentatively assigned male specimen. Relevant IBRA 7.0 bioregional acronyms are as follows: AVW, Avon Wheatbelt; COO, Coolgardie; ESP, Esperance Plains; GES, Geraldton Sandplains; HAM, Hampton; JAF, Jarrah Forest; MAL, Mallee; MUR, Murchison; NUL, Nullarbor; SWA, Swan Coastal Plain; YAL, Yalgoo.

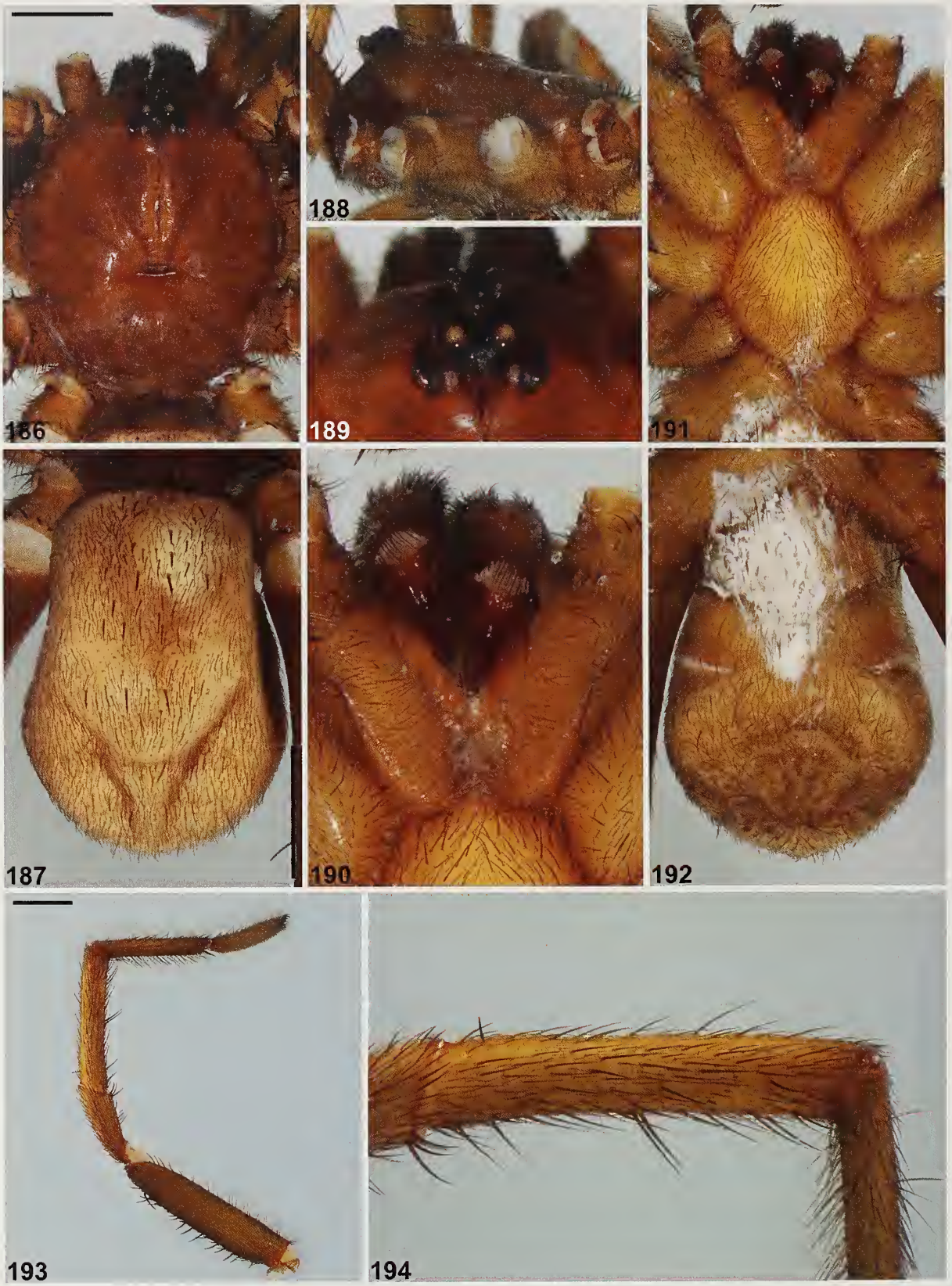


Figures 186–194.—*Bungulla fusca* sp. nov., male holotype (WAM T142947) from junction of Neds Corner and Yerritup Roads (Western Australia: ESP), somatic morphology: 186–187, carapace and abdomen, dorsal view; 188, cephalothorax, lateral view; 189, eyes, dorsal view; 190, mouthparts, ventral view; 191–192, cephalothorax and abdomen, ventral view; 193, leg I, prolateral view; 194, leg I tibia, prolateral view. Scale bars = 2.0 mm.


Figures 195–197.—*Bungulla fusca* sp. nov., male holotype (WAM T142947) from junction of Neds Corner and Yerritup Roads (Western Australia; ESP), pedipalp: 195, retrolateral view; 196, retro-ventral view; 197, prolateral view. Scale bar = 2.0 mm.

Figs. 232, 245); from *B. disrupta* by the presence of smaller, thinner chevrons on the dorsal abdomen (Fig. 187; cf. Fig. 152), combined with the presence of more uniformly-colored (i.e., not bi-colored) legs (Fig. 193; cf. Fig. 158); and from *B. oraria* by the shape of the palpal tibia, which is more bulbous in retrolateral view, with a less strongly concave disto-ventral margin (Fig. 195; cf. Fig. 345). Females are unknown.

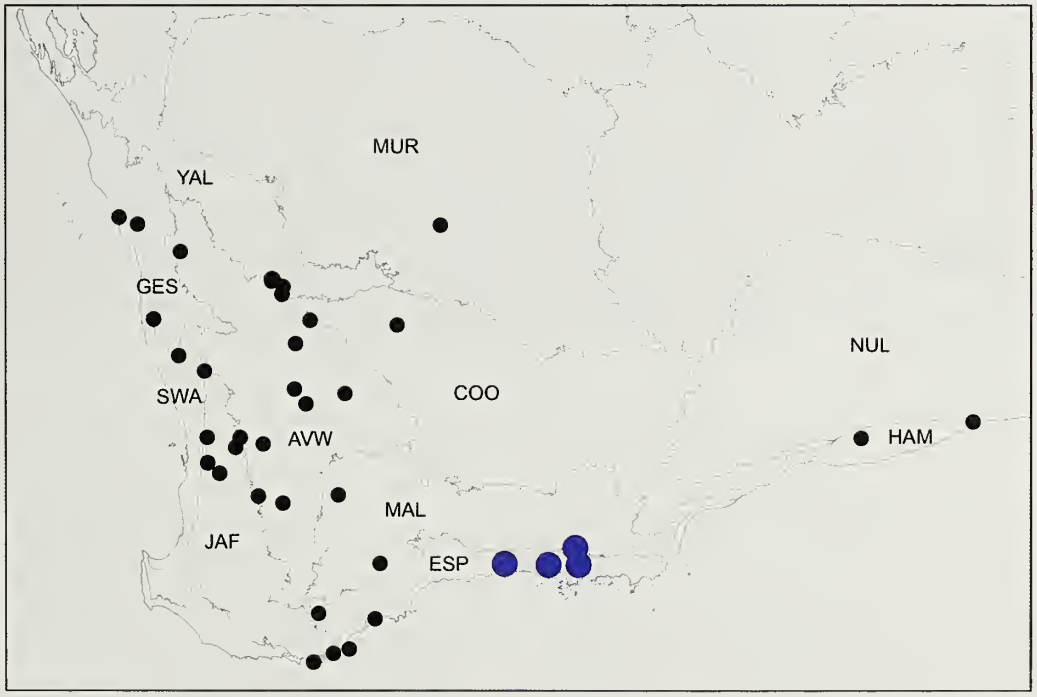


Figure 198.—Map showing collection records of *Bungulla fusca* sp. nov. (large blue circles), relative to other taxa with < 5 retrolateral spinules on the male palpal tibia (see Fig. 12). Relevant IBRA 7.0 bioregional acronyms are as follows: AVW, Avon Wheatbelt; COO, Coolgardie; ESP, Esperance Plains; GES, Geraldton Sandplains; HAM, Hampton; JAF, Jarrah Forest; MAL, Mallee; MUR, Murchison; NUL, Nullarbor; SWA, Swan Coastal Plain; YAL, Yalgoo.

**Description (male holotype).**—Total length 12.5. Carapace 6.2 long, 5.1 wide. Abdomen 5.7 long, 4.0 wide. Carapace (Fig. 186) dark chocolate-brown with black ocular region; fovea straight. Eye group (Fig. 189) trapezoidal (anterior eye row strongly procurved), 0.9 x as long as wide, PLE–PLE/ALE–ALE ratio 2.0; ALE separated by ca. half their own diameter; AME separated by less than their own diameter; PME separated by 3.4 x their own diameter; PME and PLE separated by diameter of PME, PME positioned in line with level of PLE. Maxillae slightly shrivelled, cuspules (if present) obscured (Fig. 190); labium without cuspules. Abdomen (Fig. 187) oval, beige-tan in dorsal view. Dorsal surface of abdomen (Fig. 187) with sparse arrangement of stiff, porrect black setae, each with slightly raised, dark brown sclerotic base; sclerotized sigilla absent. Legs (Figs. 193, 194) variable shades of tan, with light scopulae on tarsi I–II; tibia I largely aspinose, without prolateral clasping spurs. Leg I: femur 6.2; patella 3.1; tibia 4.8; metatarsus 4.1; tarsus 2.5; total 20.8. Leg I femur–tarsus/carapace length ratio 3.4. Pedipalpal tibia (Figs. 195–197) 2.0 x longer than wide, without retrolateral spinules; RTA absent. Cymbium (Figs. 195–197) setose, with field of curved, anteriorly-directed spine-like spinules restricted to distal half of segment. Embolus (Figs. 195–197) nearly twice length of bulb, slightly curved, with unmodified tip; embolic apophysis absent.

**Distribution and remarks.**—*Bungulla fusca* has a relatively restricted distribution in the Esperance Plains (Recherche) and south-eastern Mallee bioregions of southern Western Australia, from near Munglinup in the west, east to Coolinup Nature Reserve (Fig. 198). Nothing is known of the biology of this species.

***Bungulla gibba*** Rix, Raven & Harvey, sp. nov.
http://zoobank.org/?lsid=urn:lsid:zoobank.org:act:E98CF431-C9F1-448C-8FAC-1E328A576796
(Figs. 7–9, 14, 199–208)

**Type material.**—*Holotype female*. AUSTRALIA: *Western Australia*: Two Peoples Bay Nature Reserve, Little Beach, gully, site 15 (IBRA_JAF), 34°58′32″S, 118°12′00″E, hand collected in burrow, 30 November 2006, M.L. Moir & K.E.C. Brennan (WAM T78551$^{DNA_Voucher_95}$; GenB–COI–KY295287, GenB–CYB–KY295408, GenB–MRPL45–KY295531, GenB–RPF2–KY295652, GenB–XPNPEP3–KY295780, GenB–ITS–KY295033).

*Paratypes*. AUSTRALIA: *Western Australia*: 1 ♀, same data as holotype (WAM T78554); 1 ♀, same data (WAM T78553); 1 ♀, same data as holotype except 11 April 2017, M.G. Rix, M.S. Harvey, J.G. Cosgrove (WAM T143010).

**Other material examined.**—AUSTRALIA: *Western Australia*: 1 ♀, Bald Island (IBRA_ESP), 34°54′52″S, 118°27′37″E, edge of petrel burrow, 16 October 2003, S. Comer (WAM T58764); 1 juvenile, Mount Groper, in gully, site 5 (IBRA_ESP), 34°29′32″S, 118°53′30″E, hand collected in burrow, 25 October 2006, M.L. Moir & K.E.C. Brennan (WAM T78516$^{DNA_Voucher_282}$; GenB–COI–MG516839, GenB–CYB–MG516841, GenB–RPF2–MG516887, GenB–XPNPEP3–MG516892, GenB–ITS–MG516864).

**Etymology.**—The specific epithet is derived from the Latin 'gibbus' (adjective: 'humped', 'hump-backed' or 'protuberant'; see Brown 1956), in reference to the bulging, protuberant morphology of the fovea of this species.

**Diagnosis.**—*Bungulla gibba* is known from only six female specimens, for which sequence data are available (Fig. 14). It can be distinguished from the other two species known only from females – *B. bella* and *B. harrisonae* (and all other known species of *Bungulla*) – by the strongly efoveate carapace morphology (Figs. 7, 199, 201; cf. Figs. 76, 222).

**Description (female holotype).**—Total length 15.6. Carapace 5.6 long, 4.5 wide. Abdomen 7.4 long, 4.8 wide. Carapace (Fig. 199) chocolate-brown with slightly darker ocular region; fovea strongly everted into adpressed horn-like protrusion (Fig. 201). Eye group (Fig. 202) trapezoidal (anterior eye row strongly procurved), 0.7 x as long as wide, PLE–PLE/ALE–ALE ratio 1.7; ALE separated by their own diameter; AME separated by their own diameter; PME separated by 2.8 x their own diameter; PME and PLE separated by diameter of PME, PME positioned in line with level of PLE. Maxillae with field of cuspules confined to inner corner (Fig. 203); labium without cuspules. Abdomen (Fig. 200) oval, dark grey-brown in dorsal view with beige-grey mottling, two pairs of beige-grey sigilla spots, and three pairs of beige-grey chevrons posteriorly, each divided along midline; sclerotized sigilla absent. Legs (Figs. 205, 206) variable shades of tan; thick scopulae present on tarsi and metatarsi I–II; tibia I with distal cluster of 5 stout prolateral macrosetae, 3 retro-ventral spine-like macrosetae and 6 shorter retro-ventral macrosetae; metatarsus I with 2 stout pro-ventral macrosetae and 7 mostly longer retro-ventral macrosetae; tarsus I with distal cluster of 3 stout ventral macrosetae. Leg I: femur 3.2; patella 2.2; tibia 1.8 metatarsus 1.4; tarsus 1.2; total 9.8. Leg 1 femur–tarsus/carapace length ratio 1.8. Pedipalp tan, spinose on tibia and tarsus, with thick tarsal scopula. Genitalia (Fig. 207) with pair of obliquely-angled, handle-shaped spermathecae.

**Distribution and remarks.**—*Bungulla gibba* is known from only three locations along the southern coastline of Western Australia, at Little Beach (Two Peoples Bay Nature Reserve), Bald Island and Mount Groper (Fig. 208). Genetic data reveal that *B. gibba* is likely closely related to *B. disrupta*, together forming a deeply-divergent clade sister to all other *Bungulla* (Fig. 14). This relationship is further evidenced by the unusual morphology of the spermathecae (Fig. 207; cf. Fig. 171). A female with an egg sac was collected in late November, and at Little Beach burrows are built in the sandy banks of a coastal gully, with a burrow entrance morphology similar to that of *B. harrisonae* (Figs. 8, 9; cf. Figs. 5, 6). All sites at which *B. gibba* has been found are within 1 km of the Southern Ocean coastline, suggesting that the preferred habitat may be coastal, sandy gullies. It is unknown why this species has evolved an 'efoveate' carapace morphology, although analogous modifications are found in species of *Eucyrtops* and *Idiosoma*, including an undescribed *Eucyrtops* species closely sympatric or parapatric with *B. gibba* at Two Peoples Bay Nature Reserve and Bald Island.

***Bungulla hamelinensis*** Rix, Raven & Harvey, sp. nov.
http://zoobank.org/?lsid=urn:lsid:zoobank.org:act:35057156-

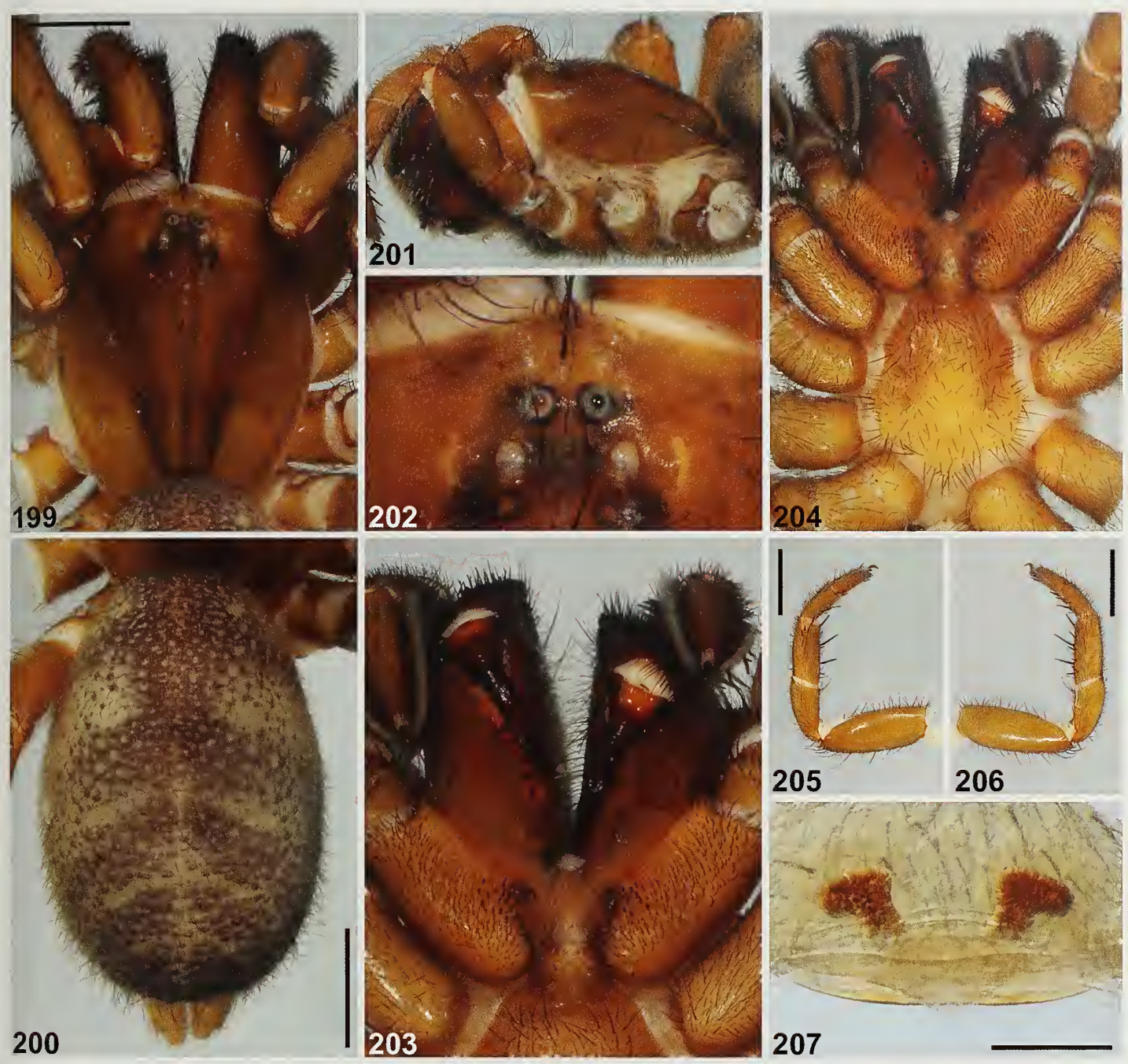


Figures 199–207.—*Bungulla gibba* sp. nov., female holotype (WAM T78551) from Two Peoples Bay Nature Reserve, Little Beach (Western Australia; JAF): 199–200, carapace and abdomen, dorsal view; 201, cephalothorax, lateral view; 202, eyes, dorsal view; 203, mouthparts, ventral view; 204, cephalothorax, ventral view; 205, leg I, prolateral view; 206, leg I, retrolateral view; 207, spermatheeae, dorsal view. Scale bars = 2.0 mm (199–200, 205–206), 0.5 mm (207).

2279-4AD1-8659-495F74E302D2
(Figs. 13, 209–221)

**Type material.**—*Holotype male*. AUSTRALIA: *Western Australia*: Nanga Station, site NA1 (IBRA_CAR), 26°28′40.2″S, 114°04′33.6″E, wet pitfall trap, 11 May–30 August 1995, N. Hall, WAM/CALM Carnarvon Survey (WAM T98562).

*Paratypes*. AUSTRALIA: *Western Australia*: 4 ♂, same data (WAM T98563).

**Etymology.**—The specific epithet is a reference to the type locality of this species, near Hamelin Pool (Western Australia).

**Diagnosis.**—Males of *Bungulla hamelinensis* can be distinguished from all other known congeners with > 10 retrolateral spinules on the palpal tibia (Fig. 13) – except *B. banksia*, *B. bertmaini*, *B. bidgemia*, *B. iota*, *B. laevigata*, *B. quobba*, *B. weld* and *B. yeni* – by the shape of the proximal half of the palpal tibia, which is without a pronounced ventral bulge (Fig. 218), combined with the absence of a medial 'ledge' on the palpal

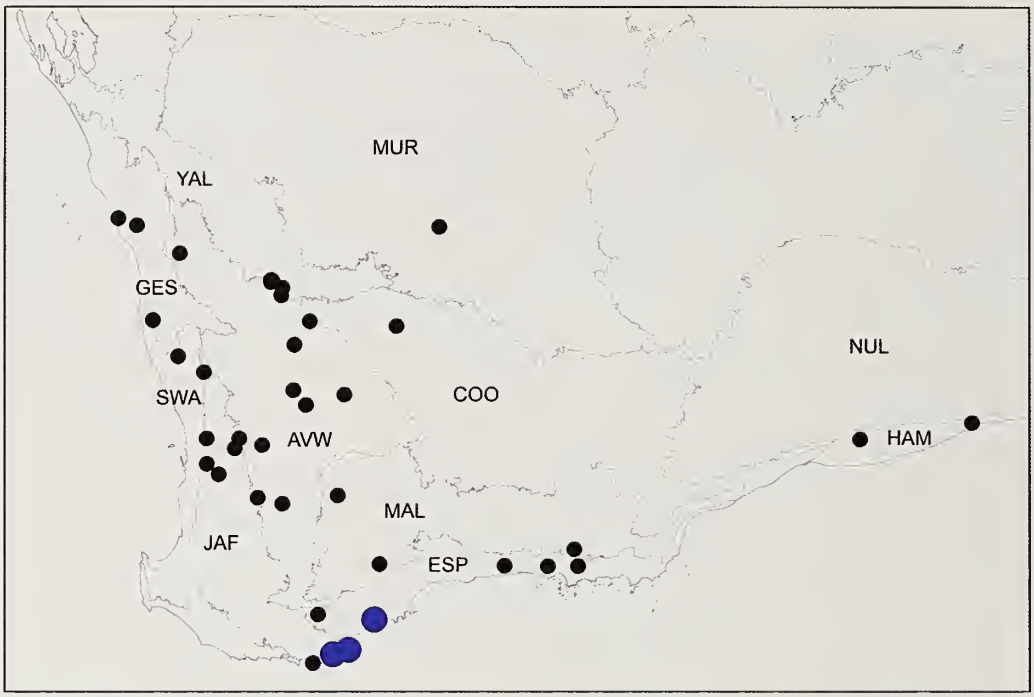


Figure 208.—Map showing collection records of *Bungulla gibba* sp. nov. (large blue circles), relative to other taxa with < 5 retrolateral spinules on the male palpal tibia (see Fig. 12). Relevant IBRA 7.0 bioregional acronyms are as follows: AVW, Avon Wheatbelt; COO, Coolgardie; ESP, Esperance Plains; GES, Geraldton Sandplains; HAM, Hampton; JAF, Jarrah Forest; MAL, Mallee; MUR, Murchison; NUL, Nullarbor; SWA, Swan Coastal Plain; YAL, Yalgoo.

tibia (Figs. 218, 219) (palpal tibia is with a ledge or bulges ventrally in other species). *Bungulla hamelinensis* can be further distinguished from *B. banksia* by the larger field of retrolateral spinules on the palpal tibia (Fig. 218; cf. Fig. 72); from *B. bertmaini*, *B. laevigata* and *B. quobba* by the shape of the embolus, which is relatively short (i.e., ~as long as bulb) (Fig. 218; cf. Figs. 24, 319, 371); and from *B. bidgemia*, *B. iota*, *B. weld* and *B. yeni* by the morphology of the cymbial spinules, which are thinner with a more filiform morphology (Figs. 218–220; cf. Figs. 95, 267, 419, 445). Females are unknown.

**Description (male holotype).**—Total length 6.7. Carapace 2.3 long, 2.0 wide. Abdomen 3.6 long, 2.1 wide. Carapace (Fig. 209) tan, with darker pars cephalica and slightly darker ocular region; fovea straight. Eye group (Fig. 212) trapezoidal (anterior eye row strongly procurved), 0.9 x as long as wide, PLE–PLE/ALE–ALE ratio 1.3; ALE separated by ca. half their own diameter; AME separated by less than their own diameter; PME separated by 3.0 x their own diameter; PME and PLE separated by diameter of PME, PME positioned in line with level of PLE. Maxillae with field of cuspules confined to inner corner (Fig. 213); labium without cuspules. Abdomen (Fig. 210) elongate-oval, damaged, faded beige in dorsal view. Dorsal surface of abdomen (Fig. 210) with sparse arrangement of stiff, porrect black setae, each with slightly raised, dark brown sclerotic base; sclerotized sigilla absent. Legs (Figs. 216, 217) variable shades of tan, with light scopulae on semi-incrassate tarsi I–II; tibia I spinose, without prolateral clasping spurs. Leg I: femur 2.8; patella 1.2; tibia 2.2; metatarsus 1.9; tarsus 1.5; total 9.6. Leg I femur–tarsus/carapace length ratio 4.2. Pedipalpal tibia (Figs. 218–220) 2.0 x longer than wide; field of retrolateral spinules large and asymmetrically crescent-shaped ('wave-shaped') in retrolateral view, positioned medially–distally (along most of retro-ventral margin), consisting of ca. 45 spinules of largely similar length; RTA absent. Cymbium (Figs. 218–220) setose, with field of slightly curved and relatively poorly developed (almost filiform) spinules covering most of dorsal surface. Embolus (Figs. 218–220) as long as bulb, slightly curved, with unmodified tip; embolic apophysis absent.

**Distribution and remarks.**—*Bungulla hamelinensis* (formerly known by WAM identification code 'MYG140') is a rare, highly restricted and extremely small species known only from Nanga Station, in the far southern Carnarvon (Wooramel) bioregion of Western Australia (Fig. 221). The type and only known locality of this species is situated on an unusual, near-tidal sandplain at the far southern tip of the Hamelin Pool Marine Reserve, 13 km south-west of Hamelin Pool. This site is also home to the similarly restricted species *B. laevigata*. Nothing else is known of the biology of *B. hamelinensis*, other than that the known male specimens were collected wandering in search of females in winter or possibly late autumn.

***Bungulla harrisonae*** Rix, Raven & Harvey, sp. nov.
http://zoobank.org/?lsid=urn:lsid:zoobank.org:act:F63F9B16-7E37-4C94-BF20-8B0F21E2AC15
(Figs. 5, 6, 14, 222–231)

**Type material.**—*Holotype female*. AUSTRALIA: *Western Australia*: John Forrest National Park, off Park Road, N. of Great Eastern Highway (IBRA_JAF), 31°53′54″S, 116°05′49″E, dug from burrow in jarrah forest, 231 m, 11 February 2013, S.E. Harrison & M.G. Rix (WAM T129257$^{DNA_Voucher_EC}$; GenB–COI–KY295236, GenB–

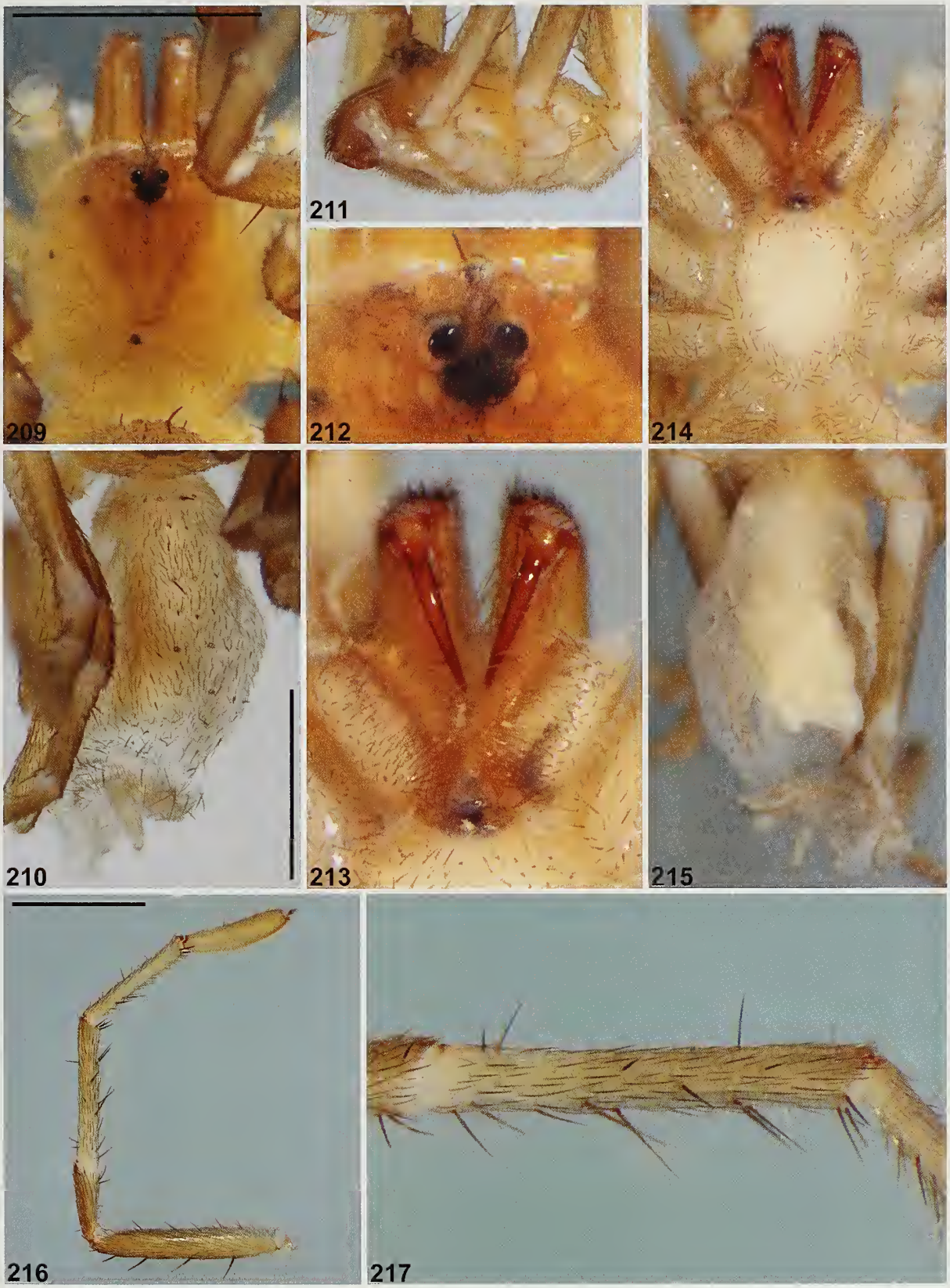


Figures 209–217.—*Bungulla hamelinensis* sp. nov., male holotype (WAM T98562) from Nanga Station (Western Australia; CAR), somatic morphology: 209–210, carapace and abdomen, dorsal view; 211, cephalothorax, lateral view; 212, eyes, dorsal view; 213, mouthparts, ventral view; 214–215, cephalothorax and abdomen, ventral view; 216, leg I, prolateral view; 217, leg I tibia, prolateral view. Scale bars = 2.0 mm.

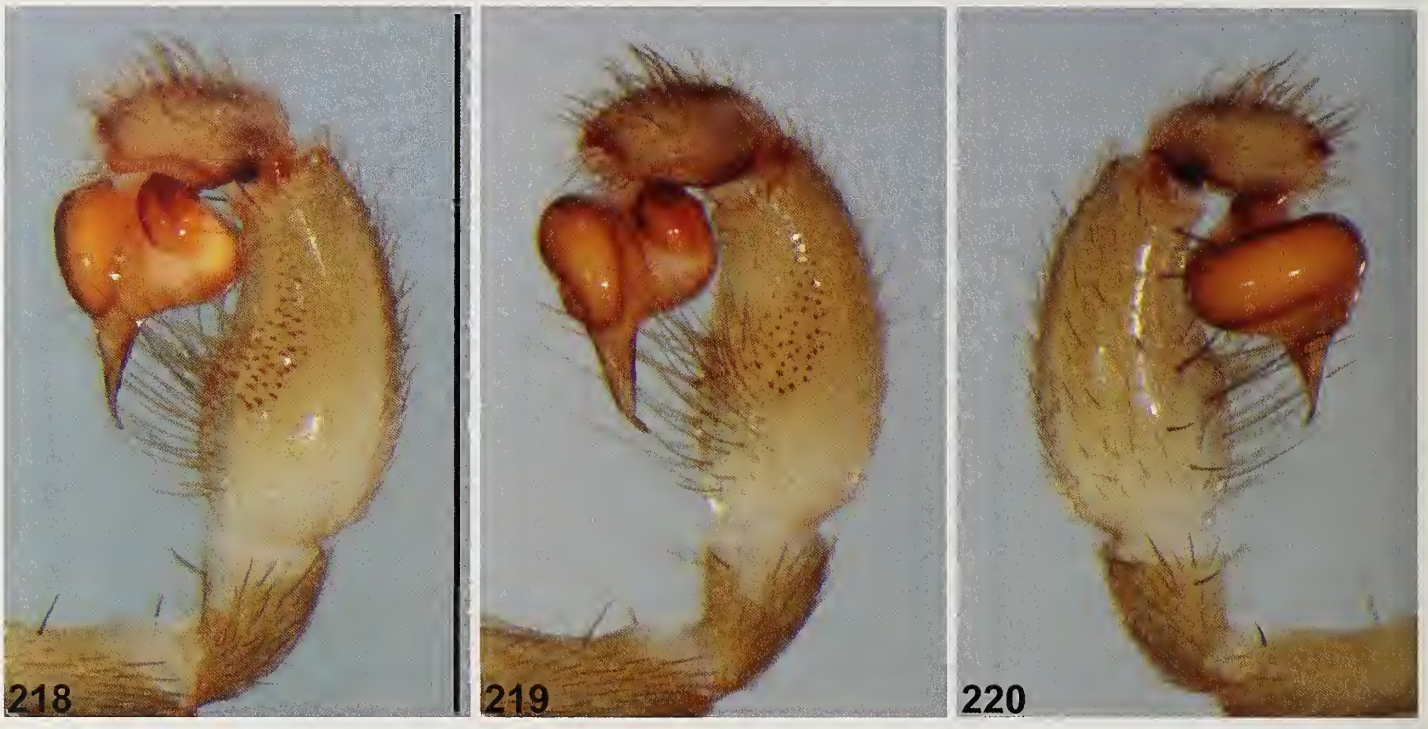


Figures 218–220.—*Bungulla hamelinensis* sp. nov., male holotype (WAM T98562) from Nanga Station (Western Australia; CAR), pedipalp: 218, retrolateral view; 219, retro-ventral view; 220, prolateral view. Scale bar = 2.0 mm.

MRPL45–KY295483, GenB–RPF2–KY295602, GenB–XPNPEP3–KY295730, GenB–ITS–KY294982).

**Etymology.**—This species is named in honor of Sophie Harrison, in recognition of her contributions to idiopid systematics, especially the taxonomy of *Blakistonia* Hogg, 1902, and for discovering the holotype and only known specimen of this species.

**Diagnosis.**—*Bungulla harrisonae* is known from only a single female specimen, for which sequence data are available (Fig. 14). It can be distinguished from the other two species known

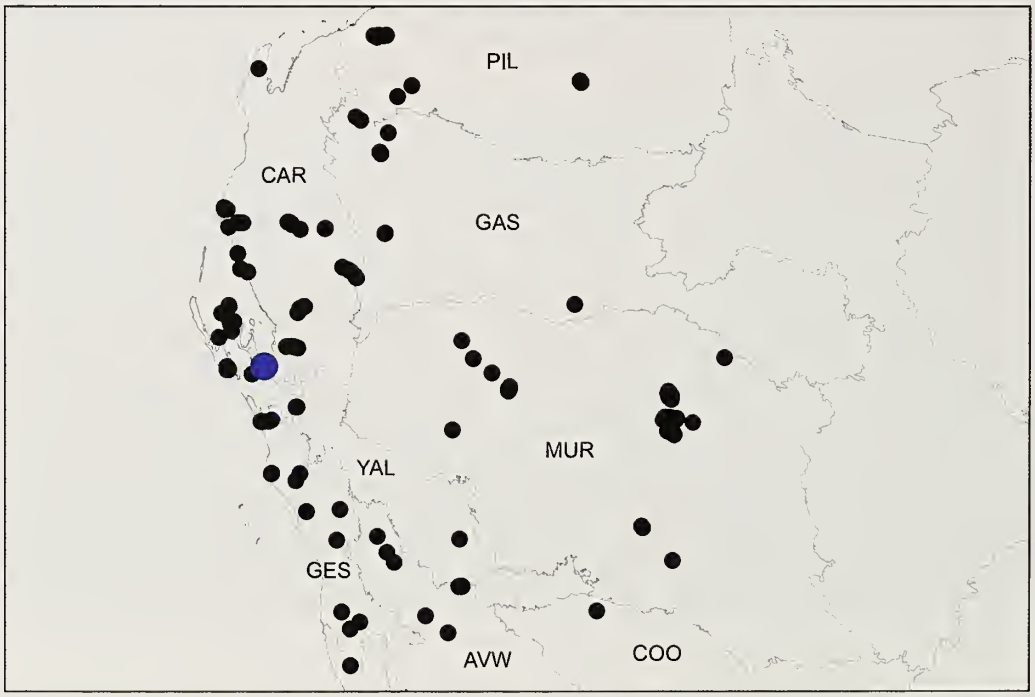


Figure 221.—Map showing collection records of *Bungulla hamelinensis* sp. nov. (large blue circles), relative to other taxa with > 10 retrolateral spinules on the male palpal tibia (see Fig. 13). Relevant IBRA 7.0 bioregional acronyms are as follows: AVW, Avon Wheatbelt; CAR, Carnarvon; COO, Coolgardie; GAS, Gascoyne; GES, Geraldton Sandplains; MUR, Murchison; PIL, Pilbara; YAL, Yalgoo.

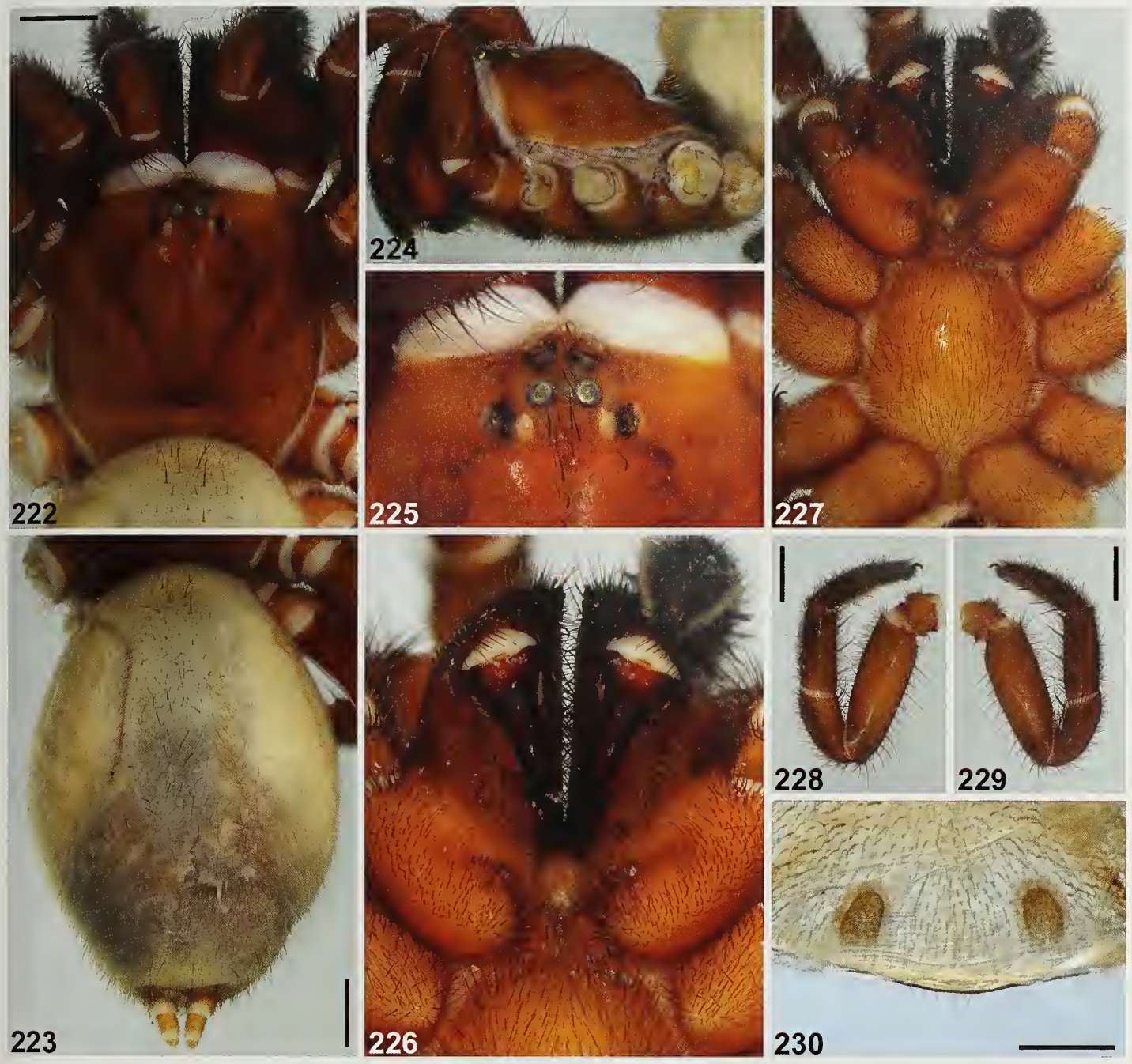


Figures 222–230.—*Bungulla harrisonae* sp. nov., female holotype (WAM T129257) from John Forrest National Park (Western Australia; JAF): 222–223, carapace and abdomen, dorsal view; 224, cephalothorax, lateral view; 225, eyes, dorsal view; 226, mouthparts, ventral view; 227, cephalothorax, ventral view; 228, leg I, prolateral view; 229, leg I, retrolateral view; 230, spermatheeae, dorsal view. Scale bars = 2.0 mm (222–223, 228–229), 0.5 mm (230).

only from females – *B. bella* and *B. gibba* – by the relatively uniform coloration of the dorsal abdomen (Fig. 223) (cf. *B. bella*; Fig. 77) and the unmodified morphology of the fovea (Fig. 222) (cf. *B. gibba*; Fig. 199). While it is possible that *B. harrisonae* may be conspecific with a species here described separately from male specimens, we consider this highly unlikely given the size, coloration and morphology of those few congeners known from the vicinity of the type locality.

**Description (female holotype).**—Total length 24.1. Carapace 7.6 long, 6.9 wide. Abdomen 13.2 long, 9.3 wide. Carapace (Fig. 222) chocolate-brown with slightly darker ocular region; fovea strongly procurved. Eye group (Fig. 225) trapezoidal (anterior eye row strongly procurved), 0.7 x as long as wide, PLE–PLE/ALE–ALE ratio 2.0; ALE separated by ca. half their own diameter; AME separated by nearly their own diameter; PME separated by 3.6 x their own diameter; PME and PLE separated by diameter of PME, PME positioned in line with level of PLE. Maxillae with field of cuspules confined to inner corner (Fig. 226); labium without cuspules. Abdomen (Fig. 223) oval, slightly damaged, beige and grey in dorsal

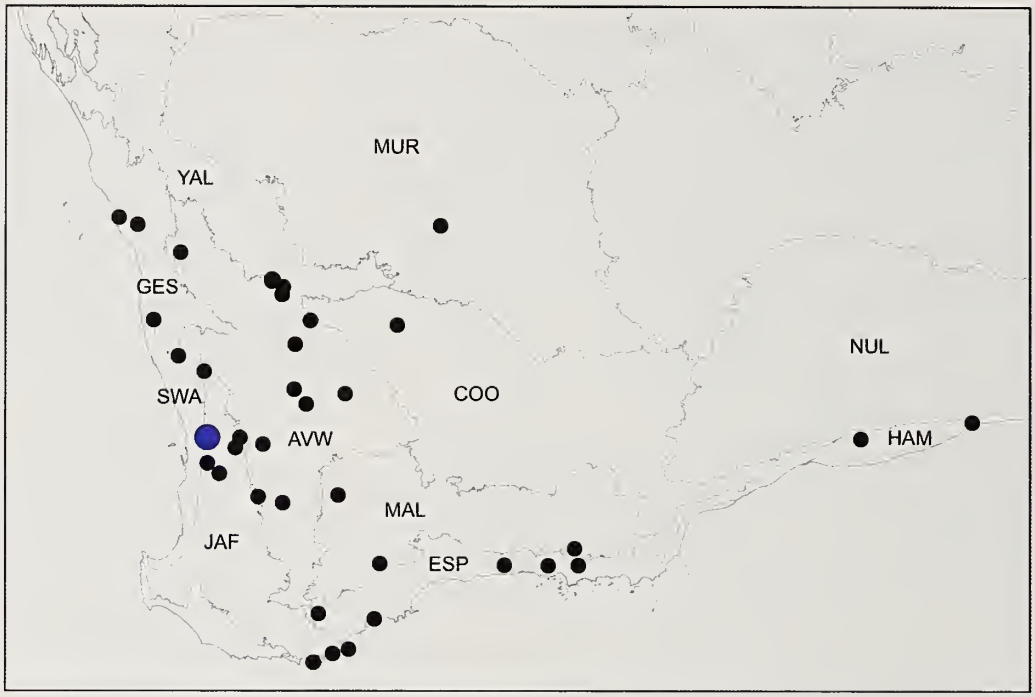


Figure 231.—Map showing collection records of *Bungulla harrisonae* sp. nov. (large blue circle), relative to other taxa with < 5 retrolateral spinules on the male palpal tibia (see Fig. 12). Relevant IBRA 7.0 bioregional acronyms are as follows: AVW, Avon Wheatbelt; COO, Coolgardie; ESP, Esperance Plains; GES, Geraldton Sandplains; HAM, Hampton; JAF, Jarrah Forest; MAL, Mallee; MUR, Murchison; NUL, Nullarbor; SWA, Swan Coastal Plain; YAL, Yalgoo.

view; sclerotized sigilla absent. Legs (Figs. 228, 229) variable shades of dark tan; thick scopulae present on tarsi and metatarsi I–II; tibia I with 5 stout prolateral macrosetae and 4 retro-ventral spine-like macrosetae; metatarsus I with 3 stout pro-ventral macrosetae and 3 longer retro-ventral macrosetae; tarsus I with distal cluster of 5 stout ventral macrosetae. Leg I: femur 5.2; patella 3.3; tibia 3.0; metatarsus 2.4; tarsus 1.8; total 15.8. Leg I femur–tarsus/carapace length ratio 2.1. Pedipalp dark tan, spinose on tibia and tarsus, with thick tarsal scopula. Genitalia (Fig. 230) with pair of short, widely spaced, bud-shaped spermathecae.

**Distribution and remarks.**—*Bungulla harrisonae* is an extremely rare species known only from John Forrest National Park, in the northern jarrah forest due east of Perth (Fig. 231). Genetic data reveal that *B. harrisonae* is closely related to *B. bella* (Fig. 14), the latter found much further inland in the vicinity of Mount Richardson (Fig. 85). Little is known of the biology of this species, other than the unusual morphology of the burrow, the latter of which consists of a highly camouflaged, convex lid with a broadly flanged lower 'lip' around the burrow entrance (Figs. 5, 6).

***Bungulla lillyerae*** Rix, Raven & Harvey, sp. nov.
http://zoobank.org/?lsid=urn:lsid:zoobank.org:act:738C1B6C-8C8B-4AD9-AF7A-6AF2C203A8F7
(Figs. 4, 12, 232–244)

**Type material.**—*Holotype male.* AUSTRALIA: *Western Australia*: Madura Caravan Park, Roe Plain (IBRA_HAM), 31°54′02″S, 127°01′14″E, running on ground at night, 11 September 2017, M.J. Hillyer (WAM T144352).

**Other material examined.**—AUSTRALIA: *Western Australia*: 1 ♂, Eucla Campsite (IBRA_HAM), 31°40′S, 128°53′E, A.R. Main (WAM T142983).

**Etymology.**—This species is named in honor of Mia Hillyer, in recognition of her contributions to molecular systematics, and for discovering the holotype specimen of this species.

**Diagnosis.**—Males of *Bungulla hillyerae* can be distinguished from all other known congeners with < 5 retrolateral spinules on the palpal tibia (Fig. 12) – except *B. disrupta*, *B. fusca*, *B. inermis*, *B. oraria* and *B. parva* – by the shape of the cymbial spinules, which are curved, anteriorly-directed and restricted to the distal half of the cymbium (Figs. 241–243) (spinules are porrect, thorn-like, and cover most of the dorsal surface of the cymbium in other species). *Bungulla hillyerae* can be further distinguished from *B. parva* by its larger body size (carapace width > 4.0) (Fig. 232; cf. Fig. 349); from *B. disrupta*, *B. fusca* and *B. oraria* by the lighter carapace coloration (depending on the state of preservation; see Supplementary File 1) (Fig. 232; cf. Figs. 151, 186, 336); and from *B. inermis* by the presence of a row of small macrosetae on the prolateral tarsus I (Fig. 239; cf. Fig. 252), and by the almost contiguous ALE (Fig. 235; cf. Fig. 248). Females are unknown.

**Description (male holotype).**—Total length 12.2. Carapace 5.7 long, 5.2 wide. Abdomen 5.4 long, 3.7 wide. Carapace (Fig. 232) dark mottled tan, with darker brown pars cephalica, dark brown lyre-like pattern on pars cephalica, dark grey lateral rims and black ocular region (carapace brown-black and dark maroon-brown in life; Fig. 4); fovea straight. Eye group (Fig. 235) trapezoidal (anterior eye row strongly procurved), 0.8 x as long as wide, PLE–PLE/ALE–ALE ratio 1.8; ALE almost contiguous; AME separated by less than their own diameter;

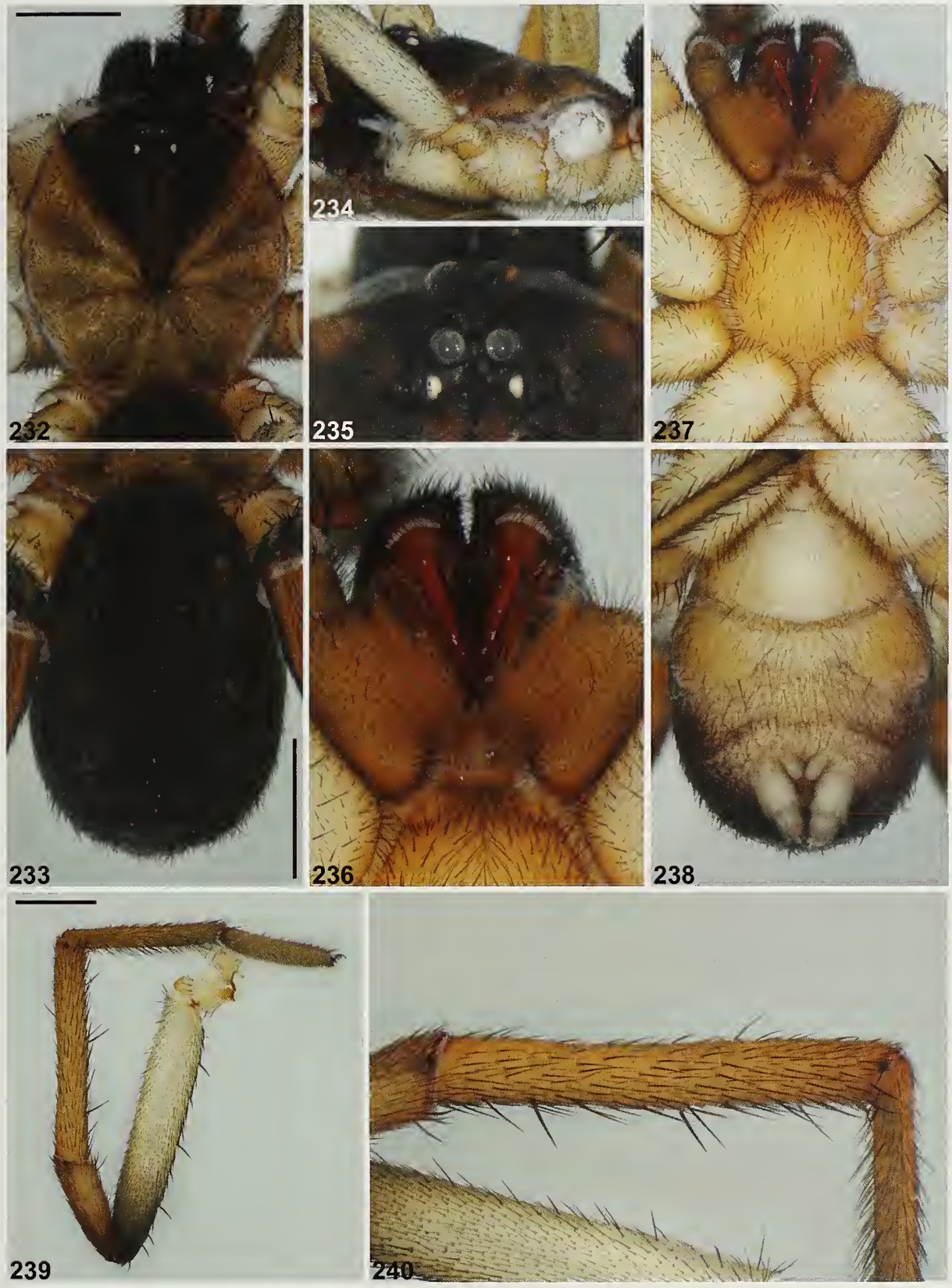


Figures 232–240.—*Bungulla hillyerae* sp. nov., male holotype (WAM T144352) from Madura Caravan Park (Western Australia; HAM), somatic morphology: 232–233, carapace and abdomen, dorsal view; 234, cephalothorax, lateral view; 235, eyes, dorsal view; 236, mouthparts, ventral view; 237–238, cephalothorax and abdomen, ventral view; 239, leg I, prolateral view; 240, leg I tibia, prolateral view. Scale bars = 2.0 mm.


Figures 241–243.—*Bungulla lillyerae* sp. nov., male holotype (WAM T144352) from Madura Caravan Park (Western Australia; HAM), pedipalp: 241, retrolateral view; 242, retro-ventral view; 243, prolateral view. Scale bar = 2.0 mm.

PME separated by 3.0 x their own diameter; PME and PLE separated by diameter of PME, PME positioned in line with level of PLE. Maxillae with field of cuspules confined to inner corner (Fig. 236); labium without cuspules. Abdomen (Fig. 233) oval, dark charcoal-black in dorsal view with beige mottling (as in life; Fig. 4), two pairs of tan sigilla spots and two pairs of faint beige chevrons posteriorly, each divided along midline. Dorsal surface of abdomen (Fig. 233) with

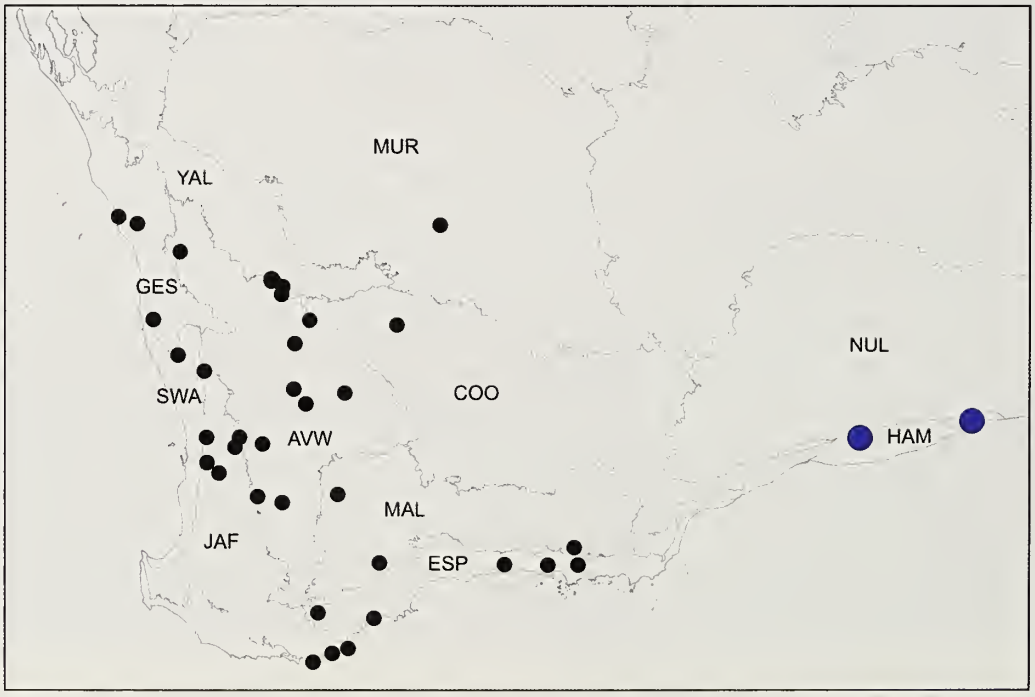


Figure 244.—Map showing collection records of *Bungulla lillyerae* sp. nov. (large blue circles), relative to other taxa with < 5 retrolateral spinules on the male palpal tibia (see Fig. 12). Relevant IBRA 7.0 bioregional acronyms are as follows: AVW, Avon Wheatbelt; COO, Coolgardie; ESP, Esperance Plains; GES, Geraldton Sandplains; HAM, Hampton; JAF, Jarrah Forest; MAL, Mallee; MUR, Murchison; NUL, Nullarbor; SWA, Swan Coastal Plain; YAL, Yalgoo.

sparse arrangement of stiff, porrect black setae, each with slightly raised, dark brown sclerotic base; sclerotized sigilla absent. Legs (Figs. 239, 240) variable shades of tan, with lighter femora and light scopulae on tarsi I–II; tibia I largely aspinose, without prolateral clasping spurs. Leg I: femur 6.6; patella 3.1; tibia 5.3; metatarsus 4.1; tarsus 2.8; total 21.9. Leg I femur–tarsus/carapace length ratio 3.8. Pedipalpal tibia (Figs. 241–243) 2.0 x longer than wide, without retrolateral spinules; RTA absent. Cymbium (Figs. 241–243) setose, with field of curved, anteriorly-directed spine-like spinules restricted to distal half of segment. Embolus (Figs. 241–243) slightly longer than bulb, slightly curved, with unmodified tip; embolic apophysis absent.

**Distribution and remarks.**—*Bungulla hillyerae* is known from only two locations in the Hampton bioregion of south-eastern Western Australia, at Eucla (near the Western Australian/South Australian border), and on the Roe Plain at Madura (Fig. 244). However, the precise collection locality of the Eucla specimen is unknown given the municipal changes that have occurred in the Eucla region since the dismantling of the Old Telegraph Station in the 1950s. Nothing is known of the biology of this species, other than that the holotype male specimen was collected wandering in search of females in mid-September (Fig. 4).

***Bungulla inermis*** Rix, Raven & Harvey, sp. nov.
http://zoobank.org/?lsid=urn:lsid:zoobank.org:act:E878F99E-34B2-4402-8F4B-63AB049D43D8
(Figs. 12, 245–257)

**Type material.**—*Holotype male*. AUSTRALIA: *Western Australia*: 2 km N. of Bunce Bin, N. of Beacon [ca. junction of Bimbijy & Stone Roads] (IBRA_AVW), 30°11′S, 117°49′E, 28 June–26 July 1985, B.Y. Main (WAM T142953).

**Other material examined.**—AUSTRALIA: *Western Australia*: 1 ♂, Lake Mollerin, west, site BE 10 (IBRA_AVW), 30°31′41″S, 117°33′54″E, wet pitfall traps, 15 September 1998–25 October 1999, P. Van Heurck, CALM Survey (WAM T142952); 1 ♂, Mount Gibson iron-ore mine, Banded Ironstone Range, Extension Hill, west facing (IBRA_AVW), 29°34′33″S, 117°09′38″E, wet pitfall trap, 30 April–11 May 2005, S. Thompson (WAM T71639); 1 ♂, same data except Iron Hill, west facing, 29°36′13″S, 117°10′17″E (WAM T72318); 1 ♂, same data except woodlands 3 (C), impact site, 29°34′38″S, 117°11′19″E, 30 April–11 May 2005 (WAM T71638); 1 ♂, Talgomine Reserve (south), N. of Merredin, site MN 11 (IBRA_AVW), 31°15′24″S, 118°23′46″E, wet pitfall traps, 15 December 1997–22 September 1998, N. Guthrie, CALM Survey (WAM T142951).

**Etymology.**—The specific epithet is derived from the Latin 'inermis' (adjective: 'unarmed', 'defenseless' or 'toothless'; see Brown 1956), in reference to the smooth morphology of the male palpal tibia, which is devoid of spinules.

**Diagnosis.**—Males of *Bungulla inermis* can be distinguished from all other known congeners with < 5 retrolateral spinules on the palpal tibia (Fig. 12) – except *B. disrupta*, *B. fusca*, *B. hillyerae*, *B. oraria* and *B. parva* – by the shape of the cymbial spinules, which are curved, anteriorly-directed and restricted to the distal half of the cymbium (Figs. 254–256) (spinules are porrect, thorn-like, and cover most of the dorsal surface of the cymbium in other species). *Bungulla inermis* can be further distinguished from *B. parva* by its larger body size (carapace width > 3.0) (Fig. 245; cf. Fig. 349); from *B. disrupta*, *B. fusca* and *B. oraria* by the lighter carapace coloration (depending on the state of preservation; see Supplementary File 1) (Figs. 245; cf. Figs. 151, 186, 336); and from *B. hillyerae* by the absence of a row of small macrosetae on the prolateral tarsus I (Fig. 252; cf. Fig. 239), and by the more widely separated ALE (Fig. 248; cf. Fig. 235). Females are unknown.

**Description (male holotype).**—Total length 13.2. Carapace 5.3 long, 4.3 wide. Abdomen 6.2 long, 3.2 wide. Carapace (Fig. 245) tan, with slightly darker pars cephalica, darker brown lyre-like pattern on pars cephalica and mostly black ocular region; fovea straight. Eye group (Fig. 248) trapezoidal (anterior eye row strongly procurved), 0.9 x as long as wide, PLE–PLE/ALE–ALE ratio 1.5; ALE separated by their own diameter; AME separated by less than their own diameter; PME separated by 3.0 x their own diameter; PME and PLE separated by slightly less than diameter of PME, PME positioned in line with level of PLE. Maxillae and labium without cuspules (Fig. 249). Abdomen (Fig. 246) oval, slightly damaged, dark grey in dorsal view. Dorsal surface of abdomen (Fig. 246) with sparse arrangement of stiff, porrect black setae, each with slightly raised, dark brown sclerotic base; sclerotized sigilla absent. Legs (Figs. 252, 253) variable shades of tan, with light scopulae on tarsi I–II; tibia I largely aspinose, without prolateral clasping spurs. Leg I: femur 5.7; patella 2.5; tibia 4.5; metatarsus 4.3; tarsus 2.8; total 19.8. Leg I femur–tarsus/carapace length ratio 3.7. Pedipalpal tibia (Figs. 254–256) 2.0 x longer than wide, without retrolateral spinules; RTA absent. Cymbium (Figs. 254–256) setose, with field of curved, anteriorly-directed spine-like spinules restricted to distal half of segment. Embolus (Figs. 254–256) ca. 1.5 x length of bulb, slightly curved, with unmodified tip; embolic apophysis absent.

**Distribution and remarks.**—*Bungulla inermis* (formerly known by WAM identification code 'MYG147') has a relatively restricted distribution in the north-eastern Avon Wheatbelt bioregion of south-western Australia, from Mount Gibson south to Merredin (Fig. 257). Nothing is known of the biology of this species, other than that the known male specimens were collected wandering in search of females in late autumn and winter.

***Bungulla iota*** Rix, Raven & Harvey, sp. nov.
http://zoobank.org/?lsid=urn:lsid:zoobank.org:act:58F78F41-5403-485A-9843-7B700AAFF615
(Figs. 13, 258–270)

**Type material.**—*Holotype male*. AUSTRALIA: *Western Australia*: Woodleigh Station, site MO4 (IBRA_CAR), 26°11′31.1″S, 114°30′33.0″E, wet pitfall trap, 17 May–21 August 1995, N. Hall, WAM/CALM Carnarvon Survey (WAM T142984).

*Paratypes*. AUSTRALIA: *Western Australia*: 6 ♂, same data as holotype (WAM T98534).

**Etymology.**—The specific epithet is a noun in apposition derived from the Greek 'iota' ('anything very small'; see Brown 1956), in reference to the very small size of this species.

**Diagnosis.**—Males of *Bungulla iota* can be distinguished from all other known congeners with > 10 retrolateral spinules on the palpal tibia (Fig. 13) – except *B. banksia*, *B. bertmaini*, *B. hamelinensis*, *B. iota*, *B. laevigata*, *B. quobba*, *B.*

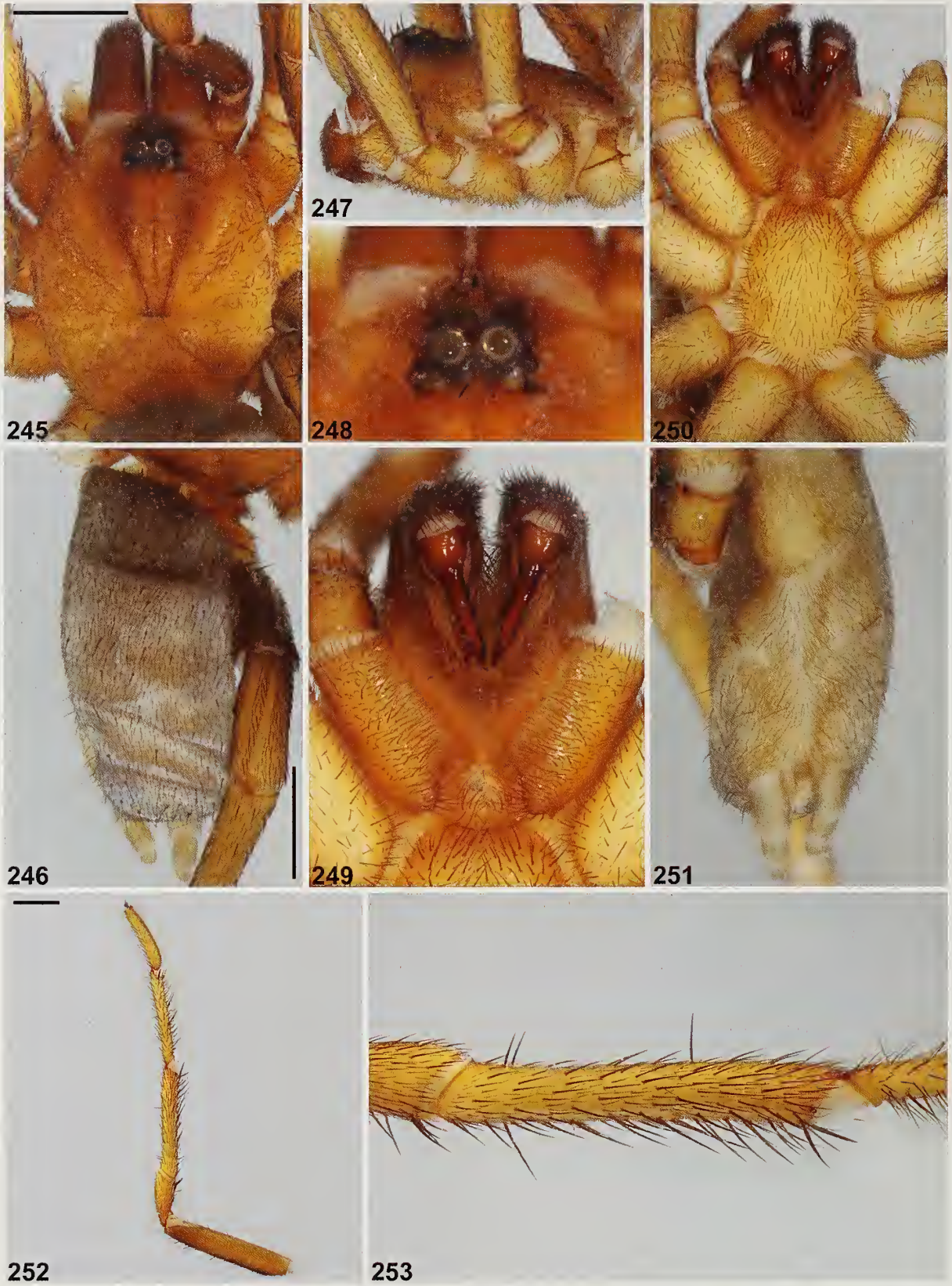


Figures 245–253.—*Bungulla inermis* sp. nov., male holotype (WAM T142953) from 2 km N. of Bunce Bin, N. of Beacon (Western Australia; AVW), somatic morphology: 245–246, carapace and abdomen, dorsal view; 247, cephalothorax, lateral view; 248, eyes, dorsal view; 249, mouthparts, ventral view; 250–251, cephalothorax and abdomen, ventral view; 252, leg I, prolateral view; 253, leg I tibia, prolateral view. Scale bars = 2.0 mm.


Figures 254–256.—*Bungulla inermis* sp. nov., male holotype (WAM T142953) from 2 km N. of Bunce Bin, N. of Beacon (Western Australia; AVW), pedipalp: 254, retrolateral view; 255, retro-ventral view; 256, prolateral view. Scale bar = 2.0 mm.

*weld* and *B. yeni* – by the shape of the proximal half of the palpal tibia, which is without a pronounced ventral bulge (Fig. 267), combined with the absence of a medial 'ledge' on the palpal tibia (Figs. 267, 268) (palpal tibia is with a ledge or bulges ventrally in other species). *Bungulla iota* can be further distinguished from *B. banksia* by the larger field of retrolateral spinules on the palpal tibia (Fig. 267; cf. Fig. 72); from *B. bertmaini*, *B. laevigata* and *B. quobba* by the shape of the

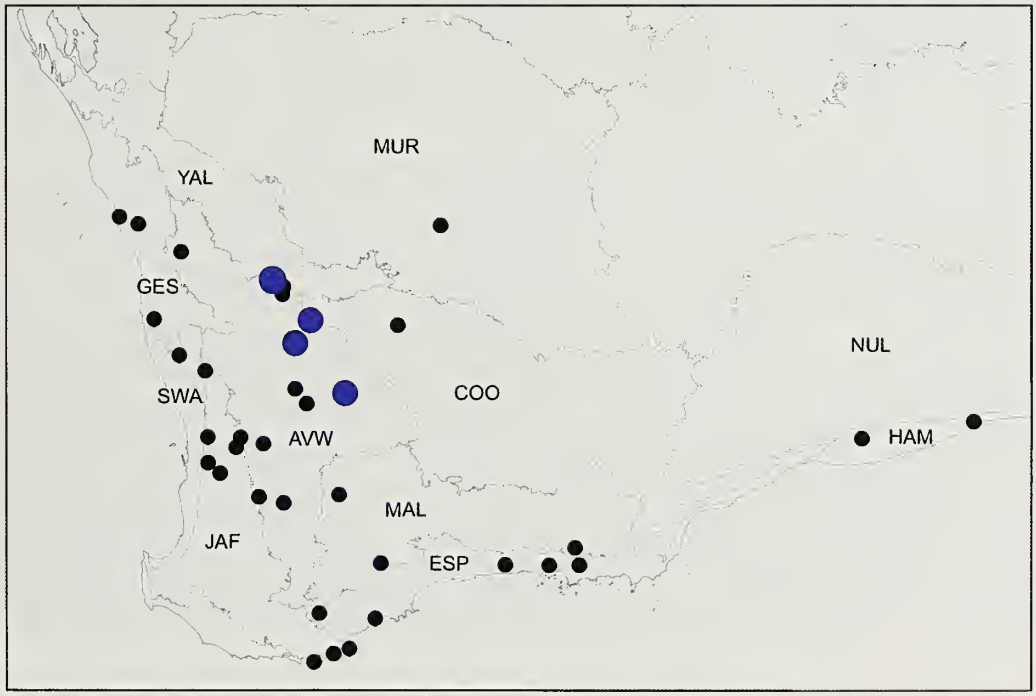


Figure 257.—Map showing collection records of *Bungulla inermis* sp. nov. (large blue circles), relative to other taxa with < 5 retrolateral spinules on the male palpal tibia (see Fig. 12). Relevant IBRA 7.0 bioregional aeronyms are as follows: AVW, Avon Wheatbelt; COO, Coolgardie; ESP, Esperance Plains; GES, Geraldton Sandplains; HAM, Hampton; JAF, Jarrah Forest; MAL, Mallee; MUR, Murchison; NUL, Nullarbor; SWA, Swan Coastal Plain; YAL, Yalgoo.

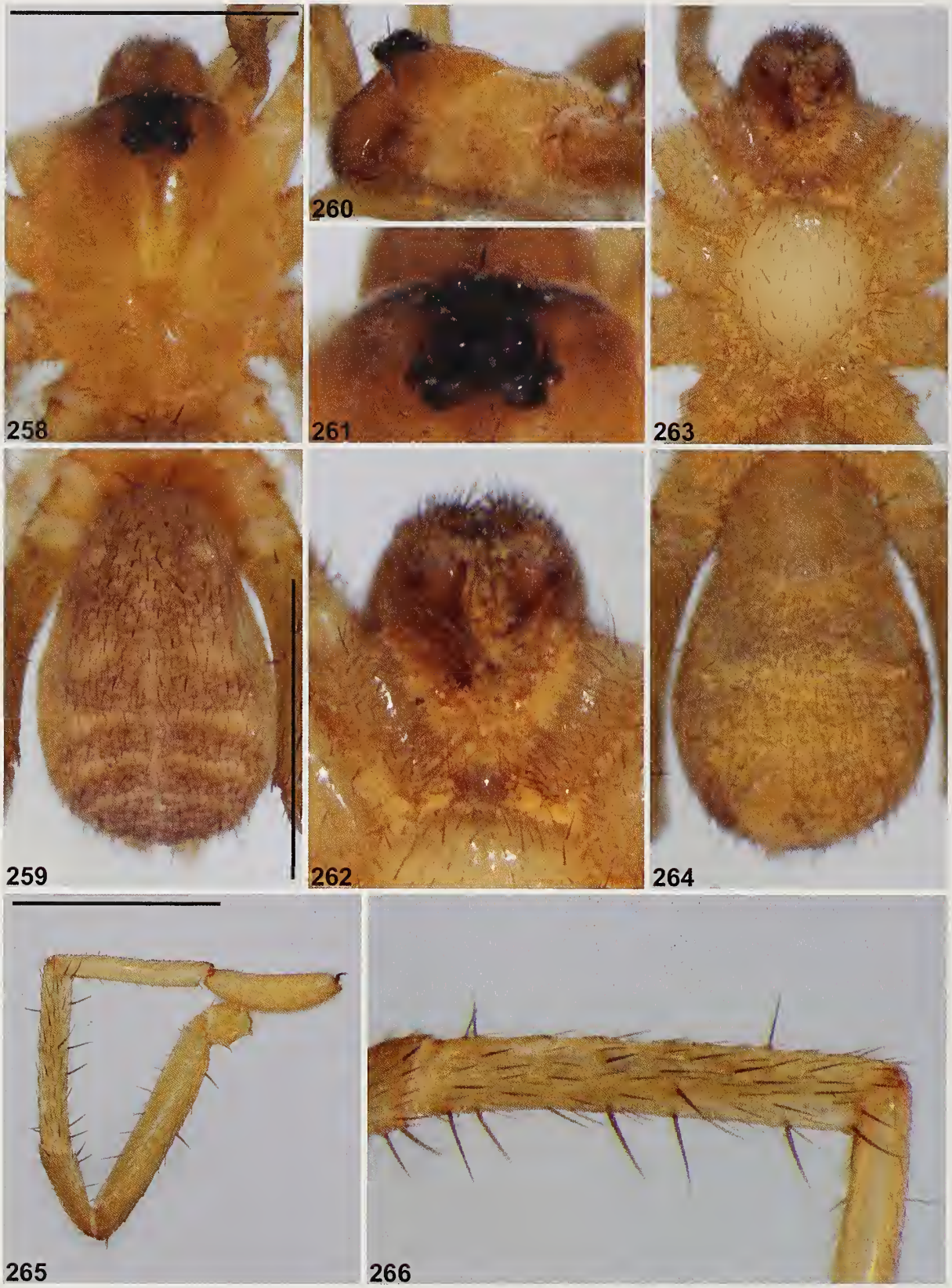


Figures 258–266.—*Bungulla iota* sp. nov., male holotype (WAM T142984) from Woodleigh Station (Western Australia; CAR), somatic morphology: 258–259, carapace and abdomen, dorsal view; 260, cephalothorax, lateral view; 261, eyes, dorsal view; 262, mouthparts, ventral view; 263–264, cephalothorax and abdomen, ventral view; 265, leg I, prolateral view; 266, leg I tibia, prolateral view. Scale bars = 2.0 mm.


Figures 267–269.—*Bungulla iota* sp. nov., male holotype (WAM T142984) from Woodleigh Station (Western Australia; CAR), pedipalp: 267, retrolateral view; 268, retro-ventral view; 269, prolateral view. Scale bar = 2.0 mm.

embolus, which is relatively short (i.e., ~as long as bulb) (Fig. 267; cf. Figs. 24, 319, 371); from *B. hamelinensis* by the morphology of the cymbial spinules, which are thicker and more spine-like (Figs. 267–269; cf. Figs. 218–220); from *B. yeni* and by the presence of a larger, crescent-shaped field of retrolateral spinules on the palpal tibia (Fig. 267; cf. Fig. 445); from *B. weld* by the presence of relatively symmetric field of retrolateral spinules on the palpal tibia (Fig. 267; cf. Fig. 419); and from *B. bidgemia* by the smaller body size (carapace width < 2.0) (Fig. 258; cf. Fig. 86), combined with the absence of

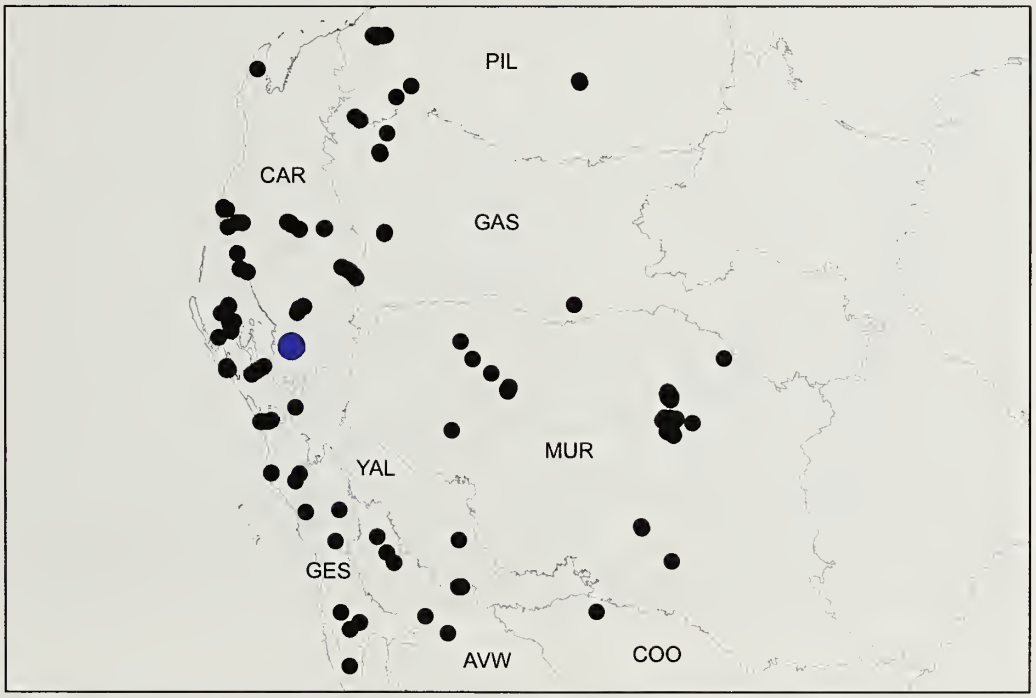


Figure 270.—Map showing collection records of *Bungulla iota* sp. nov. (large blue circles), relative to other taxa with > 10 retrolateral spinules on the male palpal tibia (see Fig. 13). Relevant IBRA 7.0 bioregional acronyms are as follows: AVW, Avon Wheatbelt; CAR, Carnarvon; COO, Coolgardie; GAS, Gascoyne; GES, Geraldton Sandplains; MUR, Murchison; PIL, Pilbara; YAL, Yalgoo.

marginal lateral indentations on the carapace between coxae II–III (Fig. 258; cf. Fig. 86). Females are unknown.

**Description (male holotype).**—Total length 5.0. Carapace 2.2 long, 1.7 wide. Abdomen 2.4 long, 1.6 wide. Carapace (Fig. 258) tan, with darker pars cephalica and mostly black ocular region; fovea straight. Eye group (Fig. 261) trapezoidal (anterior eye row strongly procurved), 0.9 x as long as wide, PLE–PLE/ALE–ALE ratio 1.4; ALE almost contiguous; AME separated by less than their own diameter; PME separated by 2.2 x their own diameter; PME and PLE separated by diameter of PME, PME positioned in line with level of PLE. Maxillae partially covered by debris, cuspules (if present) obscured (Fig. 262); labium without cuspules. Abdomen (Fig. 259) oval, pale olive-brown in dorsal view with beige-tan mottling, two pairs of beige-tan sigilla spots and three pairs of beige-tan chevrons posteriorly, each divided along midline. Dorsal surface of abdomen (Fig. 259) with sparse arrangement of stiff, porrect black setae, each with slightly raised, dark brown sclerotic base; sclerotized sigilla absent. Legs (Figs. 265, 266) variable shades of tan, with light scopulae on incrassate tarsi I–II; tibia I spinose, without prolateral clasping spurs. Leg I: femur 2.2; patella 1.1; tibia 1.8; metatarsus 1.6; tarsus 1.2; total 7.8. Leg 1 femur–tarsus/carapace length ratio 3.5. Pedipalpal tibia (Figs. 267–269) 2.2 x longer than wide; field of retrolateral spinules large and symmetrically crescent-shaped in retrolateral view, positioned medially–distally (along most of retro-ventral margin), consisting of ca. 40 spinules of largely similar length; RTA absent. Cymbium (Figs. 267–269) setose, with sparse field of spine-like spinules covering most of dorsal surface. Embolus (Figs. 267–269) as long as bulb, slightly curved, with unmodified tip; embolic apophysis absent.

**Distribution and remarks.**—*Bungulla iota* (formerly confused with WAM identification code 'MYG138') is known only from Nerren Nerren Station, in the southern Carnarvon (Wooramel) bioregion of Western Australia (Fig. 270). Nothing is known of the biology of this species, other than that the known male specimens were collected wandering in search of females in winter or possibly late autumn.

***Bungulla keigheryi*** Rix, Raven & Harvey, sp. nov.
http://zoobank.org/?lsid=urn:lsid:zoobank.org:act:F95533E3-2AC2-4124-B3BA-6A3A9D7C2B27
(Figs. 13, 271–283)

**Type material.**—*Holotype male.* AUSTRALIA: *Western Australia*: Bidgemia Station, Gascoyne Junction, site GJ3 (IBRA_CAR), 25°07′08.1″S, 115°25′33.1″E, wet pitfall trap, 6 June–20 August 1995, wet pitfall trap, N. Hall, WAM/CALM Carnarvon Survey (WAM T98531).

**Other material examined.**—AUSTRALIA: *Western Australia*: 3 ♂, same data as holotype except site GJ4, 25°05′17.4″S, 115°22′48.0″E (WAM T98532).

**Etymology.**—This species is named in honor of Greg Keighery, in recognition of his contributions to the Southern Carnarvon Basin Survey (Burbidge et al. 2000) and to the study of Australian biodiversity.

**Diagnosis.**—Males of *Bungulla keigheryi* can be distinguished from all other known congeners with > 10 retrolateral spinules on the palpal tibia (Fig. 13) – except *B. biota*, *B. burbidgei*, *B. dipsodes*, *B. kendricki*, *B. sampeyae* and *B. westi* – by the shape of the proximal half of the palpal tibia, which has a pronounced RTA-like ventral bulge in retrolateral view (Fig. 280) (palpal tibia is piriform and unmodified in other species). *Bungulla keigheryi* can be further distinguished from *B. biota*, *B. burbidgei*, *B. dipsodes*, *B. kendricki* and *B. sampeyae* by the shape of the RTA-like bulge of the palpal tibia, which is developed into a relatively acute, attenuate process (Fig. 280; cf. Figs. 108, 134, 147, 306, 406); and from *B. westi* by the absence of spinules on the disto-dorsal margin of the palpal tibia (Fig. 280; cf. Fig. 432). Females are unknown.

**Description (male holotype).**—Total length 6.1. Carapace 2.8 long, 2.2 wide. Abdomen 2.8 long, 1.8 wide. Carapace (Fig. 271) pale tan, with slightly darker pars cephalica and mostly black ocular region; fovea slightly procurved. Eye group (Fig. 274) trapezoidal (anterior eye row strongly procurved), 0.8 x as long as wide, PLE–PLE/ALE–ALE ratio 1.3; ALE separated by their own diameter; AME separated by less than their own diameter; PME separated by 2.9 x their own diameter; PME and PLE separated by slightly less than diameter of PME, PME positioned in line with level of PLE. Maxillae and labium without cuspules (Fig. 275). Abdomen (Fig. 272) elongate-oval, beige-tan in dorsal view with beige mottling and faint pattern of chevrons posteriorly. Dorsal surface of abdomen (Fig. 272) with sparse arrangement of stiff, porrect black setae, each with slightly raised, dark brown sclerotic base; sclerotized sigilla absent. Legs (Figs. 278, 279) variable shades of tan, with light scopulae on incrassate tarsi I–II; tibia 1 largely aspinose, without prolateral clasping spurs. Leg 1: femur 2.8; patella 1.3; tibia 2.2; metatarsus 2.1; tarsus 1.4; total 9.8. Leg I femur–tarsus/carapace length ratio 3.5. Pedipalpal tibia (Figs. 280–282) stout, bulbous, 1.8 x longer than wide, with pronounced RTA-like ventral bulge proximally, the latter developed into a relatively acute, attenuate process; field of retrolateral spinules reverse L-shaped in retrolateral view, positioned medially (on and adjacent to RTA-like bulge), consisting of ca. 45 spinules, the latter longest at apex of RTA-like bulge; RTA absent. Cymbium (Figs. 280–282) setose, with field of porrect, thorn-like spinules covering most of dorsal surface. Embolus (Figs. 280–282) slightly longer than bulb, curved, with slightly expanded tip; embolic apophysis absent.

**Distribution and remarks.**—*Bungulla keigheryi* (formerly known by WAM identification code 'MYG137') is known only from Bidgemia Station in the far eastern Carnarvon bioregion (Western Australia), just south of the Gascoyne River ca. 10 km south-east of Bidgemia Station Homestead (Fig. 283). Nothing is known of the biology of this species, other than that the known male specimens were collected wandering in search of females in winter.

***Bungulla keirani*** Rix, Raven & Harvey, sp. nov.
http://zoobank.org/?lsid=urn:lsid:zoobank.org:act:5035E1FA-F6D5-450B-B155-BC3A1655C70B
(Figs. 13, 284–296)

**Type material.**—*Holotype male.* AUSTRALIA: *Western Australia*: Nanga Station, site NA2 (IBRA_CAR), 26°29′23.0″S, 114°03′24.3″E, wet pitfall trap, 11 May–30 August 1995, N. Hall, WAM/CALM Carnarvon Survey (WAM T142982).

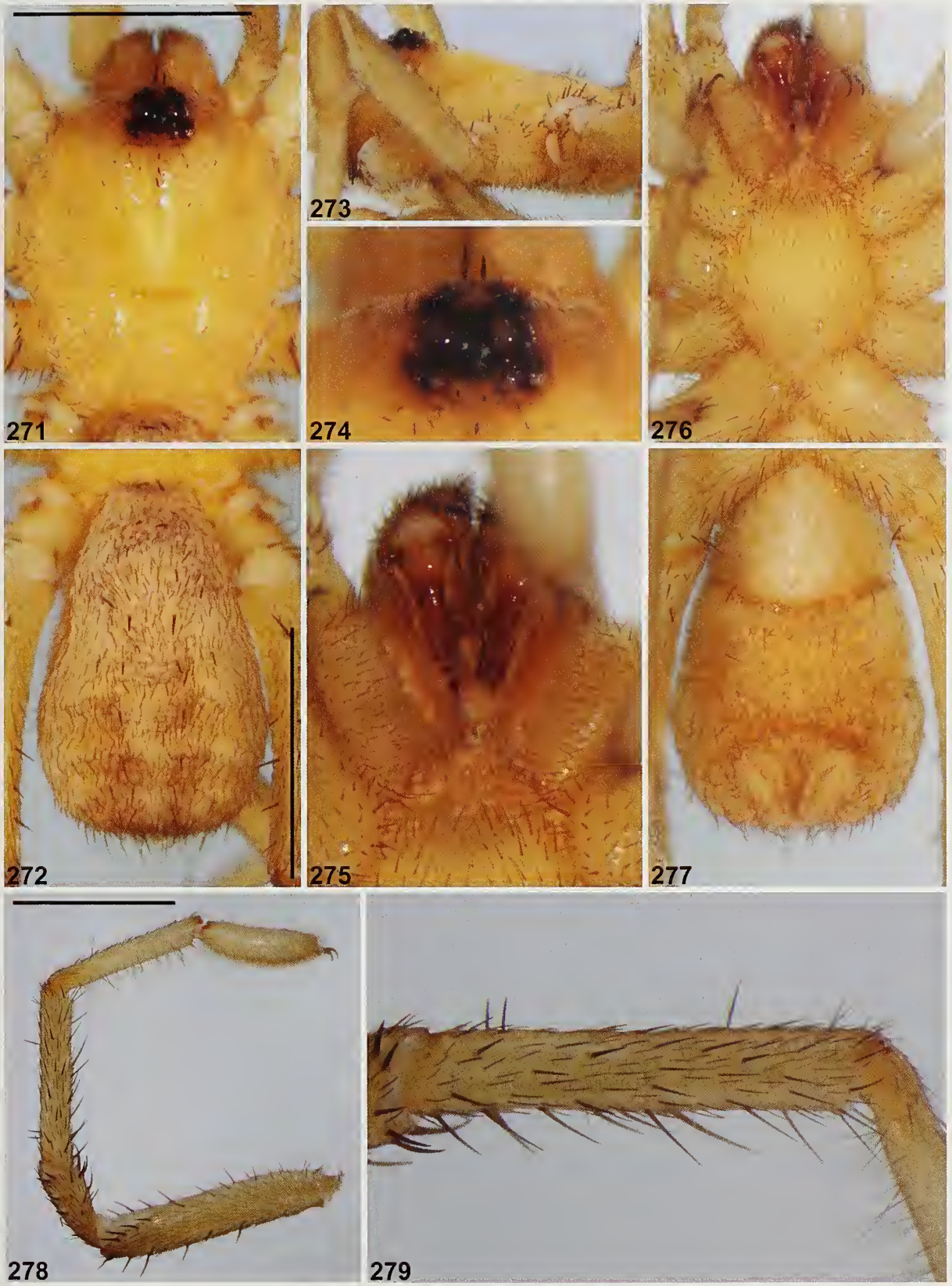


Figures 271–279.—*Bungulla keigheryi* sp. nov., male holotype (WAM T98531) from Bidgemia Station, Gascoyne Junction (Western Australia; CAR), somatic morphology: 271–272, carapace and abdomen, dorsal view; 273, cephalothorax, lateral view; 274, eyes, dorsal view; 275, mouthparts, ventral view; 276–277, cephalothorax and abdomen, ventral view; 278, leg 1, prolateral view; 279, leg 1 tibia, prolateral view. Scale bars = 2.0 mm.

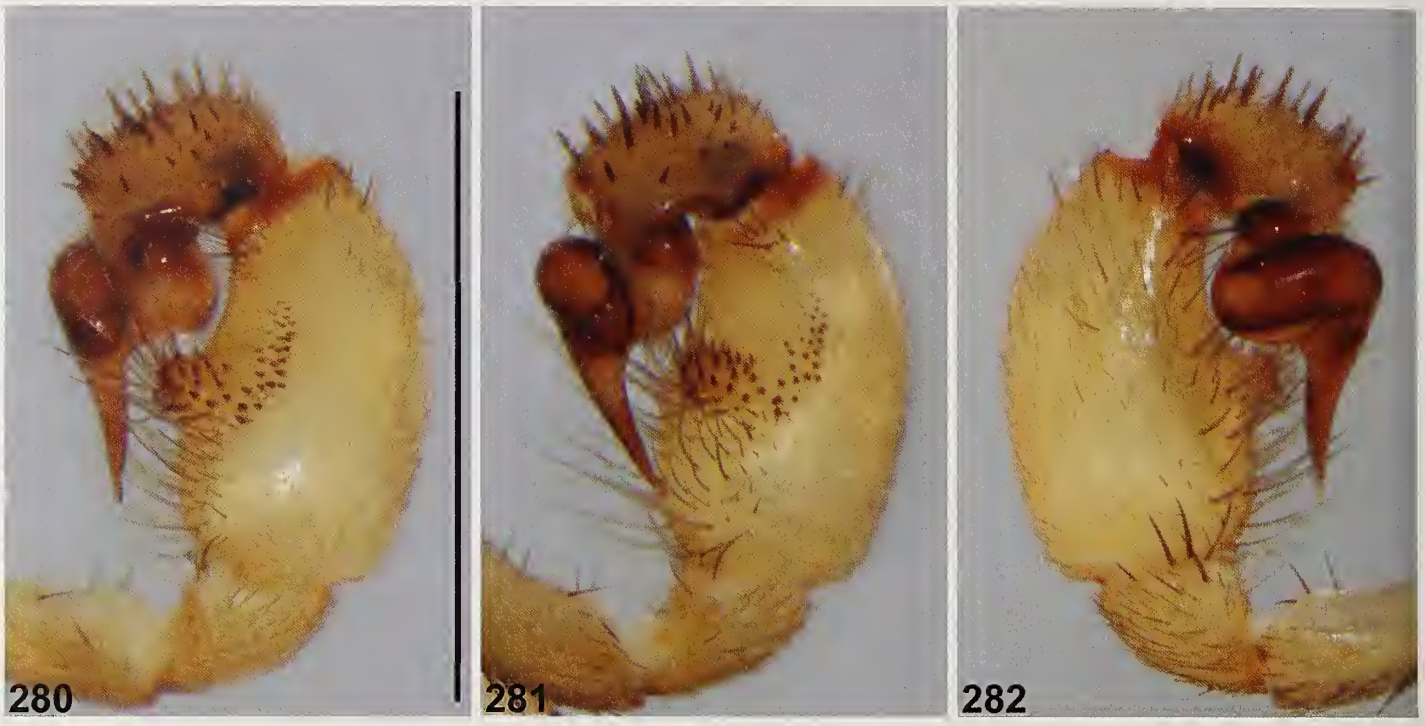


Figures 280–282.—*Bungulla keigheryi* sp. nov., male holotype (WAM T98531) from Bidgemia Station, Gascoyne Junction (Western Australia: CAR), pedipalp: 280, retrolateral view; 281, retro-ventral view; 282, prolateral view. Scale bar = 2.0 mm.

*Paratypes.* AUSTRALIA: *Western Australia*: 3 ♂, same data as holotype (WAM T98655).

**Other material examined.**—AUSTRALIA: *Western Australia*: 2 ♂, Nanga Station, site NA4 (IBRA_YAL), 26°32′47.3″S, 113°57′47.0″E, wet pitfall trap, 11 May–30 August 1995, N. Hall, WAM/CALM Carnarvon Survey (WAM T98656); 15 ♂, same data except site NA5, 26°35′31.8″S, 113°53′22.3″E (WAM T98654); 1 ♂, Chilimony Road, east, SW. of Binnu, site NO 10 (IBRA_GES), 28°06′09″S, 114°34′09″E, wet pitfall traps, 15 September 1998–18 October 1999, N. Guthrie,

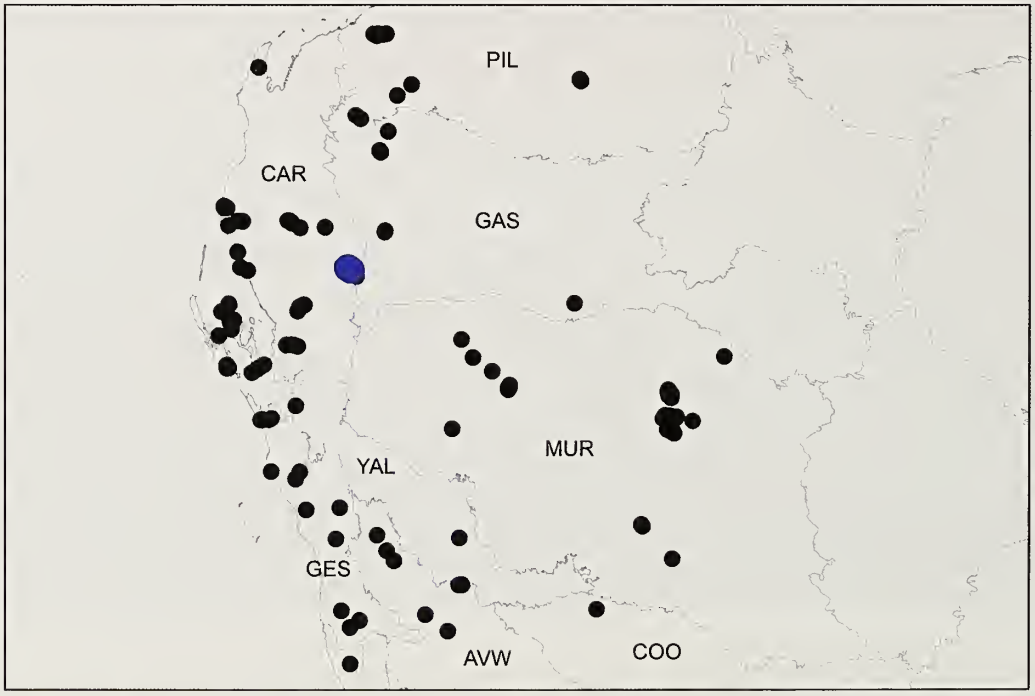


Figure 283.—Map showing collection records of *Bungulla keigheryi* sp. nov. (large blue circles), relative to other taxa with > 10 retrolateral spinules on the male palpal tibia (see Fig. 13). Relevant IBRA 7.0 bioregional acronyms are as follows: AVW, Avon Wheatbelt; CAR, Carnarvon; COO, Coolgardie; GAS, Gascoyne; GES, Geraldton Sandplains; MUR, Murchison; PIL, Pilbara; YAL, Yalgoo.

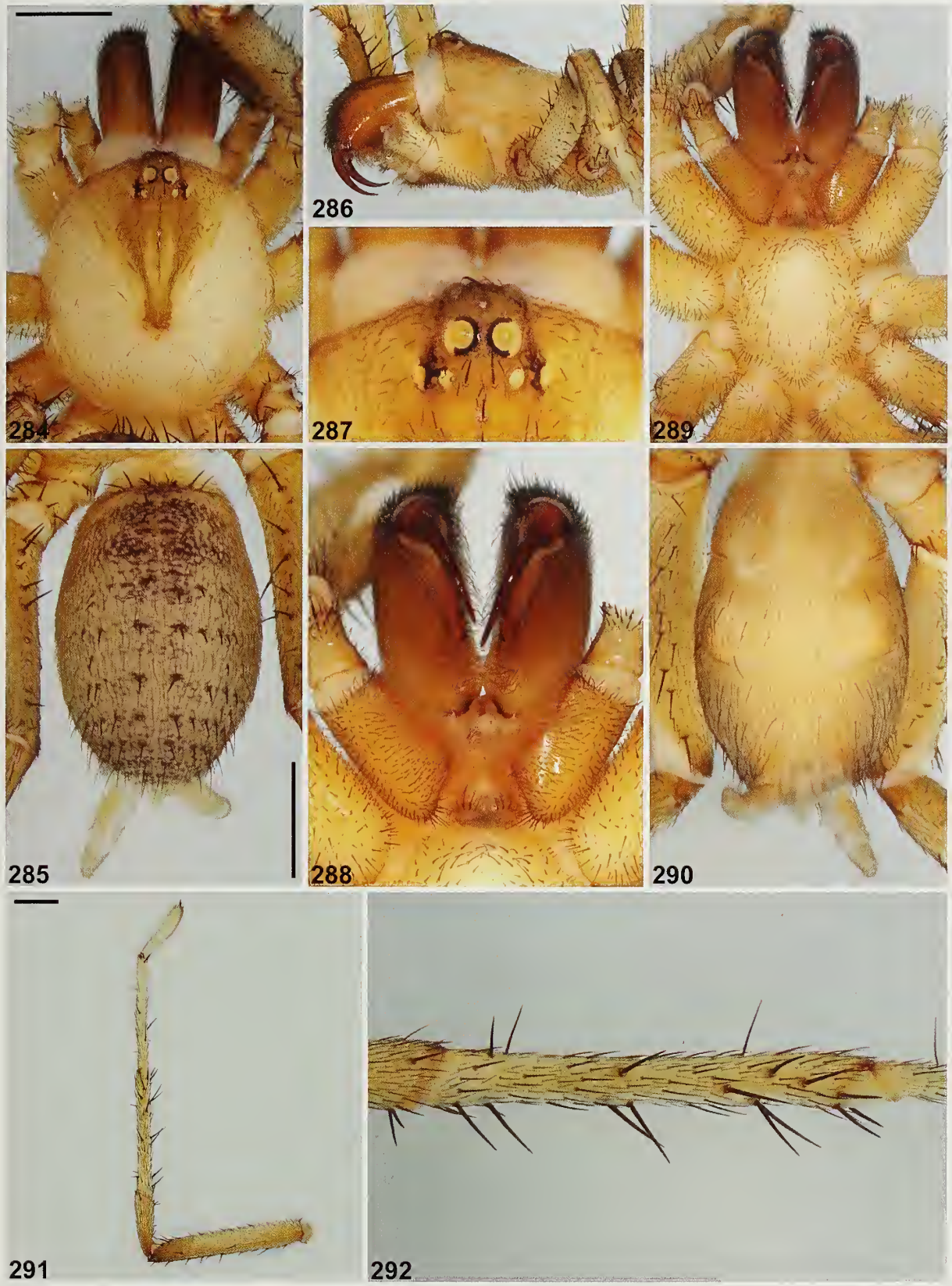


Figures 284–292.—*Bungulla keirani* sp. nov., male holotype (WAM T142982) from Nanga Station, site NA2 (Western Australia; CAR), somatic morphology: 284–285, carapace and abdomen, dorsal view; 286, cephalothorax, lateral view; 287, eyes, dorsal view; 288, mouthparts, ventral view; 289–290, cephalothorax and abdomen, ventral view; 291, leg I, prolateral view; 292, leg I tibia, prolateral view. Scale bars = 2.0 mm.


Figures 293–295.—*Bungulla keirani* sp. nov., male holotype (WAM T142982) from Nanga Station, site NA2 (Western Australia; CAR), pedipalp: 293, retrolateral view; 294, retro-ventral view; 295, prolateral view. Scale bar = 2.0 mm.

CALM Survey (WAM T142939); 2 ♂, Francois Peron National Park, site PE3 (IBRA_CAR), 25°49′14.1″S, 113°32′24.3″E, wet pitfall trap, 24 May–30 August 1995, N. Hall, WAM/CALM Carnarvon Survey (WAM T98652); 2 ♂, Zuytdorp Nature Reserve, site ZU2 (IBRA_GES), 27°15′41″S, 114°01′47.6″E, wet pitfall trap, 18 May–17 August 1995, N. Hall, WAM/CALM Carnarvon Survey (WAM T98646); 1 ♂, same data except 26 August–15 October 1995 (WAM T98647); 1 ♂, Zuytdorp, site ZU1 (IBRA_GES), 27°15′42″S, 114°01′09″E, wet pitfall trap, 18 May–17 August

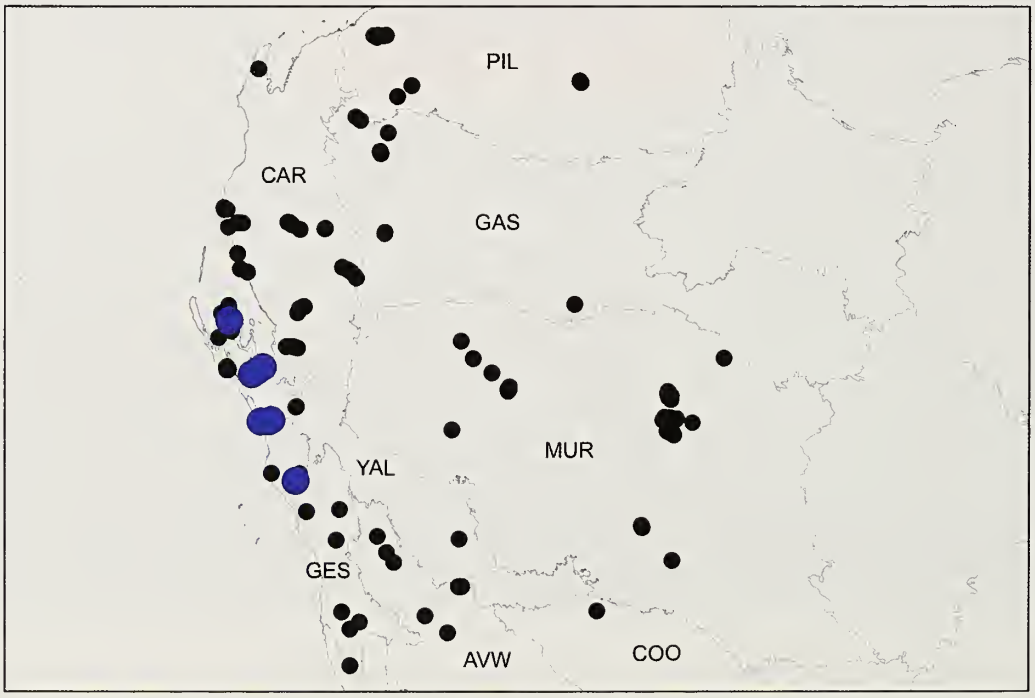


Figure 296.—Map showing collection records of *Bungulla keirani* sp. nov. (large blue circles), relative to other taxa with > 10 retrolateral spinules on the male palpal tibia (see Fig. 13). Relevant IBRA 7.0 bioregional acronyms are as follows: AVW, Avon Wheatbelt; CAR, Carnarvon; COO, Coolgardie; GAS, Gascoyne; GES, Geraldton Sandplains; MUR, Murchison; PIL, Pilbara; YAL, Yalgoo.

1995, N. Hall, WAM/CALM Carnarvon Survey (WAM T98644); 1 ♂, same data (WAM T98645); 1 ♂, same data except site ZU3, 27°15′49.9″S, 114°04′13.7″E, 18 May–16 August 1995 (WAM T98648); 3 ♂, same data except site ZU4, 27°15′45.1″S, 114°09′12.9″E (WAM T98649); 4 ♂, same data (WAM T98650); 2 ♂, same data except site ZU5, 27°14′42.9″S, 114°11′36.1″E, 17 May–16 August 1995 (WAM T98651).

**Etymology.**—This species is named in honor of the late Keiran McNamara (1954–2013), in recognition of his considerable efforts in securing funding for the Biological Survey of the southern Carnarvon Basin (run by the then Department of Conservation and Land Management from 1994–1995), which resulted in the collection of this and numerous other species of *Bungulla*.

**Diagnosis.**—Males of *Bungulla keirani* can be distinguished from all other known congeners with > 10 retrolateral spinules on the palpal tibia (Fig. 13) – except *B. ajana*, *B. aplini* and *B. mckenziei* – by the shape of the proximal half of the palpal tibia, which is without a pronounced ventral bulge (Fig. 293), combined with the presence of a medial 'ledge' on the palpal tibia, this ledge situated closely proximal to the field of retrolateral spinules and bearing a brush of filiform setae (Figs. 293, 294) (palpal tibia is without a ledge or bulges ventrally in other species). *Bungulla keirani* can be further distinguished from *B. ajana* by the shape of the palpal tibia, which is longer, less bulbous and less strongly arched dorsally (Fig. 293; cf. Fig. 46); and from *B. aplini* and *B. mckenziei* by the morphology of the cymbial spinules, which are short and thorn-like (Figs. 293–295; cf. Figs. 59–61, 332–334). Females are unknown.

**Description (male holotype).**—Total length 13.3. Carapace 5.5 long, 4.8 wide. Abdomen 5.3 long, 3.6 wide. Carapace (Fig. 284) pale tan, with darker pars cephalica, darker olive-brown lyre-like pattern on pars cephalica and slightly darker ocular region; postero-lateral corners near abdomen each with pair of porrect black setae; fovea straight. Eye group (Fig. 287) trapezoidal (anterior eye row strongly procurved), 0.8 x as long as wide, PLE–PLE/ALE–ALE ratio 1.6; ALE separated by their own diameter; AME separated by less than their own diameter; PME separated by 3.5 x their own diameter; PME and PLE separated by diameter of PME, PME positioned in line with level of PLE. Maxillae with field of cuspules confined to inner corner (Fig. 288); labium without cuspules. Abdomen (Fig. 285) oval, sandy-beige in dorsal view with darker olive-brown markings anteriorly and seven pairs of thin, spotted, faint olive-brown chevrons posteriorly, each divided along midline. Dorsal surface of abdomen (Fig. 285) with sparse arrangement of stiff, porrect black setae, each with slightly raised, dark brown sclerotic base; sclerotized sigilla absent. Legs (Figs. 291, 292) variable shades of tan, with light scopulae on tarsi I–II; metatarsus I and tarsus I lighter in color; tibia 1 heavily spinose, without prolateral clasping spurs. Leg 1: femur 7.0; patella 3.1; tibia 5.5; metatarsus 5.2; tarsus 2.8; total 23.5. Leg 1 femur–tarsus/carapace length ratio 4.3. Pedipalpal tibia (Figs. 293–295) relatively long, 2.4 x longer than wide, with small medial 'ledge' bearing a brush of filiform setae; field of retrolateral spinules rectangular in shape, positioned distally (distal to medial ledge), consisting of 20 spinules of largely similar length; RTA absent. Cymbium (Figs. 293–295) setose, with field of short, porrect, thorn-like spinules covering most of dorsal surface. Embolus (Figs. 293–295) as long as bulb, relatively straight, with unmodified tip; embolic apophysis absent.

**Distribution and remarks.**—*Bungulla keirani* (formerly known by WAM identification code 'MYG155') is a large species with a relatively restricted distribution in the northern Geraldton Sandplains, north-western Yalgoo and southern Carnarvon bioregions of Western Australia, from Zuytdorp north to the Peron Peninsula (Fig. 296). Nothing is known of the biology of this species, other than that known male specimens were collected wandering in search of females in winter or possibly late autumn.

***Bungulla kendricki*** Rix, Raven & Harvey, sp. nov.
http://zoobank.org/?lsid=urn:lsid:zoobank.org:act:2F87D1B8-EE30-4917-9C97-E1D526365891
(Figs. 13, 297–309)

**Type material.**—*Holotype male*. AUSTRALIA: *Western Australia*: Barlee Range Nature Reserve, quadrat 7 (IBRA_GAS), 23°22′45″S, 115°52′50″E, wet pitfall trap, August 1993, S. van Leeuwen & B. Bromilow (WAM T98565).

*Paratypes*. AUSTRALIA: *Western Australia*: 1 ♂, Barlee Range Nature Reserve, quadrat 6 (IBRA_GAS), 23°23′21″S, 115°53′12″E, wet pitfall trap, June 1994, S. van Leeuwen & B. Bromilow (WAM T44352); 1 ♂, same data except site BRNR5, Emu Spring Creek, 23°24′41″S, 115°53′39″E, dry pitfall trap, open *Acacia citrinoviridis*/*Eucalyptus terminalis* woodland, 11–14 June 1994, P.G. Kendrick & G.W. Kendrick (WAM T31149); 1 ♂, same data except site BRNR7, Snappy Gum Hills, 23°22′45″S, 115°52′50″E, *Eucalyptus leucophloeia* woodland over *Triodia* (WAM T31150); 1 ♂, same data except site BRNR8, Snakewood on Cracking Clays, 23°22′31″S, 115°52′57″E, *Acacia ziphophylla* over sparse *Triodia* (WAM T31151).

**Etymology.**—This species is named in honor of the late George Kendrick (1929–2014), for collecting a number of the paratypes of this species, and in recognition of his contributions to the study of fossil invertebrates.

**Diagnosis.**—Males of *Bungulla kendricki* can be distinguished from all other known congeners with > 10 retrolateral spinules on the palpal tibia (Fig. 13) – except *B. biota*, *B. burbidgei*, *B. dipsodes*, *B. keigheryi*, *B. sampeyae* and *B. westi* – by the shape of the proximal half of the palpal tibia, which has a pronounced RTA-like ventral bulge in retrolateral view (Fig. 306) (palpal tibia is piriform and unmodified in other species). *Bungulla kendricki* can be further distinguished from *B. biota* by the shape of the embolus, which is without a truncate tip (Figs. 306, 307; cf. Fig. 108); from *B. burbidgei* by the absence of dagger-like spinules at the apex of the RTA-like bulge (Fig. 306; cf. Fig. 134); from *B. keigheryi* by the broadly-rounded shape of the RTA-like bulge (Fig. 306; cf. Fig. 280); from *B. sampeyae* by the coloration of the dorsal abdomen, which is bi-colored (i.e., pale tan in color with dark anterior markings and dark posterior chevrons) (Fig. 298; cf. Fig. 398 and Supplementary File 1); from *B. dipsodes* by the shape of the palpal tibia, which is strongly arched dorsally, with a 'pistol-like' profile in retrolateral view (Fig. 306; cf. Fig. 147); and from *B. westi* by the absence of spinules on the disto-dorsal

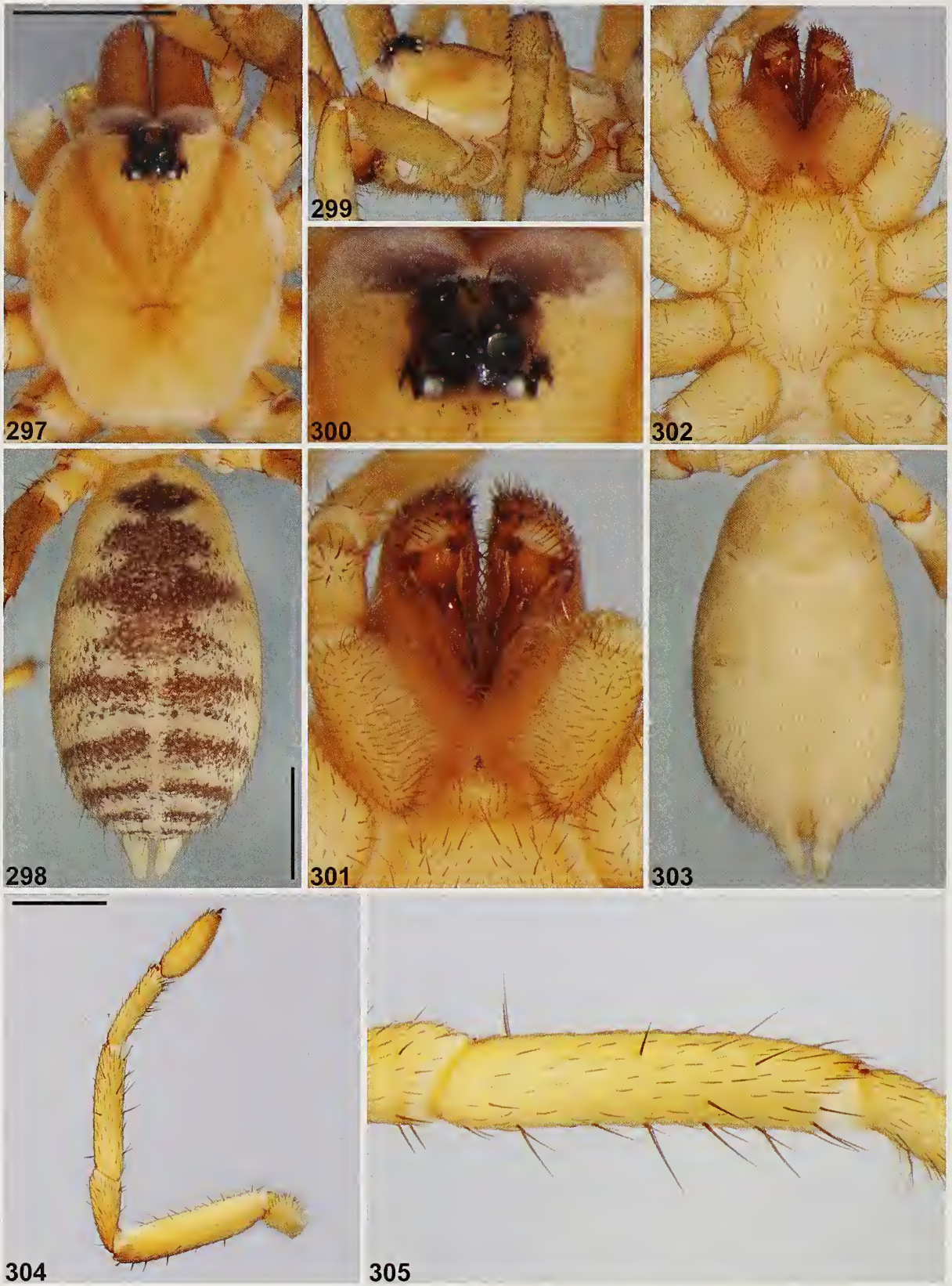


Figures 297–305.—*Bungulla kendricki* sp. nov., male holotype (WAM T98565) from Barlee Range Nature Reserve (Western Australia; GAS), somatic morphology: 297–298, carapace and abdomen, dorsal view; 299, cephalothorax, lateral view; 300, eyes, dorsal view; 301, mouthparts, ventral view; 302–303, cephalothorax and abdomen, ventral view; 304, leg I, prolateral view; 305, leg I tibia, prolateral view. Scale bars = 2.0 mm.


Figures 306–308.—*Bungulla kendricki* sp. nov., male holotype (WAM T98565) from Barlee Range Nature Reserve (Western Australia: GAS), pedipalp: 306, retrolateral view; 307, retro-ventral view; 308, prolateral view. Scale bar = 2.0 mm.

margin of the palpal tibia (Figs. 306–308; cf. Fig. 432). Females are unknown.

**Description (male holotype).**—Total length 11.6. Carapace 3.6 long, 3.0 wide. Abdomen 6.7 long, 3.8 wide. Carapace (Fig. 297) pale tan with mostly black ocular region; fovea slightly recurved. Eye group (Fig. 300) trapezoidal (anterior eye row strongly procurved), 0.8 x as long as wide, PLE–PLE/ALE–ALE ratio 1.3; ALE separated by nearly their own diameter:

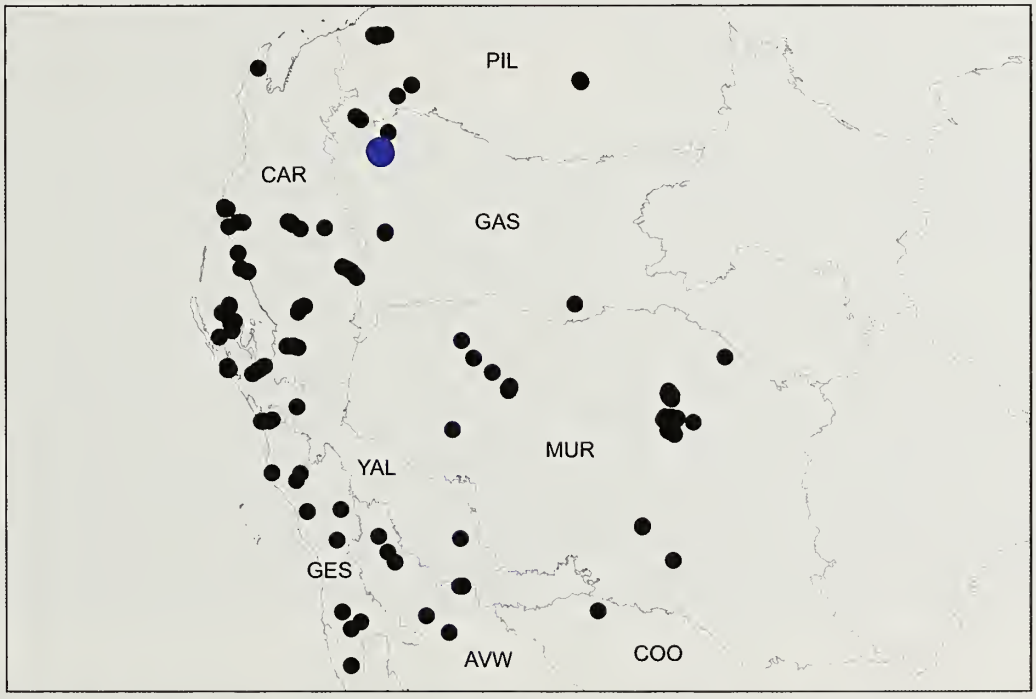


Figure 309.—Map showing collection records of *Bungulla kendricki* sp. nov. (large blue circles), relative to other taxa with > 10 retrolateral spinules on the male palpal tibia (see Fig. 13). Relevant IBRA 7.0 bioregional acronyms are as follows: AVW, Avon Wheatbelt; CAR, Carnarvon; COO, Coolgardie; GAS, Gascoyne; GES, Geraldton Sandplains; MUR, Murchison; PIL, Pilbara; YAL, Yalgoo.

AME separated by less than their own diameter; PME separated by 2.7 x their own diameter; PME and PLE separated by slightly less than diameter of PME, PME positioned in line with level of PLE. Maxillae with field of cuspules confined to inner corner (Fig. 301); labium without cuspules. Abdomen (Fig. 298) elongate-oval, beige-tan in dorsal view with contrasting pattern of four darker brown markings anteriorly and five pairs of thin brown chevrons posteriorly, each divided along midline. Dorsal surface of abdomen (Fig. 298) with sparse arrangement of stiff, porrect black setae, each with slightly raised, dark brown sclerotic base; sclerotized sigilla absent. Legs (Figs. 304, 305) variable shades of pale tan, with light scopulae on incrassate tarsi I–II; tibia 1 largely aspinose, without prolateral clasping spurs. Leg 1: femur 3.3; patella 1.8; tibia 2.7; metatarsus 2.0; tarsus 1.6; total 11.5. Leg I femur–tarsus/carapace length ratio 3.2. Pedipalpal tibia (Figs. 306–308) stout, bulbous and strongly arched dorsally, with 'pistol-like' profile in retrolateral view, 1.6 x longer than wide, with rounded RTA-like ventral bulge proximally; field of retrolateral spinules broadly crescent-shaped, positioned medially (on and adjacent to RTA-like bulge), consisting of ca. 40 spinules, the latter longest at apex of RTA-like bulge; RTA absent. Cymbium (Figs. 306–308) setose, with field of porrect, thorn-like spinules covering most of dorsal surface. Embolus (Figs. 306–308) slightly longer than bulb, strongly curved, with slightly expanded tip; embolic apophysis absent.

**Distribution and remarks.**—*Bungulla kendricki* (formerly known by WAM identification code 'MYG154') is known only from the Barlee Range, in the north-western Gascoyne bioregion of Western Australia (Fig. 309). Nothing is known of the biology of this species, other than that the known male specimens were collected wandering in search of females in winter.

***Bungulla laevigata*** Rix, Raven & Harvey, sp. nov.
http://zoobank.org/?lsid=urn:lsid:zoobank.org:act:D8198EBB-C26F-4DFB-92A6-F3545B93B4FC
(Figs. 13, 310–322)

**Type material.**—*Holotype male.* AUSTRALIA: *Western Australia*: Nanga Station, site NA1 (IBRA_CAR), 26°28′40.2″S, 114°04′33.6″E, wet pitfall trap, 11 May–30 August 1995, N. Hall, WAM/CALM Carnarvon Survey (WAM T143001).

*Paratypes.* AUSTRALIA: *Western Australia*: 2 ♂, same data as holotype (WAM T142994); 3 ♂, same data (WAM T142995).

**Etymology.**—The specific epithet is derived from the Latin 'laevigatus' (adjective: 'smooth'; see Brown 1956), in reference to the glabrous morphology of the carapace of this species.

**Diagnosis.**—Males of *Bungulla laevigata* can be distinguished from all other known congeners with > 10 retrolateral spinules on the palpal tibia (Fig. 13) – except *B. banksia*, *B. bertmaini*, *B. bidgemia*, *B. hamelinensis*, *B. iota*, *B. quobba*, *B. weld* and *B. yeni* – by the shape of the proximal half of the palpal tibia, which is without a pronounced ventral bulge (Fig. 319), combined with the absence of a medial 'ledge' on the palpal tibia (Figs. 319, 320) (palpal tibia is with a ledge or bulges ventrally in other species). *Bungulla laevigata* can be further distinguished from *B. banksia*, *B. bidgemia*, *B. iota*, *B. hamelinensis*, *B. weld* and *B. yeni* by the shape of the embolus, which is relatively long (i.e., longer than the bulb) (Fig. 319; cf. Figs. 72, 95, 218, 267, 419, 445); from *B. quobba* by the shape of the embolus, which is slightly longer and more strongly curved in standard retrolateral view (Fig. 319; cf. Fig. 371); and from *B. bertmaini* by the morphology of the pars cephalica, which is glabrous with relatively few setae (Fig. 310; cf. Fig. 15), combined with the lighter 'sandy' coloration of the dorsal abdomen (Fig. 311; cf. Fig. 16 and Supplementary File 1). Females are unknown.

**Description (male holotype).**—Total length 8.7. Carapace 3.6 long, 2.9 wide. Abdomen 3.9 long, 2.5 wide. Carapace (Fig. 310) pale tan, with slightly darker pars cephalica, pale olive-brown lyre-like pattern on pars cephalica and slightly darker ocular region; fovea slightly procurved. Eye group (Fig. 313) trapezoidal (anterior eye row strongly procurved), 0.9 x as long as wide, PLE–PLE/ALE–ALE ratio 1.4; ALE separated by nearly their own diameter; AME separated by less than their own diameter; PME separated by 2.9 x their own diameter; PME and PLE separated by slightly less than diameter of PME, PME positioned in line with level of PLE. Maxillae with field of cuspules confined to inner corner (Fig. 314); labium without cuspules. Abdomen (Fig. 311) oval, sandy-beige in dorsal view with faint charcoal-brown mottling and faint posterior chevrons. Dorsal surface of abdomen (Fig. 311) with sparse arrangement of stiff, porrect black setae, each with slightly raised, dark brown sclerotic base; sclerotized sigilla absent. Legs (Figs. 317, 318) variable shades of tan, with light scopulae on tarsi I–II; tibia I spinose, without prolateral clasping spurs. Leg I: femur 4.0; patella 1.7; tibia 3.0; metatarsus 2.9; tarsus 2.0; total 13.6. Leg 1 femur–tarsus/carapace length ratio 3.8. Pedipalpal tibia (Figs. 319–321) 2.2 x longer than wide; field of retrolateral spinules oval in shape, positioned medially, consisting of 18 spinules, the latter longest proximally; RTA absent. Cymbium (Figs. 319–321) setose, with field of relatively short, porrect, thorn-like spinules covering most of dorsal surface. Embolus (Figs. 319–321) ca. 1.5 x length of bulb, slightly curved, with unmodified tip; embolic apophysis absent.

**Distribution and remarks.**—*Bungulla laevigata* is a rare and highly restricted species known only from Nanga Station, in the far southern Carnarvon (Wooramel) bioregion of Western Australia (Fig. 322). The type and only known locality of this species is situated on an unusual, near-tidal sandplain at the far southern tip of the Hamelin Pool Marine Reserve, 13 km south-west of Hamelin Pool. This site is also home to the similarly restricted species *B. hamelinensis*. Nothing else is known of the biology of *B. laevigata*, other than that the known male specimens were collected wandering in search of females in winter or possibly late autumn.

***Bungulla mckenziei*** Rix, Raven & Harvey, sp. nov.
http://zoobank.org/?lsid=urn:lsid:zoobank.org:act:B2489421-A09A-457D-A25F-24C6B17CC1C6
(Figs. 13, 323–335)

**Type material.**—*Holotype male.* AUSTRALIA: *Western Australia*: Zuytdorp, site ZU5 (IBRA_GES), 27°14′42.9″S, 114°11′36.1″E, wet pitfall trap, 17 May–16 August 1995, N. Hall, WAM/CALM Carnarvon Survey (WAM T142978).

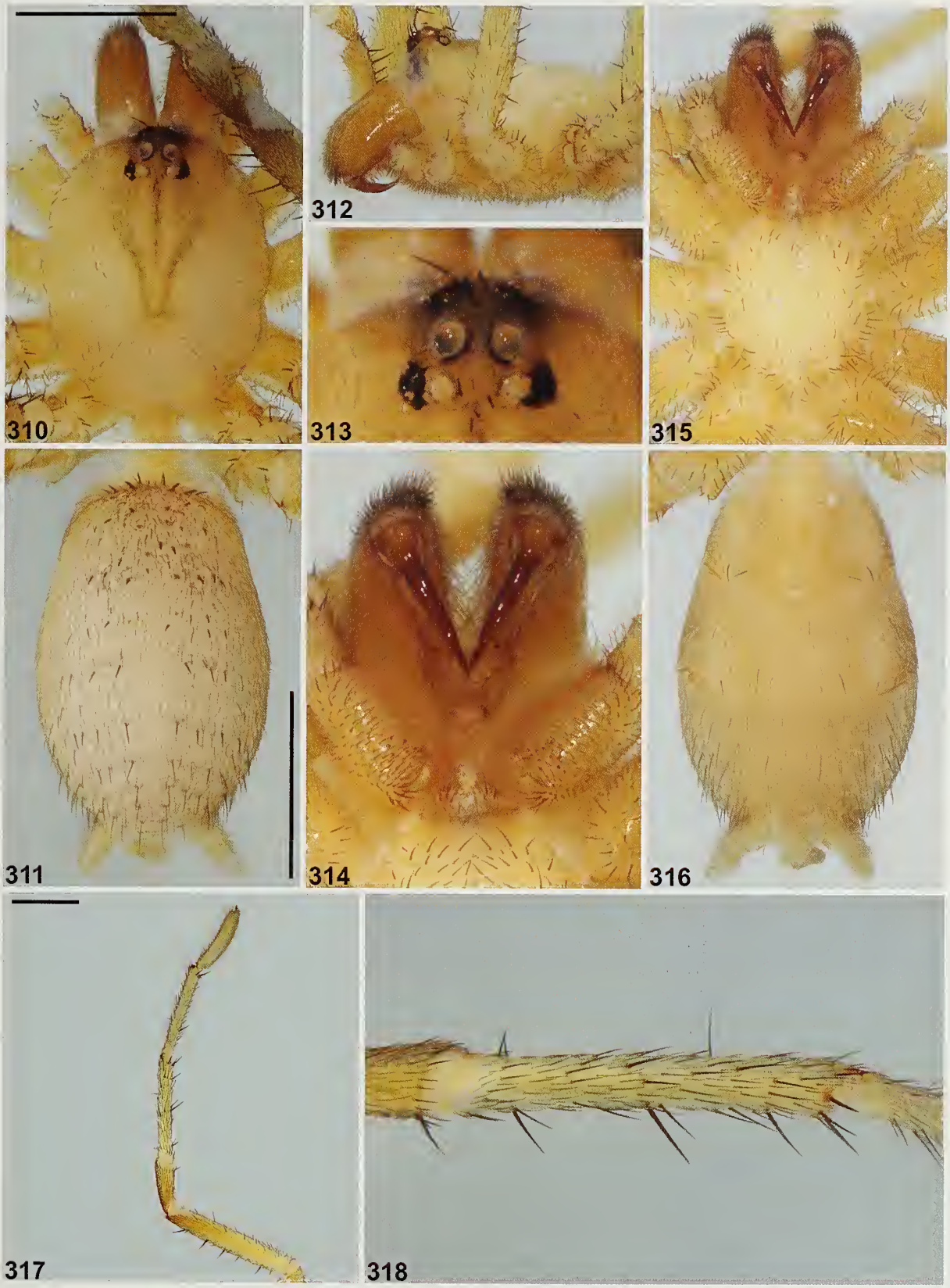


Figures 310–318.—*Bungulla laevigata* sp. nov., male holotype (WAM T143001) from Nanga Station (Western Australia; CAR), somatic morphology: 310–311, carapace and abdomen, dorsal view; 312, cephalothorax, lateral view; 313, eyes, dorsal view; 314, mouthparts, ventral view; 315–316, cephalothorax and abdomen, ventral view; 317, leg I, prolateral view; 318, leg I tibia, prolateral view. Scale bars = 2.0 mm.


Figures 319–321.—*Bungulla laevigata* sp. nov., male holotype (WAM T143001) from Nanga Station (Western Australia; CAR), pedipalp: 319, retrolateral view; 320, retro-ventral view; 321, prolateral view. Scale bar = 2.0 mm.

*Paratypes*. AUSTRALIA: *Western Australia*: 3 ♂, same data as holotype (WAM T98556).

**Other material examined.**—AUSTRALIA: *Western Australia*: 1 ♂, Zuytdorp Nature Reserve, site ZU2 (IBRA_GES), 27°15′41″S, 114°01′47.6″E, wet pitfall trap, 18 May–17 August 1995, N. Hall, WAM/CALM Carnarvon Survey (WAM T98528); 1 ♂, Zuytdorp, site ZU1 (IBRA_GES), 27°15′42″S, 114°01′09″E, wet pitfall trap, 19 May–17 August 1995, N. Hall, WAM/CALM Carnarvon Survey (WAM T98554); 2 ♂, same data except site ZU3, 27°15′49.9″S, 114°04′13.7″E, 18

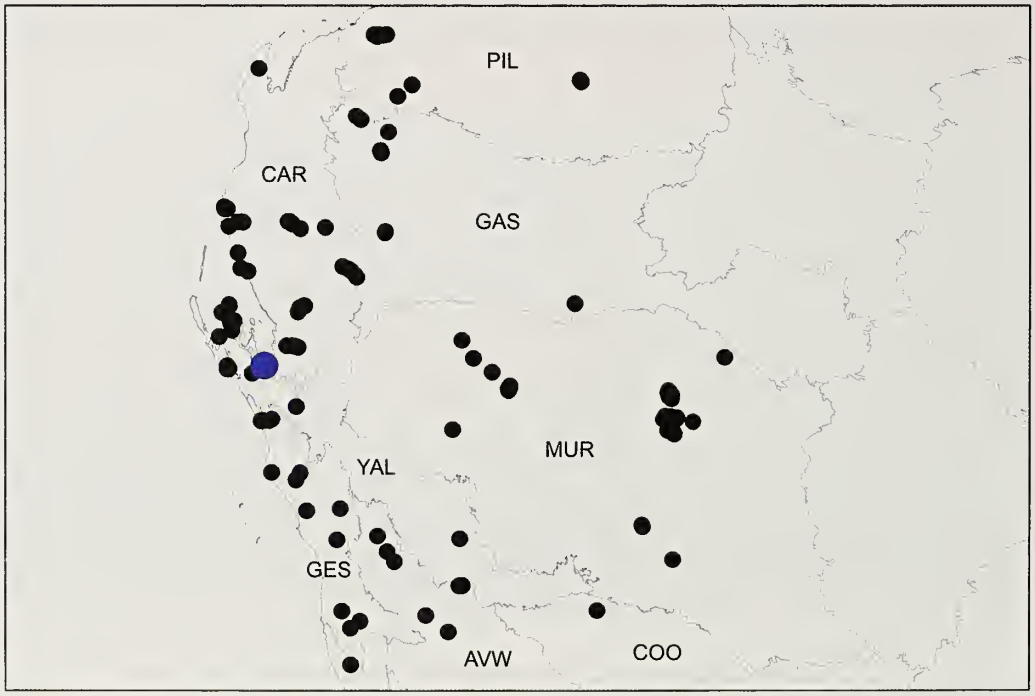


Figure 322.—Map showing collection records of *Bungulla laevigata* sp. nov. (large blue circles), relative to other taxa with > 10 retrolateral spinules on the male palpal tibia (see Fig. 13). Relevant IBRA 7.0 bioregional acronyms are as follows: AVW, Avon Wheatbelt; CAR, Carnarvon; COO, Coolgardie; GAS, Gascoyne; GES, Geraldton Sandplains; MUR, Murchison; PIL, Pilbara; YAL, Yalgoo.

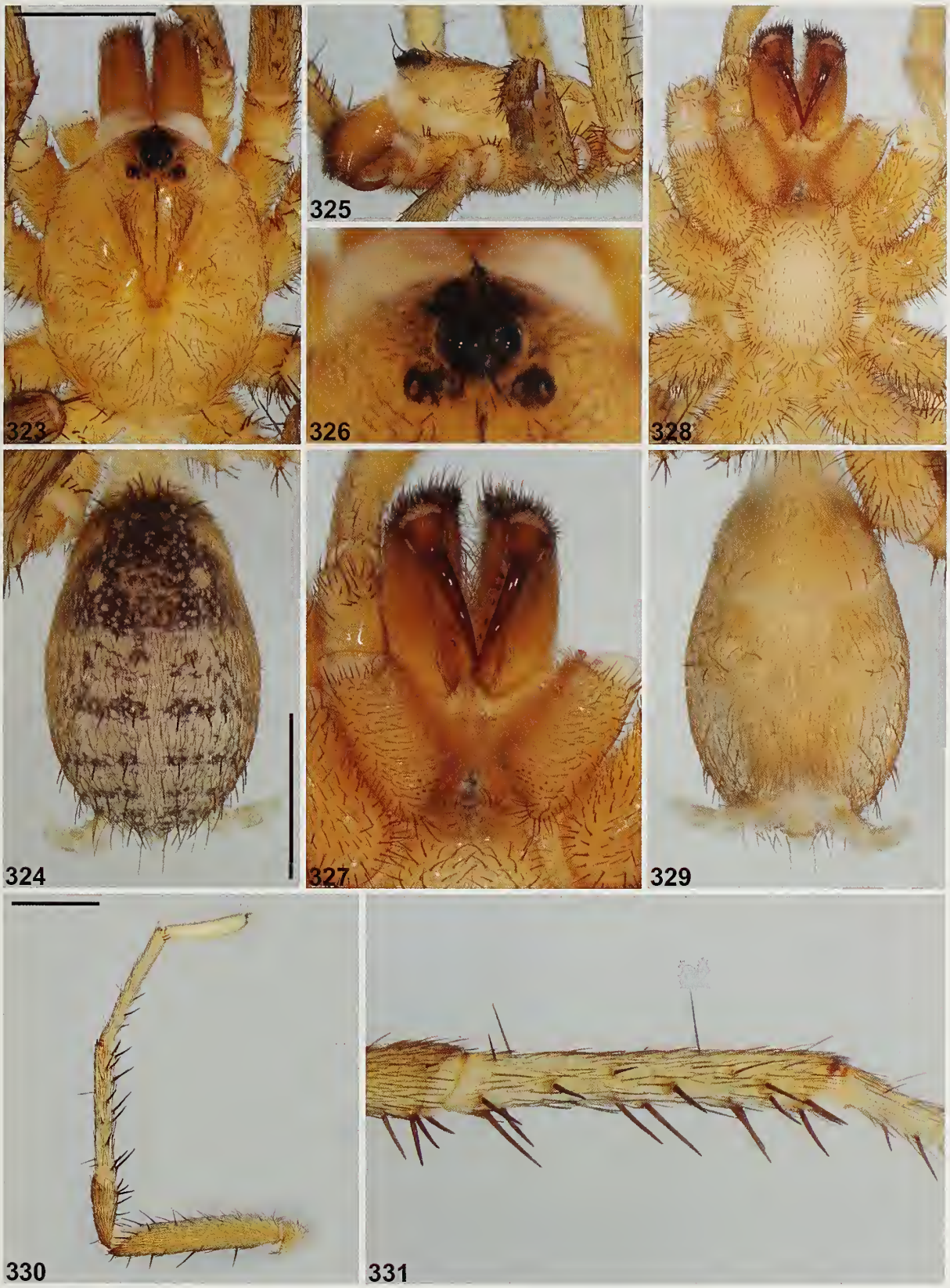


Figures 323–331.—*Bungulla mckenziei* sp. nov., male holotype (WAM T142978) from Zuytdorp (Western Australia; GES), somatic morphology: 323–324, carapace and abdomen, dorsal view; 325, cephalothorax, lateral view; 326, eyes, dorsal view; 327, mouthparts, ventral view; 328–329, cephalothorax and abdomen, ventral view; 330, leg 1, prolateral view; 331, leg I tibia, prolateral view. Scale bars = 2.0 mm.


Figures 332–334.—*Bungulla mckenziei* sp. nov., male holotype (WAM T142978) from Zuytdorp (Western Australia: GES), pedipalp: 332, retrolateral view; 333, retro-ventral view; 334, prolateral view. Scale bar = 2.0 mm.

May–16 August 1995 (WAM T98527); 1 ♂, same data except site ZU4, 27°15′45.1″S, 114°09′12.9″E, 19 May–16 August 1995 (WAM T98555); 1 ♂, Cape Lesueur, North Peron Peninsula (IBRA_CAR), 25°43′S, 113°25′E, pitfall trap, 4 August 1989, G. Harold (WAM T22313); 1 ♂, Edel Land (IBRA_YAL), 26°03′45″S, 113°22′30″E, 15–20 September 1989, G. Harold (WAM T22819); 1 ♂, Edel Land, site EL2 (IBRA_YAL), 26°31′39″S, 113°31′40″E, wet pitfall trap, 9 May–30 August 1995, N. Hall, WAM/CALM Carnarvon Survey (WAM T98557); 1 ♂, False Entrance Well, near stone

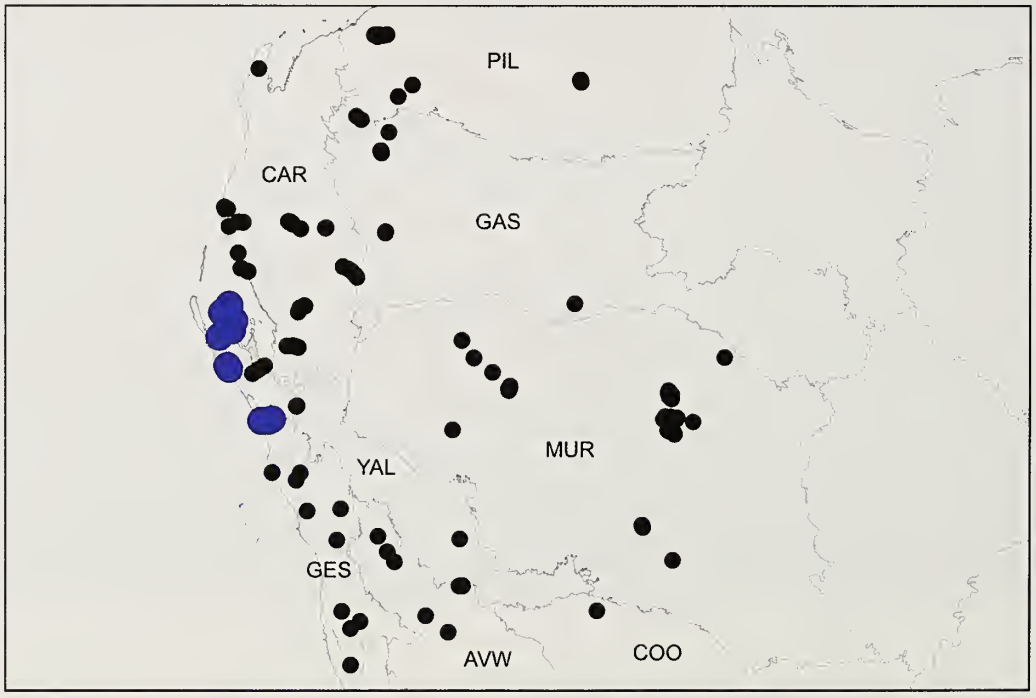


Figure 335.—Map showing collection records of *Bungulla mckenziei* sp. nov. (large blue circles), relative to other taxa with > 10 retrolateral spinules on the male palpal tibia (see Fig. 13). Relevant IBRA 7.0 bioregional acronyms are as follows: AVW, Avon Wheatbelt; CAR, Carnarvon; COO, Coolgardie; GAS, Gascoyne; GES, Geraldton Sandplains; MUR, Murchison; PIL, Pilbara; YAL, Yalgoo.

tank, Carrarang Station, W. side of Shark Bay (IBRA_YAL), 26°29′S, 113°30′E, pitfall trap, 31 May–2 June 1980, D. King & J.D. Roberts (WAM T142980); 1 ♂, Francois Peron National Park, site PE2 (IBRA_CAR), 25°52′30.9″S, 113°32′59.0″E, wet pitfall trap, 25 May–30 August 1995, N. Hall, WAM/CALM Carnarvon Survey (WAM T98558); 1 ♂, same data (WAM T98559); 2 ♂, same data except site PE3, 25°49′14.1″S, 113°32′24.3″E (WAM T98560); 1 ♂, same data except 24 August–11 October, A. Sampey et al., WAM/CALM Carnarvon Survey (WAM T133857); 1 ♂, same data except site PE4, 25°50′20.0″S, 113°36′23.1″E, 23 May–30 August 1995, N. Hall, WAM/CALM Carnarvon Survey (WAM T98561); 1 ♂, same data except site PE5, 25°58′33.6″S, 113°34′14.7″E, 26 May–30 August 1995 (WAM T98526); 1 ♂, Herald Bight (IBRA_CAR), 25°37′30″S, 113°31′50″E, pitfall trap, 30 July 1989, G. Harold (WAM T22820); 1 ♂, same data (WAM T22821); 1 ♂, same data except 25°36′30″S, 113°31′40″E (WAM T27096).

**Etymology.**—This species is named in honor of Norm McKenzie, in recognition of his contributions to the Southern Carnarvon Basin Survey (Burbidge et al. 2000) and to the study of Australian biodiversity.

**Diagnosis.**—Males of *Bungulla mckenziei* can be distinguished from all other known congeners with > 10 retrolateral spinules on the palpal tibia (Fig. 13) – except *B. ajana*, *B. aplini* and *B. keirani* – by the shape of the proximal half of the palpal tibia, which is without a pronounced ventral bulge (Fig. 332), combined with the presence of a medial 'ledge' on the palpal tibia, this ledge situated closely proximal to the field of retrolateral spinules and bearing a brush of filiform setae (Figs. 332, 333) (palpal tibia is without a ledge or bulges ventrally in other species). *Bungulla mckenziei* can be further distinguished from *B. ajana* by the shape of the palpal tibia, which is longer, less bulbous and less strongly arched dorsally (Fig. 332; cf. Fig. 46); from *B. keirani* by the morphology of the cymbial spinules, which are poorly developed and more filiform (Figs. 332–334; cf. Figs. 293–295); and from *B. aplini* by the shape of the palpal tibia, which is broader proximally (Fig. 332; cf. Fig. 59), combined with the presence of a crescent-shaped field of spinules distally (Fig. 332; cf. Fig. 59). Females are unknown.

**Description (male holotype).**—Total length 9.8. Carapace 4.1 long, 3.2 wide. Abdomen 4.2 long, 2.6 wide. Carapace (Fig. 323) tan, with slightly darker pars cephalica, darkened lateral rims and mostly black ocular region; postero-lateral corners near abdomen each with pair of porrect black setae; fovea straight. Eye group (Fig. 326) trapezoidal (anterior eye row strongly procurved), 0.9 x as long as wide, PLE–PLE/ALE–ALE ratio 1.6; ALE separated by ca. half their own diameter; AME separated by less than their own diameter; PME separated by 3.5 x their own diameter; PME and PLE separated by diameter of PME, PME positioned in line with level of PLE. Maxillae with field of cuspules confined to inner corner (Fig. 327); labium without cuspules. Abdomen (Fig. 324) oval, sandy-beige in dorsal view with darker brown-black markings anteriorly and six pairs of thin, spotted, brown-black chevrons posteriorly, each divided along midline. Dorsal surface of abdomen (Fig. 324) with sparse arrangement of stiff, porrect black setae, each with slightly raised, dark brown sclerotic base; sclerotized sigilla absent. Legs (Figs. 330, 331) variable shades of tan, with light scopulae on tarsi I–II; metatarsus I and tarsus I lighter in color; tibia I heavily spinose, without prolateral clasping spurs. Leg I: femur 3.8; patella 1.7; tibia 3.1; metatarsus 2.9; tarsus 1.8; total 13.4. Leg I femur–tarsus/carapace length ratio 3.3. Pedipalpal tibia (Figs. 332–334) relatively long, 2.3 x longer than wide, with small medial 'ledge' bearing a brush of filiform setae; field of retrolateral spinules crescent-shaped, positioned distally (separated from retro-ventral margin in retrolateral view), consisting of ca. 60 spinules of largely similar length; RTA absent. Cymbium (Figs. 332–334) setose, with field of relatively poorly developed (almost filiform) spinules covering most of dorsal surface. Embolus (Figs. 332–334) as long as bulb, strongly curved, with unmodified tip; embolic apophysis absent.

**Distribution and remarks.**—*Bungulla mckenziei* (formerly known by WAM identification codes 'MYG134' and 'MYG135') has a relatively restricted distribution in the northern Geraldton Sandplains, Yalgoo and southern Carnarvon bioregions of Western Australia, from Zuytdorp north to the Peron Peninsula (Fig. 335). Nothing is known of the biology of this species, other than that the known male specimens were collected wandering in search of females in winter, spring and possibly late autumn.

***Bungulla oraria*** Rix, Raven & Harvey, sp. nov.
http://zoobank.org/?lsid=urn:lsid:zoobank.org:act:84F1D51F-FE7E-4DB5-9240-7500AD4E4BE7
(Figs. 12, 336–348)

*Bungulla* sp. 'Torndirrup National Park' Rix et al., 2017d: 603, figs 146–147, 151, 154, 157.

**Type material.**—*Holotype male.* AUSTRALIA: *Western Australia*: Torndirrup National Park (IBRA_WAR), 35°06′S, 117°52′E, pitfall trap, 1983, P. Dyon & J. Lyon (WAM T139595).

*Paratype.* AUSTRALIA: *Western Australia*: 1 ♂, same data as holotype (WAM T142945).

**Etymology.**—The specific epithet is derived from the Latin 'orarius' (adjective: 'of the coast'; see Brown 1956), in reference to the coastal distribution of this species at Torndirrup National Park.

**Diagnosis.**—Males of *Bungulla oraria* can be distinguished from all other known congeners with < 5 retrolateral spinules on the palpal tibia (Fig. 12) – except *B. disrupta*, *B. fusca*, *B. hillyerae*, *B. inermis* and *B. parva* – by the shape of the cymbial spinules, which are curved, anteriorly-directed and restricted to the distal half of the cymbium (Figs. 345–347) (spinules are porrect, thorn-like, and cover most of the dorsal surface of the cymbium in other species). *Bungulla oraria* can be further distinguished from *B. parva* by its larger body size (carapace width ≥ 4.5) (Fig. 336; cf. Fig. 349); from *B. hillyerae* and *B. inermis* by the darker carapace coloration (depending on the state of preservation; see Supplementary File 1) (Fig. 336; cf. Figs. 232, 245); and from *B. disrupta* and *B. fusca* by the shape of the palpal tibia, which is sub-rectangular in retrolateral view, with a strongly concave disto-ventral margin (Fig. 345; cf. Figs. 160, 195).

**Description (male holotype).**—Total length 15.3. Carapace 7.1 long, 5.7 wide. Abdomen 7.2 long, 4.5 wide. Carapace (Fig.

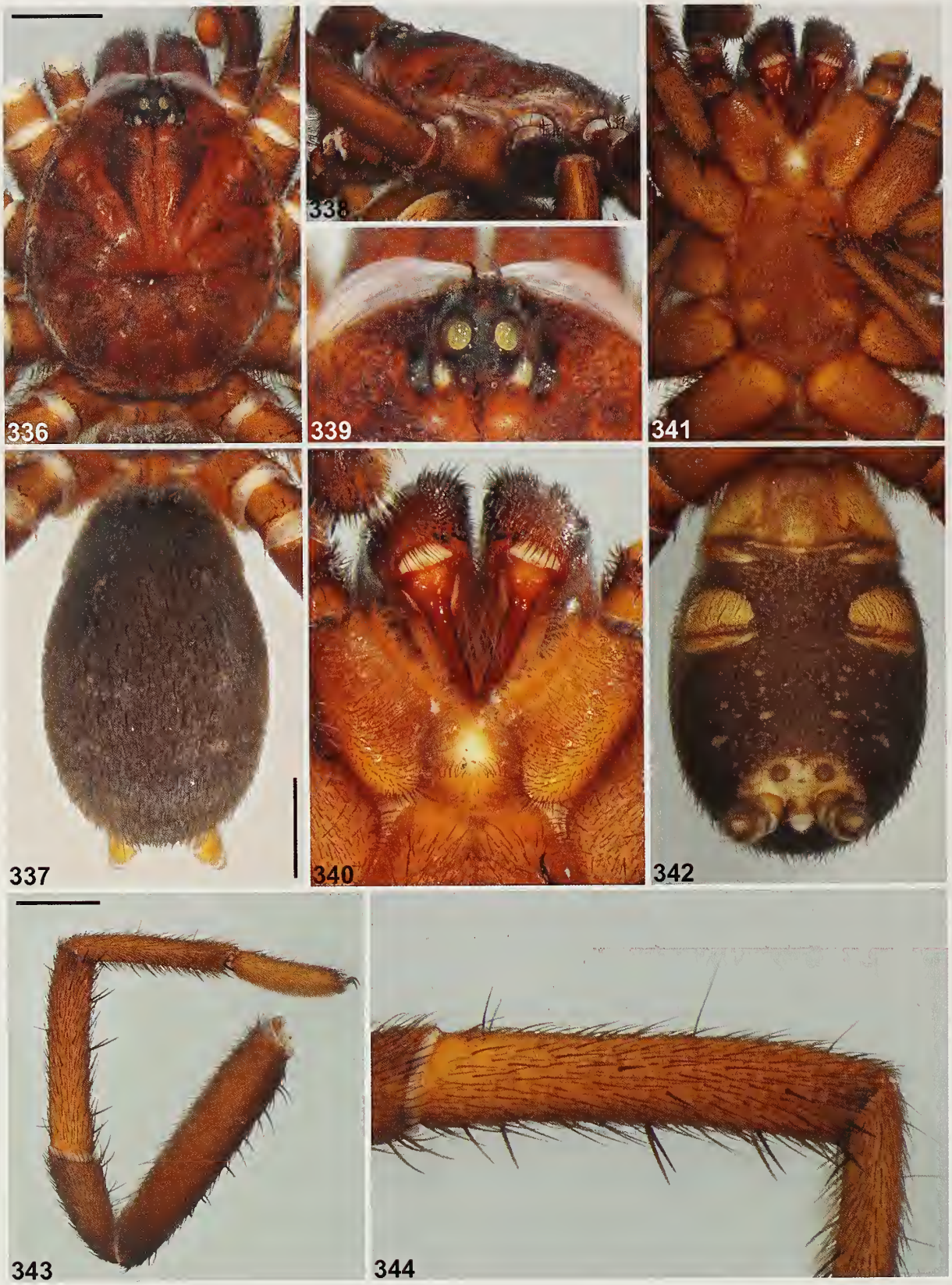


Figures 336–344.—*Bungulla oraria* sp. nov., male holotype (WAM T139595) from Torndirrup National Park (Western Australia; WAR). somatic morphology: 336–337, carapace and abdomen, dorsal view; 338, cephalothorax, lateral view; 339, eyes, dorsal view; 340, mouthparts, ventral view; 341–342, cephalothorax and abdomen, ventral view; 343, leg I, prolateral view; 344, leg I tibia, prolateral view. Scale bars = 2.0 mm.


Figures 345–347.—*Bungulla oraria* sp. nov., male holotype (WAM T139595) from Torndirrup National Park (Western Australia; WAR), pedipalp: 345, retrolateral view; 346, retro-ventral view; 347, prolateral view. Scale bar = 2.0 mm.

336) dark chocolate-brown, with darker brown lyre-like pattern on pars cephalica and black ocular region; fovea straight. Eye group (Fig. 339) trapezoidal (anterior eye row strongly procurved), 0.8 x as long as wide, PLE–PLE/ALE–ALE ratio 1.8; ALE separated by nearly their own diameter; AME separated by less than their own diameter; PME separated by 3.0 x their own diameter; PME and PLE separated by slightly less than diameter of PME, PME

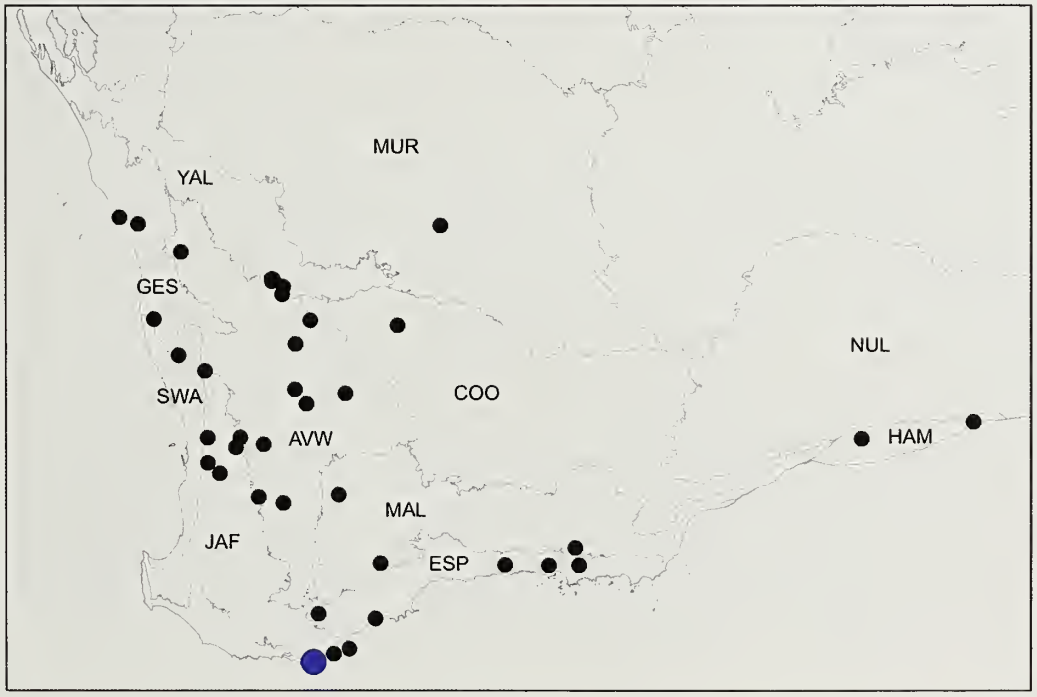


Figure 348.—Map showing collection records of *Bungulla oraria* sp. nov. (large blue circles), relative to other taxa with < 5 retrolateral spinules on the male palpal tibia (see Fig. 12). Relevant IBRA 7.0 bioregional acronyms are as follows: AVW, Avon Wheatbelt; COO, Coolgardie; ESP, Esperance Plains; GES, Geraldton Sandplains; HAM, Hampton; JAF, Jarrah Forest; MAL, Mallee; MUR, Murchison; NUL, Nullarbor; SWA, Swan Coastal Plain; YAL, Yalgoo.

positioned in line with level of PLE. Maxillae with field of cuspules confined to inner corner (Fig. 340); labium without cuspules. Abdomen (Fig. 337) oval, dark brown-black in dorsal view with faint beige-tan mottling, two pairs of small beige-tan sigilla spots and two indistinct pairs of beige-tan chevrons posteriorly, each divided along midline. Dorsal surface of abdomen (Fig. 337) with sparse arrangement of stiff, porrect black setae, each with slightly raised, dark brown sclerotic base; sclerotized sigilla absent. Legs (Figs. 343, 344) variable shades of dark tan on tibiae–tarsi, with slightly darker brown femora–patellae and light scopulae on tarsi I–II; tibia I spinose, without prolateral clasping spurs. Leg I: femur 6.5; patella 3.2; tibia 4.8; metatarsus 4.2; tarsus 2.6; total 21.2. Leg I femur–tarsus/carapace length ratio 3.0. Pedipalpal tibia (Figs. 345–347) sub-rectangular, 2.0 x longer than wide, without retrolateral spinules; RTA absent. Cymbium (Figs. 345–347) setose, with field of curved, anteriorly-directed spine-like spinules restricted to distal half of segment. Embolus (Figs. 345–347) slightly longer than bulb, slightly curved, with unmodified tip; embolic apophysis absent.

**Distribution and remarks.**—*Bungulla oraria* is a rare and highly restricted species known only from the Torndirrup Peninsula, near Albany (Western Australia) (Fig. 348). Nothing is known of the biology of this species.

***Bungulla parva*** Rix, Raven & Harvey, sp. nov.
http://zoobank.org/?lsid=urn:lsid:zoobank.org:act:D1ED4C2C-E5CE-4D3C-9ECD-5DA27B92F4A7
(Figs. 12, 349–361)

**Type material.**—*Holotype male*. AUSTRALIA: *Western Australia*: Mount Cooke (IBRA_JAF), 32°25′S, 116°18′E, hand collected, 31 July 1991, M.S. Harvey & J.M. Waldock (WAM T27102).

*Paratypes*. AUSTRALIA: *Western Australia*: 1 ♂, same data as holotype (WAM T27104); 1 ♂, same data (WAM T27105).

**Other material examined.**—AUSTRALIA: *Western Australia*: 1 ♂, ALCOA minesite and forests, N. and NW. of Jarrahdale (IBRA_JAF), 32°16′S, 116°06′E, 1 March–1 August 1993, S.J. Simmonds (WAM T31782).

**Etymology.**—The specific epithet is derived from the Latin 'parvus' (adjective: 'little'; see Brown 1956), in reference to the very small size of this species.

**Diagnosis.**—Males of *Bungulla parva* can be distinguished from all other known congeners with < 5 retrolateral spinules on the palpal tibia (Fig. 12) – except *B. distrupta*, *B. fusca*, *B. hillyerae*, *B. inermis* and *B. oraria* – by the shape of the cymbial spinules, which are curved, anteriorly-directed and restricted to the distal half of the cymbium (Figs. 358–360) (spinules are porrect, thorn-like, and cover most of the dorsal surface of the cymbium in other species). *Bungulla parva* can be further distinguished from *B. distrupta*, *B. fusca*, *B. hillyerae*, *B. inermis* and *B. oraria* by its very small body size, with a carapace width of < 2.5 (Fig. 349; cf. Figs. 151, 186, 232, 245, 336). Females are unknown.

**Description (male holotype).**—Total length 6.2. Carapace 2.9 long, 2.3 wide. Abdomen 2.9 long, 2.1 wide. Carapace (Fig. 349) chocolate-brown, with darker pars cephalica and black ocular region; fovea straight. Eye group (Fig. 352) trapezoidal (anterior eye row strongly procurved), 0.8 x as long as wide, PLE–PLE/ALE–ALE ratio 1.4; ALE separated by ca. half their own diameter; AME separated by less than their own diameter; PME separated by 3.9 x their own diameter; PME and PLE separated by slightly less than diameter of PME, PME positioned in line with level of PLE. Maxillae with field of cuspules confined to inner corner (Fig. 353); labium without cuspules. Abdomen (Fig. 350) oval, dark olive-brown in dorsal view with beige-tan mottling, two pairs of beige-tan sigilla spots and four pairs of beige-tan chevrons posteriorly, each divided along midline. Dorsal surface of abdomen (Fig. 350) with sparse arrangement of stiff, porrect black setae, each with slightly raised, dark brown sclerotic base; sclerotized sigilla absent. Legs (Figs. 356, 357) variable shades of tan, with light scopulae on semi-incrassate tarsi I–II; tibia I largely aspinose, without prolateral clasping spurs. Leg I: femur 2.3; patella 1.2; tibia 1.8; metatarsus 1.3; tarsus 1.0; total 7.7. Leg I femur–tarsus/carapace length ratio 2.7. Pedipalpal tibia (Figs. 358–360) nearly 2.0 x longer than wide, without retrolateral spinules; RTA absent. Cymbium (Figs. 358–360) setose, with field of curved, anteriorly-directed spine-like spinules restricted to distal half of segment. Embolus (Figs. 358–360) twice length of bulb, relatively straight, with unmodified tip; embolic apophysis absent.

**Distribution and remarks.**—*Bungulla parva* (formerly known by WAM identification code 'MYG151') is known only from the northern Jarrah Forest bioregion of south-western Australia, from Jarrahdale south to Mount Cooke (Fig. 361). Nothing is known of the biology of this small and extremely rare species, other than that the known male specimens were collected wandering in search of females in winter, spring and possibly autumn.

***Bungulla quobba*** Rix, Raven & Harvey, sp. nov.
http://zoobank.org/?lsid=urn:lsid:zoobank.org:act:8F3279ED-4910-4F24-9EA2-C55B869A03D0
(Figs. 13, 362–374)

**Type material.**—*Holotype male*. AUSTRALIA: *Western Australia*: Cape Cuvier, Quobba Station, site CU4 (IBRA_CAR), 24°13′27.1″S, 113°27′40.8″E, wet pitfall trap, 30 May–24 August 1995, N. Hall, WAM/CALM Carnarvon Survey (WAM T142996).

**Other material examined.**—AUSTRALIA: *Western Australia*: 1 ♂, Cape Cuvier, Quobba Station, site CU3 (IBRA_CAR), 24°13′25.3″S, 113°29′30.7″E, wet pitfall trap, 30 May–24 August 1995, N. Hall, WAM/CALM Carnarvon Survey (WAM T142998); 1 ♂, same data except site CU5, 24°11′34.0″S, 113°27′17.4″E, 29 May–25 August 1995 (WAM T142997).

**Etymology.**—The specific epithet is a noun in apposition, in reference to the type locality of this species.

**Diagnosis.**—Males of *Bungulla qnobba* can be distinguished from all other known congeners with > 10 retrolateral spinules on the palpal tibia (Fig. 13) – except *B. banksia*, *B. bertmaini*, *B. bidgemia*, *B. hamelinensis*, *B. iota*, *B. laevigata*, *B. weld* and *B. yeni* – by the shape of the proximal half of the palpal tibia, which is without a pronounced ventral bulge (Fig. 371), combined with the absence of a medial 'ledge' on the palpal tibia (Figs. 371, 372) (palpal tibia is with a ledge or bulges ventrally in other species). *Bungulla qnobba* can be further distinguished from

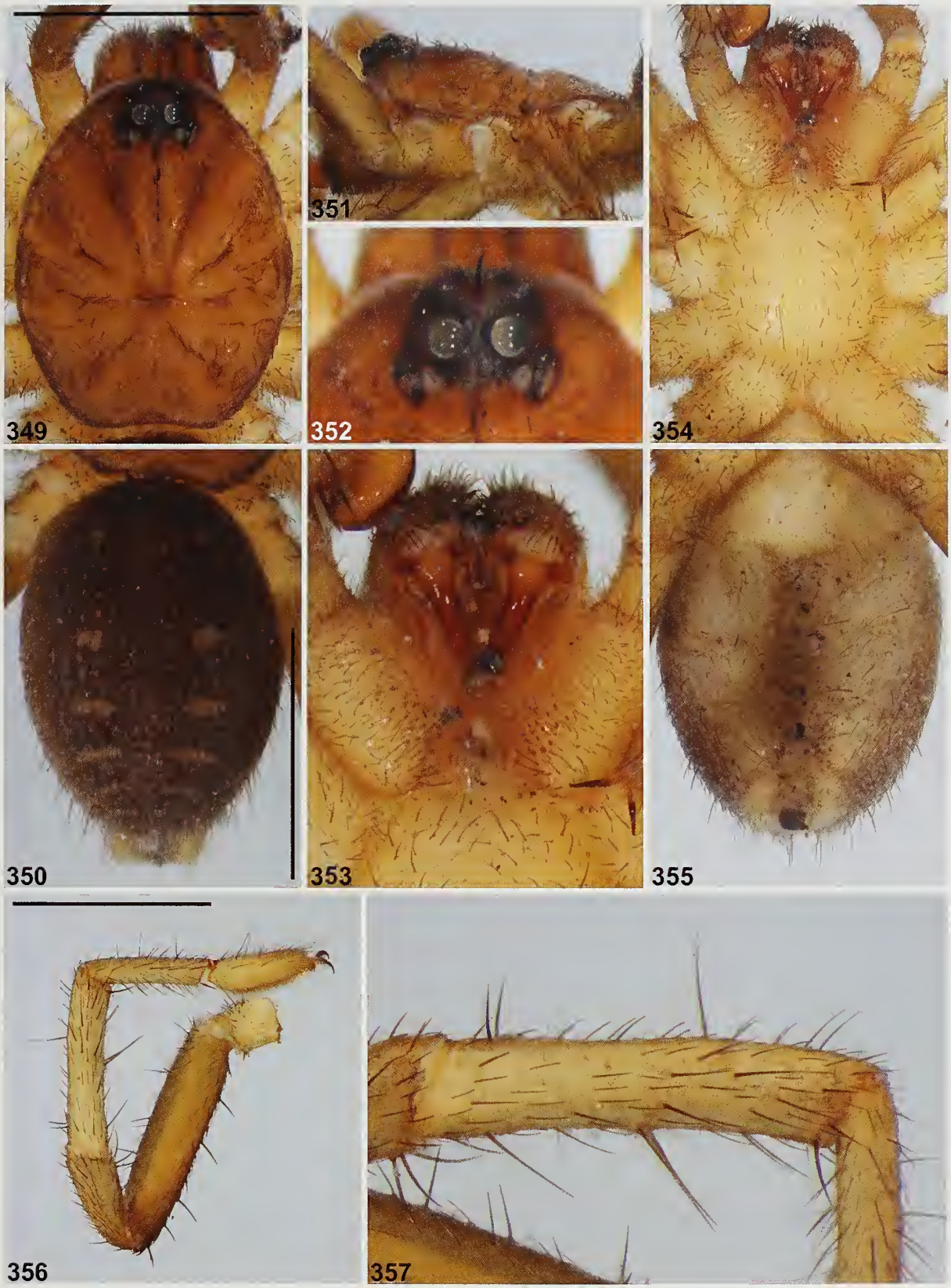


Figures 349–357.—*Bungulla parva* sp. nov., male holotype (WAM T27102) from Mount Cooke (Western Australia: JAF), somatic morphology: 349–350, carapace and abdomen, dorsal view; 351, cephalothorax, lateral view; 352, eyes, dorsal view; 353, mouthparts, ventral view; 354–355, cephalothorax and abdomen, ventral view; 356, leg I, prolateral view; 357, leg 1 tibia, prolateral view. Scale bars = 2.0 mm.


Figures 358–360.—*Bungulla parva* sp. nov., male holotype (WAM T27102) from Mount Cooke (Western Australia; JAF), pedipalp: 358, retrolateral view; 359, retro-ventral view; 360, prolateral view. Scale bar = 2.0 mm.

*B. banksia*, *B. bidgemia*, *B. iota*, *B. hamelinensis*, *B. weld* and *B. yeni* by the shape of the embolus, which is relatively long (i.e., longer than the bulb) (Fig. 371; cf. Figs. 72, 95, 218, 267, 419, 445); and from *B. bertmaini* and *B. laevigata* by the shape of the embolus, which is slightly shorter and relatively straight in standard retrolateral view (Fig. 371; cf. Figs. 24, 319), combined with the shape of the palpal tibia, which is extended distally (distal to spinules), with a strongly concave

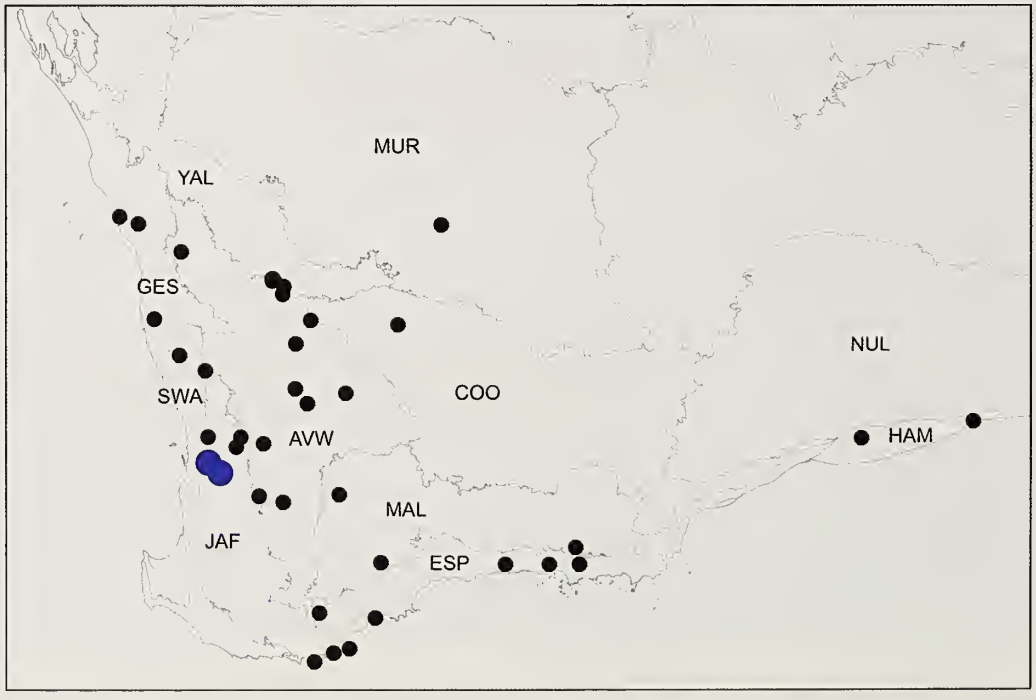


Figure 361.—Map showing collection records of *Bungulla parva* sp. nov. (large blue circles), relative to other taxa with < 5 retrolateral spinules on the male palpal tibia (see Fig. 12). Relevant IBRA 7.0 bioregional acronyms are as follows: AVW, Avon Wheatbelt; COO, Coolgardie; ESP, Esperance Plains; GES, Geraldton Sandplains; HAM, Hampton; JAF, Jarrah Forest; MAL, Mallee; MUR, Murchison; NUL, Nullarbor; SWA, Swan Coastal Plain; YAL, Yalgoo.

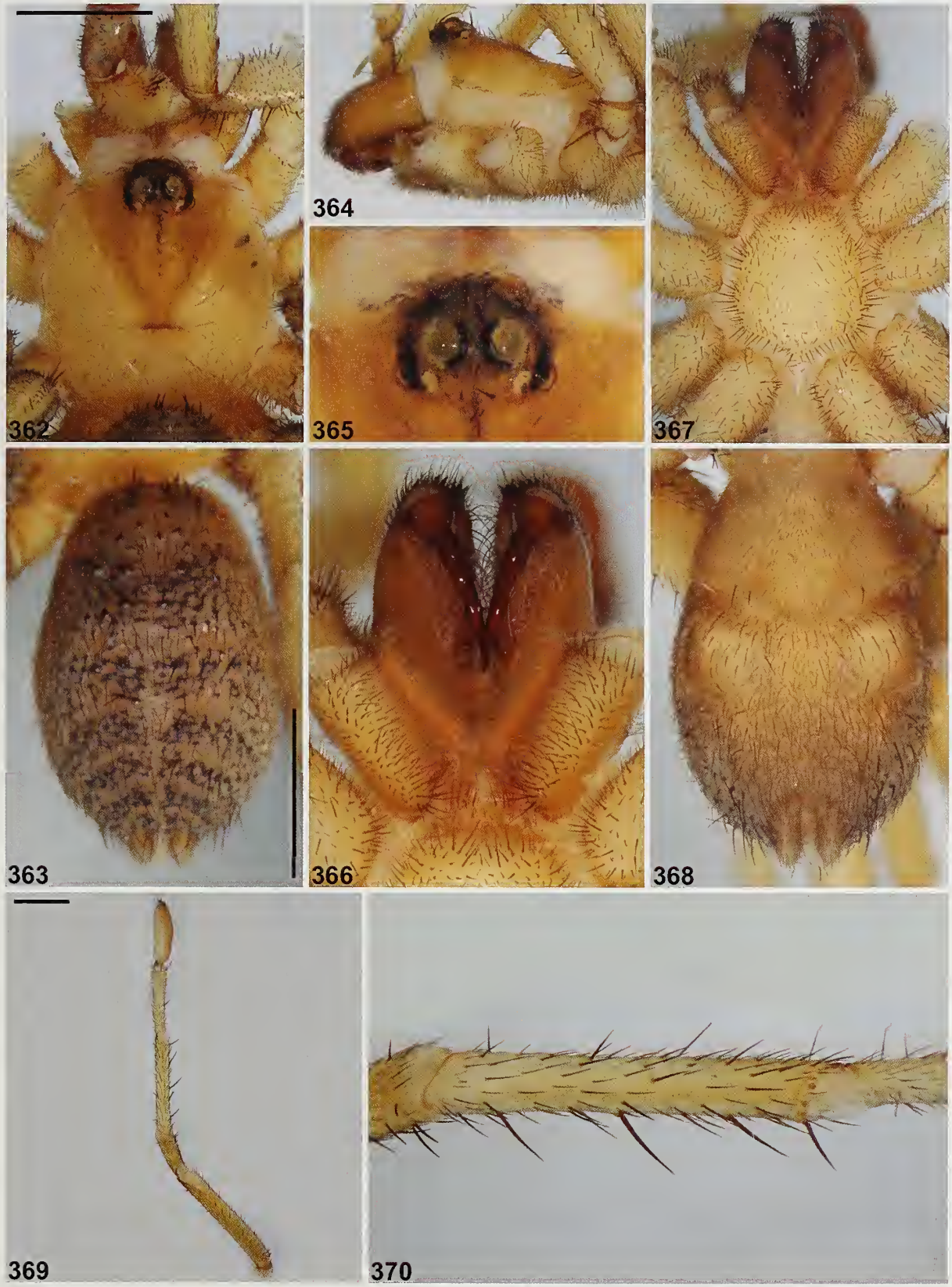


Figures 362–370.—*Bungulla quobba* sp. nov., male holotype (WAM T142996) from Cape Cuvier, Quobba Station (Western Australia; CAR), somatic morphology: 362–363, carapace and abdomen, dorsal view; 364, cephalothorax, lateral view; 365, eyes, dorsal view; 366, mouthparts, ventral view; 367–368, cephalothorax and abdomen, ventral view; 369, leg I, prolateral view; 370, leg I tibia, prolateral view. Scale bars = 2.0 mm.


Figures 371–373.—*Bungulla quobba* sp. nov., male holotype (WAM T142996) from Cape Cuvier, Quobba Station (Western Australia; CAR), pedipalp: 371, retrolateral view; 372, retro-ventral view; 373, prolateral view. Scale bar = 2.0 mm.

disto-ventral margin in retrolateral view (Fig. 371; cf. Figs. 24, 319). Females are unknown.

**Description (male holotype).**—Total length 10.0. Carapace 3.8 long, 3.3 wide. Abdomen 4.2 long, 2.9 wide. Carapace (Fig. 362) pale tan, with darker pars cephalica, darker tan lyre-like pattern on pars cephalica and mostly grey-black ocular region; fovea straight. Eye group (Fig. 365) trapezoidal (anterior eye row strongly procurved), 0.7 x as long as wide, PLE–PLE/

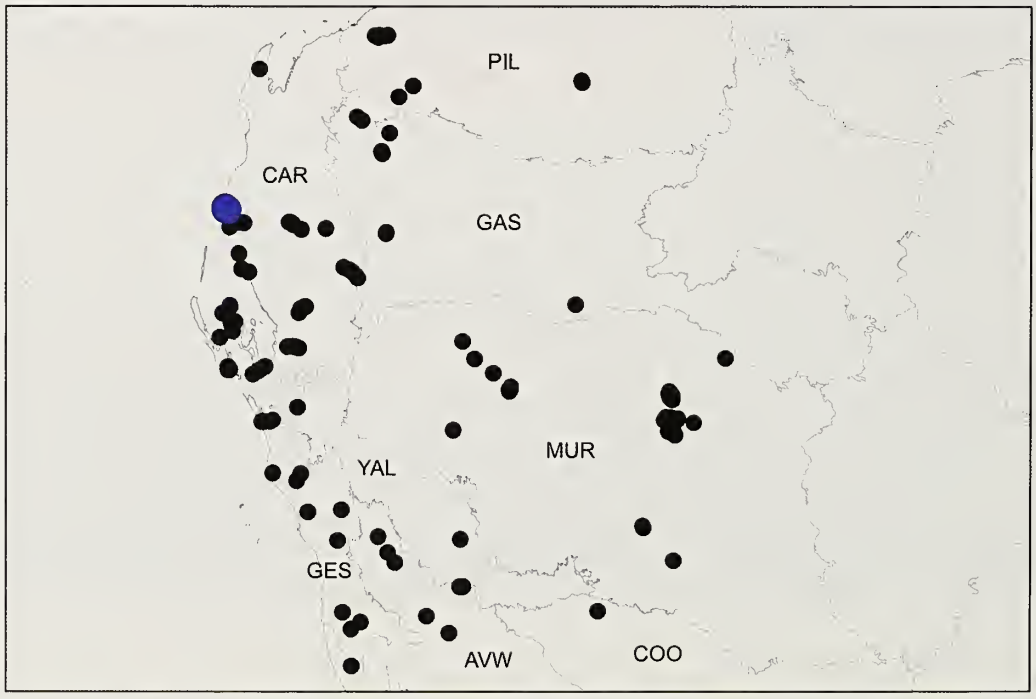


Figure 374.—Map showing collection records of *Bungulla quobba* sp. nov. (large blue circles), relative to other taxa with > 10 retrolateral spinules on the male palpal tibia (see Fig. 13). Relevant IBRA 7.0 bioregional acronyms are as follows: AVW, Avon Wheatbelt; CAR, Carnarvon; COO, Coolgardie; GAS, Gascoyne; GES, Geraldton Sandplains; MUR, Murchison; PIL, Pilbara; YAL, Yalgoo.

ALE–ALE ratio 1.5; ALE separated by ca. their own diameter; AME separated by less than their own diameter; PME separated by 4.3 x their own diameter; PME and PLE separated by diameter of PME, PME positioned slightly posterior to level of PLE. Maxillae and labium without cuspules (Fig. 366). Abdomen (Fig. 363) oval, sandy-tan in dorsal view with darker brown-black markings anteriorly and five pairs of spotted, brown-black chevrons posteriorly, each divided along midline. Dorsal surface of abdomen (Fig. 363) with sparse arrangement of stiff, porrect black setae, each with slightly raised, dark brown sclerotic base; sclerotized sigilla absent. Legs (Figs. 369, 370) variable shades of tan, with light scopulae on tarsi I–II; tibia I spinose, without prolateral clasping spurs. Leg I: femur 4.3; patella 1.9; tibia 3.3; metatarsus 2.5; tarsus 2.1; total 14.2. Leg 1 femur–tarsus/carapace length ratio 3.7. Pedipalpal tibia (Figs. 371–373) nearly 2.0 x longer than wide; field of retrolateral spinules oval in shape, positioned medially, consisting of 18 spinules, the latter longest proximally; RTA absent. Cymbium (Figs. 371–373) setose, with field of spine-like spinules covering most of dorsal surface. Embolus (Figs. 371–373) ca. 1.5 x length of bulb, relatively straight, with unmodified tip; embolic apophysis absent.

**Distribution and remarks.**—*Bungulla quobba* is known only from Quobba Station, on the Cuvier Peninsula north of Carnarvon (Western Australia) (Fig. 374). Nothing is known of the biology of this species, other than that the known male specimens were collected wandering in search of females in winter or possibly late autumn.

***Bungulla riparia*** (Main, 1957)
(Figs. 12, 375–396)

*Eucyrtops riparius* Main, 1957: 419, figs 3A, 4D–F, 7B, 8A (NB. figs 5D, 8D, 8E probably not conspecific).
*Bungulla riparia* (Main): Rix et al., 2017d: 607, figs 150, 155, 156.

**Type material.**—*Holotype female*. AUSTRALIA: *Western Australia*: 1 mile S. of Mount Misery, W. of Moora (IBRA_GES), 30°42′S, 115°37′E, 26 May 1954, B.Y. Main (WAM T3961; examined).

*Paratype*. AUSTRALIA: *Western Australia*: 1 ♂, same data as holotype except 5 April 1956 (WAM T17708).

**Other material examined.**—AUSTRALIA: *Western Australia*: 1 ♂, Mount Misery, W. of Moora (IBRA_GES), 30°42′S, 115°37′E, 5 April 1956, B.Y. Main (WAM T139594); 1 ♂, same data (WAM T142933); 1 ♂, same data (WAM T142934); 1 ♂, same data (WAM T142935); 1 ♂, same data (WAM T142936); 1 ♂, Mount Lesueur (IBRA_GES), 30°10′S, 115°12′E, pitfall trap, 1989, K. Gaul (WAM T142932).

**Diagnosis.**—Males of *Bungulla riparia* can be distinguished from all other known congeners with < 5 retrolateral spinules on the palpal tibia (Fig. 12) – except *B. bringo* and *B. ferraria* – by the shape of the cymbial spinules, which are porrect, thorn-like, and cover most of the dorsal surface of the cymbium (Figs. 393–395) (spinules more curved, anteriorly-directed and restricted to distal half of cymbium in other species). *Bungulla riparia* can be further distinguished from *B. bringo* by the absence of retrolateral spinules on the palpal tibia (Fig. 393; cf. Figs. 121, 122); and from *B. ferraria* by the presence of ≥ 4 prolateral (medial) spine-like setae on tibia I (Fig. 392; cf. Fig. 181), combined with the shape of the palpal tibia, which is relatively stout, without a strongly concave disto-ventral margin in retrolateral view (Fig. 393; cf. Fig. 182).

**Description (female holotype).**—Total length 18.7. Carapace 6.5 long, 5.4 wide. Abdomen 10.2 long, 7.5 wide. Carapace (Fig. 375) tan with slightly darker ocular region; fovea strongly procurved. Eye group (Fig. 378) trapezoidal (anterior eye row strongly procurved), 0.8 x as long as wide, PLE–PLE/ALE–ALE ratio 1.6; ALE separated by nearly their own diameter; AME separated by their own diameter; PME separated by 3.1 x their own diameter; PME and PLE separated by diameter of PME, PME positioned slightly anterior to level of PLE. Maxillae with field of cuspules confined to inner corner (Fig. 379); labium without cuspules. Abdomen (Fig. 376) oval, olive-brown in dorsal view, with two pairs of beige sigilla spots, and three pairs of beige chevrons posteriorly, each divided along midline; sclerotized sigilla absent. Legs (Figs. 381, 382) variable shades of tan; thick scopulae present on tarsi and metatarsi I–II; tibia I with 6 stout prolateral macrosetae, 4 retro-ventral spine-like macrosetae and 5 shorter retro-ventral macrosetae; metatarsus I with 3 stout pro-ventral macrosetae and 7 mostly longer retro-ventral macrosetae; tarsus I with distal cluster of 2 stout ventral macrosetae. Leg I: femur 4.6; patella 2.8; tibia 2.8; metatarsus 2.1; tarsus 1.4; total 13.7. Leg I femur–tarsus/carapace length ratio 2.1. Pedipalp tan, spinose on tibia and tarsus, with thick tarsal scopula. Genitalia (Fig. 383) with pair of short, widely spaced, bud-shaped spermathecae.

**Description (male WAM T139594).**—Total length 12.3. Carapace 5.4 long, 4.4 wide. Abdomen 5.5 long, 3.6 wide. Carapace (Fig. 384) tan, with slightly darker pars cephalica and slightly darker ocular region; postero-lateral corners near abdomen each with marginal cluster of longer black setae; fovea straight. Eye group (Fig. 387) trapezoidal (anterior eye row strongly procurved), 0.9 x as long as wide, PLE–PLE/ALE–ALE ratio 1.4; ALE separated by ca. half their own diameter; AME separated by less than their own diameter; PME separated by 3.9 x their own diameter; PME and PLE separated by diameter of PME, PME positioned in line with level of PLE. Maxillae with field of cuspules confined to inner corner (Fig. 388); labium without cuspules. Abdomen (Fig. 385) oval, dark olive-brown in dorsal view with beige-tan mottling, two pairs of small beige-tan sigilla spots, and three indistinct pairs of beige-tan chevrons posteriorly, each divided along midline. Dorsal surface of abdomen (Fig. 385) with sparse arrangement of stiff, porrect black setae, each with slightly raised, dark brown sclerotic base; sclerotized sigilla absent. Legs (Figs. 391, 392) variable shades of tan, with light scopulae on tarsi I–II; tibia I spinose, without prolateral clasping spurs. Leg I: femur 5.5; patella 2.7; tibia 4.0; metatarsus 3.6; tarsus 2.6; total 18.4. Leg I femur–tarsus/carapace length ratio 3.4. Pedipalpal tibia (Figs. 393–395) stout, 2.0 x longer than wide, without retrolateral spinules; RTA absent. Cymbium (Figs. 393–395) setose, with field of porrect, thorn-like spinules covering most of dorsal surface. Embolus (Figs. 393–395) as long as bulb, slightly curved, with unmodified tip; embolic apophysis absent.

**Distribution and remarks.**—*Bungulla riparia* has a relatively restricted distribution in the southern Geraldton Sandplains

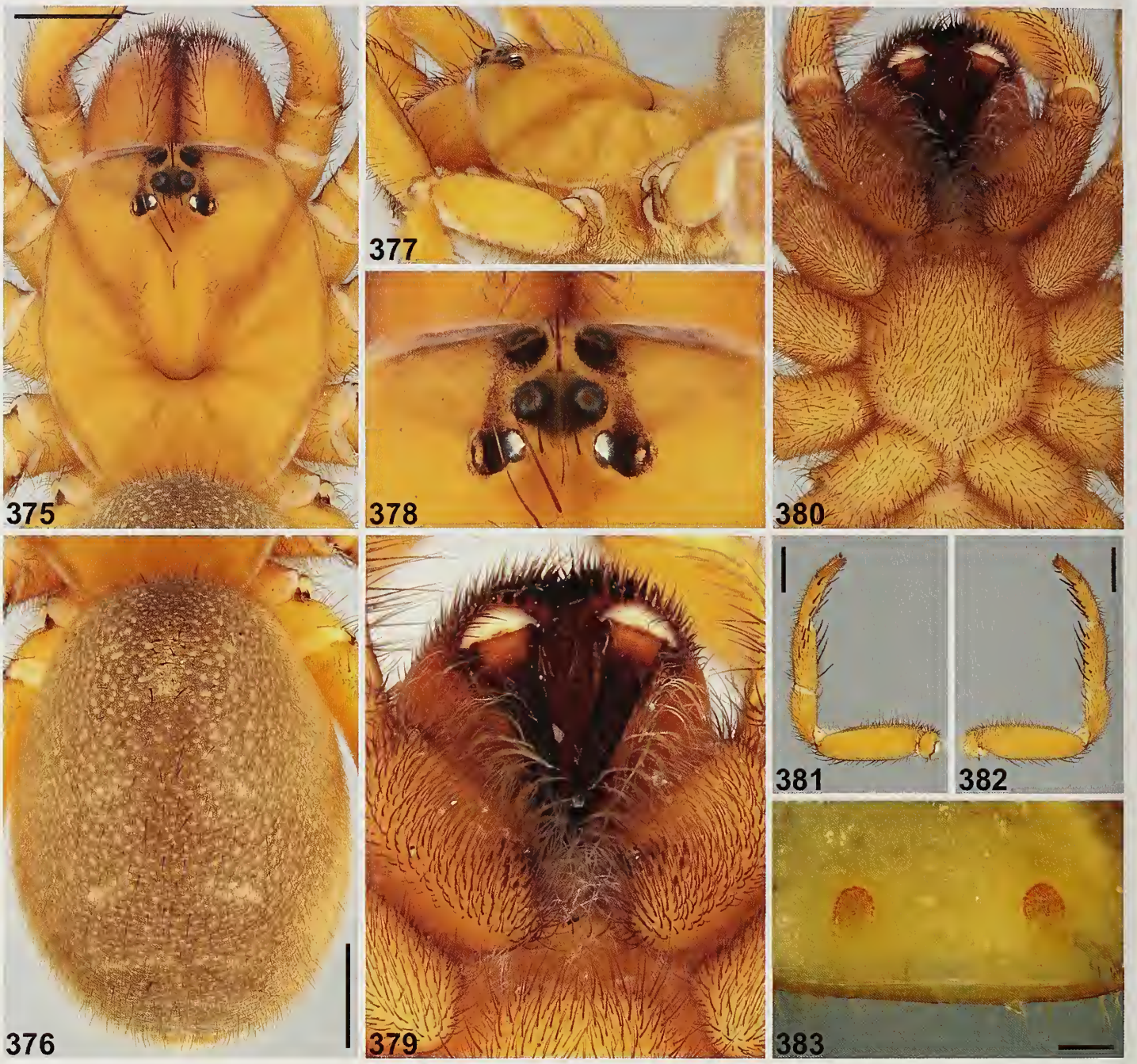


Figures 375–383.—*Bungulla riparia* (Main, 1957), female holotype (WAM T3961) from S. of Mount Misery, W. of Moora (Western Australia; GES): 375–376, carapace and abdomen, dorsal view; 377, cephalothorax, lateral view; 378, eyes, dorsal view; 379, mouthparts, ventral view; 380, cephalothorax, ventral view; 381, leg I, prolateral view; 382, leg I, retrolateral view; 383, spermatheeae, dorsal view. Scale bars = 2.0 mm (375–376, 381–382), 0.5 mm (383).

bioregion of south-western Australia, from Lesueur National Park, south to Mount Misery (Fig. 396). Burrows were documented by Main (1957, pl. 1, fig. 1), who reported collecting specimens from a creek bank, and known male specimens were collected (wandering in search of females or possibly in burrows) in mid- to late autumn.

***Bnngnlla sampeyae*** Rix, Raven & Harvey, sp. nov.
http://zoobank.org/?lsid=urn:lsid:zoobank.org:act:468B7133-7938-4215-A499-948CF1F78662
(Figs. 13, 397–409)

**Type material.**—*Holotype male*. AUSTRALIA: *Western Australia*: Zuytdorp, site ZU4 (IBRA_GES), 27°15′45.1″S, 114°09′12.9″E, wet pitfall trap, 18 May–16 August 1995, N. Hall (WAM T98523).

**Other material examined.**—AUSTRALIA: *Western Australia*: 3 ♂, Edel Land, site EL1 (IBRA_YAL), 26°31′44″S,

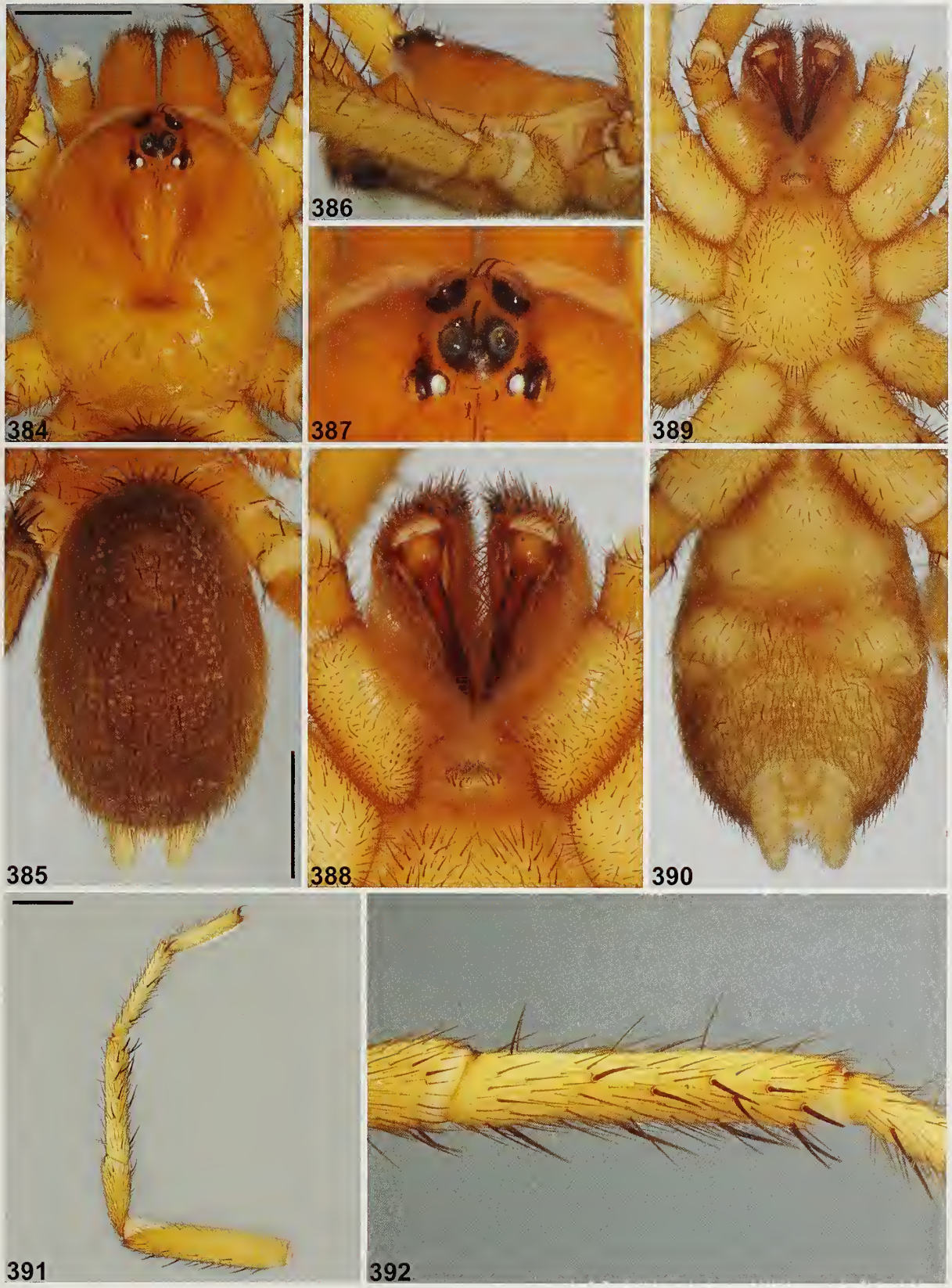


Figures 384–392.—*Bungulla riparia* (Main, 1957), male (WAM T139594) from Mount Misery, W. of Moora (Western Australia; GES), somatic morphology: 384–385, carapace and abdomen, dorsal view; 386, cephalothorax, lateral view; 387, eyes, dorsal view; 388, mouthparts, ventral view; 389–390, cephalothorax and abdomen, ventral view; 391, leg I, prolateral view; 392, leg I tibia, prolateral view. Scale bars = 2.0 mm.


Figures 393–395.—*Bungulla riparia* (Main, 1957), male (WAM T139594) from Mount Misery, W. of Moora (Western Australia; GES), pedipalp: 393, retrolateral view; 394, retro-ventral view; 395, prolateral view. Scale bar = 2.0 mm.

113°29′56″E, wet pitfall trap, 9 May–30 August 1995, N. Hall (WAM T98525); 1 ♂, same data except site EL2, 26°31′39″S, 113°31′40″E (WAM T142985); 1 ♂, same data (WAM T142986); 1 ♂, Nanga Station, site NA4 (IBRA_YAL), 26°32′47.3″S, 113°57′47.0″E, wet pitfall trap, 11 May–30 August 1995, N. Hall (WAM T98524).

**Etymology.**—This species is named in honor of Alison Sampey, in recognition of her herculean efforts in setting and

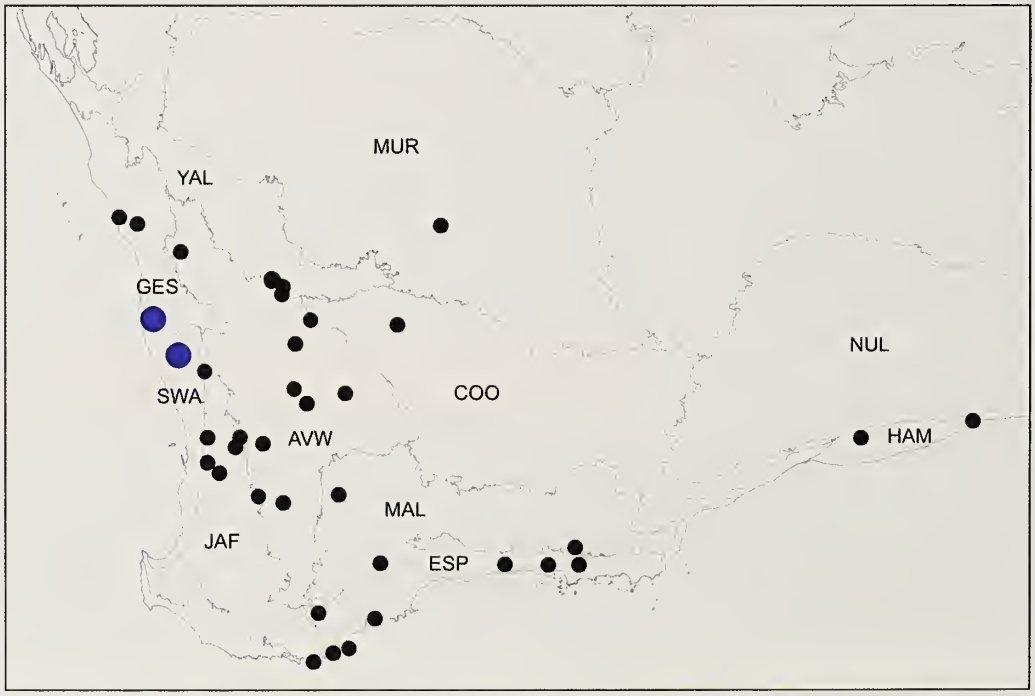


Figure 396.—Map showing collection records of *Bungulla riparia* (Main, 1957) (large blue circles), relative to other taxa with < 5 retrolateral spinules on the male palpal tibia (see Fig. 12). Relevant IBRA 7.0 bioregional acronyms are as follows: AVW, Avon Wheatbelt; COO, Coolgardie; ESP, Esperance Plains; GES, Geraldton Sandplains; HAM, Hampton; JAF, Jarrah Forest; MAL, Mallee; MUR, Murchison; NUL, Nullarbor; SWA, Swan Coastal Plain; YAL, Yalgoo.

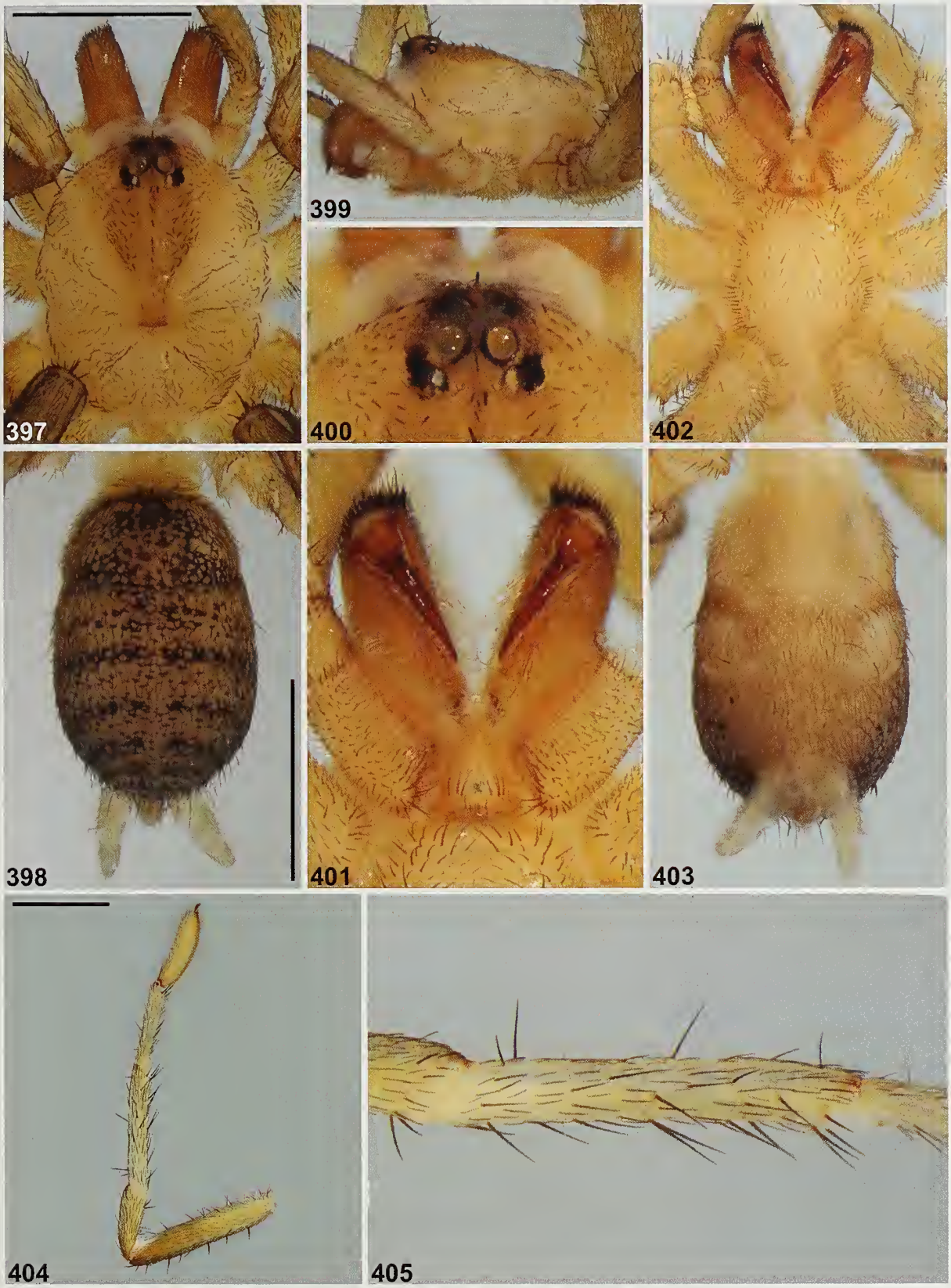


Figures 397–405.—*Bungulla sampeyae* sp. nov., male holotype (WAM T98523) from Zuytdorp (Western Australia; GES), somatic morphology: 397–398, carapace and abdomen, dorsal view; 399, cephalothorax, lateral view; 400, eyes, dorsal view; 401, mouthparts, ventral view; 402–403, cephalothorax and abdomen, ventral view; 404, leg I, prolateral view; 405, leg I tibia, prolateral view. Scale bars = 2.0 mm.


Figures 406–408.—*Bungulla sampeyae* sp. nov., male holotype (WAM T98523) from Zuytdorp (Western Australia; GES), pedipalp: 406, retrolateral view; 407, retro-ventral view; 408, prolateral view. Scale bar = 2.0 mm.

monitoring pitfall traps during the Carnarvon Biological Survey (1994–1995), and for assisting in the analysis and publication of the resulting data (see Harvey et al. 2000; Main et al. 2000).

**Diagnosis.**—Males of *Bungulla sampeyae* can be distinguished from all other known congeners with > 10 retrolateral spinules on the palpal tibia (Fig. 13) – except *B. biota*, *B. burbidgei*, *B. dipsodes*, *B. keigheryi*, *B. kendricki* and *B. westi* – by the shape of the proximal half of the palpal tibia,

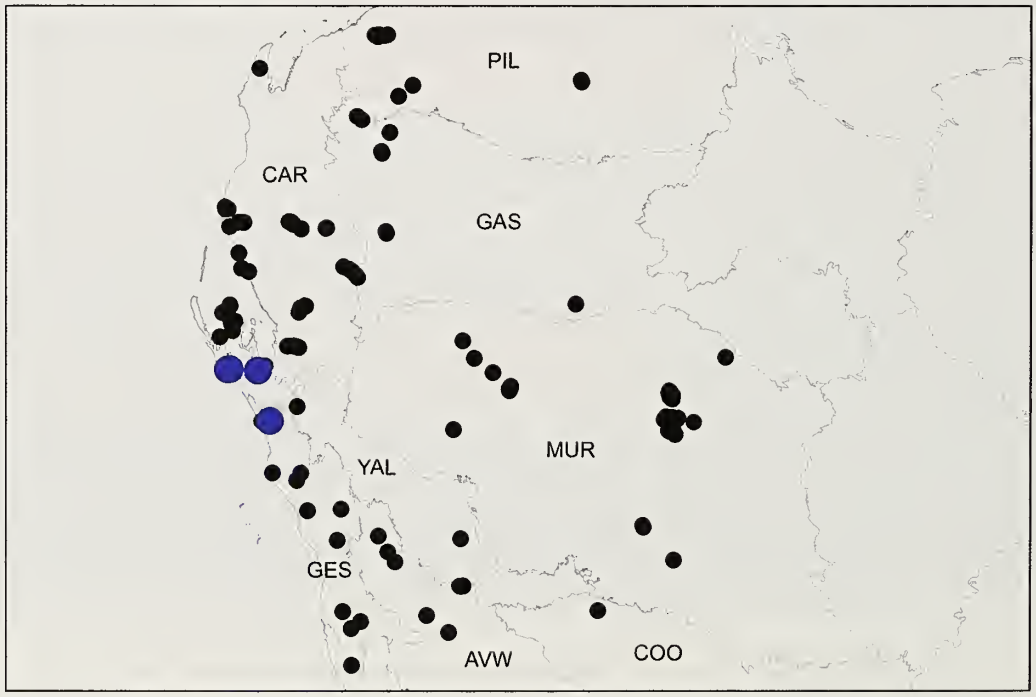


Figure 409.—Map showing collection records of *Bungulla sampeyae* sp. nov. (large blue circles), relative to other taxa with > 10 retrolateral spinules on the male palpal tibia (see Fig. 13). Relevant IBRA 7.0 bioregional acronyms are as follows: AVW, Avon Wheatbelt; CAR, Carnarvon; COO, Coolgardie; GAS, Gascoyne; GES, Geraldton Sandplains; MUR, Murchison; PIL, Pilbara; YAL, Yalgoo.

which has a pronounced RTA-like ventral bulge in retrolateral view (Fig. 406) (palpal tibia is piriform and unmodified in other species). *Bungulla sampeyae* can be further distinguished from *B. biota* by the shape of the embolus, which is without a truncate tip (Figs. 406, 407; cf. Fig. 108); from *B. burbidgei* by the absence of dagger-like spinules at the apex of the RTA-like bulge (Fig. 406; cf. Fig. 134); from *B. keigheryi* by the broadly-rounded shape of the RTA-like bulge (Fig. 406; cf. Fig. 280); from *B. dipsodes* and *B. keudricki* by the coloration of the dorsal abdomen, which is mottled and 'sandy' colored with thin chevrons (Fig. 398; cf. Figs. 139, 298 and Supplementary File 1); and from *B. westi* by the absence of spinules on the disto-dorsal margin of the palpal tibia (Figs. 406–408; cf. Fig. 432). Females are unknown.

**Description (male holotype).**—Total length 7.5. Carapace 3.1 long, 2.6 wide. Abdomen 3.1 long, 2.0 wide. Carapace (Fig. 397) pale tan, with slightly darker pars cephalica, darker tan lyre-like pattern on pars cephalica and slightly darker ocular region; fovea straight. Eye group (Fig. 400) trapezoidal (anterior eye row strongly procurved), 0.8 x as long as wide, PLE–PLE/ALE–ALE ratio 1.8; ALE separated by ca. half their own diameter; AME separated by less than their own diameter; PME separated by 3.7 x their own diameter; PME and PLE separated by diameter of PME, PME positioned in line with level of PLE. Maxillae with field of cuspules confined to inner corner (Fig. 401); labium without cuspules. Abdomen (Fig. 398) oval, sandy-tan in dorsal view with darker brown-black markings anteriorly and six pairs of thin, spotted, brown-black chevrons posteriorly, each divided along midline. Dorsal surface of abdomen (Fig. 398) with sparse arrangement of stiff, porrect black setae, each with slightly raised, dark brown sclerotic base; sclerotized sigilla absent. Legs (Figs. 404, 405 variable shades of tan, with light scopulae on tarsi I–II; tibia I spinose, without prolateral clasping spurs. Leg I: femur 3.2; patella 1.6; tibia 2.5; metatarsus 1.8; tarsus 1.6; total 10.6. Leg I femur–tarsus/carapace length ratio 3.4. Pedipalpal tibia (Figs. 406–408) stout, 1.6 x longer than wide, with broadly rounded RTA-like ventral bulge proximally; field of retrolateral spinules oval-subtriangular in shape, positioned medially (on and adjacent to RTA-like bulge), consisting of ca. 45 spinules, the latter longest at apex of RTA-like bulge; RTA absent. Cymbium (Figs. 406–408) setose, with field of relatively short, spine-like spinules covering most of dorsal surface. Embolus (Figs. 406–408) slightly longer than bulb, strongly curved, with unmodified tip; embolic apophysis absent.

**Distribution and remarks.**—*Bungulla sampeyae* (formerly known by WAM identification code 'MYG133') is a rare species with a relatively restricted distribution in the northern Geraldton Sandplains and north-western Yalgoo bioregions of Western Australia, from Zuytdorp north to the Carrarang Peninsula (Fig. 409). Nothing is known of the biology of this species, other than that the known male specimens were collected wandering in search of females in winter or possibly late autumn.

***Bungulla weld*** Rix, Raven & Harvey, sp. nov.
http://zoobank.org/?lsid=urn:lsid:zoobank.org:act:310E0AED-91A5-4FC3-B99B-B5229ECB0DD8
(Figs. 13, 410–422)

**Type material.**—*Holotype male.* AUSTRALIA: *Western Australia*: Weld Range North mine lease, site WN 8, 64 km SW. of Meekatharra (IBRA_MUR), 26°47′50.21″S, 117°53′38.97″E, wet pitfall trap, 31 August 2007, Ecologia staff (WAM T130911).

**Other material examined.**—AUSTRALIA: *Western Australia*: 2 ♂, Weld Range North mine lease, site WN 1, 63 km SW. of Meekatharra (IBRA_MUR), 26°46′13.67″S, 117°53′59.65″E, wet pitfall trap, 30 August 2007, Ecologia staff (WAM T130917); 1 ♂, Weld Range (no specific locality) (IBRA_MUR), 24 August–24 November 2006, Ecologia staff (WAM T142965).

**Etymology.**—The specific epithet is a noun in apposition, in reference to the type locality of this species.

**Diagnosis.**—Males of *Bungulla weld* can be distinguished from all other known congeners with > 10 retrolateral spinules on the palpal tibia (Fig. 13) – except *B. banksia*, *B. bertmaini*, *B. bidgemia*, *B. hamelinensis*, *B. iota*, *B. laevigata*, *B. quobba* and *B. yeni* – by the shape of the proximal half of the palpal tibia, which is without a pronounced ventral bulge (Fig. 419), combined with the absence of a medial 'ledge' on the palpal tibia (Figs. 419, 420) (palpal tibia is with a ledge or bulges ventrally in other species). *Bungulla weld* can be further distinguished from *B. banksia* by the larger field of retrolateral spinules on the palpal tibia (Fig. Fig. 419; cf. Fig. 72); from *B. bertmaini*, *B. laevigata* and *B. quobba* by the shape of the embolus, which is relatively short (i.e., ~as long as bulb) (Fig. 419; cf. Figs. 24, 319, 371); from *B. hamelinensis* by the morphology of the cymbial spinules, which are thicker and more spine-like (Figs. 419–421; cf. Figs. 218–220); from *B. yeni* and by the presence of a larger, crescent-shaped field of retrolateral spinules on the palpal tibia (Fig. 419; cf. Fig. 445); and from *B. bidgemia* and *B. iota* by the presence of a relatively asymmetric ('wave-shaped') field of retrolateral spinules on the palpal tibia (Fig. 419; cf. Figs. 95, 267). Females are unknown.

**Description (male holotype).**—Total length 5.3. Carapace 2.6 long, 2.0 wide. Abdomen 2.3 long, 1.7 wide. Carapace (Fig. 410) pale tan, with slightly darker pars cephalica and mostly black ocular region; fovea slightly procurved. Eye group (Fig. 413) trapezoidal (anterior eye row strongly procurved), 0.8 x as long as wide, PLE–PLE/ALE–ALE ratio 1.4; ALE separated by ca. half their own diameter; AME separated by less than their own diameter; PME separated by 3.2 x their own diameter; PME and PLE separated by diameter of PME, PME positioned in line with level of PLE. Maxillae with field of cuspules confined to inner corner (Fig. 414); labium without cuspules. Abdomen (Fig. 411) oval, slightly shrivelled, beige-tan in dorsal view with three darker brown markings anteriorly and four pairs of thin, spotted, dark brown chevrons posteriorly, each divided along midline . Dorsal surface of abdomen (Fig. 411) with sparse arrangement of stiff, porrect black setae, each with slightly raised, dark brown sclerotic base; sclerotized sigilla absent. Legs (Figs. 417, 418) variable shades of pale tan, with light scopulae on semi-incrassate tarsi I–II; tibia I spinose, without prolateral clasping spurs. Leg I: femur 2.5; patella 1.2; tibia 1.9; metatarsus 1.5; tarsus 1.4; total 8.4. Leg

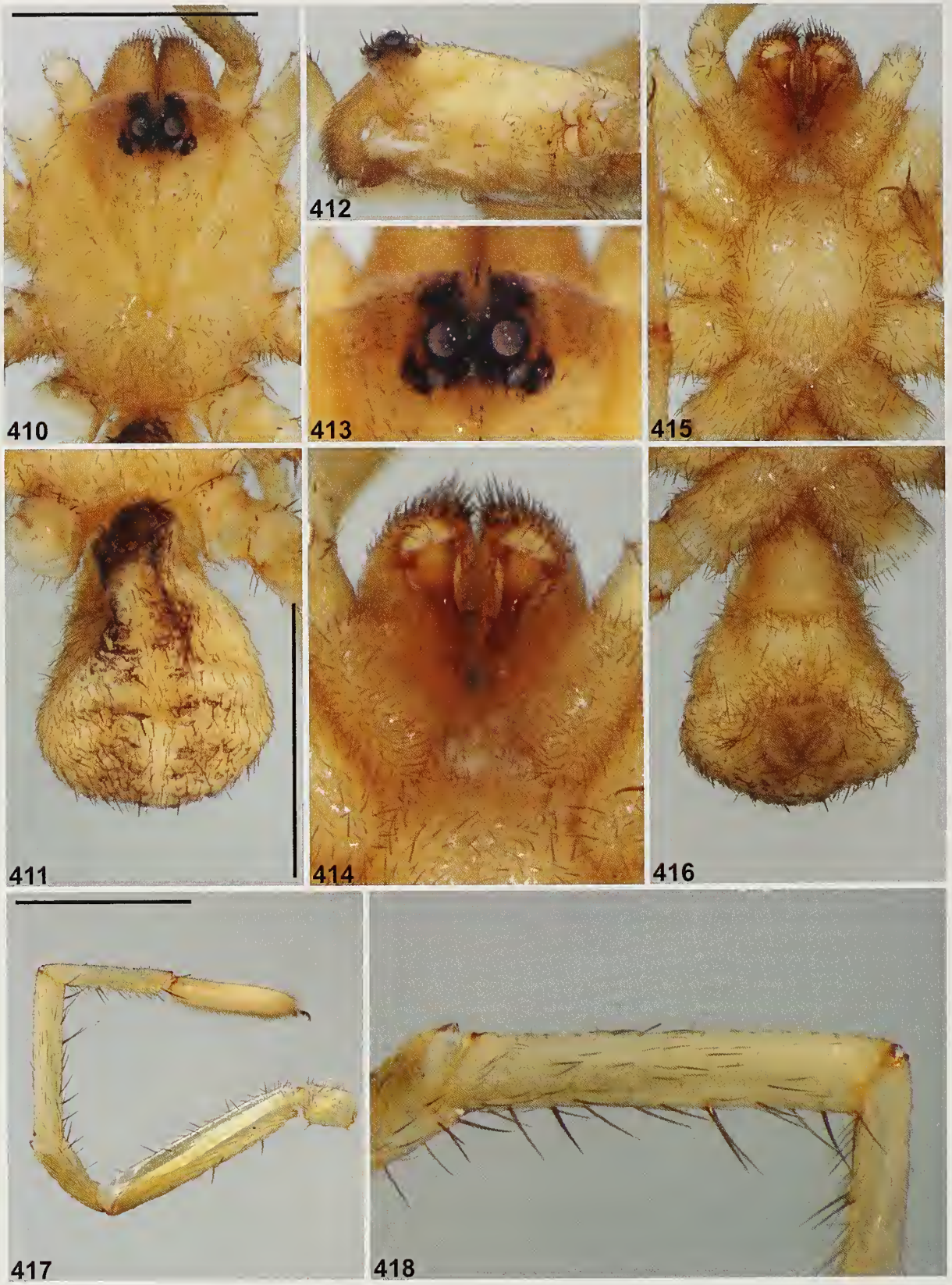


Figures 410–418.—*Bungulla weld* sp. nov., male holotype (WAM T130911) from Weld Range North mine lease (Western Australia; MUR), somatic morphology: 410–411, carapace and abdomen, dorsal view; 412, cephalothorax, lateral view; 413, eyes, dorsal view; 414, mouthparts, ventral view; 415–416, cephalothorax and abdomen, ventral view; 417, leg 1, prolateral view; 418, leg 1 tibia, prolateral view. Scale bars = 2.0 mm.


Figures 419–421.—*Bungulla weld* sp. nov., male holotype (WAM T130911) from Weld Range North mine lease (Western Australia; MUR), pedipalp: 419, retrolateral view; 420, retro-ventral view; 421, prolateral view. Scale bar = 2.0 mm.

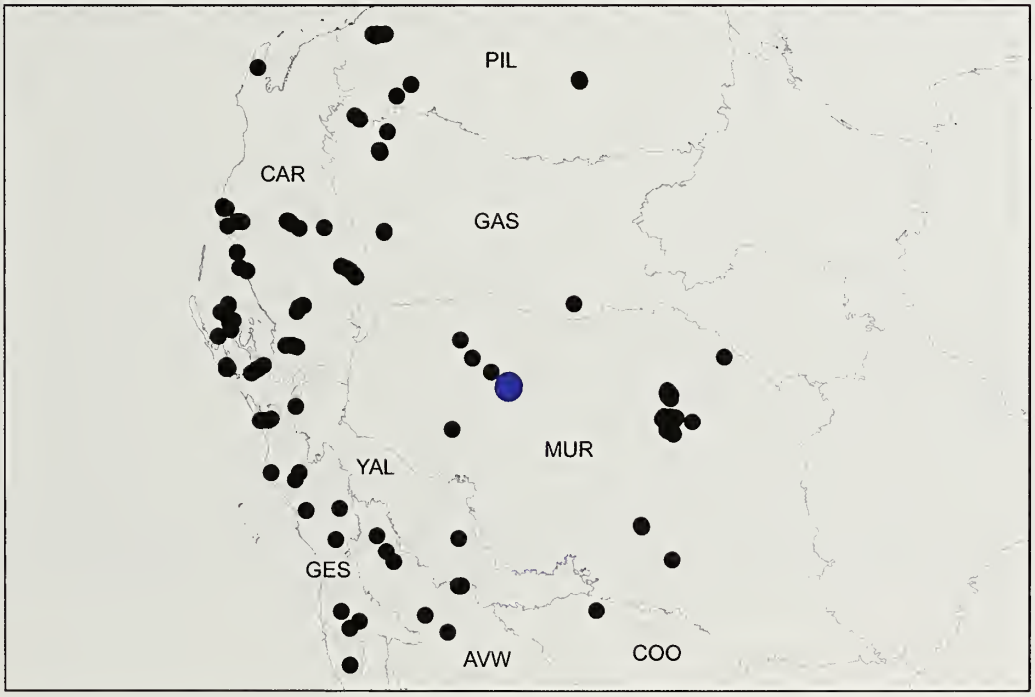


Figure 422.—Map showing collection records of *Bungulla weld* sp. nov. (large blue circles), relative to other taxa with > 10 retrolateral spinules on the male palpal tibia (see Fig. 13). Relevant IBRA 7.0 bioregional acronyms are as follows: AVW, Avon Wheatbelt; CAR, Carnarvon; COO, Coolgardie; GAS, Gascoyne; GES, Geraldton Sandplains; MUR, Murchison; PIL, Pilbara; YAL, Yalgoo.

I femur–tarsus/carapace length ratio 3.3. Pedipalpal tibia (Figs. 419–421) nearly 2.0 x longer than wide; field of retrolateral spinules large and asymmetrically crescent-shaped ('wave-shaped') in retrolateral view, positioned medially–distally (along most of retro-ventral margin), consisting of ca. 50 spinules of largely similar length; RTA absent. Cymbium (Figs. 419–421) setose, with sparse field of spine-like spinules covering most of dorsal surface. Embolus (Figs. 419–421) as long as bulb, slightly curved, with unmodified tip; embolic apophysis absent.

**Distribution and remarks.**—*Bungulla weld* is known only from the Weld Range, in the western Murchison bioregion of Western Australia (Fig. 422). Nothing is known of the biology of this species, other than that the known male specimens were collected wandering in search of females in late winter and spring.

***Bungulla westi*** Rix, Raven & Harvey, sp. nov.
http://zoobank.org/?lsid=urn:lsid:zoobank.org:act:011A73B9-B5C7-498E-9068-1CB0EB9144BD
(Figs. 13, 423–435)

**Type material.**—*Holotype male.* AUSTRALIA: *Western Australia*: Zuytdorp, site ZU1 (IBRA_GES), 27°15′42″S, 114°01′09″E, wet pitfall trap, 16–21 May 1995, M.S. Harvey et al., WAM/CALM Carnarvon Survey (WAM T98537).

*Paratypes.* AUSTRALIA: *Western Australia*: 1 ♂, same data as holotype except 11 January–19 May 1995 (WAM T98539); 2 ♂, same data except 19 May–17 August 1995, N. Hall, WAM/CALM Carnarvon Survey (WAM T98538).

**Other material examined.**—AUSTRALIA: *Western Australia*: 1 ♂, Zuytdorp Nature Reserve, site ZU2 (IBRA_GES), 27°15′41″S, 114°01′47.6″E, wet pitfall trap, 16–21 May 1995, M.S. Harvey et al., WAM/CALM Carnarvon Survey (WAM T98540); 1 ♂, Zuytdorp, site ZU4 (IBRA_GES), 27°15′45.1″S, 114°09′12.9″E, wet pitfall trap, 18 May–16 August 1995, N. Hall, WAM/CALM Carnarvon Survey (WAM T98541); 3 ♂, Francois Peron National Park, site PE2 (IBRA_CAR), 25°52′30.9″S, 113°32′59.0″E, wet pitfall trap, 25 May–30 August 1995, N. Hall, WAM/CALM Carnarvon Survey (WAM T98553); 1 ♂, Meedo Station, site MD4 (IBRA_CAR), 25°40′49.1″S, 114°37′19.8″E, wet pitfall trap, 18 May–22 August 1995, N. Hall, WAM/CALM Carnarvon Survey (WAM T98542); 1 ♂, same data (WAM T98543); 3 ♂, same data except site MD5, 25°42′41.6″S, 114°35′58.5″E, 19 May–22 August 1995 (WAM T98544); 1 ♂, Nanga Station, site NA2 (IBRA_CAR), 26°29′23.0″S, 114°03′24.3″E, wet pitfall trap, 11 May–30 August 1995, N. Hall, WAM/CALM Carnarvon Survey (WAM T98536); 2 ♂, same data except site NA3 (IBRA_YAL), 26°31′20.9″S, 114°00′08.3″E, 12 May–30 August 1995 (WAM T98545); 1 ♂, same data except site NA4, 26°32′47.3″S, 113°57′47.0″E, 11 May–30 August 1995 (WAM T98535); 1 ♂, same data except site NA5, 26°35′31.8″S, 113°53′22.3″E (WAM T98546); 2 ♂, Nerren Nerren Station, site NE1 (IBRA_YAL), 27°03′23.6″S, 114°35′21.3″E, wet pitfall trap, 11 May–18 August 1995, N. Hall, WAM/CALM Carnarvon Survey (WAM T98547); 1 ♂, same data except site NE2, 27°03′24.1″S, 114°34′22.6″E (WAM T98548); 3 ♂, Woodleigh Station, site WO1 (IBRA_CAR), 26°13′01.2″S, 114°35′59.4″E, wet pitfall trap, 17 May–21 August 1995, N. Hall, WAM/CALM Carnarvon Survey (WAM T98549); 2 ♂, same data except site WO3, 26°11′44.5″S, 114°32′14.4″E (WAM T98550); 1 ♂, same data except site WO4, 26°11′31.1″S, 114°30′33.0″E (WAM T98551); 2 ♂, same data (WAM T98552).

**Etymology.**—This species is named in honor of Paul West, in recognition of his herculean efforts in setting and monitoring pitfall traps during the Carnarvon Biological Survey (1994–1995), and for assisting in the analysis and publication of the resulting data (see Harvey et al. 2000; Main et al. 2000).

**Diagnosis.**—Males of *Bungulla westi* can be distinguished from all other known congeners by the presence of thorn-like spinules on the disto-dorsal margin of the palpal tibia (Figs. 432–434) (disto-dorsal spinules absent in other species). Females are unknown.

**Description (male holotype).**—Total length 7.5. Carapace 3.3 long, 2.6 wide. Abdomen 3.4 long, 2.0 wide. Carapace (Fig. 423) pale tan with black ocular region; fovea slightly recurved. Eye group (Fig. 426) trapezoidal (anterior eye row strongly procurved), as long as wide, PLE–PLE/ALE–ALE ratio 1.3; ALE separated by ca. half their own diameter; AME separated by less than their own diameter; PME separated by 3.1 x their own diameter; PME and PLE separated diameter of PME, PME positioned in line with level of PLE. Maxillae with field of cuspules confined to inner corner (Fig. 427); labium without cuspules. Abdomen (Fig. 424) oval, dark olive-brown in dorsal view, with beige mottling, two large pairs of beige-tan sigilla spots, and four pairs of large chevrons posteriorly, each divided along midline. Dorsal surface of abdomen (Fig. 424) with sparse arrangement of stiff, porrect black setae, each with slightly raised, dark brown sclerotic base; sclerotized sigilla absent. Legs (Figs. 430, 431) variable shades of pale tan, with light scopulae on tarsi I–II; tibia I spinose, without prolateral clasping spurs. Leg I: femur 3.5; patella 1.8; tibia 2.6; metatarsus 2.4; tarsus 1.8; total 12.1. Leg I femur–tarsus/carapace length ratio 3.7. Pedipalpal tibia (Figs. 432–434) stout and bulbous, 1.9 x longer than wide, with pronounced RTA-like ventral bulge proximally, the latter developed into a relatively acute, attenuate process; field of retrolateral spinules reverse C-shaped, positioned medially–distally (along distal third of retro-ventral margin), consisting of ca. 35 spinules, the latter longest at apex of RTA-like bulge; tibia also with field of porrect, thorn-like spinules on disto-dorsal margin; RTA absent. Cymbium (Figs. 432–434) setose, with field of porrect, stout, thorn-like spinules covering most of dorsal surface. Embolus (Figs. 432–434) slightly longer than bulb, strongly curved, with distinctly expanded tip; embolic apophysis absent.

**Distribution and remarks.**—*Bungulla westi* has a relatively restricted distribution in the greater Shark Bay region of Western Australia, from Zuytdorp (Geraldton Sandplains bioregion) north to Meedo Station in the southern Carnarvon bioregion (Fig. 435). Nothing is known of the biology of this species, other than that the known male specimens were collected wandering in search of females in late autumn and winter.

***Bungulla yeni*** Rix, Raven & Harvey, sp. nov.
http://zoobank.org/?lsid=urn:lsid:zoobank.

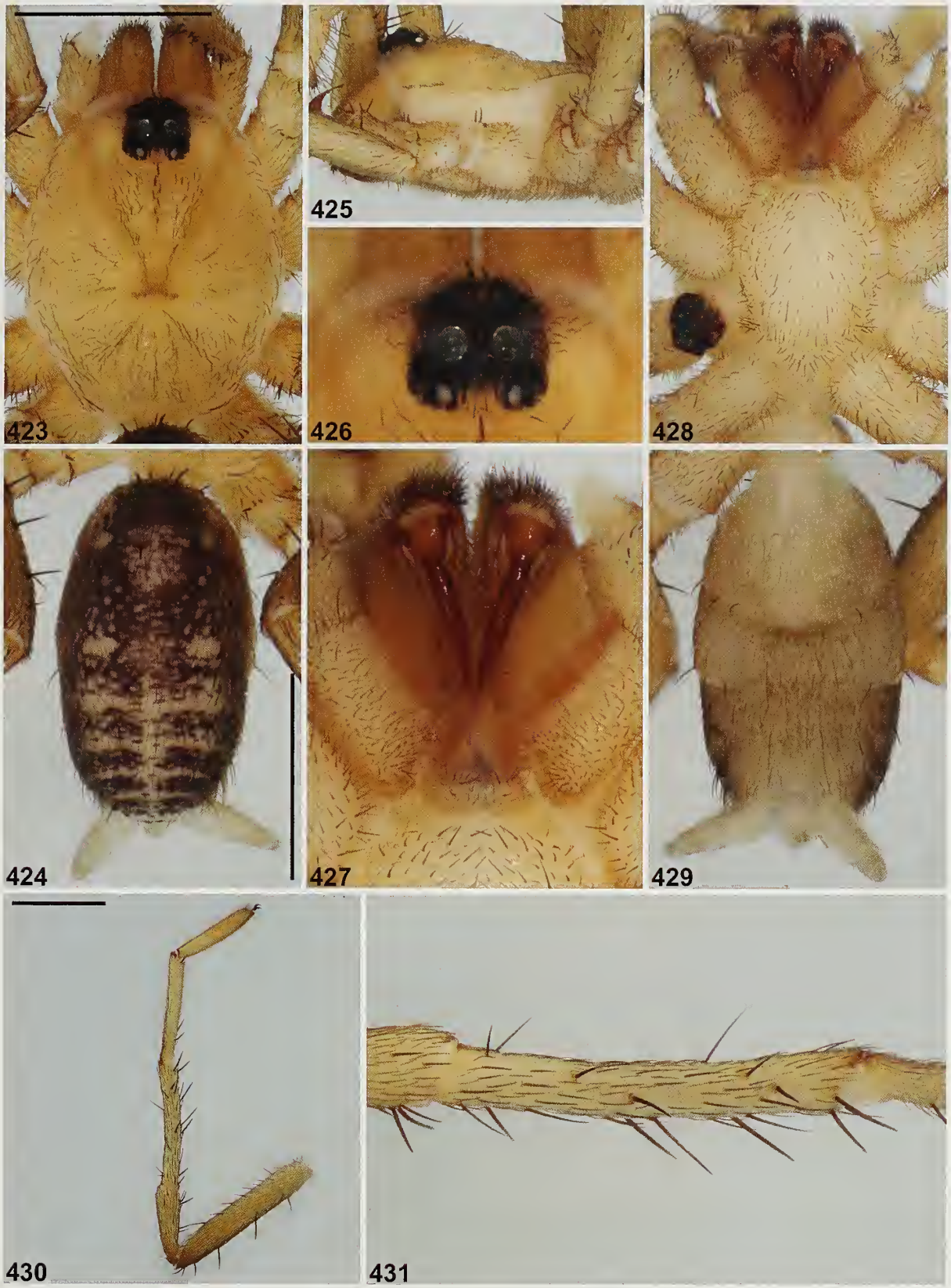


Figures 423–431.—*Bungulla westi* sp. nov., male holotype (WAM T98537) from Zuytdorp, site ZU1 (Western Australia; GES), somatic morphology: 423–424, carapace and abdomen, dorsal view; 425, cephalothorax, lateral view; 426, eyes, dorsal view; 427, mouthparts, ventral view; 428–429, cephalothorax and abdomen, ventral view; 430, leg I, prolateral view; 431, leg I tibia, prolateral view. Scale bars = 2.0 mm.


Figures 432–434.—*Bungulla westi* sp. nov., male holotype (WAM T98537) from Zuytdorp, site ZU1 (Western Australia; GES), pedipalp: 432, retrolateral view; 433, retro-ventral view; 434, prolateral view. Scale bar = 2.0 mm.

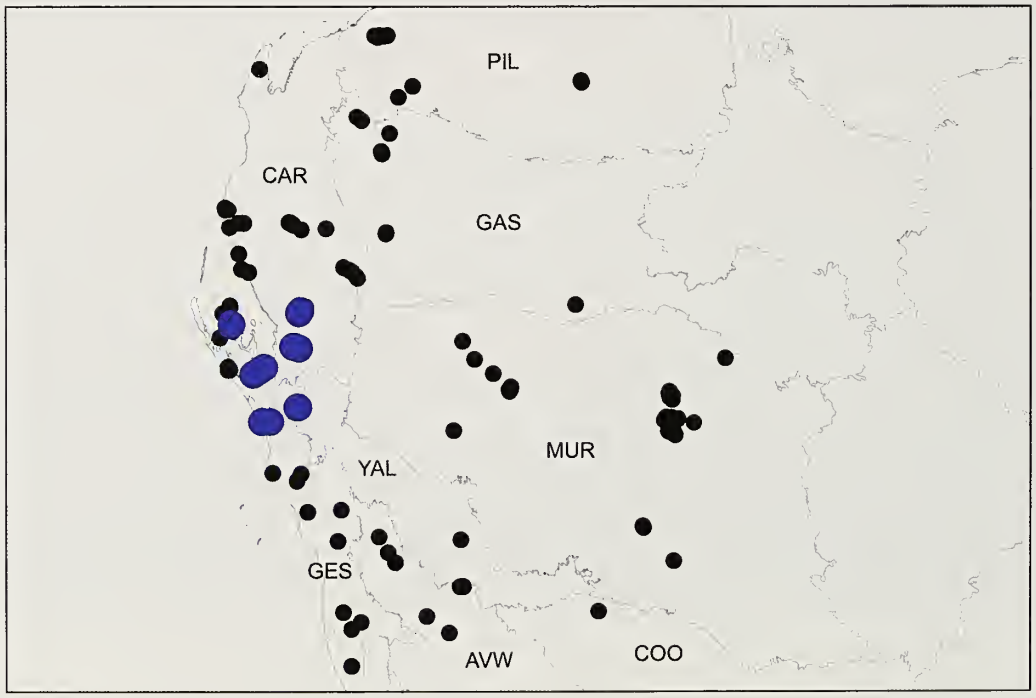


Figure 435.—Map showing collection records of *Bungulla westi* sp. nov. (large blue circles), relative to other taxa with > 10 retrolateral spinules on the male palpal tibia (see Fig. 13). Relevant IBRA 7.0 bioregional acronyms are as follows: AVW, Avon Wheatbelt; CAR, Carnarvon; COO, Coolgardie; GAS, Gascoyne; GES, Geraldton Sandplains; MUR, Murchison; PIL, Pilbara; YAL, Yalgoo.

org:act:A6BF6A12-AEF4-41CC-BDD5-25D1CBCED629
(Figs. 13, 14, 436–448)

*Bungulla* sp. 'Albion Downs' Rix et al., 2017d: 603, figs 148, 149, 153, 158.

**Type material.**—*Holotype male*. AUSTRALIA: *Western Australia*: Albion Downs, 84.1 km NNW. of Leinster (IBRA_MUR), 27°14′17″S, 120°18′43″E, dry pitfall trap, 30 August 2008, Z Hamilton & R. Teale (WAM T96263[DNA_Voucher_204]; GenB–COI–KY295251, GenB–CYB–KY295375, GenB–MRPL45–KY295499, GenB–RPF2–KY295618, GenB–XPNPEP3–KY295745, GenB–ITS–KY294997).

*Paratypes*. AUSTRALIA: *Western Australia*: 1 ♂, same data as holotype (WAM T96264); 1 ♂, same data except 28 August–3 September 2008 (WAM T96328); 1 ♂, same data except 55.8 km NNW. of Leinster, 27°27′26″S, 120°27′41″E (WAM T96301[DNA_Voucher_207]; GenB–COI–MG516835, GenB–CYB–MG516846, GenB–MRPL45–MG516869, GenB–RPF2–MG516880, GenB–XPNPEP3–MG516897, GenB–ITS–MG516861); 1 ♂, same data except 62.7 km NNW. of Leinster, 27°25′02″S, 120°23′41″E (WAM T96306[DNA_Voucher_206]; GenB–COI–MG516836, GenB–CYB–MG516848, GenB–MRPL45–MG516870, GenB–RPF2–MG516882, GenB–XPNPEP3–MG516899, GenB–ITS–MG516862); 1 ♂, same data (WAM T96300); 1 ♂, same data (WAM T96350); 1 ♂, same data except 78.3 km NNW. of Leinster, 27°15′26″S, 120°24′29″E, 30 August 2008 (WAM T96268[DNA_Voucher_205]; GenB–COI–MG516837, GenB–CYB–MG516847, GenB–MRPL45–MG516871, GenB–RPF2–MG516881, GenB–XPNPEP3–MG516898, GenB–ITS–MG516863); 1 ♂, same data (WAM T96269).

**Other material examined.**—AUSTRALIA: *Western Australia*: 1 ♂, Albion Downs, 60.4 km NNW. of Leinster (IBRA_MUR), 27°25′13″S, 120°26′23″E, dry pitfall trap, 30 August 2008, Z Hamilton & R. Teale (WAM T96262); 1 ♂, same data except 62.6 km NNW. of Leinster, 27°25′03″S, 120°23′45″E, 28 August–3 September 2008 (WAM T96305); 1 ♂, same data (WAM T96298); 1 ♂, same data (WAM T96299); 1 ♂, same data except 78.6 km NNW. of Leinster, 27°14′18″S, 120°27′41″E, 30 August 2008 (WAM T96265); 1 ♂, same data except 28 August–3 September 2008 (WAM T96291); 1 ♂, same data except 79.2 km NNW. of Leinster, 27°13′21″S, 120°30′01″E (WAM T96324); 1 ♂, same data (WAM T96325); 1 ♂, same data except 30 August 2008 (WAM T96261); 1 ♂, same data except 81.2 km NNW. of Leinster, 27°15′32″S, 120°19′50″E, 28 August–3 September 2008 (WAM T96364); 1 ♂, same data (WAM T96295); 1 ♂, same data except 84.9 km NNW. of Leinster, 27°14′40″S, 120°16′54″E, 30 August 2008 (WAM T96267); 1 ♂, Lake Way Station, Honeymoon Well lease (IBRA_MUR), 26°56′13″S, 120°24′35″E, glycol pitfall trap in spinifex, 20 October 2006, S. Thompson (WAM T80606); 1 ♂, same data except 26°53′49″S, 120°25′07″E, mulga-spinifex (WAM T80607); 1 ♂, ca. 10 km NW. of Lake Way homestead, spinifex site 1 (IBRA_MUR), 26°55′41″S, 120°23′59″E, wet pitfall trap, 20 October 2006, S. Thompson (WAM T94066); 1 ♂, ca. 7 km W. of Lake Way homestead, spinifex site 4 (IBRA_MUR), 26°56′05″S, 120°24′11″E, wet pitfall trap, 20 October 2006, S. Thompson (WAM T94197).

**Etymology.**—This species is named in honor of the late Alan Yen (1950–2017), in recognition of his seminal contributions to systematics and invertebrate conservation in Australia.

**Diagnosis.**—Males of *Bungulla yeni* can be distinguished from all other known congeners with > 10 retrolateral spinules on the palpal tibia (Fig. 13) – except *B. banksia*, *B. bertmaini*, *B. bidgemia*, *B. hamelinensis*, *B. iota*, *B. laevigata*, *B. quobba* and *B. weld* – by the shape of the proximal half of the palpal tibia, which is without a pronounced ventral bulge (Fig. 445), combined with the absence of a medial 'ledge' on the palpal tibia (Figs. 445, 446) (palpal tibia is with a ledge or bulges ventrally in other species). *Bungulla yeni* can be further distinguished from *B. banksia* by the larger field of retrolateral spinules on the palpal tibia (Fig. 445; cf. Fig. 72); from *B. bertmaini*, *B. laevigata* and *B. quobba* by the shape of the embolus, which is relatively short (i.e., ~as long as bulb) (Fig. 445; cf. Figs. 24, 319, 371); from *B. hamelinensis* by the morphology of the cymbial spinules, which are thicker and more spine-like (Figs. 445–447; cf. Figs. 218–220); and from *B. bidgemia*, *B. iota* and *B. weld* by the presence of a relatively small, rectangular field of retrolateral spinules on the distal half of the palpal tibia (Fig. 445; cf. Figs. 95, 267, 419). Females are unknown.

**Description (male holotype).**—Total length 8.2. Carapace 3.2 long, 2.5 wide. Abdomen 3.7 long, 2.5 wide. Carapace (Fig. 436) tan, with slightly darker pars cephalica, pale olive lyre-like pattern on pars cephalica and mostly black ocular region; fovea straight. Eye group (Fig. 439) trapezoidal (anterior eye row strongly procurved), 0.9 x as long as wide, PLE–PLE/ALE–ALE ratio 1.4; ALE separated by ca. half their own diameter; AME separated by less than their own diameter; PME separated by 3.0 x their own diameter; PME and PLE separated by slightly less than diameter of PME, PME positioned in line with level of PLE. Maxillae with field of cuspules confined to inner corner (Fig. 440); labium without cuspules. Abdomen (Fig. 437) elongate-oval, beige-tan in dorsal view with contrasting pattern of three darker black markings anteriorly and five pairs of spotted black chevrons posteriorly, each divided along midline. Dorsal surface of abdomen (Fig. 437) with sparse arrangement of stiff, porrect black setae, each with slightly raised, dark brown sclerotic base; sclerotized sigilla absent. Legs (Figs. 443, 444) variable shades of tan, with light scopulae on incrassate tarsi I–II; tibia 1 spinose, without prolateral clasping spurs. Leg 1: femur 2.8; patella 1.3; tibia 2.3; metatarsus 2.0; tarsus 1.6; total 10.0. Leg 1 femur–tarsus/carapace length ratio 3.1. Pedipalpal tibia (Figs. 445–447) 1.9 x longer than wide; field of retrolateral spinules relatively small and rectangular in shape, positioned medio-distally (on distal half of tibia), consisting of 31 spinules of largely similar length; RTA absent. Cymbium (Figs. 445–447) setose, with sparse field of spine-like spinules covering most of dorsal surface. Embolus (Figs. 445–447) as long as bulb, curved, with unmodified tip; embolic apophysis absent.

**Distribution and remarks.**—*Bungulla yeni* (formerly known by WAM identification code 'MYG029') is known only from the Albion Downs region north of Leinster, in the central Murchison bioregion of Western Australia (Fig. 448). Nothing is known of the biology of this species, other than that the known male specimens were collected wandering in search of females in late winter and spring.

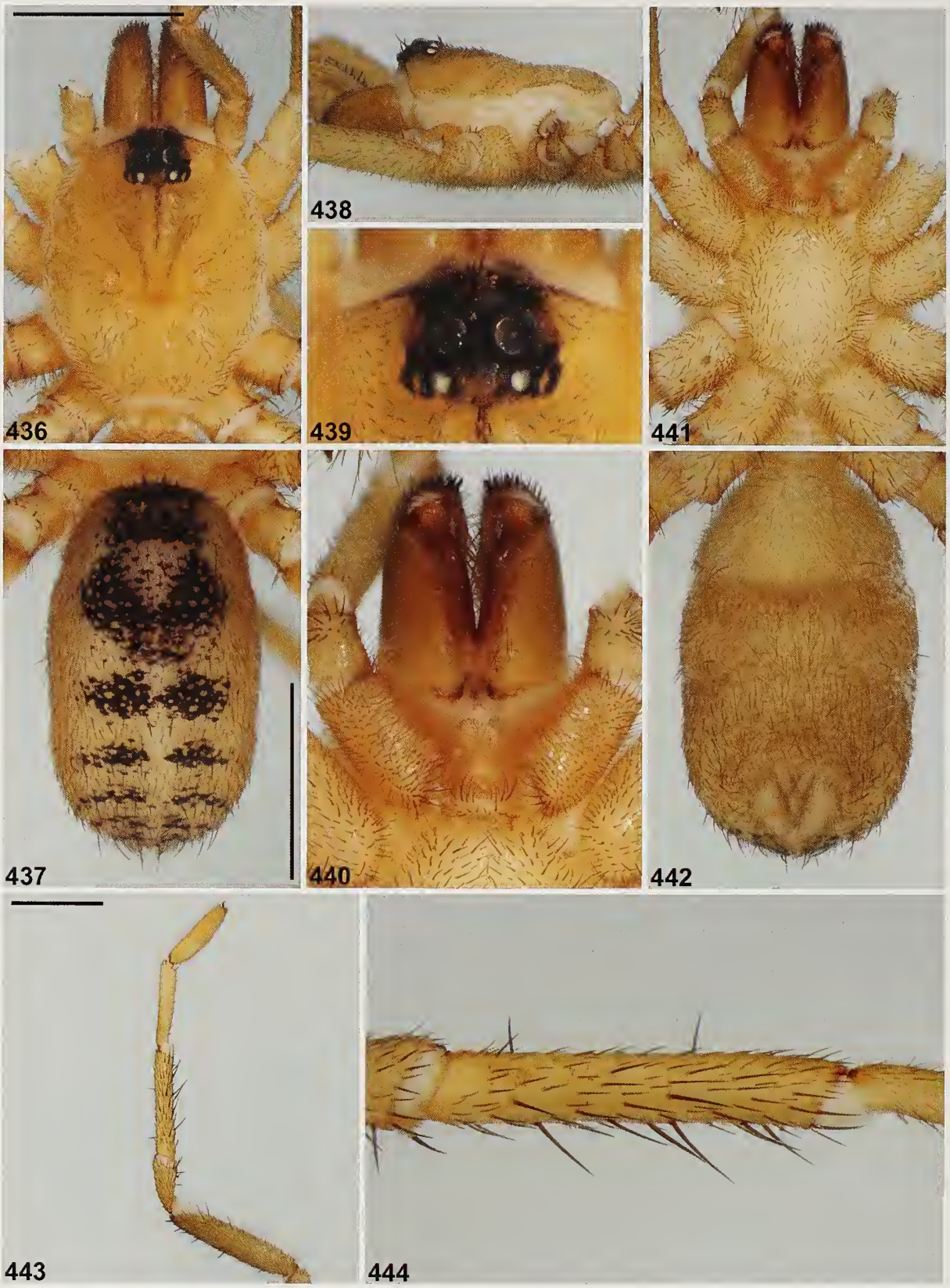


Figures 436–444.—*Bungulla yeni* sp. nov., male holotype (WAM T96263) from Albion Downs, NNW. of Leinster (Western Australia; MUR), somatic morphology: 436–437, carapace and abdomen, dorsal view; 438, cephalothorax, lateral view; 439, eyes, dorsal view; 440, mouthparts, ventral view; 441–442, cephalothorax and abdomen, ventral view; 443, leg I, prolateral view; 444, leg I tibia, prolateral view. Scale bars = 2.0 mm


Figures 445–447.—*Bungulla yeni* sp. nov., male holotype (WAM T96263) from Albion Downs, NNW. of Leinster (Western Australia; MUR), pedipalp: 445, retrolateral view; 446, retro-ventral view; 447, prolateral view. Scale bar = 2.0 mm.

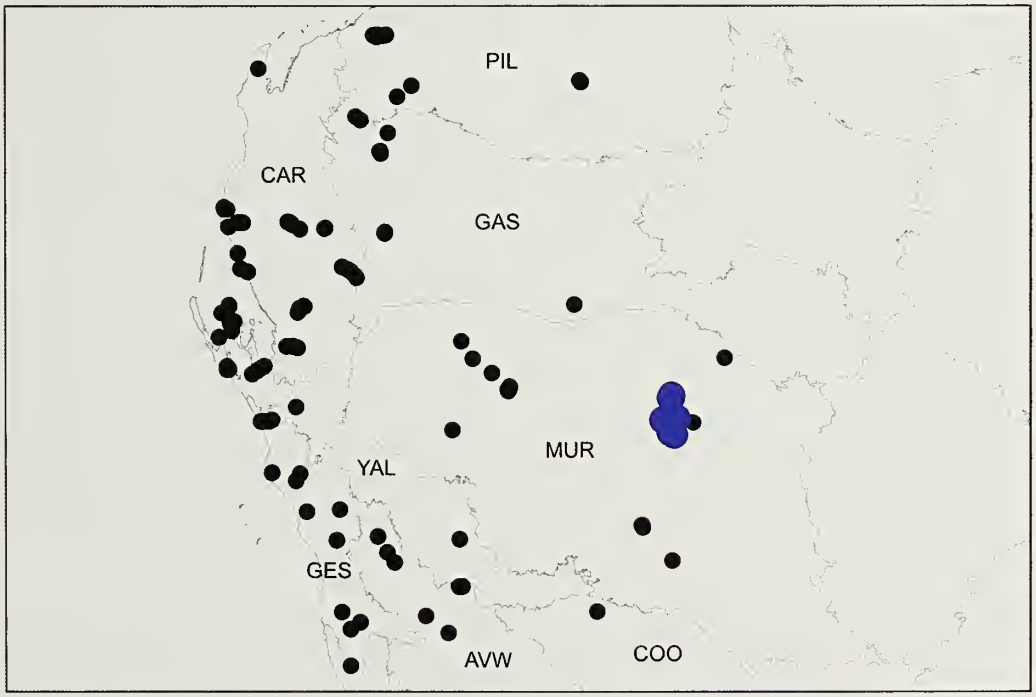


Figure 448.—Map showing collection records of *Bungulla yeni* sp. nov. (large blue circles), relative to other taxa with > 10 retrolateral spinules on the male palpal tibia (see Fig. 13). Relevant IBRA 7.0 bioregional acronyms are as follows: AVW, Avon Wheatbelt; CAR, Carnarvon; COO, Coolgardie; GAS, Gascoyne; GES, Geraldton Sandplains; MUR, Murchison; PIL, Pilbara; YAL, Yalgoo.

## ACKNOWLEDGMENTS

This work would have been significantly diminished without the collections provided by the then CALM (Department of Conservation and Land Management) 'Biodiversity Survey of the Southern Carnarvon Basin', run from 1994–1995. Other important specimens were provided by CALM's 'Salinity Action Plan Survey' (later 'State Salinity Strategy') of the Western Australian Agricultural Zone (1997–2000), and by numerous other individual collectors, especially Roy Teale, Zoe Hamilton and Barbara Main. Thanks also to Roy Teale for providing his images of a live male *B. biota*, and to Jeremy Wilson for his contribution to the development of the 'Atlas' approach to mygalomorph systematics. This work was funded by an Australian Biological Resources Study (ABRS) Taxonomy Research Grant (No. RF21506) to MGR, RJR and MSH, an Australian Research Council (ARC) Linkage Grant (No. LP120200092) to ADA, MGR, SJBC and MSH, and a Bioplatforms Australia (BPA) Grant to ADA and SJBC.

## LITERATURE CITED

Burbidge, A.H., N.L. McKenzie & M.S. Harvey. 2000. A biogeographic survey of the southern Carnarvon Basin, Western Australia: background and methods. Records of the Western Australian Museum Supplement 61:1–12.

Brown, R.W. 1956. Composition of Scientific Words: A Manual of Methods and a Lexicon of Materials for the Practice of Logotechnics. Smithsonian Books, Washington, D.C.

de Queiroz, K. 2007. Species concepts and species delimitation. Systematic Biology 56:879–886.

Harvey, M.S., A. Sampey, P.L.J. West & J.M. Waldock. 2000. Araneomorph spiders from the southern Carnarvon Basin, Western Australia: a consideration of regional biogeographic relationships. Records of the Western Australian Museum Supplement 61:295–321.

Huelsenbeck, J.P. & F. Ronquist. 2001. MRBAYES: Bayesian inference of phylogenetic trees. Bioinformatics 17:754–755.

Keighery, G.J. 2004. State Salinity Strategy biological survey of the Western Australian wheatbelt: background. Records of the Western Australian Museum Supplement 67:1–6.

Lanfear, R., B. Calcott, S.Y.W. Ho & S. Guindon. 2012. PartitionFinder: combined selection of partitioning schemes and substitution models for phylogenetic analyses. Molecular Biology and Evolution 29:1695–1701.

Main, B.Y. 1957. Biology of aganippine trapdoor spiders (Mygalomorphae: Ctenizidae). Australian Journal of Zoology 5:402–473.

Main, B.Y., A. Sampey & P.L.J. West. 2000. Mygalomorph spiders of the southern Carnarvon Basin, Western Australia. Records of the Western Australian Museum Supplement 61:281–293.

McKenzie, N.L., S. van Leeuwen & A.M. Pinder. 2009. Introduction to the Pilbara Survey, 2002–2007. Records of the Western Australian Museum Supplement 78:3–89.

Miller, M.A., W. Pfeiffer & T. Schwartz. 2010. Creating the CIPRES Science Gateway for inference of large phylogenetic trees. Proceedings of the Gateway Computing Environments Workshop (GCE), 14 Nov. 2010, pp. 1–8, New Orleans, LA.

Rambaut, A., M.A. Suchard, D. Xie & A.J. Drummond. 2014. Tracer v1.6. Available online at http://beast.bio.ed.ac.uk/Tracer (accessed June 2017).

Rix, M.G., K. Bain, B.Y. Main, R.J. Raven, A.D. Austin, S.J.B. Cooper & M.S. Harvey. 2017a. Systematics of the spiny trapdoor spiders of the genus *Cataxia* (Mygalomorphae: Idiopidae) from south-western Australia: documenting a threatened fauna in a sky-island landscape. Journal of Arachnology 45:395–423.

Rix, M.G., S.J.B. Cooper, K. Meusemann, S. Klopfstein, S.E. Harrison, M.S. Harvey et al. 2017b. Post-Eocene climate change across continental Australia and the diversification of Australasian spiny trapdoor spiders (Idiopidae). Molecular Phylogenetics and Evolution 109:302–320.

Rix, M.G., D.L. Edwards, M. Byrne, M.S. Harvey, L. Joseph & J.D. Roberts. 2015. Biogeography and speciation of terrestrial fauna in the south-western Australian biodiversity hotspot. Biological Reviews 90:762–793.

Rix, M.G., J. Huey, B.Y. Main, J.M. Waldock, S.E. Harrison, S. Comer et al. 2017e. Where have all the spiders gone? The decline of a poorly known invertebrate fauna in the agricultural and arid zones of southern Australia. Austral Entomology 56:14–22.

Rix, M.G., B.Y. Main, R.J. Raven & M.S. Harvey. 2018. Systematics of the spiny trapdoor spiders of the genus *Eucanippe* (Mygalomorphae: Idiopidae: Aganippini) from south-western Australia: documenting a poorly-known lineage from Australia's biodiversity hotspot. Journal of Arachnology 46:133–154.

Rix, M.G., R.J. Raven, B.Y. Main, S.E. Harrison, A.D. Austin, S.J.B. Cooper et al. 2017d. The Australasian spiny trapdoor spiders of the family Idiopidae (Mygalomorphae: Arbanitinae): a relimitation and revision at the generic level. Invertebrate Systematics 31:566–634.

Ronquist, F. & J.P. Huelsenbeck. 2003. MrBayes 3: Bayesian phylogenetic inference under mixed models. Bioinformatics 19:1572–1574.

*Manuscript received 27 July 2017, revised 16 November 2017.*

2018. Journal of Arachnology 46:345 354

# Two new species of cave-adapted pseudoscorpions (Pseudoscorpiones: Neobisiidae, Chthoniidae) from Guangxi, China

**Zhizhong Gao**[1], **J. Judson Wynne**[2] and **Feng Zhang**[1]: [1]The Key Laboratory of Invertebrate Systematics and Application, College of Life Sciences, Hebei University, Baoding, Hebei 071002, P. R. China; [2]Department of Biological Sciences, Merriam-Powell Center for Environmental Research, Northern Arizona University, Flagstaff, Arizona 86011, U.S.A.; E-mail: jut.wynne@nau.edu

**Abstract.** Two new troglomorphic pseudoscorpion species, *Bisetocreagris maomaotou* sp. nov. (Family Neobisiidae) and *Tyrannochthonius chixingi* sp. nov. (Family Chthoniidae) are described from one cave in the tower karst of northern Guangxi Province, China. This cave is located at close proximity to a village and an adjacent urban area. As with many caves in the South China Karst, this feature occurs at an elevation slightly above agriculture and rural activities; thus, we suggest it may be partially buffered from human activities in the lowland areas. We discuss the likelihood of narrow range endemism and provide research and conservation recommendations to guide future management of these two species.

**Keywords:** *Bisetocreagris*, *Tyrannochthonius*, troglobionts, cave conservation

http://zoobank.org/?lsid=urn:lsid:zoobank.org:pub:68745C67-FE8B-4EF1-B139-F9E968FC683A

Southeast Asia is postulated to yield the highest diversity of troglomorphic animals among the well-sampled tropical regions of the globe (Clements et al. 2006). Yet despite research conducted over the past three decades, few areas in the region have been sufficiently investigated, and knowledge of cave biological diversity and ecological processes is limited (Deharveng & Bedo 2000). The expansive South China Karst represents one of these regions (Chen et al. 2001; Clarke 2006). Among the four administrative units in China where this formation occurs, Guangxi Zhuang Autonomous Region (Guangxi) is considered the most taxonomically well-studied region. At least 99 troglomorphic (cave-adapted) arthropods have been identified; with over half (or 58 species) considered single-cave endemic species (Wynne, unpublished data).

Our knowledge of cave-dwelling pseudoscorpions in this karst area is equally limited. To date, 19 troglomorphic pseudoscorpion species (including the two described here), representing three families (Chernetidae, Chthoniidae, and Neobisiidae), have been described (Schawaller 1995; Mahnert 2003, 2009; Mahnert & Li 2016; Gao et al. 2017; Table 1). All of these animals are known from southern China – occurring within the Guizhou, Hubei, Sichuan, and Yunnan Provinces, and the Chongqing Municipality.

In the paper, we describe two new species of troglomorphic pseudoscorpions (Families Chthoniidae and Neobisiidae) representing the first cave-adapted pseudoscorpions described from Guangxi. We also provide recommendations to guide future research and management efforts.

## METHODS

**Study area.**—Located in southwest China, Guangxi encompasses ~236,400 km$^2$. Once an ancient shallow sea during the middle Cambrian to Late Triassic periods, this region is now largely characterized by a massive karst (limestone) stratum over 10,000 m thick (Cao et al. 2007) with steep-sided mountains called "tower karst" protruding skyward. As a result of the subtropical climate and rock stratum, Guangxi supports at least 600 dissolution caves.

We sampled four caves in the northeastern most extent of Guangxi within a 30 km radius of the city of Guilin, China. Caves were selected based upon two criteria – sufficient length to support deep zone conditions and the availability of a current cave map. Cave deep zones are defined as completely dark regions with relatively stable temperature, low to no airflow, and a near water-saturated atmosphere with a negligible evaporation rate (Howarth 1980, 1982). While we recognize other factors may contribute to the occurrence of cave deep zones (e.g., maze-like and/or constricted passageways, small or partially rock-fall obstructed entrances, and cave structure in general), we used these criteria because logistics prevented us from selecting study caves based upon site visit evaluations. None of these sites had been previously inventoried for cave-adapted arthropods.

Of the four caves sampled, only one yielded the two undescribed pseudoscorpion species described here (Figs. 1–6). All caves occurred at low elevations within tower karst formations. While extensive agriculture, and rural village and suburban habitation characterized the surrounding lowland plains, vegetation on the tower karst represented a marginally disturbed combination of native and introduced plant and tree species.

**Field sampling.**—We collected cave-dwelling arthropods at four caves from 15 to 18 November 2016. Approximately eight hours (2 observers at 4 hours per observer) per cave was spent conducting direct intuitive searches within estimated cave deep zones. Given the four caves varied in size and the diversity of arthropods encountered, the area sampled varied. We also opportunistically collected arthropods as encountered while transiting from entrance to estimated deep zones.

**Analysis and preparation.**—Specimens were collected and preserved in 75% ethanol and deposited in the Museum of Hebei University (MHBU), Baoding City, China. Photographs were taken using a Leica M205A stereomicroscope

Table 1.—Troglomorphic pseudoscorpions described from southern China. Family, genus and species, name of administrative province(s), number of caves (to suggest a level of potential endemism), and names of taxonomic authority are provided.

| Family, genus, species | Province | # Caves | Authority |
|---|---|---|---|
| Family Chernetidae | | | |
| *Megachernes glandulosus* | Sichuan | 1 | Mahnert (2009) |
| *Megachernes tuberosus* | Sichuan | 1 | Mahnert (2009) |
| *Nudochernes troglobius* | Sichuan | 2 | Mahnert (2009) |
| *Nudochernes lipase* | Yunnan | 1 | Mahnert (2009) |
| Family Chthoniidae | | | |
| *Tyrannochthonius akalens* | Sichuan | 1 | Mahnert (2009) |
| *Tyrannochthonius ganshuanensis* | Sichuan, Hubei | 3 | Mahnert (2009) |
| *Tyrannochthonius antridraconis* | Sichuan | 3 | Mahnert (2009) |
| *Tyrannochthonius chixingi* | Guangxi | 1 | this study |
| Family Neobisiidae | | | |
| *Bisetocreagris baozinensis* | Sichuan | 1 | Mahnert & Li (2016) |
| *Bisetocreagris cavernarum* | Chongqing | 1 | Mahnert & Li (2016) |
| *Bisetocreagris chinacavernicola* | Sichuan | 2 | Schawaller (1995) |
| *Bisetocreagris chinaensis* | Guizhou | 2 | Mahnert & Li (2016) |
| *Bisetocreagris gracilenta* | Guizhou | 1 | Schawaller (1995) |
| *Bisetocreagris guangshanensis* | Guizhou | 1 | Gao et al. (2017) |
| *Bisetocreagris jianxinae* | Sichuan | 1 | Mahnert & Li (2016) |
| *Bisetocreagris maomaoton* | Guangxi | 1 | this study |
| *Bisetocreagris martii* | Yunnan | 1 | Mahnert (2003) |
| *Bisetocreagris scaurum* | Yunnan | 1 | Mahnert (2003) |
| *Bisetocreagris titanium* | Yunnan | 1 | Mahnert (2003) |

equipped with a Leica DFC550 camera and LAS software (Ver. 4.6). We used a Leica M205A stereomicroscope for drawings (with a drawing tube) and measurements. Detailed examination of characters was carried out using an Olympus BX53 general optical microscope. Temporary slide mounts were prepared in glycerol.

**Cave locations.**—We recognize standard practice for new species description is to provide ample locality information including georeference data to facilitate future collecting, interpretation and research. Because caves are sensitive resources, we provided general geographical information and offset the latitude and longitude coordinates by ~1 km. This level of detail provided is sufficient for future comparative studies, while protecting the precise location of the cave.

**Terminology.**—Cave ecosystems typically consist of four zonal environments (Howarth 1980, 1983): (1) *entrance zone* – combination of surface and cave environmental conditions; (2) *twilight zone* – both diminished light conditions and influence of

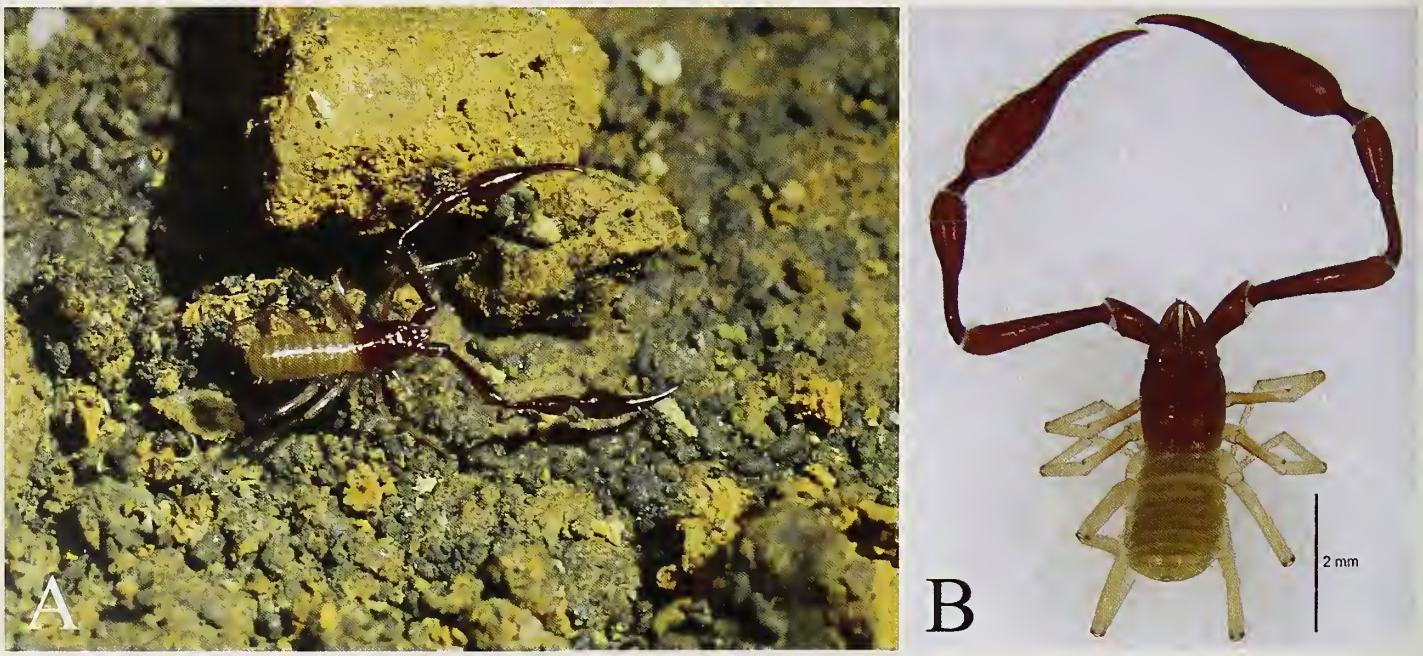


Figure 1.—*Bisetocreagris maomaoton*, sp. nov., A. Image of animal traversing cave floor. B. holotype female, dorsal view.

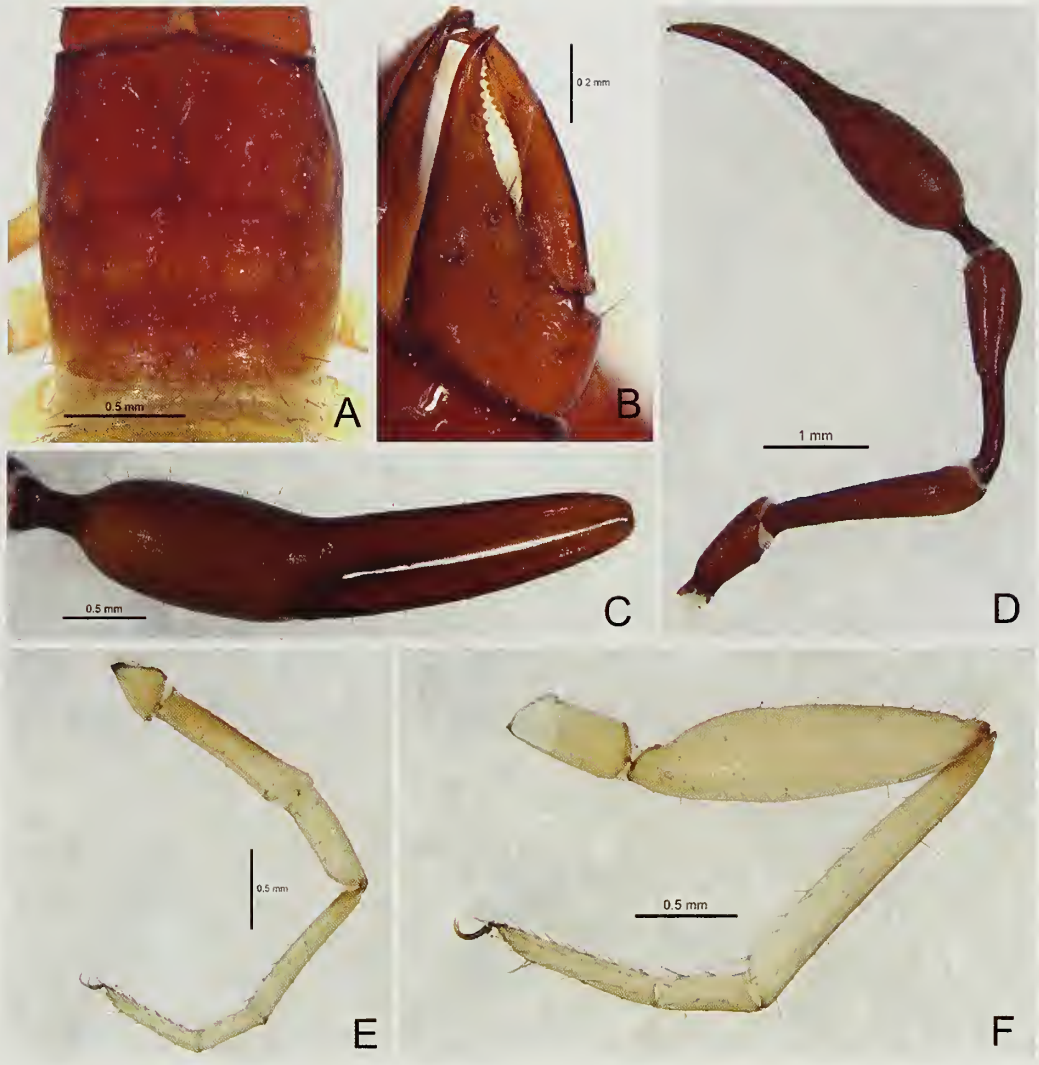


Figure 2.—*Bisetocreagris maomaotou* sp. nov., holotype female: A. Carapace (dorsal view); B. Right chelicerae (dorsal view); C. Chela (lateral view); D. Pedipalp (lateral view); E. Leg I (lateral view); F. Leg IV (lateral view). Scale bars: 0.20 mm (B); 0.50 mm (A, C, E F); 1.00 mm (D).

surface environment; (3) *transition zone* – aphotic, yet barometric and diurnal shifts are observed at a significantly diminished rate approaching near stable climatic conditions; and, (4) *deep zone* – complete darkness, high environmental stability, constant temperature, and near water-saturated atmosphere with low to no airflow (typically occurs in the deepest portion of the cave). While there are four primary cave specific functional groups generally recognized, the specimens discussed are *troglomorphic* (cave-adapted) organisms known as *troglobionts*. These animals are obligate cave dwellers that require the stable environmental conditions of the deep zone to complete their life cycle and exhibit morphological characteristics indicative of cave adaptation. We also reference *troglophiles* (or *troglophilous* organisms) – non-troglomorphic animals that occur facultatively within caves and complete their life cycles there, but also exist in similar cave-like habitats on the surface.

Pseudoscorpion terminology and measurements largely follow Chamberlin (1931) with some minor modifications to the terminology of the trichobothria (Harvey 1992) and chelicera (Judson 2007). The chela and chelal hand are measured in dorsal (for Neobidiidae) and lateral (for Chthoniidae) view and all measurements are in millimeters (mm) unless noted otherwise.

The following abbreviations are used for the trichobothria: *b* = basal; *sb* = sub-basal; *st* = sub-terminal; *t* = terminal; *ib* = interior basal; *isb* = interior sub-basal; *ist* = interior sub-terminal; *it* = interior terminal; *eb* = exterior basal; *esb* = exterior sub-basal; *est* = exterior sub-terminal; *et* = exterior terminal.

## TAXONOMY

**Family Neobisiidae** Chamberlin, 1930

***Bisetocreagris*** Ćurčić, 1983

*Bisetocreagris* Ćurčić 1983: 25.
*Chinacreagris* Ćurčić 1983: 30–31.
*Pedalocreagris* Ćurčić, 1985: 349–350.

**Type species.**—*Bisetocreagris*: *Microcreagris annamensis* Beier, 1951, by original designation.

*Chinacreagris*: *Microcreagris chinensis* Beier, 1943, by original designation.

*Pedalocreagris*: *Pedalocreagris tethys* Ćurčić, 1985, by original designation.

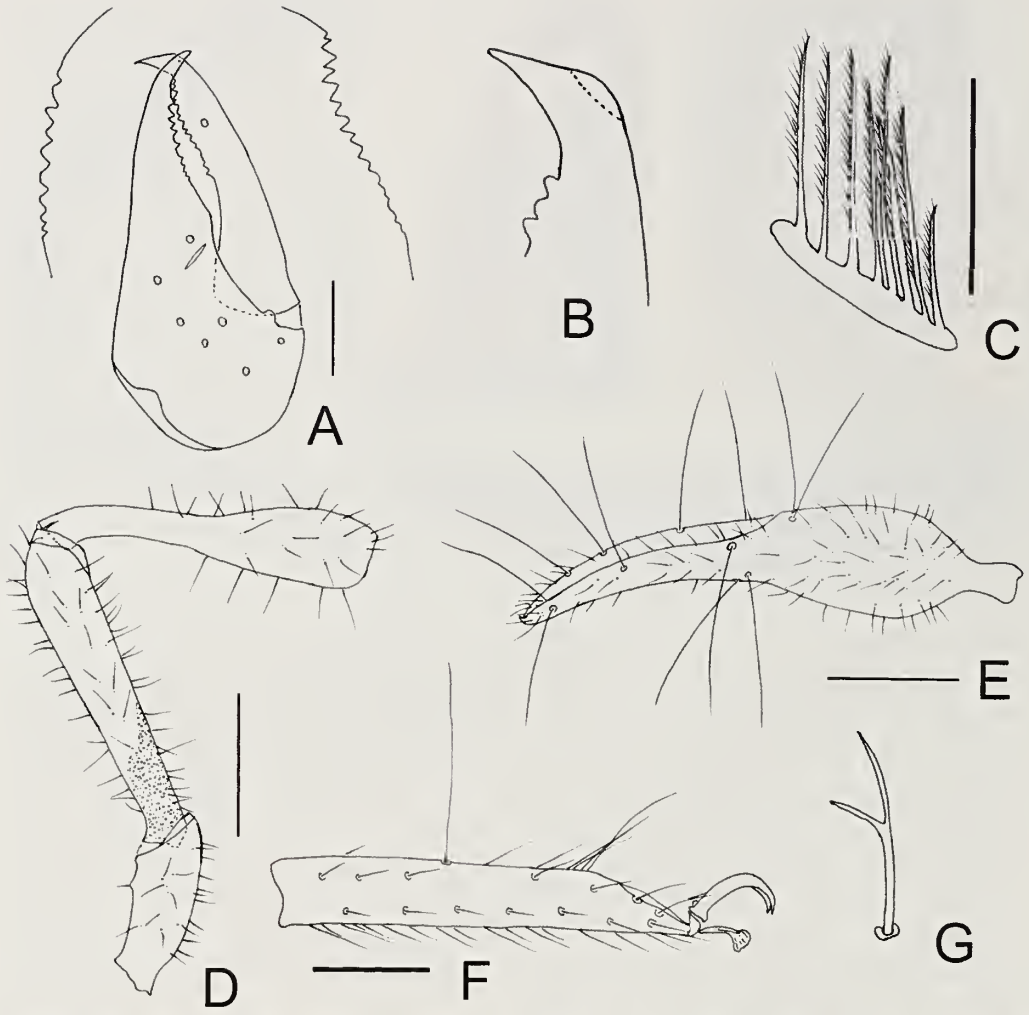


Figure 3.—*Bisetocreagris maomaotou* sp. nov., holotype female: A. Right chelicerae (dorsal view); B. Tip of movable finger of chelicerae (dorsal view); C. Rallum; D. Right pedipalp (minus chela, dorsal view); E. Right chela (lateral view); F. Telotarsus of leg IV (lateral view); G. Subterminal tarsal seta. Scale bars: 0.10 mm (C); 0.25 (A, F); 1.00 mm (D E).

**Remarks.**—Species of *Bisetocreagris* can be identified by both the two small setae each on either side of the anteromedian groove of sternite III in the male (Jia et al. 2010) and the trichobothrial pattern: *et-it* near distal finger tip, *est* isolated in distal half of fixed finger, *ib-isb-ist* grouped closely together at the finger base, *eb-esb* on lateral distal side of hand; thus five trichobothria grouped basally (Mahnert & Li 2016).

Consisting of 34 species and one subspecies, *Bisetocreagris* is widely distributed across Asia and includes 21 species from China (including the species described below). Of these, ten species exhibit troglomorphic characters (Harvey 2013; Mahnert & Li 2016; Gao et al. 2017; this study) while one species is an unnamed troglophile (*Bisetocreagris* sp.; Mahnert & Li 2016).

***Bisetocreagris maomaotou*** sp. nov.
http://zoobank.org/?lsid=urn:lsid:zoobank.org:act:516F187A-E76C-459C-8509-603AFD0422AA
(Figs. 1–3)

**Type material.**—*Holotype female:* **China:** *Guangxi Zhuang Autonomous Region:* Xiufeng District, Maomaotou cave, deep zone, [25°18′46.12″N, 110°16′12.64″E], alt. 225 m, 15 November 2016, J.J. Wynne (Ps.-MHBU-GX16121501).

**Diagnosis.**—Troglomorphic habitus; carapace without eyes or eyespots; epistome triangular and small; carapace with 8 setae on posterior margin; pedipalp smooth excepted for femur which is finely granular in basal part; pedipalp slender, both chelal fingers with 108–109 teeth; femur 5.20 times (length 2.29), patella 4.30 times (length 2.28) longer than broad, pedicel about half of total length of patella.

**Description.**—Female. Carapace, chelicerae and pedipalps reddish brown; abdomen and legs yellowish.

Carapace: Smooth, 1.16 times longer than broad, with a total of 34 setae, including 6 on anterior margin and 8 on posterior margin; without eyes or eyespots; epistome very small, triangular.

Chelicera: Hand with 7 setae, movable finger with one submedial seta; fixed finger with 10 teeth; movable finger with 14 teeth. Galea replaced by a small rounded transparent spinneret. Rallum with 8–9 pinnate setae, distal rallum without expanded base.

Pedipalps: Apex of coxa rounded, with 4 setae on each side. Femur with granulations basally, patella smooth, chelal hand

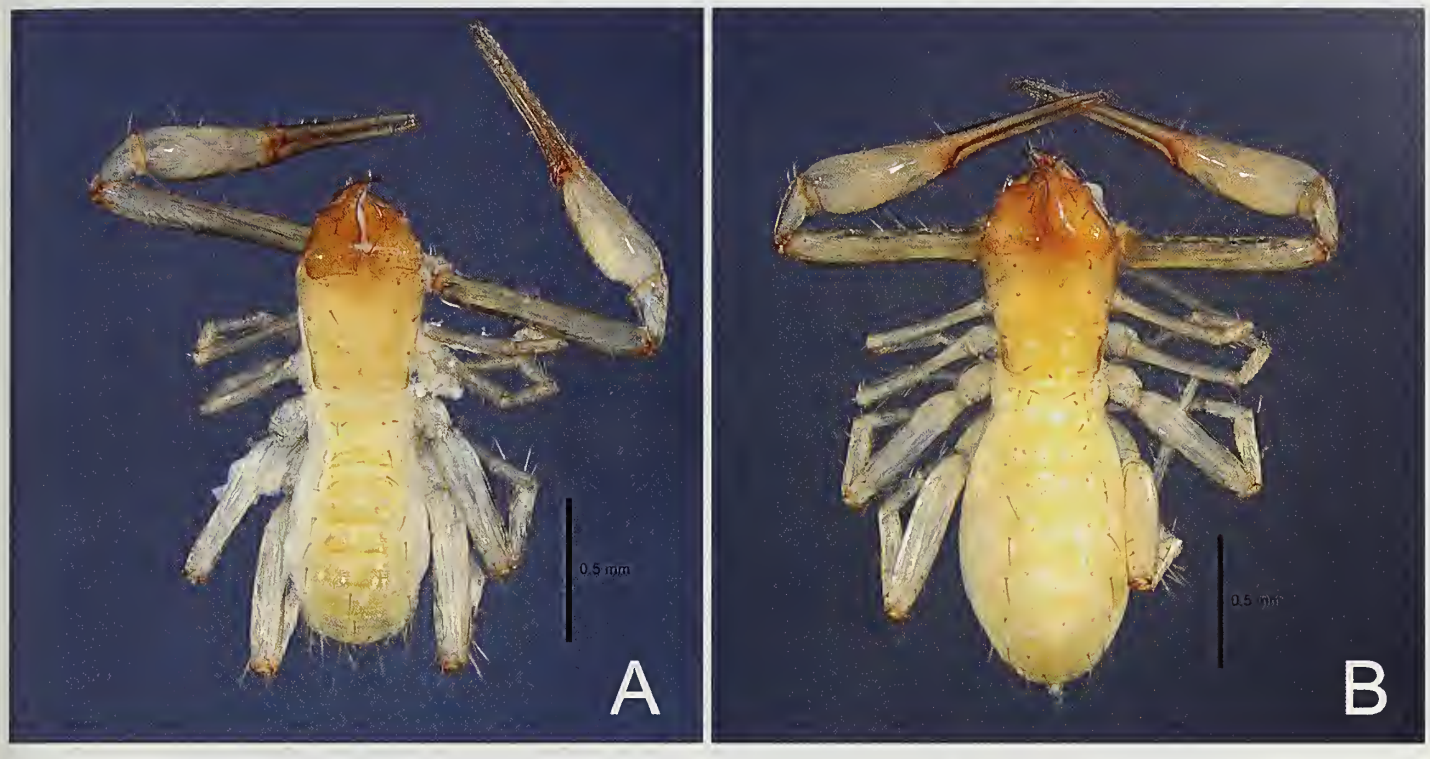


Figure 4.—*Tyrannochthonius chixingi* sp. nov., A. Male holotype, dorsal view; B. Female paratype, dorsal view.

with fine granulations on medial face. Trochanter 2.73, femur 5.20, patella 4.30, chela (with pedicel) 4.75, chela (without pedicel) 4.24 times longer than wide, movable finger 1.38 times longer than hand (without pedicel). Fixed chelal finger with 8 trichobothria, movable finger with 4, *eb* and *esb* on lateral margin of hand; *ib*, *isb* and *ist* on basal half, *et* and *it* on distal half, *est* almost on the middle of fixed finger; *t* and *st* on distal half, *sb* and *b* on basal half of movable finger. Venom apparatus present only in fixed chelal finger, venom duct short. Fixed chelal finger with 109 teeth, movable finger with 108 teeth.

Abdomen: Pleural membrane granulated. Tergal chaetotaxy (I–XI): 11: 11: 11: 11: 13: 12: 12: 13: 12: 15: 8; sternal chaetotaxy (IV–XI): 8: 15: 16: 14: 15: 14: 11: 7; stigmata with 5–6 setae around; anal cone with 2 dorsal and 2 ventral setae. Female genitalia: sternite II with 3–4 setae on each side and a row of 6 setae on the posterior margin; sternite III with a row of 8 setae on the posterior margin.

Legs: Leg I and Leg IV typical. Tibia IV with one submedial tactile seta (TS=0.43), basitarsus IV with one basal tactile seta (TS=0.14), telotarsus IV with one tactile seta (TS = 0.37). Subterminal tarsal seta bifurcate; arolium not divided, shorter than the slender and simple claws.

*Measurements:* (length/breadth or depth in mm; ratios for most characters in parentheses). Female. Body length 3.63. Carapace 1.16 (1.47/1.27). Pedipalpal trochanter 2.73 (1.23/0.45), femur 5.20 (2.29/0.44), patella 4.30 (2.28/0.53), chela (with pedicel) 4.75 (3.75/0.79), chela (without pedicel) 4.24 (3.35/0.79), hand length (without pedicel) 1.41, movable finger length 1.94 (1.38 times longer than hand without pedicel). Leg I: trochanter 1.41 (0.41/0.29), femur 3.93 (1.06/0.27), patella 3.27 (0.72/0.22), tibia 6.69 (1.07/0.16), basitarsus 3.38 (0.44/0.13), telotarsus 5.38 (0.70/0.13). Leg IV: trochanter 2.14 (0.62/0.29), femur + patella 3.91 (1.80/0.46), tibia 7.61 (1.75/0.23), basitarsus 2.83 (0.51/0.18), telotarsus 5.38 (0.86/0.16 ).

**Remarks.**—*Bisetocreagris maomaotou* is a cave-adapted member of the genus, whose pedipalpal pedicel on the patella is about half as long as patella (or about the same length as club). The new species resembles *B. chinacavernicola* but is distinguished by the complete lack of eyes or eyespots (*B. chinacavernicola* has a single small eyespot without lens on each side), epistome triangular (rounded in *B. chinacavernicola*) and the female pedipalpal femur 5.20 times longer than broad (5.7 times in *B. chinacavernicola*), patella 4.30 times longer than broad (4.75 times in *B. chinacavernicola*; Schawaller 1995).

*Bisetocreagris maomaotou* also resembles *B. cavernarum*, but once again, *B. maomaotou* lacks eyes or eyespots; *B. cavernarum* has four eyes and the anterior two have indistinct lenses, the posterior eyes reduced; *B. maomaotou* has a triangular and small epistome, while the epistome is absent in *B. cavernarum*; the new species may be further distinguished from *B. cavernarum* by the stouter pedipalpal femur (in *B. maomaotou*: femur 5.2, chela with pedicel 4.75 times longer than broad, in *B. cavernarum*: femur 5.80, chela with pedicel 5.3–5.4 times longer than broad; Mahnert & Li 2016).

**Etymology.**—The name, a noun in apposition, refers to Maomaotou cave – the type locality where this species occurs.

**Family Chthoniidae** Daday, 1888
***Tyrannochthonius*** Chamberlin, 1929
*Tyrannochthonius* Chamberlin 1929:74.
*Parachthonius* Caporiacco 1949:317.
*Paraliochthonius (Pholeochthonius)* Beier 1976:209.

**Type species.**—*Tyrannochthonius*: *Chthonius terribilis* With, 1906, by original designation.

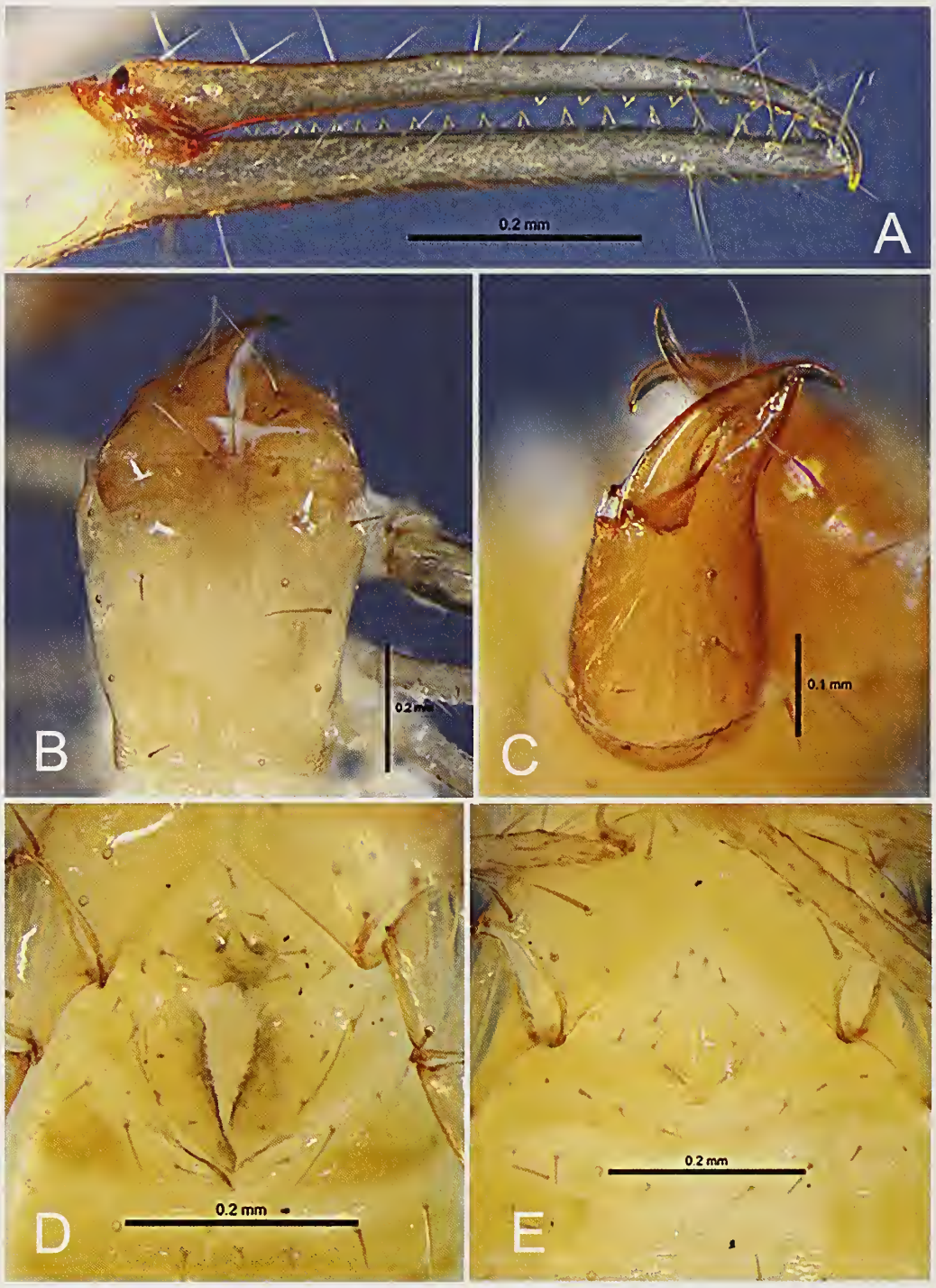


Figure 5.—*Tyrannochthonius chixingi* sp. nov., holotype male (A–D), female paratype (E): A. Chelal fingers (lateral view); B. Carapace (dorsal view); C. Left chelicerae (dorsal view); D. Male genital (ventral view); E. Female genital (ventral view).

*Parachthonius*: *Parachthonius meneghettii* Caporiacco, 1949, by monotypy.

*Paraliochthonius (Pholeochthonius)*: *Paraliochthonius (Pholeochthonius) cavernicola* Beier, 1976, by original designation.

**Remarks.**—*Tyrannochthonius* is a globally distributed genus occurring primarily in tropical and subtropical regions. It represents one of the largest chthoniid genera with about 140 recognized species (Edward & Harvey 2008). Of these, seven species (including the one described below) and one subspecies are known from China including four troglomorphic species (Mahnert 2009; this study).

***Tyrannochthonius chixingi*** sp. nov.
http://zoobank.org/?lsid=urn:lsid:zoobank.org:act:27F8FCC8-5F74-4AD0-8D81-6DA23309F55C
Figs. 4–6

**Type material.**—*Holotype male:* **China:** *Guangxi Zhuang Autonomous Region:* Xiufeng District, Maomaotou cave, deep

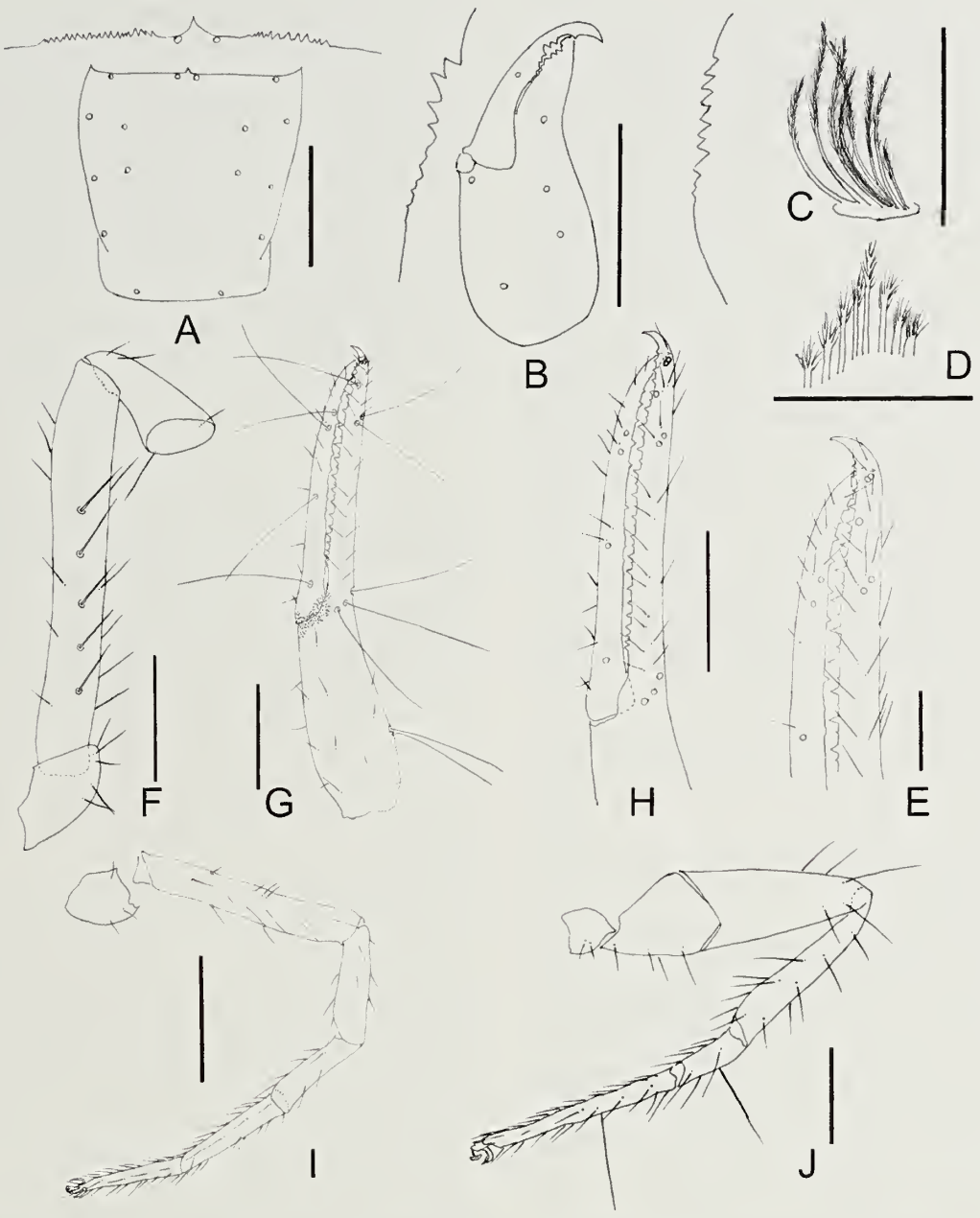


Figure 6.—*Tyrannochthonius chixingi* sp. nov., holotype male: A. Carapace (dorsal view); B. Left chelicerae (dorsal view); C. Rallum; D. Coxal spines on coxae II (ventral view); E. Finger tips of chela (lateral view); F. Left pedipalp (minus chela, dorsal view); G. Left chela (lateral view); H. Chelal fingers (lateral view, showing the teeth); I. Leg I (lateral view); J. Leg IV (lateral view). Scale bars: 0.10 mm (C E); 0.25 mm (A B, F J).

zone, [25°18′46.12″, 110°16′12.64″], alt. 225 m, 15 November 2016, J.J. Wynne (Ps.-MHBU-GX16121502).

*Paratypes:* **China:** *Guangxi Zhuang Autonomous Region:* 1 ♂, 1 ♀, collected with holotype (Ps.-MHBU-GX16121503–GX16121504).

**Diagnosis.**—Moderately sized troglomorphic species; carapace without eyes or eyespots, anterior margin toothed, posterior margin with 2 setae, epistome very pointed and small; anterior tergites (I–II) with 4 setae; intercalary teeth only present on chelal fixed finger, movable finger with 6–7 teeth; lacking chemosensory setae on dorsum of chelal hand.

**Description.**—Adult male.

Colour: Generally pale yellow, chelicera and pedipalp slightly darker, soft parts pale.

Chelicera: Five setae on hand, all setae acuminate; movable finger with one medial seta; fixed finger and movable finger with nine teeth; galea represented by a very slight bump on movable finger; rallum consisting of 7–8 blades, the most anterior blade slightly denticulate, other blades long and well bipinnate.

Pedipalp: All setae acuminate; femur 5.54–6.15, patella 2.14–2.38, chela 5.55–5.74, hand 2.35–2.53 times longer than broad; movable finger 1.27–1.36 times longer than hand, without large basal apodeme (Fig. 6G), only slightly sclerotized section is present; Fig. 6H shows complete teeth.

Femur without tactile setae. Fixed chelal finger and hand with eight trichobothria, movable chelal finger with four trichobothria: *ib* and *isb* situated close together, medially on dorsum of chelal hand; *eb*, *esb* and *ist* forming a straight oblique row sublaterally at base of fixed chelal finger; *it* slightly distal to *est*, situated subdistally; *et* slightly near to tip of fixed finger, very close to chelal teeth; *xs* situated distal to *et*, each seta obviously smaller than those of other trichobothria; microsetae (chemosensory setae) absent on both pedipalpal fingers; trichobothrium *st* of movable finger situated close to the base; *sb* situated slightly closer to *b* than to *st*; *b* and *t* situated subdistally, *t* situated at same level as *it*; *b* situated basal to *est*. Sensilla and venom apparatus absent. Chelal teeth heterodentate: fixed finger with 22–23 large, erect, well-spaced teeth, plus 9 small intercalary teeth; movable finger with 6–7 middle sized well-spaced smooth teeth, without intercalary teeth.

Cephalothorax: Carapace 1.11–1.14 times longer than broad; anterior margin toothed; lateral margins constricted posteriorly; without any traces of eyes; epistome very pointed and small; with 16 setae arranged 4: 4: 4: 2: 2; without furrows. Chaetotaxy of coxae: 4: 4: 4: 5; manducatory process with two acuminate distal setae, anterior seta less than 1/2 length of medial seta; coxae II with seven terminally incised coxal spines on each side, set in oblique row; intercoxal tubercle absent; without sub-oral seta.

Abdomen: Pleural membrane papillostriate. Tergites and sternites undivided; setae uniseriate and acuminate. Tergal chaetotaxy (I–XI): 4: 4: 4: 4: 4: 4: 4: 5: 5: 4: 2. Sternal chaetotaxy V–XI: 6: 6: 6: 6: 8: 8:2.

Legs: Typical. Femur + patella of leg IV 3.14–3.35 times longer than broad; arolium slightly shorter than the claws, not divided; claws simple.

*Measurements:* (length/breadth or depth in mm, ratios for most characters provided in parentheses). Male holotype and paratype: Body length 1.24–1.30. Pedipalps: trochanter 1.62–1.92 (0.21–0.23/0.12–0.13), femur 5.54–6.15 (0.72–0.80/0.13), patella 2.14–2.38 (0.30–0.31/0.13–0.14), chela 5.55–5.74 (1.09–1.11/0.19–0.20), hand length 2.35–2.53 (0.47–0.48/0.19–0.20), movable finger length 0.61–0.64. Carapace 1.11–1.14 (0.49–0.50/0.43–0.45). Leg I: femur 7.00–7.50 (0.42–0.45/0.06), patella 4.00–4.50 (0.24–0.27/0.06), tibia 3.67–4.00 (0.20–0.22/0.05–0.06), tarsus 8.40–9.40 (0.42–0.47/0.05). Leg IV: femur + patella 3.14–3.35 (0.67–0.69/0.20–0.22), tibia 5.67 (0.51/0.09), basitarsus 3.33–3.83 (0.20–0.23/0.06), telotarsus 11.00–13.25 (0.53–0.55/0.04–0.05).

Female paratype: Body length 1.64. Pedipalps: trochanter 1.86 (0.26/0.14), femur 6.69 (0.87/0.13), patella 2.00 (0.34/0.17), chela 5.39 (1.24/0.23), hand length 2.26 (0.52/0.23), movable finger length 0.72. Carapace 1.04 (0.56/0.54). Leg I: femur 6.25 (0.50/0.08), patella 3.86 (0.27/0.07), tibia 4.00 (0.24/0.06), tarsus 11.00 (0.55/0.05). Leg IV: femur + patella 3.30 (0.76/0.23), tibia 6.33 (0.57/0.09), basitarsus 2.63 (0.21/0.08), telotarsus 11.40 (0.57/0.05).

**Remarks.**—All Chinese cave-dwelling *Tyrannochthonius* species lack eyes or eyespots (Mahnert 2009; this study). The new species resembles *T. ganshuanensis* but can be distinguished by the toothed anterior margin of carapace (not toothed in *T. ganshuanensis*); movable finger of pedipalp without intercalary teeth in the new species, while present in *T. ganshuanensis*; the tergal chaetotaxy on anterior tergites is also different (tergites I–III with four setae in the new species, while only two in *T. ganshuanensis*; Mahnert 2009).

*Tyrannochthonius chixingi* shares the character of anterior tergites with four marginal setae with *T. antridraconis* but is differentiated by the slightly wider pedipalps (e.g., femur 6.69 times vs. 7.3–7.8 times, patella 2.0 times vs. 2.20–2.60 times, chela 5.39 vs. 7.9–8.0 times longer than broad in males). This animal seems to be further distinguished from *T. antridraconis* by a smaller body size (*T. chixingi* males range from 1.24 to 1.30 and the female specimen is 1.64, while *T. antridraconis* is at least 1.80; Mahnert 2009).

**Etymology.**—This species name, *chixingi*, was derived from the Latinized Mandarin phrase for "toothed." *Chǐ xíng* (齿形) refers to the toothed anterior margin of the carapace.

## DISCUSSION

The low number of cave-dwelling pseudoscorpions in southern China is potentially more reflective of limited biospeleological research rather than low diversity within this group. With the descriptions of the first known cave-adapted pseudoscorpions from Guangxi, we increase the total number of southern China cave-adapted pseudoscorpions to 19 species. Most of these species (14 of 19) were detected in only one cave (Table 1). Given our limited knowledge of regional cave biology (Chen et al. 2001; Clarke 2006; Whitten 2009) and that their type localities were either not sampled intensively or field sampling methodologies were not provided, we are unable to draw strong inference concerning whether any of these species may be reasonably considered single cave endemics.

While the Guangxi pseudoscorpions currently known only from their type locality may also occur in other regional caves, it is improbable they are wide-ranging species. In general, troglomorphic species are well documented as being either single endemics or having small distributional ranges (Christman et al. 2005; Deharveng et al. 2008; Latella & Chen 2008; Tian 2011; Borges et al. 2012; Harvey & Wynne 2014). Wynne (unpublished data) found that of the 99 known, cave-adapted arthropods for Guangxi, over half (or 58 species) were identified from one cave. Interestingly, in the eastern United States, Christman et al. (2005) found Pseudoscorpionida retained the highest rate of single-cave endemism (69%) across the arthropod groups examined.

Concerning other caves where these species may occur, there are at least seven caves within a 5 km radius of Maomaotou Cave (Y. Zhang, personal communication, 2017). Three of these caves occur within the same tower karst formation (Maomaotou Hill) but were not surveyed because they did not meet our study site selection criteria. We suggest these two new species likely occur throughout Maomaotou Hill within the subterranean network of interconnected fissures ranging in size from microcaverns (< 0.1 cm) to macrocaverns (> 20 cm; Howarth 1983), and thus may have once occurred within these three caves when habitat conditions were suitable.

Based upon extensive human activities in one cave and expert opinion describing environmental conditions of the other two caves, we deduced it is unlikely that troglomorphic organisms presently occur within these caves. Reed Flute Cave has been a popular tourist cave since the 1980s and has been significantly modified for tourism (E. Lynch, personal

communication, 2017). Modifications include lighted and paved concrete walking pathways, colored lighting to illuminate speleothem formations, and excavation of a second entrance, which have likely altered airflow and relative humidity. Additionally, increased cave temperatures have been correlated with intensive human visitation (Pulido-Bosch et al. 1997; Song et al. 2000; Fernandez-Cortes et al. 2011).

The other two caves are relatively small through caves (i.e., tunnel caves; Zhu et al. 1988). One is located at the base of the hill approximately 0.5 km north by northeast of Maomaotou Cave, and is ~100 m in length with a small side passage (~80m in length). The second cave is ~300 m in length. Airflow has been observed in both of these caves (Y. Zhang, personal communication, 2017), and were excluded from survey because the climatic conditions seemed too variable to support deep zone conditions.

Maomaotou Hill is surrounded by human activities. It is likely that agricultural and rural activities in this region span millennia. Today, urban development sprawls to the south and east, and agriculture, suburban areas and rural village habitation occur to the north and west. Subsequently, these two new cave-adapted pseudoscorpion species may have been restricted to this limestone formation for thousands of years.

To obtain a better understanding of these species' distributional ranges, we recommend additional arthropod surveys be conducted at the seven regional caves within a 5 km radius of Maomaotou Cave. Such an effort will be required to help constrain whether these species are single-cave or regional endemics, as well as to obtain the information necessary to make science-based recommendations for conservation and management. However, because our two species are cave-adapted and thus endemic, we consider these species to be of management concern.

We have limited information regarding the cave-dwelling arthropod community within which these two species occur. Through better characterizing this community, researchers and managers may elucidate the pseudoscorpions' role in the community, as well as better define the distribution of these two species within Maomaotou Cave based upon the distributions of suitable habitat and potential prey species. As our sampling was temporally constrained (2 people at ~ 4 hours) during one site visit and employed a single technique, we suggest applying multiple techniques with multiple site visits conducted during the appropriate time of year to garner a more comprehensive picture of the cave arthropod community (Wynne & Voyles 2014; Wynne et al. 2018). If this is not possible, we minimally suggest the deep zone of Maomaotou Cave be intensively and systematically sampled using baits (Howarth et al. 2007), leaf-litter traps (Slaney & Weinstein 1996), and direct intuitive searches using a similar sampling protocol proposed by Wynne et al. (2014) and Wynne et al. (2018).

**Conservation and management.**—These two new pseudoscorpion species are presumed to have restricted distributional ranges and are subsequently sensitive to human disturbance. Presently, there are no cave management strategies in place to mitigate impacts associated with trampling by human visitation, surface contamination or other human activities. Although we did not observe a significant amount of litter within this cave, we did observe trampled areas associated with recent visitation. Additionally, this cave is well known as evidenced by the old Mandarin inscriptions believed to be at least 100 years old and contemporary graffiti along the cave walls, as well as garbage both around the entrance and along the trail leading to the cave. Given that future human activity will probably intensify rather than diminish, increased human visitation is anticipated to further challenge the persistence of these species, the arthropod community within which they occur, and the other sensitive cave biological resources occurring within this cave.

Regarding other human impacts, this cave is situated at a slightly higher elevation than human development, so it may be partially insulated from human activities including runoff associated with fertilizer and pesticide use, siltification from vegetation conversion and agriculture, and other related human activities.

Finally, an earlier attempt was made to restrict human access as evidenced from a now dilapidated cave gate. While gates can be effective in deterring some of the proximal effects of human activities (inadvertently trampling arthropod habitats, contamination including spray paint used for graffiti, etc.) and repairing the gate is advisable, an outreach program to educate both villagers and visitants regarding the sensitive biological resources within the cave should also be considered. The local karst research institute in Guilin could possibly host a meeting in the Yujiacun village (the village below the cave) to discuss these new discoveries and stress the sensitivities of cave-restricted animal populations to human disturbance. Additionally, we recommend establishing an educational display on the sensitivities of cave-adapted animals and the threats human activities pose at the Reed Flute Cave Visitor's Center. We further suggest posting signage within the village and at Maomaotou cave entrance describing the sensitivity of cave resources, the presence of sensitive endemic species, and cave etiquette protocols describing how to reduce human impacts. Through both additional research and the management recommendations elucidated here, we may be able to make strides towards evidence-based conservation and management including the protection of Chinese cave-adapted animal populations such as the Maomaotou pseudoscorpions.

## ACKNOWLEDGMENTS

This work was supported by the National Natural Science Foundation of China (No. 31372154), and also by the Ministry of Science and Technology of the People's Republic of China (MOST Grant No. 2015FY210300). Data collection was partially supported by Wang Jietao at the Wuhan Center, China Geological Survey. Fieldwork was recognized as an Explorers Club flag expedition.

## LITERATURE CITED

Beier, M. 1976. The pseudoscorpions of New Zealand, Norfolk and Lord Howe. New Zealand Journal of Zoology 3:199 246.

Borges, P.A.V., P. Cardoso, I.R. Amorim, F. Pereira, J.P. Constância, J.C. Nunes et al. 2012. Volcanic caves: Priorities for conserving the Azorean endemic troglobiont species. International Journal of Speleology 41:101 112.

Cao, J., D. Yang, C. Zhang & Z. Jiang. 2007. Karst ecosystem of Guangxi Zhuang Autonomous Region Constrained by Geological Setting: Relationship between carbonate rock exposure and

vegetation coverage. International Conference on Karst Hydrogeology and Ecosystems, USA:211–218.

Caporiacco, L. di 1949. Aracnidi della Colonia del Kenya raccolti da Toschi e Meneghetti negli anni 1944–1946. Commentationes Pontificiae Academia Scientarum 13:309–492.

Chamberlin, J.C. 1929. A synoptic classification of the false scorpions or chela-spinners, with a report on a cosmopolitan collection of the same. Part 1. The Heterosphyronida (Chthoniidae) (Arachnida-Chelonethida). Annals and Magazine of Natural History [series 10] 4:50–80.

Chamberlin, J.C. 1931. The arachnid order Chelonethida. Stanford University Publications. Biological Sciences 7:1–284.

Chen, Z., V. Deeu, C. Juberthie & S.I. Ueno. 2001. China. Pp. 1763–1781. *In* Encyclopaedia Biospeologica, Part III. (C. Juberthie & V. Deeu, eds.). Société Internationale de Biospéologie, Moulis, France.

Christman, M.C., D.C. Culver, M.K. Madden & D. White. 2005. Patterns of endemism of the eastern North American cave fauna. Journal of Biogeography 32:1441–1452.

Clarke, A.K. 2006. Guangxi 2005 cave fauna report (China Caves Project). YRC Bulletin, Autumn 2006.

Clements, R., N.S. Sodhi, M. Schilthuizen & P.K. Ng. 2006. Limestone karsts of Southeast Asia: imperiled arks of biodiversity. Bioscience 56:733–742.

Ćurčić, B.P.M. 1983. A revision of some Asian species of *Microcreagris* Balzan, 1892 (Neobisiidae, Pseudoscorpiones). Bulletin of the British Arachnological Society 6:23–36.

Ćurčić, B.P.M. 1985. A revision of some species of *Microcreagris* Balzan, 1892 (Neobisiidae, Pseudoscorpiones) from the USSR and adjacent regions. Bulletin of the British Arachnological Society 6:331–352.

Deharveng L. & A. Bedo. 2000. The cave fauna of Southeast Asia: Origin, evolution and ecology. Pp. 603–632. *In* Ecosystems of the World 30: Subterranean Ecosystems (H. Wilkens, D.C. Culver, W.F. Humphreys, eds.). Elsevier, Amsterdam.

Deharveng, L.O., F. Bréhier, A.N. Bedos, M.Y. Tian, Y.B. Li, F. Zhang et al. 2008. Mulun and surrounding karsts (Guangxi) host the richest cave fauna of China. Subterranean Biology 6:75–79.

Edward, K.L., & M.S. Harvey. 2008. Short-range endemism in hypogean environments: the pseudoscorpion genera *Tyrannochthonius* and *Lagynochthonius* (Pseudoscorpiones: Chthoniidae) in the semiarid zone of western Australia. Invertebrate Systematics 22:259–293.

Fernandez-Cortes, A., S. Cuezva, S. Sanchez-Moral, J.C. Cañaveras, E. Porca, V. Jurado et al. 2011. Detection of human-induced environmental disturbances in a show cave. Environmental Science and Pollution Research 18:1037–1045.

Gao, Z., H. Chen & F. Zhang. 2017. Description of two new cave-dwelling *Bisetocreagris* species (Pseudoscorpiones, Neobisiidae) from China. Turkish Journal of Zoology 41:615–623.

Harvey, M.S. 1992. The phylogeny and classification of the Pseudoscorpionida (Chelicerata: Arachnida). Invertebrate Taxonomy 6:1373–1435.

Harvey, M.S. 2013. Pseudoscorpions of the World, version 3.0. Western Australian Museum, Perth. Online at http://museum.wa.gov.au/catalogues-beta/pseudoscorpions Accessed 12 June 2017.

Harvey, M.S. & J.J. Wynne. 2014. Troglomorphic pseudoscorpions (Arachnida: Pseudoscorpiones) of northern Arizona, with descriptions of two new short-range endemic species. Journal of Arachnology 42:205–219.

Howarth, F.G. 1980. The zoogeography of specialized cave animals: A bioclimatic model. Evolution 34:394–406.

Howarth, F.G. 1982. Bioclimatic and geological factors governing the evolution and distribution of Hawaiian cave insects. Entomologia Generalis 8:17–26.

Howarth, F.G. 1983. Ecology of cave arthropods. Annual Review of Entomology 28:365–389.

Howarth, F.G., S.A. James, W. McDowell, D.J. Preston & C.T. Imada. 2007. Identification of roots in lava tube caves using molecular techniques: implications for conservation of cave arthropod faunas. Journal of Insect Conservation 11:251–261.

Jia, Y., Y.W. Zhao & M.S. Zhu. 2010. A new species of the pseudoscorpion genus *Bisetocreagris* from China (Arachnida: Pseudoscorpiones: Neobisiidae). Zootaxa 2340: 65–68.

Judson, M.L.I. 2007. A new and endangered species of the pseudoscorpion genus *Lagynochthonius* from a cave in Vietnam, with notes on chelal morphology and the composition of the Tyrannochthoniini (Arachnida, Chelonethi, Chthoniidae). Zootaxa 1627:53–68.

Latella, L. & H. Chen. 2008. Biological investigation of the Museo Civico di Storia Naturale of Verona in South China caves. Pp. 65–88. *In* Research in South China Karst (L. Latella & R. Zorzin, eds.). Memorie del Museo Civico di Storia Naturale di Verona-2. Serie – Monografie Naturalistiche 3.

Mahnert, V. 2003. Four new species of pseudoscorpions (Arachnida, Pseudoscorpiones: Neobisiidae, Chernetidae) from caves in Yunnan Province, China. Revue suisse de Zoologie 110:739–748.

Mahnert, V. 2009. New species of pseudoscorpions (Arachnida, Pseudoscorpiones, Chthoniidae, Chernetidae) from caves in China. Revue Suisse de Zoologie 116:185–201.

Mahnert, V. & Y.C. Li. 2016. Cave-inhabiting Neobisiidae (Arachnida: Pseudoscorpiones) from China, with description of four new species of *Bisetocreagris* Ćurčić. Revue Suisse de Zoologie 123:259–268.

Pulido-Bosch, A., W. Martin-Rosales, M. López-Chicano, C.M. Rodriguez-Navarro & A. Vallejos. 1997. Human impact in a tourist karstic cave (Aracena, Spain). Environmental Geology 31:142–149.

Schawaller, W. 1995. Review of the pseudoscorpion fauna of China (Arachnida: Pseudoscorpionida). Revue Suisse de Zoologie 102:1045–1063.

Slancy, D.P. & P. Weinstein. 1996. Leaf litter traps for sampling orthopteroid insects in tropical caves. Journal of Orthoptera Research 5:51–52.

Song, L., X. Wei & F. Liang. 2000. The influence of cave tourism on $CO_2$ and temperature in Baiyun Cave, Hebei, China. International Journal of Speleology 29:77–87.

Tian, M. 2011. A new subgenus and two new species of the troglobitic genus *Dongodytes* Deuve from Guangxi, China (Coleoptera, Carabidae). Subterranean Biology 8:57–64.

Whitten, T. 2009. Applying ecology for cave management in China and neighboring countries. Journal of Applied Ecology 46:520–523.

Wynne, J.J. & K.D. Voyles. 2014. Cave-dwelling arthropods and vertebrates of North Rim Grand Canyon, with notes on ecology and management. Western North American Naturalist 74:1–17.

Wynne, J.J., E.C. Bernard, F.G. Howarth, S. Sommer, F.N. Soto-Adames, S. Taiti et al. 2014. Disturbance reliefs in a rapidly changing world: the Rapa Nui (Easter Island) factor. BioScience 64:711–718.

Wynne, J.J., S. Sommer, F.G. Howarth, B.G. Dickson & K.D. Voyles. 2018. Capturing arthropod diversity in complex cave systems. Diversity and Distributions DOI: 10.1111/ddi.12772.

Zhu X.W., X.Y. Wang, D.H. Zhu, Z. Gong, & H. Qin. 1988. Research of Guilin Karst Geomorphology and Caves. Geological Publishing House, Beijing, China. ISBN: 7-116-00122-0 (In Mandarin).

*Manuscript received 9 August 2017, revised 8 November 2017.*

2018. Journal of Arachnology 46:355–369

# Clarification of three species of *Discocyrtus* Holmberg, 1878 with convoluted taxonomic histories (Opiliones: Laniatores: Gonyleptidae: Pachylinae)

**Adriano B. Kury**[1], **Ricardo Pinto-da-Rocha**[2], **Jürgen Gruber**[3] and **Rafael N. Carvalho**[1]: [1]Departamento de Invertebrados, Museu Nacional (UFRJ), 20.940-040, Rio de Janeiro, Rio de Janeiro, Brazil; E-mail: adrianok@gmail.com; [2]Departamento de Zoologia, Instituto de Biociências, Universidade de São Paulo (USP), 05422-970 São Paulo, São Paulo, Brazil; [3]Naturhistorisches Museum, [3]Zoologische Abteilung, P.O.B. 417, Burgring 7, A-1010, Wien, Austria.

**Abstract.** *Gouyleptes curvipes* Kollar, in C.L. Koch, 1839 has taxonomic problems: it is a primary junior homonym of *Gouyleptes curvipes* Guérin-Méneville, 1837; the holotype of *G. curvipes* Kollar was cited twice by Roewer (1913) under two genera, one being a misidentification of an undescribed species and a new combination under *Discocyrtus* Holmberg, 1878; Koch labeled another unreported specimen as *Gouyleptes curvipes*. However, this specimen belongs to a species described later by Roewer as *D. crenulatus* Roewer, 1913. In 2003, Kury transferred *G. curvipes* sensu Roewer to *Discocyrtus* and, to avoid homonymic collision with *D. curvipes* sensu Roewer, proposed the new name *D. confusus* as a replacement name. *Discocyrtus confusus* was later considered an invalid replacement name and was used to newly describe the species named by Kollar and Koch. *Discocyrtus flavigranulatus* B. Soares, 1944 is here considered a new junior subjective synonym of *G. curvipes* Kollar, but which is the next oldest available synonym. *Discocyrtus confusus* thus also becomes a junior synonym of *D. flavigranulatus*. Here we discuss the history and identity of three species of *Discocyrtus*: *D. flavigranulatus* B. Soares, 1944; *D. crenulatus* Roewer, 1913; and *D. fenax* sp. nov. from Santa Catarina state, Brazil (misidentified by Roewer as *D. curvipes*).

**Keywords:** Arachnida; harvestmen; Grassatores; Neotropics; Brazil.

ZooBank LSID: urn:lsid:zoobank.org:pub:041B7A98-FE0B-482B-B99A-125B638CBCD0

The Neotropical harvestmen genus *Discocyrtus* Holmberg, 1878 is the most diverse of the Gonyleptidae, and is among the top ten most diverse genera of Opiliones in the world (Kury 2002+), with ca. 70 valid species (Kury 2003; Kury & Carvalho 2016). This accounts for 10% of the valid Gonyleptidae and is caused by real diversity and also by generalized use of meristic formulas in Laniatores (the so-called Roewerian system), which has been widely favored by subsequent authors. Due to this diversity and lack of taxonomic resolution, already in the 1940s Mello-Leitão (pers. comm. to H. Soares, reported to A. Kury in the 1990s) had given up identifying *Discocyrtus* to species, leaving most as "*Discocyrtus* sp.", while B. and H. Soares also avoided a direct confrontation with the subject. Modern expeditions to all parts of the Brazilian Atlantic Forest often retrieve many specimens with different morphotypes, which mostly remain as identified as "*Discocyrtus* sp." More recently, some distinct groups are being little by little removed from *Discocyrtus* and given generic status (e.g., Kury & Carvalho 2016; Carvalho & Kury 2018).

Three *Discocyrtus* species are remarkably entangled in the literature – involving, among others, the names *D. curvipes* Kollar, 1839, *D. crenulatus* Roewer, 1913, *D. flavigranulatus* B. Soares, 1944, *D. confusus* Kury, 2011 and one as yet undescribed species. In the present work, an extensive study of the material used to describe the species associated with these names is made and we present new diagnoses of two valid species, while a third one is formally described.

## METHODS

Descriptions of colors use the standard names of the 267 Color Centroids of the NBS/IBCC Color System (Jaffer 2001+) as described in Kury & Orrico (2006). Scanning Electron Microscopy was carried out with a JEOL JSM-6390LV at the Center for Scanning Electron Microscopy of Museu Nacional/Universidade Federal do Rio de Janeiro (UFRJ). All measurements are in mm.

The diagnoses given here are comparative among the three relevant species, but they are not especially similar to one another. Additionally, we have compared them with the type species, *D. testudineus* (Holmberg, 1876). The confusion of those three species with one another is merely an historical artifact. The two questions: (1) "Are any of these species more similar to other species not included in the manuscript?" and (2) "Are there sympatric species that could be confused with any of these three?" are not addressed here, but rather in ongoing reviews of several species groups.

The answers to the questions in the preceding paragraph have significance for the diagnoses the authors use for each species. It would be odd to diagnose the mutual differences among three random, allopatric species when species that are more similar and perhaps sympatric are simply ignored. Diagnoses should be applicable to identification among all relevant species, especially sympatric or potentially sympatric ones, not simply which happen to share a peculiar nomenclatural past.

Abbreviations of the repositories cited are: IBSP (Instituto Butantan, São Paulo), MNRJ-HS (Private Collection Helia Soares, presently in MNRJ), IRSNB (Institut Royal des Sciences Naturelles de Belgique, Brussels), MNRJ (Museu Nacional, Rio de Janeiro), MZSP (Museu de Zoologia da Universidade de São Paulo, São Paulo), NHMW (Naturhistorisches Museum Wien, Vienna), SMF (Senckenberg Natur-Museum und Forschungsinstitut, Frankfurt). Other abbrevi-

ations used: DS = dorsal scutum, CL = carapace length, CW = carapace width, AL = abdominal scutum length, AW = abdominal scutum width, Ch = chelicera, Pp = pedipalpus, Cx = coxa, Tr = trochanter, Fe = femur, Pa = patella, Ti = tibia, Mt = metatarsus, Ta = tarsus, MS = macrosetae.

Tarsal formula: numbers of tarsomeres in tarsus I to IV, when an individual count is given, order is from left to right side (figures in parentheses denote number of tarsomeres only in the distitarsus I–II).

## HISTORICAL TAXONOMIC BACKGROUND

Guérin-Méneville (1837) described the species *Gonyleptes curvipes* from Chile; a few years later (Gervais 1844: 101) it was synonymized with *G. chilensis* Gray, 1833 (currently *Pachylus chilensis*). Guérin-Méneville's work *Iconographie du Règne Animal* appeared in separate parts over many years. Based on Cowan (1971), we can establish that the first publication of *G. curvipes* was in Planche 4, Livraison 45 (December 1837), although the corresponding complete text only appeared on September 7, 1844.

Sometime between 1818 and 1824, Johann Natterer collected arachnids in several localities in eastern Brazil. The specimens (pinned and dry) arrived in Vienna by at least 1836, but probably earlier.

In the 1830s, the Austrian biologist Vinzenz Kollar planned to publish descriptions of Natterer material (in 1833, he presented the Monograph of mainly Austrian phalangids – also remaining unpublished), then at some time the material was sent to German arachnologist Carl Ludwig Koch in Regensburg, for further description and preparing hand-coloured figures, before being returned to Vienna. There must have been accompanying documentation (labels, preliminary descriptions by Kollar) but seemingly no precise locality data. As currently known, nothing remains of this presumed documentation.

C.L. Koch (1839a) examined a male among the NHMW harvestman material previously studied by Kollar, and described the then new species *G. curvipes* (C.L. Koch 1839a, pp. 36–38, plate CCXXIV [= 224], fig. 555). He provided a Latin diagnosis by Kollar with his German translation, a longer German description, and a mock life-like colored illustration (Fig. 1A). The type locality of the specimen is reported only as "Brasilien". His illustration allows recognition of what is today called a typical Atlantic *Discocyrtus* with features of a species still recognizable. Although not reported in the description, the accession number of this specimen is 1847.II.49 (therefore given 8 years later) and currently (during a 1965 inventory by J. Gruber) renumbered NHMW 3127 (Figs. 1D–E, 2). There are no original labels associated with the specimen remaining in NHMW, which may have been discarded by the "Korrespondent" (that is, a voluntary coworker) E. Reimoser in early 20th century. This specimen was originally pinned and conserved dry, but later transferred to ethanol (see below).

C.L. Koch (1839b: 13) repeated the diagnosis of *G. curvipes* in a synopsis of Opiliones.

Kollar entered in the accession book of NHMW sub 1847. Februar, II., numbers 1. and 2. two samples of Crustacea from Brazil. On the same page further below we find a "Nachtrag" (addendum) (and, curiously, "Arachnoidea" stricken out!) – a list of Brazilian Arachnida numbered consecutively (!) "3 – 63.", clearly written by another person about 50 years later (as evidenced by the names of authors Ausserer and W[illiam] S[orensen]). Present in this list are the names "47 Discocyrtus crenulatus W.S." and "49 Gonyleptes curvipes Kllr".

Bertkau (1880) synonymized *G. curvipes* Kollar, in C.L. Koch, 1839 with *G. horridus* Kirby, 1819, which was refuted by all subsequent authors.

W. Sorensen (1884: 603), commenting on some species of *Gonyleptes*, stated [our translation]: "*G. curvipes* does not match *G. horridus*. But *G. horridus* (of Kirby), *Phalangium acanthopus* Quoy & Gaimard [1824] and *G. horridus* (sensu Koch 1839b), all appear to be the same species." At that time, he had not examined any material from Vienna, including the type of *G. curvipes*.

Around 1891 (as evidenced by the annual report of curator Karl Koebel in Hauer 1892: 40), Sorensen studied material lodged in NHMW. Besides studying the holotype of *G. curvipes* (NHMW 3127) (Figs. 1D–E, 2), he studied another male specimen, numbered 1847.II.47 (currently NHMW 3126) (Figs. 3A–B). He assigned both specimens to the genus *Discocyrtus*, labeling NHMW 3126 as *D. crenulatus* W.S. [in schedula] and NHMW 3127 as *D. curvipes*. Sorensen never published these data (he died in 1916).

In the late 1890s, T. Adensamer and A. Penther, the NHMW curators, prepared a card index for arachnids which now serves as a surrogate for the lost original labels. These cards are shown here for *D. crenulatus* W.S. [in schedula] (Figs. 3C–D) and *D. curvipes* (Figs. 1B–C).

About twenty years after Sorensen, C.-F. Roewer (1913) studied both NHMW specimens along with new material from his own collection. (The annual reports of NHMW from 1910 and following years mention loans to Roewer). Roewer names were incorporated in the newer catalogue version by Penther (and later Reimoser) and written on "Reimoser format" specimen labels – any older (original?) labels were lost in this era.

Under the heading *Discocyrtus curvipes* [then a new combination] Roewer (1913: 107, fig. 49) provided a redescription and a new illustration (Fig. 4A). In the "material examined" section he listed two lots belonging to two different species – "1 ♂ (verstümmelt) – (Type Koch's im Mus. Wien – durch Soerensen mit: "Discocyrtus curvipes" beschriftet – gesehen!) [1 ♂ (Vienna Museum, broken), Koch's type, determined as *Discocyrtus curvipes* by Sorensen]" [that is NHMW 3127, see index card based on Sorensen's identification in Figs. 1B–C] and 1 ♂ (Roewer's collection, "Brasilien – S. Paulo", no number reported – currently this specimen is SMF RI 812), but both the description and his illustration fig. 49 are only based on SMF RI 812 (Fig. 4A).

A few pages below (Roewer 1913: 112, fig. 51) described a new species, *D. crenulatus*, using Sorensen's unpublished name (Fig. 4B). Roewer based his description on: 1 ♂ (broken) which is NHMW 3126 (Figs. 3A–B), plus "many ♂ and ♀ in my collection, from Brasilien: S. Paulo", which would be the 6 ♂ (SMF RI 764), labeled by Roewer as "D. crenulatus: Type" (Figs. 8A–D). Some of these are beta males, which probably were thought to be females by Roewer. However, the locality label states "Brasilien: Petropolis" (Fig. 8D), which is


Figure 1.—*Discocyrtus flavigranulatus* B. Soares, 1944, male holotype of synonym *Discocyrtus curvipes* (Kollar in C.L. Koch, 1839), from "Brazil" (NHMW 1847.II.49, currently NHMW 3127): A. Original illustration by C.L. Koch; B. Old catalogue index card after Sorensen with the transfer from *Gonyleptes* to *Discocyrtus*; C. Cross-reference old catalogue index card after Sorensen; D. Specimen, dorsal scutum, dorsal view; E. Same, dorso-posterior view.

consistent with what is now known for this species. The illustration provided is clearly based on one of SMF RI 764 specimens. The NHMW specimen has only minor differences with the material in SMF, which will be addressed below.

Roewer (1913: 113) also wrote that while Koch mentioned only one male of *G. curvipes*, there were two specimens in NHMW, and that he found that one was the type of *D. curvipes*, the other was a specimen of *D. crenulatus*.

Roewer (1913: 231) apparently forgot he had described a *Discocyrtus curvipes* and described once again the same NHMW 3127 (Figs. 1D–E, 2) material as *Gonyleptes curvipes*, using Koch's name, but this time combined in the genus *Gonyleptes* as Koch had done. His illustration is unfaithful, but even so it is possible to recognize NHMW 3127 (Fig. 4C). Apart from NHMW 3127, he also cited a syntype male in IRSNB (Bertkau's material).

The Brazilian arachnologist Benedicto Soares—reporting the study of many spiders from Monte Alegre (Soares 1944)—in the last pages described the new species of harvestman *D. flavigranulatus* B. Soares, 1944, based on a male and a female MZSP 569 (Fig. 5), and providing an artistic rendering of the habitus in dorsal view.

Around 1965, Gruber transferred some pinned and dry specimens of NHMW into ethanol and wrote new museum labels based on information contained in "Reimoser labels," the Penther catalogue, the old card index, and the accession ledger's entries ("entered afterwards").

Acosta (1996) published on Roewer's types of Pachylinae and mentioned NHMW 3126 (Figs. 3A–B) as a syntype of *D. crenulatus*.

Kury (2003) noted that Roewer's *G. curvipes* Kollar, 1839 [*G. curvipes* sensu Roewer] (Figs. 1D–E, 2) should be assigned to *Discocyrtus* and made this combination, but this created a homonymy with the same *Discocyrtus curvipes* (Fig. 4A), treated by Roewer (1913) as a different species in the same paper. Kury then proposed the replacement name *Discocyrtus confusus* for the junior homonym.

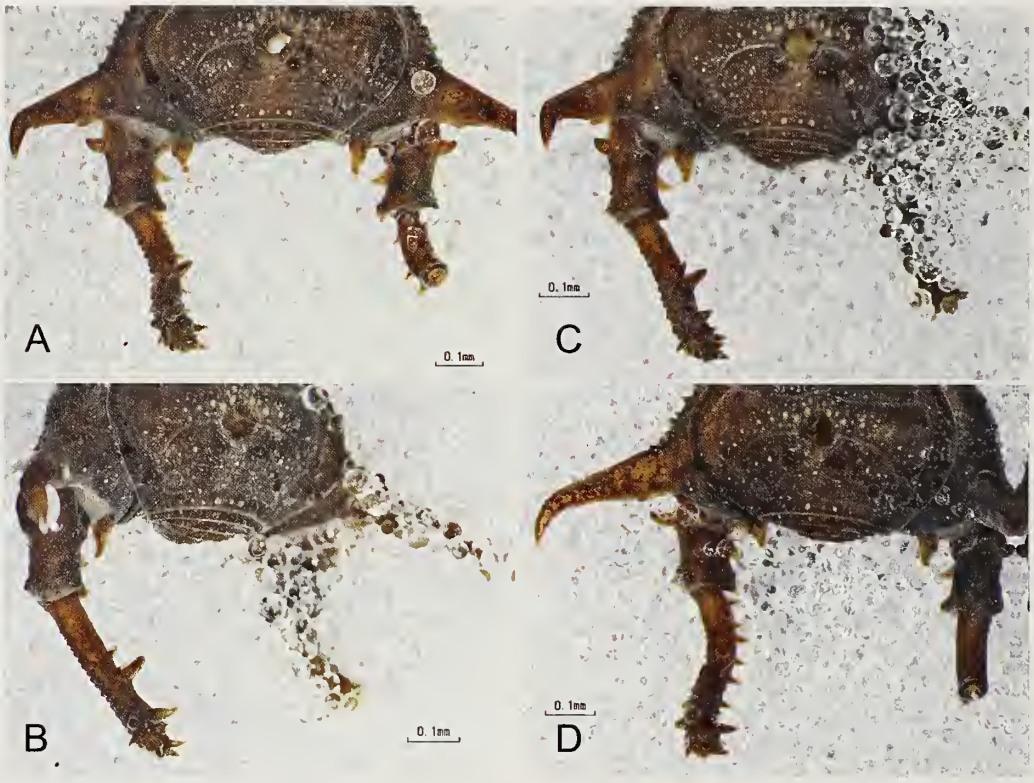


Figure 2.—*Discocyrtus flavigranulatus* B. Soares, 1944, male holotype of synonym *Discocyrtus curvipes* (Kollar in C.L. Koch, 1839), from "Brazil" (NHMW 1847.II.49, currently NHMW 3127), posterior part of dorsal scutum and leg IV up to femur: A. Dorsal flat; B. Oblique, prolateral/dorsal; C. Same, with less rotation; D. Prolateral-dorsal.

Kury & Alonso-Zarazaga (2011) explained that *D. confusus* Kury, 2003 is unavailable, because *Gouyleptes curvipes* sensu Roewer, 1913 is a misidentification, and replacement names can only be proposed for available names (Art. 13.1.3). So, they formally described *Discocyrtus confusus* as a new species, with the authority attributed to Kury only.

## SYSTEMATICS

### Genus *Discocyrtus* Holmberg, 1878

*Discocyrtus* Holmberg 1878: 74; Kury 2003: 159 (see extensive synonymy therein).

**Type species.**—*Gouyleptes testudineus* Holmberg, 1876, by monotypy.

### *Discocyrtus flavigranulatus* B. Soares, 1944

(Figs. 1, 2, 4C, 5, 6, 7, 12)

*Gouyleptes curvipes* Kollar, in C.L. Koch 1839: 36, pl. 224, fig. 555; Roewer 1913: 231, fig. 96 [junior primary homonym of *Gonyleptes curvipes* Guérin-Méneville, 1837, first detected here].

*Discocyrtus flavigranulatus* B. Soares 1944: 165, fig 11.

*Discocyrtus confusus* Kury 2003: 161 [unavailable replacement name for *Gouyleptes curvipes*, thought to have been based on other type material].

*Discocyrtus confusus* Kury, in Kury & Alonso-Zarazaga 2011: 56 [first valid description]. **Syn. nov.**

**Type material.**—*Discocyrtus flavigranulatus*: Holotype male: Monte Alegre do Sul, São Paulo, Brazil, 27 September 1942, F. Lane (MZSP 569, examined). Paratype: 1 female: same data (MZSP 569, examined).

*Discocyrtus confusus*: Holotype male: Brazil, without further locality data (NHMW 3127 = 1847.II.49, examined) – determined by Sorensen as *Discocyrtus curvipes*, recognized by Roewer as syntype of *Gouyleptes curvipes*.

**Other material cited in literature.**—1 ♂ (IRSNB, not examined) Rio de Janeiro, Tijuca. Conspecificity unknown.

**Material examined.**—BRAZIL: *Minas Gerais*: 1 ♂, 1 ♀, Lavras, Cachoeira de Farias, 18 February 1993, R. L. C. Baptista (MNRJ 2401); 4 ♂, 3 ♀, Lavras, Reserva Municipal Poço Bonito, 12 May 1992, R. L. C. Baptista (MNRJ 6754); 6 ♂, 4 ♀, Poços de Caldas, 22 February 1967, I. Becker (MNRJ 9269); 1 ♂, Poços de Caldas, Morro São Domingos, 19 July 1967, I. Becker (MNRJ 0032); 1 ♂, 1 ♀, Poços de Caldas, Morro São Domingos, 18 January 1968, I. Becker (MNRJ 9271); 1 ♂, Poços de Caldas, Morro São Domingos, 18 January 1968, I. Becker (MNRJ 9279); 1 ♂, Poços de Caldas, Recanto Japonês, 1200 m, 11–13 March 2001, A.B. Kury (MNRJ 4503); 1 ♂, 4 ♀, Poços de Caldas, Santana, 31 July 1967, I. Becker, O. Roppa & O. Leoncini (MNRJ 0035); *São Paulo:* 2 ♂, Serra Negra, Cachoeira dos Sonhos, 15–16 March 2001, A. B. Kury (MNRJ 4505).

**Distribution.**—BRAZIL: Minas Gerais, Lavras; Poços de Caldas; São Paulo, Serra Negra.

**Diagnosis.**—Mesotergum with prominent granules forming a cross pattern (*D. crenulatus* with mesotergum practically all covered by the prominent granules, *D. testudineus* and *D. fenax* sp. nov. without prominent granules on mesotergum).


Figure 3.—*Discocyrtus crenulatus* Roewer, 1913, male, second specimen of *Gonyleptes curvipes* of Koch from "Brazil" (NHMW 1847.II.47, currently NHMW 3126), not used in the description, but regarded as a syntype of *D. crenulatus* by Roewer: A. Dorsal scutum, partial, and basal legs, dorsal view; B. Coxa IV, stigmatic area and basal leg IV, ventral view; C. Old catalogue index card after Sorensen with the indication of the new species in schedula *Discocyrtus crenulatus*; D. Cross-reference old catalogue index card after Sorensen.

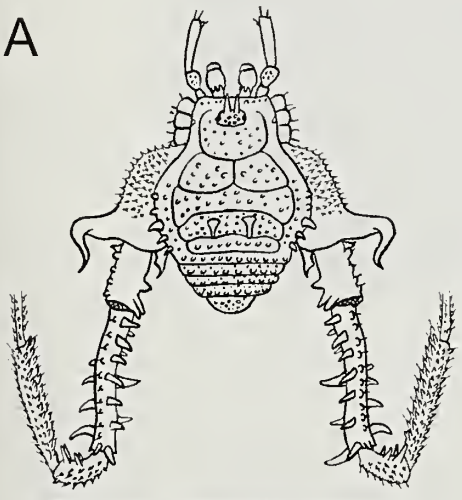


Fig. 544. *Discocyrtus curvipes* ♂.
Körper dorsal mit 4. Bein bis zur Tibia.

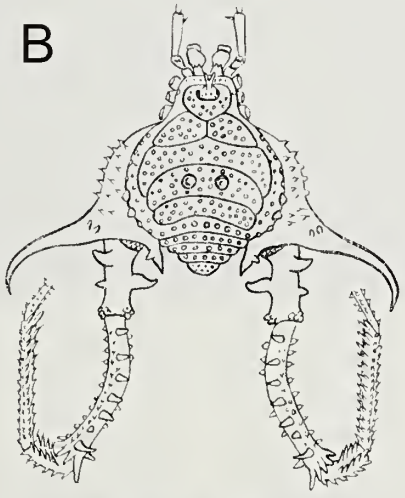


Fig. 546. *Discocyrtus crenulatus* ♂.
Körper dorsal mit 4. Bein bis zur Tibia.

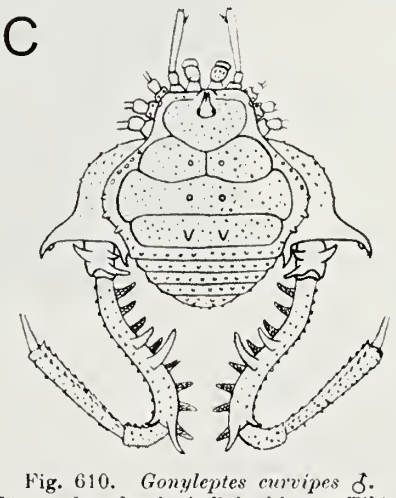


Fig. 610. *Gonyleptes curvipes* ♂.
Körper dorsal mit 4. Bein bis zur Tibia.
(Nach Typ.)

Figure 4.—Illustrations of the three species involved with the names as given by Roewer (1913/1923): A. *Discocyrtus curvipes* ("Koch"), based on SMF RI 812 [here called *D. fenax*]; B. *Discocyrtus crenulatus* Roewer, based on SMF RI 764; C. *Gonyleptes curvipes* "Kollar MS", based on NHMW 3127 [here called *D. flavigranulatus*].

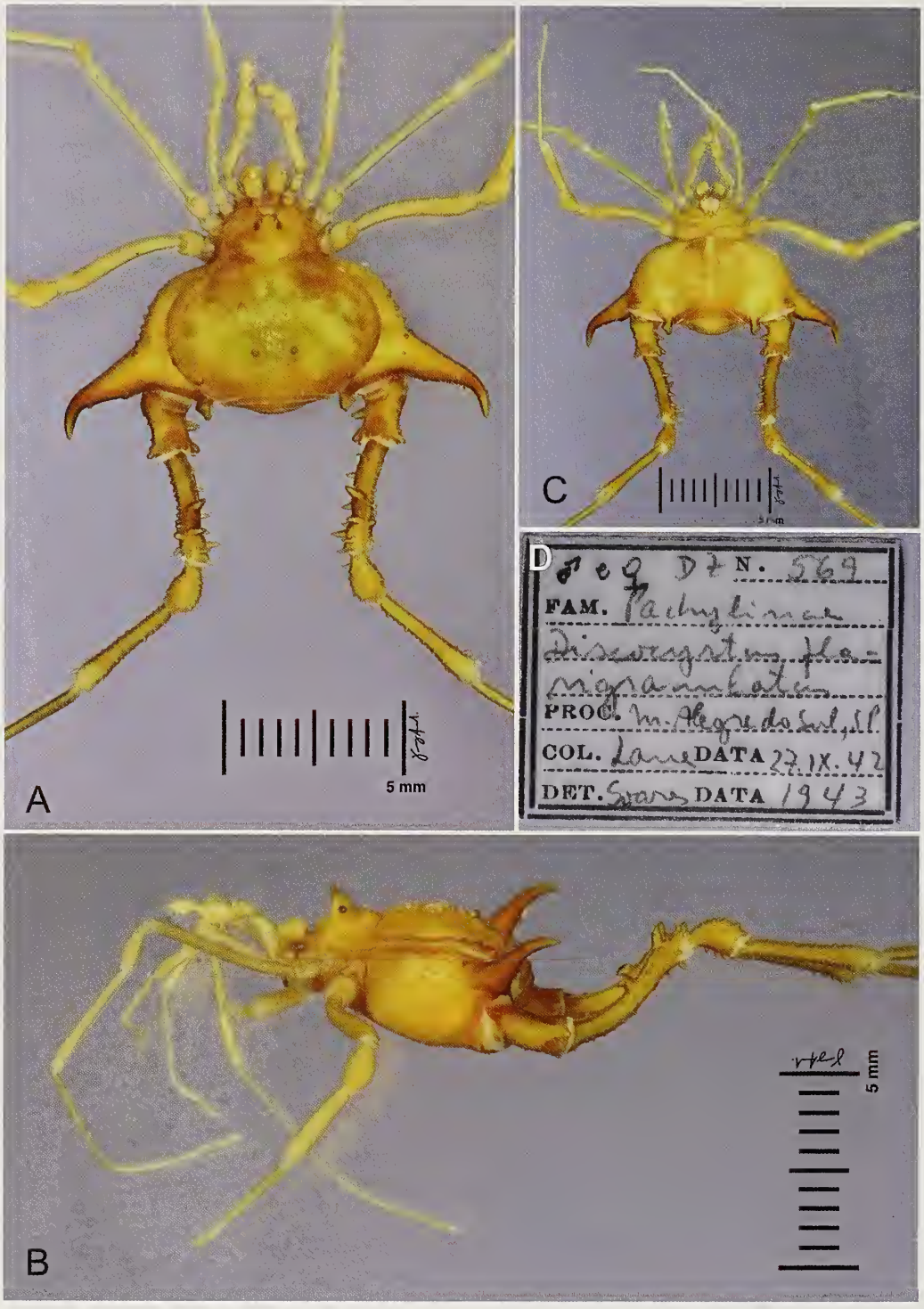


Figure 5.—*Discocyrtus flavigranulatus* B. Soares, 1944, male holotype from Monte Alegre do Sul (MZSP 569): A. Habitus, dorsal view; B. Same, lateral view; C. Same, ventral view; D. Original label by Soares. Scale bars = 5 mm. Photo: Enrique Leopardi.

Paramedian tubercles of area III dome-shaped (the same in *D. crenulatus*, conical with non-acuminate apex in *D. testudineus*, conical acuminate with distal curvature to the posterior region in *D. fenax*). Apophysis of Cx IV with a swollen basal-medial branch, forming an angle of almost 90° with the axis of the body, with a backward curvature at the apex (*D. testudineus* with a swollen apophysis forming a 135° angle with the axis of the body, *D. crenulatus* with elongate and non-swollen apophysis, *D. feuax* with sigmoid medial-distal portion). Tr IV square (rectangular in *D. testudineus*, *D. crenulatus* and *D. feuax*). Fe IV dorsally with medial-distal armature of two spines curved to retrolateral (spines not curved in *D. crenulatus*, spines not present in *D. testudineus* and *D. feuax*).

**Redescription.**—*Male holotype (MZSP 569), also MNRJ 4603 (some photographs) and MNRJ 9279 (genitalic illustrations):* DS measurements: CW 3.0, CL 2.0; AW 6.5, AL 3.6.

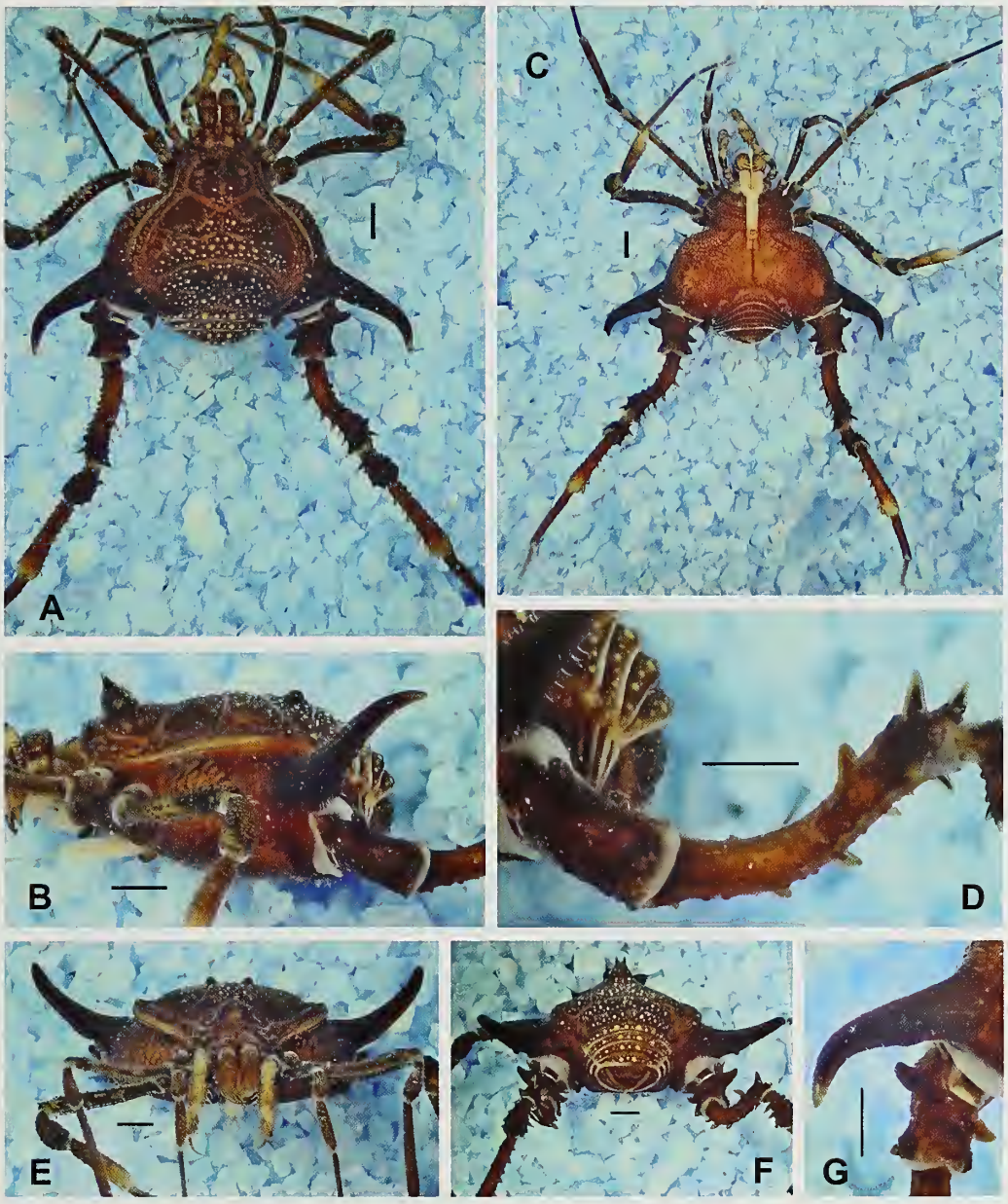


Figure 6.—*Discocyrtus flavigranulatus* B. Soares, 1944, male from Poços de Caldas (MNRJ 4503): A. Habitus, dorsal view; B. Same, lateral view; C. Same, ventral view; D. Tr and Fe IV, prolateral view; E. Habitus, anterior view; F. Same, posterior view; G. Cx IV, prodorsal distal apophysis. Scale bars = 1 mm.

Fe measurements: I = 2.2, II = 4.8, III = 3.9, IV = 3.6. Right / left tarsal (distitarsal) counts, ♂ holotype: 6(3) / 6(3) - 9(3) / 10(3) - 7 / 7 - 7 / 7; ♀ paratype – / 6(3) - – / 8(3) - 7 / 7 - 7 / 7.

Dorsum: Dorsal scutum almost as long as wide, abdominal scutum with lateral margins strongly convex (Fig. 6A), widest and highest at area II (Fig. 6B). Carapace with few tubercles on posterior region, with a pair of paramedian higher tubercles (Fig. 6A). Cheliceral sockets shallow, with a small apophysis in the center. Eye mound elliptical, high, slightly inclined frontwards, placed in the middle of the carapace, armed with a pair of divergent high spines fused at baseline and inclined frontwards (Figs. 6A–B, E–F). Mesotergum divided into four clearly defined areas. Areas I and IV divided into left and right halves by median groove. Area II anterior lateral border invading space of area I and posterior lateral border invading the space of area III. AS lateral borders with ordinary tubercles from area I backwards (Fig. 6A). All areas with many tubercles, area I with three pairs of paramedian tubercles higher than the others. Area II with six paramedian tubercles higher than the others (two at anterior portion and four at posterior portion) (Fig. 6A). Area III with a pair of paramedian rounded higher tubercles (Figs. 6A–B, E–F). Posterior border of dorsal scutum and free tergites with a horizontal row of ordinary tubercles, with a paramedian pair of highlighted tubercles (Figs. 6A–B, D, F).

Venter: Cx I–III parallel to each other; each with ventral transverse rows of 7–11 setiferous tubercles (Cx I rows with higher and sharper tubercles). Cx II retroventral distal with a

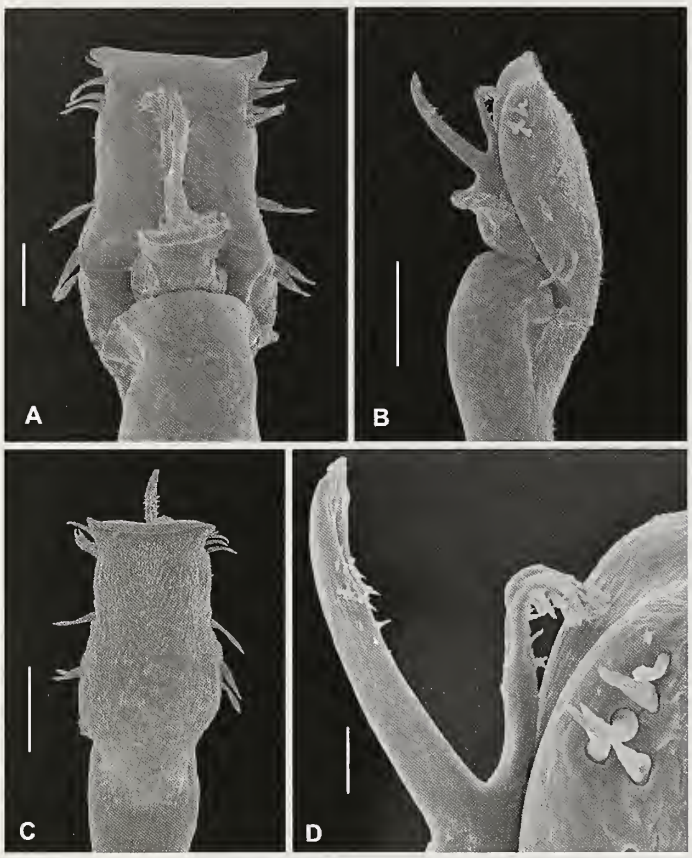


Figure 7.—*Discocyrtus flavigranulatus* B. Soares, 1944, male from Poços de Caldas (MNRJ 9279), penis, distal part: A. Dorsal view; B. Lateral view; C. Ventral view; D. Detail of stylus and ventral process, lateral view. Scale bars = 50 μm (A); 100 μm (B, C); 20 μm (D).

row of two acuminate tubercles. Cx III retroventral distal with a row of seven acuminate tubercles. Cx IV much larger than the others, directed obliquely (Fig. 6C). Stigmatic area Y-shaped, clearly sunken relative to distal part of coxa IV. Intercoxal bridges well marked. Stigmata clearly visible. Free sternites and anal operculum each with one transverse row of tubercles (Figs. 6B–D).

Chelicera: Basichelicerite elongate, bulla well marked (Figs. 6A–B), with marginal setiferous tubercles—two ectal, one posterior, two mesal; hand not swollen.

Pedipalpus (Figs. 6A, C, E): Tr with two geminate ventral setiferous tubercles. Fe with a prolateral apical setiferous tubercle and one ventral basal setiferous tubercle. Pa unarmed. Ti with two rows of setiferous tubercles; four (iiIi) ventro-mesal and (IiIi) ventroectal. Ta with two rows of setiferous tubercles; three (IiI) ventro-mesal and four (IIIi) ventro-ectal.

Legs: Tr I–III each with several ventral tubercles. Fe I–II straight (Figs. 6A, C). Fe and Ti I–II with two rows (proventral and retroventral) of small tubercles. Leg III sub-straight (Figs. 6A, C). Fe III and Ti III with two rows (proventral and retroventral) of acuminate tubercles. Fe III with a developed prodorsal and retrodorsal distal spore (Figs. 6A, C, E). Cx IV ending distally at area IV of dorsal scutum (Fig. 6A). Cx IV with 1) a prolateral apophysis thick, with distal curvature on the apical portion and 2) a retroventral spiniform apophysis with secondary branch (Figs. 6A–C, E–G). Cx IV prodorsal, prolateral, proventral and ventral with rows of acuminate tubercles (Figs. 6A–C, E). Tr IV apophysis retrolateral proximal and distal (geminate). Tr IV apophysis prolateral distal (Figs. 6A, G). Tr IV ventrally covered by tubercles along its entire length. Fe IV sinuous, curved from the proximal-distal region toward dorsal (Figs. 6A, C–D, F). Fe IV proventral and retrolateral with row of small tubercles (Fig. 6C). Fe IV dorsal–prodorsal medial distal with three spines (IIi) curved toward retrolateral portion (Fig. 6A). Fe IV prolateral with a row of tubercles, which grow in size towards the distal portion, terminated with a small spur (Figs. 6A, C). Fe IV retrolateral with row of six equidistant spines (IIiIII) (Figs. 6A, C). Pa IV proventral and retroventral with row of five and three spines, respectively (Fig. 6C). Pa IV retrolateral proximal with a spine (Figs. 6A, C). Ti IV prodorsal, proventral, retrodorsal, retrolateral and retroventral with row of acuminate tubercles (Figs. 6A, C). Mt IV proventral and retroventral distal with spur.

Color (in ethanol): Dorsal scutum background Moderate Brown (58), with grooves and reticles Moderate Orange (53). Granules of scutum and free tergites Brilliant Orange Yellow (67). All legs background Moderate Brown (58) with Brownish Black (65) reticle. Ch and Pp background Moderate Greenish Yellow (102), with honeycombed Deep Brown (56) reticle.

Male genitalia (MNRJ 9279): VP subrectangular, distal half with parallel sides, with basal half quite convex, distal border substraight (Figs. 7A, C). Ventral surface with entire field of microsetae (Fig. 7C). Truncus slender (thinner than podium plus VP) (Fig. 7A). Macrosetae C1–C3 cylindrical with apex beveled, forming longitudinal row, unequally spaced, subapical on laterals of VP (Figs. 7A–D). Macrosetae A1–A3 forming triangle, with one more dorso-distal than the other two (Figs. 7A–C). MS B inserted ventrally, proximal to A2 (Figs. 7B–C). MS D very short, inserted on lateral border of VP, close to C1–C3 (Figs. 7A–B). MS E1–E2 extremely reduced, located on latero-distal flange of VP (Figs. 7B–C). Stylus and the axis of its ventral process fused basally (forming long pedestal) at an acute angle (V-shaped) (Figs. 7A–B, D). Ventral process of stylus shorter than it, *in situ* not reaching distal border of VP (Figs. 7A–B, D). Stylus straight, without clearly defined head, armed with a few small sub-distal setae (Figs. 7A–D). Flabellum curved proximally, fan-shaped, occupying about 40% length of free portion of process (Figs. 7A–B, D).

**Variation.**—Specimen MZSP 569 (Fig. 5) has a callus instead of prolateral basal apophysis on Tr IV.

**Female.**—*Paratype of* D. flavigranulatus *(MZSP 569)*: CW 2.5, CL 1.7; AW 4.9, AL 3.2. Cx IV with much weaker armature, prodorsal apophysis reduced to a simple spine and retroventral absent. Fe IV thinner and less curved when compared to male. Fe IV with fewer spines on distal retrolateral axis and a retrolateral distal spur.

### *Discocyrtus crenulatus* Roewer, 1913
(Figs. 3, 4B, 8, 9, 12)

*Discocyrtus crenulatus* Roewer 1913: 111, fig. 51.

**Type material.**—*Lectotype male*: Petrópolis, Rio de Janeiro, Brazil (SMF R1 764, examined).


Figure 8.—*Discocyrtus crenulatus* Roewer, 1913, male syntype from Petrópolis (SMF RI 764): A. Habitus, dorsal view; B. Same, dorso-lateral view; C. Same, ventral view; D. Original label by Roewer.

*Paralectotypes*: 5 males, collected with lectotype (SMF RI 764, examined; incorrectly reported as ♂ and ♀ in original description); 1 male, from Brazil, without further locality data (NHMW 3126 = 1847.II.47, examined; identified as "G. curvipes = D. crenulatus" by Sørensen, syntype of *D. crenulatus*).

**Other material examined.**—BRAZIL: *Rio de Janeiro:* 4 ♂, 6 ♀, Nova Friburgo, Três Picos, 16 November 1991, R. L. C. Baptista (MNRJ 6736); 5 ♂, 3 ♀, Nova Friburgo, Campo do Coelho, Três Picos, -22.368°, -42.678°, 1150 m, 11 April 2015, A. Garcia, A. Kury, M. Medrano & A. Pinto (MNRJ 8635); 1 ♂, 1 ♀, Nova Friburgo, Mury, Debossan, 950 m, 30 July 1996, R.S. Bérnils (MZSP 15252); 1 ♂, same county (Rio Bengalas), 21–23 August 1996, R. S. Bérnils (MZSP 15122); 1 ♂, Teresópolis, Parque Nacional da Serra dos Órgãos (MNRJ 0193); 13 ♂, 5 ♀, Teresópolis, Parque Nacional da Serra dos Órgãos, Trilhas Rancho Frio e Pedra do Sino, 20–23 October 2006, Expedição Arachné (MNRJ 18711); 2 ♂, Teresópolis, Subaio, antigo Hotel Sayonara, 20–22 April 1995, R. L. C. Baptista & M. I. Landim (MNRJ 5380).

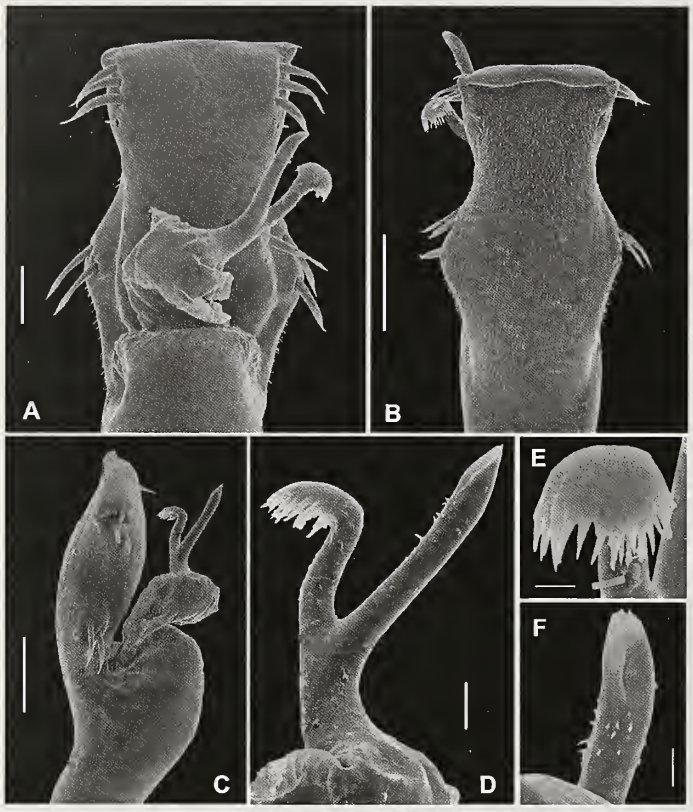


Figure 9.—*Discocyrtus crenulatus* Roewer, 1913, male from Teresópolis (MNRJ 5380), penis, distal part: A. Dorsal view; B. Ventral view; C. Lateral view; D. Detail of stylus and ventral process, lateral view; E. Flabellum, apico-ventral view; F. Stylus, apico-ventral view. Scale bars = 50 μm (A); 100 μm (B, C); 20 μm (D); 10 μm (E, F).

**Distribution.**—BRAZIL: Rio de Janeiro, Nova Friburgo; Teresópolis.

**Diagnosis.**—Mesotergum with prominent granules covering practically all its extension (mesotergum of *D. flavigranulatus* with prominent granules in cross pattern, *D. testudineus* and *D. fenax* without prominent granules on mesotergum). Paramedian tubercles of area III dome-shaped (the same in *D. flavigranulatus*, conical with non-acuminate apex in *D. testudineus*, conical acuminate with distal curvature to the posterior region in *D. fenax*). Apophysis of the Cx IV with basal-medial branches forming an angle of 135° in relation to the axis of the body, elongated, with apex longitudinally exceeding the height of Tr IV (*D. testudineus* and *D. flavigranulatus* with swollen basal-medial branch, *D. fenax* with medial-distal portion sigmoid, all three with apex not exceeding longitudinally the height of Tr IV). Fe dorsal IV armed with four equidistant spines (*D. flavigranulatus* with two spines in the medial-distal portion, curved to retrolateral; *D. fenax* with six spines in the proximal-medial portion, curved to retrolateral, spines not present in *D. testudineus*).

**Description.**—*Male lectotype (SMF RI 764), except for color in vivo and genitalia):* DS measurements: CW 3.7, CL 2.5; AW 6.9, AL 4.0. Fe measurements: I = 3.2, II = 6.9, III = 5.1, IV = 6.1. Right / Left tarsal (distitarsal) counts, ♂ lectotype: 6(3) / 6(3) - 9(3) / 10(3) - – / 7 - 7 / 7.

Dorsum: Dorsal scutum almost as long as wide, abdominal scutum with lateral margins strongly convex (Fig. 8A), widest and highest at area III. AS posterior margin strongly concave (Figs. 8A–B). Carapace with few tubercles on posterior region, with two pairs of paramedian higher tubercles (Figs. 8A–B). Cheliceral sockets shallow, with a small apophysis in the center. Eye mound elliptical, high, slightly inclined frontwards, placed in the middle of the carapace, armed with a pair of divergent high spines fused at baseline and inclined frontwards (Figs. 8A–B). Mesotergum divided into four clearly defined areas (Figs. 8A–B). Areas I and IV divided into left and right halves by median groove. Area II posterior lateral border strongly invading the space of area III. AS lateral borders with ordinary tubercles from area I frontwards. All areas with many tubercles (Figs. 8A–B). Area I with pair of paramedian tubercles higher than the others. Area II with row of tubercles on posterior portion. Area III with a pair of paramedian rounded higher tubercles (Figs. 8A–B). Posterior border of dorsal scutum and free tergites with a horizontal row of ordinary tubercles, with a paramedian pair of highlighted tubercles (Fig. 8A).

Venter: Cx I–III parallel to each other; each with ventral transverse rows of 9–12 setiferous tubercles (Cx I two rows with higher and sharper tubercles). Cx II retroventral distal with a row of three acuminate tubercles. Cx III retroventral distal with a row of seven acuminate tubercles. Cx IV much larger than the others, directed obliquely (Fig. 8C). Stigmatic area Y-shaped, clearly sunken relative to distal part of coxa IV. Intercoxal bridges well marked. Stigmata clearly visible. Stigmatic area posterior portion with row of 11 tubercles that stand out. Free sternites and anal operculum each with one transverse row of tubercles (Fig. 8C).

Chelicera: Basichelicerite elongate, bulla well marked (Fig. 8A), with marginal setiferous tubercles—three ectal, two posterior, one mesal; hand not swollen.

Pedipalpus: Tr with two geminate ventral setiferous tubercles. Fe with a prolateral apical setiferous tubercle and one ventral basal setiferous tubercle. Pa unarmed. Ti with two rows of setiferous tubercles; four (IiIi) ventro-mesal and ventro-ectal. Ta with two rows of setiferous tubercles; three (III) ventro-mesal and five (IiIii) ventro-ectal.

Legs: Tr I–III each with several ventral tubercles (Fig. 8C). Fe I–II straight (Figs. 8A–C). Fe and Ti I–II with all axis containing rows of small tubercles. Leg III sub-straight (Figs. 8A–C). Fe III with two rows (proventral and retroventral) of acuminate tubercles. Fe III with a developed prodorsal and retrodorsal distal spore (Figs. 8A–B). Cx IV ending distally posterior to the border of the dorsal scutum (Fig. 8A). Cx IV with (1) a long prolateral apophysis (forming an obtuse angle in relation to Cx) with medial–distal curvature to posterior on the apical portion, and (2) a spiniform retroventral apophysis with secondary branch (Figs. 8A–C). Cx IV prodorsal, prolateral, proventral and ventral with rows of acuminate tubercles (Figs. 8A–C). Tr IV with conical proximal retrolateral apophysis (Figs. 8A–C). Tr IV with conical proximal retrolateral apophysis (proximal 3x larger than the others) (Figs. 8A, C). Tr IV prodorsal distal apophysis shaped as a screwdriver apex (Figs. 8A–B). Tr IV ventrally covered by tubercles along its entire length (Fig. 8C). Fe IV C-shaped, retrolateral convex (Figs. 8A–C). Fe IV prodorsal, prolateral, proventral, retroventral and retrodorsal with row of small


Figure 10.—*Discocyrtus fenax* sp. nov., male holotype from Itajaí (MZSP 18158): A. Habitus, dorsal view; B. Same, ventral view; C. Same, lateral view; D. Same, dorso-lateral view; E. Tr and Fe IV, prodorsal view; F. Same, proventral view; G. Same, retroventral view; H. Same, retrolateral view. Scale bars = 2 mm.

tubercles (Figs. 8A–C). Fe IV dorsal with six equidistant spines (iIiIIi) (Figs. 8A–B). Fe IV retrolateral distal with four spines (IiII) (Fig. 8C). Fe IV proventral and retrolateral distal with a spine (Fig. 8C). Fe IV prodorsal distal with a spur (Figs. 8A–B). Pa IV proventral and retroventral with row of four and three spines, respectively (Fig. 8C). Pa IV in dorsal view covered by spines (Figs. 8A–B). Ti IV prodorsal, proventral, retrodorsal, retrolateral and retroventral with row of acuminate tubercles (Figs. 8A–C). Mt IV proventral and retroventral distal with spur.

Color (*in vivo*): Mesotergum background Dark Greenish Yellowish Green (151) with granules Moderate Yellow Green (120). Leg IV, carapace and rim of abdominal scutum Deep Yellowish Brown (75). Legs I–III Dark Greenish Gray (156). Pp and Ch background Light Olive (106) with dense reticle Dark Olive Green (126).

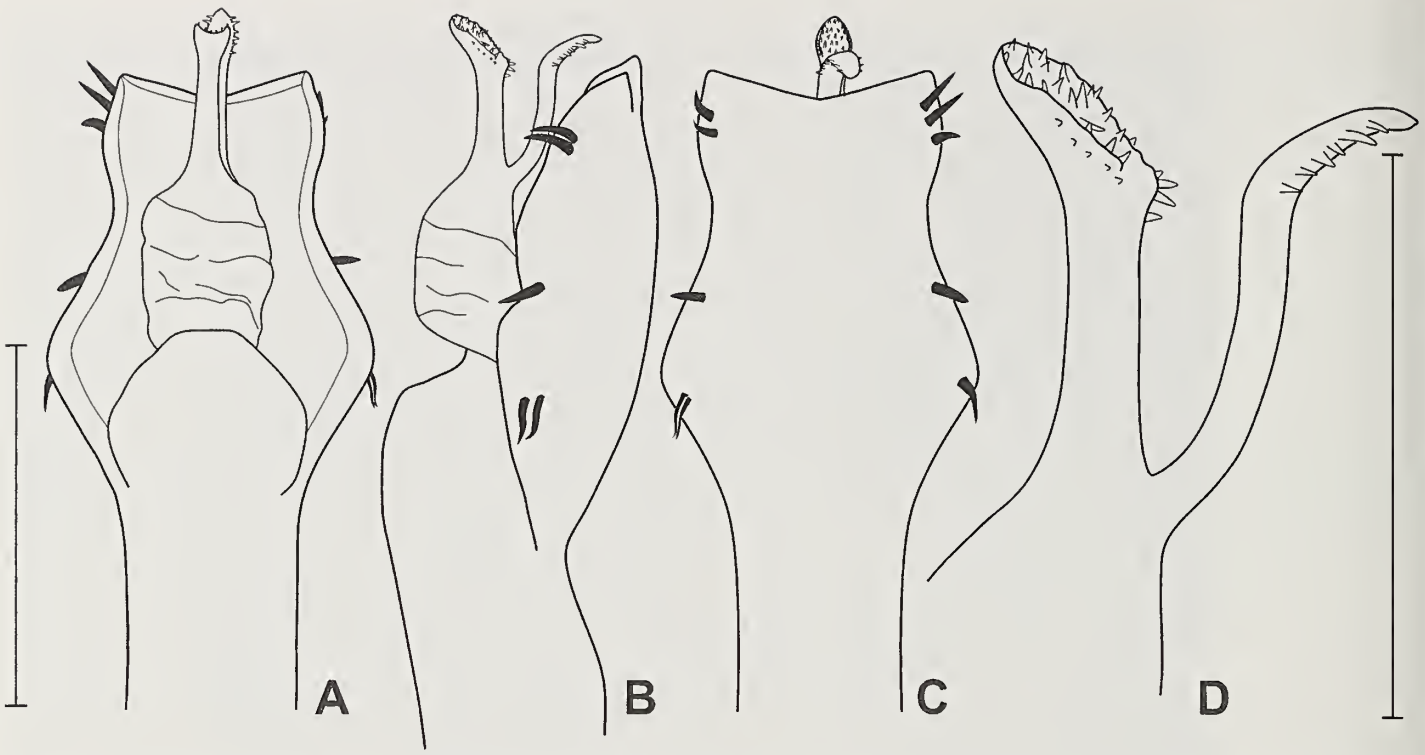


Figure 11.—*Discocyrtus fenax* sp. nov., male paratype from Joinville (SMF RI 812), distal part of penis: A. Dorsal view; B. Lateral view; C. Ventral view; D. Detail of glans and stylus. Scale bars = 100 μm (A, B, C); 50 μm (D).

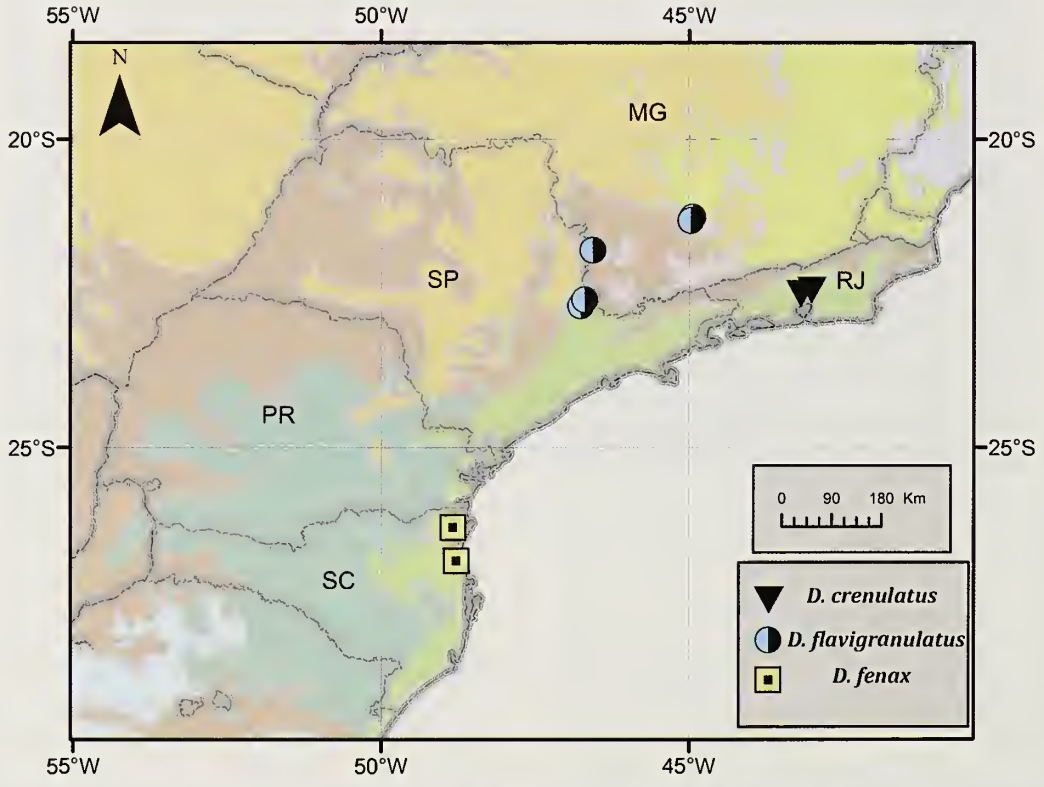


Figure 12.—South-southeastern Brazil showing distribution of the three *Discocyrtus* species treated here. Standard abbreviations of the relevant Brazilian states are: MG (Minas Gerais), PR (Paraná), RJ (Rio de Janeiro), SC (Santa Catarina), SP (São Paulo). Shaded areas on the background are WWF terrestrial eco-regions.

Color (in ethanol): Body and appendages background uniform Light Brown (57) with mesotergal granules Moderate Yellow Green (120). Pp, Ch and legs I–III Deep Greenish Yellow (100).

Genitalia (MNRJ 6380): VP subrectangular, distal half with parallel sides, with basal half quite convex, distal border substraight (Figs. 9A–B). Ventral surface with entire field of microsetae (Figs. 9B). Truncus slender (thinner than podium plus VP) (Figs. 9A, C). Macrosetae C1–C3 cylindrical with apex beveled, forming longitudinal row, equally spaced, subapical on laterals of VP (Figs. 9A–C). Macrosetae A1–A3 forming triangle, with one more dorso-distal than the other two (sides asymmetrical in this specimen) (Figs. 9A–C). MS B much reduced, clustered with A (Figs. 9B–C). MS D very short, inserted on lateral border of VP, extremely close to C1–C3 (Figs. 9B–C). MS E1–E2 extremely reduced, located on latero-distal flange of VP (Figs. 9B–C). Stylus and the axis of its ventral process fused basally (forming long pedestal) at an acute angle (V-shaped) (Figs. 9A, C–D). Ventral process of stylus shorter than it, *in situ* not reaching distal border of VP (Figs. 9A, C). Stylus straight, without clearly defined head, armed with a few small subdistal setae (Figs. 9A, C–D, F). Flabellum curved proximally, fan-shaped, occupying about 40% length of free portion of process (Figs. 9A–E).

**Female.**—(MNRJ 6736): CW 3.3, CL 2.4; AW 6.0, AL 3.8. AS widest at area II. Area III with the median region elevated, with apex bringing a pair of large conical spines. Cx IV with much weaker armature and prodorsal apophysis reduced to a simple spine. Fe IV straight. Fe IV retrolateral with row of six spines. Tr IV apophysis retrolateral proximal absent.

**Remarks.**—The designation of a lectotype, as explained in ICZN, fixes the status of the specimen as the sole name-bearing type of that nominal taxon. The type series is composed of alpha and beta males (so that Roewer even mistakenly reported males and females). The specimen illustrated by Roewer was clearly an alpha male, and in a group with such plasticity (and convoluted taxonomy) as *Discocyrtus*, it is important not to leave the slightest margin of chance for further confusion.

***Discocyrtus fenax*** Kury, Pinto-da-Rocha & Carvalho sp. nov.
(Figs. 4A, 10, 11, 12)
urn:lsid:zoobank.org:act:06AB3468-BBBB-44E9-8E0E-5BE209291D85

*Discocyrtus curvipes* Kollar: Roewer 1913: 107, fig. 49 [non Kollar, 1839 – misidentification of *D. fenax*]; Kury 2003: 162.

**Type material.**—*Holotype male*: close to road BR470, near Itajaí, Santa Catarina, Brazil, 10 March 1999, A. Kury, R. Pinto-da-Rocha, A. Giupponi (MZSP 18158). *Paratype:* 1 ♂, Joinville, Santa Catarina, Brazil (SMF R1 812).

**Distribution.**—BRAZIL: Santa Catarina, Itajaí; Joinville.

**Etymology.**—Species name is a masculine noun in apposition, from Greek φέναξ, κος (impostor).

**Diagnosis.**—Mesotergum without granules (the same in *D. testudineus*, in *D. flavigranulatus* prominent granules forming a cross pattern, *D. crenulatus* with mesotergum nearly all covered by the prominent granules). Paramedian tubercles of area III conical and acuminate with distal curvature backwards (dome-shaped in *D. crenulatus* and *D. flavigranulatus*, conical with blunt apex in *D. testudineus*). Distal region of the apophysis of Cx IV sigmoid (with slight curvature for the posterior region in *D. crenulatus*, *D. flavigranulatus* and *D. testudineus*). Dorsum of Fe IV with six spines on proximal to medial portion, curved to retrolateral (*D. crenulatus* armed with four equidistant spines, *D. flavigranulatus* with two spines in the medial-distal portion, curved to retrolateral, spines not present in *D. testudineus*). Ventral process of the stylus thinner than the stylus itself (both with basically the same diameter in *D. crenulatus*, *D. flavigranulatus* and *D. testudineus*).

**Description.**—*Male holotype:* DS measurements. CW 3.1, CL 2.3; AW 6.0, AL 3.3. Fe measurements: I = 2.7, II = 5.1, III = 3.1, IV = 4.6. Tarsal (distitarsal, right side) counts, ♂ holotype: 6(3) - 11(3) - 7 - 7.

Dorsum: Dorsal scutum almost as long as wide, abdominal scutum with lateral margins strongly convex, widest and highest at area III (Figs. 10A, C–D). Anterior margin with 4 tubercles each side (Figs. 10A, C–D). Carapace with few tubercles on posterior region, with a pair of paramedian higher tubercles (Figs. 10A, C–D). Cheliceral sockets shallow, with a small apophysis in the center (Fig. 10A). Eye mound elliptical, high, slightly inclined frontwards, placed in the middle of the carapace, armed with a pair of divergent high spines inclined frontwards (Figs. 10A, C–D). Mesotergum divided into four clearly defined areas (Fig. 10A). Area I divided into left and right halves by median groove. Area II and posterior lateral border strongly invading the space of area III. AS lateral borders with ordinary tubercles from area I backwards. All areas with many tubercles. Area III with a pair of paramedian conical higher tubercles, curved backwards, with a rounded apex (Figs. 10A, C–D). Posterior border of dorsal scutum and free tergites with a horizontal row of ordinary tubercles (Figs. 10A, D).

Venter: Cx I–III parallel to each other; each with ventral transverse rows of 8–12 setiferous tubercles (Cx I two rows with higher and sharper tubercles). Cx II retroventral distal with a row of eight acuminate tubercles. Cx III retroventral distal with a row of seven acuminate tubercles (Fig. 10B). Cx IV much larger than the others, directed obliquely. Stigmatic area Y-shaped, clearly sunken relative to distal part of coxa IV. Intercoxal bridges well marked. Stigmata clearly visible. Free sternites and anal operculum each with one transverse row of tubercles (Fig. 10B).

Chelicera: Basichelicerite elongate, bulla well marked, with marginal setiferous tubercles—three ectal, three posterior, one mesal; hand not swollen (Fig. 10A).

Pedipalpus (Figs. 10A–B): Tr with two geminate ventral setiferous tubercles. Fe with a prolateral apical setiferous tubercle and one ventral basal setiferous tubercle (Fig. 10B). Pa unarmed (Figs. 10A–B). Ti with two rows of setiferous tubercles: four (IiIi) ventro-mesal and ventroectal. Ta with two rows of setiferous tubercles; three (IIi) ventro-mesal and ventro-ectal.

Legs: Cx I–III each with ventral transverse rows of 8–12 setiferous tubercles. Tr I–III each with several ventral tubercles (Fig. 10B). Fe I–II straight (Figs. 10A–B). Fe and Ti I–II with two rows (proventral and retroventral) of small tubercles (Fig. 10B). Leg III sub-straight (Fig. 10B). Fe III and Ti III with two rows (proventral and retroventral) of acuminate tubercles (Fig. 10B). Cx IV ending distally at

posterior border of dorsal scutum (Fig. 10A). Cx IV with 1) a prodorsal apophysis conical, with curvature on the medial portion and distal portion sigmoid and 2) a retroventral spiniform apophysis with secondary branch (Figs. 10A–D). Cx IV prodorsal, prolateral, proventral and ventral with rows of acuminate tubercles (Figs. 10A–D). Tr IV with retrolateral and prolateral proximal apophysis (Figs. 10A–D). Tr IV distal prolateral border posterior covered by conical tubercles (Fig. 10A). Tr IV ventrally covered by tubercles along its entire length (Figs. 10B–D, F–G). Fe IV sinuous, curved from the proximal-distal region toward dorsal and medial-distal toward prolateral (Figs. 10A–B, E, G). Fe IV proventral and retroventral with row of acuminate tubercles (retroventral twice the size of the proventral) (Figs. 10B, G). Fe IV dorsal-medial with six spines (IiIIIi) curved toward retrolateral portion (Figs. 10A, D, F–G). Fe IV prolateral with a row of tubercles, which increase in size towards the medial portion and decreasing to distal (Figs. 10A–F). Fe IV retrolateral proximal-medial with row of six spines (iiiIII), which the last three are curved toward dorsal portion (Figs. 10A–B, G–H). Pa IV proventral and retroventral with row of five and two spines, respectively (Figs. 10E–H). Pa IV covered by acuminate spines in dorsal view (Fig. 10C). Ti IV prodorsal, proventral, retrodorsal, retrolateral and retroventral with row of acuminate tubercles (Figs. 10E–H). Mt IV proventral and retroventral distal with spur.

Color (in ethanol): Dorsal scutum and legs I–III (except Tr) background Grayish Olive (110), with grooves, arcoles and reticulation Grayish Yellow (90). Pp, Ch, Tr I–III background Pale Greenish Yellow (104) with reticle Dark Grayish Olive (111). Leg IV background Grayish Olive (110), with varied mottling and apex of apophyses Dark Grayish Brown (62).

Male genitalia (SMF RI 812, paratype): VP subrectangular, distal half with convex sides, with basal half angular, distal border concave (Figs. 11A, C). Truncus thick (as thick as podium plus VP) (Fig. 11). Macrosetae C1–C3 cylindrical with apex beveled, forming longitudinal row, unequally spaced, subapical on laterals of VP (Fig. 11). Macrosetae A1–A3 forming triangle, with one more dorso-distal than the other two (Figs. 11A, C). MS B not visible. MS D very short, inserted on lateral border of VP, close to C1–C3 (Fig. 11A). MS E1–E2 extremely reduced, located on latero-distal flange of VP (Fig. 11C). Stylus and the axis of its ventral process fused basally (forming short pedestal) at an acute angle (V-shaped) (Fig. 11B). Ventral process of stylus is slightly sinuous, thinner and as long as the stylus, *in situ* reaching distal border of VP (Fig. 11B). Stylus straight, but distal third abruptly angled, defining a head densely covered (lateral and ventral) with small setae (Fig. 11). Flabellum very narrow, only slightly curved proximally, provided with short serrulations, and occupying less than 30% of length of free portion of process (Figs. 11B–C).

*Female:* unknown.

**Remarks.**—The male paratype from Joinville was used by Roewer to base his description of *Discocyrtus curvipes*. Roewer's inclusion of NHMW 3127 is mistaken, as that material belongs to *D. curvipes*.

## DISCUSSION

**Roewer's procedure.**—When splitting a species into two others in different genera, Roewer had the complicating habit of baptizing the second one with the same specific epithet and the authority wrongly ascribed to the original author, or later even to himself with the wrong date. This procedure was never explained, and was not immediately obvious to subsequent reviewers, who were plunged into a hopeless tangle of synonymies. This is prone to cause confusion, especially with subsequent citations. We may cite four cases where Roewer split an original species keeping the same name: *Metascotolemon jaqueti* (Corti, 1905) X *Scotolemon jaqueti* Roewer, 1915; *Ibalonius impudens* Loman, 1906 X *Ibalonianus impudens* Roewer, 1923; *Pseudobiantes japonicus* Hirst, 1911 X *Ataminius japonicus* Roewer, 1938; and *Algidia nigriflava* (Loman, 1902) X *Nuncia (Corinuncia) nigriflava nigriflava* Roewer, 1923. In all of them, Roewer applied the incorrect authority.

However, it is clear that the present case is different from the others: There was some dispute among the authors and colleagues over three contrasting courses of action: the characterization of *D. curvipes* by Roewer (1913) could be considered (1) a valid species description, by using the same name as Koch (similarly to the four cases related above), (2) a misidentification, or (3) Roewer never intended to recognize a second morphospecies, he just forgot that he had mentioned Koch's species before. We support the third alternative and accordingly, we have described *Discocyrtus fenax* as a distinct new species.

**The holotype of *G. curvipes*.**—Roewer studied the holotype of *G. curvipes* twice, including it in two different genera in two separate subfamilies: as a secondary material of his *Discocyrtus curvipes* (while illustrating the other specimen); and as the primary illustrative material of *Gonyleptes curvipes*. This occurred because of the ambiguity of the scutal area count and its critical role in determining subfamilies in Roewer's system. This problem has been already abundantly commented in literature (e.g., Kury 1990).

**Homogeneity of typical *D. crenulatus*.**—The male specimen in vial NHMW 3126 exhibits a few differences with respect to other typical *D. crenulatus*: the apophyses of the stigmatic area are large (as opposed to small; Figs. 3B, 8C); the basal prolateral apophysis of Tr IV is large and pointed posteriorly (as opposed to smaller and pointed anteriorly; Figs. 3B, 8A); and the prodorsal apical apophysis of coxa IV is shorter, sharply bent in a straight angle and with a well-developed flange (as opposed to extremely elongate, gently curved, and small flanged; Figs. 3A, 8A). All of these three features fall within the variation found in the material examined of this species. Therefore, it is possible to determine that this male specimen is conspecific with the other *D. crenulatus* in Frankfurt.

## CONCLUSIONS

Kollar and C.L. Koch studied two specimens in Vienna belonging to two species, A (NHMW 3127) (Figs. 1, 2) and B (NHMW 3126) (Fig. 3) of what is now called *Discocyrtus*. Species A has been described and illustrated by C.L. Koch (1839, assigning the authorship to Kollar) as *Gonyleptes curvipes*. Species B was not described by Koch but was also labeled *G. curvipes*.

The same name *G. curvipes* had been used two years before (Guérin-Méneville 1837), and even though the species had been since long synonymized with *Pachylus chilensis* (Gray,

1833) (species D), *G. curvipes* is an invalid name due to homonymy.

Roewer (1913) called species A *G. curvipes* Kollar and illustrated the holotype (NHMW 3127).

Roewer (1913) also included NHMW 3127 (the holotype of *G. curvipes*) as part of the material of his *D. curvipes* (mixed with undescribed species C, Fig. 4A), otherwise described and illustrated upon SMF RI 812. It might be regarded either as a misidentification of *G. curvipes* Kollar or as a new species named *D. curvipes* described by Roewer with the authority wrongly ascribed to Kollar.

Roewer (1913) described *D. crenulatus* (species B) partly based on NHMW 3126 (not illustrated), but actually described upon material SMF RI 764.

Kury (2003) transferred species A to *Discocyrtus*, which caused species C to become a secondary homonym of species A, proposing a replacement name.

Kury & Alonso-Zarazaga (2011) wrongly assumed NHMW 3126 was Kollar's type of *G. curvipes* and described the real holotype of *G. curvipes* (NHMW 3127) as *D. confusus*.

The following synonymies are in order:

Species A is *D. curvipes* (Kollar, in Koch, 1839), a name invalid by homonymy; *Discocyrtus flavigranulatus* B. Soares, 1944, is a junior subjective synonym which is taken here as the most senior synonym and *D. confusus* Kury, 2011 is a junior objective synonym.

Species B is *D. crenulatus* Roewer, 1913. The syntype male (NHMW 3126) matches the hitherto known morphological variation of *D. crenulatus*. The lectotype herein chosen for this species is taken from SMF RI 764.

Species C is *D. fenax* sp. nov., which had been previously confused with *D. curvipes* sensu Roewer (misidentification).

Species D is *Pachylus chilensis* (Gray, 1833) which contains in its synonymy a *Gonyleptes curvipes* Guérin-Méneville 1837, long removed from *Gonyleptes* but which still competes for homonymy with *Gonyleptes curvipes* Kollar, in Koch, 1839.

## ACKNOWLEDGMENTS

This study has been supported by grant #306411/2015-6 from the Conselho Nacional de Desenvolvimento Científico e Tecnológico (CNPq) to ABK and scholarship # 134421/2016-7 (CNPq) to RNC; CNPq, FAPESP (#2012/02969-6, #2013/50297-0), National Science Foundation (NSF, DOB #1343578) and NASA supported RPR. The SEM micrographs were taken in the SEM Lab of Marine Diversity of the MNRJ (financed by PETROBRAS), with the kind assistance of Amanda Veiga and Beatriz Cordeiro. Edmund Schiller provided images of the old NHMW types. Enrique Leopardi produced the photographs of the holotype of *D. flavigranulatus* in MZSP. We also thank two anonymous referees for welcome suggestions that improved our final draft.

## LITERATURE CITED

Acosta, L.E. 1996. Die Typus-Exemplare der von Carl-Friedrich Roewer beschriebenen Pachylinae (Arachnida: Opiliones: Gonyleptidae). Senckenbergiana Biologica 76:209–225.

Bertkau, P. 1880. Verzeichniss der von Prof. Ed. van Beneden auf seiner im Auftrage der Belgischen regierung unternommenen wissenschaftlichen Reise nach Brasilien und La Plata i. J. 1872–1875 gesammelten Arachniden. Mémoires couronnées et mémoires des savants étrangers, publiés par l'Académie royale des sciences, des lettres et des beaux-arts de Belgique 43:1–120 + pls 1, II.

Carvalho, R.N. & Kury, A.B. 2018. Further dismemberment of *Discocyrtus* with description of a new Amazonian genus and a new subfamily of Gonyleptidae (Opiliones, Laniatores). European Journal of Taxonomy 393: 1–32.

Cowan, C.F. 1971. On Guérin's *Iconographie*: particularly the insects. Journal of the Society for the Bibliography of Natural History 6:18–29.

Gervais, P. 1844. Acères Phrynéides, Scorpionides, Solpugides, Phalangides et Acarides: Dicères Épizoïques, Aphaniptères et Thysanoures. Pp. 94–131, Atlas 3 pls 28–30 and 4 pls 46–47. *In* Histoire naturelle des Insectes Aptères. (C.A. Walckenaer, ed.) Librairie Encyclopédique de Roret, Paris.

Guérin-Méneville, F.E. 1837. Iconographie du Règne Animal de Cuvier ou Représentation d'après nature de l'une des especes les plus remarquables et souvent non encore figurées de chaque genre d'animaux. ["1829–1844"]. Vol. 2. Planches des Animaux Invertebrés, ftsp. + 226 pls. J. B. Baillière, Paris, Livraison 45 – Arachnides pl. 2, 4, 5, 6. [Issued Dec 1837].

Hauer, F.R. von 1892. Jahresbericht für 1891. Annalen des k. k. Naturhistorischen Hofmuseums 7:27–99.

Holmberg, E.L. 1878. Notas aracnologicas sobre los Solpugidos argentinos. El Naturalista argentino 1:69–74.

Jaffer, A. 2001 [and onward]. NBS/ISCC Centroids. *In* Color-Name Dictionaries. Online at http://people.csail.mit.edu/jaffer/Color/Dictionaries#nbs-isec/

Koch, C.L. 1839a. Die Arachniden getreu nach der Natur abgebildet und beschrieben. C. H. Zeh, 7:1–130, 36 pls.

Koch, C.L. 1839b. Übersicht des Arachnidensystems. Zweites Heft. C.H. Zeh, 1–38, 6 pls.

Kury, A.B. 1990. [Notes on Mitobatinae I]. Synonymic notes on *Mitobates* Sund. with redescription of the type species *M. conspersus* (Perty) (Opiliones: Gonyleptidae). Bulletin of the British Arachnological Society 8:194–200.

Kury, A.B. 2002 [and onward]. Checklist of valid genera of Opiliones of the World. Museu Nacional/UFRJ website. Online at http://www.museunacional.ufrj.br/mndi/Aracnologia/checklaniator.htm/

Kury, A.B. 2003. Annotated catalogue of the Laniatores of the New World (Arachnida, Opiliones). Revista Ibérica de Aracnología, vol. especial monográfico 1:1–337.

Kury, A.B. & M.-A. Alonso-Zarazaga. 2011. Addenda and corrigenda to the "Annotated catalogue of the Laniatores of the New World (Arachnida, Opiliones)". Zootaxa 3034:47–68.

Kury, A.B. & R.N. Carvalho. 2016. Revalidation of the Brazilian genus *Discocyrtanus*, with description of two new species (Opiliones: Gonyleptidae: Pachylinae). Zootaxa 4111:126–144.

Kury, A.B. & V.G.D. Orrico. 2006. A new species of *Lacronia* Strand, 1942 from the highlands of Rio de Janeiro (Opiliones, Gonyleptidae, Pachylinae). Revista Ibérica de Aracnologia 13:147–153.

Roewer, C.F. 1913. Die Familie der Gonyleptiden der Opiliones-Laniatores. Archiv für Naturgeschichte, Abt. A, Original-Arbeiten 79:1–256, pl. 1a.

Soares, B.A.M. 1944. Aracnídeos de Monte Alegre. Papéis avulsos do Departamento de Zoologia 4:151–168.

Sorensen, W.E. 1884. Opiliones Laniatores (Gonyleptides W. S. olim) Musei Hauniensis. Naturhistorisk Tidsskrift 14:555–646.

*Manuscript received 20 August 2017, revised 5 April 2018.*

2018. Journal of Arachnology 46:370–372

## SHORT COMMUNICATION

# Web asymmetry in the tetragnathid orb spider *Metellina mengei* (Blackwell, 1869) is determined by web inclination and web size

**Nicholas Tew**[1,2] and **Thomas Hesselberg**[1]: [1]Department of Zoology, University of Oxford, South Parks Road, Oxford, OX1 3PS, United Kingdom; E-mail: thomas.hesselberg@zoo.ox.ac.uk; [2]Department of Life Sciences, Imperial College London, Buckhurst Road, Ascot, SL5 7PY, United Kingdom

**Abstract.** Vertical asymmetry is a widespread feature of orb webs, with the lower part larger than the upper, although its adaptive value is not fully understood. Gravity is thought to play a major role in the generation of asymmetry through increased running speed downwards from the hub. The relationship between spider orientation and gravity has been relatively well studied. However, webs' inclination from vertical has been less studied. Here we conducted a field study on the tetragnathid orb spider *Metellina mengei* Blackwall, 1869, which constructs webs that show a marked variation in inclination. Our findings revealed a significant influence of the degree of web inclination and web area on the level of vertical asymmetry, while environmental variables did not have any effect. Thus, our results support the hypothesis that the asymmetry in upwards and downwards running speeds due to gravity is an important determinant of web asymmetry.

**Keywords:** Vertical web asymmetry, spider running speeds, effects of gravity, optimal foraging theory

The majority of webs from both major orb spider families (Araneidae and Tetragnathidae) are asymmetric with the area below the hub being larger than the area above (Masters & Moffat 1983; ap Rhiziart & Vollrath 1994; Kuntner et al. 2010b). This vertical web asymmetry is primarily thought to arise from an asymmetry in running speed caused by gravity, which allows for faster downwards running speeds than upwards against gravity, as has been observed in a number of araneids in the laboratory (Masters & Moffat 1983; ap Rhiziart & Vollrath 1994; Nakata & Zschokke 2010). Given this asymmetry in running speed, it follows from optimal foraging theory that spiders optimise their prey capture rate by investing more time and silk resources in web construction below the hub compared to above (Maciejewski 2010; Gregoric et al. 2013). Another hypothesis relating to gravity that has been proposed to explain web asymmetry is that web-building costs should be higher in the upper part of the web (Herberstein & Heiling 1999), although this has not been supported by empirical data (Coslovsky & Zschokke 2009).

A number of predictions arise from the gravity-determined running speed asymmetry hypothesis: *i)* Spiders should be orientated downwards to gain full advantage of the faster downward gravity-assisted running speeds. This prediction is supported by a range of studies that demonstrate a link between vertical asymmetry and spider orientation, including studies that show that the few spider species facing upwards in the hub often have reversed asymmetries with the area above the hub being larger than below (Nakata & Zschokke 2010; Zschokke & Nakata 2010), although this is not always the case (Rao et al. 2011). *ii)* Larger and heavier spiders should build more asymmetric webs as heavier spiders should experience a larger asymmetry in running speeds due to gravity's impact on mass. Studies comparing different sized adults and different ontogenetic stages confirm that larger spiders build more asymmetric webs (Herberstein & Heiling 1999; Hesselberg 2010; Kuntner et al. 2010a). Spiders that build webs with reversed asymmetry build more symmetric webs with increasing size (Nakata 2010), further supporting the notion that upwards running speed is slower in heavier spiders. Alternatively, it has been suggested that web asymmetry is an evolutionary derived trait and that spiders recapitulate this during individual development (the biogenetic law) such that young spiders build symmetric webs and older spiders asymmetric webs even in the absence of any adaptive advantage (Eberhard et al. 2008), but a number of studies specifically tested this hypothesis without finding any support (Hesselberg 2010; Kuntner et al. 2010a; Nakata 2010; Gregoric et al. 2013). *iii)* Since gravity acts vertically in the direction of the center of the Earth, spiders building webs that are not completely vertical should experience less of a difference in upwards and downwards running speed and therefore should build more symmetric webs. This is supported by experimental studies on horizontal web building in the araneid *Araneus diadematus* Clerck, 1757, which normally builds vertical webs (Zschokke 2011) and by observational studies of the tetragnathid *Leucauge venusta* (Walckenaer, 1841) webs classified into three inclination groups (Gregoric et al. 2013). The importance of gravity is further supported by observations of two *A. diadematus* building symmetric webs in space on board Skylab (Witt et al. 1977). *iv)* Web vertical asymmetry should only depend on the gravity-determined differences in running speed (predictions *i* to *iii* above), suggesting that the majority of other variables known to affect overall orb web geometry, but not expected to affect the asymmetry in running speeds, should not affect web asymmetry. This is the case for spatial constraints (Hesselberg 2013), but has not been specifically studied for other variables such as climatic factors (Vollrath et al. 1997), leg loss (Pasquet et al. 2011) and exposure to neurotoxins (Hesselberg & Vollrath 2004). However, some factors may affect web asymmetry without directly affecting running speed asymmetry, including factors such as experiences of prey capture success in different parts of the web (Heiling & Herberstein 1999), inter- and intra-individual variability in web-building behaviour (Heiling & Herberstein 2000), possibly related to differences in behavioural syndromes (Kralj-Fiser & Schneider 2012) and perceived predation risk (Nakata & Mori 2016).

Most of the above-mentioned studies focus on the effect of only one variable in a highly controlled laboratory study (but see Kuntner et al. 2010a) and use araneids with predominantly vertical webs (but see Gregoric et al. 2013). Here we investigate the asymmetry of webs of the tetragnathid *Metellina mengei* (Blackwall, 1869) in the field measuring a range of different web and climatic variables with the specific aim of testing the third and fourth prediction of the gravity-determined running speed asymmetry hypothesis (see above). To our knowledge, this is the first study to compare the effect of inclination on web asymmetry with both measured as continuous variables.

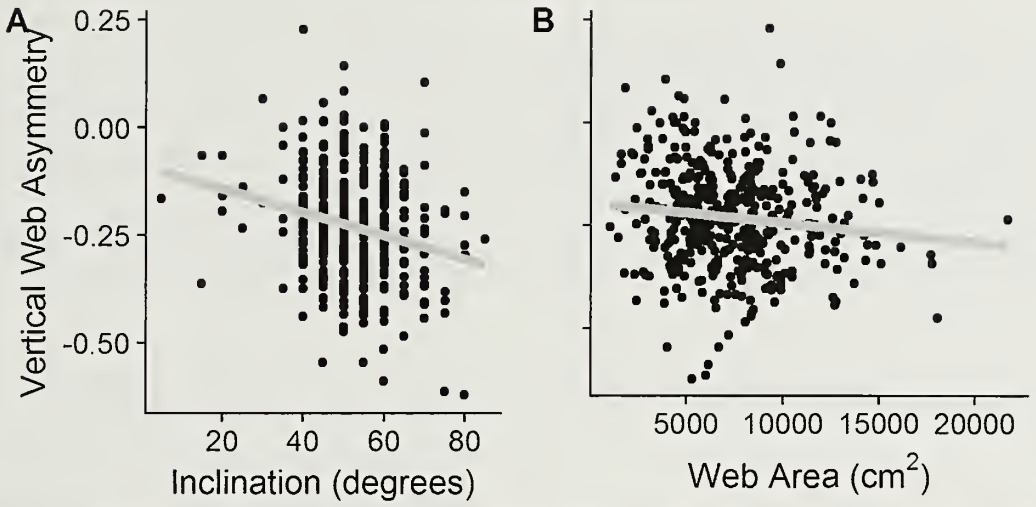


Figure 1.—The vertical asymmetry of field webs of the tetragnathid *Metellina mengei* as a function of (A) The inclination of the webs to horizontal ($n = 430$) and (B) The area of the capture spiral ($n = 430$). The grey regression lines were calculated from a simple linear regression between the two variables.

*Metellina mengei* is a medium sized orb spider common in woodland understory in Western and Central Europe in the early spring (in summer and autumn, it is replaced by the very similar *M. segmentata* (Clerck, 1757)). It builds relatively small webs that show a large variation in inclination. In this study, we observed webs ranging from 5° to 85° (but with 85% of 430 measured webs between 40° and 60°). *Metellina* spiders always (when present in the hub) face downwards (Tew & Hesselberg, pers. obs.). The data used come from a larger study by Tew and Hesselberg (2017), but here we focus on webs from the edge of the forest, where climatic conditions were more variable than in the forest interior. We recorded 430 webs of adult and subadult *M. mengei* on three 200-m transects in Wytham Woods, Oxfordshire, UK (51° 78′ N, 01° 34′ W) during 10 days in May and June 2015 and measured the following variables: the inclination of the web to horizontal (0° = horizontal, 90° = vertical) measured to the nearest 5° with a protractor kept level by placing it on a clipboard, web height above ground level, the vertical and horizontal diameters of web, the upper radius of the web, horizontal diameter of web, the vertical diameter of the free zone. From the latter variables, we calculated vertical web asymmetry with the formula: $(R_U - R_L)/(R_U + R_L)$, where $R_U$ is the upper and $R_L$ the lower radius of the web (Zschokke 1993; Hesselberg 2010), and the area of the capture spiral (web area), with the Ellipse-Hub equation (Herberstein & Tso 2000). In addition, we measured the following climatic variables at the start of each transect (three times each study day): temperature, humidity, pressure and wind speed. See Tew & Hesselberg (2017) for a more detailed description of the methodology.

In order to determine the influence of web and climatic variables on web asymmetry, we used the statistical programming language R (R Core Team 2016) to build a general linear mixed model with web asymmetry as response variable and inclination, web area, web height, wind speed, temperature, pressure and humidity as predictor variables. First order interactions between the first four variables were also included in the model. The study day and transect number were included as random factors. The model was validated following Thomas et al. (2013). Non-significant terms were removed from the full model following the marginal rule until the final model with the lowest AIC score was found. *P*-values were determined with Type II Wald F tests with Kenward-Roger degrees of freedom. The conditional ($R_c^2$ fixed and random effects) and marginal ($R_m^2$, fixed effects only) coefficients of determination were estimated based on the method by Nakagawa & Schielzeth (2013).

We found a clear negative relationship between the degree of inclination and vertical asymmetry ($F = 17.76$, $df = 1$, $n = 430$, $P < 0.001$), which supports prediction *iii* above. The less inclined (more horizontally orientated) a *M. mengei* web was, the more symmetric it was (Fig. 1A). We furthermore found a significant effect of web area ($F = 8.54$, $df = 1$, $n = 430$, $P = 0.004$) in that larger webs were significantly more asymmetric (Fig. 1B). This lends support to prediction *ii*, since larger webs are usually built by larger and heavier spiders (Heiling & Herberstein 1998). We furthermore found support for prediction *iv* in that none of the climatic variables tested (wind speed, temperature, humidity and pressure) or height of web above the ground were found to have a significant effect on web asymmetry (Wind speed: $F = 1.02$, $df = 1$, $n = 430$, $P = 0.340$; Temperature: $F = 0.88$, $df = 1$, $n = 430$, $P = 0.371$; Humidity: $F = 1.33$, $df = 1$, $n = 430$, $P = 0.289$; Pressure: $F = 0.20$, $df = 1$, $n = 430$, $P = 0.672$; Height: $F = 0.64$, $df = 1$, $n = 413$, $P = 0.423$). However, height did have an indirect effect on web asymmetry in that its interaction with inclination was significant ($F = 9.89$, $df = 1$, $n = 413$, $P = 0.002$) such that webs build lower in the vegetation did not show a clear relationship between inclination and web asymmetry. Similarly, we found a significant interaction between inclination and web area ($F = 6.24$, $df = 1$, $n = 413$, $P = 0.013$) such that only larger webs showed a clear relationship between inclination and web asymmetry. None of the first order interactions including wind speed, were significant and neither was the interaction between height and web area (results not shown). The full model with fixed and random factors explained 12% of the variance ($R_c^2 = 0.124$), while the fixed factors alone explained 9% ($R_m^2 = 0.089$). Thus, the model developed in this study only explained about 12% of the variation in the observed web asymmetry. This suggests that although inclination and web area significantly influence web asymmetry, it is also influenced by a range of other factors not measured in this study such as spider size (although this is partly taken into account by the use of web-size (Heiling & Herberstein 1998), intra- and inter-individual variation in web-building (Heiling & Herberstein 2000), spider age, ontogeny and reproductive status (Hesselberg 2010; Anotaux et al. 2012).

Despite the relatively large number of studies on web asymmetry in orb spiders, there is still much we do not know, especially in relation to webs in the wild. In this study, we focussed on some of the mechanistic factors influencing the asymmetry, but there is also a need to look at the functional aspects. In particular it would be interesting to study prey capture success and the resulting growth rate and reproductive success in spiders that build webs of different

inclination (and hence asymmetry) in greater detail as our previous study suggests that inclination is a significant determinant of prey capture success in the webs of this species (Tew & Hesselberg 2017). The webs of *M. uengei* that were measured in this study varied quite significantly in both inclination and asymmetry (with 3% of webs even having larger upper parts than lower parts – see figure 1). If a given inclination and web asymmetry provides the largest return in terms of prey capture, why do webs in the wild show such a large variation? One intriguing possibility is that predation risk may affect the degree of web asymmetry in that asymmetric webs are posited to be more complex and take longer time to build than symmetric webs causing spiders to build more symmetric webs when they perceive a risk of predation (Nakata & Mori 2016). However, our previous study did not show any differences in the asymmetry of webs between the more exposed forest edge with presumably higher predation risk and the more sheltered interior of the forest (Tew & Hesselberg 2017).

## LITERATURE CITED


Anotaux, M., J. Marchal, N. Chaline, L. Desquilbet, R. Leborgne, C. Gilbert et al. 2012. Ageing alters spider orb-web construction. Animal Behaviour 84:1113–1121.

ap Rhiziart, A. & F. Vollrath. 1994. Design features of the orb web of the spider, *Araneus diadematus*. Behavioral Ecology 5:280–287.

Coslovsky, M. & S. Zschokke. 2009. Asymmetry in orb-webs: an adaptation to web building costs? Journal of Insect Behavior 22:29–38.

Eberhard, W.G., G. Barrantes & Madrigal-Brenes, R. 2008. Vestiges of an orb-weaving ancestor? The "biogenetic law" and ontogenetic changes in the webs and building behavior of the black widow spider *Latrodectus geometricus* (Araneae Theridiidae) Ethology Ecology & Evolution 20:211–244.

Gregoric, M., H.C. Kiesbuy, S.G. Quiñones Lebron, A. Rozmann, I. Agnarsson & M. Kuntner. 2013. Optimal foraging, not biogenetic law, predicts spider orb web allometry. Naturwissenschaften 100:263–268.

Heiling, A.M. & M.E. Herberstein. 1998. The web of *Nuctenea sclopetaria* (Araneae, Araneidae): relationship between body size and web design. Journal of Arachnology 26:91–96.

Heiling, A.M. & M.E. Herberstein. 1999. The role of experience in web-building spiders (Araneidae). Animal Cognition 2:171–177.

Heiling, A.M. & M.E. Herberstein. 2000. Interpretations of orb-web variability: a review of past and current ideas. Ekológia 19:97–106.

Herberstein, M.E. & A.M. Heiling. 1999. Asymmetry in spider orb webs: a result of physical constraints? Animal Behaviour 58:1241–1246.

Herberstein, M.E. & I-M. Tso. 2000. Evaluation of formulae to estimate the capture area of orb webs (Araneoidea, Araneae). Journal of Arachnology 28:180–184.

Hesselberg, T. 2010. Ontogenetic changes in web design in two orb-web spiders. Ethology 116:535–545.

Hesselberg, T. 2013. Web-building flexibility differs in two spatially constrained orb spiders. Journal of Insect Behavior 26:283–303.

Hesselberg, T. & F. Vollrath. 2004. The effects of neurotoxins on web-geometry and web-building behaviour in *Araneus diadematus* Cl. Physiology & Behavior 82:519–529.

Kralj-Fiser, S. & J. Schneider. 2012. Individual behavioural consistency and plasticity in an urban spider. Animal Behaviour 84:197–204.

Kuntner, M., M. Gregoric & D. Li. 2010a. Mass predicts web asymmetry in *Nephila* spiders. Naturwissenschaften 97:1097–1105.

Kuntner, M., S. Krajl-Fiser & M. Gregoric. 2010b. Ladder webs in orb-web spiders: ontogenetic and evolutionary patterns in Nephilidae. Biological Journal of the Linnean Society 99:849–866.

Maciejewski, W. 2010. An analysis of the orientation of an orb-web spider. Journal of Theoretical Biology 265:604–608.

Masters, M. & A. Moffat. 1983. A functional explanation of top-bottom asymmetry in vertical orb webs. Animal Behaviour 31:1043–1046.

Nakagawa, S. & H. Schielzeth. 2013. A general and simple method for obtaining $R^2$ from generalized linear mixed-effects models. Methods in Ecology and Evolution 4:133–142.

Nakata, K. 2010. Does ontogenetic change in orb web asymmetry reflect biogenetic law? Naturwissenschaften 97:1029–1032.

Nakata, K. & Y. Mori. 2016. Cost of complex behaviour and its implications in antipredator defence in orb-web spiders. Animal Behaviour 120:115–121.

Nakata, K. & S. Zschokke. 2010. Upside-down spiders build upside-down orb webs: web asymmetry, spider orientation and running speeds in *Cyclosa*. Proceeding of the Royal Society of London. Series B. 277:3019–3025.

Pasquet, A., M. Anotaux & R. Leborgne. 2011. Loss of legs: is it or not a handicap for an orb-weaving spider? Naturwissenschaften 98:557–564.

R Core Team. 2016. R: A language and environment for statistical computing. R Foundation for Statistical Computing, Vienna, Austria. URL https://www.R-project.org/.

Rao, D., O.C. Fernandez, E. Casteñedo-Barbosa & F. Diaz-Fleischer. 2011. Reverse positional orientation in a neotropical orb-web spider, *Verrucosa arenata*. Naturwissenschaften 98:699–703.

Tew, N. & T. Hesselberg. 2017. The effect of wind exposure on the web characteristics of a tetragnathid orb spider. Journal of Insect Behavior 30:273–286.

Thomas, R., I. Vaughan & J. Lello. 2013. Data Analysis with R statistical Software: A Guidebook for Scientists. – Eco-Explore, Newport.

Vollrath, F., M. Downes & S. Krackow. 1997. Design variability in web geometry of an orb-weaving spider. Physiology & Behavior 62:735–743.

Witt, P. N., M.B. Searboro, R. Daniels, D.B. Peakall & R.L. Gause. 1977. Spider web-building in outer space: evaluation of records from the Skylab experiment. Journal of Arachnology 4:115–124.

Zschokke, S. 1993. The influence of the auxiliary spiral on the capture spiral in *Araneus diadematus* Clerck (Araneidae). Bulletin of the British Arachnological Society 9:169–173.

Zschokke, S. 2011. Spiral and web asymmetry in the orb webs of *Araneus diadematus* (Araneae: Araneidae). Journal of Arachnology 39:358–362.

Zschokke, S. & K. Nakata. 2010. Spider orientation and hub position in orb web. Naturwissenschaften 97:43–52.


*Manuscript received 15 August 2017, revised 21 December 2017.*

2018. Journal of Arachnology 46:373–375

## SHORT COMMUNICATION

# A method for accurately estimating social spider numbers without colony damage

**Bharat Parthasarathy** and **Hema Somanathan**: IISER-TVM Centre for Research and Education in Ecology and Evolution (ICREEE), School of Biology, Indian Institute of Science Education and Research, Thiruvananthapuram, Kerala 695011, India. E-mail: bharat@iisertvm.ac.in

**Abstract.** Ecologists are often required to accurately estimate the number of individuals residing in groups of variable sizes inside opaque shelters. Here, we have used x-rays as a non-destructive solution to this problem in social spiders which reside within collectively built opaque, silken, nest-like retreats. Social spiders are model systems for understanding social organization, collective behaviours and population genetics of inbred populations. Such studies often require an accurate determination of the number of individuals, developmental stages and orientation of individuals within the colony which is difficult without compromising the integrity of their retreat or affecting colony behaviour. We demonstrate the effectiveness of x-rays in accurately estimating colony size in the social spider *Stegodyphus sarasinorum* Karsch, 1892 (Eresidae). This method can also be applied to evaluate body sizes, developmental stages and individual orientation within the colony. We show that this technique does not alter spider prey-capture behaviour or short-term survival compared to control colonies.

**Keywords:** Animal-built shelters, colony size, social animals, X-rays

Studies in diverse fields such as ecology, behaviour, animal architecture and biocontrol often require screening opaque material for the presence of macroscopic animals without inducing damage to individuals within them. In the recent past, several technological advances such as near-infrared spectroscopy or three dimensional x-ray technologies have been used in studying infestation of cereal kernel (Maghirang et al. 2003; Aldrich et al. 2007) or in studying bee behaviour inside natural colonies, respectively (Greco et al. 2005). X-rays have been used in the past to detect hidden insects, largely wood-boring pest species (Fischer & Tasker 1940; Berryman & Stark 1962) by the pest management industry. However its application in ecology and behavioural investigations is rare. Here, we describe an inexpensive and efficient method that we have used to accurately quantify social spider numbers. Our method can be used to quantify developmental stages, measure body sizes and spatial orientation within colonies of social spiders or shelters of other animal groups.

Social spiders are rare and an interesting model organism for the following reasons. Unlike eusocial insects, social spiders lack morphological castes, but show personality types in certain behaviours (Pruitt et al. 2008, 2010; Pruitt & Reichert 2009), at least in certain contexts (Beleyur et al. 2015; Lichtenstein et al. 2016). Their colonies have highly female-biased sex ratios and inbreed with natal kin, which is believed to have led to a dramatic reduction in diversification rates (Lubin & Bilde 2007). Studies of social spiders often require a reliable, quick and inexpensive method to determine the numbers of individuals without undesirable effects on the colony. Because social spiders live in dense silken colonies, it is impossible to visualize their numbers, developmental stages and spatial orientation inside the colony without severely damaging the retreat. In the past, indirect methods such as estimating retreat/nest volume to infer colony size has been employed (Powers & Avilés 2007), however, this requires standardisation for every species being studied and may not give accurate estimates due to dispersal or immigration. In this study, we examine whether x-rays can be reliably used to determine social spider numbers and whether colonies subjected to x-rays have altered survival and behavioural responses.

We collected twenty colonies of *Stegodyphus sarasinorum* Karsch, 1892 of varying sizes (numbers of resident spiders) in and around Kuppam (12.75° N, 78.37° E), Andhra Pradesh, India in January 2014. Whole colonies were removed by carefully cutting the branch of the plant which contained their retreats. The colonies were immediately transferred into well-ventilated rectangular plastic containers (25 × 18 × 10 cm). The spiders remained within the retreat during this process. We subjected twenty colonies to x-rays (hereafter referred to as x-ray colonies) at 60 kV and 100 mA for 0.4 *s* (Allengers 325/525) at a local medical x-ray facility close to the field site and obtained digital images of the radiogram (Fig. 1). The cost of each x-ray was approximately 7.5 USD (approximately 500 Indian rupees). The colony was placed at an angle of $90^0$ from the incident x-ray beam. From these images, we later counted spider numbers. To verify the degree of accuracy of our estimates, we also did manual counts by opening up the retreat structure. Intra-class correlation (ICC) between the spiders counted from the x-rays film and from the manual counts were very similar (ICC = 0.975, $P = 0.0003$, $n = 20$ colonies each; Mean ± SD from x-ray films = 30.8 ± 20.30 and manual count = 33.3 ± 20.94). The means from the two counts were comparable (paired sample *t*-test after 5000 bootstrap runs: $t = 1.83$, $P = 0.110$, $n = 10$ colonies each; Fig. 2).

Next, we randomly transferred 30 spiders from each of 10 out of the 20 colonies subjected to x-rays into separate well-ventilated plastic containers. For controls, we transferred another 30 spiders from 10 colonies collected from the same area and not subjected to x-radiation into identical plastic containers. Controls and x-ray colonies built dense capture webs inside the box after two days. From the third day onwards, we performed prey capture experiments for six consecutive days as follows: A live honey bee, *Apis cerana*, (maintained inside hive boxes in the field) was added as prey to each box containing spiders. The time taken for the first attack and the number of attackers were recorded for five minutes. The mean number of attackers was similar in controls and x-ray colonies (Mean ± SD = 3.08 ± 2.53 and 3.04 ± 3.10 respectively, Mann Whitney $U = 1039.50$, $P = 0.506$, $n = 10$ colonies each). The mean time to initiate prey capture was also similar between the control and x-ray colonies (34.23 ± 71.04 *s* for control and 25.81 ± 48.73 *s* for x-ray colonies; $U = 1060.50$, $P = 0.614$, $n = 10$ colonies each). We built separate general linear mixed models (GLMM) in R (version 3.0.2, R Core Team 2013) with number of attackers or prey capture time as response variables and treatment (x-rays or control) as binary dependent variable, colony number and trial number as random effects, and compared these against the null

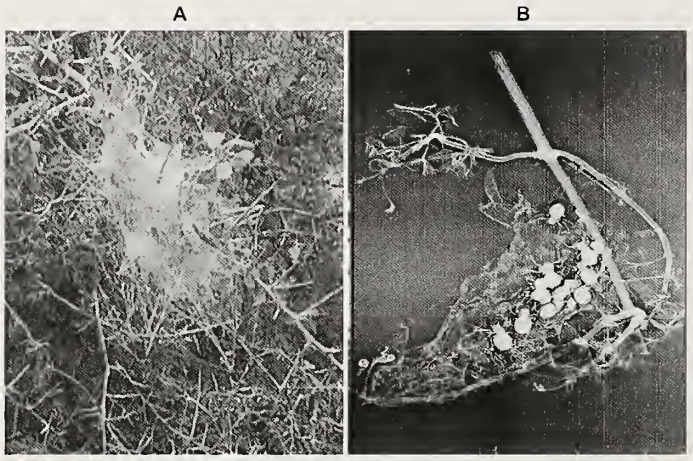


Figure 1.—Retreat of *Stegodyphus sarasinorum*. A. Picture of a spider retreat in the field. Spiders live within the dense opaque silken retreat. B. X-ray image of a spider retreat showing spiders. Twenty colonies were subjected to x-radiation at 60 kV and 100 mA for 0.4 *s*. Social spiders which reside within the dense silken retreat are clearly visible here and the numbers were estimated by counting individuals in the image. The count from the x-ray image was 10 while the actual numbers (from manual count) were 11.

model (without the dependent variable). The number of spiders attacking prey was similar in controls and in x-ray colonies as evidenced from non-significant $\chi^2$ values after model comparisons ($\chi^2 = 0.04$, $P = 0.836$). So was the latency to attack between the two groups ($\chi^2 = 0.53$, $P = 0.466$). Survival in x-ray and control colonies was followed over a 10-day period and no mortality was recorded over this duration. Moreover, during this 10-day period, spiders laid four egg sacs in x-ray colonies and three egg sacs in control colonies. In a long-term study on dispersal, we found that x-ray colonies showed similar frequency and timing of dispersal as normal colonies (Parthasarathy and Somanathan 2018), and also produced viable eggs sacs as in normal colonies (unpublished data).

Thus, we demonstrate a reliable and accurate method using x-rays to ascertain social spider colony sizes which does not require opening of retreats, and minimizes disturbance that can trigger dispersal from retreats when colonies are counted manually. Branches containing the retreat, when carefully cut can be returned to the field for further studies after x-rays are taken. If experiments require intact capture webs then portable x-ray machines may be used. As long as the x-rays penetrate the entire retreat, the angle of x-ray beams is not of consequence to count the number of individuals or to examine their spatial orientation within the retreat. We also show that spiders subjected to x-rays behave similar to control colonies in performing collective prey capture, suggesting that x-rays do not alter behavioural responses. Moreover, colonies did not suffer mortality over the short term (10 days) due to the x-ray treatment; they built normal capture webs as in control colonies within two days and also reproduced. Only continuous exposure to x-rays may cause mutagenesis as shown by numerous studies in invertebrates (e.g., Muller 1928; Herskowitz 1950). It is essential to note that it would suffice to subject social spider colonies (or other insects) to x-radiation only once in order to ascertain their numbers, without suffering such consequences. The cost of an x-ray was approximately 7.5 USD in our field site in southern India, however the costs are likely to vary a lot across countries/sites where social spiders are found. Researchers often collect entire retreats containing spiders in boxes and transport them over long distances. In such cases the x-ray can be taken later (through the box), at a convenient time and facility, thus avoiding the use of more invasive methods.

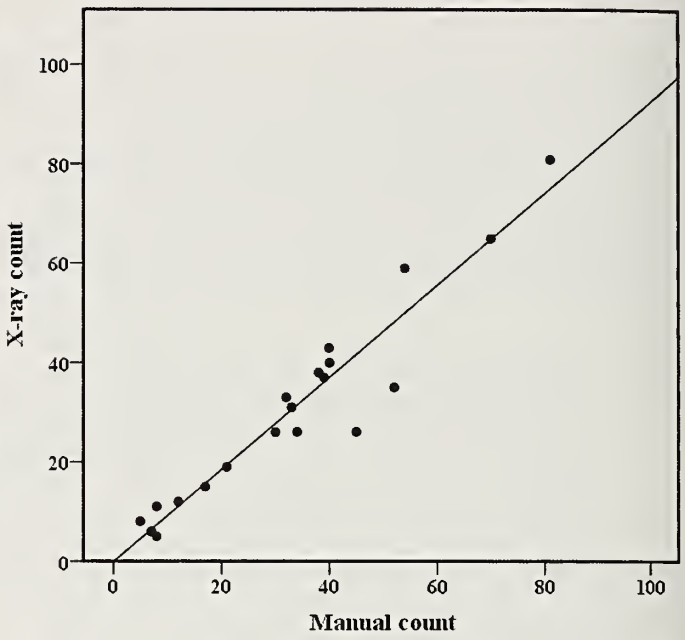


Figure 2.—Plots comparing social spider numbers determined from x-ray films (y-axis) and manual counts (x-axis). Mean ± SD for manual and x-rays count were 33.3 ± 20.94 and 30.8 ± 20.30 respectively ($n = 20$, ICC = 0.975, $P = 0.0003$). The regression equation was 0.927 ± 0.067.

In summary, we suggest that x-radiation may be used to census insects and other invertebrates living within opaque shelters. Thus, this method can also be extended to examine spatial organisation of individuals within communal shelters, developmental stages, presence or absence of kleptoparasites and so on without compromising the integrity of the shelter structure.

## ACKNOWLEDGMENTS

We thank Sheheer Ali and Chinmay Joshi for help with experiments. We also thank Dr. Srikanta Dani and two anonymous reviewers for their useful comments on the manuscript. BP thanks IISER TVM for the PhD fellowship and the partial support from the American Arachnology Society. This study was supported by a grant to HS from Council for Industrial and Scientific Research (CSIR), India and intramural funds from IISER TVM.

## LITERATURE CITED

Aldrich, B.T., E.B. Maghirang, F.E. Dowell & S. Kambhampati. 2007. Identification of termite species and subspecies of the genus *Zootermopsis* using near-infrared reflectance spectroscopy. Journal of Insect Science 7:18.

Beleyur, T., D.U. Bellur & H. Somanathan. 2015. Long term behavioural consistency in prey capture but not in web maintenance in a social spider. Behavioural Ecology and Sociobiology 69:1019–1028.

Berryman, A.A. & R.W. Stark. 1962. Radiography in forest entomology. Annals of the Entomological Society of America 55:456–466.

Fisher, R.C. & H.S. Tasker. 1940. The detection of wood-boring insects by means of x-rays. Annals of Applied Biology 27:92–100.

Greco, M., R. Spooner-Hart & P. Holford. 2005 A new technique for monitoring *Trigona carbonaria* nest contents, brood and activity using x-ray computerized tomography. Journal of Apicultural Research 44:97–100.

Herskowitz, I.H. 1950. The genetic basis of x-rays induced recessive lethal mutations. Genetics 36:356–363.

Lichtenstein, J.L.L., N. Dirienzo, K. Knutson, C. Kuo, K.C. Zhao, H.A. Brittingham et al. 2016. Prolonged food restriction decreases body condition and reduces repeatability in personality traits in web-building spiders. Behavioral Ecology and Sociobiology 70:1793–1803.

Lubin, Y. & T. Bilde. 2007. The evolution of sociality in spiders. Advances in the Study of Behaviour 37:83–145.

Maghirang, E.B., F.E. Dowell, J.E. Baker & J.E. Throne. 2003. Automated detection of single wheat kernels containing live or dead insects using near–infrared reflectance spectroscopy. Transactions of the American Society of Agricultural Engineers 46:1277.

Muller, H.J. 1928. The production of mutations by x-rays. Proceedings of the Natural Academy of Sciences 14:714–726.

Parthasarathy, B. & H. Somanathan. 2018. Body condition and food shapes group dispersal but not solitary dispersal in a social spider. Behavioral Ecology doi:10.1093/beheco/ary013

Powers, K.S. & L. Avilés. 2007. The role of prey size and abundance in the geographical distribution of spider sociality. Journal of Animal Ecology 76:995–1003.

Pruitt, J.N. & S.E. Riechert. 2009. Sex matters: sexually dimorphic fitness consequences of a behavioural syndrome. Animal Behaviour 78:175–181.

Pruitt, J.N., S.E. Riechert, G. Iturralde, M. Vega, B.M. Fitzpatrick & L. Aviles. 2010. Population differences in behaviour are explained by shared within-population trait correlations. Journal of Evolutionary Biology 23:748–756.

Pruitt, J.N., S.E. Riechert & T.C. Jones. 2008. Behavioural syndromes and their fitness consequences in a socially polymorphic spider, *Anelosimus studiosus*. Animal Behaviour 76:871–879.

R Core Team. 2013. R: A language and environment for statistical computing. R foundation for Statistical Computing, Vienna, Austria.

*Manuscript received 17 September 2017, revised 30 October 2017.*

2018. Journal of Arachnology 46:376–379

## SHORT COMMUNICATION

# Assessing spider diversity in grasslands – does pitfall trap color matter?

**Sascha Buchholz**[1,3] and **Maria Möller**[2]: [1]Department of Ecology, TU Berlin, Rothenburgstraße 12, 12165 Berlin, Germany; E-mail: sascha.buchholz@tu-berlin.de; [2]Zoological Institute and Museum, University of Greifswald, Loitzer Str. 26, 17489 Greifswald, Germany; [3]Berlin-Brandenburg Institute of Advanced Biodiversity Research (BBIB), 14195 Berlin, Germany

**Abstract.** We analyzed effects of pitfall trap color on spider catches using four different pitfall trap colors (white, yellow, green, brown). For each color, we installed 17 pitfall traps at two grassland sites, respectively, and sampled 77 species from 6,202 individuals. Number of species showed no significant differences but Shannon- and Simpson-diversity were significantly higher in green and brown traps while number of individuals increased in white ones. Species inventories were not complete in the different pitfall trap colors but species accumulation increased significantly slower in white and brown traps. Trap color significantly affected hunting type with ground hunters being associated with bright and web-builders associated with dark colors. Attractiveness of different trap colors may arise due to differences in biological preconditions, albedo and microclimate which in turn can affect diversity and community structure of spiders. Trap color has a significant impact on spider catches and should be considered when planning surveys. We recommend the use of a combination of white and brown (or transparent) pitfall traps to gain complete and diverse species inventories in spiders.

**Keywords:** Araneae, by-catch, capture efficiency, functional traits, sampling design

Pitfall trapping is one of the most commonly used methods to sample ground-dwelling arthropods. The method is easy to use, time-efficient, associated with low costs and suitable for studying the occurrence and relative abundance of ground-dwelling arthropods (New 1999). Moreover, pitfall trap catches are rich in both species and individuals (Spence & Niemelä 1994) and therefore yield reliable data for a broad range of ecological and biological studies (Sonoda et al. 2013; Coreuera et al. 2016; Yekwayo et al. 2016).

However, capture efficiency of pitfall traps depends strongly on properties such as trap size and the fluid employed (see Brown & Matthews 2016 for a comprehensive review). Interestingly, effects of pitfall trap color have rarely been investigated (but see Buchholz et al. 2010). This could be a drawback, since colored traps could either attract or deter specific taxa as it is known for other types of traps such as pan traps (Heneberg & Bogusch 2014; Moreira et al. 2016). Buchholz et al. (2010) observed that brightly colored pitfall traps (white, yellow) caught significantly more spiders and beetles than more inconspicuous colors such as brown and green. This is of concern, since most studies on epigeal invertebrates use white-colored plastic cups (e.g., Schirmel et al. 2010; Kataja-aho et al. 2016; Meriste et al. 2016) or transparent glass jars (then perceived as brown or soil color) (e.g., Negro et al. 2009; Sadler et al. 2006; Buchholz & Hartmann 2008), thus yielding significantly different catch sums. However, since these results were merely based on individual sums rather than on diversity, it should be valuable to provide a more detailed analysis on species and functional level. Based on the data of Buchholz et al. (2010), we therefore evaluated possible effects of pitfall trap colors (four colors; two dark-shaded, two bright-shaded) on (1) alpha-diversity, (2) species composition of spider communities, and (3) life-history traits.

The study was conducted close to the city of Münster (51°57′46.6″N, 7°37′43.3″E) in North Rhine-Westphalia, Germany. The sub-oceanic climate in this region has a mean annual temperature of 7.9°C and an annual precipitation of 758 mm (Landesanstalt für Ökologie, Bodenordnung und Forsten NRW, 2005). Two sites with a homogeneous vegetation structure were selected that consisted of (1) a sparsely vegetated, dry grassland (Corynephoretum: nutrient-poor grassland on inland dunes; coverage of herbaceous plants [CH] = 20%, height of herbaceous plants [HH] = 15 cm), and (2) a densely vegetated grassland site (Lolio-Cynosuretum: mesotrophic grasslands; CH = 100%, HH = 50–60 cm). In total, 68 colored pitfall traps made of plastic jars and filled with a 3% formalin solution and detergent were set. The traps with a diameter of 9 cm and a height of 12 cm were brown, green, white, or yellow and arranged in a grid in rotational order (white–yellow–green–brown, yellow–green–brown–white, green–brown–white–yellow, brown–white–yellow–green). The distance between the traps was 5 m. At the dry grassland site, 24 pitfall traps (6 traps per color) were set and 44 at the densely vegetated grassland site (11 traps per color) (see Buchholz et al. 2010 for more details). These traps were used to catch spiders from 24 April to 6 June 2009 and emptied fortnightly.

Spiders were preserved in ethyl alcohol and determined using standard references (Roberts 1998). For all subsequent analyses, we took into account only adult specimens. To express alpha-diversity, we calculated the observed species numbers and Shannon and Simpson diversity indices.

To assess whether there were significant differences in alpha-diversity among the four pitfall colors (explaining variable: pitfall trap color), we used generalized linear models (GLM) and Holm-Sidak post-hoc tests for pairwise comparisons. Furthermore, species accumulation curves have been calculated with 10,000 permutations to evaluate the completeness of species inventories for each pitfall trap color. We tested differences in curve growth applying a repeated measures ANOVA and Holm-Sidak pairwise-tests. For this, we took data series for each curve and calculated growth between each data point resulting in sixteen growth values per curve.

To determine whether pitfall trap color affected species composition, we applied permutational multivariate analysis of variance (R function: adonis in VEGAN package) (10,000 permutations). Finally, we calculated lightness association for each species. First, we referred to the HSL categorization of colors (Wyszecki & Stiles 2000) and took the lightness values for each color (white = 100%, yellow = 50%, green = 34%, brown = 31%). Second, we calculated Pearson correlation coefficients to express lightness association of spider species. Significance levels of correlations were computed using permutations tests (number of permutations = 99999). Based on Pearson correlation

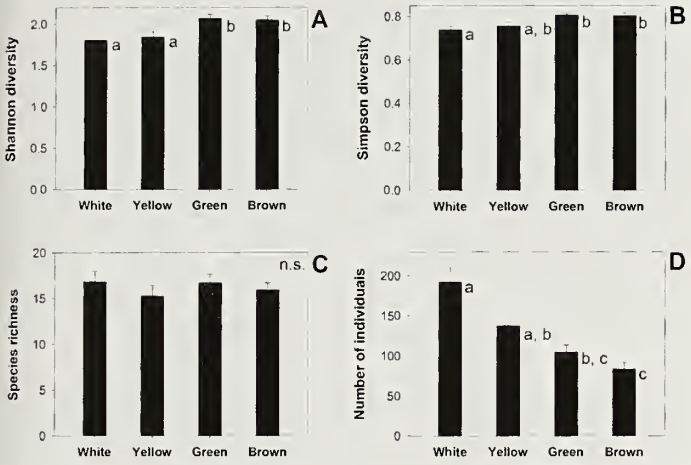


Figure 1.—Alpha-diversity of grassland assemblages differed among pitfall trap color in terms of Shannon- (**A:** GLM, $F = 6.7$, $df = 3$, $P = 0.0009$) and Simpson-diversity (**B:** GLM, $F = 5.5$, $df = 3$, $P = 0.003$), species richness (**C:** GLM, n.s.) and number of individuals (**D:** GLM, $F = 15.5$, $df = 3$, $P < 0.0001$). Pairwise differences (Holm-Sidak, $P < 0.05$) are presented with lower case letters; values with the same letter are not significantly different.

coefficients, we ran further GLMs to assess whether life-history traits (hunting mode and daily activity) had different light associations. All statistical analyses were performed using the R software environment (version 3.3.1, R Core Team 2016).

A total of 6,202 spiders belonging to 77 species were determined (grassland = 54, dry grassland = 37) (See appendix S1 online at http://dx.doi.org/10.1636/JoA-S-16-062.s1). Most abundant species in grassland sites were *Pardosa prativaga* (L. Koch, 1870) ($n = 1{,}962$), *Pardosa amentata* (Clerck, 1757) ($n = 1{,}417$), *Pachygnatha degeeri* Sundevall, 1830 ($n = 489$), and *Pardosa pullata* (Clerck, 1757) ($n = 468$). In dry grasslands, most abundant species were *Xerolycosa miniata* (C. L. Koch, 1834) ($n = 269$), *Pardosa hyginis* (Walckenaer, 1802) ($n = 108$), and *Drassyllus pusillus* (C. L Koch, 1833) ($n = 16$).

Although the number of species showed no significant differences among pitfall trap colors, Shannon-diversity (GLM, $F = 6.7$, $df = 3$, $P = 0.0009$) and Simpson-diversity (GLM, $F = 5.5$, $df = 3$, $P = 0.003$) were significantly higher in dark-colored (green and brown) than in bright pitfall traps (Fig. 1). In contrast, the number of individuals (GLM, $F = 15.5$, $df = 3$, $P < 0.0001$) decreased by 42% from bright to dark traps (Fig. 1).

Species correlations to pitfall trap color were generally missing except for *Pardosa prativaga* and *Trochosa terricola* Thorell, 1856, which were associated with bright colors and *Palliduphantes pallidus* (O. Pickard-Cambridge, 1871), which was associated with dark colors (Appendix S1).

Species inventories were not complete, that is, the species accumulation curves indicated that the complete diversity of (rarer) species had not been sampled in any of the different pitfall trap colors. However species accumulation curves increased significantly more slowly in white (2.04 ± 0.49, mean ± SEM, repeated measures ANOVA: $F = 124.9$, $df = 3$, $P < 0.001$) and brown pitfall traps (2.20 ± 0.45) than in yellow (2.79 ± 0.43) and green ones (2.52 ± 0.44) (Fig. 2).

Pitfall trap color association differed among hunting types (GLM, $F = 3.7$, $df = 4$, $P = 0.009$) but pairwise comparisons indicated significant differences only between ground hunters and web builders (Fig. 3). The former had a higher association with bright colors while the latter were associated with dark traps. Regarding activity patterns (diurnal, nocturnal or diurnal-nocturnal), no significant differences

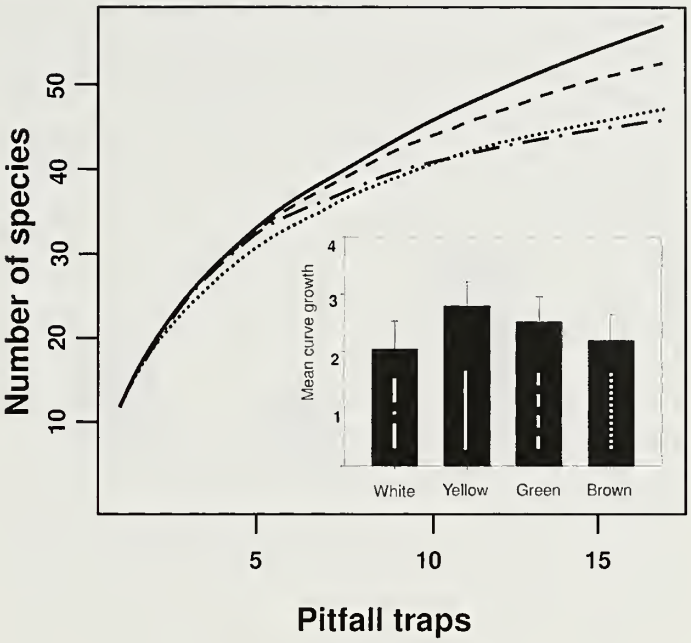


Figure 2.—Sample-based species accumulation curves of the different pitfall trap colors (white = dot-dashed line, yellow = line, green = dashed line, brown = dotted line). X-axis = number of traps. Growth of accumulation curves differed significantly among pitfall trap colors (repeated measures ANOVA, $F = 124.9$, $df = 3$, $P < 0.001$; all pairwise comparisons are significant with $P < 0.01$).

were found in pitfall trap color association (GLM, $F = 0.9$, $df = 2$, $P = 0.41$) (Fig. 4).

Previous work revealed that catches among different pitfall trap colors significantly differ in terms of total numbers of individuals captured (Buchholz et al. 2010). However, this study shows that analyzing alpha diversity, community structure and trait composition yielded a more nuanced result which should be considered when using pitfall traps. One main insight from this study is that hunting guilds

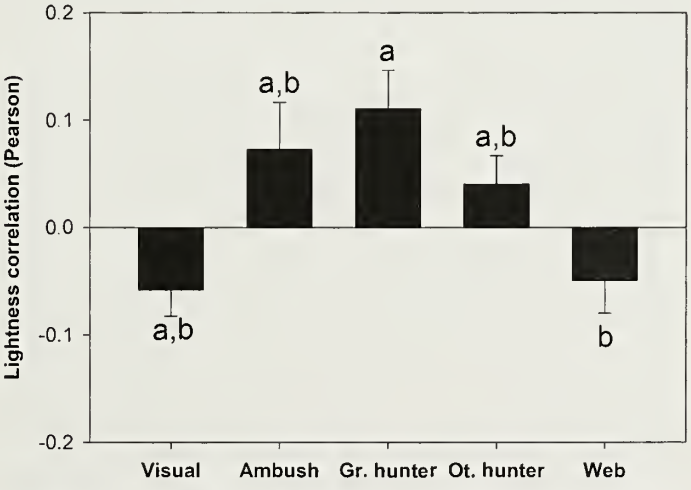


Figure 3.—Differences in lightness correlation among hunting types (GLM, $F = 3.7$, $df = 4$, $P = 0.009$). Pairwise comparisons (Holm-Sidak, $P < 0.05$) are presented with lower case letters, indicating significant differences only between ground hunters and web builders. Gr. Hunter = ground hunter, Ot. Hunter = other hunter. See appendix S1 online at http://dx.doi.org/10.1636/JoA-S-16-062.s1 for species assigned to each hunting style.

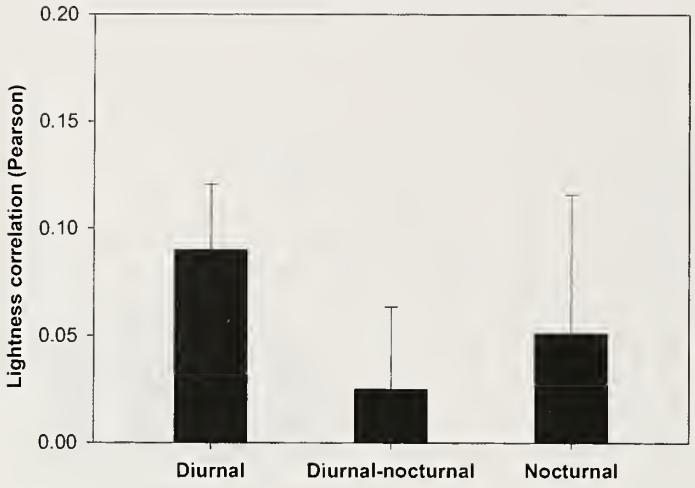


Figure 4.—Lightness correlation among activity categories (GLM, $F = 0.9$, $dF = 2$, $P = 0.41$). See appendix S1 online at http://dx.doi.org/10.1636/JoA-S-16-062.s1 for species assigned to each activity category.

significantly responded to different pitfall trap colors since ground hunters showed higher association to bright colors while web-builders were associated with dark ones. One explanation could be that ground hunters are able to distinguish colors to some extent and to notice contrasts (Foelix 2011; Zopf et al. 2013; Zurek et al. 2015). Attraction to bright trap colors could therefore be due to an improved visibility of prey on a bright background. Another reason could be a higher albedo of bright surfaces making white and yellow pitfall traps clearly visible points of orientation for ground-hunting spiders. In turn, web-builders might prefer green and brown due to lower albedo and color pattern similar to herbal layer where they commonly install their webs. Finally, differences in color are associated with different temperatures in the surroundings of pitfall traps. In this context, microclimate is known to significantly affect pitfall trap catches, their diversity, species composition and even trait distribution (Saska et al. 2013). Differences in trait signals can result in species-turnover among pitfall trap colors as for example two ground hunting species (*Pardosa prativaga* and *Trochosa terricola*) were related to bright colors, contrary to web-building *Palliduphantes pallidus* occurring in dark colors.

In terms of diversity, Shannon and Simpson diversity were significantly higher in dark compared to bright colors. Both indices are known to be sensitive to evenness of individuals per species, with higher values in communities having even individual sums (Magurran & McGill 2011). Hence, Shannon and Simpson diversity were lower in bright pitfall traps due to high individual sums of few wolf spiders (e.g., *Pardosa amentata*, *P. prativaga*, Appendix S1). Species inventories were not complete in any pitfall trap color but significantly lower growth of species accumulation curves in white and brown pitfall traps indicates a higher completeness in these traps.

Buchholz et al. (2010) concluded that the use of bright pitfall traps should increase spider capture efficiency and therefore enhance the level of precision of species inventories. Diversity analyzes showed that although overall individual sums were lower in green and brown pitfall traps, alpha diversity was nevertheless highest at these colors. However, given that diversity indices can be biased by individual sums, and that observed species richness was similar, these results should not be overrated. One practical implication is that species-rich spider communities can be also sampled in inconspicuous traps while avoiding unnecessary high individual catches at the same time. These findings are important, since avoiding unintentional by-catches should be intended in science due to animal welfare, ethics, and species protection (New 1999). Correspondingly, in their review, Brown & Matthews (2016) recommended transparent pitfall traps for all ground-active arthropods. This is in line with our findings, as transparent plastic cups or jars should be perceived as brown, environment, or soil color by spiders. In parallel, another practical implication is that white pitfall traps yield a higher biomass and – more important – attract more ground hunting spiders. Furthermore, white pitfall traps yielded a more complete species inventory, followed by brown ones. Considering all this, the main recommendation is to use a combination of white and brown (or transparent) pitfall traps for complete and diverse species inventories.

## ACKNOWLEDGMENTS

We would like to thank A.-M. Corman, F. Hertenstein, K. Mantel and J. Schirmel for help with the fieldwork and two anonymous reviewers as well as M. Entling and L. Fischer for valuable comments on the manuscript.

## LITERATURE CITED

Brown, G.I. & I.M. Matthews. 2016. A review of extensive variation in the design of pitfall traps and a proposal for a standard pitfall trap design for monitoring ground-active arthropod biodiversity. Ecology and Evolution: doi: 10.1002/ece3.2176.

Buchholz, S. 2010. Factors determining daily rhythms of epigeic arthropods - activity patterns of spiders in dry open habitats. Entomologia Generalis 32:251–264.

Buchholz, S. & V. Hartmann. 2008. Spider fauna of semi-dry grasslands on a military training base in Northwest Germany (Münster). Arachnologische Mitteilungen 35:51–60.

Buchholz, S., A.M. Jess, F. Hertenstein & J. Schirmel. 2010. Effect of the colour of pitfall traps on their capture efficiency of carabid beetles (Coleoptera: Carabidae), spiders (Araneae) and other arthropods. European Journal of Entomology 107:277–280.

Cardoso, P., S. Pekar, R. Joeque & J.A. Coddington. 2011. Global patterns of guild composition and functional diversity of spiders. Plos One 6(6):e21710. (Cited in appendix S1 online at http://dx.doi.org/10.1636/JoA-S-16-062.s1)

Corcuera, P., P.L. Valverde, M.L. Jimenez, A. Ponce-Mendoza, G. De La Rosa & G. Nieto. 2016. Ground spider guilds and functional diversity in native pine woodlands and *Eucalyptus* plantations. Environmental Entomology 45:292–300.

Foelix, R. 2011. Biology of Spiders. 3rd edition. Oxford University Press, USA.

Henatsch, B. & T. Blick. 1993. Zur tageszeitlichen Laufaktivität der Laufkäfer, Kurzflügelkäfer und Spinnen in einer Hecke und einer angrenzenden Brachfläche (Carabidae, Staphylinidae, Araneae). Mitteilungen der deutschen Gesellschaft für Allgemeine und Angewandte Entomologie 8:529–536. (Cited in appendix S1 online at http://dx.doi.org/10.1636/JoA-S-16-062.s1)

Heneberg, P. & P. Bogusch. 2014. To enrich or not to enrich? Are there any benefits of using multiple colors of pan traps when sampling aculeate Hymenoptera? Journal of Insect Conservation 18:1123–1136.

Kataja-aho, S., P. Hannonen, T. Liukkonen, H. Rosten, M.J. Koivula, S. Koponen et al. 2016. The arthropod community of boreal Norway spruce forests responds variably to stump harvesting. Forest Ecology and Management 371:75–83.

Kreuels, M. 2001. Die Tagesphänologie epigäischer Spinnen (Arachnida: Araneae) im NSG Hasental-Kregenberg bei Marsberg (NRW). Arachnologische Mitteilungen 22:19–28. (Cited in appendix S1 online at http://dx.doi.org/10.1636/JoA-S-16-062.s1)

Landesanstalt für Ökologie, Bodenordnung und Forsten NRW (LÖBF) 2005. Natur und Landschaft in Nordrhein-Westfalen 2005. Grundlagen – Zustand – Entwicklung. LÖBF-Mitteilungen 4/2005.

Magurran A.E. & B.J. McGill. 2011. Biological Diversity: Frontiers in Measurement and Assessment. Oxford University Press, Oxford.

Meriste, M., A. Helm & M. Ivask. 2016. Ground-dwelling spider fauna of flooded meadows in Matsalu, Estonia. Wetlands 36:525–537.

Moreira, E.F., R.L. Da Silva Santos, U.L. Penna, C. Angel-Coca, F.F. De Oliveira & B.F. Viana. 2016. Are pan traps colors complementary to sample community of potential pollinator insects? Journal of Insect Conservation 20:583–596.

Negro, M., M. Isaia, C. Palestrini & A. Rolando. 2009. The impact of forest ski-pistes on diversity of ground-dwelling arthropods and small mammals in the Alps. Biodiversity and Conservation 18:2799–2821.

New, T.R. 1999. By-catch, ethics and pitfall traps. Journal of Insect Conservation 3:1–3.

R Core Team. 2016. R: A language and environment for statistical computing. R Foundation for Statistical Computing, Vienna, Austria. Online at https://www.R-project.org/

Roberts, M.J. 1998. Spinnengids. Tirion Natuur Baarn, Netherlands.

Sadler, J.P., E.C. Small, H. Fiszpan, M.G. Telfer & J. Niemelä. 2006. Investigating environmental variation and landscape characteristics of an urban-rural gradient using woodland carabid assemblages. Journal of Biogeography 33:1126–1138.

Saska, P., W. van der Werf, L. Hemerik, M.L. Luff, T.D. Hatten, A. Honek et al. 2013. Temperature effects on pitfall catches of epigeal arthropods: a model and method for bias correction. Journal of Applied Ecology 50:181–189.

Schirmel, J., S. Lenze, S. Katzmann & S. Buchholz. 2010. Capture efficiency of pitfall traps is highly affected by sampling interval. Entomologia Experimentalis et Applicata 136:206–210.

Sonoda, S., J. Yamashita, Y. Koshiyama, Y. Kohara & T. Enomoto. 2013. Short-term effects of mowing on insect communities in Japanese peach orchards. Applied Entomology and Zoology 48:65–72.

Spence, J.R. & J.K. Niemelä. 1994. Sampling carabid assemblages with pitfall traps: the madness and the method. Canadian Entomologist 126:881–894.

Wyszecki, G. & W.S. Stiles. 2000. Color Science: Concepts and Methods, Quantitative Data and Formulae, 2nd Edition. Wiley, Germany.

Yekwayo, I., J.S. Pryke, F. Roets & M.J. Samways. 2016. Conserving a variety of ancient forest patches maintains historic arthropod diversity. Biodiversity and Conservation 25:887–903.

Zopf, L.M., A. Schmid, D. Fredman & B.J. Eriksson. 2013. Spectral sensitivity of the etenid spider *Cupiennius salei*. Journal of Experimental Biology 216:4103–4108.

Zurek, D.B., T.W. Cronin, L.A. Taylor, K. Byrne, M.L.G. Sullivan & N.I. Morehouse. 2015. Spectral filtering enables trichromatic vision in colorful jumping spiders. Current Biology 25:403–404.

*Manuscript received 23 September 2016, revised 28 February 2018.*

2018. Journal of Arachnology 46:380–383

## SHORT COMMUNICATION

# Reproductive strategy of a cave-living arachnid with indeterminate growth (*Phrynus longipes*; Amblypygi: Phrynidae)

**Kenneth James Chapin** and **Emily Katherine Chen**: Department of Ecology & Evolutionary Biology, University of California, Los Angeles, 612 Charles E. Young Drive East, Los Angeles, CA 90095-7246; E-mail: chapinkj@gmail.com.

**Abstract.** Natural selection predicts that organisms should maximize reproductive fitness by exhibiting a tradeoff between the quantity and quality of offspring. While many species clearly show this tradeoff, it is not a ubiquitous phenomenon. Indeed, observing this tradeoff in different organisms is contingent on life history traits, reproductive strategy, parental investment, and physiological constraints. We tested for a tradeoff between the number and quality of offspring in the amblypygid *Phrynus longipes* (Pocock, 1894)—a long-lived, iteroparous arachnid with indeterminate growth, post-ultimate molts, and parental care. We measured the size of gravid females and the mass and number of eggs in their clutches. Egg count, but not mass, was predicted by female size, indicating that we did not detect an offspring quantity-quality tradeoff. We posit that larger female *P. longipes* are laying more eggs rather than increasing investment in each egg. This study is the first of its kind in any amblypygid species.

**Keywords:** Amblypygid, egg, parental investment, reproduction, reproductive tradeoff

Natural selection predicts that organisms should maximize reproductive fitness by optimizing the tradeoff between the quantity and quality of offspring (Lack 1947, 1954; Smith & Fretwell 1974). This was intuitively posited because organisms have limited resources available in the environment with which to produce offspring. Thus, increasing the quantity of offspring decreases the investment available for each offspring. This tradeoff between quantity and quality has resulted in different reproductive strategies, e.g., r- and K-selection (Pianka 1970). Here, we test for a tradeoff between offspring quality and quantity in the amblypygid *Phrynus longipes* (Pocock, 1894).

Species of the order Amblypygi (Arachnida) have a unique combination of life history traits that provide no clear intuition about the likelihood of exhibiting a tradeoff. Unlike nearly all other arthropods, amblypygids have indeterminate growth and continue to molt after sexual maturity (Weygoldt 2000; Chapin & Hebets 2016). Thus, unlike most other arthropods, amblypygid initial egg size is unlikely to determine final adult size (Smith 1997). Many arthropods with indeterminate growth produce higher quality offspring as they age (Fox & Czesak 2000). For example, older female water fleas (order: Cladocera) with indeterminant growth produce eggs that are larger than the optimal size (Bell 1983; Boersma 1997). Amblypygids are long-lived (perhaps 7–10 years), iteroparous, and produce 10–90 eggs per clutch (Fig. 1; Chapin & Hebets 2016). Amblypygids exhibit high parental care relative to arthropods that typically exhibit a quantity-quality tradeoff (Chapin & Hebets 2016). Females carry the eggsac on the ventral opisthosoma (Fig. 1a). After hatching, young emerge and climb onto the back of the female where they molt before becoming free-living (Figs. 1b,c; Weygoldt 2000; Chapin & Hebets 2016). Thus, amblypygids provide postembryonic parental investment that may limit clutch size and obscure the quantity-quality tradeoff (Boyce & Perrins 1987; Oksanen et al. 2001; Gilbert & Manica 2010; but see Walker et al. 2008). Evolutionary history also provides no clear hypothesis for a tradeoff occurring in *P. longipes*; the closely related Araneae tend to not show the tradeoff, but scorpions do (Killebrew & Ford 1985; Marshall & Gittleman 1994; Brown 2003; Skow & Jakob 2003), and the phenomenon is common among other arthropod groups (Berrigan 1991; Fox & Czesak 2000).

The tradeoff is often detected in semelparous species that exhibit low parental care and use larval-acquired resources to produce eggs (Ford & Seigel 1989; Fox & Czesak 2000). However, the tradeoff is often not detected in taxa with iteroparity and parental care as these factors complicate life history and obscure existing tradeoffs (Gilbert & Manica 2010). In addition, the quantity-quality tradeoff is more obvious in oviparous species, which, unlike viviparous species, allocate a discrete amount of resources to offspring upon or soon after fertilization (Ford & Seigel 1989; King 1993). Egg-laying animals provide finite resources to developing young, which should emphasize energetic constraints on offspring number and quality (Parker & Begon 1986). Spider egg mass scales geometrically with egg diameter and spider eggs have constant energy density (Anderson 1990). We assume the same is true for whip spiders, such that larger eggs require greater energy investment, but often have higher survivability. Larger eggs experience lower rates of desiccation (Anderson 1990; Sota & Mogi 1992). In addition, progeny that arise from larger eggs have better feeding performance (Walker et al. 2003) and may be less resistant to starvation (Gliwicz & Guisande 1992; Wallin et al. 1992). Thus, we tested whether the amblypygid, *Phrynus longipes*, exhibits a tradeoff between the quality and quantity of offspring, with the goal of expanding our understanding of variation in parental investment across arthropods.

We collected twenty-four egg-carrying *Phrynus longipes* from Cueva Matos (*ca.* 18.38°N, 66.68°), Arecibo, Puerto Rico in August 2014. We measured the maximum prosoma width of each female using digital calipers to the nearest 0.1 mm ± 0.1 mm. The prosoma shows allometric growth throughout the life of amblypygids and correlates well with body mass (Chapin 2011; Chapin & Hebets 2016). We stored specimens in 95% ethanol and shipped them to our laboratory at UCLA for further analysis. We recorded the total number of eggs per female and dry mass of eggs from each clutch. We placed individual eggs in microcentrifuge tubes and dried them in a drying oven at 60°C for 120 h. We weighed dried eggs with a microbalance scale to the nearest 1 μg ± 1μg (Orion Cahn C-33). Further, we determined the developmental stage of each egg, and if the embryo was developing.

We compared generalized linear models (GLM) of egg mass predicting egg count with female size as a covariate using Akaike's information criterion corrected for small sample size (AICc) and Akaike's weights ($w_i$; Burnham et al. 2011; Symonds & Mousalli 2011). We used post hoc linear regressions to examine the relationship between mean egg mass, total egg count, and female size separately.

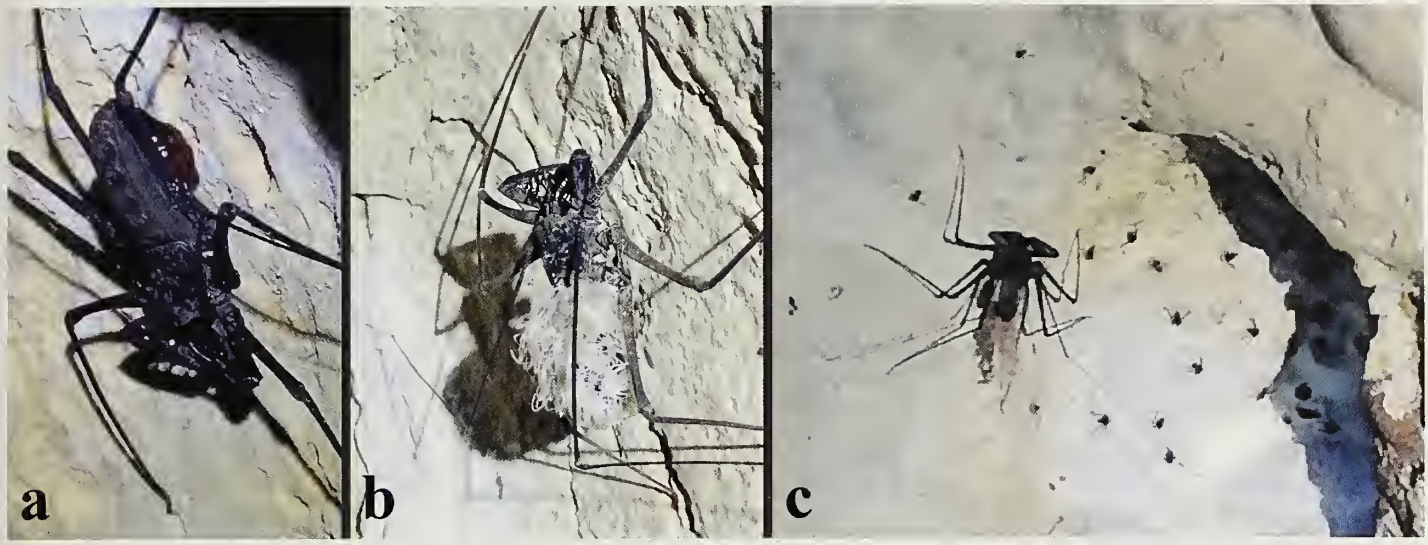


Figure 1.—*Phrynus longipes* (a) with an egg clutch attached to the ventral opisthosoma (b) with offspring on the dorsum and (c) with free-living offspring.

*Phrynus longipes* had a clutch size of 67 ± 3.3 eggs ($\bar{x} \pm s$; range: 29–94; $n = 24$ clutches). Overall, eggs mass was 4.01 ± 0.12 mg (Range: 3.10–5.21 mg) and the prosoma width of females was 15.80 ± 0.36 mm (range: 12.3–18.9 mm). The best GLM predicting egg count included only female size, not mass (Table 1; estimate ± $s = 5.806 \pm 1.473$, $t_{23} = 3.940$, $P < 0.001$). Larger females (measured as prosoma width) laid more eggs per clutch (adjusted $r^2 = 0.435$, $F_{1, 21} = 17.96$, $P < 0.001$; Fig. 2a) but female prosoma width failed to predict egg mass (adjusted $r^2 = 0.012$, $F_{1, 21} = 1.268$, $P = 0.273$; Fig. 2b). Egg developmental stage or the proportion of embryos that developed did not improve model results.

We did not detect a quality-quantity tradeoff in *P. longipes* (Fig. 2). Larger females had a higher number of eggs but not lower quality offspring, measured as egg mass. Larger females invest more resources into producing more eggs rather than investing more into each egg. Our results support the findings of Fox and Czesak (2000): species that do not show a quantity-quality tradeoff are often iteroparous, use adult-acquired resources for reproduction, or provide postembryonic parental care, all of which are characteristics of *P. longipes* (Fox & Czesak 2000).

Our results generally align with patterns seen in Araneae with few differences that can be attributed to life-history (Killebrew & Ford 1985; Marshall & Gittleman 1994; Brown et al. 2003; Skow & Jakob 2003; Barrantes 2015). Larger, and therefore older, *P. longipes* females laid larger clutches. This is the opposite pattern seen in many arthropods, including Araneae, which lay smaller successive clutches with age (Marshall & Gittleman 1994; Fox & Czesak 2000; Brown et al. 2003). Female Araneae generally lay only a few clutches in their lifetime while female amblypygids can generally produce one to three clutches a year over their lifetime of perhaps as many as 10 years (Weygoldt 2000; Chapin & Hebets 2016). Clutches are expected to become smaller with age in arthropods that acquire resources as larva

Table 1.—Multimodel comparisons of generalized linear models predicting egg count ($n = 24$) in clutches of *Phrynus longipes*. The full model includes egg mass, female size, and their interaction as predictor variables. Female size, but not mass, best predicted egg count.

| Model | AICc | $k$ | ΔAICc | $w_i$ |
|---|---|---|---|---|
| mass × size | 199.12 | 4 | 0.00 | 0.06 |
| mass + size | 196.22 | 3 | −2.90 | 0.26 |
| size | 194.33 | 2 | −4.80 | 0.67 |
| mass | 204.93 | 2 | 5.81 | < 0.001 |
| intercept only | 204.76 | 1 | 5.63 | < 0.001 |

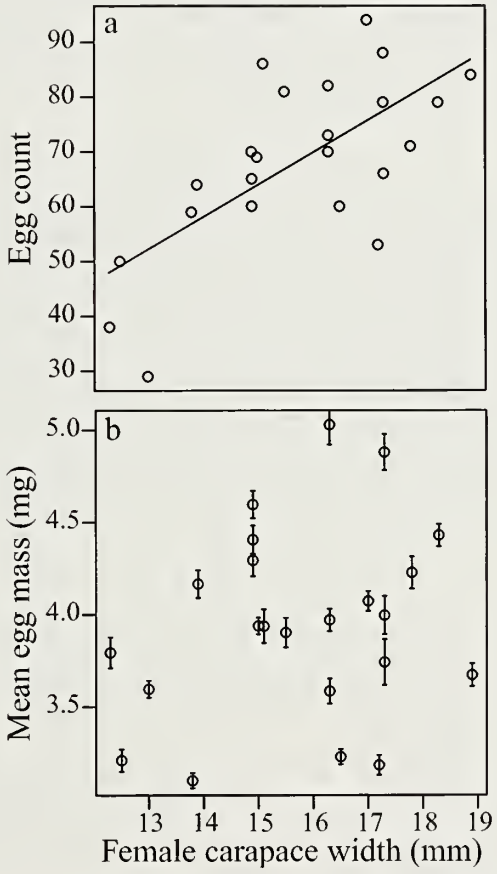


Figure 2.—Plots of egg clutch and female measurements for *Phrynus longipes*: (a) Total egg count per clutch predicted by female carapace width (adjusted $r^2 = 0.44$, $F_{1,21} = 17.96$, $P < 0.001$). (b) Mean egg mass predicted by female carapace width (adjusted $r^2 = 0.01$, $F_{1,21} = 1.27$, $P = 0.273$).

and deplete reserves with age (Wasserman & Asami 1985; Boggs 1986; Fox 1993) or where short or variable lifespans make future reproduction uncertain. *Phrynus longipes*, however, has a long lifespan and survivorship probabilities likely increase with age.

Amblypygids exhibit indeterminate growth and continue to molt after maturity. Many arthropods with indeterminate growth produce higher quality offspring as they age (Bell 1983; Boersma 1997; Fox & Czesak 2000;). Surprisingly, older, larger female *P. longipes* produce more but not larger eggs. Amblypygi eggs might already be of an optimal size, such that provisioning resources to eggs might not benefit offspring. Instead, amblypygids invest in a great number of offspring.

Our cave study site provides exceptionally high levels of prey, so we assumed there would be low variation in resource acquisition (Chapin 2015; Chapin & Hill-Lindsay 2016). This is important, because variation in resource acquisition can obscure a tradeoff between size and quantity (van Noordwijk & de Jong 1986). For example, resource scarcity results in unequal rates of resource acquisition and investment in clutches among female conspecifics which may conceal an existing tradeoff (van Noordwijk & de Jong 1986). Intraspecific experiments indicated a tradeoff under high, but not low, resources abundance (Brown 2003). Variable resource acquisition, however, can mask these effects. Despite this, no tradeoff was detected in *P. longipes* between egg size and quantity. Although females are unlikely to be limited by resource acquisition, other factors could potentially prevent a tradeoff from being detected.

Future research should quantify how egg mass impacts survivorship and reproductive fitness. For example, egg size may be influenced by physiological constraints on eggs, including oxygen absorption, nutritional accessibility, and desiccation. Further investigation into factors influencing egg size in amblypygids will provide insight into the diversity of parental investment in arthropods and reveal the unique life history of amblypygids.

## ACKNOWLEDGMENTS

This research was funded by a Student Research Grant from the Animal Behavior Society, the American Philosophical Society's Lewis and Clark Fund for Exploration and Research, the Explorers Club Exploration Fund, the UCLA Latin American Institute via a donation from the Fawcett Catalyst Fund, the UCLA's Edwin W. Pauley Fellowship, and the Department of Ecology and Evolutionary Biology Fellowship. Thanks to Peter Nonacs and the Nonacs Lab for advice and feedback. Thanks also to field assistants Alma Baseo, Laura Caicedo, Patrick Casto, Kimberly Dolphin, Jose Sanchez, Chelsea Vretenar, and Daniel E. Winkler. Research was conducted under the Puerto Rico Department of Natural Resources and the Environment permit number 2012-IC-064.

## LITERATURE CITED

Anderson, J.F. 1990. The size of spider eggs and estimates of their energy content. Journal of Arachnology 18:73–78.

Barrantes, G. 2015. Effect of body size and maternal care on clutch size and egg size in theridoids. Boletin de la Sociedad zoological del Uruguay 24:81–90.

Bell, G. 1983. Measuring the cost of reproduction. III. The correlation structure of the early life history of *Daphnia pulex*. Oecologia 60:378–383.

Berrigan, D. 1991. The allometry of egg size and number in insects. Oikos 60:313–321.

Boersma, M. 1997. Offspring size and parental fitness in *Daphnia magna*. Evolutionary Ecology 11:439–450.

Boggs, C.L. 1986. Reproductive strategies of female butterflies: variation in and constraints on fecundity. Ecological Entomology 11:7–15.

Boyce, M.S. & C.M. Perrins. 1987. Optimizing great tit clutch size in a fluctuating environment. Ecology 68:142–153.

Brown, C.A. 2003. Offspring size-number trade-off in scorpions: an empirical test of the Van Noordwijk and de Jung Model. Evolution 57:2184–2190.

Brown, C.A., B.M. Sanford & R.R. Swerdon. 2003. Clutch size and offspring size in the wolf spider *Pirata sedentarius* (Araneae, Lycosidae). Journal of Arachnology 31:285–296.

*Burnham, K.P., D.R. Anderson & K.P. Huyvaert. 2011. AIC model selection and multimodel inference in behavioral ecology: some background, observations, and comparisons. Behavioral Ecology & Sociobiology 65:23–35.

Chapin, K.J. 2011. Ecology and natural history of the tree-inhabiting social amblypygid *Heterophrynus batesii* (Butler 1873; Amblypygi: Phrynidae) in eastern Amazonian Ecuador MS Thesis, West Texas A&M University, Canyon, Texas.

Chapin, K.J. 2015. Cave-epigean behavioral variation of the whip spider *Phrynus longipes* (Arachnida: Amblypygi) evidenced by activity, vigilance, and aggression. Journal of Arachnology 43:214–219.

Chapin, K.J. & E.A. Hebets. 2016. Behavioral ecology of amblypygids. Journal of Arachnology 44:1–14.

Chapin, K.J. & S. Hill-Lindsay. 2016. Territoriality evidenced by asymmetric intruder-holder motivation in an amblypygid. Behavioural Processes 122:110–115.

Ford, N.B. & R.A. Seigel. 1989. Relationships among body size, clutch size, and egg size in three species of oviparous snakes. Herpetologica 45:75–83.

Fox, C.W. 1993. The influence of maternal age and mating frequency on egg size and offspring performance in *Callosobruchus maculatus* (Coleoptera: Bruchidae). Oecologia 96:139–146.

Fox, C.W. & M.E. Czesak. 2000. Evolutionary ecology of progeny size in arthropods. Annual Review of Entomology 45:341–369.

Gilbert, J.D.J. & Manica A. 2010. Parental care trade-offs and life-history relationships in insects. American Naturalist 176:212–226.

Gliwicz, Z.M. & C. Guisande. 1992. Family planning in *Daphnia*: resistance to starvation in offspring born to mothers grown at different food levels. Oecologia 91:463–467.

Killebrew, D.W. & N.B. Ford. 1985. Reproductive tactics and female body size in green lynx spider, *Peucetia viridans* (Araneae, Oxyopidae). Journal of Arachnology 13:375–382.

King, R.B. 1993. Determinants of offspring number and size in the brown snake, *Storeria dekayi*. Journal of Herpetology 27:175–185.

Lack, D. 1947. The significance of clutch size. Ibis 89:302–352.

Lack, D. 1954. The Natural Regulation of Animal Numbers. Oxford University Press, Oxford.

Marshall, S.D. & J.L. Gittleman. 1994. Clutch size in spiders: is more better? Functional Ecology 8:118–124.

Oksanen, T.A., P. Jonsson, E. Koskela & T. Mappes. 2001. Optimal allocation of reproductive effort: manipulation of offspring number and size in the bank vole. Proceedings of the Royal Society of London B: Biological Sciences 268:661–666.

Parker, G.A. & M. Begon. 1986. Optimal egg size and clutch size: effects of environment and maternal phenotype. American Naturalist 128:573–592.

Pianka, E.R. 1970. On r- and K-Selection. American Naturalist 104:592–597.Skow, C.D. & E.M. Jakob. 2003. Effects of maternal body size on clutch size and egg weight in a pholcid spider (*Holocnemus pluchei*). Journal of Arachnology 31:305–308.

Smith, C.C. & S.D. Fretwell. 1974. The optimal balance between size and number of offspring. American Naturalist 108:499–506.

Smith, R.L. 1997. Evolution of paternal care in the giant water bugs (Heteroptera: Belostomatidae). Pp. 116–149. *In* The Evolution of Social Behaviour in Insects and Arachnids. (J.C. Choe, B.J. Crespi, eds). Cambridge University Press, Cambridge.

Sota, T. & M. Mogi. 1992. Interspecific variation in desiccation

survival time of *Aedes* (*Stegomyia*) mosquito eggs is correlated with habitat and egg size. Oecologia 90:353–358.

Symonds, M.R.E. & A. Mousalli. 2011. A brief guide to model selection, multimodel inference, and model averaging in behavioral ecology using Akaike's information criterion. Behavioral Ecology & Sociobiology 65:13–21.

van Noordwijk, A.J. & G. de Jong. 1986. Acquisition and allocation of resources: their influence on variation in life history tactics. American Naturalist 128:137–142.

Walker, R.S., M. Gurven, O. Burger & M.J. Hamilton. 2008. The trade-off between number and size of offspring in humans and other primates. Proceedings of the Royal Society of London B: Biological Sciences 275:827–834.

Walker S.E., A.L. Rypstra & S.D. Marshall. 2003. The relationship between offspring size and performance in the wolf spider *Hogna helluo* (Araneae: Lycosidae). Evolutionary Ecology Research 5:19–28.

Wallin H., P.A. Chiverton, B.S. Ekmob & A. Borg. 1992. Diet, fecundity and egg size in some polyphagous predatory carabid beetles. Entomologia Experimentalis et Applicata 65:129–140.

Wasserman, S.S. & T. Asami. 1985. The effect of maternal age upon fitness of progeny in the southern cowpea weevil, *Callosobruchus maculatus*. Oikos 45:191–196.

Weygoldt, P. 2000. Whip Spiders (Chelicerata: Amblypygi): Their Biology, Morphology and Systematics. Apollo Books, Stenstrup.

*Manuscript received 8 August 2017, revised 26 January 2018.*

2018. Journal of Arachnology 46:384–387

## SHORT COMMUNICATION

# Capturing the elusive camel spider (Arachnida: Solifugae): effective methods for attracting and capturing solifuges

**Paula E. Cushing**[1] and **Edmundo González-Santillán**[2,3]: [1]Department of Zoology, Denver Museum of Nature & Science, 2001 Colorado Boulevard, Denver, Colorado 80205 USA; E-mail: Paula.Cushing@dmns.org; [2]Departamento de Medicina Molecular y Bioprocesos, Instituto de Biotecnología, Universidad Nacional Autónoma de México (UNAM), Av. Universidad 2001, Colonia Chamilpa C.P. 62210, Cuernavaca, Morelos, México; [3]Laboratorio de Aracnología, Facultad de Ciencias, UNAM, Circuito Exterior s/n, Colonia Copilco el Bajo, C.P. 04510 Del. Coyoacán, CDMX, México.

**Abstract.** Camel spiders (Arachnida: Solifugae) are a notoriously difficult group of arachnids to study. They are almost all strictly nocturnal, fast moving predators that are difficult to find, collect, and rear. In this paper, we present methods for both attracting solifuges in desert field sites and collecting them efficiently using a combination of light attraction and pitfall trapping techniques. Although many of these methods have been used by solifuge collectors for decades, they are not typically described in detail in the literature nor have the methods been consolidated in a single paper. We hope that doing so will enable others to more efficiently target this group of arachnids.

**Keywords:** Solpugids, wind scorpions, pitfall trap, light trap

Solifugae, known colloquially as camel spiders, are mostly nocturnal arachnids known for their powerful two-segmented chelicerae, voracious appetites, and fast running speeds (Punzo 1998a; Beccaloni 2009). They are dominant predators in arid habitats worldwide (Banta & Marer 1972; Cloudsley-Thompson 1977; Polis & McCormick 1986; Wharton 1987; Punzo 1994). Solifuges are also notoriously difficult to study. They are challenging to keep alive in a laboratory setting and nearly impossible to raise to maturity in captivity, with only one researcher reporting some small success in rearing (Punzo 1998b). As a result of challenges inherent in the study of camel spiders, only the first author's lab regularly publishes on their phylogeny, taxonomy, and biology (Brookhart & Cushing 2002, 2004, 2005, 2008; Cushing et al. 2005, 2014, 2015; Catenazzi et al. 2009; Conrad & Cushing 2011; Cushing & Casto 2012; Cushing & Brookhart 2016). Herein we present methods, many adopted from capture techniques for other taxonomic groups (particularly reptiles), that we have co-opted and further developed over the years that have proven effective in attracting and capturing these elusive arachnids in an attempt to encourage other researchers to begin collecting and studying these animals so that we may learn more about the many aspects of solifuge biology that remain mysteries. Many of these techniques, such as light trapping and pitfall trapping, have been used for decades to attract and collect solifuges; however, at best, researchers refer to these techniques in passing in their methods sections and have not provided details about these collecting techniques. Thus, the authors felt it would be useful to consolidate successful collecting techniques for these elusive arachnids into one paper.

Two methods that have been used to attract and collect solifuges are light attraction and pitfall trap sampling. It has long been known that solifuges are attracted to light, where they hunt insects that are also attracted to this stimulus (Pocock 1897; Turk 1947; Cloudsley-Thompson 1961, 1977; Punzo 1998a; Catenazzi et al. 2009; Conrad & Cushing 2011; Belozorov 2013). It is not known what draws the solifuges to the light source – whether it is the light itself or the vibrations from insect prey. Nevertheless, setting light stimuli in arid habitats or visiting permanent lights such as buildings in these environments is a good way to find hunting solifuges. Solifuges typically begin visiting these light sources after sunset when insects have begun swarming the lights. Solifuges that come to the lights can be grabbed by hand if the collector is fast enough and if the collector wants to keep the animals alive. Alternatively, they can be shot with a focused stream of 70–75% ethanol (Hewitt 1919). Spraying with alcohol has proved to be a very effective method for slowing and killing solifuges. A squirt bottle filled with water could be used to slow down solifuges if the collector wants to keep the animals alive (but the moisture should be wicked from the animal in that case). If a site lacks permanent lights on buildings or structures, temporary lights can be hung on tripods in the field to create a concentrated pool of light (Fig. 1). Lights are illuminated just after sunset; insects and solifuges begin appearing at this light pool one to two hours after that (Fig. 1). Table 1 provides the success rate for collecting at both temporary lights such as those shown in Fig. 1 or permanent lights. As can be seen in Table 1, more solifuges can be collected around permanent lights than around temporary lights. Solifuges are typically found hunting near permanent lights just after sunset. It takes collectors several hours waiting and watching around temporary lights to collect as many solifuges as are found in one hour around permanent lights.

For years, solifuges have been collected from field sites using pitfall traps (Muma 1980; Griffin 1990). A modified pitfall trap array using drift fences was used for solifuges by Xavier & Suesdek Rocha (2001) (Fig. 2). This pitfall trap array traces its origin to the field of herpetology (Gibbons & Semlitsch 1981; Bury & Corn 1987; Corn 1994) and the capture of solifuges as bycatch of herpetological pitfall sampling is evident from collecting label data. This technique has been used successfully by the first author's lab for the past 12 years. The drift fences are 12–13 cm wide plastic landscape fencing; pitfall traps are 13 cm diameter, 9.5 cm deep plastic Tupperware containers one-third to one-half filled with lab-grade propylene glycol. Vink et al. (2005) demonstrated the effectiveness of propylene glycol for molecular tissue preservation. One pitfall trap is placed at the end of each of the three drift fence arms, which are each approximately 10 m long; one pitfall trap is placed in the middle of the array where the three arms converge; and two pitfall traps are placed on either side of the approximate center of each drift fence arm, as close to the fence as possible. This arrangement maximizes capture success of any cursorial arthropod (including solifuges) out hunting in the general


Figures 1–4.—1. Creating a pool of light to attract solifuges in a desert habitat. 2. A 10-cup pitfall trap array using three 10 m long pieces of landscape fencing. One pitfall trap is placed at the intersection of the three drift fence arms; two are placed on either side of the middle of each arm; and one is placed at the end of each of the three drift fence arms. Pitfall traps are one-third to one-half filled with lab-grade propylene glycol. The array can be left in place for up to four weeks, depending on habitat and conditions (i.e. in very hot deserts during the height of the summer, the preservative will evaporate if not re-filled before four weeks). 3. Butterfly Light Trap. Small drift fence segments (plastic landscape fencing) link pairs of small pitfall traps half filled with 96% ethanol. Individual drift fence segments can be placed around individual small pitfall traps set in between the linked traps, creating a discontinuous ring of fencing (these individual drift fence pieces are missing in the photo). This arrangement allows the light from the center suspended lamps to continue attracting approaching arthropods. Pitfall traps should be placed at the outer edge of the pool of light. Inset: Diagram of Butterfly Light Trap. The object in the middle is the light source, the curved structures represent the drift fence segments, black circles represent the pitfall cups. Pitfalls can be filled with 95% ethanol since researchers will check traps the following morning. 4. Caterpillar Light Trap. Small drift fence segments are arranged in a long line with small pitfalls placed in between segments. Pitfalls are half filled with 95% ethanol. Lights are suspended at the ends of the line of fencing and in the middle in order to illuminate the entire line of fencing.

Table 1.—Efficacy of permanent light collecting versus temporary light collecting as documented from field notes recorded between 2005–2017.

| Method | Total # Locations Between 2005–2017 | Mean # Solifuges per hour ± SD | Range (# specimens coll. per hour) |
|---|---|---|---|
| Permanent Lights | 41 | 3.8 ± 3.10 | 0–11 |
| Temporary Lights | 65 | 1.2 ± 1.9 | 0–8 |

Table 2.—Efficacy of 10-cup pitfall arrays as documented from field notes recorded between 2005–2017. Total number of arrays set between 2005–2017 = 70.

| Trap duration and Solifuge Capture Efficiency | Mean ± SD | Range |
|---|---|---|
| Trap duration (days) | 34.5 ± 14.6 days | 2–58 days |
| # Solifuges Captured | 11.3 ± 12.0 solifuges | 0–50 solifuges |

vicinity. Lids of some sort should be suspended over the pitfall traps to keep out rainwater and debris, minimize evaporation, and minimize interference by larger animals investigating the liquid inside the cups. Propylene glycol is harmless to mammals; but some mammals may be attracted to the odor or the sweet taste of this preservative. We suspend wooden lids over our pitfall traps using three nails inserted into three corners of the wooden lid and then extending into small square wooden "feet" that suspend the lids about 2–3 cm above the soil. The diameter of containers utilized as pitfall traps should be wide enough that larger species of solifuges can be captured. We do not recommend the use of small diameter jars, tubes, or other containers for this reason. The lids suspended over the cups should be larger than the diameter of the cup itself to minimize rainwater from entering the cup. The pitfall trap array can be left in place for up to four weeks. It is not recommended to leave the pitfalls in place for longer than that time. In very hot deserts during the middle of the hottest part of the season, the preservative will evaporate if left in place for four weeks and should be checked and replaced well before that time. Pitfall traps are not effective ways to collect live solifuges since solifuges will readily climb out of dry traps and/or will cannibalize one another in the trap before they can be removed. Table 2 presents the success rate of these pitfall arrays used by the first author since 2005.

Recently, during a collecting trip in the Chihuahuan Desert of central Mexico, the authors used a modified light-trapping method for solifuges that utilizes both lights and pitfall traps. Such a combined technique was suggested and illustrated in a letter from R.F. Lawrence to Jack O. Brookhart (DMNS Research Associate) written in 1963. Lawrence suggests suspending a light directly over a pitfall trap (a copy of this letter was provided to PEC). The modified light-trapping design we developed, which we call the "Butterfly Light Trap," consists of a ring of small pitfall traps placed around the pool of light cast by three or four lamps suspended on a cluster of tripods (Fig. 3 and inset). Small flexible segments of drift fence about 1 m in length are bent such that the ends connect adjacent pitfall traps. Gaps are left in between drift fence segments or additional small sections of drift fence can be bent around individual pitfall traps placed in between the linked pairs such that a small piece of drift fence is placed behind the individual pitfalls (Fig. 3 inset). By thus creating breaks in the drift fence encircling the pool of light, a light stimulus can still be seen by a small arthropod approaching the light pool (if the drift fence sections were completely encircling the pool of light, then the light stimulus might disappear in shadow as a small ground-dwelling arthropod approaches). The second modified light trap we call the "Caterpillar Light Trap." The second author noted that since illuminated buildings in desert environments serve as strong attractants to hunting solifuges, we could create an artificial "building" by laying small 1 m segments of drift fence interspersed with pitfall traps and shining lights directly on this small artificial "wall" (Fig. 4). In both modified light trap designs, we used very small pitfalls and filled these with 96% ethanol since the pitfalls would be left in place just for one or two nights. Adding drift fences and pitfall traps to a light stimulus increases the efficacy of the light stimulus in not only attracting solifuges but also capturing them, since otherwise collectors must rely on seeing approaching solifuges before the animals run out of the pool of light. We tested the Butterfly Light Trap design on two consecutive nights at field sites in Mexico during the summer of 2017. During the first night, we set up the traps but otherwise did not stay up to monitor them. In the morning, we found 1 solifuge in the pitfall traps and the second night, we collected three solifuges from the traps. This success rate is on par with multiple observers monitoring the pools of light for 4–6 hours during the night. We tested the Caterpillar Light Trap at only one field site in Mexico and found 1 solifuge in a trap the next morning. The lights we used were low-power solar light with two-three hour duration (the only lights we had available during that field expedition). Using stronger lights that have a longer duration would certainly prove more effective. The advantage of these modified Light/Pitfall trap designs is that collectors can set them up but do not have to monitor the lights for many hours in order to capture the low number of solifuges attracted to such temporary light sources (Table 1).

When placing Butterfly Light Traps, Caterpillar Light Traps, or pitfall trap arrays in field sites, multiple traps should be utilized at each site to maximize the potential different habitats or corridors sampled since solifuges are known to be habitat or substrate specific (e.g., Lawrence 1963; Crawford 1988; Griffin 1990; Dean & Griffin 1993). For example, if you are sampling in a dune system, one trap system should be placed on top of the dunes; another between dune ridges to maximize topographic variability existing at a site and, by extension, to increase possible taxonomic diversity sampled. Although solifuges are a challenging group of arachnids to study, we hope that presenting effective methodology in one place for attracting these animals and collecting them may encourage more researchers to explore the biology of this poorly understood taxon.

## ACKNOWLEDGMENTS

Funding for solifuge research at the DMNS was supported by NSF grant DEB-0640245 awarded to PEC and funding from the Kenneth King Foundation and the DMNS curator grant support. Thanks also to Henry Carmona who provided help and advice during the 2017 collecting expedition to Chihuahuan Desert sites in Mexico. Thanks also to Jack Brookhart for providing helpful suggestions on an earlier draft of this manuscript and to Wendell Icenogle for helpful suggestions in the field over the years. Thanks also to two anonymous reviewers who provided helpful suggestions for improving this manuscript.

## LITERATURE CITED

Banta, B.H. & P.J. Marer. 1972. An attack by a solpugid on an iguanid lizard hatchling. British Journal of Herpetology 4:266–267.

Beccaloni, J. 2009. Solifugae: camel spiders, wind spiders, wind scorpions, sun spiders. Pp. 291–309. *In* Arachnids. University of California Press, Berkeley, Los Angeles, California.

Belozerov, V.N. 2013. Seasonal aspects of the life cycle of solifuges (Arachnida, Solifugae) as compared with pseudoscorpions (Arachnida, Pseudoscorpiones). Entomological Review 93:1050–1072.

Brookhart, J.O. & P.E. Cushing. 2002. New species of Eremobatidae

(Arachnida, Solifugae) from North America. Journal of Arachnology 30:84–97.

Brookhart, J.O. & P.E. Cushing. 2004. The systematics of the *Eremobates scaber* species-group (Solifugae, Eremobatidae). Journal of Arachnology 32:284–312.

Brookhart, J.O. & P.E. Cushing. 2005. Three new species of Solifugae from North America and a description of the female of *Branchia brevis* (Arachnida, Solifugae). Journal of Arachnology 33:127–133.

Brookhart, J.O. & P.E. Cushing. 2008. The *Hemerotrecha banksi* group (Arachnida, Solifugae), a diurnal group of solifuges from North America. Journal of Arachnology 36:49–64.

Bury, R.B. & P.S. Corn. 1987. Evaluation of pitfall trapping in northwestern forests: trap arrays with drift fences. Journal of Wildlife Management 5:112–119.

Catenazzi, A., J.O. Brookhart & P.E. Cushing. 2009. The natural history of coastal Peruvian solifuges with a redescription of *Chinchippus peruvianus* and an additional new species (Arachnida, Solifugae, Ammotrechidae). Journal of Arachnology 37:151–159.

Cloudsley-Thompson, J.L. 1961. Some aspects of the physiology and behaviour of *Galeodes arabs*. Entomologia Experimentalis et Applicata 4:257–263.

Cloudsley-Thompson, J.L. 1977. Adaptational biology of Solifugae (Solpugida). Bulletin of the British Arachnological Society 4:61–71.

Conrad, K.R. & P.E. Cushing. 2011. Observations on hunting behavior of juvenile *Chanbria* (Solifugae, Eremobatidae). Journal of Arachnology 39:183–184.

Corn, P.S. 1994. Straight-line drift fences and pitfall traps. Pp. 109–117. *In* Measuring and Monitoring Biological Diversity: Standard Methods for Amphibians. (W.R. Heyer, M.A. Donnelly, R.W. McDiarmid, L.C. Hayek & M.S. Foster, eds.). Smithsonian Institution Press, Washington DC.

Crawford, C.S. 1988. Surface-active arthropods in a desert landscape: Influences of microclimate, vegetation, and soil texture on assemblage structure. Pedobiologia 32:373–385.

Cushing, P.E. & J.O. Brookhart. 2016. Nine new species of the *Eremobates scaber* species group of the North American camel spider genus *Eremobates* (Solifugae, Eremobatidae). Zootaxa 4178:503–520.

Cushing, P.E., J.O. Brookhart, H.-J. Kleebe, G. Zito & P. Payne. 2005. The suetorial organ of the Solifugae (Arachnida, Solifugae). Arthropod Structure & Development 34:397–406.

Cushing, P.E. & P. Casto. 2012. Preliminary survey of the setal and sensory structures on the pedipalps of camel spiders (Arachnida, Solifugae). Journal of Arachnology 40:123–127.

Cushing, P.E., P. Casto, E.D. Knowlton, S. Royer, D. Laudier, D.D. Gaffin, L. Prendini & J.O. Brookhart. 2014. Comparative morphology and functional significance of setae called papillae on the pedipalps of male camel spiders (Arachnida, Solifugae). Annals of the Entomological Society of America 107:510–520.

Cushing, P.E., M.R. Graham, L. Prendini & J.O. Brookhart. 2015. A multilocus molecular phylogeny of the endemic North American camel spider family Eremobatidae (Arachnida: Solifugae). Molecular Phylogenetics and Evolution 92:280–293.

Dean, W.R.J. & E. Griffin. 1993. Seasonal activity patterns and habitats in Solifugae (Arachnida) in the southern Karoo, South Africa. South African Journal of Zoology 28:91–94.

Gibbons, J.W. & R.D. Semlitsch. 1981. Terrestrial drift fences with pitfall traps: an effective technique for quantitative sampling of animal populations. Brimleyana 7:1–16.

Griffin, E. 1990. Seasonal activity, habitat selection and species richness of Solifugae (Arachnida) on the gravel plains of the central Namib Desert. Transvaal Museum Monograph 7:77–82.

Hewitt, T. 1919. A short survey of the Solifugae of South Africa. Annals of the Transvaal Museum 7:1–76.

Lawrence, R.F. 1963. The Solifugae of South West Africa. Cimbebasia 8:1–28.

Muma, M.H. 1980. Comparison of three methods for estimating solpugid (Arachnida) populations. Journal of Arachnology 8:267–270.

Pocock, R.I. 1897. On the genera and species of tropical African arachnids of the order Solifugae with notes upon the taxonomy and habits of the group. Annals and Magazine of Natural History [Sixth Series] 20:249–272.

Polis, G.A. & S.J. McCormick. 1986. Scorpions, spiders, and solpugids: predation and competition among distantly related taxa. Oecologia 71:111–116.

Punzo, F. 1994. Trophic and temporal niche interactions in sympatric populations of *Eremobates palpisetulosus* Fichter and *Eremobates mortuous* (Roewer) (Solpugida: Eremobatidae). Psyche, Cambridge 101:187–194.

Punzo, F. 1998a. The Biology of Camel Spiders (Arachnida, Solifugae). Kluwer Academic Publishers, Boston/Dordrecht/London.

Punzo, F. 1998b. Natural history and life cycle of the solifuge *Eremobates marathoni* Muma & Brookhart (Solifugae, Eremobatidae). Bulletin of the British Arachnological Society 11:111–118.

Turk, F.A.V. 1947. On two new species of the family Galeodidae (Solifuga) from Asia. Journal of Natural History 14:74–80.

Vink, C.J., S.M. Thomas, P. Paquin, C.Y. Hayashi & M. Hedin. 2005. The effects of preservatives and temperatures on arachnid DNA. Invertebrate Systematics 19:99–104.

Wharton, R.A. 1987. Biology of the diurnal *Metasolpuga picta* (Kraepelin) (Solifugae, Solpugidae) compared with that of nocturnal species. Journal of Arachnology 14:363–383.

Xavier, E. & L. Suesdek Rocha. 2001. Autoecology and description of *Mummucia mamyi* (Solifugae, Mummucciicae), a new solifuge from Brazilian semi-arid Caatinga. Journal of Arachnology 29:127–134.

*Manuscript received 15 August 2017, revised 8 November 2017.*

# INSTRUCTIONS TO AUTHORS

(revised January 2018)

**All manuscripts are submitted online at**
http://www.editorialmanager.com/arachno

***General:*** The *Journal of Arachnology* publishes scientific articles reporting novel and significant observations and data regarding any aspect of the biology of arachnid groups. Articles must be scientifically rigorous and report substantially new information. Submissions that are overly narrow in focus (e.g., local faunal lists, descriptions of a second sex or of a single species without additional discussion of the significance of this information), that have poorly substantiated observational data, or that present no new information will not be considered. Book reviews will not be published.

Manuscripts must be in English and should use the active voice throughout. Authors should consult a recent issue of the *Journal of Arachnology* for additional points of style. Manuscripts longer than three printed journal pages (12 or more double-spaced manuscript pages) should be prepared as Feature Articles, shorter papers as Short Communications. Invited Reviews will be published from time to time and unsolicited reviews are also welcomed. All reviews will be subject to the same review process as other submissions.

***Submission:*** Manuscripts should be prepared in Microsoft Word and submitted electronically via our online system, *PeerTrack* (http://www.editorialmanager.com/arachno). *PeerTrack* will guide you through the step-by-step process including uploading the manuscript and all of its parts. The paper can be uploaded as one piece, with tables, figures, and appendices embedded, or as text, then tables, figures, and appendices, each uploaded individually. Ultimately, *PeerTrack* will assemble all parts of the paper into a PDF that you, as corresponding author, will need to approve before the submission process can be completed. Supplemental Materials (see below) can also be uploaded, but they are not bundled into the PDF. If the manuscript is accepted for publication, authors are responsible for ensuring that all figures are submitted as individual image files that meet the required resolution and dimensions (see "**Illustrations**" below). These may be submitted to *PeerTrack* or directly to the editor-in-chief.

***Voucher Specimens:*** Specimens of species used in your research should be deposited in a recognized scientific institution. All type material *must* be deposited in a recognized collection/institution and the identity of the collection must be given in the text of the manuscript.

*Checklist—Common Formatting Errors* is available as a PDF at http://www.americanarachnology.org/JOA.html#instructions

## FEATURED ARTICLES

**Title page.**—The title page includes the complete name, address, and e-mail address of the corresponding author; the title in bold text and sentence case; each author's name and address; and the running head.

**Running head.**—This should be in all capital letters, not exceeding 60 characters and spaces, and placed at the top of the title page. It should be composed of the authors' surnames and a short title. Examples: SMITH—SALTICIDS OF PANAMA; SMITH & CRUZ—SALTICIDS... ; SMITH ET AL.—SALTICIDS...

**Abstract.**—Length: ≤ 250 words for Feature Articles; ≤ 150 words for Short Communications.

**Keywords.**—Give 3–5 appropriate keywords or phrases following the abstract. *Keywords should not duplicate words in the title.*

**Text.**—Double-space text, tables, legends, etc. throughout. Except for titles and headers, all text should be left-justified. Do not add line numbers—they are automatically added by *PeerTrack*. Three levels of heads are used.

- The first level (METHODS, RESULTS, etc.) is typed in capitals and centered on a separate line.
- The second level head begins a paragraph with an indent, is in bold type, and is separated from the text by a period and a dash.
- The third level may or may not begin a paragraph but is italicized and separated from the text by a colon.

Use only the metric system unless quoting text or referencing collection data. If English measurements are used when referencing collection data, then metric equivalents should also be included parenthetically. All decimal fractions are indicated by a period (e.g., 3.141). Include geographic coordinates for collecting locales if possible, using one of the following formats: 0°12′32″S, 29°52′17″E or 0.2089°S, 29.8714°E.

***Citation of references in the text:*** Cite only papers already published or in press. Include within parentheses the surname of the author followed by the date of publication. A comma separates multiple citations by the same author(s) and a semicolon separates citations by different authors, e.g., (Smith 1970), (Jones 1988; Smith 1993), (Smith & Jones 1986, 1987; Jones et al. 1989). Include a letter of permission from any person who is cited as providing unpublished data in the form of a personal communication.

***Citation of taxa in the text:*** Include the complete taxonomic citation (author, year) for each arachnid genus and/or species name when it first appears in the abstract and text proper. For example, *Araneus diadematus* Clerck, 1757. For Araneae, this information can be found online at www.wsc.nmbe.ch. Citations for scorpions can be found in the *Catalog of the Scorpions of the World (1758–1998)* by V. Fet, W.D. Sissom, G. Lowe & M.E. Braunwalder. Citations for the smaller arachnid orders (pseudoscorpions, solifuges, whip scorpions, whip spiders, schizomids, ricinuleids and palpigrades) can be found at museum.wa.gov.au/catalogues-beta/. Citations for some species of Opiliones can be found in the *Annotated Catalogue of the Laniatores of the New World (Arachnida,Opiliones)* by A.B. Kury.

**Literature cited.**—Use the following style and formatting exactly as illustrated; include the full unabbreviated journal title.

Personal web pages should not be included in Literature Cited. These can be cited within the text as (John Doe, pers. website) without the URL. Institutional websites may be included in Literature Cited. If a citation includes more than six authors, list the first six and add "et al." to represent the others.

Binford, G. 2013. The evolution of a toxic enzyme in sicariid spiders. Pp. 229–240. *In* Spider Ecophysiology. (W. Nentwig, ed.). Springer-Verlag, Heidelberg.

Cushing, P.E., P. Casto, E.D. Knowlton, S. Royer, D. Laudier, D.D. Gaffin et al. 2014. Comparative morphology and functional significance of setae called papillae on the pedipalps of male camel spiders (Arachnida, Solifugae). Annals of the Entomological Society of America 107:510–520.

Harvey, M.S. & G. Du Preez. 2014. A new troglobitic ideoroncid pseudoscorpion (Pseudoscorpiones: Ideoroncidae) from southern Africa. Journal of Arachnology 42:105–110.

World Spider Catalog. 2015. World Spider Catalog. Version 16. Natural History Museum, Bern. Online at http://wsc.nmbe.ch/

Roewer, C.F. 1954. Katalog der Araneae, Volume 2a. Institut Royal des Sciences Naturelles de Belgique, Bruxelles.

Rubio, G.D., M.O. Arbino & P.E. Cushing. 2013. Ant mimicry in the spider *Myrmecotypus iguazu* (Araneae: Corinnidae), with notes about myrmecomorphy in spiders. Journal of Arachnology 41:395–399.

**Footnotes.**—Footnotes are permitted on the first page, only to give current address or other author information, and at the bottom of tables (see below).

**Taxonomic articles.**—Consult a recent taxonomic article in the *Journal of Arachnology* for style or contact a Subject Editor for Systematics. Papers containing original descriptions of focal arachnid taxa should be listed in the Literature Cited section.

**Tables.**—Each table, with the legend above, should be placed on a separate manuscript page. Only horizontal lines (usually no more than three) should be included. When necessary, tables may have footnotes, for example, to specify the meanings of symbols about particular data.

**Illustrations.**—Original illustrations include photographs, line drawings, maps, and other graphic representations. All should be considered figures and numbered consecutively with other figures. You should ensure that all illustrations, at submission, are at high enough resolution to be useful to editors and reviewers: 300 dpi is usually sufficient. When preparing images, consider the final dimensions of the image on a printed page. Images may be printed at a width of one column (20.8 picas, 3.45 inches or 8.8 cm), one and a half columns (31.3 picas, 5.2 inches or 13.25 cm) or two columns (43.3 picas, 7.2 inches or 18.3 cm). Maximum height for all printed images is 49.8 picas, 8.3 inches or 21.08 cm. Thus, if a figure must be printed two columns wide to be legible, its corresponding vertical dimension cannot be greater than 21.08 cm.

At the discretion of the Editor-in-Chief, a figure can be rendered in color in the online version but in monochrome in the journal's printed version, or in color in both versions if warranted by the figure's context and content. Address all questions concerning illustrations to the Editor-in-Chief of the *Journal of Arachnology*: **Deborah R. Smith, Editor-in-Chief** [*E-mail:* debsmith@ku.edu].

**Legends for illustrations** should be placed together on the same page(s). Each plate must have only one legend, as indicated below:

Figures 1–4. *A-us x-us*, male from Timbuktu: 1. Left leg. 2. Right chelicera. 3. Dorsal aspect of genitalia. 4. Ventral aspect of abdomen.

The following alternate Figure numbering is also acceptable:

Figure 1a–e. *A-us x-us*, male from Timbuktu: a. Left leg. b. Right chelicera. c. Dorsal aspect of genitalia. d. Ventral aspect of abdomen.

**Assemble manuscript.**—The manuscript should be assembled in the following sequence: title page, abstract, text, tables with legends, figure legends, figures. As noted above, at the time of submission the paper can be uploaded as one piece, with tables, figures, and appendices embedded, or as text, then tables, figures, and appendices, each uploaded individually. However, if manuscripts are accepted for publication, figures (or plates) must be provided in individual files.

**Supplemental materials.**—Authors may submit materials for online publication that importantly augment the contents of a manuscript. These may be audio files (e.g., .mp3, .m4a, .aif, .wav), video files (e.g., .mov, .m4v, .flv, .avi), or Word documents (e.g., .doc, .docx) for large tables of data. Consult with the Editor-in-Chief if you are considering submitting other kinds of files. Audio and video files should be carefully edited before submission to eliminate leaders, trailers, and other extraneous content. Individual files may not exceed 10MB; no more than five files may be included as supplemental materials for a manuscript.

Supplemental materials will be considered by reviewers and therefore must be included at the time of manuscript submission. Supplemental materials are published online at the discretion of the editors.

## SHORT COMMUNICATIONS

Short Communications are usually limited to 3–4 journal pages, including tables and figures (11 or fewer double-spaced manuscript pages including Literature Cited; no more than 2 figures or tables). Internal headings (METHODS, RESULTS, etc.) are omitted. Short communications must include an abstract and keywords.

**Page charges.**—Page charges are voluntary, but authors who are not members of the American Arachnological Society are strongly encouraged to pay in full or in part for their articles ($75 per journal page).

**Proofs.**—The Journal's expectation is that the final revision of a manuscript, the one that is ultimately accepted for publication, will not require substantive changes. Accordingly, the corresponding author will be charged for excessive numbers of changes made in the proofs.

**Reprints.**—PDFs of papers published in the *Journal of Arachnology* are available to AAS members at the society's web site. They are also available through BioOne (www.bioone.org) and JSTOR (www.jstor.org) if you or your institution is a member of BioOne or JSTOR. PDFs of articles older than one year are freely available from the AAS website.

## COVER ARTWORK

Authors are encouraged to send high quality color photographs to the Editor-in-Chief to be considered for use on the cover. Images should be at least 300 dpi.

# CONTENTS

Journal of Arachnology

Volume 46 Number 2

## Invited Review

A review of the mechanisms and functional roles of male silk use in spider courtship and mating
**by Catherine E. Scott, Alissa G. Anderson & Maydianne C.B. Andrade** ..... 173

## Featured Articles

Sexual dimorphism in the spinning apparatus of *Allocosa senex* (Araneae: Lycosidae), a wolf spider with a reversal in typical sex roles
**by Andrea Albín, Anita Aisenberg, Miguel Simó & Petr Dolejš** ..... 207

Morphology of setae on the coxae and trochanters of theraphosine spiders (Mygalomorphae: Theraphosidae)
**by Arthur Galleti Lima & José Paulo Leite Guadanucci** ..... 214

Response of the eastern sand scorpion, *Paruroctonus utahensis*, to air movement from a moth analog
**by Kathryn Ashford, Raven Blankenship, Wyatt Carpenter, Isaac Wheeler & Douglas Gaffin** ..... 226

From storage to delivery: sperm volume and number of spermatozoa inside storage organs and ejaculates in males of *Timogenes elegans* (Scorpiones: Bothriuridae)
**by David Eduardo Vrech, Paola Andrea Olivero, Camilo Iván Mattoni & Alfredo Vicente Peretti** ..... 231

A new, relictual *Antilloides* from Mexican caves: first mainland record of the genus and revised placement of the fossil *Misionella didicostae* (Araneae: Filistatidae)
**by Ivan L. F. Magalhaes** ..... 240

Systematics of the spiny trapdoor spider genus *Bungulla* (Mygalomorphae: Idiopidae): revealing a remarkable radiation of mygalomorph spiders from the Western Australian arid zone
**by Michael G. Rix, Robert J. Raven, Andrew D. Austin, Steven J. B. Cooper & Mark S. Harvey** ..... 249

Two new species of cave-adapted pseudoscorpions (Pseudoscorpiones: Neobisiidae, Chthoniidae) from Guangxi, China
**by Zhizhong Gao, J. Judson Wynne & Feng Zhang** ..... 345

Clarification of three species of *Discocyrtus* Holmberg, 1878 with convoluted taxonomic histories (Opiliones: Laniatores: Gonyleptidae: Pachylinae)
**by Adriano B. Kury, Ricardo Pinto-da-Rocha, Jürgen Gruber & Rafael N. Carvalho.** ..... 355

## Short Communications

Web asymmetry in the tetragnathid orb spider *Metellina mengei* (Blackwell, 1869) is determined by web inclination and web size
**by Nicholas Tew & Thomas Hesselberg** ..... 370

A method for accurately estimating social spider numbers without colony damage
**by Bharat Parthasarathy & Hema Somanathan** ..... 373

Assessing spider diversity in grasslands – does pitfall trap color matter?
**by Sascha Buchholz & Maria Möller** ..... 376

Reproductive strategy of a cave-living arachnid with indeterminate growth (*Phrynus longipes*; Amblypygi: Phrynidae)
**by Kenneth James Chapin & Emily Katherine Chen** ..... 380

Capturing the elusive camel spider (Arachnida: Solifugae): effective methods for attracting and capturing solifuges
**by Paula E. Cushing & Edmundo González-Santillán** ..... 384

*Instructions to Authors* ..... 388